



AGRICULTURAL RESEARCH INSTITUTE

PUSA

E
L
E
C
T
R
O
N
I
C
S
&
T
E
L
E
C
O
M
M
U
N
I
C
A
T
I
O
N
E
N
G
I
N
E
E
R
I
N
G
D
I
V
I
S
I
O
N

JOURNAL OF THE INSTITUTION OF ENGINEERS (INDIA)

79234



IARI



VOLUME 45

NUMBER 1

PART ET 1

SEPTEMBER 1964



PUBLISHED BY THE INSTITUTION
8 GOKHALE ROAD CALCUTTA

Rs. 2.50 .



NOW ...
WE GO
UNDERGROUND WITH
A BRAND-NEW
CABLE
ALIND SOLIDAL!

Here's an exciting new design in aluminium cable construction which is yet another classic example of Alind's forward-thinking!

Making the fullest possible use of the properties of aluminium as a conductor and pvc as an insulant, ALIND SOLIDAL will be a light, compact, easy-on-the-budget, easy-to-lay-and-joint cable!

Alind will gladly send you further information on this new type of cable



THE ALUMINIUM INDUSTRIES LTD.
India's largest manufacturers of aluminium conductors and accessories
Registered Office: Kundara (Kerala)
Plants: Kundara • Hirakud • Hyderabad
Managing Agents
SFSHASAYEE BROS. (TRAY) PRIVATE LIMITED

THE JOURNAL

OF

The Institution of Engineers (India)

SECRETARY & EDITOR : B. SESHADRI, B.Sc., A.I.I.Sc., D.I.C., M.Sc.(Eng.), M.I.E.

The Institution of Engineers (India) as a body accepts no responsibility for the statements made by the individual authors.

The Institution of Engineers (India) subscribes to the Fair Copying Declaration of the Royal Society and reprints of any portion of this publication may be made provided that reference thereto be quoted.

Vol. XLV

SEPTEMBER 1964

No. 1, Pt. ET 1

CONTENTS

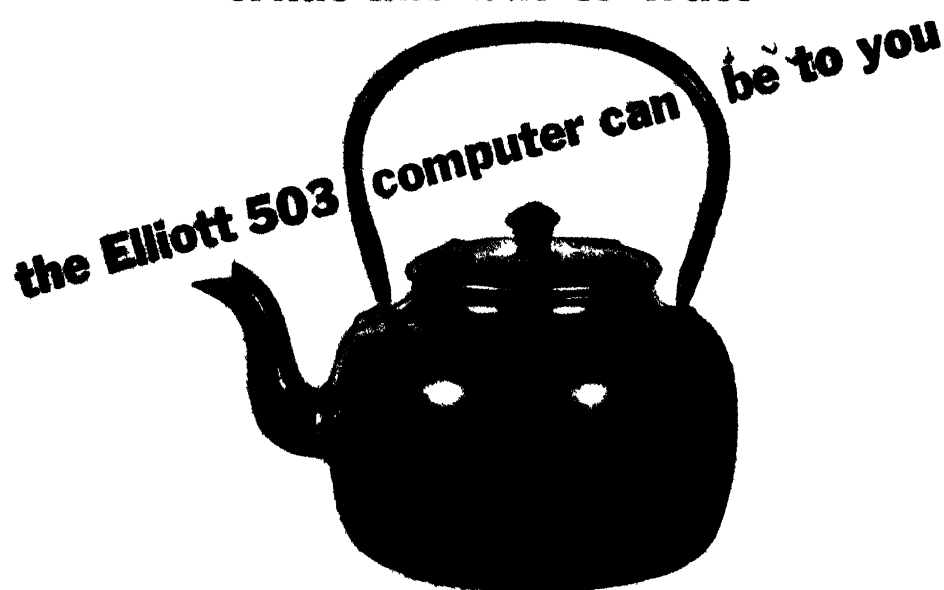
Page

ELECTRONICS AND TELECOMMUNICATION ENGINEERING DIVISION

Dr. A. K. Chatterjee (M.), *Chairman*

1. Propagation of Space Charge Waves in Accelerated Electron Beams. G. R. Babu, <i>Non-member</i> , and Dr. M. Chaudhuri, <i>Non-member</i> ..	1
2. Control System Stability by the Direct Method of Lyapunov. B. Chatterjee, <i>Non-member</i>	11
3. Computerization of Mitrovic's Method of Analysis and Synthesis of Feedback Control Systems. Dr. S. Das Gupta, <i>Associate Member</i> , and R. Chandra, <i>Non-member</i>	17
4. An Aspect of the Bang-Bang Control Problem. N. K. Gupta, <i>Non-member</i> , and B. P. Bhattacharyya, <i>Associate Member</i>	24
5. A Study of Backlash in Feedback Control Systems. I. J. Nagrath, <i>Non-</i> <i>member</i> , and D. C. Surana, <i>Non-member</i>	40
6. Gain Compensation of a Phase-Compensated Third Order Type-1 System. V. Seshadri, <i>Associate Member</i>	67
7. Transistor Operational Amplifier. R. Sundar, <i>Non-member</i>	77
8. Solution to Third Order Differential Equations with One Operational Amplifier. L. K. Wadhwa, <i>Non-member</i>	85
Corrigenda	90

What this was to Watt



A puff of steam, the mind of a genius—and a revolutionary discovery is made. Just like that. Today, discovery of this nature is virtually impossible. The problems are more complex—and to solve them we need more than steaming kettles, Archimedean bathtubs or falling apples. We need computers!

These days, great breakthroughs in science or engineering are usually only possible with the help of computers. In ten short years they are revolutionizing the daily life of every one of us.

At every stage in computer development Elliotts have led the way, solving the increasingly complex problems of tomorrow. Now Elliotts introduce a companion to their highly successful 803 computer—the 503, the greatest computer of its class ever produced.

ELLIOTT 503
computer

ELLIOTT COMPUTING DIVISION, ELLIOTT BROTHERS (LONDON) LIMITED

Sole Selling Agents LARSEN & TOUBRO LIMITED

P.O. BOX 278, BOMBAY 1

ALSO AT: CALCUTTA • NEW DELHI • MADRAS • BANGALORE • COCHIN
AHMEDABAD • LUCKNOW • HYDERABAD • BHOPAL • GOA • RAURKELA

THE JOURNAL

OF

The Institution of Engineers (India)

SECRETARY & EDITOR : B SESHADRI, B.Sc., A.I.I.Sc., D.I.C., M.Sc. (Eng.), M.I.E.

The Institution of Engineers (India) as a body accepts no responsibility for the statements made by the individual authors.

The Institution of Engineers (India) subscribes to the Fair Copying Declaration of the Royal Society and reprints of any portion of this publication may be made provided that reference thereto be quoted.

Vol. XLV

JANUARY 1965

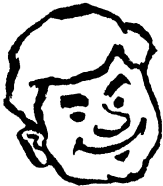
No. 5, Pt. ET 2

CONTENTS

Page

ELECTRONICS AND TELECOMMUNICATION ENGINEERING DIVISION

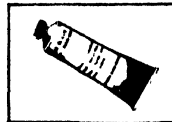
1. Transistorized Definite Time-Lag Relay Using Constant Current Charging Source. S. K. Basu, *Non-member* .. 91
2. Microwave Spectrometer. M. M. Rao, *Non-member*, and S. K. Chatterjee, *Non-member* . 98
3. Design of Electron Optical Systems for Collimators and Deflectors. C. S. Upadhyay, *Non-member* 111
4. Simulation of Fourth Order Systems with Double Lead by Single Operational Amplifier. L. K. Wadhwa, *Non-member*, and Maj. S. P. Sharma, *Associate Member* .. 120



Joining materials for Insulated Aluminium Conductors

KERALITE GREASE

This special conducting and moisture inhibiting grease when applied to bare aluminium wire terminals and accessories removes oxide film, precludes moisture and ensures permanent and efficient connection.



KERALITE ANTI-CORROSIVE TAPE (KAT)

Special adhesive cotton tape coated with water-repellent chemicals. Absolutely waterproof, quickly and easily applied, KAT ensures practically a permanent protection against atmospheric, chemical and electrolytic corrosion, and can be used with advantage on aluminium-to-aluminium or aluminium-to-copper connections, and for service connections, from distribution mains.

KERALITE SOLDER

For soldering of aluminium conductors



We stock the full range of joining materials ..also carry the complete tool kit for Insulated cable jointing.



ALIND

... where forward thinking
is a fact of habit

THE ALUMINIUM INDUSTRIES LTD.

India's largest manufacturers of
aluminium conductors and accessories

Registered Office: Kundara (Kerala)

Plants: Kundara • Mirakud • Hyderabad

Managing Agents

SESHASAYEE BROS. (TRAV.) PRIVATE LIMITED

PROPAGATION OF SPACE CHARGE WAVES IN ACCELERATED ELECTRON BEAMS*

G. R. Babu

Non-member

and

Dr. M. Chaudhuri

Non-member

*Department of Electronics and Telecommunication Engineering,
Birla College of Engineering, Pilani*

Summary

Theoretical investigation of space charge waves in an accelerated or decelerated electron stream is presented in this paper using one-dimensional small signal approximation. An attempt is made to obtain certain general differential equations of fluctuations. Equations of space charge waves for the case where the potential distribution is independent of the space charge of the beam are deduced. These general equations are verified for some of the special cases, e.g., (i) uniformly accelerated electron beam, (ii) space charge limited diode, (iii) space charge waves in constant potential drift space, and (iv) space charge waves in velocity jump.

1. Notations

u_0 = D.C. velocity component,

v = A.C. (fluctuating) velocity component,

I_0 = D.C. beam current,

i = A.C. (fluctuating) beam current,

$\eta = \frac{e}{m}$ = specific charge of an electron,

i_ω = fluctuating current component at frequency, ω ,

v_ω = fluctuating velocity component at frequency, ω ,

ρ_0 = D.C. beam density,

ρ = A.C. (fluctuating) beam density,

θ = transit angle,

ω_p = plasma angular frequency, and

ω = angular frequency of A.C. quantities.

* Written discussion on this paper will be received until November 30, 1964.

This paper was received on March 24, 1964.

2. Introduction

There are two theories concerning the propagation of fluctuations in an electron beam. The theory of Hahn and Ramo¹ treats fluctuations in an electron beam flowing in a constant potential drift space and shows that they are constituted by a velocity modulation wave and a current modulation wave travelling as standing waves, 90° apart in phase with each other. The other one is Llewellyn-Peterson's formulations known as 'L-P' equations² which express the relationship between several A.C. quantities in a diode at high frequencies.

The mechanism of amplification in space charge wave tubes and the generation of noise in beam type amplifiers are both analyzed by these theories. The L-P equations have a serious defect in spite of their great utility that the D.C. potential distribution of a beam is completely decided by its space charge condition. Generally, however, the D.C. potential distribution in electron gun region of a beam type amplifier depends mainly upon the shape and arrangement of the gun electrodes and is nearly independent of the space charge of the electron beam. So, a solution of fluctuations in problems concerning some special distribution of potential along the beam is needed.

With this objective in view, a general differential equation of fluctuations is obtained. This general equation leads to the well known equations of space charge waves for the case where the potential distribution is independent of the space charge of the beam. From this equation of space charge waves in general, solutions for the following particular cases are also obtained :

- (i) Uniformly accelerated beam ;
- (ii) Space charge limited diode ;
- (iii) Space charge waves in constant potential drift space ; and
- (iv) Space charge waves in velocity jump region.

3. General equation of space charge waves

The following assumptions are made to simplify the theory :

- (i) An electron beam has a velocity component in the z -direction only (z is the direction of propagation) and is extended infinitely on a plane transverse to the z -direction ;
- (ii) All A.C. and D.C. quantities have uniform values on a plane perpendicular to the z -axis ;
- (iii) A.C. quantities are sufficiently small compared with the corresponding D.C. quantities ;
- (iv) No relativistic velocities are used (i.e., the D.C. velocity of the electrons is small compared with the velocity of light) ; and
- (v) Emission velocities of electrons are assumed to be negligible and the electrons start with zero velocities at the cathode.

The fundamental laws on which the theory is based are :

- (i) Newton's laws of motion ;
- (ii) Equation of continuity of current ;
- (iii) Poisson's equation ; and
- (iv) Equation relating current density, charge density and electron velocity.

These are expressed in mathematical terms as

$$\frac{d}{dt}(u_0 + v) = -\eta(E_0 + E) \quad (1)$$

$$\frac{\delta i}{\delta z} = -\frac{\delta \rho}{\delta t} \quad (2)$$

$$\frac{\delta E}{\delta z} = \frac{\rho}{\epsilon} \quad (3)$$

$$-I_0 + i = (\rho_0 + \rho)(u_0 + v) \quad (4)$$

$$I_0 = -\rho_0 u_0 \quad (5)$$

$$\eta = \frac{e}{m} \quad (6)$$

where the subscript, 0, represent the D.C. quantities.

Eliminating ρ from equations (2) and (3), we get

$$i + j\omega \epsilon E = J \quad (7)$$

where the integration constant, J , means the total current density physically, i.e., J is the current flowing along the external circuit connected between two parallel plane electrodes where an electron beam flows between them. So if the impedance of such an external circuit is infinitely large, we may assume that $J = 0$. Moreover, the A.C. components vary with time as $\exp(j\omega t)$ and u_0 and ρ_0 are functions of z .

Hence, in general the equations may be written as

$$v_x = u_0 + v_\omega \exp(j\omega t) \quad (8)$$

$$i_x = i_\omega \exp(j\omega t) \quad (9)$$

$$E_x = E_0 + E_\omega \exp(j\omega t) \quad (10)$$

$$\rho = \rho_\omega \exp(j\omega t) \quad (11)$$

Substituting the variable, z , by the electron transit angle, θ , given by

$$\theta = \int_0^z \frac{\omega}{u_0} dz \quad (12)$$

and introducing a change of variable

$$i = y e^{-j\theta} \quad (13)$$

from equation (1), we get

$$\frac{1}{u_0} \frac{\delta}{\delta \theta} \left(u_0^2 \frac{\delta y}{\delta \theta} \right) + \frac{\eta}{\epsilon} \frac{I_0}{\omega^2} y = 0 \quad (14)$$

and

$$v_\omega = j \frac{u_0}{I_0} \frac{\delta y}{\delta \theta} e^{-j\theta} \quad (15)$$

Equations (13), (14) and (15) are the general equations for the space charge waves. To get solutions of these equations the relationship between u_0 and θ is to be known. It means that the distribution of D.C. potential, V , should be assumed.

4. Solution of general equations for $V \propto z^n$

In a space charge limited diode the D.C. potential is proportional to $\frac{4}{3}$ power of the distance from the cathode. Extending this idea, solutions of space charge waves when the D.C. potential is proportional to the n th power of the distance from the cathode may be derived. Assuming

$$\frac{V}{z^n} = \frac{V_1}{z_1^n} = F \quad (16)$$

and using equation (13) and $u_0^2 = 2 \eta V$, the following relationships can be established :

$$u_0 = (2 \eta F)^{\frac{1}{2}} z^{\frac{n}{2}} \quad (17)$$

$$\theta = \frac{\omega}{(2 \eta F)^{\frac{1}{2}}} \frac{z^{\frac{2-n}{2}}}{1 - \frac{n}{2}} \quad (18)$$

With the help of equations (17) and (18), the following differential equation is obtained from equation (14) :

$$\frac{\partial}{\partial \theta} \left(\theta^{\frac{2n}{2-n}} \frac{\delta y}{\partial \theta} \right) + \frac{\eta I_0}{\omega^2 \epsilon B} \theta^{\frac{n}{2-n}} y = 0 \quad (19)$$

where

$$B = \left\{ 2 \eta F \left(\frac{1 - \frac{n}{2}}{\omega} \right)^n \right\}^{\frac{1}{2-n}} \quad (20)$$

Equation (19) can be solved if it can be modified to the form

$$\frac{\partial^2 y}{\partial x^2} + \frac{1-2\nu}{x} \frac{\partial y}{\partial x} + y = 0 \quad (21)$$

since the solution of equation (21) is given by

$$y = x^\nu P J_{\nu}(x) + Q N_{\nu}(x) \quad (22)$$

where P and Q are the constants.

In order to transform equation (19) to the form of equation (21), a new variable x is introduced, x being related to θ as given by

$$x = C \theta^\xi \quad (23)$$

where C and ξ are constants and

$$C^2 \xi^2 = \frac{\eta I_0}{\omega^2 \epsilon B} \quad (24)$$

Using equations (23) and (24), equation (19) can easily be transformed as

$$\frac{\delta^2 y}{\delta x^2} + \frac{1}{\theta C \xi \theta (\xi - 1)} \left(\frac{2n}{2 - n} + \xi - 1 \right) \frac{\delta y}{\delta x} + \frac{\theta n - 2}{\theta (2\xi - 2)} y = 0 \quad (25)$$

In order to make equation (25) identical to equation (21), the following conditions have to be satisfied :

- (i) The coefficient of the term, y , in equation (25) must be unity ; and
- (ii) The coefficient of $\frac{\delta y}{\delta x}$ in equation (25) must be equated to $\frac{1 - 2\nu}{x}$.

Condition (i) leads to

$$\xi = \frac{3n - 4}{2(n - 2)} \quad (26)$$

Condition (ii) with the help of equations (23) and (26) leads to

$$\nu = \frac{n - 2}{n} \quad (27)$$

Equations (26) and (27) show that the constants, ξ and ν , are functions of n and hence the potential distribution in the beam.

The values of i and ν are obtained from equations (13) and (15), once the value of y is known, which is of course given by the solution expressed in equation (22). The constants, P and Q , of equation (22) can be determined by substituting equation (22) in equation (13) and (15) with $i = i_1$ and $\nu = \nu_1$ where i_1 and ν_1 being are the values of i and ν respectively at a distance, $z = z_1$. With the expression for P and Q thus determined, the general expression for i and ν can be written in the matrix form as

$$\begin{bmatrix} i \\ \nu \end{bmatrix} = \begin{bmatrix} E^* & F^* \\ H^* & I^* \end{bmatrix} \begin{bmatrix} i_1 \\ \nu_1 \end{bmatrix} \quad (28)$$

The matrix elements E^* , F^* , H^* and I^* are given by the following relationship which are obtained with the help of the expressions for P and Q determined as

$$E^* = \left(\frac{x}{x_1} \right)^\nu \frac{J_{|\nu|}(x) N_{|\nu-1|}(x_1) - J_{|\nu-1|}(x_1) N_{|\nu|}(x)}{J_{|\nu|}(x_1) N_{|\nu-1|}(x_1) - J_{|\nu-1|}(x_1) N_{|\nu|}(x_1)} \quad [29(a)]$$

$$F^* = \mp \frac{I_0 \theta_1}{\xi u_1} \frac{1}{x_1} \left(\frac{x}{x_1} \right)^\nu \frac{J_{|\nu|}(x) N_{|\nu|}(x_1) - J_{|\nu|}(x_1) N_{|\nu|}(x)}{J_{|\nu|}(x_1) N_{|\nu-1|}(x_1) - J_{|\nu-1|}(x_1) N_{|\nu|}(x_1)} \quad [29(b)]$$

$$H^* = \mp \frac{\xi U_0}{I_0 \theta} x \left(\frac{x}{x_1} \right)^\nu \frac{J_{|\nu-1|}(x) N_{|\nu-1|}(x_1) - J_{|\nu-1|}(x_1) N_{|\nu-1|}(x)}{J_{|\nu|}(x_1) N_{|\nu-1|}(x_1) - J_{|\nu-1|}(x_1) N_{|\nu|}(x_1)} \quad [29(c)]$$

$$I^* = - \frac{u_0 \theta_1}{u_1 \theta} \left(\frac{x}{x_1} \right)^{\nu+1} \frac{J_{|\nu-1|}(x) N_{|\nu|}(x_1) - J_{|\nu|}(x_1) N_{|\nu-1|}(x)}{J_{|\nu|}(x_1) N_{|\nu-1|}(x_1) - J_{|\nu-1|}(x_1) N_{|\nu|}(x_1)} \quad [29(d)]$$

For F^* and H^* , the negative sign is to be taken when ν is positive and *vice versa*.

5. Applications of general equations

Uniformly accelerated electron beam

In this case, the potential V is proportional to z and therefore $n = 1$. Substitution of $n = 1$ in equations (26) and (27) gives $\xi = \frac{1}{2}$ and $\nu = -1$.

Introducing the plasma frequency, ω_p , given by

$$\omega_p = \left[\frac{I_0 e}{u_0 m \epsilon} \right]^{\frac{1}{2}} = \left[\frac{I_0 \eta}{u_0 \epsilon} \right]^{\frac{1}{2}} \quad (30)$$

in equation (24), we get

$$C \xi = \frac{\omega_p}{\omega} \sqrt{\frac{u_0}{B}} \quad (31)$$

Writing $u_0 = (2 \eta F)^{\frac{1}{2}} z^2$ and

$$B = \left\{ 2 \eta F \left(\frac{1 - \frac{n}{2}}{\omega} \right)^n \right\}^{\frac{n}{n-2}}$$

it can be shown that

$$\sqrt{\frac{u_0}{B}} = \left(\frac{1}{\theta} \right)^{\frac{n}{n-2}}$$

so that equation (31) can be rewritten as

$$C \xi = \frac{\omega_p}{\omega} \left(\frac{1}{\theta} \right)^{\frac{n}{n-2}} \quad (32)$$

Putting $\xi = \frac{3n-4}{2(n-2)}$ in equation (23) and using equation (32), it can easily be shown that

$$x = \frac{4 - \frac{2n}{3}}{\frac{4n}{3} - \frac{\omega_p}{\omega}} \theta \quad (33)$$

Since in the present case $n = 1$, we get

$$x = \frac{2 \omega_p}{\omega} \theta$$

Thus, putting $\nu = -1$, $\xi = \frac{1}{2}$ and $x = \frac{2 \omega_p}{\omega} \theta$ in the equations [29(a)] to [29(d)] the matrix elements for the case under investigation are given as

$$E^* = \frac{J_1(x) N_2(x_1) - J_2(x_1) N_1(x)}{x \{ J_1(x_1) N_2(x_1) - J_2(x_1) N_1(x_1) \}} \quad [34(a)]$$

$$F^* = j \frac{2G}{x} \frac{J_1(x_1) N_1(x) - J_1(x) N_1(x_1)}{J_1(x_1) N_2(x_1) - J_2(x_1) N_1(x_1)} \quad [34(b)]$$

$$H^* = j \frac{x_1}{2G} \frac{N_2(x) J_2(x_1) - N_2(x_1) J_2(x)}{J_1(x_1) N_2(x_1) - J_2(x_1) N_1(x_1)} \quad [34(c)]$$

$$I^* = \frac{J_1(x_1) N_2(x) - J_2(x) N_1(x_1)}{J_1(x_1) N_2(x_1) - J_2(x_1) N_1(x_1)} \quad [34(d)]$$

where

$$\left. \begin{aligned} G &= \frac{I_0 \theta}{u_0} = \frac{I_0 \theta_1}{u_1} \\ \text{and} \quad \frac{x}{\theta} &= \frac{x_1}{\theta_1} = \frac{2 \omega_p}{\omega} \end{aligned} \right\} \quad (35)$$

Equations (34) are similar to those obtained by Tien and Field.³

Space charge waves in constant potential drift space

Different methods were adopted by earlier investigators for deriving the equations for space charge waves in a constant potential drift space. But with the help of the general equation derived and discussed in earlier sections it is easy to deduce the equation for space charge waves in a constant potential drift space. Here the D.C. velocity u_0 is independent of θ and so equation (14) is written as

$$\frac{\partial^2 y}{\partial \theta^2} + \left(\frac{\omega_p}{\omega} \right)^2 y = 0 \quad (36)$$

Solving equation (36), the following matrix relationship is obtained with the initial conditions $i = i_1$ and $v = v_1$ as

$$\begin{bmatrix} i \\ v \end{bmatrix} = \begin{bmatrix} \cos \frac{\omega_p}{\omega} \theta & -j \frac{I_0}{u_0} \frac{\omega}{\omega_p} \sin \frac{\omega_p}{\omega} \theta \\ -j \frac{u_0}{I_0} \frac{\omega_p}{\omega} \sin \frac{\omega_p}{\omega} \theta & \cos \frac{\omega_p}{\omega} \theta \end{bmatrix} \begin{bmatrix} i_1 \\ v_1 \end{bmatrix} \quad (37)$$

This is a well known relationship to be found in text books.⁴

Space charge waves in velocity jump region

Field and Watkins⁵ have shown that when an electron beam passes through a narrow gap in which the beam is rapidly accelerated or decelerated, the current fluctuation of the beam is not affected but the velocity fluctuation is either increased or decreased in an inverse proportion to the change of the D.C. velocity the beam. This relationship was obtained by them from the Llewellyn-Peterson equations or the energy relationship. The same can however be arrived at with the help of equations (34). In a narrow gap, the potential distribution may be considered to be nearly linear, so the relationship between input and output fluctuations is expressed by the limits that the potential gradient becomes infinitely large and θ and θ_1 become infinitely small in equations (34). Substituting these limiting values and making use of the following simplifying expressions for the Bessel functions which are valid for small argument, we get

$$\left. \begin{aligned} J_{\nu}(x) &= \frac{x^{\nu}}{2^{\nu} \Gamma(\nu+1)} \\ N_{\nu}(x) &= -\frac{(\nu-1)!}{\pi x^{\nu}} \end{aligned} \right\} \quad (38)$$

the following well established relationships⁴ are obtained :

$$\left. \begin{aligned} i &= i_1 \\ v &= \frac{u_1}{u_0} v_1 \end{aligned} \right\} \quad (39)$$

6. Solution for cases where general equation breaks down

Case for $n = \frac{4}{3}$

For $n = \frac{4}{3}$, $V = F z^{\frac{4}{3}}$ and this represents the case where the current is purely space charge limited. When $n = \frac{4}{3}$, equations (26) and (27) show that ξ and ν become respectively zero and infinity and so the matrix relationships given in equation (29) can not be used. In order to solve for this case the following expedient can be followed.

Let a new variable ζ be introduced in place of θ , but which is related to θ by the relationship

$$\theta = e^{\zeta} \quad (40)$$

Using equation (40) with $n = \frac{4}{3}$, equation (19) is modified as

$$\frac{\delta^2 y}{\delta \zeta^2} + 3 \frac{\delta y}{\delta \zeta} + \frac{\eta I_0}{\omega^2 \epsilon B} y = 0 \quad (41)$$

Since the space charge limited current is given by

$$I_0 = \frac{4}{9} \epsilon \sqrt{2} \eta \frac{V_1^{\frac{3}{2}}}{z_1^{\frac{3}{2}}}$$

the above relationship can be rewritten as

$$\eta \frac{I_0}{\epsilon} = \frac{2}{9} (2 \eta F)^{\frac{3}{2}} \quad (42)$$

where F is given by

$$V_1 = F z_1^{\frac{4}{3}}$$

With the help of equations (20) and (40), the coefficient of y in equation (41) can be simplified as

$$\frac{\eta I_0}{\omega^2 \epsilon B} = 2$$

with $n = \frac{4}{3}$.

Equation (41) ultimately becomes

$$\frac{\delta^2 y}{\delta \zeta^2} + 3 \frac{\delta y}{\delta \zeta} + 2 y = 0$$

its solution being

$$y = A e^{-\zeta} + B e^{-2\zeta} \quad [43(a)]$$

$$\nu = \frac{A}{\theta} + \frac{B}{\theta^2} \quad [43(b)]$$

Using equation [43(b)] with equations (13) and (15) for $i = i_1$ and $v = v_1$ at $z = z_1$ ($\theta = \theta_1$), the constants A and B are evaluated, whence the matrix elements for i and v are obtained as

$$E^* = \frac{\theta_1 (2\theta - \theta_1)}{\theta^2} \quad [44(a)]$$

$$F^* = -jG_1 \frac{(\theta - \theta_1)}{\theta^2} \quad [44(b)]$$

$$H^* = -jG_1 \frac{1}{\theta} \frac{2\theta_1 (\theta - \theta_1)}{\theta} \quad [44(c)]$$

$$I^* = -\frac{\theta - 2\theta_1}{\theta} \quad [44(d)]$$

where

$$G_1 = \frac{I_o \theta}{u_o} \quad (45)$$

Space charge limited diode

Using the L-P equations, the equation for fluctuations in a space charge limited diode can be obtained on the same lines as developed by Pierce.⁷ From the discussion in the previous sections, the same equation can be arrived at easily.

Putting $\theta_1 = 0$ in equation (44) and using the resultant matrix elements in the matrix equations for i and v , we get

$$i = -j \frac{I_o \theta}{u_o} v_1 \quad [46(a)]$$

and

$$v = -v_1 \quad [46(b)]$$

Equations (46) are similar to those obtained by Pierce.⁷

7. Acknowledgment

The authors thank Shri V. Lakshminarayanan, Principal, Birla College of Engineering, Pilani, for his encouragement and permission to publish this paper.

8. References

1. S. Ramo. 'Electronic Wave Theory of Velocity Modulation Tubes'. *Proceedings of the Institution of Radio Engineers*, vol. 27, no. 12, December 1939, p. 757.
2. F. B. Llewellyn and L. C. Peterson. 'Vacuum Tube Network'. *Proceedings of the Institution of Radio Engineers*, vol. 32, no. 3, March 1944, p. 144.
3. L. M. Field and P. K. Tien. 'Space Charge Waves in an Accelerated Electron Stream for Amplification of Microwave Signals'. *Proceedings of the Institution of Radio Engineers*, vol. 40, no. 6, June 1952, p. 688.

4. R. G. Hutter. 'Beam and Wave Electronics in Microwave Tubes'. *D. Van Nostrand Co., Inc.*, 1960.
5. L. M. Field, P. K. Tien and D. A. Watkins. 'Amplification by Acceleration and Deceleration of a Single-Velocity Stream'. *Proceedings of the Institution of Radio Engineers*, vol. 39, no. 2, February 1951, p. 194.
6. D. A. Watkins. 'Travelling Wave Tube Noise Figure'. *Proceedings of the Institution of Radio Engineers*, vol. 40, no. 1, January 1952, p. 65.
7. J. R. Pierce. 'Travelling Wave Tubes'. *D. Van Nostrand Co., Inc.*, 1950.

CONTROL SYSTEM STABILITY BY THE DIRECT METHOD OF LYAPUNOV*

B. Chatterjee

Non-member

*Department of Electronics and Electrical Communication Engineering,
Indian Institute of Technology, Kharagpur*

Summary

In this paper, the direct (or second) method of Lyapunov, as used to study the stability of control systems, is discussed. As this method does not require a solution of the system equations, it is specially useful for studying the stability of nonlinear systems, the differential equations for which are often not amenable to analytical solutions. Another important advantage of this method is that it considers stability in a region and not at an equilibrium point, thus giving stability in the large.

Introduction

Control systems, which are essentially negative feedback devices, may get unstable at one or more frequencies within the system passband, due to phase shifts in its different parts. For proper operation, a control system must remain stable at all frequencies within its passband, and the study of stability is the most important one. The commonly used methods of analyzing the stability of a system, e.g., Nyquist criterion, Routh test, etc., are applicable to linear systems only. Unfortunately, however, all physical systems are essentially nonlinear in character, due to the effects of saturation, threshold, backlash, hysteresis, etc. Some simpler systems may approximately be treated as linear over some limited ranges of operation. But for many control systems used in practice, this approximation can, at the most, give a rough idea of system stability. Again, in many control systems for industrial and military applications, nonlinearities are purposely introduced for improving system performances. In all such cases, the nonlinear nature of the system has to be taken into account for studying the system stability.

But the study of stability of a nonlinear system is rather involved, as in general, the corresponding differential equations cannot be solved analytically. Stability analysis of nonlinear systems (and nonlinear equations) are primarily based on the perturbation method of Poincaré¹ or the second (or direct) method of Lyapunov.²

Poincaré¹ has developed his theory of stability from the 'variational equations' where stability is analyzed with respect to singular points (critical points) and limit cycles. For the former, the stability concerns the equilibrium (asymptotic stability), whereas for the latter, it relates to a stationary motion on the limit cycle (orbital stability). If the system comes back to its original singular point or limit cycle after being

* Written discussion on this paper will be received until November 30, 1964.

This paper was received on April 24, 1963.

perturbed slightly, the system is stable at that point or gives a stable oscillation at that cycle. But if the perturbation or deviation increases with time, it is unstable. As an infinitesimal perturbation is assumed in studying stability, it is called 'infinitesimal stability,' in contrast to stability in the large as given by the method of Lyapunov.

The direct method (second method) of Lyapunov is based on the properties of definiteness of certain functions associated with the differential equation (linear or nonlinear) in such a manner that it is possible to know whether the solution remains in a certain region or not.³ As the condition of stability or instability is determined for a certain region and not for a singular point, this method is well suited for the investigation of stability in the large.

Analysis of stability

The object of the direct method of Lyapunov in analyzing stability of a system is to answer the question of stability of the differential equation (or equations) by utilizing the given form of the equation but without an explicit knowledge of its solutions. It is more a point of view or philosophy of approach, rather than a systematic method.⁴ But it is very useful for studying the stability of nonlinear and/or non-stationary systems, the differential equations for which cannot be solved easily.

The principal idea of the method is that if the rate of change, $\frac{dE(x)}{dt}$ of the energy, $E(x)$ (or equivalent), of an isolated physical system is negative for any possible state, X , except for a single equilibrium state, X_e , then the energy will continuously decrease till it reaches the minimum value, $E(X_e)$. Under that condition, the system will be stable. Physically it means that a dissipative system, perturbed from its equilibrium state, will always return to it.

It is to be noted that for a general equation of motion in a purely mathematical form, there is no natural way of defining energy. As such, to investigate the stability, a suitable scalar function, $V(X)$, is considered instead. This particular function, $V(X)$, is called 'Lyapunov function.' Occasionally, but not necessarily always, V and E are identical.

The generalized differential equation of a control member may be written as

$$J \frac{d^2\mu}{dt^2} + R \frac{d\mu}{dt} + K \mu = f^*(\sigma) \quad (1)$$

where μ is the generalized coordinate of the control member, and J , R and K are its constant parameters (inertia, damping and restoring force respectively). The force function, $f^*(\sigma)$, is often a nonlinear function of the actuating signal, σ . The actuating signal, in turn, is the arithmetic difference of the applied signal and the feedback signal, $(r - \mu)$, i.e.,

$$\sigma = \sum_{\alpha=1}^m p_{\alpha} h_{\alpha} - r \mu \quad (2)$$

where h is the generalized coordinate of the physical system in question and r the feedback coefficient.

Also, we have

$$\frac{dh_i}{dt} = \sum_{\alpha=1}^n b_{i\alpha} h_{\alpha} + h \mu \quad (3)$$

where $i = 1, \dots, n$.

For investigating stability, the above equations are put in proper canonical forms after suitable transformation of variables. The Lyapunov function, $V(X)$, may be written as³

$$V = \phi + \Psi + \int_0^{\sigma} f(\sigma) d\sigma \quad (4)$$

where

$$\Psi = \sum_{k=1}^{n+1} \sum_{i=1}^{n+1} \frac{a_k a_i}{\rho_k + \rho_i} x_k x_i \quad (5)$$

$$\phi = \frac{1}{2} (A_1 x_1^2 + \dots + A_n x_n^2) + c_1 x_{n+1} x_{n+2} + \dots + c_{n-1} x_n x_{n+1} \quad (6)$$

where the ρ 's are the roots of the characteristic equations and a , A and C the constants.

After simplification, we get

$$\frac{dV}{dt} = -[F_1] - [F_2] + f(\sigma) [(F_3) + (F_4)] \quad (7)$$

where (F_1) and (F_2) contain only positive terms and the essence of the method is to set both (F_3) and (F_4) to zero, for stability. In that case, $\frac{dV}{dt}$ will always be negative in the given region and the Lyapunov condition of stability will be satisfied.

In explicit form

$$\left. \begin{aligned} (F_3) &= A_i + B_i + 2\sqrt{r} a_i + 2 a_i \sum_{k=1}^{n+1} \frac{a_k}{\rho_k + \rho_i} = 0 \\ (F_4) &= C_{\alpha} + B_{s+\alpha} + 2\sqrt{r} a_{s+\alpha} + 2 a_{s+\alpha} \sum_{k=1}^{n+1} \frac{a_k}{\rho_k + \rho_{\alpha}} \end{aligned} \right\} \quad (8)$$

where A_i , C_{α} , a , etc. are constants. Equations (8) give sufficient condition for stability by the Lyapunov method.

Evidently, equation (8) define a certain region, G , in the parameter space in which $(F_3) \leq 0$ and $(F_4) \leq 0$ is satisfied and hence the system is stable over a certain region, thus giving stability in the large. Two simple examples⁴ are given below.

Example 1

Let us consider the case of a simple harmonic oscillator whose frequency has been normalized to unity. The differential equation is given below.

or,

$$\left. \begin{aligned} \frac{d^2 x_1}{dt^2} + x_1 &= 0 \\ \frac{d^2 x_2}{dt^2} &= -x_1 \end{aligned} \right\} \quad (9)$$

Putting $\frac{dx_1}{dt} = x_2$, we get (10)

$$\frac{d^2 x_1}{dt^2} = \frac{dx_2}{dt} = -x_1 \quad (11)$$

If we define

$$V(x) = x_1^2 + x_2^2 = E(x)$$

then from equations (10) and (11) we get

$$\frac{dV(x)}{dt} = 2x_1 \frac{dx_1}{dt} + 2x_2 \frac{dx_2}{dt} = 2x_1 x_2 - 2x_1 x_2 = 0$$

That is, the system is a conservative one and the point moves on a steady limit cycle in the parameter space. In other words, this is a case of orbital stability as depicted in Fig. 1.

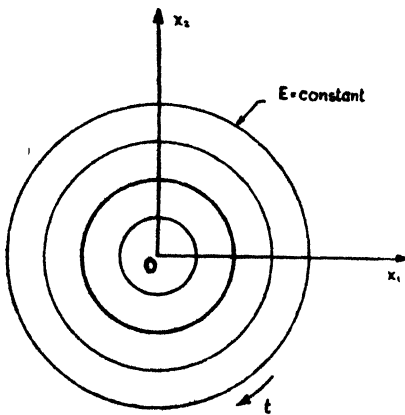


Fig. 1
Phase-plane trajectory

The above solution is for a simple linear system and can be found out easily by methods other than that of Lyapunov, as given above. But the advantage of Lyapunov's method will be more evident for a nonlinear case, as illustrated below.

Example 2

Let us take a simple system with nonlinear damping, the differential equation of which is given by

$$x_2 \frac{dx_1}{dt} - x_1 \frac{dx_2}{dt} = x_1^2 + x_2^2 \quad (12)$$

Such an equation cannot be solved easily and the Lyapunov's method is useful here.

Putting

$$\frac{dx_1}{dt} = +x_2 - a x_1 (x_1^2 + x_2^2)$$

we get

$$\frac{dx_2}{dt} = -x_1 - a x_2 (x_1^2 + x_2^2) \quad (13)$$

where a is a positive constant. Taking the Lyapunov function as

$$V(x) = x_1^2 + x_2^2$$

and substituting from equation (13), we get

$$\frac{dV(x)}{dt} = 2x_1 \frac{dx_1}{dt} + 2x_2 \frac{dx_2}{dt} = -2a(x_1^2 + x_2^2)^2 = -2aV^2(x) \quad (14)$$

and hence is negative for all values of x_1 and x_2 except for $x_1 = x_2 = 0$, the trivial solution.

Hence, $V(X)$ satisfies the condition of a Lyapunov function for all values of x_2 and x_1 (i.e., all points in the parameter space) and the system is unconditionally stable. Any point in the parameter space will ultimately move to the origin corresponding to $V(X) = 0$ as shown in Fig. 2. Figs. 1 and 2 show respectively the phase-plane trajectories corresponding to the differential equations (9) and (12).

Many more such problems may be worked out. Letov⁵ has given many such examples on control system problems, which may be consulted.

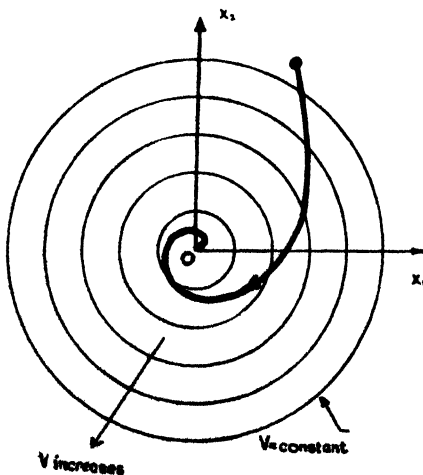


Fig. 2
Phase-plane trajectory

Conclusions

One of the principal advantages of Lyapunov's method is that it provides a tool for studying stability and transient behaviours of dynamic systems without solving the differential equations of the system. This is of special importance to nonlinear and/or non-stationary systems, where it is very difficult and often impossible to have any analytical solution of the equations. Another great advantage of the method is that it gives stability in a region, i.e., stability in the large, instead of stability in the neighbourhood of equilibrium positions, as in the classical methods.

The difficult part of the method is to find the Lyapunov function, $V(X)$. The method does not give any means of determining $V(X)$, but merely states that if such a function exists, the stability conditions are satisfied. Although an explicit expression for the Lyapunov function can be found for the linear stationary case [from equation (4)], no such straightforward method is yet available for the nonlinear or non-stationary cases. Further applied mathematical research may some day solve this problem, but still it is a matter of intuition and ingenuity to find the Lyapunov function of a nonlinear or non-stationary system.

The direct method of Lyapunov is more a unifying principle and a philosophy of approach than a real method, but it can give valuable information on stability in the large, which is of so much importance in many control system applications.

References

1. H. Poincare. 'Les Methodés Nouvelles de la Mécanique Céleste'. T-1, Gauthier-Villars, Paris, 1892.
2. A. M. Lyapunov. 'General Problems of Stability of Motion'. Charkov, 1892.
3. N. Minorsky. 'Nonlinear Oscillations'. D. Van Nostrand Co., Inc., 1962.
4. R. E. Kalman and J. E. Bertram. 'Control System Analysis and Design via the Second Method of Lyapunov'. *Proceedings of the American Society of Mechanical Engineers*, vol. 82 D, no. 2, June 1960, p. 371.
5. A. I. Lourje. 'Nonlinear Problems in the Theory of Automatic Regulation'. Moscow, 1951.
6. A. M. Letov. 'Stability of Nonlinear Control Systems'. Princeton University Press, 1961.

COMPUTERIZATION OF MITROVIC'S METHOD OF ANALYSIS AND SYNTHESIS OF FEEDBACK CONTROL SYSTEMS*

Dr. S. Das Gupta

Associate Member

Professor, Department of Electrical Engineering, Jadavpur University

and

R. Chandra

Non-member

Department of Electrical Engineering, University of Roorkee, Roorkee

Summary

A recent approach to the problem of analysis of feedback control systems suggested by Mitrovic holds considerable promise. The analysis of linear systems according to this method primarily depends on evaluating two variables—essentially polynomials of the real variables ρ and ω_n . In this paper, a scheme is suggested for a computer set-up which could evaluate both the variables. Two control system problems are actually set up according to this scheme and the corresponding Mitrovic curves plotted. These curves are then compared with those obtained by desk calculator computations. The results are satisfactory for all practical purposes. The roots of the characteristic equation of an overdamped system are graphically determined in one case from the curves drawn from experimental results and, these also check closely with the actual values of the roots.

Introduction

The analysis of a feedback control system for its performance means investigation of stability, damping, transient overshoot, settling time, etc. Several methods were devised earlier for this purpose. A more recent analytic approach holding considerable promise is suggested by Mitrovic.^{2,3} His method is, in fact, equivalent to many of the previous methods taken together. It approaches the problem algebraically by handling the equation with Laplace transform. The most important advantages are:

- (i) All the operations are effected in the real domain;
- (ii) The coefficients of the characteristic equation are adjusted without any calculation; and
- (iii) All the roots of the characteristic equation may be determined almost simultaneously.

The method is easy to apply for analysis and synthesis. It is especially suitable for the design of systems in which settling time and damping ratio are specified. It may be applied to sampled-data servo systems also.

* Written discussion on this paper will be received until November 30, 1964.

This paper was received on August 29, 1963.

The method is described in this paper briefly without giving the details of the proof. In a later section of the paper, an analogue computer method according to Mitrovic's theory is suggested. Two simple type-1 servo systems are taken as examples and actual computer set-ups are made. The computer solution and the calculated results are compared. A discussion of this analysis and the results are given elsewhere in this paper.

Mitrovic's method

The characteristic equation of a linear feedback control system is given by

$$\begin{aligned} f(s) &= a_n s^n + a_{n-1} s^{n-1} + \dots + a_2 s^2 + a_1 s + a_0 \\ &= A(s) + a_1 s + a_0 \text{ (say)} \end{aligned} \quad (1)$$

Now, in the above equation, it is assumed that the constant coefficients a_1 and a_0 are just a set of constant values of a set of variables ξ and η , such that for all values of complex variables, these two real variables ξ and η attain values to make

$$A(s) + \xi s + \eta = 0 \quad (2)$$

Applying the transformation

$$T(s) = \omega_n e^{j\left(\frac{\pi}{2} + \theta\right)} = -\omega_n \sin \theta + j\omega_n \cos \theta = -\omega_n \zeta + j\omega_n \sqrt{1 - \zeta^2} \quad (3)$$

where $0 \leq \theta < \frac{\pi}{2}$ and $0 \leq \zeta \leq 1$, to equation (2) and equating the real and imaginary parts, we get

$$\xi = \sum_{i=2}^n a_i \bar{\Phi}_i(\zeta) \omega_n^{i-1} \quad (4)$$

$$\eta = - \sum_{i=2}^n a_i \bar{\Phi}_{i-1}(\zeta) \omega_n^i \quad (5)$$

The functions $\Phi_i(\zeta)$ are independent of the coefficients, a_i . These functions, Φ_i [the symbol Φ_i is henceforth used for indicating $\Phi_i(\zeta)$ for brevity] may be very easily calculated from

$$\Phi_i = - [2 \zeta \Phi_{i-1} + \Phi_{i-2}] \quad (6)$$

with

$$\Phi_0 = 0 \text{ and } \Phi_1 = -1$$

Evidently, these functions are dependent only on the damping ratio, ζ . Thus, these coefficients could be calculated once for all in a tabular form for various values of ζ ranging from 0 to 1.

Equations (4) and (5) are of fundamental importance in Mitrovic's method. It is observed from these equations that a curve could be plotted with ξ as the independent variable and η as the dependent one, with ω_n as the parameter. Also, for $\omega_n = 0$, both $\xi = 0$ and $\eta = 0$. In other words, corresponding to $\omega_n = 0$, the point in the ξ - η plane is its origin. If now for a constant ζ , ω_n is increased, the value of s changes in the direction shown in the s -plane [Fig. 1(a)]. Fig. 1(b) shows the corresponding trans-

formed curve in ξ - η plane. This curve is designated as $\bar{\zeta}$ curve. If all the coefficients a_i in equation (1) are present and are greater than zero, the $\bar{\zeta}$ curve encloses a region, in the positive-half plane, between the $\bar{\zeta}$ curve and the ξ -axis, as shown shaded in Fig. 1(b). Further increase in ω_n makes η negative and the $\bar{\zeta}$ curve enters the fourth quadrant. It was shown by Mitrovic² that a point, M, having coordinates (a_1, a_0) will fall within the shaded region provided that all the roots of equation (1) will fall within the domain shown in full line in the s -plane in Fig. 2, bounded by the contour C. Evidently, as we are tacitly assuming that all a 's in equation (1) are present and are greater than zero, the roots contained within the domain bound by the contour C is also contained by the contour C' shown in broken lines in Fig. 2. Thus, for instance if a plot of $\bar{0}$ curve is obtained as in Fig. 3, and if the values of the constants, a_1 and a_0 , are such that the point M with coordinates (a_1, a_0) lies within the shaded region, then the system is stable. Any point M' falling outside the region naturally indicates instability. Finally, the point M'' indicates that the system is oscillatory. Thus $\bar{0}$ plot is in essence the counterpart of the frequency response in the KG-plane.

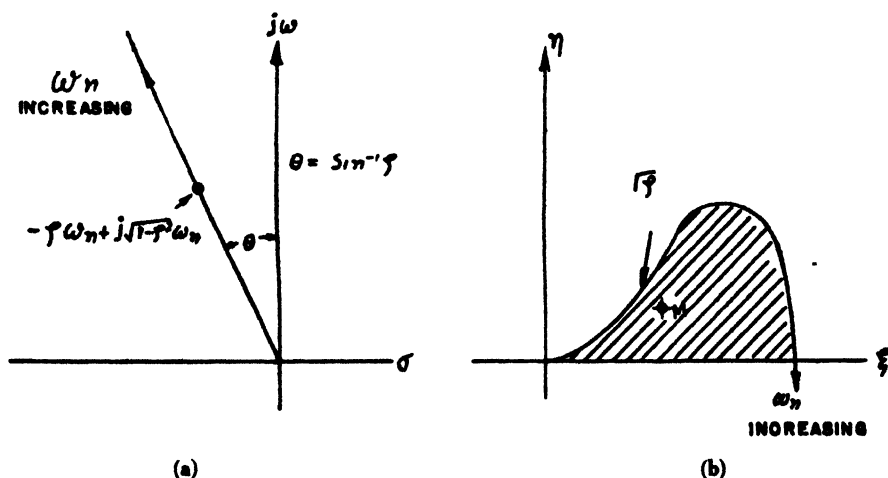


Fig. 1

Locus of s and corresponding $\bar{\zeta}$ curve

Similarly, if now a $\bar{1}$ curve is drawn along with a $\bar{0}$ curve, as in Fig. 4, then a point M as shown will mean an underdamped solution, as although all the possible roots are in the left-half of the s -plane, there are at least some roots which are not on the real axis (as this point is not enclosed by the $\bar{1}$ curve). Thus, the region external to the $\bar{1}$ curve but included within $\bar{0}$ curve is the underdamped region. The point M' on the other hand represents overdamped systems with all real negative (and also distinct) roots. Finally, a point M'' represents a critically damped system. Evidently, if a $\bar{\zeta}$ curve is drawn and the characteristic point M lies on it, then, according equation (2), the characteristic equation in question has a pair of complex roots, $-\zeta \omega_n \pm j\sqrt{1-\zeta^2} \omega_n$.

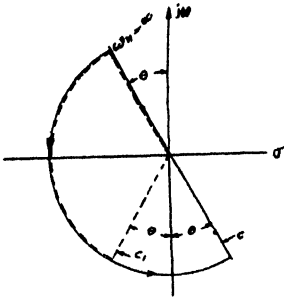


Fig. 2

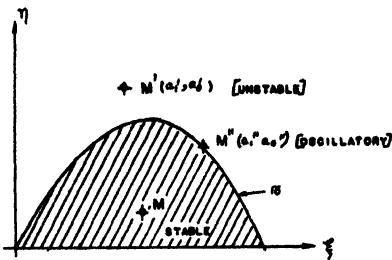
Curve showing contours C and dC_1 

Fig. 3

Typical 0 curve

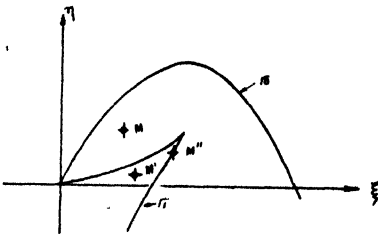


Fig. 4

0 and π curves for typical system

Scope of the present work

It will be seen from the foregoing considerations that a computer set-up to describe the characteristic equation in the Mitrovic form will be of great use. In what follows, one such scheme is suggested which is simple enough to set. Mitrovic equations (4) and (5) for a few simple systems are set up according to this scheme, and the corresponding Mitrovic curves obtained. These curves are then compared with the curves obtained by desk calculator computations. The result, as seen from the plots, is satisfactory for all practical purposes.

Mitrovic suggested a scheme for automatic plotting of the Mitrovic curves which is based on a different principle.⁴ It is found that the scheme suggested in this paper, although not particularly suitable for automatic plotting, is probably more advantageous for its inherent simplicity and is quite adequate for the purpose of computing equations (4) and (5), for various values of ρ and ω_n . Also, in this scheme, the use of the two-position servo as required in Mitrovic's scheme is avoided. To the best of our knowledge, Mitrovic's scheme has not yet been set up on a computer.

Computer circuit

The circuit shown in Fig. 5, is a modification of a potentiometric machine in which operational amplifiers with unity feedback are used for isolating adjacent sections of potentiometer circuits to avoid the loading effect. The potentiometer gang, P, fixes the value of ω_n . The potentiometers labelled as a_2, a_3 , etc., are used to set the values of the respective coefficients of the characteristic equation (1). The gang switch, S_1 , (inclusive of S_{11}, S_{12} , etc.) chooses the correct circuitry for either equation (4) or (5), i.e., for either the variable ξ or η respectively, as shown in Fig. 5. The potentiometers labelled as $|\Phi_1|, |\Phi_2|$, etc. set the magnitudes of the factors Φ_1, Φ_2 , respectively for the value of damping ratio under consideration. Since these potentiometers, in effect, constitute a set of input impedances of an operational amplifier, it is possible to set values of $|\Phi|$ both greater and less than one. The switches S_2 , etc. are provided for the sign of the variable Φ . For instance, for a certain value of ζ , if the value of Φ is positive, the corresponding sign switch is switched on to the positive side, and so on.

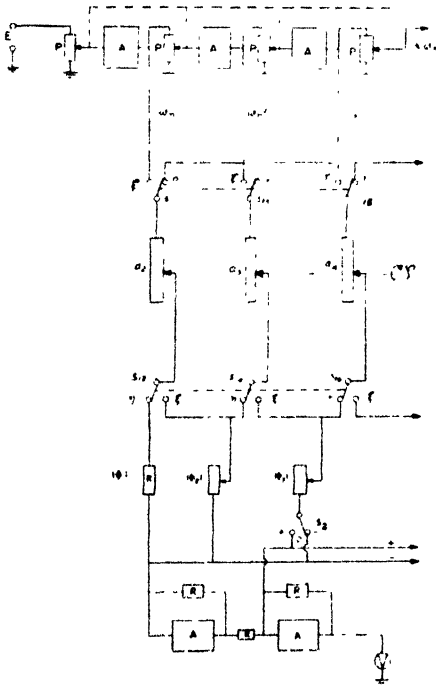


Fig. 5
Schematic diagram of analogue
computer set-up

The two operational amplifiers, connected as adders, sum up all the components of the equation in question and the output voltage is measured by a voltmeter as shown.

The ratio, $\frac{V}{E}$, gives the value of ξ or η according to the position of switch S_1 .

Scaling of equations

The values of a_2, a_3 , etc., and ω_n (or σ for $\sqrt{1}$ curve) being set on potentiometers, require that these should be each less than one. Naturally, the equations have to be scaled down whenever required. In such a case, it is only a matter of a constant factor, normally a round figure, by which the output result is to be multiplied.¹

Experimental results

Two type-1 systems are taken as example problems out of those worked out by Mitrovic.¹ The open-loop transfer function of these systems are :

$$G(s) = \frac{K}{s(s+2)(s+3)} \quad (7)$$

$$G(s) = \frac{K}{s(s+2)(s+1.2)} \quad (8)$$

The Γ_0 and Γ_1 curves for the systems above are given in Figs. 6 and 7 respectively. These curves drawn from the calculated and experimental data are reasonably close for all practical purposes.

The point, M_1 , in Fig. 7 corresponds to an overdamped solution. The three tangent lines drawn from the point M_1 (each tangent shown with an arrow head at their tips) has slopes equal to the negative of the three respective roots of the overdamped characteristic equation.

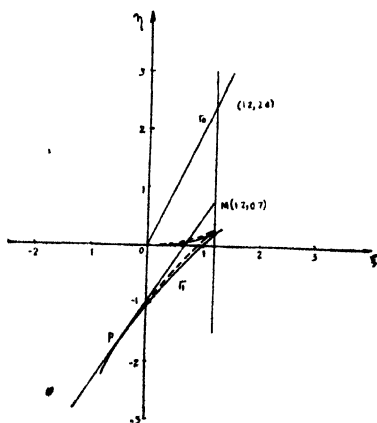


Fig. 6

Γ_0 and Γ_1 curves for type-1 system

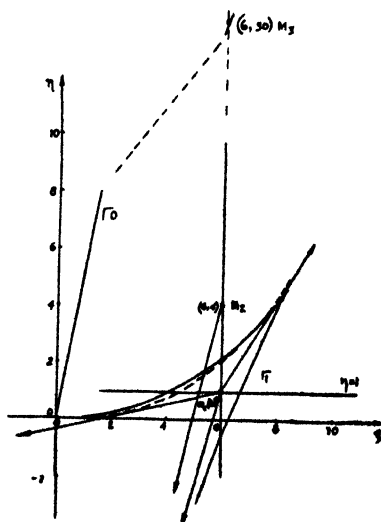


Fig. 7

Γ_0 and Γ_1 curves for type-1 system

The values of the roots obtained from the experimental solution are -0.2 , -1.5 , and -3.3 . The roots calculated, correct to three significant digits, are -0.198 , -1.552 , and -3.25 respectively. A very high accuracy is possibly due to the fact that the point M_1 has been chosen almost in the middle of the region. A point, M , chosen closer to the Γ_1 contour however will not give such high accuracy.

The point M_2 is an operating point corresponding to an underdamped oscillation. The real root is at $s = -3.65$. Finally, M_3 corresponds to a purely oscillatory condition in the system.

Conclusions

An analogue computer scheme is presented to obtain the Mitrovic curves for various values of damping ratio with the natural frequency as a parameter on the curve.

Two type-1 systems are set up in a computer according to this scheme and the results given. The computer results check closely with the calculated results.

The roots of the characteristic equation of an overdamped system are obtained in one case from the curves from the experimental results. These are also in close agreement with the calculated values.

Acknowledgments

The authors thank the authorities of Bengal Engineering College for providing them the facilities to design and build a differential analyzer and carry out the work presented in this paper.

References

1. R. Chandra. 'An Analogue Computer Approach for Mitrovic's Method of Analysis of Linear Feedback Control Systems'. Thesis submitted to the University of Calcutta for the Master's degree, 1961.
2. D. Mitrovic. 'Graphical Analysis of Feedback Control Systems'. *Proceedings of the American Institute of Electrical Engineers*, vol. 77, pt. 2, no. 40, January 1959, p. 476.
3. G. J. Thaler and R. G. Brown. 'Analysis and Design of Feedback Control Systems'. *McGraw-Hill Book Co., Inc.*, 1960.
4. D. Mitrovic. 'Automatic Plotting of Characteristic Curves and Analogue Solution of Algebraic Equations'. *Proceedings of the American Institute of Electrical Engineers*, vol. 80, pt. 1, no. 58, January 1962, p. 701.

AN ASPECT OF THE BANG-BANG CONTROL PROBLEM***N. K. Gupta***Non-member*

and

B. P. Bhattacharyya*Associate Member**Department of Electrical Engineering, Bengal Engineering College, Howrah***Summary**

In this paper, a special case of bang-bang control is considered wherein the higher order derivatives of the controlled variable are 'quenched' at the switching instants. The idea was first put forward by Chang (1955), who showed that such systems have faster response-time compared with what is obtainable by conventional minimal-time systems. The approach seems to have received scant attention in the control literature, and is discussed here in connection with optimizing (by the bang-bang principle) a third order system having a pair of complex open-loop poles. Problems associated with quenching of higher order derivatives in such systems are discussed.

1. Introduction

In recent years, the problem of optimal control has engaged extensive interest. The basic task in such systems is that certain performance index of the system behaviour is either to be minimized or maximized.

In a large number of applications, the index of performance is taken to be the 'time' needed for the physical system to move from a given initial state to some desired final state. The system is said to behave in an 'optimal fashion' if, subject to certain constraints in the forcing capabilities, the time required to perform such task is minimized. Such systems have been variably termed as minimal-time systems, time-optimal systems, or final value systems.

A characteristic feature of such systems is that the control force referred to is always worked at extremes. Typically, if a motor is driven utilizing its maximum permissible torque in either direction, always the system behaves in the best possible manner. Earlier works of Bushaw,¹ Bellman, *et al*,² lent mathematical credence to this intuitive idea and a great spurt of activity has ensued since then in this field.

It is not the purpose of this paper to cover this extensive background of studies made on the problem to date. Rather, attention is drawn to one promising aspect of the problem which has, apparently, escaped attention in the control literature.

* Presented at the First Conference of Automation and Computation Scientists of India, Sindri, February 22-24, 1963.

In order to bring the process to any desired final state, it is necessary to reverse the direction of the control force at certain specified instants. When the force is thus reversed, it is assumed that all the components of the process state are continuous. If, instead of maintaining the continuity of all the components some are quenched at the instant of switching reversal, a system having faster response-time compared with conventional minimal-time systems will result. The practical problems associated with such quenching will have to be resolved with ingenuity depending upon the physical nature of the process. But the aspect which holds promise is the simplification attainable in implementing the decision rule (with attendant simplification of computer hardware) when 'quenching' is resorted to. In a subsequent section, this aspect is dealt with in some detail. The consideration that lead Chang³ propose the idea of 'quenching' is given below.

2. Review of Chang's approach

Chang considered a system (Fig. 1) in which the process (the motor-load combination) transfer characteristics is given by a linear differential equation of the form

$$T_\phi \frac{d^3 e}{dt^3} + \frac{d^2 e}{dt^2} = \delta \frac{T_m}{J} \quad (1)$$

where T_ϕ is the field time constant, T_m the maximum allowable torque, J the inertia of the motor and load torque, and e the error equal to $(\theta_i - \theta_o)$, and δ represents the switching condition and has a value of ± 1 .

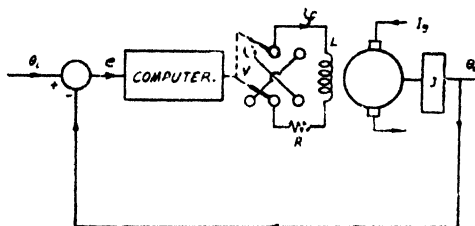


Fig. 1

Block diagram of system

Derivation of equation

The motor is a D.C. field-controlled machine where armature current i_a is assumed to be a constant. Assuming a linear relationship between field current, i_f and flux ϕ , the motor torque is given by, $T = K i_f$. Also, neglecting friction, $T = J \frac{d^2 \theta_o}{dt^2}$. The forcing voltage, δV , and the field current, i_f , are related by

$$R i_f + L \frac{di_f}{dt} = \delta V \quad (2)$$

Combining the equations, we get

$$T_\phi \frac{d^3 \theta_o}{dt^3} + \frac{d^2 \theta_o}{dt^2} = -\delta \frac{T_m}{J} \quad (3)$$

where $T_\phi = \frac{L}{R}$ and $T_m = \frac{KV}{R}$. For $\theta_i = 0$, equation (1) is obtained, since $\theta_i - \theta_o = e$.

The problem is to devise a switching logic which brings $|e|$ to zero in minimum time. This problem was also treated by Bogner and Kazda⁴ who derived the equations for the switching surface and the zero trajectory, assuming continuity of $\frac{de}{dt}$ and $\frac{d^2e}{dt^2}$ before and after switching reversal.

Chang imposed constraints on the continuity of $\frac{d^2e}{dt^2}$ by making $\frac{d^2e}{dt^2} = 0$ at the switching instant. Physically, the constraint is realized by keeping the contacts of the field-circuit open for a small period during switching reversal. By means of anti-arcing devices the current, i_f , may be brought to zero in an interval of time equal to approximately 1 or 2% of the field time constant. The field current, i_f vs. time is shown qualitatively in Figs. 2(a) and (b) for close-circuit and open-circuit switching. Since acceleration ($\frac{d^2\theta}{dt^2}$ or $\frac{d^2e}{dt^2}$ equivalently) is proportional to i_f , for all practical purposes, $\frac{d^2\theta}{dt^2}$ may be quenched in a negligibly small time.

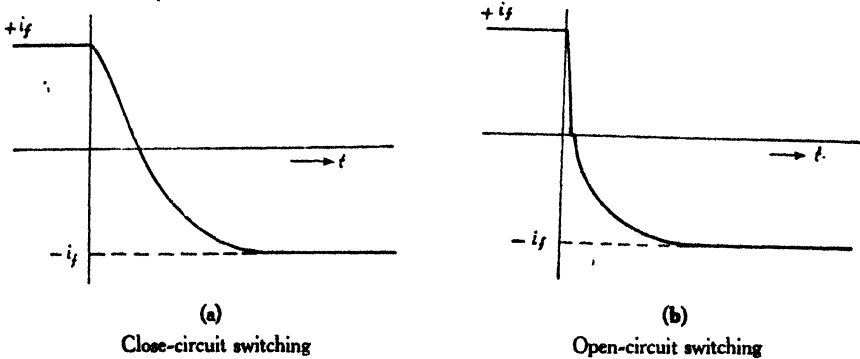


Fig. 2

Curve of field current vs. time

Let $e = U_1$, $\frac{de}{dt} = U_2$ and $\frac{d^2e}{dt^2} = \frac{dU_2}{dt}$ denote the phase-space variables. Then the solution to equation (1) in terms of U_1 and U_2 , with the condition

$$\frac{dU_2}{dt} = 0 \text{ at } t = 0 \quad (4)$$

is

$$U_1 = \frac{\delta T_m T_\phi^2}{J} \left(\frac{t^2}{2 T_\phi^2} + 1 - \frac{t}{T_\phi} - \epsilon^{-\frac{t}{T_\phi}} \right) + U_{20} + U_{10} \quad (5)$$

$$U_2 = \frac{\delta T_m T_\phi}{J} \left(\frac{t}{T_\phi} - 1 + \epsilon^{-\frac{t}{T_\phi}} \right) + U_{20} \quad (6)$$

where U_{10} and U_{20} are the initial state where the trajectory starts, and t is the time required to reach any state, U_1, U_2 .

If U_1 and U_2 are the desired final state of the system, the origin, say, then on substitution of the final values in equations (5) and (6), the set of initial points is obtained by a reverse process, wherefrom all trajectories converge to the final state. The locus of these points constitutes the critical boundary in question. It should be pointed out that the critical boundary derived in this manner is not a trajectory, as in the case where the constraint in equation (4) is not satisfied. In a three-dimensional phase-space, it is a surface [Fig. 3(a)] dividing the space in two regions over which the polarity of the forcing function has opposite signs. The projection of switching surface and zero-trajectories in U_1 - U_2 plane as derived by Chang is shown in Fig. 3(b). The response of this system is compared with the case where continuity of the state variables is maintained (Fig. 4).

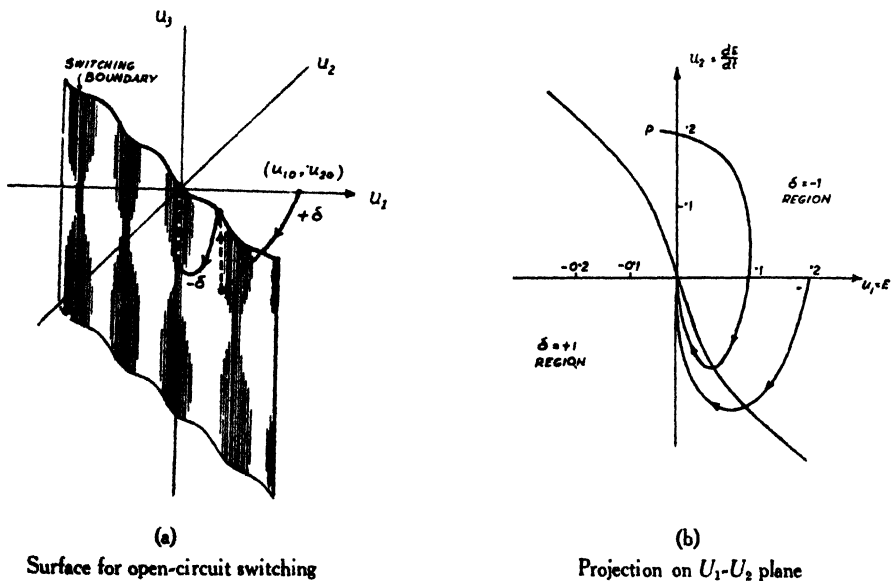


Fig. 3
Diagram of switching surface and zero-trajectory

The result is significant for two reasons. First by the response time is about 20% faster in this case. The second and the more important reason is the reduction in the number of switchings required with the consequent simplification attained in devising the switching logic. If all the higher order derivatives are brought to zero whenever their components e and $\frac{de}{dt}$ become equal to those specified by the critical boundary, then only one switching reversal is required irrespective of the order of the system. In practical cases, however, it might be difficult to force all the higher order derivatives to zero simultaneously at the time of switching reversal. At present, it is difficult to establish exactly how many switching reversals will be required for varying degrees of quenching.

But it is certain from physical considerations that the time required to reach the origin will still be less than the continuous-state case.

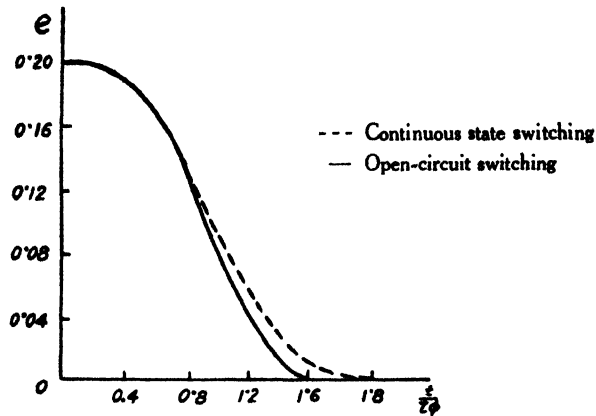


Fig. 4

Comparison of time responses of systems

In a subsequent section, the difficulties in realizing these conditions are explained. However, in the following section, this simplification in deriving the switching boundary for two other third order cases is utilized.

3. Critical boundary for other third order systems

Case 1 : Third order type-zero system with all real roots

Referring to Fig. 5, the plant transfer function is taken as

$$G(S) = \frac{K_1}{(S + \alpha_1)(S + \alpha_2)(S + \alpha_3)} \quad (7)$$

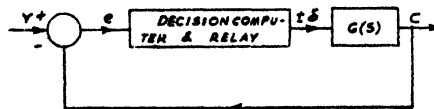


Fig. 5

Block diagram of system

The differential equation of the system in terms of θ_0 is

$$\frac{d^3\theta_0}{dt^3} + (\alpha_1 + \alpha_2 + \alpha_3) \frac{d^2\theta_0}{dt^2} + (\alpha_1\alpha_2 + \alpha_2\alpha_3 + \alpha_3\alpha_1) \frac{d\theta_0}{dt} + \alpha_1\alpha_2\alpha_3\theta_0 = \pm \delta K_1 \quad (8)$$

For $r(t) = 0$, the equation in terms of error, e , is

$$\frac{d^3e}{dt^3} + (\alpha_1 + \alpha_2 + \alpha_3) \frac{d^2e}{dt^2} + (\alpha_1\alpha_2 + \alpha_2\alpha_3 + \alpha_3\alpha_1) \frac{de}{dt} + (\alpha_1\alpha_2\alpha_3)e = \pm K_1\delta \quad (9)$$

The problem is particularized at this point by assuming $\alpha_1 = 1$, $\alpha_2 = 2$, $\alpha_3 = 3$ and $K \triangleq 6$. The equation becomes

$$e + 6 \frac{d^2 e}{dt^2} + 11 \frac{de}{dt} + 6e = \pm 6\delta \quad (10)$$

The solution of this differential equation is

$$e = A_1 e^{-t} + A_2 e^{-2t} + A_3 e^{-3t} \pm \delta \quad (11)$$

where A_1 , A_2 , and A_3 are arbitrary constants to be determined from initial conditions.

Substituting

$$\left. \begin{aligned} e &= U_1 \\ \frac{de}{dt} &= U_2 \\ \frac{d^2 e}{dt^2} &= U_3 = \frac{dU_2}{dt} \end{aligned} \right\} \quad (12)$$

we get

$$\left. \begin{aligned} U_1 &= A_1 e^{-t} + A_2 e^{-2t} + A_3 e^{-3t} + \delta \\ U_2 &= -A_1 e^{-t} - 2A_2 e^{-2t} - 3A_3 e^{-3t} \\ \frac{dU_2}{dt} &= A_1 e^{-t} + 4A_2 e^{-2t} + 9A_3 e^{-3t} \end{aligned} \right\} \quad (13)$$

Assuming the conditions at the time of switching as

$$\left. \begin{aligned} U_1 &= U_{10} \\ U_2 &= U_{20} \\ \frac{dU_2}{dt} &= 0 \end{aligned} \right\} \quad (14)$$

and substituting these values in equation (13), the time being initially taken as zero, we get

$$U_{10} = A_1 + A_2 + A_3 \pm \delta \quad [15(a)]$$

$$U_{20} = -A_1 - 2A_2 - 3A_3 \quad [15(b)]$$

$$0 = A_1 + 4A_2 + 9A_3 \quad [15(c)]$$

If the values of A_1 , A_2 and A_3 are known, the value of U_{10} and U_{20} can be calculated from above. The locus of U_{10} and U_{20} thus found can be used as the switching boundary. Our interest is at present restricted to calculation of this boundary. For this purpose, A_1 , A_2 and A_3 are calculated for positive as well as negative values of δ using equation (13) and assigning U_1 , $U_2 = 0$ therein. Under this condition, equation (13) becomes

$$A_1 e^{-t} + A_2 e^{-2t} + A_3 e^{-3t} \pm \delta = 0 \quad [16(a)]$$

$$-A_1 e^{-t} - 2A_2 e^{-2t} - 3A_3 e^{-3t} = 0 \quad [16(b)]$$

By assigning various arbitrary values to time t , the values of A_1 , A_2 and A_3 are calculated from equations [15(c)], [16(a)] and [16(b)]. These values are again substituted in equations [15(a)] and [15(b)] for obtaining corresponding values for U_{10} and U_{20} .

When these values of U_{10} and U_{20} are plotted in the U_1 - U_2 plane, the resulting critical boundary is obtained as shown in Fig. 6. The curve in the fourth quadrant is the boundary corresponding to positive δ and that in the second quadrant corresponds to negative δ . Fig. 7(a) shows a typical optimum trajectory with discontinuous switching and Fig. 7(b) the corresponding time response for an initial error of 0.53 units.

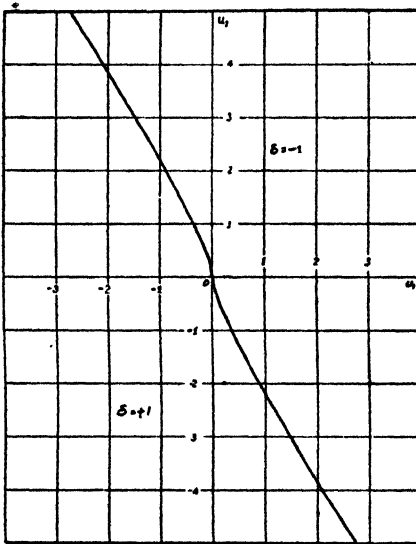


Fig. 6
Critical boundary for third order
type-0 system

Case 2: Third order system with complex roots

As is well known, if the roots of the characteristic equation of a control system are complex, the switching trajectory becomes very complicated even for the second order case.⁵ Lotz and Titus⁶ has adopted certain approximation techniques for a third order system with complex roots. It is shown in this paper that using Chang's idea the derivation of the switching boundary for such cases becomes a straightforward procedure. This is best illustrated by considering an example.

In Fig. 5, let

$$G(S) = \frac{K}{(S + 0.5)[(S + 6)^2 + 64]} \quad (17)$$

with $K = 1$ (say).

As before, if $r(t) = 0$, the differential equation in terms of the system error, e , is given by

$$\frac{d^3 e}{dt^3} + 12.5 \frac{d^2 e}{dt^2} + 106 \frac{de}{dt} + 50 e = \pm \delta \quad (18)$$

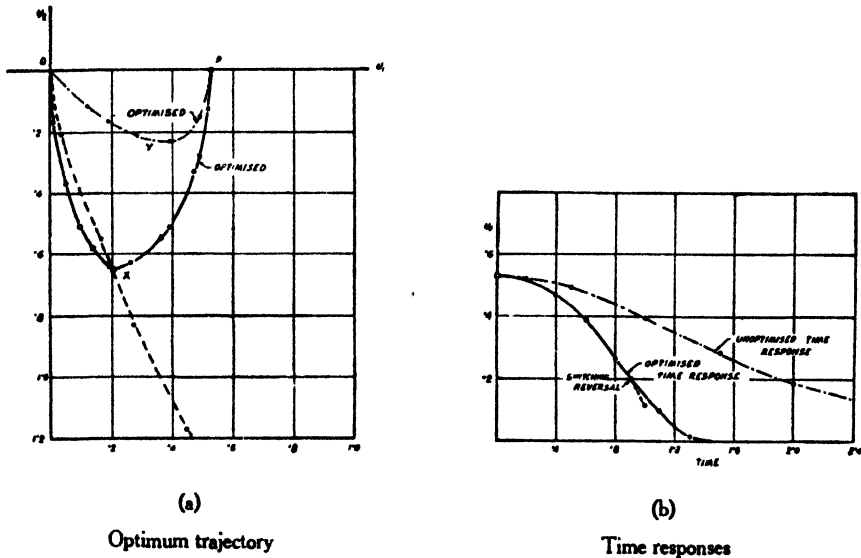


Fig. 7

Curves for discontinuous switching

The solution is conveniently expressed as

$$e = \pm \frac{\delta}{50} + K_1 e^{-0.5t} + e^{-8t} (K_2 \cos 8t + K_3 \sin 8t)$$

Also,

$$\frac{de}{dt} = -0.5 K_1 e^{-0.5t} + (8 K_2 - 6 K_3) e^{-8t} \cos 8t - (8 K_2 + 6 K_3) e^{-8t} \sin 8t \quad (19)$$

Using the same assumptions as in equation (14), we get

$$\left. \begin{aligned} U_{10} &= \frac{\delta}{50} + K_1 + K_2 \\ U_{20} &= -0.5 K_1 + 8 K_2 - 6 K_3 \\ 0 &= 0.25 K_1 - 28 K_2 - 96 K_3 \end{aligned} \right\} \quad (20)$$

 The values of K_1 , K_2 and K_3 in terms of U_{10} and U_{20} are obtained from equation (20) as

$$\begin{aligned} K_1 &= 1.06 U_{10} + 0.1278 U_{20} - 0.0212 \delta \\ K_2 &= -0.06 U_{10} - 0.1278 U_{20} + 0.0012 \delta \\ K_3 &= 0.02125 U_{10} + 0.0374 U_{20} - 0.000425 \delta \end{aligned}$$

 Substituting these values of K_1 , K_2 and K_3 in equation (19), we get

$$\left. \begin{aligned} U_1 = e &= A_1 \delta + A_2 U_{10} + A_3 U_{20} \\ U_2 = \frac{de}{dt} &= B_1 \delta + B_2 U_{10} + B_3 U_{20} \end{aligned} \right\} \quad (21)$$

where

$$A_1 = 0.02 - 0.0212 e^{-0.5t} + e^{-6t} (0.0012 \cos 8t - 0.000425 \sin 8t)$$

$$A_2 = 1.06 e^{-0.5t} - e^{-6t} (0.06 \cos 8t - 0.02125 \sin 8t)$$

$$A_3 = 0.1278 e^{-0.5t} - e^{-6t} (0.1278 \cos 8t - 0.0374 \sin 8t)$$

$$B_1 = 0.0106 e^{-0.5t} - e^{-6t} (0.0106 \cos 8t + 0.00705 \sin 8t)$$

$$B_2 = -0.53 e^{-0.5t} - e^{-6t} (0.53 \cos 8t + 0.3525 \sin 8t)$$

$$B_3 = -0.0639 e^{-0.5t} + e^{-6t} (1.064 \cos 8t + 0.7980 \sin 8t)$$

By assigning various values to t in above and solving for U_{10} and U_{20} with $U_1 = U_2 = 0$ in equation (21), the critical boundary for a third order system with a pair of complex open-loop poles (Fig. 8) is obtained.

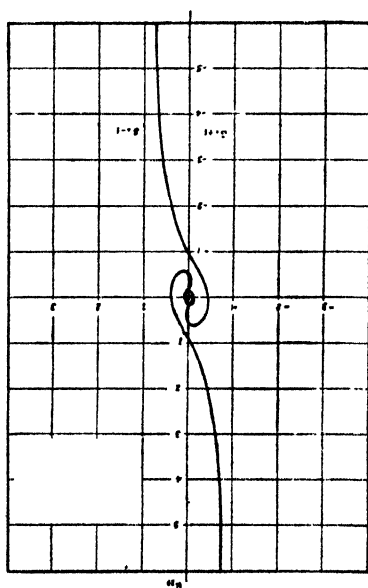


Fig. 8
Critical boundary for third
order system

It is noted that the switching boundary for this case is a complicated curve, being multi-valued in the proximity of the origin. The switching characteristics in this region will require involved experimentation. It is not intended in this paper to present any such results. However, in the following section a simplified procedure for designing the decision computer is given. Experimental results of quenched state bang-bang system of the type discussed in case 1 is presented.

4. Computer mechanization of quenched state system

General

One of the main problems in implementing an optimization scheme is the design of the decision element. The decision element has to perform the task of continuously sensing the state of the system and actuating the relay (with proper polarity) at an instant when a specified function of the state variables satisfies a given relationship. In

a quenched state system, the element has to perform the additional task of momentarily forcing the higher order derivatives to zero at the same instant.

With the progress of analogue computing techniques in the last decade, a host of special purpose computing units and other sophisticated devices have been put into use for such purposes. The use of digital computers has also been advantageously employed in many cases.

The experimental results obtained by using a simplified procedure are presented in this paper. The main idea of the suggested computer mechanization is contained in Figs. 9 and 10. In Fig. 9, block A shows a function generator on which the switching boundary may be simulated. For the type of switching boundary obtained in case 1, a universal function generator of the series biased diode type gives a segmental approximation of the switching boundary. By choosing an appropriate number of segments, a close approximation of the switching boundary (Fig. 6) is obtained.

For the switching boundary of the type as obtained in case 2, a cathode-ray tube with a suitable stylus and a photoelectric cell⁷ may be conveniently adopted.

The input to the function generator is e and the output is $[f(e)]$. Block B (Fig. 9) is a comparator circuit. Its primary function is to sense the sign of $[f(e) - e]$. Depending upon whether this quantity is positive or negative the comparator switches correspondingly a positive or negative voltage. The comparator output voltage energizes the coil of a bipolar electromagnetic relay (Fig. 10) which has separate contacts for instantaneous grounding of the second derivative of the error, or, of the output. The complete simulation diagram of the system is shown in Fig. 11 and the details of the segmental approximation of the switching boundary are shown in Fig. 12.

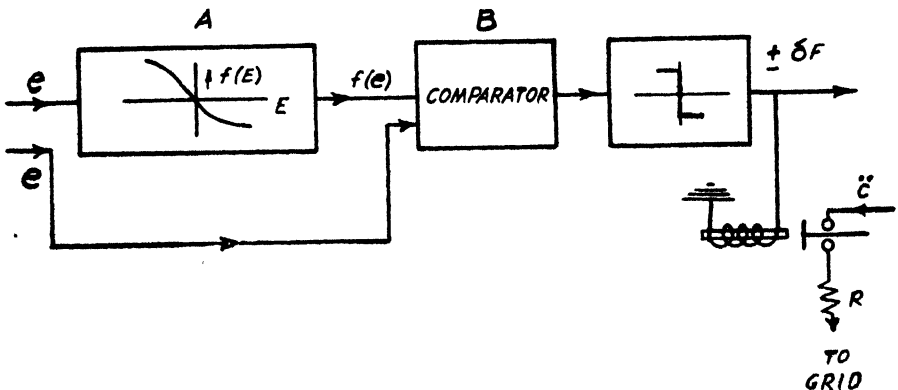


Fig. 9

Block diagram of decision computer

Experimental results

Although it was assumed that $\frac{d^2c}{dt^2}$ is quenched completely, the manner in which it is actually realized in the computer affects the experimental response critically. If, for

example, the output of the amplifier giving $\frac{d^2c}{dt^2}$ is solidly grounded at the time of reversal, a discontinuity in the time response is observed (Fig. 13). To minimize this undesirable effect, the integrator voltage is discharged through a resistance of suitable value. The integrator discharges at a rate determined by the resultant time constant. Consequently, there is some time delay in affecting complete discharge of the condenser of the $\frac{d^2c}{dt^2}$ integrator within the reversal time of the switch; $\frac{d^2c}{dt^2}$ is therefore only partially

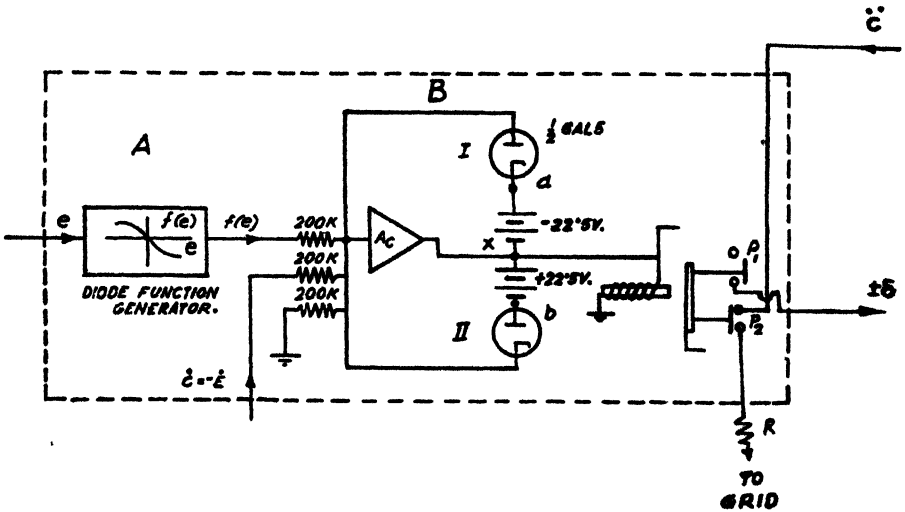
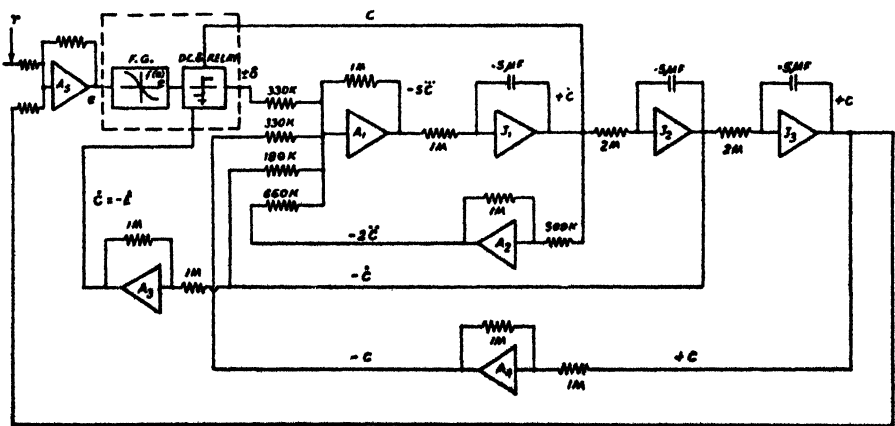


Fig. 10

Details of decision computer



A = ADDER OR SIGN REVERSING AMPLIFIER
B.C. = DECISION COMPUTER

I = INTEGRATOR. F.G. = FUNCTION GENERATOR

Fig. 11

Complete simulation diagram of system

quenched. The effect of such partial quenching is shown in Figs. 14 (a) and (b). The step magnitude of error in both the cases is 0.53 units. Possibly because of such partial realization of the switching conditions, the resulting response exhibits small magnitude oscillations near the origin.

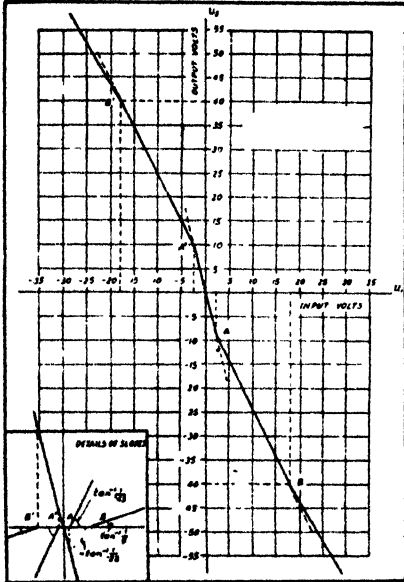


Fig. 12

Segmental approximation of switching boundary

A compromise between these two extreme cases may be realized by adopting the following switching sequence. Initially, $\frac{d^2c}{dt^2}$ is grounded through a suitable resistance to avoid the discontinuity, and immediately after the switching reversal has taken place $\frac{d^2c}{dt^2}$ is connected to ground momentarily. The corresponding time response is shown in Fig. 15. A comparison of the open-loop response (top-half of the loop curve) and the optimized response (bottom-half of the loop curve) as obtained in this manner is shown in Fig. 16.

The experimental response of Fig. 15 may be compared with the theoretical response (assuming ideal quenching) of Fig. 7(b). It may be concluded that such 'graded quenching' does not affect the response time adversely to any great degree.

An interesting case arises when the system acceleration is never brought to zero but is allowed to have a free travel. The resulting response is shown in Fig. 17(a). It may be explained in this manner: referring to Fig. 17(b) the trajectory starts from the initial error point, p (0.53 units of error) and meets the switching boundary at the point a , where the sign reversal of the forcing function is effected, but $\frac{d^2c}{dt^2}$ is not quenched. Due

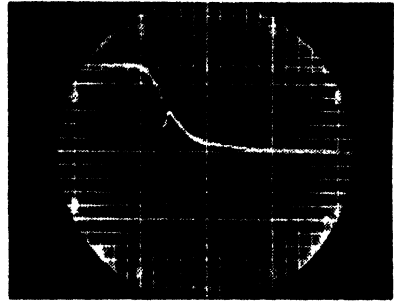
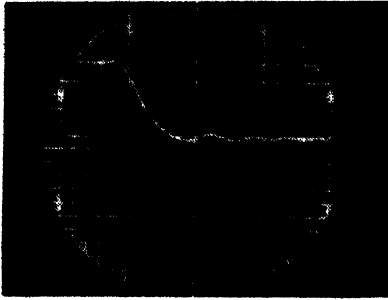


Fig. 13

Effect of type of quenching on time response

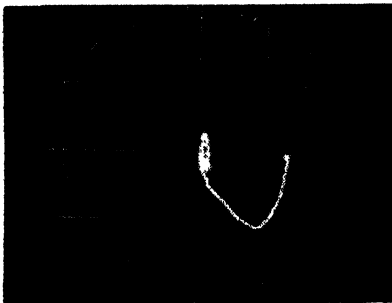


(a)



Fig. 16

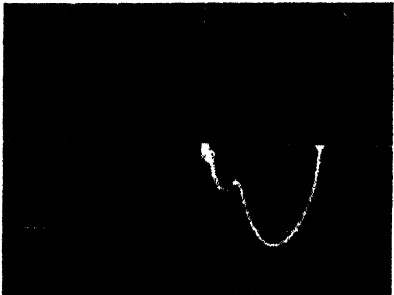
Comparison of experimental responses



(b)

Fig. 14

Effects of partial quenching



(a)

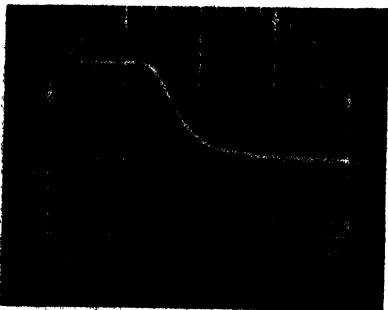
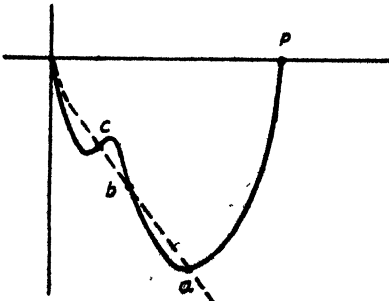


Fig. 15

Time response for graded quenching



(b)

Fig. 17

System response with free travel

to this departure from assumption the resultant trajectory is moved away from the boundary wherefrom it might have been brought to the origin. So, instead of reaching the origin, the state-point again meets the trajectory at the point, b, and a second switching reversal takes place. But as the new forcing function requires the trajectory to move in opposite direction the system state-point, after an initial overshoot, again meets the switching boundary at the point, c. A third reversal takes the system to the origin, the value of $\frac{d^2\theta_o}{dt^2}$ having been substantially reduced meanwhile.

5. Problems of implementation of quenching scheme

In the system considered by Chang, quenching of the second derivatives of the output or the error posed no problem since motor friction was neglected. If such assumptions are not permitted, as, for example, if the system is like the one as discussed in case 2 of section 3, then isolated quenching of $\frac{d^2\theta_o}{dt^2}$ is not a straightforward task.

Referring to Fig. 18, the relationship between the variables, m_2 and m_3 , of the system is given by

$$m_3 = \frac{K_2}{S^2 + 2\alpha_2 S + (\alpha_2^2 + \beta_2^2)} m_2 \quad (23)$$

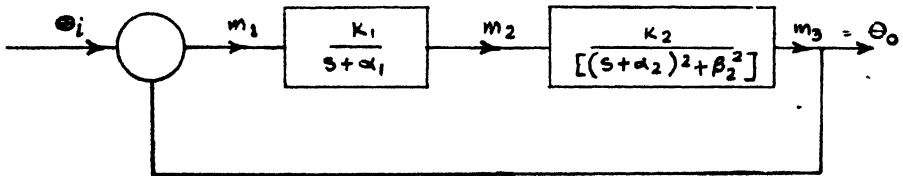


Fig. 18

Relationships between variables for a third order complex root system

Writing in the form of a differential equation we get

$$\frac{d^2\theta_o}{dt^2} + 2\alpha_2 \frac{d\theta_o}{dt} + (\alpha_2^2 + \beta_2^2) \theta_o = K_2 m_2 \quad [24(a)]$$

Re-writing, we get

$$\frac{d^2\theta_o}{dt^2} = K_2 m_2 - [2\alpha_2 \frac{d\theta_o}{dt} + (\alpha_2^2 + \beta_2^2) \theta_o] \quad [24(b)]$$

With the help of equations (24), the quenching problem can be analyzed further. Two cases may arise. In the first case, $K_2 m_2$ may be made equal to zero (i.e., Chang's open-circuit switching scheme is adopted and i_f is made equal to 0 at the switching instant). The state variables then satisfy the relationship

$$\frac{d^2\theta_o}{dt^2} + 2\alpha_2 \frac{d\theta_o}{dt} + (\alpha_2^2 + \beta_2^2) \theta_o = 0$$

where $\frac{d^2\theta_o}{dt^2}$ might undergo partial quenching, but in order that the above relationship is

satisfied, $\frac{d\theta_o}{dt}$ and θ_o will also change values. This means that the state-point has shifted from the critical boundary, hence it is not liable to reach the origin after the polarity reversal.

This is the problem which was earlier referred to as the problem of partial quenching, and its exact effect can be ascertained only after involved experimentation.

In the second case, a reference to equation [24(b)] suggests that $\frac{d^2\theta_o}{dt^2}$ may be made zero if the following condition is satisfied :

$$K_2 m_2 = [2 \alpha_2 \frac{d\theta_o}{dt} + (\alpha_2^2 + \beta_2^2) \theta_o] \quad (25)$$

In terms of the D.C. field-controlled machine, this does not imply open-circuit switching, but necessitates a close-circuit switching scheme in which the value of i_f (or, $K_2 m_2$, equivalently) at the switching instant is modified in such a manner as to satisfy equation (25). Since the expression of the right-hand side is a function of $\frac{d\theta_o}{dt}$ and θ_o , a computer with decision capability is needed. Its function will be to calculate $[2 \alpha_2 \frac{d\theta_o}{dt} + (\alpha_2^2 + \beta_2^2) \theta_o]$ at the switching time and insert a resistance in the field circuit of a value appropriate to satisfy equation (25). This may be built-in for different sets of values of $\frac{d\theta_o}{dt}$ and θ_o on the switching boundary and a predesigned resistor selected for insertion in the circuit. This aspect also merits further study.

6. Conclusions

The paper emphasizes the idea of quenched state bang-bang systems. Analogue computer results are presented and it is seen that these agree reasonably well with the theoretically derived response of a system dealt with by Chang. The idea has been extended for deriving the switching boundary of a third order system with a pair of complex open-loop poles. Further investigations, both analytical and experimental, are necessary before quenched state systems may be established as a new philosophy in optimization theory.

7. Acknowledgment

The authors thank the authorities of the Bengal Engineering College, Howrah for providing facilities to carry out the experiments in connection with the work presented in this paper.

8. References

1. D. W. Bushaw. 'Differential Equations with a Discontinuous Forcing Term Experimental Towing Tank.' Stevens Institute of Technology Report no. 469, January 1953.
2. R. Bellman, I. Glicksberg and O. Gross. 'On the Bang-Bang Control Problem.' *Quarterly of Applied Mathematics*, vol. 14, no. 1, April 1956, p. 11.

3. S. S. L. Chang. 'Optimum Switching Criteria for Higher Order Contactor Servo with Interrupted Circuits.' *Proceedings of the American Institute of Electrical Engineers*, vol. 74, pt. 2, 1955, p. 273.
4. I. Bogner and L. Kazda. 'An Investigation of Switching Criteria for Higher Order Contactor Servomechanisms'. *Proceedings of the American Institute of Electrical Engineers*, vol. 73, pt. 2, 1954, p. 118.
5. P. Chandaket and C. T. Leondes. 'Synthesis of Quasi-Stationary Optimum Nonlinear Control Systems'. *Proceedings of the American Institute of Electrical Engineers*, vol. 80, pt. 2, 1961, p. 313.
6. I. F. Lotz and H. A. Titus. 'Optimum and Quasi-Optimum Control of Third and Fourth Order Systems'. J.A.C.C.-ASME-IFAC, paper no. IX-2, 1963.
7. A. M. Hopkin. 'A Phase-Plane Approach to the Compensation of Saturating Systems'. *Proceedings of the American Institute of Electrical Engineers*, vol. 70, pt. 1, 1951, p. 631.

A STUDY OF BACKLASH IN FEEDBACK CONTROL SYSTEMS***Prof. I. J. Nagrath***Non-member*

and

D. C. Surana*Non-member**Department of Electrical Engineering, Birla College of Engineering, Pilani***Summary**

In this paper, a phase-plane technique for the solution of generalized backlash problem in a feedback control system with inertia, and viscous and coulomb friction on both sides of backlash is described. The general time solutions are given for determining the time required to take up backlash and for the case of backlash with no coulomb friction on either side, a numerical method based on phase-plane technique is given. By this method, an overall study of several cases involving inertia and viscous friction on one or both sides of backlash is carried out and general results obtained. In addition, the cases of an instrument servo with only coulomb friction and with both viscous and coulomb friction on motor side are analyzed. A simple method of investigating the existence, location and amplitude of limit cycles is presented.

Notations J = inertia, f = viscous friction, C = coulomb friction,

$$a = \frac{C}{K},$$

 ζ = damping ratio,

$$\omega = \sqrt{\frac{K}{J}} = \text{natural frequency,}$$

$$T = \frac{J}{f} = \frac{1}{2} \zeta \omega = \text{time constant, and}$$

 N = trajectory slope for an isocline.**Suffixes used with the above symbols**

No suffix indicates the combined system (motor and load moving together) quantities with inertia and friction referred to the motor shaft,

*Presented at the Paper Meetings in the Electronics and Telecommunication Engineering Division, 44th Annual Convention, Hyderabad, February 8-13, 1964.

Suffix M indicates motor quantities, and

Suffix L indicates load quantities.

$$J_r = \frac{J_L}{J_M} = \text{inertia ratio,}$$

(Notations contd.)

$$x = \frac{T_L}{T_M} = \text{time constant ratio,}$$

$$\theta_L = \text{load angle,}$$

$$\theta_M = \text{motor angle,}$$

$$\theta_R = \text{input angle,}$$

$$E = (\theta_L - \theta_R) = \text{error,}$$

$$\frac{d\theta_M}{dt}$$

$$n = \frac{\frac{d\theta_M}{dt}}{\frac{d\theta_L}{dt}} = \text{gear ratio,}$$

$$\Delta = \text{angle of backlash,}$$

$$t = \text{time,}$$

$$t_d = \text{time to take up backlash,}$$

$$\gamma = \frac{8 \zeta_M^3 \omega_M \Delta}{\left(\frac{d\theta_M}{dt}\right)_1}$$

$$\alpha = \frac{4 \zeta_M^2 \Delta}{E_1'}$$

State points

P_1 = position of state point when load just separates from motor,

P_2 = position of state point just before recombination of load and motor, and also indicates both P_2 and P_3 when they lie in the same position just before and just after recombination in instrument servo,

P_3 = position of state point just after recombination of load and motor, and

P_4 = state point where the load is just going to separate from motor once again.

Coordinate systems

The various coordinate systems used are $\left(\theta_L, \frac{d\theta_L}{dt}\right)$, $\left(E, \frac{dE}{dt}\right)$ and (X, Y) , or, (ρ, Ψ) .

In any coordinate system, suffixes 1, 2, 3 and 4 refer to the points P_1 , P_2 , P_3 and P_4 respectively.

$$X = \rho \cos \Psi = \omega \sqrt{1 - \zeta^2} (1 - \theta_L) = \omega \sqrt{1 - \zeta^2} E$$

$$Y = \rho \sin \Psi = -\left(\frac{d\theta_L}{dt}\right)_1 + \zeta \omega (1 - \theta_L) = \frac{dE}{dt} + \zeta \omega E$$

Introduction

Backlash is a discontinuous, multivalued nonlinearity and occurs commonly in the mechanical linkages which are not connected rigidly as in a gear train. It is similar in nature to hysteresis. In the presence of backlash the drive gear has to move a finite distance before making contact with the load gear. If the gear train forms part of a feedback control system, the system operates open-loop while the backlash is being taken up. The effect of backlash is destabilizing and therefore, a system with backlash may exhibit a limit cycle. Phase-plane method of analysis was used by a number of authors^{2,3} to study the effects of backlash in a second order control system. Pastel and Thaler³ have analyzed an instrument servo with backlash in the forward loop under the simplifying assumption that the load inertia is negligible and a small but finite amount of stiction is present at the load end of the gear train. The result of their analysis shows that such a system is always stable for a motor damping ratio of more than 0.29 and exhibits a limit cycle for lower values of damping ratio. It is further inferred that the stability criteria are independent of the forward loop natural frequency. Pastel and Thaler⁴ have developed a phase-plane technique for analyzing the case, where load inertia and friction are present. Their approach consists mostly of computing dividing lines (backlash, separation, recombination, etc.) and then drawing the phase trajectories by using any of the well known techniques of construction. As many as three dividing lines are required to be computed before the phase trajectories can be drawn and the limit cycle obtained by a tedious graphical trial and error method. A complete study with variation of different system parameters becomes prohibitive by this method.

Generalized backlash problem (second order system)

Consider a second order feedback control system with inertia, viscous and coulomb frictions on both sides of backlash as shown in Fig. 1. The system of Fig. 1 can be converted to an equivalent system with a gear ratio of unity as shown in Fig. 2. The system can now be analyzed between θ_R and θ_L . When the system is moving with the backlash taken up, the total inertia and friction referred to the motor shaft are :

$$\left. \begin{aligned} J &= J_M + \frac{J_L'}{n^2} = J_M + J_L \\ f &= f_M + \frac{f_L'}{n^2} = f_M + f_L \\ C &= C_M + \frac{C_L'}{n^2} = C_M + C_L \end{aligned} \right\} \quad (1)$$

where the gear ratio is

$$\frac{1}{n} = \frac{\frac{d\theta_L'}{dt}}{\frac{d\theta_M}{dt}} \quad (\text{with backlash taken up})$$

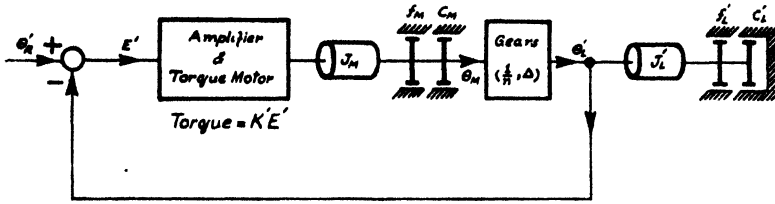


Fig. 1

Second order feedback control system

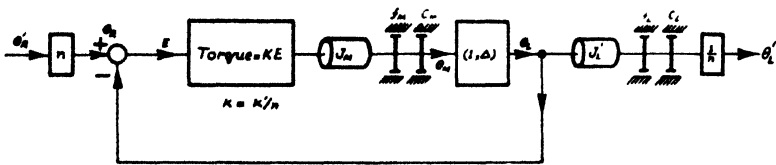


Fig. 2

Equivalent system with unity gear ratio

The differential equation describing the motion of the system with backlash taken up is

$$J \frac{d^2\theta_M}{dt^2} + f \frac{d\theta_M}{dt} + C \operatorname{sign} \frac{d\theta_M}{dt} = K E \quad (2)$$

Since the motor and load are moving together, we get

$$\theta_L = \theta_M$$

Also,

$$E = \theta_R - \theta_L$$

Equation (2) can thus be written as

$$J \frac{d^2\theta_L}{dt^2} + f \frac{d\theta_L}{dt} + K \theta_L = K \left(\theta_R - a \operatorname{sign} \frac{d\theta_L}{dt} \right) \quad (3)$$

$$a = \frac{C}{K}$$

When the system is moving in the backlash region, the motor and the load move in accordance with the equations given below.

For the load,

$$J_L \frac{d^2\theta_L}{dt^2} + f_L \frac{d\theta_L}{dt} + C_L \operatorname{sign} \frac{d\theta_L}{dt} = 0 \quad (4)$$

For the motor,

$$J_M \frac{d^2\theta_M}{dt^2} + f_M \frac{d\theta_M}{dt} + C_M \operatorname{sign} \frac{d\theta_M}{dt} = K (\theta_R - \theta_L)$$

or,

$$J_M \frac{d^2\theta_M}{dt^2} + f_M \frac{d\theta_M}{dt} = K \left(\theta_R - \theta_L - a_M \operatorname{sign} \frac{d\theta_M}{dt} \right)$$

where

$$a_M = \frac{C_M}{K} \quad (5)$$

When the system is moving with backlash taken up, the phase trajectory is defined by the second order equation (3).

Its isoclines are given by

$$\frac{d\theta_L}{dt} = \frac{K \left(\theta_R - a \operatorname{sign} \frac{d\theta_L}{dt} \right)}{(N J + f)} - \frac{K \theta_L}{N J + f} \quad (6)$$

The isoclines, according to equation (6), are two families of straight lines passing through

$$[(\theta_R - a), 0] \text{ for } \frac{d\theta_L}{dt} > 0$$

and

$$[(\theta_R + a), 0] \text{ for } \frac{d\theta_L}{dt} < 0$$

These isoclines are shown in Fig. 3 with the foci at A_1 and A_2 respectively.

Starting from the state point O, the load and motor gears move together and separation would occur, when the slope of the combined system trajectory becomes equal to the slope of the drifting load trajectory (load moving without contact with motor gears).

The isoclines of the drifting load described by equation (4) are given by

$$\frac{d\theta_L}{dt} = - \frac{a_L K \operatorname{sign} \frac{d\theta_L}{dt}}{(N_L J_L + f_L)} \quad (7)$$

These isolines are, therefore, a family of straight lines parallel to θ_L -axis.

Let the separation of motor and load gears occur when the state point reaches P_1 defined by $\left[\theta_{L1}, \left(\frac{d\theta_L}{dt} \right)_1 \right]$ or $\left[\theta_{M1}, \left(\frac{d\theta_M}{dt} \right)_1 \right]$. Using the condition of separation ($N = N_L$), we get

$$\theta_R - a \operatorname{sign} \left(\frac{d\theta_L}{dt} \right)_1 - \theta_{L1} = \frac{f}{K} \left(1 - \frac{J f_L}{J_L f} \right) \left(\frac{d\theta_L}{dt} \right)_1 - \frac{J}{J_L} a_L \operatorname{sign} \left(\frac{d\theta_L}{dt} \right)_1$$

or,

$$\theta_R - a \operatorname{sign} \left(\frac{d\theta_M}{dt} \right)_1 - \theta_{M1} = \frac{1}{\omega_M^2} \left(\frac{1}{T_M} - \frac{1}{T_L} \right) \left(\frac{d\theta_M}{dt} \right)_1 - \frac{J}{J_L} a_L \operatorname{sign} \left(\frac{d\theta_M}{dt} \right)_1 \quad (8)$$

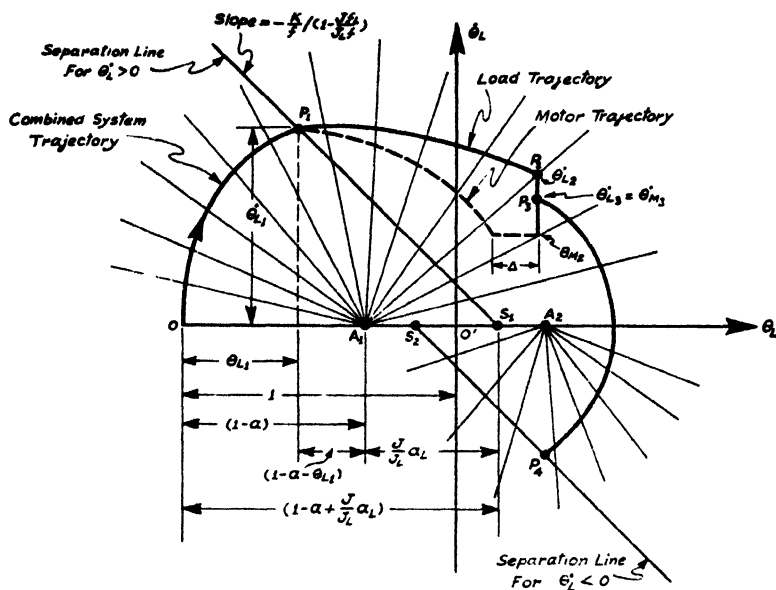


Fig. 3

Isoclines

Equation (8) shows that the separation of load from motor occurs on two lines in $(\theta_L, \frac{d\theta_L}{dt})$ plane such that

$$\text{Slope of separation lines} = \frac{-\frac{K}{f}}{\left(1 - \frac{J}{J_L} f\right)} \quad (9)$$

The separation line passes through the point

$$\left[\begin{aligned} &\left[\left(\theta_R - a + \frac{J}{J_L} a_L \right), 0 \right] \text{ for } \frac{d\theta_L}{dt} > 0 \\ &\left[\left(\theta_R + a - \frac{J}{J_L} a_L \right), 0 \right] \text{ for } \frac{d\theta_L}{dt} < 0 \end{aligned} \right] \quad (10)$$

After separation at P_1 , the load and the motor move according to equations (4) and (5) and would recombine when

$$\theta_L(t) - \theta_M(t) = \Delta \quad (11)$$

where Δ is the angle of backlash.

The trajectory for the drifting load can be drawn from its isocline equation (7), but motor trajectory can not be drawn by the method of isoclines. Even though it could be drawn by another method, equation (11) can best be satisfied by a time solution of θ_L and θ_M .

Choose $t = 0$ corresponding to the state point at P_1 . Since load and motor are just going to separate at P_1 , we get

$$\theta_{L1} = \theta_{M1}$$

and

$$\left(\frac{d\theta_L}{dt}\right)_1 = \left(\frac{d\theta_M}{dt}\right)_1 \quad (12)$$

Taking Laplace transform of equations (4) and (5) for $\theta_R = \text{unit step}$ and for $\frac{d\theta_L}{dt} > 0$,

$$\theta_L(s) = \frac{\theta_{L1}}{s} + \frac{\left(\frac{d\theta_L}{dt}\right)_1}{s\left(s + \frac{1}{T_L}\right)} - \frac{a_L \omega_L^2}{s^2\left(s + \frac{1}{T_L}\right)} \quad (13)$$

where

$$T_L = \frac{J_L}{f_L}$$

and

$$\left[s^2 \theta_M(s) - s \theta_{M1} - \left(\frac{d\theta_M}{dt}\right)_1\right] + \frac{1}{T_M} [s \theta_M(s) - \theta_{M1}] = \omega_M^2 \left[1 - \frac{a_M}{s} - \theta_L(s)\right] \quad (14)$$

where $T_M = \frac{J_M}{f_M}$ and $\omega_M^2 = \frac{K}{J_M}$.

Substituting for $\theta_L(s)$ from equation (13) in equation (14), we get

$$\begin{aligned} \theta_M(s) = \frac{\theta_{M1}}{s} + \frac{\left(\frac{d\theta_M}{dt}\right)_1}{s\left(s + \frac{1}{T_M}\right)} + \frac{(1 - a_M - \theta_{M1}) \omega_M^2}{s^2\left(s + \frac{1}{T_M}\right)} - \frac{\omega_M^2 \left(\frac{d\theta_M}{dt}\right)_1}{s^2\left(s + \frac{1}{T_M}\right)\left(s + \frac{1}{T_L}\right)} \\ + \frac{a_L \omega_L^2 \omega_M^2}{s^3\left(s + \frac{1}{T_L}\right)\left(s + \frac{1}{T_M}\right)} \quad (15) \end{aligned}$$

Taking the inverse Laplace transform of $\theta_L(s)$ and $\theta_M(s)$ and substituting in equation (11), we get

$$\begin{aligned} \Delta = \left[\left(\frac{d\theta_M}{dt}\right)_1 T_L \left(1 - e^{-\frac{t}{T_L}}\right) + a_L \omega_L^2 T_L^2 \left(1 - \frac{t}{T_L} - e^{-\frac{t}{T_L}}\right) - \left(\frac{d\theta_M}{dt}\right)_1 T_M \right. \\ \left. \left(1 - e^{-\frac{t}{T_M}}\right) + (1 - a_M - \theta_{M1}) \omega_M^2 T_M \left(1 - \frac{t}{T_M} - e^{-\frac{t}{T_M}}\right) + \left(\frac{d\theta_M}{dt}\right)_1 \right. \\ \left. \omega_M^2 T_L T_M \left\{ t - (T_L + T_M) - \frac{1}{(T_L - T_M)} \left(T_M^2 e^{-\frac{t}{T_M}} - T_L^2 e^{-\frac{t}{T_L}} \right) \right\} \right. \\ \left. - a_L \omega_L^2 \omega_M^2 T_L T_M \left\{ \frac{t^2}{2} - (T_L + T_M) t + (T_L^2 + T_M^2 + T_L T_M) \right. \right. \\ \left. \left. + \frac{1}{(T_L - T_M)} \left(T_L^2 e^{-\frac{t}{T_L}} - T_M^2 e^{-\frac{t}{T_M}} \right) \right\} \right] \quad (16) \end{aligned}$$

From equation (8),

$$(1 - a_M - \theta_{M1}) = \frac{1}{\omega_M^2} \left(\frac{1}{T_M} - \frac{1}{T_L} \right) \left(\frac{d\theta_M}{dt} \right)_1 - a_L \left(1 + \frac{J}{J_L} \right) \quad (17)$$

Substituting for $(1 - a_M - \theta_{M1})$ from equation (17) in equation (16), the value of t for recombination of the load and the motor gears can be obtained by a graphical solution for any specific problem, but a general solution is not possible.

Let $t = t_d$ be the time after which the gears recombine. Load velocity at recombination is obtained by inverse Laplace transforming $s \theta_L(s)$ in equation (13) as

$$\theta_{L2} = \left(\frac{d\theta_M}{dt} \right)_1 \epsilon^{-t_d/T_L} - a_L \omega_L^2 T_L \left(1 - \epsilon^{-t_d/T_L} \right) \quad (18)$$

Motor velocity at recombination obtained by inverse Laplace transforming $s \theta_M(s)$ in equation (15) is

$$\begin{aligned} \left(\frac{d\theta_M}{dt} \right)_2 = & \left[\left(\frac{d\theta_M}{dt} \right)_1 \epsilon^{-t_d/T_M} + (1 - a_M - \theta_{M1}) \omega_M^2 T_M (1 - \epsilon^{-t_d/T_M}) - \left(\frac{d\theta_M}{dt} \right)_1 \omega_M^3 \right. \\ & T_L T_M \left\{ 1 + \left(\frac{1}{T_L} - \frac{1}{T_M} \right) \left(T_M \epsilon^{-t_d/T_M} - T_L \epsilon^{-t_d/T_L} \right) \right\} + a_L \omega_L^2 \omega_M^2 T_L T_M \left\{ t - \right. \\ & \left. (T_L + T_M) - \left(\frac{1}{T_L} - \frac{1}{T_M} \right) \left(T_L^2 \epsilon^{-t_d/T_L} T_M^2 \epsilon^{-t_d/T_M} \right) \right\} \left. \right] \quad (19) \end{aligned}$$

On recombination, the load and the motor suddenly acquire a new common velocity in accordance with the principle of conservation of momentum. The state point on recombination corresponds to P_3 on Fig. 3. Thus,

$$\left(\frac{d\theta_L}{dt} \right)_3 = \left(\frac{d\theta_M}{dt} \right)_3 = \frac{J_L \left(\frac{d\theta_L}{dt} \right)_2 + J_M \left(\frac{d\theta_M}{dt} \right)_2}{J_L + J_M} \quad (20)$$

and

$$\theta_{L2} = \theta_{M1} + \left(\frac{d\theta_M}{dt} \right)_1 T_L \left(1 - \epsilon^{-t_d/T_L} \right) - a_L \omega_L^2 T_L \left(1 - \epsilon^{-t_d/T_L} \right) \quad (21)$$

Also,

$$\theta_{L2} = \theta_{L3} = \theta_{M3}$$

From P_3 onwards, the trajectory can be easily drawn using the isoclines corresponding to the focus A_1 for $\frac{d\theta_L}{dt} > 0$ and corresponding to the focus A_2 for $\frac{d\theta_L}{dt} < 0$, till the state point reaches P_4 , where a separation would occur in the negative velocity region.

If P_4 in fourth quadrant (origin O') lies symmetrically with respect to P_1 in the second quadrant, the trajectory from P_4 onward closes on to P_1 and so a limit cycle results. Expressed mathematically, the conditions for existence of a limit cycle are

$$\left. \begin{aligned} \left(\frac{d\theta_L}{dt} \right)_1 &= - \left(\frac{d\theta_L}{dt} \right)_4 \\ (1 - \theta_{L1}) &= - (1 - \theta_{L4}) \end{aligned} \right\} \quad (22)$$

For any specific system, the limit cycle can be determined by trying various locations of P_1 till the corresponding P_4 satisfies the conditions outlined above. On account of the large number of parameters involved (T_L , T_M , ω_L , ω_M , a_L and a_M), an overall study is prohibitive by hand computation.

Case 1

(a) No coulomb friction ($a_L = a_M = 0$)

With no coulomb friction the points A_1 , A_2 and S_1 , S_2 merge with O' in Fig. 3 and a single separation line results. The isoclines of Fig. 3 thus simplifies to those of Fig. 4.

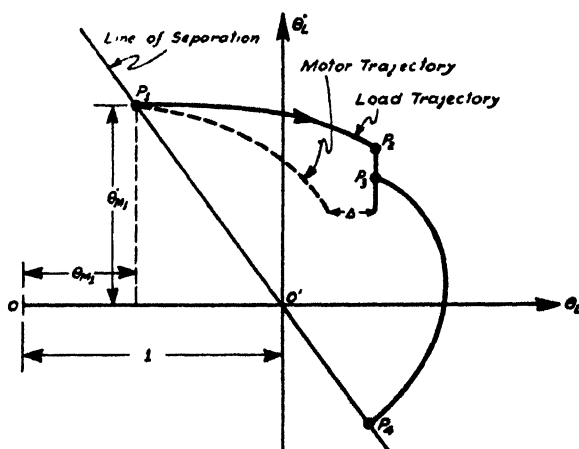


Fig. 4

Isoclines for systems with no coulomb friction

From equation (8), the separation line is given by

$$(1 - \theta_{M1}) = \frac{1}{\omega_M^2} \left(\frac{1}{T_M} - \frac{1}{T_L} \right) \left(\frac{d\theta_M}{dt} \right)_1 = \frac{2 \zeta_M}{\omega_M} \left(1 - \frac{1}{x} \right) \left(\frac{d\theta_M}{dt} \right)_1 \quad (23)$$

From equation (16) the time to take up backlash is given by

$$\begin{aligned} \delta = \frac{2 \zeta_M \omega_M \Delta}{\left(\frac{d\theta_M}{dt} \right)_1} &= x \left(1 - e^{-\frac{t}{x T_M}} \right) - \left(1 - e^{-\frac{t}{T_M}} \right) + \left(1 - \frac{1}{x} \right) \left(1 - \frac{t}{T_M} - e^{-\frac{t}{T_M}} \right) \\ &+ \frac{x}{4 \zeta_M^2} \left[\frac{t}{T_M} - (1 + x) - \frac{1}{(x-1)} \left(e^{-\frac{t}{T_M}} - x^2 e^{-\frac{t}{x T_M}} \right) \right] \quad (24) \end{aligned}$$

where

$$x = \frac{T_L}{T_M}$$

The value of $t = t_d$ depends on x and ζ_M for an assumed value of $\left(\frac{d\theta_M}{dt}\right)_1$. A three-dimensional curve is needed to represent graphically $\delta\left(x, \zeta_M, \frac{t}{T_M}\right)$.

From equation (18),

$$\left(\frac{d\theta_L}{dt}\right)_2 = \left(\frac{d\theta_M}{dt}\right)_1 \epsilon^{-\frac{t_d}{T_L}} = B \left(\frac{d\theta_M}{dt}\right)_1 \quad (25)$$

and from equation (19),

$$\begin{aligned} \left(\frac{d\theta_M}{dt}\right)_2 &= \left(\frac{d\theta_M}{dt}\right)_1 \left\{ \epsilon^{-\frac{t_d}{T_M}} + \left(1 - \frac{1}{x}\right) \left(1 - \epsilon^{-\frac{t}{T_M}}\right) - \frac{x}{4\zeta_M^2} \left[1 - \frac{1}{(x-1)} \right. \right. \\ &\quad \left. \left. \left(\epsilon^{-\frac{t_d}{T_M}} - x \epsilon^{-\frac{t_d}{T_L}} \right) \right] \right\} \\ &= A \left(\frac{d\theta_M}{dt}\right)_1 \end{aligned} \quad (26)$$

Also,

$$\theta_{L2} = \theta_{M1} + \left(\frac{d\theta_M}{dt}\right)_1 T_L \left(1 - \epsilon^{-\frac{t_d}{T_L}}\right) \quad (27)$$

Using equations (24), (25) and (26) in conjunction with the recombination equation (20), the existence of a limit cycle can be determined by a trial and error procedure. An overall system study would involve three parameters x , T_M and ζ_M . Two simple cases arise out of this case.

(b) Equal motor and load time constants

This is a case of special interest where load has been matched with motor such that

$$T_L = T_M, \text{ or, } x = 1$$

Using $x = 1$ in equation (23), we get

$$(1 - \theta_{M1}) = 0 \quad (28)$$

It means that separation always occurs on $\frac{d\theta_L}{dt}$ -axis. Equation (24) modifies to

$$\gamma = \frac{8\zeta_M^2 \omega_M \Delta}{\left(\frac{d\theta_M}{dt}\right)_1} = \left(\frac{t}{T_M} - 2 + \frac{t}{T_M} \epsilon^{-\frac{t}{T_M}} + 2 \epsilon^{-\frac{t}{T_M}} \right) \quad (29)$$

The plot of γ vs. $\frac{t}{T_M}$ according to equation (29) is given in Fig. 5. This plot is universal and can be used to determine $\left(\frac{t_A}{T_M}\right)$ for any system with $T_L = T_M$ and for any value of Δ and $\left(\frac{d\theta_M}{dt}\right)_1$.

Using $x = 1$ in equations (25) and (26), we get

$$\frac{\left(\frac{d\theta_L}{dt}\right)_2}{\left(\frac{d\theta_M}{dt}\right)_1} = e^{-\frac{t_A}{T}} \quad (30)$$

and

$$\frac{\left(\frac{d\theta_M}{dt}\right)_2}{\left(\frac{d\theta_M}{dt}\right)_1} = e^{-\frac{t_A}{T}} - \omega_M^2 T_M^2 \left(1 - e^{-\frac{t_A}{T_M}} - \frac{t}{T_M} e^{-\frac{t_A}{T_M}}\right) \quad (31)$$

Substituting these values in equation (20), we get

$$\frac{\left(\frac{d\theta_M}{dt}\right)_3}{\left(\frac{d\theta_M}{dt}\right)_1} = e^{-\frac{t_A}{T_M}} + \frac{1}{4(1+J_r)\zeta_M^2} \left(e^{-\frac{t_A}{T_M}} + \frac{t_A}{T_M} e^{-\frac{t_A}{T_M}} - 1\right) \quad (32)$$

where $J_r = \frac{J_L}{J_M}$.

From equation (27), we get

$$\theta_{L3} = \theta_{L2} = \theta_{M1} + \left(\frac{d\theta_M}{dt}\right)_1 T_M \left(1 - e^{-\frac{t_A}{T_M}}\right) \quad (33)$$

Equations (32) and (33) give the location of P_3 , for which P_4 can be determined by graphical or numerical techniques. For any specific system, two or three trial values of $\left(\frac{d\theta_M}{dt}\right)_1$ would suffice to determine the existence of a limit cycle.

The results of a specific system study with fixed J_r and Δ , and varying ζ_M are given in Table 1.

Limit cycle criterion

A limit cycle criterion can be obtained for the case of $T_L = T_M$ by considering the system behaviour for very low values of $\left(\frac{d\theta_M}{dt}\right)_1$. A limit cycle would exist if the system trajectory diverges as $\left(\frac{d\theta_M}{dt}\right)_1 \rightarrow 0$.

Table I

$J_r = 0.5$, $\omega_M = 10$ radians per sec., and $\Delta = 0.05$ radian

ζ_M	$\left(\frac{d\theta_M}{dt}\right)_1$ for a limit cycle, radian per sec.
0.10	0.55
0.20	0.30
0.30	0.10
0.35	No limit cycle

For very low values of $\left(\frac{d\theta_M}{dt}\right)_1$, γ is very large and $\frac{t}{T_M}$ as obtained from equation (25) (*vide* Fig. 5) tends to be very high, so that in the limit

$$\text{as } \left. \begin{aligned} \epsilon^{-\frac{t}{T_M}} &\rightarrow 0 \\ \left(\frac{d\theta_M}{dt}\right)_1 &\rightarrow 0 \end{aligned} \right\} \quad (34)$$

Using this limit process in equations (32) and (33), we get

$$\frac{\left(\frac{d\theta_M}{dt}\right)_3}{\left(\frac{d\theta_M}{dt}\right)_1} = -\frac{\omega_M^2 T_M^2}{1 + J_r} \quad (35)$$

and

$$\theta_{L3} = \theta_{M1} + T_M \left(\frac{d\theta_M}{dt}\right)_1 \quad (36)$$

At this stage, it is convenient to transform from $\left(\theta_L, \frac{d\theta_L}{dt}\right)$ plane to (X, Y) plane in accordance with the well known linear transformation given below.

$$\left. \begin{aligned} X &= \omega \sqrt{1 - \zeta^2} (1 - \theta_L) = \rho \cos \Psi \\ Y &= -\frac{d\theta_L}{dt} + \zeta \omega (1 - \theta_L) = \rho \sin \Psi \end{aligned} \right\} \quad (37)$$

where Ψ is measured positively in clockwise direction.

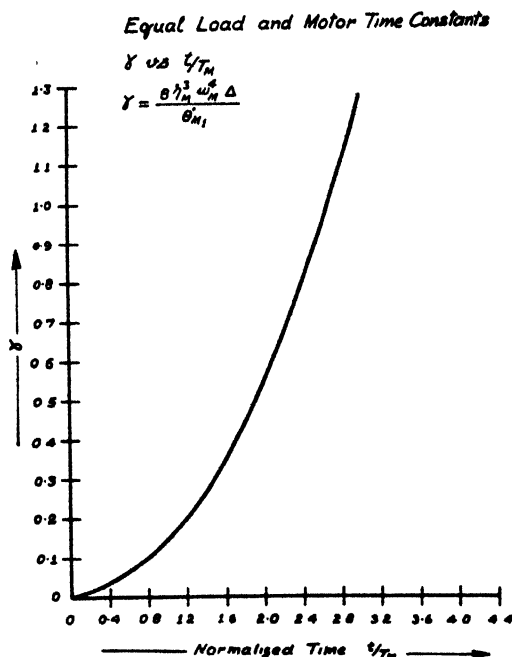


Fig. 5

Curve of γ vs. $\frac{\zeta}{T_M}$

It is obvious that the system would diverge and get into a limit cycle, if $\rho_4 > \rho_1$, which yields the condition given below (*vide* Appendix).

$$\left[\frac{1}{4\zeta^2} e^{-\frac{\zeta}{2\sqrt{1-\zeta^2}} \left(\frac{\pi}{2} - \tan^{-1} \frac{\sqrt{1-2\zeta^2}}{\zeta \sqrt{1-\zeta^2}} \right)} \right] > 1 \quad (38)$$

The solution of equation (38) yields that the system would get into a limit cycle if

$$\zeta < 0.413 \quad (39)$$

This result is verified by the data given in Table 1 according to which the limit cycle does not exist for

$$\zeta_M = 0.35$$

or,

$$\zeta = 0.425$$

since

$$\zeta = \zeta_M \sqrt{1 + J_r} = \sqrt{1.5} \zeta_M$$

Equation (38) also shows that the existence of a limit cycle depends upon damping ratio only and is not affected by any other system parameter.

(c) Zero load friction

If $f_L = 0$,

$$T_L = \frac{J_L}{f_L} = \infty, \text{ or, } x = \infty \quad (40)$$

The separation of load and motor gears now occurs at

$$(1 - \theta_{M1}) = \left(2 \frac{\zeta_M}{\omega_M} \right) \left(\frac{d\theta_M}{dt} \right)_1 \quad (41)$$

Under this condition, equation (24) modifies to

$$\frac{8 \zeta_M^3 \omega_M \Delta}{\left(\frac{d\theta_M}{dt} \right)_1} = \left[1 - \frac{t}{T_M} + \frac{1}{2} \left(\frac{t}{T_M} \right)^2 - e^{-\frac{t}{T_M}} \right] \quad (42)$$

Let

$$\gamma = \frac{8 \zeta_M^3 \omega_M}{\left(\frac{d\theta_M}{dt} \right)_1} = \frac{8 \zeta^3 \omega (1 + J_r)^2 \Delta}{\left(\frac{d\theta_M}{dt} \right)_1} \quad (43)$$

According to equation (42) the universal curve is plotted in Fig. 6 for γ vs. $\frac{t}{T_M}$ which is applicable for any system with $f_L = 0$ and for any amount of backlash and $\left(\frac{d\theta_M}{dt} \right)_1$. The normalized time $\left(\frac{t_d}{T_M} \right)$ required to take up backlash can be conveniently evaluated from Fig. 6.

Since the load friction is zero, the load velocity remains constant after separation till a recombination occurs. Thus

$$\left(\frac{d\theta_L}{dt} \right)_2 = \left(\frac{d\theta_M}{dt} \right)_1 \quad (44)$$

It follows that on recombination

$$\left(\frac{d\theta_L}{dt} \right)_3 = \left(\frac{d\theta_M}{dt} \right)_3 = \left(\frac{d\theta_M}{dt} \right)_1 \left[1 + 4 \zeta_M^2 (1 + J_r) \left(1 - \frac{t_d}{T_M} - e^{-\frac{t_d}{T_M}} \right) \right] \quad (45)$$

and

$$\theta_{L3} = \theta_{M1} + \left(\frac{d\theta_M}{dt} \right)_1 \left(\frac{t_d}{T_M} \right) T_M \quad (46)$$

Transforming to (X, Y) plane (vide Fig. 7),

$$X_3 = \left(\frac{d\theta_M}{dt} \right)_1 2 \zeta \sqrt{1 - \zeta^2} \left[1 - \left(\frac{t_d}{T_M} \right) \frac{1}{4 \zeta^2 (1 + J_r)} \right] \quad (47)$$

$$Y_3 = \left(\frac{d\theta_M}{dt} \right)_1 \left[\zeta^2 \left\{ 1 - \left(\frac{t_d}{T_M} \right) \frac{1}{4 \zeta^2 (1 + J_r)} \right\} - \frac{1 - \left(\frac{t_d}{T_M} \right) - e^{-\frac{t_d}{T_M}}}{4 \zeta^2 (1 + J_r)} - 1 \right] \quad (48)$$

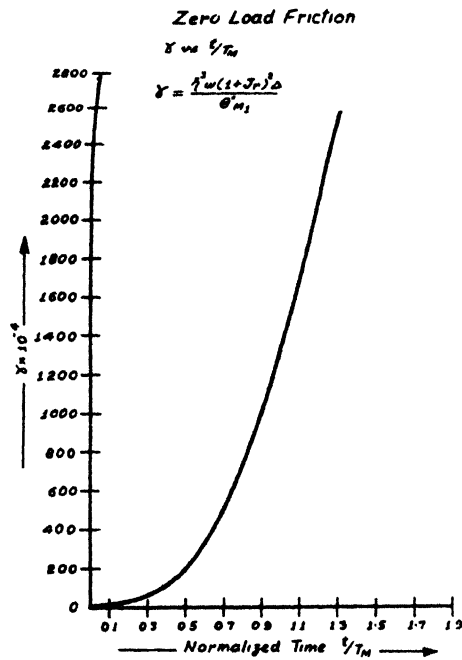


Fig. 6

Curve of γ vs. $\frac{t}{T_M}$

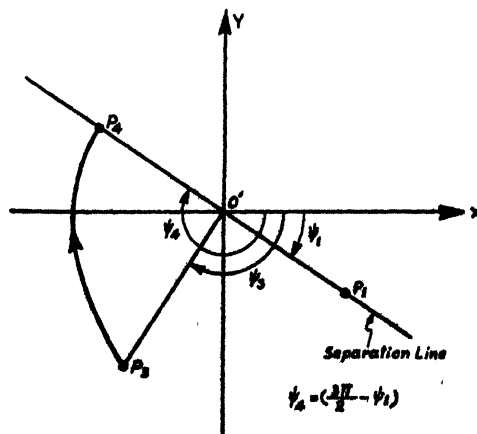


Fig. 7

Transformation to (X, Y) plane

The separation line transforms to a line passing through origin with an angle Ψ_1 , where

$$\Psi_1 = \tan^{-1} \frac{\sqrt{1-2\zeta^2}}{2\zeta\sqrt{1-\zeta^2}} \quad (49)$$

At point P_1 ,

$$\rho_1 = \left(\frac{d\theta_M}{dt} \right)_1 \quad (50)$$

Let

$$\left. \begin{aligned} X_3 &= -A \left(\frac{d\theta_M}{dt} \right)_1 \\ Y_3 &= -B \left(\frac{d\theta_M}{dt} \right)_1 \end{aligned} \right\} \quad (51)$$

and

Therefore,

$$\left. \begin{aligned} r_3 &= \theta_{M1} \sqrt{A^2 + B^2} \\ \Psi_3 &= \left(\pi - \tan^{-1} \frac{B}{A} \right) \end{aligned} \right\} \quad (52)$$

and

Referring to Fig. 7, it can be shown that

$$\rho_4 = \left(\frac{d\theta_M}{dt} \right)_1 \sqrt{A^2 + B^2} = \frac{\zeta}{\sqrt{1-\zeta^2}} \left(\frac{\pi}{2} - \Psi_1 + \tan^{-1} \frac{B}{A} \right)$$

A limit cycle exists when

$$\rho_4 = \rho_1$$

or,

$$\sqrt{A^2 + B^2} = \frac{\zeta}{\sqrt{1-\zeta^2}} \left(\frac{\pi}{2} - \tan^{-1} \frac{\sqrt{1-2\zeta^2}}{2\zeta\sqrt{1-\zeta^2}} + \tan^{-1} \frac{B}{A} \right) = 1 \quad (53)$$

Since A and B are functions of $\left(\zeta, J, \text{ and } \frac{t_d}{T_M} \right)$, the existence of limit cycle can be determined by trial and error from equation (53), but no definite conclusion is possible as in case 1(b). Allowing $\epsilon^{-\frac{t_d}{T_M}} \rightarrow 0$ does not produce any better results.

For specified values of ζ and J , $\frac{t_d}{T_M}$ is obtained graphically from equation (53) and the corresponding γ is read off from the universal curve of Fig. 6. According to equation (53), the existence of the limit cycle is independent of ω and Δ ; but the amplitude of $\left(\frac{d\theta_M}{dt} \right)_1$ at the limit cycle depends upon these two parameters according to equation (43).

The results of a study carried out with fixed J , ($J_r = 1$) and varying ζ (0 to 0.5) are plotted in Fig. 8 from which the value of γ at which the limit cycle exists can be read off. It is seen from this figure that as ζ reduces, γ increases monotonically. It means that the system always breaks into a limit cycle and never becomes stable in the range of ζ studied, i.e., 0 to 0.5. Also for specified ω and Δ , $\left(\frac{d\theta_M}{dt}\right)_1$ at the limit cycle decreases monotonically as damping ratio is increased. The maximum error amplitude of the limit cycle is plotted in Fig. 9 for ($\omega = 10$ radian per sec., $\Delta = 0.05$ radian). The error becomes less than 5% for $\zeta > 0.21$ for this case.

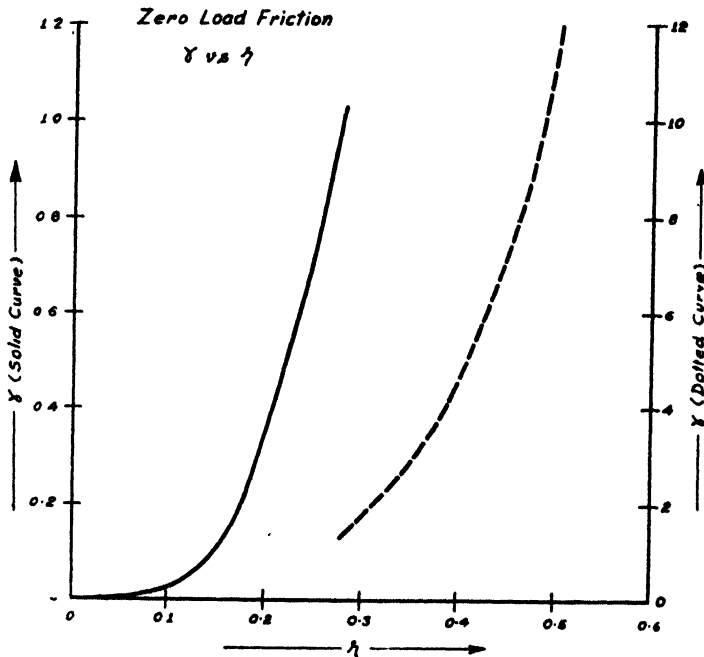


Fig. 8
Curve of γ vs. ζ

The results of a study with fixed ζ_M ($\zeta_M = 0.2$) and varying J , are plotted in Fig. 10. It is noticed that γ reduces monotonically with J , but the system never becomes stable. The maximum error amplitudes are plotted in the same figure for $\omega = 10$ radian per sec. and $\Delta = 0.05$ radian.

Case 2

(a) Instrument servo with negligible load inertia and small but finite load stiction

This case is met with in instrument servos. The small but finite stiction assumed to be present at the load shaft does not affect the damping of the combined system, but

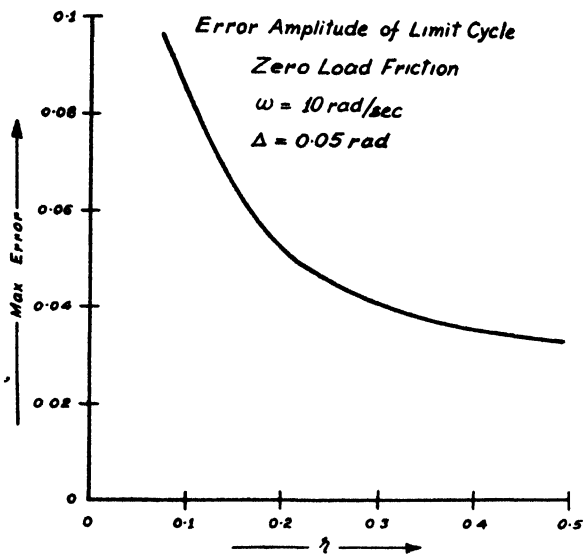


Fig. 9

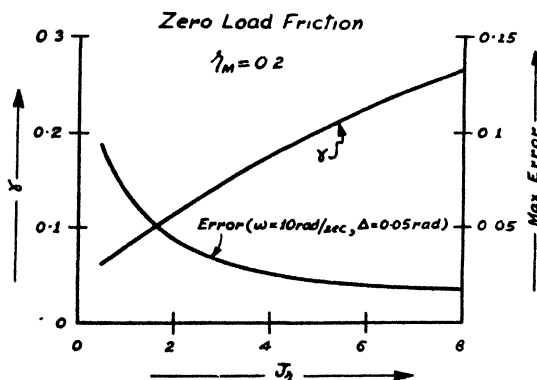
Curve of maximum error vs. ζ 

Fig. 10

Curves for fixed ζ_M and varying J_L

makes the load time constant, $T_L = 0$. From equation (23), it follows that the separation occurs at

$$\left(\frac{d\theta_M}{dt} \right)_1 = 0 \quad (54)$$

It means that the load separates from motor along θ_L -axis, when the motor velocity is passing through zero. The load stops immediately the contact with motor gears

is lost and restarts instantaneously with the motor velocity, when the backlash is taken up. This case has been analyzed by Pastel and Thaler.³ The authors have shown that a limit cycle always exists for $\zeta < 0.29$.

(b) *Instrument servo with only coulomb friction at motor shaft*

Separation of the load from the motor occurs whenever the motor goes through zero velocity. The load stops immediately and stays stationary at P_1 in Fig. 11 such that

$$\theta_{L1} = \theta_{M1} \text{ and } \left(\frac{d\theta_M}{dt} \right)_1 = 0$$

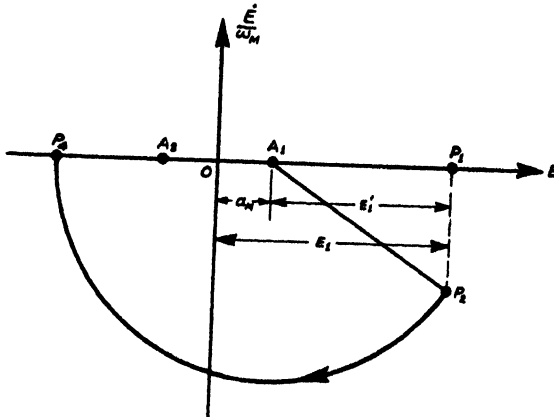


Fig. 11

System trajectory

During the separation period, the equation of the motor can be written from equation (5) as

$$J_M \frac{d^2\theta_M}{dt^2} = K \left(1 - \theta_{M1} - a_M \text{sign} \frac{d\theta_M}{dt} \right) \quad (55)$$

Considering the separation that occurs as the motor velocity changes from negative to positive, it can be shown that the time to take up backlash is given by

$$t_d = \sqrt{\frac{2 \Delta}{\omega_M^2 E_1'}} \quad (56)$$

where

$$E_1' = (1 - \theta_{M1} - a_M) \quad (57)$$

Also, the motor velocity at recombination, which equals the load velocity at recombination, since the load inertia is zero, is given by

$$\left(\frac{d\theta_L}{dt} \right)_2 = \left(\frac{d\theta_M}{dt} \right)_2 = \omega_M \sqrt{2 \Delta E_1'} \quad (58)$$

Defining

$$\left. \begin{aligned} E &= (1 - \theta_L) \\ \frac{dE}{dt} &= -\frac{d\theta_L}{dt} \end{aligned} \right\} \quad (59)$$

We get

$$\left(\frac{dE}{dt} \right)_{\omega_M} = -\sqrt{2\Delta} E_1' \quad (60)$$

It is well known that on recombination the system trajectory is a circle in $\left(\frac{dE}{dt}, E \right)$ plane centred at A_1 as shown in Fig. 11.

$$\text{Radius of circle, } A_1P_2 = \sqrt{\left[\left(\frac{dE}{dt} \right)_{\omega_M}^2 + E_1'^2} = \sqrt{2\Delta} E_1' + E_1'^2} \quad (61)$$

The system separates once again at P_1 . For stable operation,

$$OP_4 < OP_1$$

$$(A_1P_4 - a_M) < (a_M - E_1')$$

But $A_1P_4 = A_1P_2$, since P_2 and P_4 lie on a circle centred at A_1 .

For stable operation,

$$E_1 < \left(a_M + \frac{2a_M^2}{\Delta} \right) \quad (62)$$

Thus, according to equation (62), the system would be stable for errors less than $\left(a_M + \frac{2a_M^2}{\Delta} \right)$ and unstable for errors larger than this value. It implies that the system has an unstable limit cycle when

$$E_1 = \left(a_M + \frac{2a_M^2}{\Delta} \right) \text{ for } 2a_M < \Delta \quad (63)$$

The limit cycle, however, vanishes for $2a_M \geq \Delta$ and the system becomes stable. Equation (63) indicates that the condition of existence and amplitude of the unstable limit cycles are both independent of ω_M .

(c) *Instrument servo with both viscous and coulomb friction at motor shaft*

With both viscous and coulomb friction present in an instrument servo, the differential equation of motor motion during the backlash region is

$$J_M \frac{d^2\theta_M}{dt^2} + f_M \frac{d\theta_M}{dt} = K \left(1 - \theta_{M1} - a_M \text{sign} \frac{d\theta_M}{dt} \right) \quad (64)$$

The time to take up backlash is given by

$$\alpha = \frac{4\zeta_M^2 \Delta}{E_1'} = \left(-1 + \frac{t}{T_M} + \epsilon \frac{t}{T_M} \right) \quad (65)$$

where

$$E_1' = (1 - \theta_{M1} - a_M) = E_1 - \theta_{M1} \quad (66)$$

The magnitudes of θ_{M1} , E_1 , E_1' and a_M are indicated in Fig. 12(a). As shown in this figure the separation occurs at P_1 and the recombination at P_2 . From P_2 to P_4 , the system follows the linear second order trajectory with focus located at A_1 which is shifted from O' by a_M . A limit cycle would exist if

$$O'P_4 = O'P_1 \quad (67)$$

At P_2 when the backlash is taken up,

$$\left(\frac{dE}{dt} \right)_2 = - \left(\frac{d\theta_M}{dt} \right)_2 = - \frac{E_1'}{2\zeta} \left(1 - e^{-\frac{t_d}{T_M}} \right) \quad (68)$$

where $\frac{t_d}{T_M}$ the normalized time to take up back lost is obtained from the plot of equation (65).

Using the transformation from $\left(E', \frac{dE}{dt} \right)$ to (X, Y) plane, Fig. 12(a) maps in to Fig. 12(b) such that

$$\left. \begin{aligned} \rho_1 &= E_1' \\ \psi_1 &= \tan^{-1} \frac{\zeta_M}{\sqrt{1 - \zeta_M^2}} \end{aligned} \right\} \quad (69)$$

and

$$\left. \begin{aligned} \rho_2 &= \frac{\omega_M E_1'}{2\zeta_M} \left[1 - 2(1 - 2\zeta_M^2) e^{-\frac{t_d}{T_M}} + e^{-2\frac{t_d}{T_M}} \right]^{\frac{1}{2}} \\ \psi_2 &= \tan^{-1} \frac{\left(1 - e^{-\frac{t_d}{T_M}} \right) - 2\zeta_M^2}{2\zeta_M \sqrt{1 - \zeta_M^2}} \end{aligned} \right\} \quad (70)$$

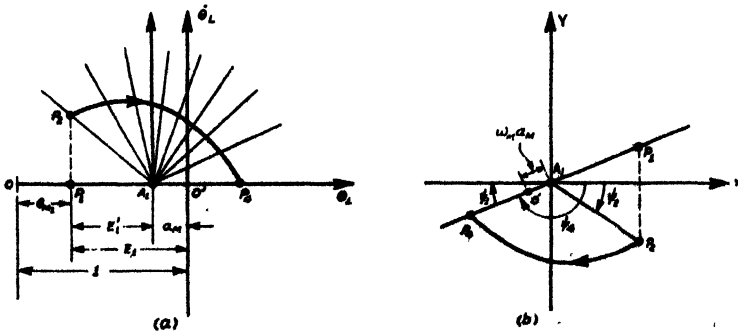


Fig. 12

Curves for case 2 (c)

Also,

$$A_1 O' = \omega_M a_M \quad (71)$$

The trajectory from P_2 to P_4 is a logarithmic spiral and it can be easily shown that

$$\rho_4 - \rho_2 \epsilon^{-\frac{\zeta_M}{\sqrt{1-\zeta_M^2}}(\pi - \Psi_1 - \Psi_2)} \quad (72)$$

Using equation (67), a limit cycle would exist if

$$\rho_4 - a_M \omega_M = \rho_1 + a_M \omega_M$$

or,

$$\frac{D}{\omega_M} = \frac{\rho_4 - \rho_1}{\omega_M} = 2 a_M \quad (73)$$

The value, $D = (\rho_4 - \rho_1)$, is the amount (in ρ, ψ plane) by which the state point diverges if $a_M = 0$, i.e., there is no coulomb friction. The divergence, D , is positive for low errors only if $\zeta_M < 0.29$. It means that a limit cycle for the system having both viscous and coulomb friction would possibly exist only if $\zeta_M < 0.29$.

It follows from equations (70), (71) and (73) that

$$\frac{D}{\omega_M} = \left[1 - 2(1 - 2\zeta_M^2) \epsilon^{-\frac{t_d}{T_M}} + \epsilon^{-\frac{2t_d}{T_M}} \right]^{\frac{1}{2}} - 1 \quad (74)$$

Since $\frac{D}{\omega_M}$ is independent of ω_M , it means that the existence of limit cycle is independent of ω_M and depends upon ζ_M and a_M only. Equation (73) would be satisfied at a particular value of $\frac{t_d}{T_M}$ and so a particular value α . It means that the amplitude of limit cycle would also be independent of ω_M .

The limit cycle is determined at a specified ζ_M by plotting $\left(\frac{D}{\omega_M}\right)$ vs. $\left(\frac{E_1'}{\Delta}\right)$.

The nature of the plot for $\zeta_M = 0.2$ is given in Fig. 13. It is seen that $\left(\frac{D}{\omega_M}\right)$ goes through a maximum positive value and finally becomes negative. The $(2 a_M)$ line on Fig. 13 shows that two limit cycles are possible. For values of $\left(\frac{E_1'}{\Delta}\right)$ less than that corresponding to the point U, the system converges and is stable; while for values of $\left(\frac{E_1'}{\Delta}\right)$ more than that corresponding to the point V, the system also converges and is stable. For values intermediate between the points U and V, the system is unstable. Thus the limit cycle defined by the point U is unstable and that defined by the point V is stable.

When $a_M = 0$, there is only a stable limit cycle corresponding to the point W in Fig. 13. As a_M is increased, the amplitude of the unstable limit cycle increases, and that of stable limit cycle decreases, till the $(2 a_M)$ line becomes tangential to $\frac{D}{\omega_M}$

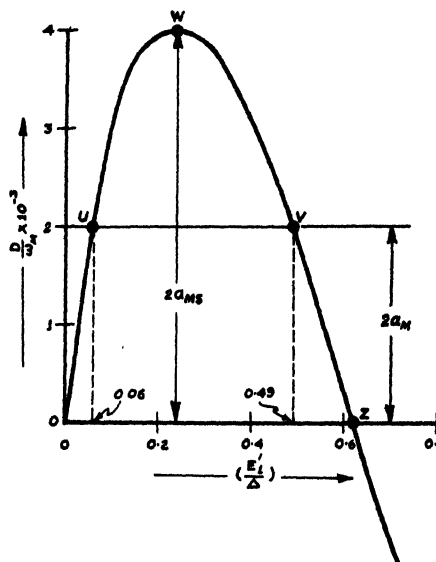


Fig. 13

Nature of $\frac{D}{\omega_M}$ vs. $\frac{E_1'}{\Delta}$ curve

curve at the point W for $a_M = a_{MS}$. For $a_M = a_{MS}$ the system becomes stable and no limit cycle exists. For $\zeta_M = 0.2$, $\omega_M = 10$ radian per sec., $\Delta = 0.05$ radian per sec. and $a_M = 1 \times 10^{-3}$

Unstable limit cycle exists at $E_1' = 0.003$ radian

Stable limit cycle exists at $E_1' = 0.0245$ radian

System becomes stable at $a_{MS} = 2$

Conclusions

The paper presents the phase-plane technique for the generalized backlash problem in a second order feedback control system with inertia, viscous and coulomb friction on both sides of backlash. The equation for separation lines and location of the foci for linear parts for the trajectory are given. The general time solution for the backlash region is derived, from which the time to take up backlash can be obtained by a graphical solution. It is shown that a limit cycle would exist, if the separation point in the region of positive $\frac{d\theta_L}{dt}$ is odd symmetrical to the corresponding point in the region of negative $\frac{d\theta_L}{dt}$. The limit cycle can be determined for any specific system by trial and error in the phase-plane. The results for a system in which the various inertias and frictions are absent can be easily derived from the general case. A number of simpler cases are studied.

The first simplification results when there is no coulomb friction. The equation of separation line and the equation for obtaining the backlash take-up time are given. An overall system study involves three independent parameters. A case of special interest arises, when load and motor are matched so as to have equal time constants. The load separates from the motor in this case always on the $\frac{d\theta_L}{dt}$ -axis. A universal plot is given for γ vs. $\frac{t}{T_M}$, from which the backlash take-up time for any initial conditions can be read off. A criterion is developed to determine the existence of a limit cycle, according to which the system breaks into a limit cycle for $\zeta < 0.413$. This result is verified by a direct system study.

For the case of negligible load friction, a universal chart is given to determine the backlash take-up time. It is found that the existence of a limit cycle is independent of the system natural frequency and the amount of backlash, while the amplitude of limit cycle $\left(\frac{d\theta_M}{dt}\right)_1$ depends directly upon these two parameters. A limit cycle criterion is developed which can be solved by numerical trial and error, and the limit cycle can be determined much quicker and more accurately than by constructing recombination lines and phase trajectory. The criterion, however, yields no clear cut conclusions directly. Two system studies are, therefore, carried out from this criterion (i) $J_r = 1$ and variable ζ (0 to 0.5) and (ii) $\zeta_M = 0.2$ and variable J_r . These studies indicate that a system with zero load friction always has a limit cycle up to the value of ζ studied, i.e., (0 to 0.5), but the error amplitude decreases monotonically with damping ratio and becomes less than 5% for $\zeta > 0.29$.

In the case of instrument servos with viscous friction only, the limit cycle criterion has been developed by Pastel and Thaler³ according to which the system becomes stable for $\zeta > 0.29$.

It is shown in the present paper that for instrument servos with only coulomb friction at motor shaft, the unstable limit cycle can exist, the amplitude of which is independent of ω_M and depends upon a_M and Δ only. The system becomes stable for $2 a_M > \Delta$.

For an instrument servo with both viscous and coulomb friction, investigation for a limit cycle needs to be carried out for $\zeta < 0.29$ only. A graphical technique is advanced for determining the existence of a limit cycle. It is found that in general two limit cycles are possible, viz., an inner unstable limit cycle and an outer stable limit cycle. As coulomb friction is increased, the two limit cycles become closer to each other and then merge into a single unstable limit cycle. The system becomes stable for larger values of coulomb friction. For $\zeta_M = 0.2$ and $\Delta = 0.05$, this happens at $a_M > 2$.

Acknowledgments

The authors are grateful to Prof. V. Lakshminarayanan, Principal, and Dr. M. Chaudhuri, Head of the Department of Electronics and Telecommunication Engineering, Birla College of Engineering, Pilani, Rajasthan, for providing facilities to carry out the investigations presented in this paper.

References

1. L. M. Vallese. 'Analysis of Backlash in Feedback Control Systems with One Degree of Freedom.' *Proceedings of the American Institute of Electrical Engineers*, vol. 74, pt. 2, no. 17, March 1955, p. 1,
2. M. P. Pastel and G. J. Thaler. 'Stability Criteria for Instrument Servomechanisms with Coulomb Friction and Stiction'. *Proceedings of the American Institute of Electrical Engineers*, vol. 78, pt. 2, no. 45, November 1959, p. 294.
3. M. P. Pastel and G. J. Thaler. 'Instrument Servomechanisms with Backlash, Coulomb Friction and Stiction'. *Proceedings of the American Institute of Electrical Engineers*, vol. 79, pt. 2, no. 49, July 1960, p. 214.
4. M. P. Pastel and G. J. Thaler. 'Analysis and Design of Nonlinear Feedback Control Systems'. *McGraw-Hill Book Co., Inc.*, 1962.

Appendix

Using the transformation of equation (37), at the point P_1

$$X_1 = \omega \sqrt{1 - \zeta^2} (1 - \theta_{M1}) = 0$$

$$Y_1 = -\frac{d\theta_M}{dt} + \zeta \omega (1 - \theta_{M1}) = -\left(\frac{d\theta_M}{dt}\right)_1$$

Therefore

and
$$\left. \begin{aligned} \rho_1 &= \left(\frac{d\theta_M}{dt}\right)_1 \\ \psi_1 &= \frac{\pi}{2} \end{aligned} \right\} \quad (75)$$

At the point P_3

$$X_3 = \omega \sqrt{1 - \zeta^2} \left[1 - \theta_{M1} - T_M \left(\frac{d\theta_M}{dt}\right)_1 \right] = -\omega \sqrt{1 - \zeta^2} T_M \left(\frac{d\theta_M}{dt}\right)_1 \quad (76)$$

$$Y_3 = \frac{\omega_M^2 T_M}{1 + J_r} \left(\frac{d\theta_M}{dt}\right)_1 + \zeta \omega (1 - \theta_{M1} - T_M \theta_{M1}) = \frac{\omega_M^2 T_M}{1 + J_r} \left(\frac{d\theta_M}{dt}\right)_1 - \zeta \omega T_M \left(\frac{d\theta_M}{dt}\right)_1 \quad (77)$$

Since

$$T_L = T_M$$

or,

$$\frac{J_L}{f_L} = \frac{J_M}{f_M}$$

we get

$$\frac{J_L}{J_M} = \frac{f_L}{f_M} = J_r \quad (78)$$

Now

$$T = \frac{J_L + J_M}{f_L + f_M} = \frac{J_M}{f_M} \left(\frac{1 + \frac{J_L}{J_M}}{1 + \frac{f_L}{f_M}} \right)$$

or,

$$T = T_M = T_L \quad (79)$$

Therefore,

$$\zeta \omega = \zeta_M \omega_M \quad (80)$$

$$\omega^2 = \frac{K}{J_L + J_M}$$

$$\omega_M^2 = \frac{K}{J_M}$$

Therefore,

$$\frac{\omega}{\omega_M} = \sqrt{\frac{J_M}{J_L + J_M}} = \sqrt{\frac{1}{1 + J_r}} \quad (81)$$

From equation (6) using equation (7), we get

$$\zeta_M = \zeta \left(\frac{\omega}{\omega_M} \right) = \frac{\zeta}{1 + J_r} \quad (82)$$

Substituting equations (80), (81) and (82) in equations (76) and (77), we get

$$X_3 = -\frac{\sqrt{1 - \zeta^2}}{2\zeta} \left(\frac{d\theta_M}{dt} \right)_1 \quad (83)$$

$$Y_3 = \frac{\sqrt{1 - 2\zeta^2}}{4\zeta^2} \left(\frac{d\theta_M}{dt} \right)_1 \quad (84)$$

Therefore,

$$\begin{aligned} \rho_3 &= \frac{1}{4\zeta^2} \left(\frac{d\theta_M}{dt} \right)_1 \\ \psi_3 &= \pi - \tan^{-1} \left(\frac{Y_3}{-X_3} \right) = \pi - \tan^{-1} \frac{\sqrt{1 - 2\zeta^2}}{2\zeta\sqrt{1 - \zeta^2}} \end{aligned} \quad (85)$$

The points P_1 , P_3 and P_4 in (ρ, ψ) plane are shown in Fig. 14.

From P_3 to P_4 , the state point follows the trajectory of the combined linear second order system, which is given by

$$\rho = C e^{-\frac{\zeta}{\sqrt{1 - \zeta^2}} \psi} \quad (86)$$

At point P_3 ,

$$\left(\frac{d\theta_M}{dt} \right)_1 = C e^{-\frac{\zeta}{\sqrt{1 - \zeta^2}} \psi_3}$$

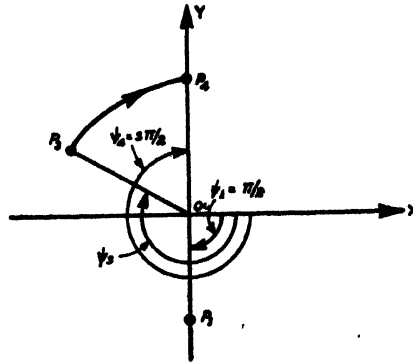


Fig. 14
Points on (ρ, ψ) plane

Therefore,

$$C = \frac{\left(\frac{d\theta_M}{dt}\right)_1}{4\zeta^2} e^{-\frac{\zeta}{\sqrt{1-\zeta^2}} \psi_2} \quad (87)$$

At point P_4

$$\psi_4 = \frac{3\pi}{2} \quad (88)$$

Therefore,

$$\rho_4 = C e^{-\frac{\zeta}{\sqrt{1-\zeta^2}} \frac{3\pi}{2}} \quad (89)$$

Substituting for C from equation (13) in (15), we get

$$\left(\frac{d\theta_M}{dt}\right)_{\rho_4} = e^{-\frac{\zeta}{\sqrt{1-\zeta^2}} \left(\frac{3\pi}{2} - \psi_2\right)} \quad (90)$$

A limit cycle would exist if

$$\rho_4 = \rho_1$$

or,

$$\frac{1}{4\zeta^2} e^{-\frac{\zeta}{\sqrt{1-\zeta^2}} \left(\frac{\pi}{2} - \tan^{-1} \frac{\sqrt{1-2\zeta^2}}{2\zeta\sqrt{1-\zeta^2}}\right)} = 1 \quad (91)$$

GAIN COMPENSATION OF A PHASE-COMPENSATED THIRD ORDER TYPE-1 SYSTEM*

V. Seshadri

Associate Member

*Assistant Professor, Electrical Engineering Department,
Birla Institute of Technology, Ranchi*

Summary

A typical position control system with the necessary phase compensation is chosen for study. A gain advancing lag network is designed for this system. The effects of shifting the corner frequencies of the lag network on the performance of the overall system with respect to input and load-disturbed transients are studied on an analogue computer set-up and the results are presented in this paper. The corresponding variations in the root-loci and frequency responses of the system are obtained by digital computation. The effects of changes in the lag network corner frequencies on system performance with respect to stability, damping, rise time of transient responses, nature of settlement of transients under input and load disturbances are evaluated from experimental results. A generalized scheme for arriving at the best choice of network corner frequencies is developed.

1. Introduction

The common form of the simple position control system, consisting essentially of an amplidyne and a servo motor, is of third order type-1 and hence requires phase and gain compensation to meet the requirements of good stability and low steady state error. Such phase and gain compensation can be accomplished satisfactorily by using lead and lag networks respectively. The paper discusses the experimental and analytical studies made to ascertain the criteria relating to the choice of lag network parameters for optimum system performance.

2. Choice of representative system

The transfer function of such a position control system is of the form

$$K G = \frac{K}{p(1 + \tau_a p)(1 + \tau_m p)} \quad (1)$$

where τ_a and τ_m are the operational time constants of the servomotor and the amplidyne respectively. When the servo motor has an externally applied torque in addition to the inertia load, its transfer function is given implicitly by the equation

$$\theta_c = \frac{k_m E_a + \tau_m L_n}{p(1 + \tau_m p)} \quad (2)$$

* Written discussion on this paper will be received until November 30, 1964.

This paper was received on November 26, 1962.

where E_a is the armature voltage and L_n the load torque per unit moment of inertia of the motor system with respect to the output shaft. The values, $K_m = 1.0$, $\tau_m = 0.1$ sec. and $\tau_a = 1.0$ sec., are chosen as representative values. After phase compensation for satisfactory stability, the overall transfer function becomes

$$K G = \frac{33}{p(1+p)(1+0.1p)} \frac{0.1(1+p)}{(1+0.1p)} \quad (3)$$

where the second factor of the product represents the lead network. Choosing an error margin of 1 degree at 5 revolutions per min., the minimum value necessary for the gain-constant required becomes 30, thus necessitating gain advancement by about 20 dB. This can be accomplished satisfactorily by using a lag network.

3. Lag network and system optimization

Fig. 1 shows a common form of lag network. With a sinusoidal input voltage, the output lags behind the input in phase. With zero source impedance and infinite load impedance, the operational transfer function of the lag network is given by

$$\frac{E_o}{E_{in}} = \frac{(1 + \tau p)}{(1 + a \tau p)} \quad (4)$$

where $\tau = R_1 C_1$ and $a = \frac{(R_1 + R_2)}{R_2}$. The network ratio, a , determines the low frequency gain advancement obtainable. By increasing the system gain by a factor, a , it is possible to increase the gain constant by a factor, a , while the insertion of the lag network retains the gain crossover frequency unaltered.

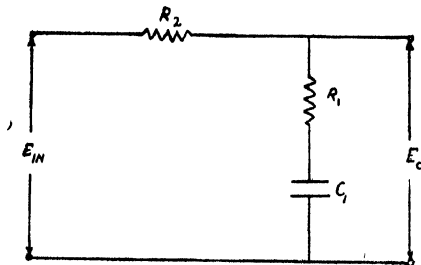


Fig. 1

A simple lag network

It is observed from equation (4) that the lag network introduces into the system a zero equal in value to its upper corner frequency, $\frac{1}{\tau}$, and a pole equal in value to its lower corner frequency, $\frac{1}{a\tau}$. These values of the corner frequencies of the lag network, relative to the poles and zeros of the rest of the system, greatly influence the overall performance of the system.

An optimum system may be defined as one having the best form of transient response to a step input. A satisfactory assessment of the degree of optimization can be made from a knowledge of the rise time and the settling time of transients under a step input. An experimental study was, therefore, undertaken by the analogue computer techniques for the purpose of determining the values of corner frequencies of the lag network for which the system gives optimum response. The effect of the lag network design on the nature of the load disturbed transients was also examined.

4. Experimental procedure

An analogue computer set-up simulating completely the basic system, the phase advancing system, and the gain advancing system is shown in Fig. 2. The simulation of the basic system follows equation (2) so as to make provision for the study of system response to load disturbances. The equalizing system (stages 2 to 5) is placed between the two parts of the basic system simulating the amplidyne (stage 1) and the servo motor (stages 6 and 7). Stages 2 and 3 represent the phase advancing system, while stages 4 and 5 simulate a variable lag network for a fixed value of gain compensation under varying values for the corner frequencies. If the value of the two capacitors of same rating, C , in stages 4 and 5 is made variable simultaneously, the variable function for the gain advancing system becomes

$$K G (\text{gain-advancer}) = \frac{10(1 + 0.5 C p)}{(1 + 5 C p)} \equiv \left(\frac{p + \frac{2}{C}}{p + \frac{1}{5C}} \right) \quad (5)$$

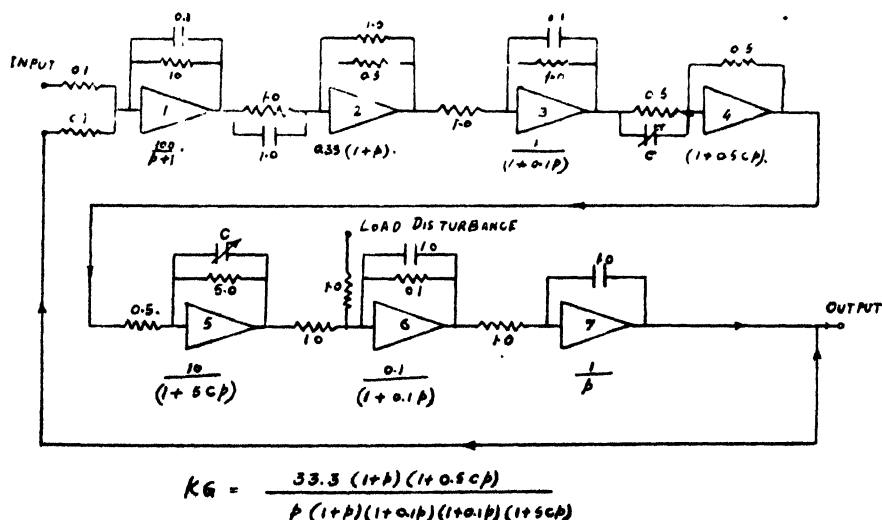


Fig. 2

Analogue set-up of compensated system with variable design lag network

Thus, by changing the value of the capacitors, the position of the lag network corners on the frequency scale can be changed over a wide range, while keeping the

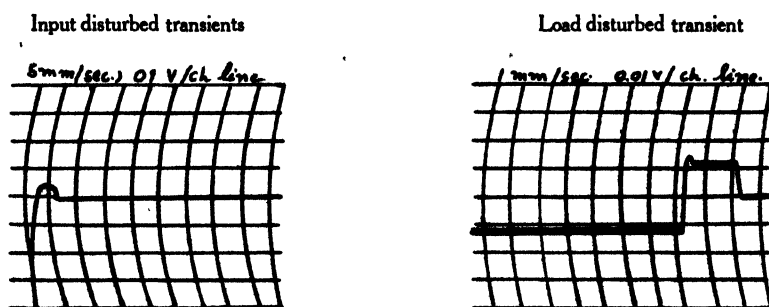
network ratio of gain advancement constant at 10. The leakage resistances of the capacitors employed were measured and allowed for in setting up the experimental analogue.

For different values of the corner frequencies of the lag network as obtained by changing the values of the capacitors, C , a low frequency square wave (0.01 cycle per sec.) signal was applied at the input terminal of the analogue set-up and the nature of the output signal was observed and recorded on a Brush recorder when the input signal was removed suddenly.

For the same amplitude of square wave signals applied at the point on the analogue corresponding to the load torque disturbances, the behaviour of the output potential was observed, when the applied signal was removed suddenly.

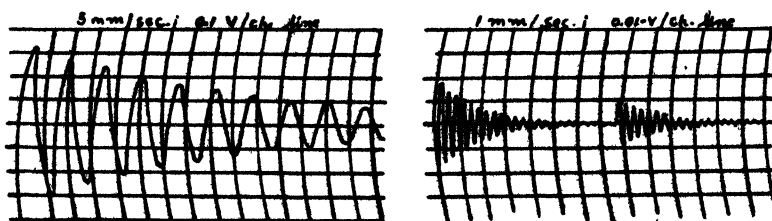
5. Discussion of results

A representative set of recorded transients under input and load-disturbances is given in Fig. 3 and Fig. 4 shows the polar plots of the frequency response and phase angle characteristics of the system for several values of the lag network corner frequencies. Fig. 5 contains the root-loci for the same functions. Data for plotting the above curves were obtained by digital computation. The results of the experiment are given in Table 1 along with relevant particulars obtained from the graphical plots.



(a)

Phase compensated system without gain compensation

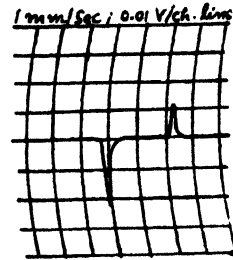
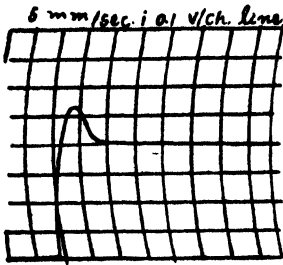


(b)

$$C = \frac{1}{2} \mu F; Z_{lag} = 4 \tau/s; P_{lag} = 0.4 \tau/s$$

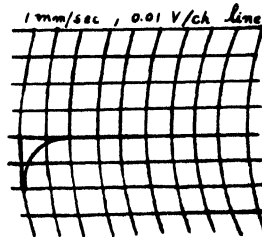
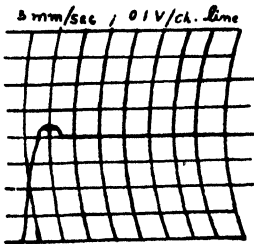
Input disturbed transients

Load disturbed transients



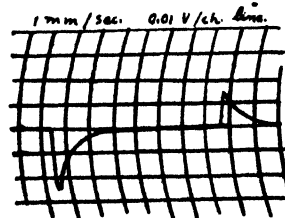
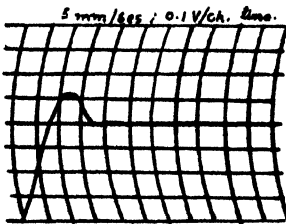
(c)

$$C = 2 \mu F ; Z_{lag} = 1.0 \text{ r/s} ; P_{lag} = 0.1 \text{ r/s}$$



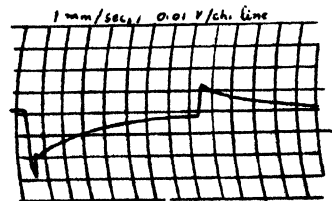
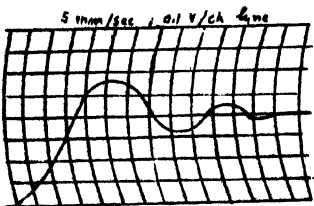
(d)

$$C = 5 \mu F ; Z_{lag} = 0.4 \text{ r/s} ; P_{lag} = 0.04 \text{ r/s}$$



(e)

$$C = 8 \mu F ; Z_{lag} = 0.25 \text{ r/s} ; P_{lag} = 0.015 \text{ r/s}$$



(f)

$$C = 30 \mu F ; Z_{lag} = 0.067 \text{ r/s} ; P_{lag} = 0.0067 \text{ r/s}$$

Fig. 3

Input and load disturbed transients for different positions of lag network on frequency scale

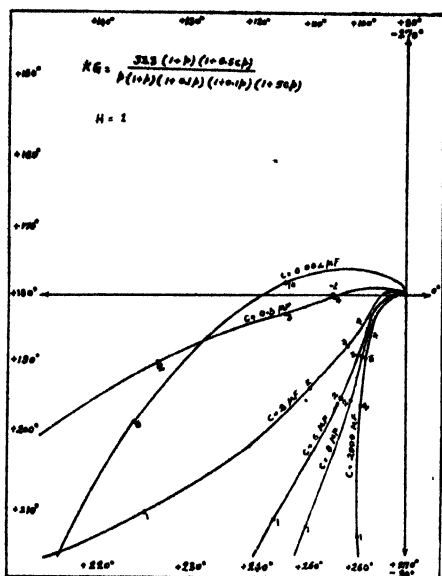


Fig. 4
Polar plots of compensated system

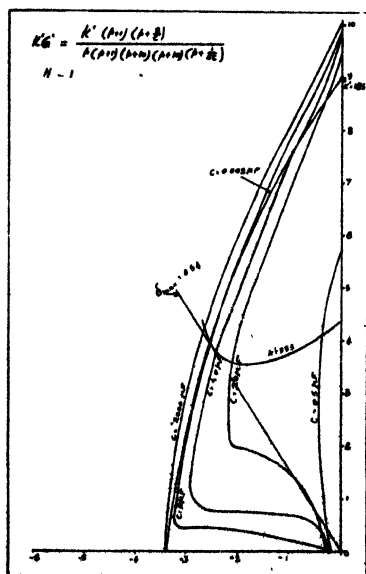


Fig. 5
Root-loci of compensated system

Table 1
Lag network and system characteristics

Value of $C, \mu F$	Corner frequency		Value of ω_d	Value of ω_{cp}	Phase margin, φ_m	Gain margin, g_m , db.	Damping ratio of least damped roots, δ	Percent- age over- shoot of input- disturbed transients	Rise time of input- disturbed transients, t_r	Settling time (to within 5%) of input- disturbed transients, t_s	Time constant of decay of load- disturbed transients, T_s
	Lower, revolu- tions per sec.	Upper, revolu- tions per sec.									
0.002	100	1,000	14.50	9.5	-26°	-9.0	Negative	—	—	—	—
0.5	0.4	4.0	4.30	5.8	6°	6.0	0.070	80	0.3	—	0
2.0	0.1	1.0	3.20	9.5	39°	15.0	0.520	29	0.5	1.0	1.0
5.0	0.04	0.4	3.15	9.5	48°	15.5	0.540	10	0.8	2.1	2.5
8.0	0.025	0.25	3.00	9.5	52°	15.5	0.535	30	1.3	2.7	4.0
2,000	0.0001	0.001	3.00	9.5	57°	16.0	0.550	—	—	—	—

The effects of a variation in lag network design on the phase compensated third order type-1 system, as borne out by experimental results, are summarized below.

Stability and damping

The system without gain advancement has a high degree of stability and damping. But it is susceptible to large errors in the steady state, as evidenced by the very low tendency for corrective action on load disturbances.

For extremely small value of C , the system is oscillatory on account of the pole of the lag network being close to the rest of the poles and zeroes of the system; this destabilizing effect is reduced as the value of C is increased. Thus, the system damping improves, as evidenced by improvements in overshoot, phase margin and the damping ratio of least damped roots. An optimum value for C appears to exist with respect to system stability and damping. A maximum value is obtained at this condition for the least damped roots. This condition is approximately represented by the point at which the tangent from the origin touches the constant-gain locus plotted over the root-loci (Fig. 5). For the system under study, this occurs for $C = 5 \mu\text{F}$, for which the corner frequencies of the lag network are 0.04 and 0.4 radian per sec.

As the values are further increased for C the stability becomes poorer, the overshoots larger and the system response more sluggish. The destabilizing effect may now be traced to the fact that the pole of the lag network approaches the origin.

Rise time of transients

There is a steady increase in the rise time of input disturbed transients as the value of C is increased, along with a corresponding decrease in gain crossover frequency. However, it is also found that an exact inverse proportionality does not exist between the rise time and gain crossover frequency under nonuniform conditions of damping and stability.

Nature of settlement of transients

A steady increase in the settling time of the input-disturbed transients as the value of C is increased indicates the increasing sluggishness of the system. This is due to the increasing time constant corresponding to the negative real root introduced by the zero of lag network into the system.

Transients under load disturbances

The absence of the lag network leads to large errors in the steady state. A load disturbance under these conditions is found to cause a large dislocation with very little corrective action.

Changes in the lag network do not have any appreciable effect on the maximum shift of the output for a given magnitude of load disturbance.

The importance of the zero of the lag network as the determinant of the settlement characteristics of the system is clearly seen in the study of load-disturbed transients. The transient disturbance of output under a step disturbance on load is found to decay exponentially with a time constant corresponding to the upper corner frequency of lag network.

6. Criteria for choice of lag network

Since the upper corner frequency of the lag network is found to largely determine the nature of settlement of transients, the designer may attempt the prediction of a lower limit on the zero of the lag network on the basis of the restrictions on settling time. Especially in the case of load-disturbed transients, where the decay of dislocation is practically exponential, a simple correlation between the settling time and the time constant is possible. It is observed that, under conditions of good damping, the settling time (5% basis) under input disturbances is found to be approximately equal to the time constant of the exponential decay of load-disturbed transients, the latter in turn being equal to the reciprocal of the upper corner frequency of the lag network. This gives an approximate empirical relationship :

$$T_m = t_s = \frac{1}{Z_{\min.}} \quad (6)$$

where T_m is the maximum value of the time constant corresponding to the zero of the lag network, t_s the maximum allowed settling time under input or load disturbances and $Z_{\min.}$ the minimum value for the upper corner frequency of the lag network. Although this relationship is approximately true only under conditions of good damping, this may nevertheless be employed for initially estimating the zero of the lag network, so that allowance for it can be made during phase compensation.

It is seen from the results that, in order to have good damping and stability and reasonably low values of rise time and settling time of transients, the choice of the lag network has to be the one with $C = 5 \mu F$ for the system under study. A study of the effect of the poles and zeroes of the system on its frequency response would suggest a simple, though empirical and approximate, relationship that would yield the optimum region of choice for the zero of the lag network in terms of the poles and zeroes of the rest of the system and the asymptotic crossover frequency required for stability. Fig. 6 indicates schematically the typical placement on a logarithmic scale of the poles and zeroes in the vicinity of the asymptotic crossover frequency. The approximate empirical relationship connecting these is

$$\log \frac{\omega_{cg}}{Z_{lag}} + \log \frac{\omega_{cg}}{Z_{lead}} - \log \frac{\omega_{cg}}{p_1} \simeq \log \frac{p_{lead}}{\omega_{cg}} + \log \frac{p_2}{\omega_{cg}} \quad (7)$$

which simplifies to an estimate of the zero of the lag network as

$$Z_{lag} \simeq \frac{(\omega_{cg})^3 p_1}{Z_{lead} p_{lead} p_2} \quad (8)$$

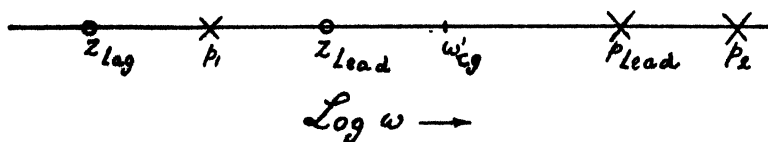


Fig. 6

Typical placement of poles and zeroes

For the case under study, with an asymptotic crossover at 3.33 radian per sec., equation (8) yields a value of 0.367 radian per sec. and this agrees well with the experimentally determined optimum value of 0.4 radian per sec. After the upper corner frequency for the lag network is thus established, the value of the lower corner frequency is easily fixed on the basis of the degree of gain compensation desired. In the case under study, the lower corner is placed at 0.04 radian per sec. for obtaining the necessary gain compensation of 20 db.

7. Conclusions

The results of the experimental and analytical studies described in this paper would serve as useful criteria in the choice of the best lag network design for the gain compensation of a phase-compensated third order type-1 system with unity feedback. The developed criteria indicate the best range of values for the lag network upper corner frequency that would optimize the system in respect of the transient response under input or load disturbances.

8. Acknowledgments

The author expresses his indebtedness to Dr. R. E. Nolte and Mr. R. T. DeWoody, of the Electrical Engineering Department of the Missouri University School of Mines and Metallurgy, Rolla, Mo., U.S.A., under whose guidance the above work was undertaken, and also to Prof. R. Lee, of the Department of Mathematics of the above school, who helped in the programming of digital computation for the analytical studies included in this paper.

9. Reference

- V. Seshadri. 'Optimization and Equalization of a Third Order Type-1 Position Control System'. Thesis submitted to the Missouri University for the Master's degree, 1960.

TRANSISTOR OPERATIONAL AMPLIFIER***R. Sundar***Non-member***Summary**

This paper describes a low drift transistorized operational amplifier designed to form the main computing element in a D.C. analogue computer being developed at the Electronics and Radar Development Establishment, of the Government of India. An analysis of the operational amplifier as a summing amplifier and as an integrator is made and the characteristics of the amplifier required to achieve a computing accuracy of 0.01% are drawn.

The amplifier in the steady state has a forward gain of approximately 1,000 volts per microamp., an output swing of ± 10 volts, and an output drift of less than 1 millivolt per hr. The principle of chopper stabilization is successfully used to achieve the low drift. Test results of the amplifier constructed on two plug in printed circuit boards indicate useful performance adequate for the normal analogue computers.

Introduction

The analogue computer is now established as the most useful aid in the investigation of problems, e.g., control of anti-aircraft fire equipment for radar. The need for greater accuracy and increasing number of parameters entering the computation has however necessitated more computing amplifiers with corresponding increase in the size of the computer. Transistorized computers provide useful solution in reducing considerably the size and power requirements of the computer with added reliability. The transistor operational amplifier forms the basic building block of the computer.

Analysis of operational amplifier

A block diagram of an operational amplifier without drift stabilization is shown in Fig. 1(a). The corresponding equivalent circuit is shown in Fig. 1(b).

The transistor is essentially a current operated device, its admittance properties bearing a close resemblance to the impedance properties in a valve. Nevertheless, it is still convenient to use a voltage analogue in preference to a current analogue. The analysis of the amplifier has been made accordingly, although the open-loop gain of the amplifier is defined by a transfer impedance instead of the normal voltage or current gain. The amplifier is represented by its input impedance, R_i , transfer impedance

$Z = \frac{\text{Output volts}}{\text{Input amp.}}$ and its output impedance, R_o .

* Presented at the First Conference of Automation and Computation Scientists of India, Sindri, February 22-24, 1963.

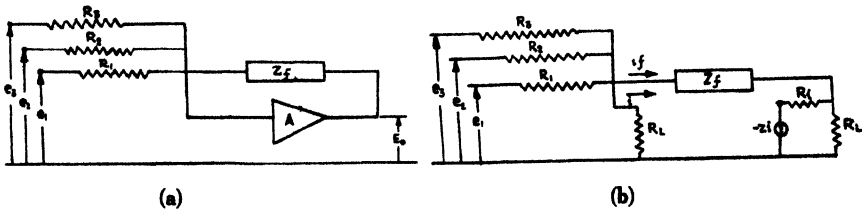


Fig. 1

Operational amplifier circuits

The output impedance, R_o , is generally made very small compared with the load that the amplifier can drive and hence, for an input current, i , flowing into the amplifier terminals, the output voltage is given by

$$e_o = -Zi \quad (1)$$

Equating the currents at the summing node, we get

$$\sum \frac{e_1 - i R_i}{R_1} = -i + \frac{i R_i + Z i}{Z_f}$$

or,

$$\sum \frac{e_1}{R_1} = i \left(1 + \frac{R_i}{Z_f} + \frac{Z}{Z_f} + \sum \frac{R_i}{R_1} \right)$$

Substituting $i = \frac{-e_o}{Z}$ and collecting terms, we get

$$e_o = \frac{Z_f}{\sum R_1} \left\{ \frac{\sum e_1}{1 + \frac{Z_f}{Z} \left(1 + \frac{R_i}{Z_f} + \sum \frac{R_i}{R_1} \right)} \right\} \quad (2)$$

The amplifier behaves as a pure summing device when the feedback impedance is a pure resistance and as summing integrator when the feedback is through a condenser.

For a perfect amplifier, the output voltage should be $e_o = -\frac{Z_f}{\sum R_1} \sum e_1$. The output would then be governed entirely by the computing components R_1, R_2, R_3 and Z_f . The other terms in the above equation then represents a computing error which decreases with an increase in the transfer ratio, $\frac{Z}{Z_f}$, and tends to zero as the transfer impedance tends to infinity. For a finite transfer impedance, the input impedance of the amplifier also contributes to the error and for the same transfer impedance should be small compared with R_1, R_2, R_3 and Z_f for a low computing error. This requirement of the operational amplifier is significantly in sharp contrast to the high impedance requirement of the vacuum tube operational amplifiers.

For the amplifier working in a summing role, equation (2) can be re-written as

$$e_o = \sum e_1 \frac{R_f}{R_1} \left\{ \frac{1}{1 + \frac{R_f}{Z} \left(1 + \sum \frac{R_i}{R_1} + \frac{R_i}{R_f} \right)} \right\}$$

The effect of R_i , R_1 , R_2 and R_3 is hence to effectively reduce the transfer impedance, Z .

Representing $\frac{Z}{1 + \Sigma \frac{R_i}{R_1} + \frac{R_i}{R_f}}$ by an equivalent transfer impedance, Z' , we get

$$e_0 = \Sigma e_1 \frac{R_f}{R_1} \left\{ \frac{1}{1 + \frac{R_f}{Z'}} \right\}$$

The error in the summing amplifier due to the finite transfer impedance can be simplified as

$$\text{Error} = \Sigma e_1 \frac{R_f}{R_1} \left(\frac{R_f}{R_f + Z'} \right) \quad (3)$$

For a single input e_1 ,

$$\% \text{ error} = \left(100 \times \frac{R_f}{R_f + Z'} \right)$$

To achieve a 0.03% computing error for a single input with a feedback resistance = 100 K, the transfer impedance is

$$Z' = \frac{100 \times R_f}{0.03} = \frac{100 \times 100 \times 10^3}{0.03} = \frac{1,000}{3} \text{ megohm}$$

For a three input summing amplifier with a loop gain of 1, for the same percentage error, the transfer impedance, Z' , would have to be 1,000 megohms.

Since $R_1 = R_2 = R_3 = R_f = 100 \text{ K}$, for an input impedance R_1 of the amplifier of the order of 2 K or less, the effective transfer impedance, $Z' \simeq Z = 1,000$ megohms.

In the above analysis, the effect of noise and zero drift of the amplifier have not been considered. The amplifier output voltage drifts with the input earthed owing to the quiescent parameters of the amplifier drifting from its set value at any instant. This also contributes an additive error in the system. Although each stage of the cascaded D.C. amplifier contributes to the total drift, the final drift voltage at the output would be more or less determined by the drift component of the input stage. If the total gain of the amplifier is made up of individual stage gains, Z_1, Z_2, \dots and the corresponding drift components are i_{d1}, i_{d2}, \dots , then it can be shown that the effective drift referred to the input would be

$$i_d = i_{d1} + \frac{i_{d2}}{Z_1} + \frac{i_{d3}}{Z_1 Z_2}$$

dependent mostly on the input stage drift. Allowing for an effective current drift, i_d , flowing into the input impedance, R_1 , of the amplifier, for the same input current, i , assumed in equation (1) the final output voltage is

$$e_0 = \frac{-Z_f}{\Sigma R_1} \left\{ \frac{\Sigma e_1}{1 + \frac{Z_f}{Z} \left(1 + \Sigma \frac{R_i}{R_1} + \frac{R_i}{Z_f} \right)} \right\} - Z_f \left\{ \frac{i_d}{1 + \frac{Z_f}{Z} \left(1 + \Sigma \frac{R_i}{R_1} + \frac{R_i}{Z_f} \right)} \right\} \quad (4)$$

The drift error is additive. For a summing amplifier with a high $\frac{Z}{R_f}$ ratio, the drift component is approximately equal to $R_f i_d$. The drift is directly dependent on the feedback resistance, R_f , and the effective input drift and independent of the close-loop gain. The D.C. drift of the system thus limits the computing accuracy of the system.

Integrator

When the feedback path in the loop is through a condenser, C , the impedance, Z_f , in the amplifier equation is equal to $\frac{1}{C_p}$ where p is the differential operator. The operational amplifier then behaves as a summing integrator. Solving the equation, we get

$$e_o = - \int_0^T \left(\frac{e_1}{R_1 C} + \frac{e_2}{R_2 C} \dots \dots \right) \left(\frac{1}{1 + \frac{1}{C Z_1}} \right) dt \quad (5)$$

The effect of the finite transfer impedance is again to introduce an integrating error in the system, the time constant being different from that determined by the computing components, R_1 and C . To achieve minimum error, the ratio $\frac{Z'}{R_1}$ should be again as large as possible.

The D.C. drift error in the integrator system is

$$V_d = Z_f i_d = \frac{i_d}{C p} = \int \frac{i_d}{C} = i_d R \frac{t}{T}$$

where $T = CR$ is the integrator time constant. The D.C. drift increases with time. For a low drift the integrator time constant should be high for a small value of input resistance, R , which indicates a high feedback capacitance. The highest value of capacitance that can be used is however limited by the stability of the overall system.

Design of amplifier

The D.C. drift of an uncompensated transistor operational amplifier is of a much higher magnitude compared with the tube amplifiers. This is mainly because the transistors are inherently temperature sensitive. The quiescent current as well as the gain parameters of the transistor have a predominant variation with temperature which contributes to the high drift. Yet since the variation in parameters follows a set pattern with temperature, it is possible to control and compensate for the zero drift unlike the vacuum tubes where the drift is random.

A conventional D.C. amplifier even when provided with matching components, and compensating elements for temperature variations, still falls short of the acceptable minimum when provided with gains of the order of 1,000 volts per microamp. A chopper amplifier, which essentially provides all the gain in the A.C. channel, is widely used in achieving low drift D.C. amplification. But its poor bandwidth capabilities preclude its use directly in high gain operational amplifiers. The chopper amplifier

is hence used along with wideband D.C. amplifier in a chopper stabilizing circuit to overcome the bandwidth limitation, yet using its low drift figures.

The block diagram of the stabilizing circuit is as shown in Fig. 2. The amplifier is made up of a comparatively drift free chopper amplifier, A_1 , feeding into a conventional D.C. amplifier, A_2 . If the input current drift of the D.C. amplifier is i_d the effective drift current referred to the input circuit of the chopper amplifier is $\left(\frac{i_d}{Z_1}\right)$

where Z_1 represents the gain of the chopper channel. The D.C. and low frequency transfer impedance of the overall amplifier is $Z_1 Z_2$. The chopper amplifier thus helps to reduce the overall drift to its gain times the D.C. amplifier drift. By making i_d sufficiently small and increasing Z_1 for the overall transfer impedance, the output drift is reduced to a negligible value. The condenser, C_1 , is included in the circuit to effectively bypass the chopper amplifier at higher frequencies and limit the gain of the overall amplifier to that of the D.C. amplifier alone. This helps in considerably improving the frequency response of the system. The individual gains of the chopper amplifier and the D.C. amplifier would depend, apart from the drift considerations, by the stability margins that would be needed in the overall loop.

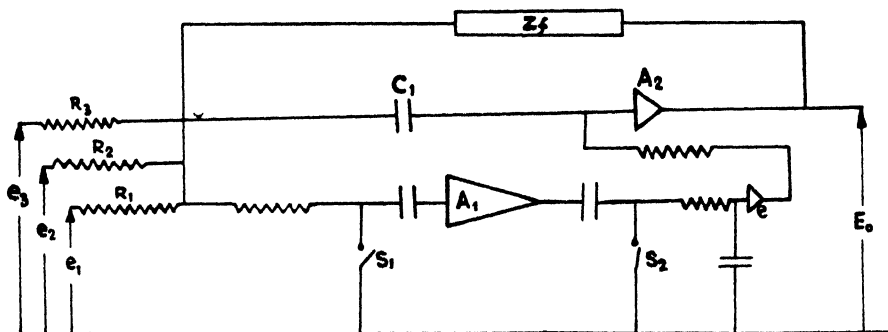


Fig. 2

Block diagram of stabilizing circuit

The D.C. amplifier is made up of two differentially cascaded stages feeding into a two-stage grounded emitter amplifier (Fig. 3). Sufficient negative feedback is provided in the individual stages to maintain repeatability in the amplifiers. Low drift, matched silicone transistors working at low collector currents have been used in the differential input stage providing a low input drift. The cascading of the differential stages reduces to a large extent the drift output at the second stage. The use of an NPN-transistor in the third stage prevents interstage loss and helps in achieving a zero output, and a large swing of -10 to $+10$ volts at the output stage. Condensers, C_2 and C_3 provide the proper shaping of the frequency response at approximately 6 dB. per octave to prevent instability and oscillations in the amplifier.

The chopper amplifier circuit is as shown in Fig. 4. It is made up of an input chopper which provides a modulated square pulse of the D.C. signal. The modulated

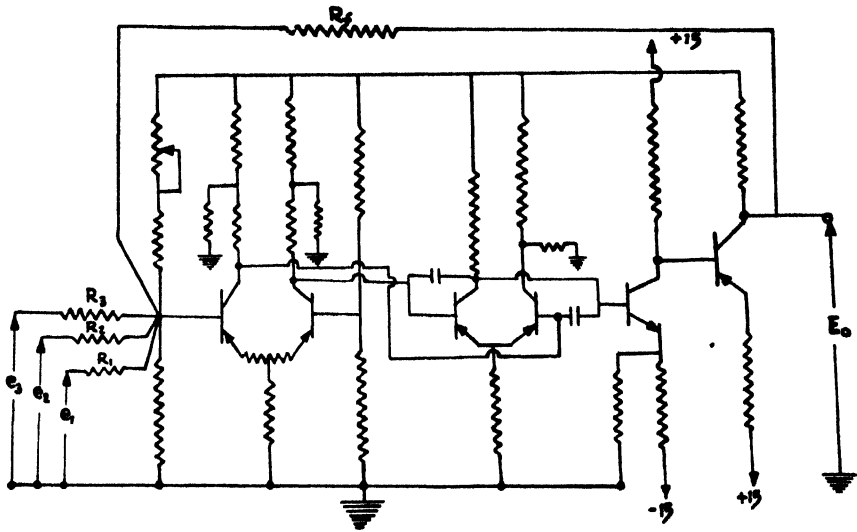


Fig. 3

Details of stabilizing circuit

pulses are amplified in a three-stage A.C. amplifier which is itself direct coupled to provide a sharp pulse at the output. The amplifier provides a net phase reversal. The amplified pulses are synchronously rectified at the output chopper, smoothed in the R - C network and fed through an emitter follower circuit to the succeeding D.C. amplifier. The input chopper as well as the output chopper are both switching transistors, driven synchronously by pulses from a built in multivibrator at a frequency of 3 kilocycles per sec. The output chopper is in anti-phase with the input chopper and with the phase reversal of the A.C. amplifier, provides an in-phase amplified D.C. signal at

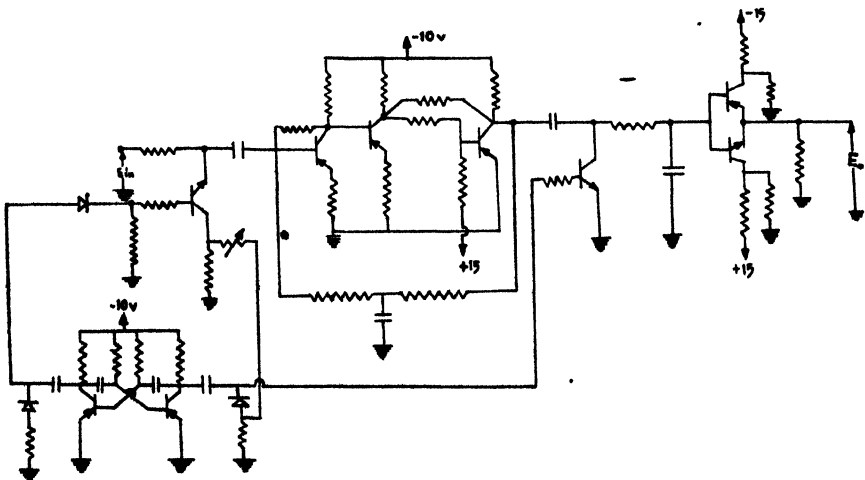


Fig. 4

Chopper amplifier circuit

the output. A high frequency of 3,000 cycles per sec. was chosen to attain good smoothing in the R - C network. High frequency transistors were preferred to prevent widening of the chopping transients in the amplifier. The chopper amplifier is however not entirely drift-free because of the temperature variations in the switching characteristics of the input chopper transistor. The overall drift is however less than 1 millivolt at the output.

The D.C. amplifier and the chopper amplifier are compact units (*vide* Figs. 5 and 6) mounted on individual printed circuit boards in rugged aluminium brackets. These can be individually plugged into 15-pin printed circuit connectors. Suitable check points of the amplifier are brought out in both the pads into small 8-pin monitoring connectors fixed on the printed circuit pad to facilitate easy checking.

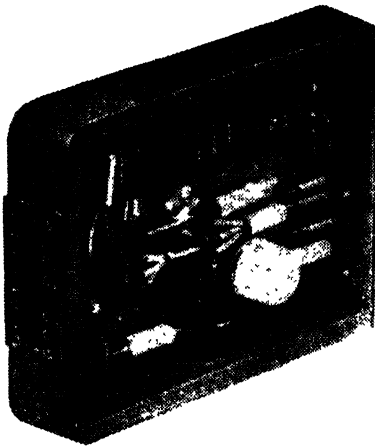
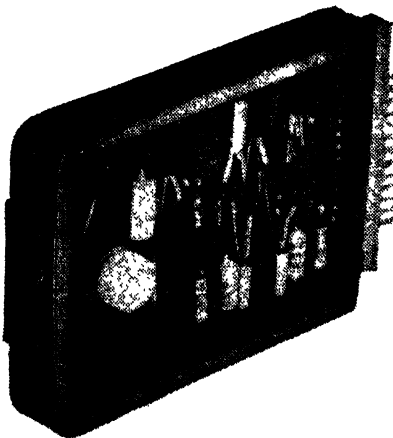
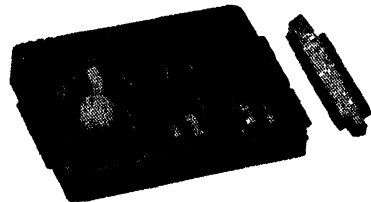


Fig. 5
Operational amplifier unit



(a)



(b)

Fig. 6
Chopper amplifier units

The amplifier provides an overall open-loop D.C. gain greater than 1,000 volts per microamp. and with a feedback impedance of 100 K has a summing accuracy greater than 0.01% for up to three inputs. The amplifier has an output voltage swing of -10 to $+10$ volts and an output drift of the order of 1 millivolt per hr. for a 10°C. change in temperature.

Conclusions

Design of a transistorized D.C. operational amplifier presents many difficulties, the chief among them being the D.C. drift due to temperature variations. This practical design shows that it is still possible to build a transistorized operational amplifier comparable with its vacuum tube counterpart.

Acknowledgments

The author thanks the authorities of the Research and Development Organization, Ministry of Defence, Government of India, for the facilities provided for carrying out the work presented in this paper and for their kind permission to publish this paper.

References

1. G. B. B. Chaplin and A. R. Owens. 'Transistor High Gain Chopper Type D.C. Amplifiers'. *Proceedings of the Institution Electrical Engineers*, vol. 105, pt. B, no. 21, May 1958, p. 258.
2. G. B. B. Chaplin and A. R. Owens. 'Transistor Input Stages for High Gain D.C. Amplifiers'. *Proceedings of the Institution of Electrical Engineers*, vol. 105, pt. B, no. 21, May 1958, p. 249.
3. F. H. Bletcher. 'Transistor Circuits for Analogue Computers'. *Bell system Technical Journal*, vol. 35, no. 2, March 1956, p. 295.
4. D. L. Davies and S. F. Miles. 'D.C. Gain of An Operational Amplifier'. *Electronic Engineering*, vol. 34, no. 410, April 1962, p. 249.
5. J. R. Baird and W. T. Matzen. 'Drift Considerations in Low Level Direct Coupled Circuits. National Convention Record, Institution of Radio Engineers, pt. 3, 1959, p. 27.
6. A. R. Kruper. 'Switching Transistors Substitute for Mechanical Low Level Choppers.' *Proceedings of the American Institute of Electrical Engineers*, vol. 74, pt. 1, March 1955, p. 141.

SOLUTION TO THIRD ORDER DIFFERENTIAL EQUATIONS WITH ONE OPERATIONAL AMPLIFIER*

L. K. Wadhwa

Non-member

Defence Research and Development Organization, New Delhi

Summary

This paper describes a method for the solution to third order linear differential equations with only one operational amplifier, three capacitors and four resistors by the techniques of operational simulation. Four circuits along with the design formulae and the conditions for their physical realizability are also presented.

Introduction

A previous paper¹ on this topic discussed the simulation of third order linear systems with one operational amplifier, three capacitors and five resistors. On re-examination of the problem, it is found that such systems can be simulated with the same basic network but employing a fewer number of resistors. Four such networks, each consisting of one operational amplifier, three capacitors, four resistors and capable of simulating systems described by third order linear differential equations, are presented in this paper.

Solution of third order differential equation

A third order linear differential equation

$$a_3 \frac{d^3 e_o}{dt^3} + a_2 \frac{d^2 e_o}{dt^2} + a_1 \frac{de_o}{dt} + e_o = -b_o e_1(t) \quad (1)$$

can be put after Laplace transformation in the operational form

$$\frac{E_o(s)}{E_1(s)} = - \frac{b_o}{a_3 s^3 + a_2 s^2 + a_1 s + 1} \quad (2)$$

provided the initial conditions on e_o and its derivatives are zero.

Now the solution to equation (1) in the differential analyzer set-up would require at least five operational amplifiers, three capacitors and eleven resistors, whereas its solution in the operational set-up, i.e., the simulation of equation (2), would require only one operational amplifier, three capacitors and four resistors.

The technique of operational simulation *vis-a-vis* that of differential analyzer solution has certain advantages and disadvantages. Since it employs fewer computing components, the simulator (i) effectively increases the capacity of small or overloaded computing installations, (ii) is compact, i.e., it weighs less and occupies less volume, (iii) has greater reliability, better precision and accuracy, and (iv) is less expensive.

* Presented at the First Conference of Automation and Computation Scientists of India, Sindri, February 22-24, 1963.

Some of the disadvantages of the method are :

- (i) Initial conditions cannot be easily introduced; and
- (ii) Parameters, e.g., the a 's in equation (1), cannot be easily varied.

Hence, if the nature of the problem is such that the parameters are known and fixed, i.e., they are not required to be varied during the problem solution, and if the system to be simulated is initially in a quiescent state, the technique of operational simulation has much to recommend itself.

A network for the simulation of third order systems is shown in Fig. 1 and its transfer function is given by²

$$\frac{E_o}{E_i} = - \frac{y_1 y_3 y_5}{y_6 (y_1 + y_2 + y_8) (y_3 + y_4 + y_5 + y_7) + y_3 y_6 (y_4 + y_5 + y_7) + y_5 y_7} \quad (3)$$

Three circuits, each capable of simulating the system of equation (2), where a_3 , a_2 , a_1 and b_0 are positive real constants, with the network of Fig. 1 and consisting of three capacitors and five resistors was presented elsewhere.¹

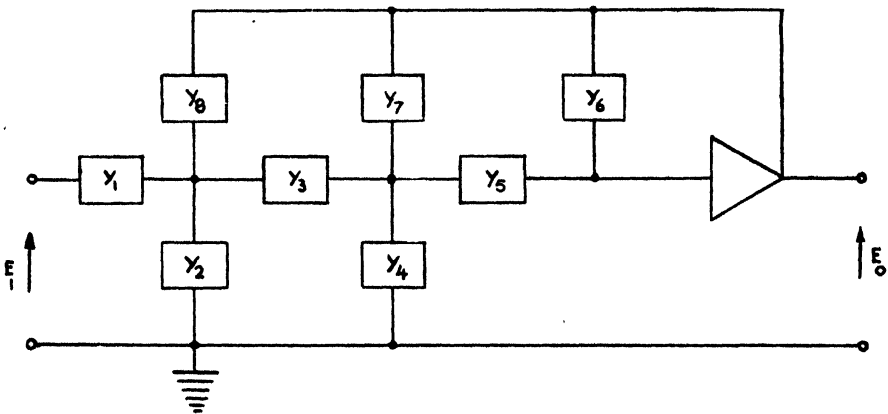


Fig. 1

Network for simulation of third order systems

An examination of equation (3) shows that the system of equation (2) can be simulated with a minimum of seven elements instead of eight as shown in Fig. 1. A circuit consisting of seven elements is obtained when any one of the four admittances, y_2 , y_4 , y_7 or y_8 , is removed and the resulting circuit can simulate the system of equation (2) if the admittances (y 's) are suitably chosen such that three of the appropriate y 's are capacitors and the remaining four are resistors.

The manner in which the design equations and the conditions of physical realizability for these circuits can be obtained is similar to that discussed earlier elsewhere¹ and, therefore these are not discussed in detail here. The circuits, each employing three capacitors and four resistors, are shown in Fig. 2 and their design formulae and the physical realizability conditions are given below.

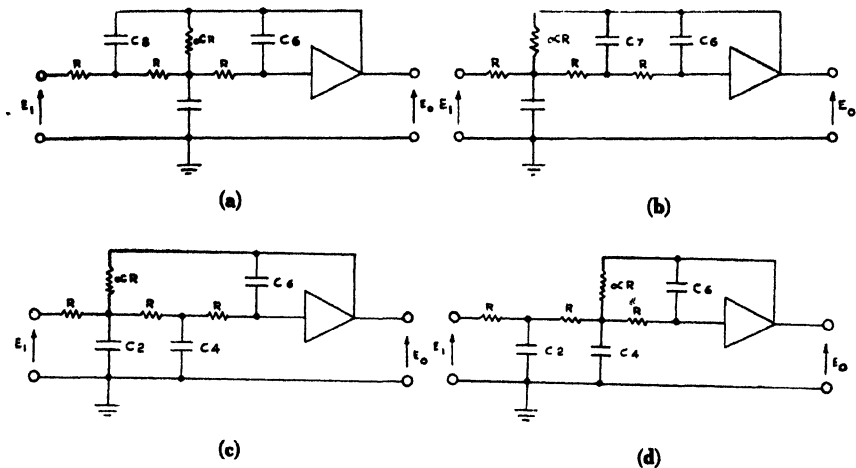


Fig. 2

Networks for simulation of $\frac{E_0}{E_1} = -\frac{b_0}{a_3 S^3 + a_2 S^2 + a_1 S + 1}$

Case 1 : For $y_2 = 0$

$$\left. \begin{aligned} y_4 &= S C_4, \quad y_6 = S C_6, \quad y_8 = S C_8 \\ y_1 &= y_3 = y_5 = \frac{1}{R} \quad \text{and} \quad y_7 = \frac{1}{\alpha R} \end{aligned} \right\}$$

$$b_0 = \frac{\alpha}{2} \quad (1)$$

$$a_1 = \left(\frac{3\alpha + 2}{2} \right) T_6 + \left(\frac{\alpha + 1}{2} \right) T_8 \quad (2)$$

$$a_2 = \alpha T_4 T_6 + \left(\frac{2\alpha + 1}{2} \right) T_6 T_8 \quad (3)$$

$$a_3 = \frac{\alpha}{2} T_4 T_6 T_8 \quad (4)$$

where

$$T_n = R C_n \quad (5)$$

$$(1 + 2b_0)(1 + 4b_0)T_8^3 - 2a_1(1 + 4b_0)T_8^2 + 4a_2(1 + 3b_0)T_8 - 8a_3(1 + 3b_0) = 0 \quad (6)$$

$$T_6 = \frac{2a_1 - (1 + 2b_0)T_8}{2(1 + 3b_0)} \quad (7)$$

under condition

$$a_1 > \frac{a_3}{a_2} (1 + 2b_0) \quad (8)$$

For the design of the network, the component values are required to be determined. The proper procedure for design would be to first check and see if the condition of equation (8) is satisfied, which signifies that the circuit of Fig. 2(a) is physically realizable. The next step then would be to solve³ the cubic of equation (6) for T_8 . The substitution of positive real T_8 in equation (7) gives the corresponding positive real T_6 ; the values of α and T_4 can be obtained directly from equations (1) and (4) respectively. Having thus determined α , T_4 , T_6 and T_8 , and choosing arbitrarily a convenient value for any one of the capacitors, the values for the remaining components may be obtained with the help of equation (5). Following the same procedure as given above, the calculations* for the particular cases of $y_4 = 0$, $y_7 = 0$ and $y_8 = 0$ are given below.

Case 2: For $y_4 = 0$

$$\left. \begin{aligned} y_2 = S C_2, y_6 = S C_6, y_7 = S C_7 \\ y_1 = y_3 = y_5 = \frac{1}{R} \text{ and } y_8 = \frac{1}{\alpha R} \end{aligned} \right\}$$

$$b_0 = \alpha$$

$$a_1 = (3\alpha + 2)T_6 + (2\alpha + 1)T_7$$

$$a_2 = 2\alpha T_2 T_6 + \alpha T_2 T_7 + (2\alpha + 1)T_6 T_7$$

$$a_3 = \alpha T_2 T_6 T_7$$

$$(2 + 3b_0)^2 T_6^4 - 2a_1(2 + 3b_0)T_6^3 + \{a_1^2 + a_2(2 + 3b_0)\}T_6^2 - (a_1 a_2 - a_3 b_0)T_6 + a_1 a_3 = 0$$

$$T_7 = \frac{a_1 - (2 + 3b_0)T_6}{(1 + 2b_0)}$$

under conditions

$$\left. \begin{aligned} a_1 &> \frac{a_3}{a_2} b_0 \\ (I^2 - 27J^2) &< 0 \end{aligned} \right\}$$

and, either

$$\left. \begin{aligned} \Delta &> 0 \\ \frac{2a_1}{3(2 + 3b_0)} &> \sqrt[3]{A} + \sqrt[3]{B} \end{aligned} \right\}$$

or,

$$\frac{2a_1}{3(2 + 3b_0)} > \text{Max.} \left[\sqrt{-\frac{p}{3} \cos \frac{\phi}{3}}, -\sqrt{-\frac{p}{3} \cos \left(\frac{\pi}{3} - \frac{\phi}{3} \right)}, -\sqrt{-\frac{p}{3} \cos \left(\frac{\pi}{3} + \frac{\phi}{3} \right)} \right]$$

$$\Delta > 0$$

where

$$I = a_1 a_3 (2 + 3b_0)^2 - \frac{a_1^3}{2} (2 + 3b_0) (a_1 a_2 - a_3 b_0) + \frac{1}{18} [a_1^2 + a_2 (2 + 3b_0)]^3$$

$$J = \begin{vmatrix} (2+3b_o)^2 & -\frac{a_1}{2}(2+3b_o) & \frac{1}{6}[a_1^2 + a_2(2+3b_o)] \\ -\frac{a_1}{2}(2+3b_o) & \frac{1}{6}[a_1^2 + a_2(2+3b_o)] & -\frac{1}{4}(a_1a_2 - a_3b_o) \\ \frac{1}{6}[a_1^2 + a_2(2+3b_o)] & -\frac{1}{4}(a_1a_2 - a_3b_o) & a_1a_3 \end{vmatrix}$$

$$\Delta = 4p_3 + 27q^2$$

$$p = \frac{a_2}{(2+3b_o)} - \frac{1}{3} \left(\frac{a_1}{2+3b_o} \right)^2$$

$$q = \frac{a_3}{2+3b_o} + \frac{1}{3} \frac{a_1a_2}{(2+3b_o)^2} - \frac{2}{27} \left(\frac{a_1}{2+3b_o} \right)^3$$

$$A = -\frac{q}{2} + \sqrt{\frac{\Delta}{108}}$$

$$B = -\frac{q}{2} - \sqrt{\frac{\Delta}{108}}$$

$$\phi = \tan^{-1} \left[\frac{-\sqrt{\Delta}}{q\sqrt{27}} \right]$$

Case 3 : For $y_7 = 0$

$$\left. \begin{aligned} y_2 = S C_2, \quad y_4 = S C_4, \quad y_6 = S C_6 \\ y_1 = y_3 = y_5 = \frac{1}{R} \text{ and } y_8 = \frac{1}{\alpha R} \\ b_o = \alpha \end{aligned} \right\}$$

$$a_1 = (3\alpha + 2) T_6$$

$$a_2 = 2\alpha T_2 T_6 + (2\alpha + 1) T_4 T_6$$

$$a_3 = \alpha T_2 T_4 T_6$$

$$T_6 = \frac{a_1}{2+3b_o}$$

$$T_4 = \frac{a_2 \pm \sqrt{a_2^2 - 8a_1a_3} \left(\frac{1+2b_o}{2+3b_o} \right)}{2a_1 \left(\frac{1+2b_o}{2+3b_o} \right)}$$

under condition

$$a_2^2 \geq 8a_1a_3 \left(\frac{1+2b_o}{2+3b_o} \right)$$

Case 4 : For $y_8 = 0$

$$\left. \begin{aligned} y_2 = S C_2, \quad y_4 = S C_4, \quad y_6 = S C_6 \\ y_1 = y_3 = y_5 = \frac{1}{R} \text{ and } y_7 = \frac{1}{\alpha R} \end{aligned} \right\}$$

$$b_0 = \frac{\alpha}{2}$$

$$a_1 = \frac{1}{2} T_2 + \frac{1}{2} (3 \alpha + 2) T_6$$

$$a_2 = \frac{1}{2} (2 \alpha + 1) T_2 T_6 + \alpha T_4 T_6$$

$$a_3 = \frac{1}{2} \alpha T_2 T_4 T_6$$

$$(1 + 4 b_0) T_2^3 - 2 a_1 (1 + 4 b_0) T_2^2 + 4 a_2 (1 + 3 b_0) T_2 - 8 a_3 (1 + 3 b_0) = 0$$

$$T_6 = \frac{2 a_1 - T_2}{2 (1 + 3 b_0)}$$

under the condition

$$a_1 > \frac{a_3}{a_2}$$

Acknowledgment

The author thanks the Director of Electronics, Defence Research and Development Organization, Government of India, for his permission to publish this paper.

References

1. L. K. Wadhwa. 'Simulation of Third Order Systems with One Operational Amplifier'. *Proceedings of the Institution of Radio Engineers*, vol. 50, no. 2, February 1962, p. 201.
2. L. K. Wadhwa. 'Simulation of Third Order Systems with One Operational Amplifier'. *Proceedings of the National Institute of Sciences, India*, vol. 29A, no. 2, March 1963, p. 213.
3. J. V. Uspensky. 'Theory of Equations'. *McGraw-Hill Book Co., Inc.*, 1948.

CORRIGENDA

TO VOL. 44, NO. 9, PT. ET 3, MAY 1964

Page 132, equation (19), instead of ' $G(s) = 1$, please read' $|G(s)| = 1$; page 133, line 6, instead of ' K ', please read ' K_1 '; page 134, line 5, instead of 'polynomial', please read 'polynomial'; page 134, line 10, instead of ' $s = \delta$ ', please read ' $s = -\delta_1$ '; and page 135, line 28, instead of '69', please read '79'.

TRANSISTORIZED DEFINITE TIME-LAG RELAY WITH CONSTANT CURRENT CHARGING SOURCE

S. K. Basu

Non-member

Lecturer, Electrical Engineering Department, Jadavpur University, Calcutta

Summary

In this paper, a circuit is developed for providing reliable and accurate time delay in a transistorized definite time-lag relay, in which the principle of charging of a capacitor from a constant current source instead of from the conventional fixed voltage source has been utilized.

1. Introduction

The charging of a capacitor^{1,2,3} or, the growth or the decay of current in an inductive circuit are well known methods of providing time delays in electrical circuits. It is also known that a time-lag relay based on such principles has several distinct components, viz., an accurate timing element, a level detector and switching circuits which operate when the voltage across the capacitor or the inductor reaches a pre-set level.

1.1. Voltage vs. current energization

The emphasis is laid on the 'accurate timing element' because when a condenser in series with a resistor is charged from a voltage source, the charging characteristic is nonlinear and for reliable operation, the work should be carried out on the approximately linear part of the charging characteristic curve near the starting point. Now

$$V_L = \frac{1}{C} \int i \, dt \quad (1)$$

where V_L is the level detector voltage, i the constant charging current and C the capacitance.

In the case of voltage energization, the charging voltage, V , should be much higher than the level detector voltage, V_L , for successful operation. Alternatively, if a constant current charging is used, the voltage across the capacitor varies linearly with time for a given constant charging current, i , and $Q = i t = C V_L$. Therefore,

$$V_L = \frac{i t}{C}$$

2. Practical circuit

Fig. 1(i) shows a circuit in which a change-over contact is used for the initiation. Here, the charging and the resetting time constants are dependent on $C R$ and $C r$ respectively. Fig. 1(ii) shows a possible way of using the circuit of Fig. 1(i). In this circuit, the transistor, T_1 , is working as a grounded base configuration and acts as a

* Written discussion on this paper will be received until March 31, 1965.

This paper was received on July 22, 1964.

constant charging source for capacitor, C . The voltage across capacitor C changes linearly with time from an initial value to the base potential of T_1 and the time setting can be very easily changed in two ways, *viz.*, either by changing the magnitude of charging current, or by altering the initial voltage across the capacitor. Thus, the resistance, r_4 , may be used to obtain a time-scale multiplier. If it is assumed that the transistor emitter base voltage drop is small (300 millivolts for OC72), then

$$i_1 = \frac{v_a - v_b}{r_4} \quad (3)$$

where v_a is the potential rail to which r_4 is connected, v_b the base potential, and i_1 the charging current.

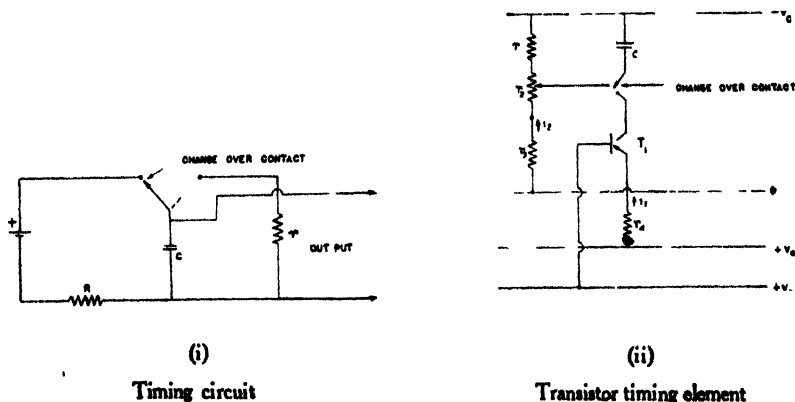


Fig. 1

Practical circuits for time-lag relay

Also, from Fig. 1(ii), we get

$$i_3 = \frac{v_c}{r_1 + r_3 + r_5} \quad (4)$$

where v_c is the capacitor voltage and i_3 the divider current.

Now, if the level detector operates when the capacitor voltage equals v_c and if $\alpha = 1$ (approximately), we get

$$t = \frac{C(v_c - v_0)}{i_1} = \frac{C(v_c - v_0)}{(v_a - v_b)} r_4 \quad (5)$$

where v_0 is the initial capacitor voltage and t the time delay. From Fig. 1(i), it can be seen that the collector current can be varied by changing r_4 and the divider current can be varied by changing the potentiometer, r_3 . Also, by increasing r_3 to a reasonably great extent, the quiescent power drain of the relay can be reduced. The capacitor discharges through the divider resistors and the resetting time varies with the position of r_3 . In the circuit, r_1 is added in series with the potentiometer to prevent the short-circuiting of the capacitor C , while resetting. The resistance, r_5 is added to prevent inadvertent operation of the relay while r_3 is varied. In practice, r_1 and r_5 are much smaller than r_3 .

Since the collector circuit of T_1 is normally open, the time delay is linearly related to the potentiometer setting. Moreover, as the relay is initiated by the closing operation of a normally open contact, the deterioration of the contact is unlikely to cause wrong operation.

2.1. Design of timing element

- (i) The maximum emitter and the collector current depends on the type of the transistors used and for OC72 they are of the order of 125 milliamp. ;
- (ii) The voltages, v_c and v_e , are usually between 10 and 20 volts, for medium power transistors like OC72 or OC76 ;
- (iii) The capacitances used should be of electrolytic type for having a higher time delay and tantalum type capacitors will have to be used for a reliable performance ;
- (iv) The charging current used is dependent on two factors :
 - (a) $i_1 > I_{co}$, i.e., the leakage current at the maximum working temperature (I_{co} is less than 80 microamp. at 55°C. for OC72) ; and
 - (b) The current, i_1 must not be less than the current needed for successful operation of the level detector. This is less than 250 microamp. for a two-stage switching amplifier. Thus, a minimum charging current of 250 microamp. should be used. If such a relay is used over a wide range of temperature, the use of silicon transistors is preferable in place of germanium transistors. The magnitude of the resistances, r_1 and r_2 , depends on the battery drainage and the resetting time constant ;
- (v) The maximum time delay is limited by the minimum permissible charging current (approximately 250 microamp. for OC72, and about 5 microamp. for silicon transistors) and the minimum time setting is limited by the consideration of stability of the circuit ; and
- (vi) The time setting multiplier can be obtained either by changing the capacitance, C , or by varying r_4 , i.e., by changing the charging current.

2.2. Level detector

Fig. 2 shows the level detector and the timing element. The latter essentially consists of a diode, D_1 , and a two-stage switching amplifier, T_2 and T_3 . Under quiescent condition, the transistor, T_2 , is fully bottomed and the potentiometer network involving r_6 , r_7 and r_8 is so arranged that the base of T_2 is positive with respect to its emitter and T_2 is under cut-off condition. Normally, the diode, D_1 , is cut off, since A is at a lower potential with respect to the base of T_2 . When the change-over contact is thrown from position 1 to position 2, the capacitor, C , starts charging and the potential of A starts becoming more positive, and when A is more positive with respect to the base of the transistor, T_2 , the diode, D_1 , conducts and the resulting current

reduces the base emitter forward current of T_2 . Then T_2 stops conducting which in effect switches T_3 to the bottoming condition, thereby operating the relay, R.

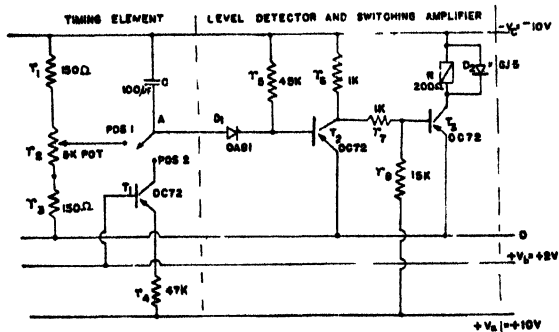


Fig. 2

Timing and level detector element

2.3. Design of level detector

The use of the transistor, T_3 , is dependent on the power needed to operate the relay, R. Since the transistor, T_3 , is used either in the fully on or in the fully off condition, an intermediate power transistor (OC72 or OC76) is suitable for driving a telephone-type relay of about 200 ohm impedance. A diode, D_2 , is used to protect the transistor from the inductive kick when the relay resets. The basic considerations for the design are :

- (i) The maximum collector current in T_2 should be much greater than I_{co} , the leakage current, at an ambient temperature of at least 40°C . ;
- (ii) The sensitivity increases but the stability decreases with an increase in the values of r_6 and $\frac{r_6}{r_7}$; and
- (iii) For a given value of r_6 , the value of r_5 can be calculated from the basic relationship :

$$\frac{V_c}{r_6} = \frac{V_c}{\alpha_{min.} r_6} + i_b \quad (6)$$

where $\alpha_{min.}$ is the minimum grounded emitter current gain for T_2 and i_b the additional base bias current necessary to stabilize the circuit against the tolerances in the resistors. The switching amplifier circuit is designed for 10% tolerances in the resistors and for a current gain of about 45.

It is, however, necessary to note that if A is connected to the common rail, the diode, D_1 , shunts the base emitter circuit of T_2 and the resulting reduction in current in T_2 may cause wrong operation of the relay. Hence, a fixed resistor, r_9 , is connected in series with the potentiometer r_2 for the prevention of accidental connection of the point, A, with the common rail.

3. Steady bias voltage

The British Standard Specification, B.S. 142 : 1953 states that the relay should work satisfactorily for a variation of supply voltage from 70 to 110% of the rated voltage. Two methods of obtaining stabilized voltage supply are possible :

- (i) Using a diode chain ; and
- (ii) Using zener diode utilizing the reverse breakdown characteristic.

In Fig. 3, a method of obtaining the stabilized voltage supply by using zener diodes is shown. Although owing to their non-availability in India, they have not been used in the prototype scheme.

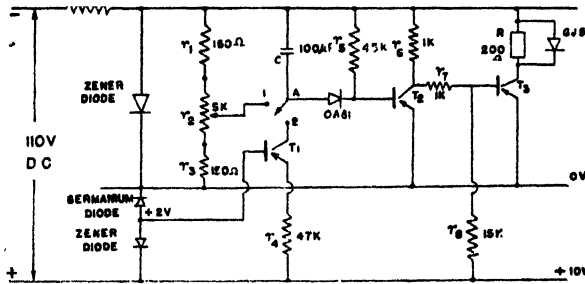


Fig. 3

Circuit of stabilized relay using zener diode

4. Effect of temperature variation

With the increase of temperature, the collector leakage current also increases (I_{co} is nearly equal to 80 to 100 microamp. for OC72 at 55°C.), hence the minimum charging current should be well above this value for satisfactory operation with the varying temperature. The current gain is not seriously dependent on the temperature variation. The level detector is designed suitably for successful operation up to about 50°C. and the input current needed is less than 250 microamp.

5. Component tolerances

- (i) The manufacturing spread in α is from 0.95 to 0.99 and this should not cause any trouble ; and
- (ii) The manufacturing spread in the electrolytic condenser and the carbon resistors may be taken as of the order of ± 10 to $\pm 20\%$. Since the time setting is linearly related to the capacitance, C , the calibration of r_3 and r_4 is needed for a few settings only. The level detector circuit is designed such that the input current needed is always less than 250 microamp. By a judicious design of the circuit, it is possible to use 10% tolerance in resistors.

6. Test results

The time-lag relay based on the considerations discussed above has been built and tested with satisfactory results. Fig. 4 shows the linear effect of variation of the

time delay with the change in the value of $K r_3$, where $K r_3$ is the resistance measured from the zero voltage bus. The linear variation is also obtained when r_4 is varied as shown in Fig. 5. Hence, either of the potentiometers, r_3 and r_4 , can be calibrated in terms of the time delay of the relay. As is obvious the maximum time depends on the minimum initial voltage, v_0 , and upon the minimum charging current of T_1 .

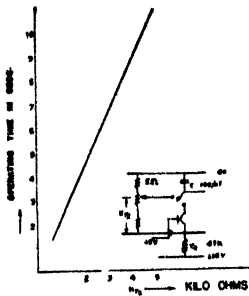


Fig. 4

Curve of operating time vs. $K r_3$

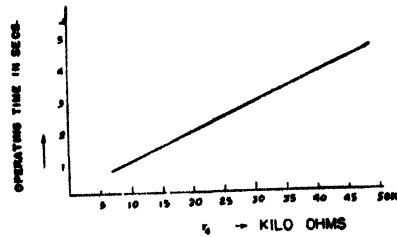


Fig. 5

Curve of operating time vs. r_4

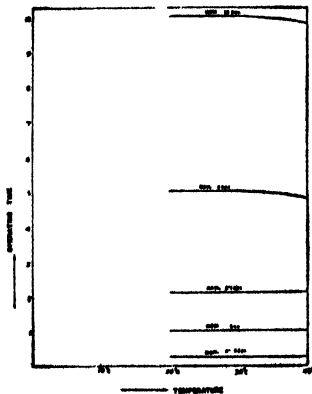


Fig. 6

Curves of operating time vs. temperature

Fig. 6 shows the effect of variation of time delay between 20° and 40°C. for different nominal values of time delay. For this test, r_1 was made variable since the change in temperature will correspondingly change the leakage current, I_{co} , and hence the operating time delay of the relay. For higher nominal values of time delay, the operating time shows a slight drooping of the characteristic curve at a temperature of 40°C. owing to the fact that the leakage current increases, resulting in an increase of the charging current. Hence, this relay will perform much more satisfactorily if the charging current is made considerably higher, i.e., the operating time delay is lower.

The resetting time of the relay depends on a variety of factors : (i) a little time delay is introduced by the diode, D_1 , shunting the relay coil ; (ii) a small time elapses before the diode, D_1 , ceases to conduct and this happens when the potential of A has

fallen to about 400 millivolts negative with respect to the common rail; (iii) the time interval before the capacitor has completely recovered and become able to measure accurately on any successive current energization (this recovery time is about three times the discharging time constant of the capacitor C); and (iv) on the resetting time of the relay, R . The actual resetting time which is the sum of all these time delays was never higher than 100 millisecc.

7. Advantages

The transistorized relay described in this paper has the following points in its favour:

- (i) Owing to the fact that the capacitor, C , is being charged from a constant current source, the voltage developed across the capacitor varies linearly with time which is a better method of achieving accurate timing control than that of using voltage energization;^{1,2,3}
- (ii) By using zener diodes for bias voltage stabilization as shown in Fig. 3, the effect of supply voltage variation will be negligible;
- (iii) The time delay is not affected by the variation of temperature from 20° to 40°C.;
- (iv) There are two methods of obtaining different time delay in the relay, viz., by controlling the charging current or by controlling the initial voltage, v_0 , across the capacitor. The maximum time delay will depend on the minimum charging current used, i.e., on the type of the transistors used and also on the type of the relay used;
- (v) Since the time setting is linearly related to C , r_3 and r_4 , the circuit of Fig. 2 is very simple to design for the spread-in components and calibration is necessary for a few settings only;
- (vi) The resetting time is small; and
- (vii) The miniaturization and encapsulation of the transistorized relay is possible.

8. Conclusions

From the investigation, it is clear that the time-lag relay based on the transistor technique is practically feasible. Accurate time settings from 50 millisecc. to about 10 sec. can be obtained using the normal component tolerances (for resistors, 10% and for capacitors, 20%). This circuit enables independent adjustment of the resetting time and the time delay is not susceptible to change due to a deterioration of the change-over contact.

9. References

1. J. F. Young. 'The Use of Transistors in Industrial Timer Circuits'. *Electronic Engineering*, vol. 35, no. 424, June 1963, p. 366.
2. S. P. Patra and S. K. Basu. 'Transistorized, Static Overcurrent Relay'. *Electrical Times*, vol. 144, no. 3751, November 14, 1963 p. 742.
3. J. J. Pinto. 'Semiconductor Time-Delay Circuits'. *Electronic Engineering*, vol. 36, no. 433, March 1964, p. 166.

MICROWAVE SPECTROMETER*

M. M. Rao

Non-member

and

S. K. Chatterjee

Non-member

*Department of Electrical Communication Engineering,
Indian Institute of Science, Bangalore*

Summary

In this paper, the theoretical and experimental considerations for the construction of a microwave spectrometer are presented. Using Snell's law and considering multiple reflections inside a dielectric sheet as well as interface reflections, the expressions for the transmission and the reflection coefficients of dielectrics are derived as functions of the angles of incidence and the thickness of the dielectrics for parallel polarized waves. The transmission and the reflection coefficients of perspex and hylam sheets for different angles of incidence of the waves are measured with the help of the spectrometer. The dielectric constant of perspex sheet is determined from the experimental data of transmission and reflection coefficients. A discussion on the sources of error associated with the spectrometer described here and the scope for its improvement are also given.

Introduction

Several authors^{1 to 4} have constructed microwave spectrometers in 1-cm. and millimetre range mainly to study the dielectric properties of the materials. The object of the present investigations is to construct a microwave spectrometer in the X-band to determine mainly the transmission and the reflection coefficients and hence the absorption coefficients of dielectric materials in the form of sheets. In this paper, only transmission and reflection coefficients are determined.

For such small wavelengths, it is natural that the size of the spectrometer should be fairly large in order to give satisfactory performance. As a preliminary experiment, a microwave spectrometer is constructed within the limited available space in the laboratory. In order to test the performance characteristics of the spectrometer, the dielectric constant of perspex was determined from transmission and reflection coefficient measurements at two different angles of incidence. It was found that the value of the dielectric constant, so obtained, agrees fairly well with the existing value at some angles of incidence. There is, however, a divergence in the value of dielectric constant from the correct value at some angles of incidence.

*Written discussion on this paper will be received until March 31, 1965.
This paper was received on October 30, 1964.

Description of spectrometer

The experimental set-up of the spectrometer is shown in Figs. 1 and 2. It mainly comprises :

- (i) Transmitter : it consists of a reflex klystron (X-band) fed from an electronically regulated power supply unit, and a square wave modulated at 1 kilocycle per sec. The power from the reflex klystron is fed through an attenuator to a pyramidal horn having a gain of about 20 dB ; and
- (ii) Receiver : it consists of the same type of pyramidal horn, as in the transmitter, connected to a crystal detector unit, the output of which is fed to a twin-tee amplifier tuned to 1 kilocycle per sec. The output of the amplifier is fed through a crystal bridge detector to a microammeter.

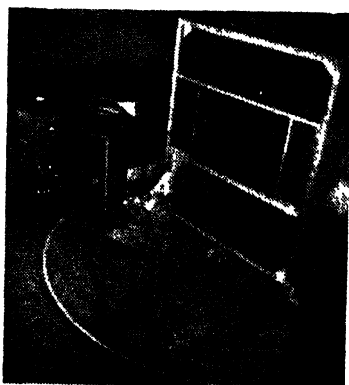


Fig. 1
View of experimental
set-up

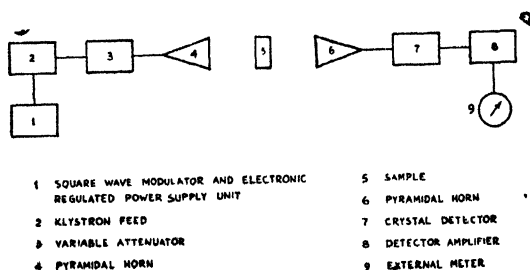


Fig. 2

Block diagram of experimental set-up

The transmitter and the receiver units are mounted independently on two separate adjustable trolleys which can be rotated through 360° on circular rails mounted on a wooden platform. The angular position of the receiver and the transmitter can be read from a metallic scale graduated in degrees and mounted on the wooden platform. The electronic circuits of the power supply unit, the square wave modulator and the twin-tee amplifier are of conventional types. The transmitter and the receiver units are also

mounted on rails fixed up on the trolleys so that they can be moved forward and backward radially. The heights of the transmitter and the receiver units are also adjustable. The dielectric sheets are fixed on a wooden framework which is fixed at the centre of the spectrometer base during the time of measurement. The wooden sample holder has also the provision for moving the sample vertically or horizontally with respect to the transmitter and the receiver.

Theoretical considerations

As the object is mainly to determine the reflection and the transmission coefficients of dielectric sheets with the help of the spectrometer, it is considered worthwhile to derive the expressions for these coefficients as functions of angles of incidence, dielectric constant and thickness of the material. The case of plane, parallel polarized wave incidence on the sheet is considered. In this case, the vector, \vec{E} , is parallel to the plane of incidence and the vector, \vec{H} , is parallel to the reflecting surface.

(i) Reflection coefficient

Applying the boundary condition, that the tangential component of \vec{E} is continuous at the interface, and applying Snell's law, the following relationship for the ratio of the reflected electric field intensity, E_r , to the incident electric field intensity, E_i , is obtained :

$$\frac{E_r}{E_i} = \frac{\eta_1 \cos \theta_1 - \eta_2 \cos \theta_2}{\eta_1 \cos \theta_1 + \eta_2 \cos \theta_2} \quad (1)$$

where θ_1 is the angle of incidence, θ_2 the angle of refraction, $\eta_1 = \sqrt{\frac{j\omega \mu_1}{\sigma_1 + j\omega \epsilon_1}}$, $\eta_2 = \sqrt{\frac{j\omega \mu_2}{\sigma_2 + j\omega \epsilon_2}}$, $\omega = 2\pi f$, f is the frequency, and ϵ_1 , μ_1 and σ_1 are the permittivity, permeability and conductivity of medium 1 respectively. Here, medium 1 is the free space. Similarly, ϵ_2 , μ_2 and σ_2 are the characteristics of medium 2. Here, medium 2 is the dielectric sheet.

The propagation constant, γ , is given by the relationship :

$$\gamma = \alpha' + j\beta' = \sqrt{j\omega \mu (\sigma + j\omega \epsilon)} \quad (2)$$

which yields

$$\frac{\beta'}{\omega} = \sqrt{\mu \epsilon} \sqrt{\frac{1 \pm \sqrt{1 + y^2}}{2}} \quad (3)$$

where $y = \frac{\sigma}{\omega \epsilon}$.

The velocity of the waves in medium 1 (free space) is

$$V_1 = \frac{\omega_1}{\beta_1} = \frac{1}{\sqrt{\mu_1 \epsilon_1}}$$

The velocity of the waves in medium 2 (dielectric sheet) is

$$V_2 = \frac{\omega_2}{\beta_2'} = \frac{1}{\sqrt{\mu_2 \epsilon_2}} \sqrt{\frac{2}{1 \pm \sqrt{1 + y_2^2}}}$$

But,

$$V_2 \sin \theta_1 = V_1 \sin \theta_2$$

Hence,

$$\frac{V_1}{V_2} = \frac{\sin \theta_1}{\sin \theta_2} = \sqrt{\frac{\epsilon_2}{\epsilon_1}} \sqrt{\frac{1 \pm \sqrt{1 + y_2^2}}{2}} \quad (4)$$

which gives

$$\cos \theta_2 = \sqrt{1 - \frac{2}{1 \pm \sqrt{1 + y_2^2}} \frac{\sin^2 \theta_1}{\epsilon_r}} \quad (5)$$

where $\epsilon_r = \frac{\epsilon_2}{\epsilon_1}$ = relative permittivity. Substituting for $\cos \theta_2$, η_1 and η_2 in equation (1) and simplifying, we get

$$\frac{E_r}{E_i} = \frac{(M \cos \theta_1 - P) - jN \cos \theta_1}{(M \cos \theta_1 + P) - jN \cos \theta_1} \quad (6)$$

where

$$M = \sqrt{\frac{\epsilon_r \sqrt{1 + y_2^2} + \epsilon_r}{2}}$$

$$N = \sqrt{\frac{\epsilon_r \sqrt{1 + y_2^2} - \epsilon_r}{2}}$$

$$P = \sqrt{1 - \frac{2}{1 \pm \sqrt{1 + y_2^2}} \frac{\sin^2 \theta_1}{\epsilon_r}}$$

Rationalizing and simplifying equation (6), we get

$$\alpha = \frac{E_r}{E_i} = \frac{\{(M^2 + N^2) \cos^2 \theta_1 - P^2\} - j2NP \cos \theta_1}{(M^2 + N^2) \cos^2 \theta_1 + P^2 + 2MP \cos \theta_1} \quad (7)$$

(ii) *Normalized electric field intensity in medium 2*

A portion of the incident wave is transmitted into the dielectric sheet. If the electric field intensity in medium 2 is denoted by E_t , then by following the same procedure as above, the normalized field intensity, $\frac{E_t}{E_i}$, in medium 2 is given by

$$\frac{E_t}{E_i} = \frac{2 \cos \theta_1}{(M \cos \theta_1 + P) - jN \cos \theta_1} \quad (8)$$

Rationalizing equation (8), we get

$$\beta = \frac{E_t}{E_i} = \frac{(2M \cos^2 \theta_1 + 2P \cos \theta_1) + j2N \cos^2 \theta_1}{(M^2 + N^2) \cos^2 \theta_1 + P^2 + 2MP \cos \theta_1} \quad (9)$$

(iii) *Effect of multiple and interface reflections*

The multiple reflections inside the dielectric sheet and the reflections at the interfaces separating the two media undergone by the incident wave is shown in Fig. 3.

Notations

d = thickness of the sample,

n = refractive index,

λ_0 = free space wavelength,

$\phi = \frac{2\pi n d'}{\lambda_0}$ = change in phase by passing through the sample a distance d' ,

$$d' = \frac{d}{\sqrt{1 - \sin^2 \theta_1}},$$

$p = e^{j\phi}$ = phase term, and

α = coefficient for internal reflection.

Calculations

Referring to Fig. 3, the resultant reflection coefficient is obtained as :

$$\frac{E_R}{E_I} = \alpha - \alpha p^2 \beta^2 (1 + \alpha^2 p^2 + \alpha^4 p^4 + \dots) \quad (10)$$

and the resultant transmission coefficient as :

$$\frac{E_T}{E_I} = p \beta^2 (1 + \alpha^2 p^2 + \alpha^4 p^4 + \dots) \quad (11)$$

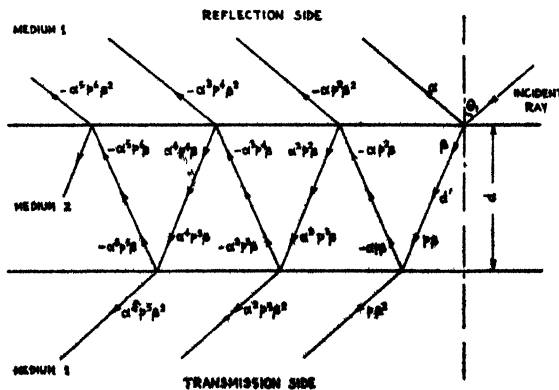


Fig. 3

Multiple reflections, interface reflections and transmission of incident wave

Equations (10) and (11) lead respectively to equations (12) and (13) given by

$$\frac{E_R}{E_I} = \frac{\{Q S (1 - \cos x) - R S \sin x\} - j\{Q S \sin x + R S (1 - \sin x)\}}{[S^2 - \{(Q^2 - R^2) \cos x + 2 Q R \sin x\}] - j\{(Q^2 - R^2) \sin x - 2 Q R \cos x\}} \quad (12)$$

where

$$Q = (M^2 + N^2) \cos^2 \theta_1 - P^2$$

$$R = 2 N P \cos \theta_1$$

$$x = 2 \phi$$

$$S = (M^2 + N^2) \cos^2 \theta_1 + P^2 + 2 M P \cos \theta_1$$

and

$$\frac{E_T}{E_I} = \frac{\left\{ (T^2 - U^2) \cos \frac{x}{2} - 2 T U \sin \frac{x}{2} \right\} + j \left\{ (T^2 - U^2) \sin \frac{x}{2} + 2 T U \cos \frac{x}{2} \right\}}{[S^2 - \{(Q^2 - R^2) \cos x + 2 Q R \sin x\}] - j\{(Q^2 - R^2) \sin x - 2 Q R \cos x\}} \quad (13)$$

where

$$T = (2 M \cos^2 \theta_1 + 2 P \cos \theta_1)$$

$$U = 2 N \cos^2 \theta_1$$

Rationalizing equations (12) and (13) respectively and taking only the amplitude, we get

$$\begin{aligned} & \{[Q S (1 - \cos x) - R S \sin x] \{S^2 - [(Q^2 - R^2) \cos x + 2 Q R \sin x]\} \\ & + \{Q S \sin x + R S (1 - \sin x)\} \{(Q^2 - R^2) \sin x - 2 Q R \cos x\}\}^2 \\ & + \{[Q S (1 - \cos x) - R S \sin x] \{(Q^2 - R^2) \sin x - 2 Q R \cos x\} \\ & - \{Q S \sin x + R S (1 - \sin x)\} \{S^2 - [(Q^2 - R^2) \cos x + 2 Q R \sin x]\}\}^2 \\ & | \frac{E_R}{E_I} | = \frac{\{S^2 - [(Q^2 - R^2) \cos x + 2 Q R \sin x]\}^2 + \{(Q^2 - R^2) \sin x - 2 Q R \cos x\}^2}{\quad} \quad (14) \end{aligned}$$

$$\begin{aligned} & \left\{ \left[\left\{ S^2 - [(Q^2 - R^2) \cos x + 2 Q R \sin x] \right\} \left\{ (T^2 - U^2) \cos \frac{x}{2} - 2 T U \sin \frac{x}{2} \right\} \right. \right. \\ & \quad \left. \left. - \left\{ (Q^2 - R^2) \sin x - 2 Q R \cos x \right\} \left\{ (T^2 - U^2) \sin \frac{x}{2} + 2 T U \cos \frac{x}{2} \right\} \right]^2 \right. \\ & \quad \left. + \left[\left\{ (Q^2 - R^2) \sin x - 2 Q R \cos x \right\} \left\{ (T^2 - U^2) \cos \frac{x}{2} - 2 T U \sin \frac{x}{2} \right\} \right. \right. \\ & \quad \left. \left. + \left\{ S^2 - [(Q^2 - R^2) \cos x + 2 Q R \sin x] \right\} \left\{ (T^2 - U^2) \sin \frac{x}{2} + 2 T U \cos \frac{x}{2} \right\} \right]^2 \right\}^{\frac{1}{2}} \\ & | \frac{E_T}{E_I} | = \frac{[S^2 - \{(Q^2 - R^2) \cos x + 2 Q R \sin x\}]^2 + \{(Q^2 - R^2) \sin x - 2 Q R \cos x\}^2}{\quad} \quad (15) \end{aligned}$$

To verify the validity of equations (14) and (15), the transmission and the reflection coefficients of perapex sheets were measured and the experimental values substituted

in the above two equations, which were then solved to give the dielectric constant of perspex. As the equations are complicated, these were solved by numerical methods. For two sets of angles of incidence : (i) 20° and 30° ; and (ii) 25° and 35° ; the dielectric constant obtained from equation (14) are 2.5 and 2.3 respectively. It is believed this difference may be due to the shortcomings of the spectrometer which needs further improvement. The above theory is based on the assumption that the incident wave is plane. But, the experimental results on wavefront measurements show that the wave is not plane. It is, however, pointed out that the ray theory as given above may be improved by making a rigorous approach to the problem with the help of the field theory.

Experimental procedures

Response characteristics of spectrometer

The response characteristics of the spectrometer obtained by keeping the position of the transmitter fixed and observing the readings in the detector for different angular positions of the receiving horn is shown in Fig. 4. The object of determining the response characteristics is to find out whether there are any spurious reflections from any nearby objects. The determination of the response characteristics was repeated for different positions of the transmitter and it was found that the response characteristics remain the same as shown in Fig. 5. The determination of the response characteristics was also repeated for slightly different heights of the transmitter and the receiver from the ground. In this case also, no noticeable change was observed in the response characteristics. It is, therefore, concluded that with the sensitivity possessed by the spectrometer, the effect of nearby objects on the response characteristics of the spectrometer, if there is any, is negligible. The experiment was conducted at a wavelength of 3.164 cm. The response characteristics are similar to the radiation characteristics of the horn observed in the set-up outside the building where all the antenna characteristics are determined. This experiment was performed without placing any sample in the spectrometer.

Standing wave pattern

In order to test whether there is any standing wave between the transmitter and the receiver due to the interaction between the transmitting and the receiving horns, an experiment was conducted by keeping the position of the transmitting horn fixed and changing the position of the receiving horn radially when the two horns are situated diametrically opposite to each other. The characteristic (Fig. 6) shows the absence of any standing wave pattern when the sample is not interposed between the transmitting and the receiving horns.

In order to test whether there is any standing wave created when a dielectric sample is placed, due to the interaction of the sample and the horn, an experiment was conducted in a similar way as above and the results are shown in Fig. 7. The results indicate the presence of a standing wave between the transmitting horn and the sample as well as between the sample and the receiving horn. It has not been possible to suppress the standing wave. So, all the succeeding readings to determine the transmission and the reflection coefficients were taken by keeping the radial positions of the two horns while

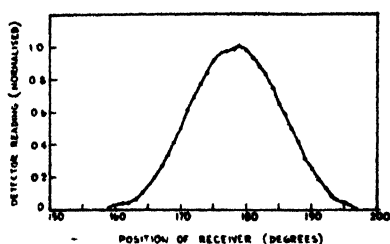


Fig. 4

Response characteristics of spectrometer
(transmitter is at 0°)

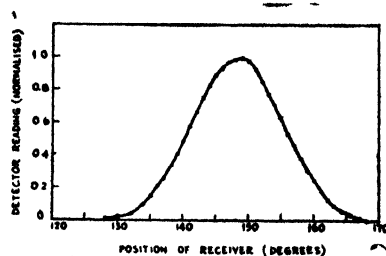


Fig. 5

Response characteristics of spectrometer
(transmitter is at 30°)

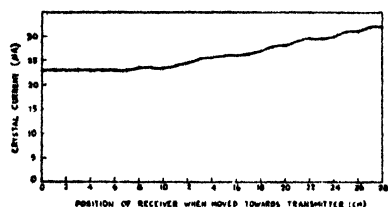


Fig. 6

Standing wave pattern between transmitter
and receiver without sample

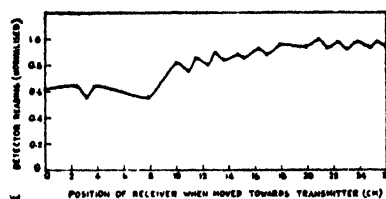


Fig. 7

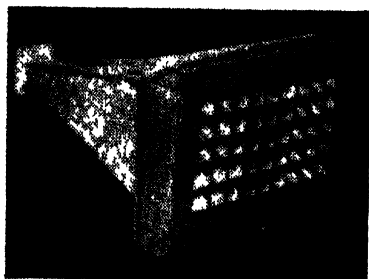
Standing wave pattern between transmitter
and receiver with sample

respect to the centre of the spectrometer fixed all throughout the experiment. It is, therefore, obvious that this may lead to some error in the experimental results.

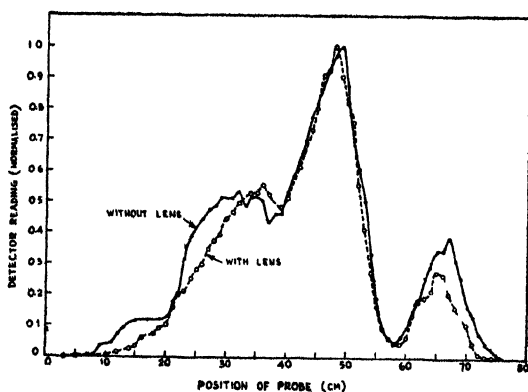
Wavefront error

It has been assumed in deriving the theory that the wave incident on the sample is plane, i.e., the sample is illuminated uniformly by the incident ray. In order to test how the intensity of the incident wave is distributed all throughout the surface of the sample, the field intensity of the emergent wave from the sample and also the field intensity very near to it were scanned with the help of a monopole probe horizontally and vertically. The experiment was conducted under two conditions, viz., the transmitting horn fitted with and without a metal plate lens. Fig. 8 shows the photograph of the lens fitted to the transmitting horn. The results of the experiment, as shown in Figs. 9 and 10, indicate clearly that the illumination of the sample is not uniform, even though the measurements are not very accurate. In the absence of any other better technique, the usual probe method of sampling the field was used.

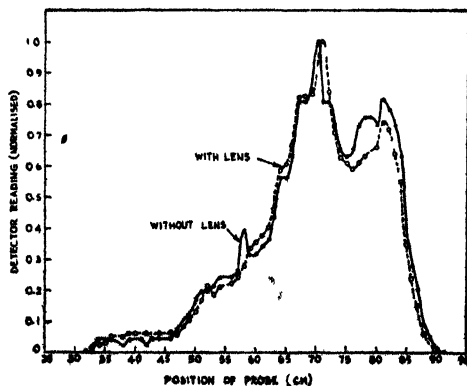
One of the reasons of such nonuniform illumination is possibly due to the very small distance between the horn and the sample. It appears that to achieve a plane wave either the size of the spectrometer has to be made prohibitively large or the wavelength of radiation has to be reduced to a very small value. Neither of these, in the present set-up, was possible with the available facilities. It is, therefore, evident that this will contribute significantly to the discrepancies in the experimental results.

**Fig. 8**

View of metal plate lens fitted
to transmitter horn

**Fig. 9**

Curves showing amplitude
of incident wave measured
by probe
(probe is moved horizontally
at centre of sample)

**Fig. 10**

Curves showing amplitude
of incident wave measured
by probe
(probe is moved vertically
at centre of sample)

Diffraction experiment

In order to determine a finite size of the sample that should be used with the spectrometer, so that the diffraction of the incident wave by the edge of the sample may not affect the readings of the detector, an experiment was conducted to observe the detector readings when the transmitter and the receiver were fixed for normal incidence

and the sample was slowly moved from the centre horizontally and vertically. The characteristics (Fig. 11) obtained from this experiment does not lead to any definite conclusion as regards the optimum size of the sample. But the experiment, conducted as mentioned in the wavefront error experiment, shows that with a sample of size 2 ft. \times 2½ ft., the intensity of the field as noted by the probe decreases sharply from the centre to the sides of the sheet in both the horizontal and the vertical directions.

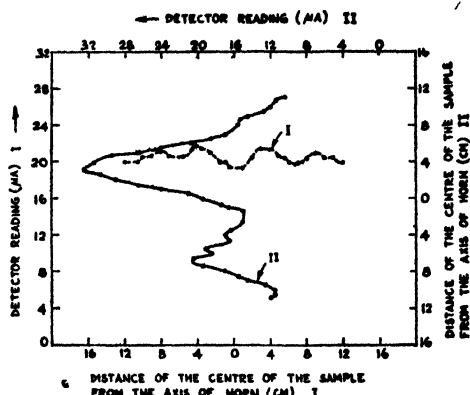


Fig. 11
Diffraction in horizontal
and vertical directions

So, it has been concluded that the effect of diffraction on the detector reading is inappreciable when the size of the sample as used in the experiment is 2 ft. \times 2½ ft. But, the characteristics shown in Fig. 11 do not show this to be the case, because, if the diffraction from the edge of the sample is negligible, the vertical and the horizontal characteristics ought to have exhibited a flat portion and not a peak, at least, up to a certain portion of the movement of the sample horizontally and vertically. This still remains to be explained.

Reflection and transmission coefficients

The reflection and the transmission coefficients of hylam sheet (2 ft. \times 2½ ft.) were measured for different thicknesses of the sample at an angle of incidence of 30°. The results are given in Fig. 12. In Fig. 12, the variation of the reflection coefficients of hylam sheet of different thicknesses when backed by a metal plate is also shown. It is seen that the nature of the curves is oscillatory. This is to be expected due to the multiple reflections that take place inside the material and to the combining of the emergent ray with the direct reflected ray from the interface with different amplitudes and phases when the thickness of the sample is varied. However, the thickness of the sample was varied by putting different sheets together. This may introduce an error in the reflection coefficient as the medium is not homogeneous due to the unavoidable presence of air in between the different sheets, even though an attempt was made to keep the sheets pressed tightly by means of a wooden frame. The theoretical value of the reflection coefficient derived above was on the assumption that the dielectric sheet is homogeneous.

Figs. 13 and 14 show the variation of the reflected power (normalized) with different thicknesses of hylam sheet for different angles of incidence. The results are also subject to the limitations as discussed above.

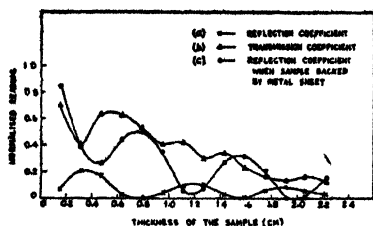


Fig. 12

Curves of normalized reading vs thickness of hylam for 30° angle of incidence

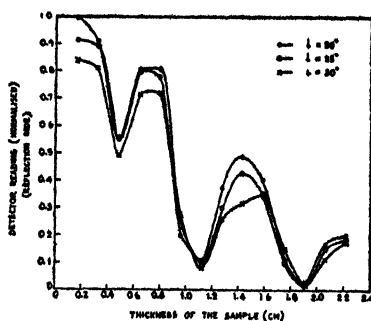


Fig. 13

Variation of reflection coefficient with thickness of hylam for various angles of incidence

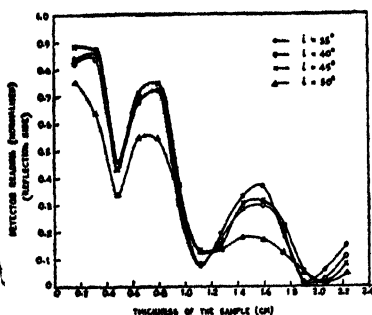


Fig. 14

Variation of reflection coefficient with thickness of hylam for various angles of incidence

In order to determine the dielectric constant of the material from the measurement of reflection and transmission coefficients, perspex sheets were chosen because of their well known value of dielectric constant. The detector reading on the reflection side as measured for perspex sheet of $\frac{1}{8}$ in. thickness for the angles of incidence of 20° , 25° , 30° and 35° are 58, 50, 42.5 and 32 microamp. respectively. As the crystal has a square law characteristics, the detector reading is directly proportional to the power. Assuming the loss-tangent of perspex to be 0.005, as given in the standard tables, the dielectric constant is evaluated with the help of equation (14). For a set of angles of incidence of 20° and 30° , the dielectric constant is found to be 2.5, and for another set of angles of incidence of 25° and 35° , it is found to be 2.3.

The value calculated from the measurement of transmission coefficient formula is very much different from the standard value and as such, has not been reported. It is observed from the values obtained from reflection measurements that for one set of angles, the value agrees favourably with the standard value of dielectric constant of perspex sheet. But the value calculated from another set of angles is different from the standard value. The reason may be due to the multiple peaks observed on the reflection side.

Multiple peaks

The values of reflected powers given above were measured at the angle of reflection corresponding to the angle of incidence given by Snell's law. However, it was observed that for a particular angle of incidence, very large number of secondary peaks are presented on the reflection side. The relative positions and amplitudes of the peaks differ for different thicknesses of the material and also for different materials. But, on the transmission side, the secondary peaks observed are only relatively few. It was also experimentally observed that the number of peaks on the reflection side for perspex sheet are more than those for hylam sheet for the same thicknesses and angles of incidence. The data in the table gives an analysis of the peaks as observed in the case of hylam sheet on the reflection and transmission sides for thicknesses varying from $\frac{1}{8}$ in. to $\frac{3}{8}$ in. in steps of $\frac{1}{8}$ in. It will be observed from the table that there is very little correlation between the relative amplitudes and the positions of the peaks. It has not been possible to explain such phenomenon of the multiple peaks. It is believed that the appearance of the multiple peaks may be due to the effect of the near-field. This phenomenon requires further investigation. For the sake of comparison, the reflection coefficients of hylam sheet when backed by a metal plate have also been given in the same table.

Conclusions

The experimental and theoretical works carried out on this spectrometer leads to the conclusion that further work is necessary to improve upon its performance characteristics. There is scope for work which would enable the elimination of the secondary peaks or would enable a theoretical evaluation of the peaks.

Acknowledgment

The authors thank Prof. S. V. C. Aiya for providing the facilities for carrying out the work presented in the paper. One of the authors (M. M. Rao) is thankful to the Ministry of Scientific Research and Cultural Affairs, Government of India, for the award of a National Research Fellowship during which period the works presented in this paper were carried out.

References

1. W. Culshaw. 'A Spectrometer for Millimetre Wave Lengths'. *Proceedings of the Institution of Electrical Engineers*, vol. 100, pt. 2A, March 1953, p. 5.
2. H. Rebbenhust. 'Messung der Dielektrischen Eigenschaften aus dem Hauptsächlich Winkel und dem Wiederhergestellten Azimut für Wellenlängen Unterhalb 3 cm.'. *Annalen der Physik*, vol. 16, pt. 6, 1955, p. 163.
3. C. A. Cochrane. 'Experimental Verifications of the Theory of Parallel Plate Media'. *Proceedings of the Institution of Electrical Engineers*, vol. 97, no. 146, March 1950, p. 72.
4. P. H. Sollom and J. Brown. 'A Centimetre Parallel Plate Spectrometer'. *Proceedings of the Institution of Electrical Engineers*, vol. 103, no. 7, pt. B, May 1956, p. 419.

Table

Data of multiple peaks observed with hylam sheet

(angle of incidence = 30° , r = angle of reflection, and t = angle of transmission)

Thickness of hylan sheet, in.	Sample backed by metal sheet			Sample not backed by metal sheet			Transmission side		
	Reflection coefficient for $r = 30^\circ$	Maximum value of re- flection co- efficient observed	Shift of r from 30° , degree	Reflection coefficient for $r = 30^\circ$	Maximum value of re- flection co- efficient observed	Shift of r from 30° , degree	Transmission coefficient for $t = 30^\circ$	Maximum value of transmission coefficient observed	Shift of t from 30° , degree
1/8	0.849	0.850	-2.5	0.063	0.068	-2.5	0.716	0.733	-0.2
1/4	0.394	0.394	0 and 1.5	0.219	0.219	0	0.400	0.400	0
3/8	0.265	0.273	-0.8 and 0.5	0.175	0.175	0	0.633	0.633	0
1/2	0.455	0.485	2	0.035	0.041	1.5	0.625	0.633	-0.5
5/8	0.515	0.576	-3	0.005	0.005	0.2, 2.5 and 3.5	0.525	0.533	-0.5 and 4.7
3/4	0.348	0.379	-2	0.050	0.054	-4.5	0.400	0.417	-0.8
7/8	0.060	0.076	1	0.100	0.100	0 and 1	0.433	0.467	-0.6
1	0.076	0.076	0	0.116	0.116	0	0.301	0.317	-1
1 1/8	0.273	0.303	0.5	0.032	0.032	0, 1 and 2.1	0.341	0.358	-0.8 and 4
1 1/4	0.318	0.364	1	0.008	0.011	-0.4 and 0.8	0.233	0.267	3
1 3/8	0.212	0.258	0.5	0.043	0.052	-2, -0.7 and 0.5	0.166	0.217	2.2
1 1/2	0	0	-	0.084	0.100	0.5	0.133	0.192	2.5
1 5/8	0.015	0.015	0	0.053	0.066	0.6	0.166	0.233	2.8
1 7/8	0.159	0.159	0	0.036	0.045	0.5	0.133	0.200	2.2

DESIGN OF ELECTRON OPTICAL SYSTEMS FOR COLLIMATORS AND DEFLECTORS*

C. S. Upadhyay

Non-member

Summary

The theoretical aspects of the design of collimators or deflectors, used in cathode-ray tubes, with minimum aberrations is put forward in this paper, taking the example of the collimator, which is a device to bring the parallel rays to a point focus. First, the condition of focusing a tube of rays to a point in a three-dimensional electrostatic field is derived. This condition is used to obtain the relationship between the focusing properties in a given plane, XZ-plane, say, and in a plane at right angles to it, i.e., YZ-plane, of an electrostatic collimator. This shows that the focal power in the YZ-plane (Y-focal power) varies with the angle of inclination, θ , with the optical axis, through which the ray is collimated in the XZ-plane. Such variation of Y-focal power, termed as transverse aberration, can be eliminated by a potential exponentially decreasing on either side of the axis in a plane, $y=\theta$. In the solution so suggested, the discontinuities in the higher order derivatives are also admissible. The evidences from the experiments, performed in the past, support the theory which is applicable for the deflectors also. Such electron optical systems could be realized by applying equipotential strips on two simple bounding surfaces by printed circuit technique.

1. Introduction

The study of higher order errors in the focusing of astigmatic electron beams in a three-dimensional electrostatic field was done by a number of authors.^{1,2} However, in the literature, only the expressions for various aberrations were derived and no thorough investigation was done regarding eliminating or even minimizing such aberrations. The straight axis astigmatic electron optical systems are being used for the deflectors and the collimators in cathode-ray tubes for general purposes and for television receivers.^{3,4} The minimization of the errors will reduce the dynamic correction circuitry used in television receivers. In the present theoretical study of straight axis electron optical systems, the problem of minimizing the errors is considered in a different way, keeping the above practical aspect in view. First, the conditions of focusing in a three-dimensional electrostatic field are derived and then the analysis of non-uniformity of the focusing properties, called transverse aberrations, due to deflection through various angles is made. A method is suggested for eliminating the transverse aberrations and thus designing an astigmatic system with minimum errors.

* Written discussion on this paper will be received until March 31, 1965.

The paper was received on October 20, 1964.

which means that F must be independent of y for identical vanishing of equation (2), i.e., ϕ must not depend on y , and

$$\frac{\delta F}{\delta x'} = \text{constant} \quad (10)$$

which means that F must be independent of x for the vanishing of equation (3), i.e., ϕ must be independent of x . This set of conditions cannot achieve focusing of parallel rays on z axis.

(ii) Or,

$$\left. \begin{aligned} F - x' \frac{\delta F}{\delta x'} - y' \frac{\delta F}{\delta y'} &= \text{constant} \\ \frac{\sqrt{\phi}}{\sqrt{1 + x'^2 + y'^2}} &= \text{constant} \end{aligned} \right\} \quad (11)$$

which from equation (4) means that F must be independent of z , i.e., ϕ must depend only on x and y . Hence, the focusing condition arrived at from condition 1 is :

$$\frac{\delta F}{\delta z} = 0 \quad (12)$$

i.e., F is independent of z and as a consequence :

$$F - x' \frac{\delta F}{\delta x'} - y' \frac{\delta F}{\delta y'} = \text{constant} \quad (13)$$

It is clear that under these conditions, the Hilbert integral becomes a perfect differential. Also, the focusing condition is nothing but the first integral of both equations (2) and (3) which is the same as Snell's law.

Condition 2

If $\text{curl } \vec{P}$ has to be zero, we must have

$$\left(\text{curl } \vec{P} \right)_x = \frac{\delta}{\delta y} \left(\frac{\sqrt{\phi}}{\sqrt{1 + x'^2 + y'^2}} \right) - \frac{\delta}{\delta z} \left(\frac{\sqrt{\phi} y'}{\sqrt{1 + x'^2 + y'^2}} \right) = 0 \quad [13(a)]$$

$$\left(\text{curl } \vec{P} \right)_y = \frac{\delta}{\delta z} \left(\frac{\sqrt{\phi} x'}{\sqrt{1 + x'^2 + y'^2}} \right) - \frac{\delta}{\delta x} \left(\frac{\sqrt{\phi}}{\sqrt{1 + x'^2 + y'^2}} \right) = 0 \quad [13(b)]$$

$$\left(\text{curl } \vec{P} \right)_z = \frac{\delta}{\delta x} \left(\frac{\sqrt{\phi} y'}{\sqrt{1 + x'^2 + y'^2}} \right) - \frac{\delta}{\delta y} \left(\frac{\sqrt{\phi} x'}{\sqrt{1 + x'^2 + y'^2}} \right) = 0 \quad [13(c)]$$

or,

$$\frac{\delta \phi}{\delta y} = \frac{\delta \phi}{\delta x} y' \quad [14(a)]$$

$$\frac{\delta \phi}{\delta z} x' = \frac{\delta \phi}{\delta x} \quad [14(b)]$$

$$\frac{\delta \phi}{\delta z} y' = \frac{\delta \phi}{\delta y} x' \quad [14(c)]$$

In order to satisfy the above condition, two possibilities may be considered. One is that each of equations (13) or (14) cancel among each other and the second is that each term of equations (13) cancels separately for an electron trajectory which satisfies equation (2) or (3). The first possibility is ruled out because on making use of any of equations (14) in Euler equations (2) or (3), trivial solutions are obtained.

Considering the possibility of the vanishing of each term of each component of $\text{curl } \vec{P}$, the same conditions as obtained previously are arrived at and for focusing to take place on z -axis, we get

$$F - y' \frac{\delta F}{\delta y'} - x' \frac{\delta F}{\delta x'} = - \frac{\sqrt{\phi}}{\sqrt{1 + x'^2 + y'^2}} = \text{constant} \quad (15)$$

This focusing condition is achieved by making ϕ independent of z -coordinate.

The focusing condition given by equation (15) ensures the bringing of a double manifold of rays in a plane to a point focus. However, this does not ensure the uniformity of focal power in a I -plane, YZ -plane, say, on rays turned through various angles. Such uniformity of focal powers is a necessary requirement of a deflecting or a collimating system.

3. Transverse aberrations in straight axis astigmatic electrostatic system

In order to study the transverse aberrations, the relationship between the focusing properties in a given plane, XZ -plane, say, and in a plane at right angles to it, YZ -plane, in the case of a collimator with straight axis is derived. The notations are shown in Fig. 1. The differential equations governing the path of electrons can be written from equations (2) and (3) as :

$$\frac{d}{dz} \left\{ \frac{\sqrt{\phi} x'}{\sqrt{1 + x'^2 + y'^2}} \right\} = \frac{\frac{\delta \phi}{\delta x}}{2\sqrt{\phi}} \sqrt{1 + x'^2 + y'^2} \quad (16)$$

$$\frac{d}{dz} \left\{ \frac{\sqrt{\phi} y'}{\sqrt{1 + x'^2 + y'^2}} \right\} = \frac{\frac{\delta \phi}{\delta y}}{2\sqrt{\phi}} \sqrt{1 + x'^2 + y'^2} \quad (17)$$

In order to have collimation, the focusing condition must be satisfied, i.e., equations (11) and (12) are to be satisfied.

For non-trivial solution, from equations (11) and (16), we get

$$\frac{dx'}{dz} = \frac{\frac{\delta \phi}{\delta x}}{2\sqrt{\phi}} (1 + x'^2 + y'^2) \quad (18)$$

Considering the case of symmetrical field about the plane, $x = 0$, and the plane, $y = 0$, and denoting the slope of the trajectory at any point by θ in the plane, $y = \text{constant}$, we get

$$\left. \begin{aligned} \frac{d}{dz} \tan \theta &= \frac{\frac{\delta \phi}{\delta x}}{2 \frac{\delta \phi}{\delta x}} (1 + x^2) \\ \frac{d\theta}{dz} &= \frac{\frac{\delta \phi}{\delta x}}{2 \frac{\delta \phi}{\delta x}} \end{aligned} \right\} \quad (19)$$

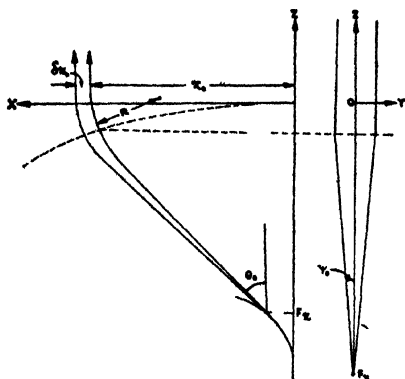


Fig. 1
Explanations of notations

In collimator, the total deflection angle is equal to the initial angle, θ_0 , which gives the design condition for collimator as :

$$\theta_0 = - \int_{-\infty}^{+\infty} \frac{\frac{\delta \phi}{\delta x}}{2 \frac{\delta \phi}{\delta x}} dz \quad (20)$$

It is assumed that the potential field is such that this design condition is satisfied for every possible ray and the consequences for narrow pencil of rays centering on a principle ray are now considered.

X-focus

In the case of a collimator which is a convergent lens in XZ -plane, the X -focal power of narrow pencil of rays on a principle ray at a distance, x_0 , can be defined as :

$$\frac{\partial \theta_0}{\partial x_0} = \frac{1}{F_x} \quad (21)$$

Under the focusing conditions, because ϕ is independent of x , we get

$$\frac{1}{F_x} = - \int_{-\infty}^{+\infty} \left\{ \frac{\partial^2 \phi}{\partial x^2} - \frac{\partial^2 \phi}{\partial z^2} \right\} dz \quad (22)$$

where the subscripts denote the partial derivation. Equation (22) gives the X -focal properties. The X -focal power must be constant in XZ -plane.

Y-focus

From equations (11) and (17), for non-trivial solution, we get

$$\frac{dy'}{dz} = \frac{\delta\varphi}{2\varphi} \sqrt{1 + x'^2 + y'^2} \quad (23)$$

For focusing of beams in the directions of y -axis, on the principal axis in $y = \text{constant}$ plane, we get

$$\Psi_0 = - \int_{-\infty}^{+\infty} \frac{\delta\varphi}{2\varphi} dz \quad (24)$$

where Ψ_0 is the angle which a ray makes with z -axis while getting collimated in the directions of y -axis. The Y -focal power can be written as :

$$\frac{1}{F_y} = \frac{\delta\Psi_0}{\delta y_0} = - \int_{-\infty}^{+\infty} \left(\frac{\varphi_{yy}}{2\varphi} - \frac{\varphi_y^2}{2\varphi^3} \right) dz \quad (25)$$

For symmetrical potential field in the plane $y = 0$, we get

$$\frac{1}{F_y} = - \int_{-\infty}^{+\infty} \frac{\varphi_{yy}}{2\varphi} dz \quad (26)$$

From Laplace equation, we get

$$\varphi_{xx} + \varphi_{yy} = 0 \quad (27)$$

Using equations (26) and (27), we get

$$\frac{1}{F_y} = - \frac{1}{F_x} + \int_{-\infty}^{+\infty} \frac{\varphi_x^2}{2\varphi^3} dz \quad (28)$$

Now

$$\frac{1}{R \cos \theta} = \frac{\varphi_x - x' \varphi_z}{2\varphi} \quad (29)$$

where $\frac{1}{R}$ denotes the curvature of the path in the plane, $y = 0$.

In the case of a collimator, $\phi_z = 0$, and hence

$$\frac{1}{R \cos \theta} = \frac{\varphi_x}{2\varphi} \quad (30)$$

Substituting equation (30) in equation (28), we get

$$\frac{1}{F_y} = - \frac{1}{F_x} + 2 \int_{-\infty}^{+\infty} \frac{1}{(R \cos \theta)^2} dz \quad (31)$$

Equations (28) and (31) give the variations of Y -focal properties with x or θ and can be termed as giving $Y(x)$ aberrations. Both $\frac{1}{F_y}$ and $\frac{1}{F_z}$ must be constant for all values of θ .

4. Elimination of transverse aberrations

In order to eliminate the transverse aberrations, the following relationships must be satisfied :

$$\frac{\varphi_{xx}}{2\varphi} - \frac{\varphi_x^2}{2\varphi^3} = \text{constant} \quad (32)$$

$$\frac{2}{(R \cos \theta)^3} = \frac{\varphi_x^2}{2\varphi^3} = \text{constant} \quad (33)$$

Both these conditions can easily be achieved in the plane, $y = 0$, by a potential field of the type given by

$$\left. \begin{aligned} \varphi &= A e^{-\alpha x} \text{ for } x > 0 \\ \varphi &= A e^{\gamma x} \text{ for } x < 0 \end{aligned} \right\} \quad (33)$$

Thus, there is discontinuity in ϕ all along the z -axis. However, this discontinuity does not make the electron trajectories discontinuous as can be seen by writing equation (13) in the form :

$$x' = k \int \frac{\delta \varphi}{\delta x} dz \quad (34)$$

Because of the continuous properties of the integral, the expression on the left-hand side, i.e., x' , is a continuous function although a discontinuity in $\frac{\delta \varphi}{\delta x}$ exists at $z = 0$.

Under the focusing condition given in equation (11), it is seen that $\frac{\delta^2 F}{\delta y^2} = 0$ and $\frac{\delta^2 F}{\delta x^2} = 0$. It is well known that under these conditions, discontinuous solutions of Euler equations (2) and (3) are admissible.⁷ In these solutions, x , x' , y and y' will be defined but the higher derivatives may be discontinuous functions of x . These discontinuities occur due to sudden changes in the potentials.

It is to be emphasized that a collimator given by equations (32) and (33) appears to be the only optimum solution. One can arrive at the potential field in the plane, $y = 0$, to get the desired Y - and X -focal lengths and this potential field can then be extrapolated on to two simple bounding surfaces/planes, $y = \pm y_1$. These equipotentials may be applied on an insulating material like ashlam by printed circuit techniques.

The evidences in support of this theory is available in the experimental development of the deflector plates for a flat cathode-ray tube.⁸ It is clear that on putting plates on top and bottom at an intermediate potential on channel-shaped deflectors, the non-uniformity in X - and Y -focal powers is minimized considerably. This has been achieved by making $\phi(x, y, z)$ independent of z . By the mathematical method as suggested, an almost perfect system can be arrived at by properly shaping the electrodes or by using printed equipotentials on simple bounding surfaces.

5. Conclusions

From the above theory, it is clear that it is possible to design an astigmatic electron optical system free from transverse aberrations. It is possible to realize such systems by applying equipotentials on simple bounding surfaces by printed circuit techniques.

6. Acknowledgments

The author thanks Dr. S. M. Dasgupta, Principal, G. S. Technological Institute, Indore, for his guidance in the work presented in the paper.

7. References

1. R. G. E. Hutter. 'The Deflection of Beams of Charged Particles'. *Advances in Electronics*, vol. 1, 1948, p. 167.
2. P. A. Sturrock. 'The Imaging Properties of Electron Beams in Arbitrary Static Electromagnetic Fields'. *Philosophical Transactions*, vol. 245A, 1952, p. 155.
3. D. Gabor, P. R. Stuart and P. G. Kalman. 'A New Cathode-Ray Tube for Monochrome and Colour Television'. *Proceedings of the Institution of Electrical Engineers*, vol. 105, pt. B, no. 24, November 1958, p. 581.
4. W. R. Aiken. 'A Thin Cathode-Ray Tube'. *Proceedings of the Institution of Radio Engineers*, vol. 45, 1957, p. 1599.
5. A. R. Forsyth. 'Calculus of Variations'. *Dover Publications, Inc.*, 1960.
6. P. A. Sturrock. 'An Introduction to Static and Dynamic Electron Optics'. *Cambridge University Press*, 1955.
7. C. Fox. 'An Introduction to the Calculus of Variations'. *Oxford University Press*, 1954.

SIMULATION OF FOURTH ORDER SYSTEMS WITH DOUBLE LEAD BY SINGLE OPERATIONAL AMPLIFIER*

L. K. Wadhwa

Non-member

and

Maj. S. P. Sharma

Associate Member

Summary

A network consisting of one operational amplifier, four capacitors and four resistors, and capable of simulating fourth order linear systems having a double zero at the origin, is presented in this paper. The design equations and the physical realizability conditions of the network are also given.

Introduction

An earlier communication¹ on this subject discussed a method for the solution of fourth order linear systems with only one operational amplifier and a network consisting entirely of resistors and capacitors and presented a circuit for the simulation of systems characterized by the transfer function :

$$F_1(s) = - \frac{b_1 s}{a_4 s^4 + a_3 s^3 + a_2 s^2 + a_1 s + 1}$$

The purpose of this paper is to discuss the simulation of another particular type of fourth order systems, i.e., systems with double lead and which are represented by a transfer function :

$$F(s) = - \frac{b_2 s^2}{a_4 s^4 + a_3 s^3 + a_2 s^2 + a_1 s + 1} \quad (1)$$

where a 's and b_2 are positive real constants.

Only one circuit, out of the many circuits possible, is presented and its design equations and physical realizability conditions are given below.

Simulation of systems with double lead

A network for the simulation of fourth order linear systems is shown in Fig. 1 and its transfer function can be shown¹ to be given by

$$\frac{E_2}{E_1} = - \frac{Y_1 Y_2 Y_3 Y_7}{Y_2 Y_3 (Y_1 + Y_2) (Y_3 + Y_4 + Y_7) + (Y_1 + Y_2 + Y_3) [Y_4 Y_5 (Y_6 + Y_7) + Y_6 Y_{10}] + (Y_4 + Y_5 + Y_7) + Y_5 Y_7 Y_{10}} \quad (2)$$

* Written discussion on this paper will be received until March 31, 1965.

This paper (re-drafted) was received on January 16, 1964.

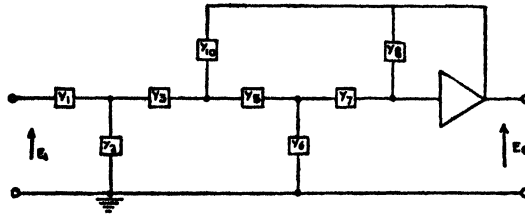


Fig. 1

Network for simulation of fourth order systems

It is possible to simulate the system of equation (1) with the network of Fig. 1, if the admittances, Y 's, are suitably chosen and furthermore, it should be obvious from equation (2) that four of the appropriate admittances would be required to be capacitive. Of the various possible circuits, each employing four capacitors and four resistors and capable of simulating, under certain conditions, the system represented by equation (1), only one circuit with :

$$\begin{aligned} Y_1 &= s c_1, & Y_3 &= s c_3, & Y_6 &= s c_6, & Y_8 &= s c_8 \\ Y_2 &= Y_5 = Y_{10} = \frac{1}{R} \text{ and } Y_7 = \frac{1}{\alpha R} \end{aligned} \quad (3)$$

is presented in this paper.

On substituting equation (3) in equation (2) and after simplification and comparison with equation (1), we get

$$b_2 = T_1 T_3 \quad (4)$$

$$a_1 = T_1 + T_3 + (\alpha + 2) T_8 \quad (5)$$

$$a_2 = (\alpha + 2) T_1 T_8 + (2\alpha + 3) T_3 T_8 + 2\alpha T_6 T_8 \quad (6)$$

$$a_3 = (\alpha + 1) T_1 T_3 T_8 + 3\alpha T_3 T_6 T_8 + 2\alpha T_1 T_6 T_8 \quad (7)$$

$$a_4 = \alpha T_1 T_3 T_6 T_8 \quad (8)$$

where

$$T_n = R c_n \quad (9)$$

Now, the simulation of the system of equation (1) with the network of Fig. 1 is possible only if the values of α , T_1 , T_3 , T_6 and T_8 obtained as the solutions of equations (4) through (8) are positive real.

The solution of equations (4) through (8) gives

$$(T_1^3 - a_1 T_1 + b_2) [T_1^4 - a_1 T_1^3 + (a_2 + 2b_2) T_1^2 - (a_1 b_2 + a_3) T_1 + (3a_4 + b_2^2)] = 0 \quad (10)$$

$$\alpha = \frac{-l_1 T_1^2 - b_2 m_1 T_1 + b_2 n_1}{l_2 T_1^3 + b_2 m_2 T_1 - b_2 n_2} \quad (11)$$

$$T_8 = \frac{l_2 T_1^3 + b_2 m_2 T_1 - b_2 n_2}{b_2^2 T_1} \quad (12)$$

It can be shown by a process of reasoning similar to that discussed elsewhere² that a set of positive real α , T_1 , T_2 , T_3 and T_4 exist, provided that

$$\left(\frac{l_2 T_1' + b_2 m_2}{n_2} \right) > \frac{b_2}{T_1'} > \left(\frac{l_1 T_1' + b_2 m_1}{n_1} \right) \quad (13)$$

where

$$l_1 = 4 a_4 - b_2^2$$

$$l_2 = 2 a_4 - b_2^2$$

$$m_1 = a_1 b_2 - 2 a_3$$

$$m_2 = a_1 b_2 - a_3$$

$$n_1 = b_2^2 - 6 a_4$$

$$n_2 = b_2^2 - 3 a_4$$

and T_1' is the positive real root of equation (10).

The design procedure³ would be to solve equation (10) and check to see if inequality (13) is satisfied; the fulfilment of which means that the circuit is physically realizable. The circuit parameters may then be obtained with the help of equations (11), (12), (4) and (8). Having thus determined α , T_2 , T_3 and T_4 and choosing arbitrarily a convenient value for any one of the capacitors, the value of the remaining components may then be determined with the help of equation (9).

Acknowledgment

The authors thank the Director of Electronics, Defence Research and Development Organization, Government of India, New Delhi, for his permission to publish this paper.

References

1. L. K. Wadhwa. 'On Simulation of Fourth Order Systems with One Operational Amplifier'. Paper read at the Conference of the Automation and Computation Scientists in India, Sindri, February 22-24, 1963.
2. L. K. Wadhwa. 'Simulation of the General Third Order Systems by a Single Operational Amplifier'. *Proceedings of the National Institute of Sciences, India*, vol. 29A, no. 6, November 1963, p. 597.
3. J. V. Uspansky. 'Theory of Equations'. *McGraw-Hill Book Co., Inc.*, 1948.

E
L
E
C
T
R
O
N
I
C
S
&
T
E
L
E
C
O
M
M
U
N
I
C
A
T
I
O
N
E
N
G
I
N
E
E
R
I
N
G
D
I
V
I
S
I
O
N

JOURNAL OF THE INSTITUTION OF ENGINEERS (INDIA)



VOLUME 45

NUMBER 9

PART ET 3

MAY 1965



PUBLISHED BY THE INSTITUTION

8 GOKHALE ROAD

CALCUTTA

Rs. 2.50

REQUIREMENTS OF PAPERS SUBMITTED FOR PUBLICATION

1. Papers should be submitted directly to the Headquarters, and all communications and enquiries concerning publications should be addressed to the Technical Officers at the Headquarters.
2. Three manuscript copies, accompanied by original Indian ink drawings and photographs, if any, should be submitted, with the author retaining one copy for his own file. The author should give his name in full, grade of membership, designation, and present address, not forgetting to intimate any change of address at a subsequent date.
3. Length of the paper should not generally exceed 7,500 words, and should include the most salient features of the work described in an orderly presentation conforming with the conventional usage in the *Journal*.
4. All copy including quotations from other works, etc. should be typed double-spaced on one side only in good quality paper of foolscap size with a generous margin at the left-hand side. Footnotes should be generally avoided.
5. No attention will be paid to loose leaflets, disorderly and handwritten manuscripts, cyclostyled texts, and anonymous contributions, not accompanied by a forwarding letter.
6. In their own interest, authors should seek prior permission of their employers or patent protection, etc., if necessary, before the paper is submitted. The Institution can accept no responsibility in this matter. Paper should be devoid of derogatory remarks or matter of advertisement value or personal interests.
7. Papers should not be submitted to another journal till a decision is given by the Institution and, when accepted, till it is published in the *Institution Journal*. The author should declare to this effect while submitting the paper. Permission should be obtained and proper acknowledgment made to the Institution if the paper is to be reprinted in any other publication.
8. The paper should have a brief title which is explanatory, commence with a summary of not more than 250 words, and end with an itemized account of findings and conclusions. The presentation should be in the third person.

(Continued on inside back cover)

THE JOURNAL

OF

The Institution of Engineers (India)

SECRETARY & EDITOR : B. Seshadri, B.Sc., A.I.I.Sc., D.I.C. M.Sc.(Eng.), M.I.E.

TECHNICAL EDITOR : B. R. Subramanyam, B.Sc., B.E., A.M.I.E.

The Institution of Engineers (India) as a body accepts no responsibility for the statements made by the individual authors.

The Institution of Engineers (India) subscribes to the Fair Copying Declaration of the Royal Society and reprints of any portion of this publication may be made provided that reference thereto be quoted.

Vol. XLV

MAY 1965

No. 9, Pt. ET 3

CONTENTS

Page

ELECTRONICS AND TELECOMMUNICATION ENGINEERING DIVISION

1. **Design and Application of Transistorized Phase Angle Meter.** S. K. Basu, *Non-member*, Dr. S. P. Patra, *Associate Member*, and Prof. J. K. Choudhury, *Associate Member* 123
2. **Party Line Telephone Working Using a New Device.** P. N. Das, *Non-member* 133
3. **Near End Infra-Red Filters for I. R. Communication Systems.** K. R. Wadhera, *Non-member* 137

Electronics & Telecommunication Engineering Division Board

The President (*Ex-officio*)

Brig. M. K. Rao (*M.*), *Chairman*

Prof. S. P. Chakravarti (*M.*)

Automatic Control Group

Prof. V. V. Sarwate, *Chairman*

Oerlikon Quick-acting Regulators

For automatic regulation of:

- * voltage * current
- * effective & reactive power
- * frequency * power factor

Oerlikon quick-acting rolling sector regulators are available in five different types to suit your specific requirements. They can be supplied as Direct Current Regulators with a moving coil measuring system instead of the normal Ferraris system.

Oerlikon quick-acting regulators are designed for semi-flush mounting on switchboards. A transparent plastic cover or a housing with glass front permits visual control of the operation of the regulator at any time and protects the active parts against dust.

Manufactured by.

OERLIKON ENGINEERING COMPANY,
Zurich, Switzerland

Sole Distributors..

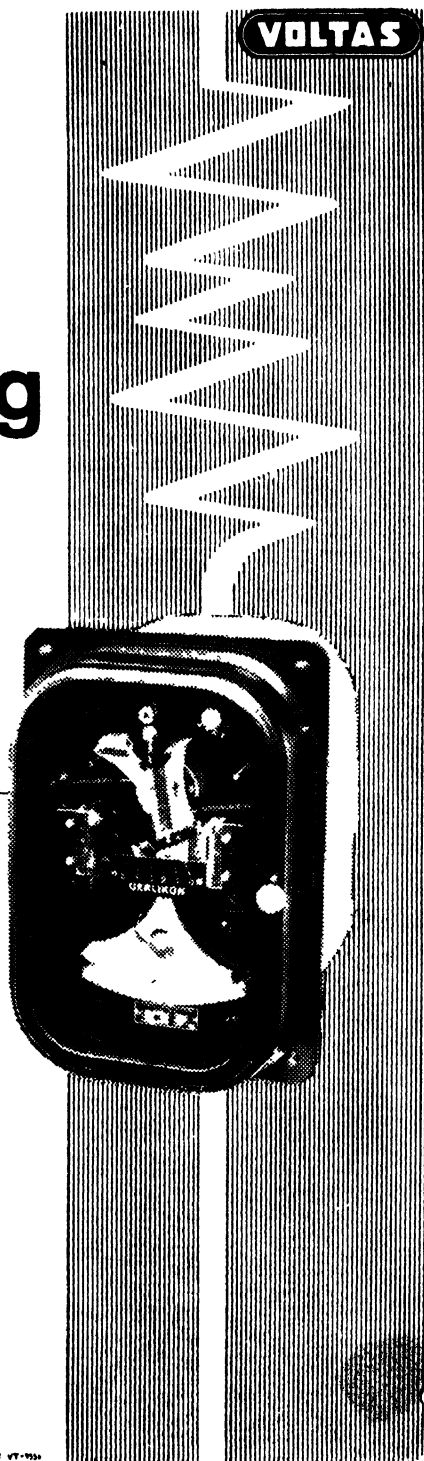
VOLTAS LIMITED, ELECTRICAL DIVISION

Head Office: Ballard Estate, Bombay 1.

Calcutta Madras New Delhi Bangalore

Lucknow Cochin Ahmedabad Secunderabad

Nagpur Jaipur Bhopal Patna



DESIGN AND APPLICATION OF TRANSISTORIZED PHASE ANGLE METER*

S. K. Basu

Non-member

Lecturer in Electrical Engineering

Dr. S. P. Patra

Associate Member

Professor of Electrical Engineering

and

Prof. J. K. Choudhury

Associate Member

Professor of Electrical Engineering

Department of Electrical Engineering, Jadavpur University, Calcutta

Summary

This paper describes the design and construction of a transistorized phase angle meter for measuring phase angle between two sinusoidal alternating voltages of the same frequency; it can also be used for measuring the power factor in an A.C. circuit. Though basically designed for use in a single-phase circuit, it can be adapted for measuring power factor in a balanced three-phase circuit. The advantages of the instrument described in this paper over the conventional electrodynamic and moving iron type power factor meters are: (i) high input impedance of voltage circuit; (ii) negligible power consumption in test circuit; and (iii) good frequency characteristics.

1. Introduction

The most commonly used instruments for the measurement of power factor of a circuit at power frequency are of cross-coil electrodynamic and moving iron types.^{1,2,3} Instruments employing electronic valve circuitry which have a wide frequency range have also been developed.^{4,5,6} This paper describes the design and construction of a transistorized phase angle meter which can be used for the measurement of phase angle between two alternating voltages of the same frequency. The same instrument can be adapted for the measurement of power factor angle in single-phase and balanced three-phase circuits. In this respect, it has definite advantages over the electrodynamic and moving iron type instruments which can be designed for use either in a single-phase or in a three-phase circuit only. The impedance of voltage circuit of the instrument described in this paper is very high; as such, it absorbs negligible power from the test circuit. Power for operating the moving system of the permanent

* Written discussion on this paper will be received until July 31, 1965.

This paper was received on August 19, 1964.

magnet moving coil type indicating meter is obtained from an auxiliary source, *viz.*, a self-contained 12-volt dry cell which also operates the circuit transistors. While electrodynamic and moving iron type power factor meters⁵ are basically power frequency devices, the transistorized phase angle meter is not affected by frequency variation between 30 and 1,000 cycles per sec. The instrument performance is also unaffected by wide variations in the magnitudes of current and voltage from their rated values. Phase angle meters using electronic valves are comparatively more bulky because of the high tension D.C. power source needed for their operation. These instruments contain fragile components and hence require considerable precautions during transit and handling. The cost of the instruments using electronic valve is quite high. The transistorized equipment described in this paper is very light, compact, portable and less costly. In this respect, it has advantages over electronic equipment, although its frequency range is comparatively limited.

2. Basic circuit and principle of operation

The principle of operation of the transistorized instrument is explained from the basic circuit shown in Fig. 1(i). Two sinusoidal alternating voltages v_1 and v_2 , are connected between the base and the emitter of the transistor T, through two high resistances R_1 and R_2 , so that either voltage can make the transistor conducting during the period of the negative half-cycle. Rectifiers D_1 and D_2 prevent short-circuiting between v_1 and v_2 . So long as the transistor conducts, the open-circuit voltage between the terminals a and b remains at zero if the small emitter-collector drop in the transistor is neglected. When the transistor stops conducting, its collector potential attains the value $(-V_c)$. It follows, therefore, that the open-circuit voltage output v_0 , across the terminals a and b remains at $(-V_c)$ during the period when both the voltages v_1 and v_2 , are simultaneously positive. During the rest of the period in each cycle, the voltage v_0 , falls to and remains at zero. Thus there will be rectangular block output voltage v_0 , in each cycle of the alternating voltages, v_1 and v_2 . It is evident from Figs. 1(ii) and (iii) that the block output is maximum when the input voltages are in phase and zero when they are 180° degrees out-of-phase. It is also obvious that the average value of the output voltage v_0 , decreases linearly from its maximum value to zero as the phase angle between v_1 and v_2 increases from 0° to 180° . Fig. 1(iv) shows the output voltage v_0 , when v_1 and v_2 are in phase. If a permanent magnet moving coil type indicating meter M, having a very high resistance is connected across a and b, its deflection indicates the average value of v_0 . In other words, a linearly calibrated scale of M gives a measure of the phase angle between the two voltages, v_1 and v_2 . It is to be noted that the maximum value of v_0 is the collector voltage $(-V_c)$, and hence the average value of v_0 over a complete cycle during the maximum output condition is $\left(-\frac{V_c}{2}\right)$ which corresponds to the full scale indication in meter M.

3. Actual circuit for phase angle measurement

The actual circuit used for the measurement of phase angle between two sinusoidal alternating voltages is shown in Fig. 2. Two similar potential transformers t_1 and t_2 , having mu-metal cores are used to derive the required voltages v_1 and v_2 , from the test voltages. Rectifiers D_3 and D_4 , are used to prevent the positive half-cycles of v_1

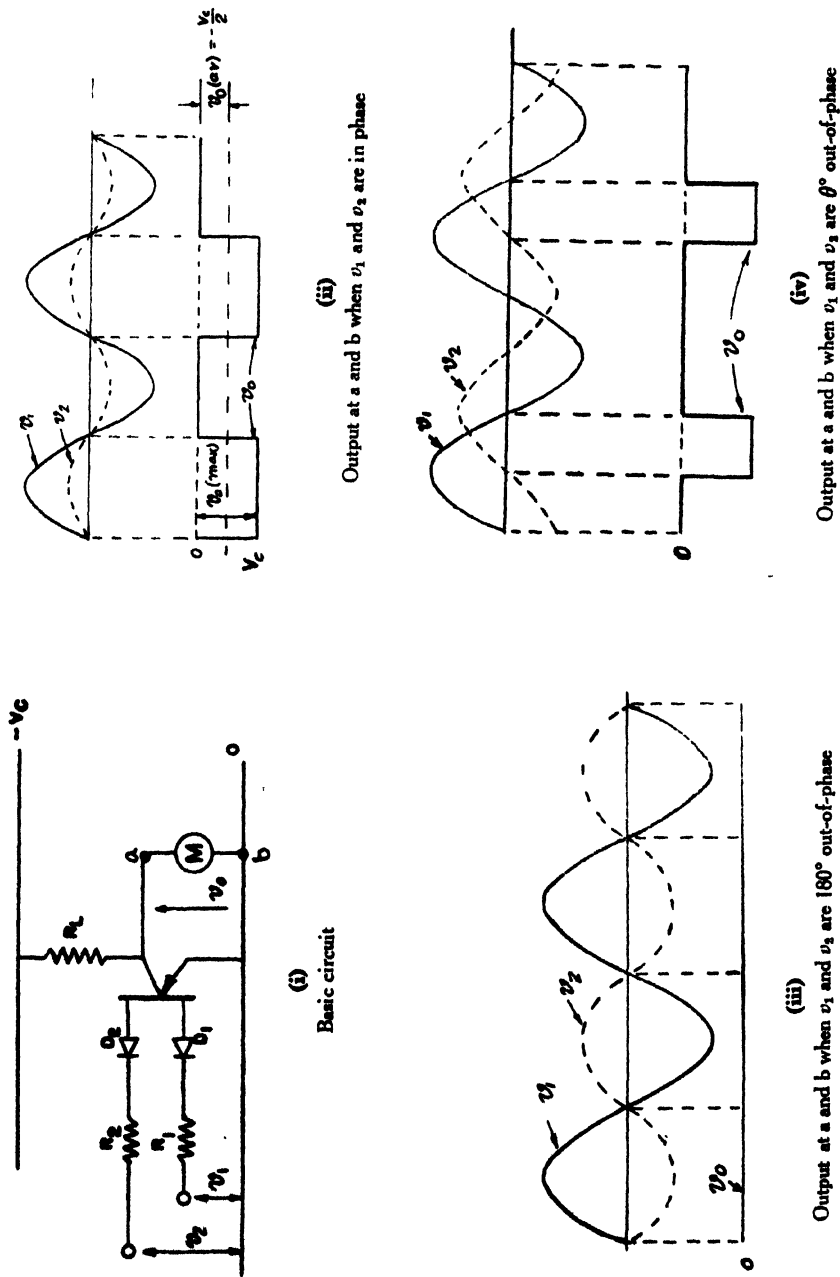


Fig. 1

Diagrams showing principle of operation of transistorized phase angle meter

and v_2 from appearing across the base and the emitter of transistor T. The rectifiers D_5 and D_6 , are used to clip the negative half-cycle of v_1 and v_2 at a convenient pre-determined value, $(-V_c)$, to avoid excessive current flow in the base-emitter circuit of transistor T.

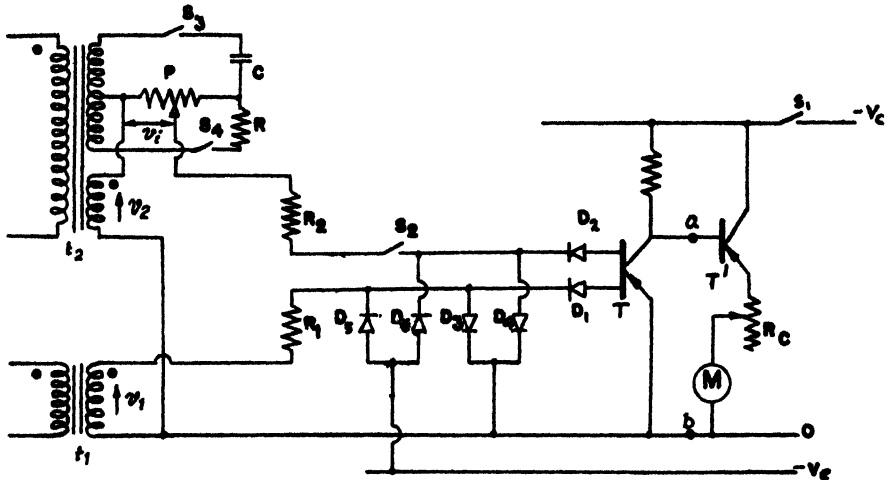


Fig. 2

Circuit for measurement of phase angle between two alternating voltages

It has already been mentioned that if a D.C. meter of very high resistance is connected across a and b, it indicates the output voltage, v_0 . This requires a highly sensitive micro-ammeter to be connected across the terminals, a and b. However, the effective input impedance of a comparatively low impedance indicating meter M, can be increased by introducing another transistor T' , connected across a and b, as shown in Fig. 2. This modification makes it possible to use a comparatively robust permanent magnet milli-ammeter M, as the indicating instrument. The switch s_1 , is used to disconnect the collector supply voltage $(-V_c)$, when the instrument is not in use.

Initial adjustment of meter deflection

From Figs. 1(i) and (ii), it is seen that the indicating meter M, always gives maximum deflection when only one of the input voltages v_1 , say, is present. Also, as has been already stated, this maximum deflection corresponds to $\left(-\frac{V_c}{2}\right)$ which is the average value of v_0 over a complete cycle of v_1 . So the calibration of meter M, is done in terms of $\left(-\frac{V_c}{2}\right)$ for full scale deflection. Since there may be small variations of the collector voltage $(-V_c)$, the meter deflection should be adjusted over full scale with only one input voltage, v_1 , say, immediately before a measurement. This adjustment is done with the help of resistance R_c , in series with meter M. Thus, every time, before any measurement is made, the indicating meter deflection

should be adjusted over full scale values by operating resistance R_c . During such an adjustment, only one input voltage v_1 , say, should operate transistor T, while the other input voltage v_2 , is cut off from the transistor circuit by switch s_2 (Fig. 2).

Leading or lagging phase angle

From Fig. 1(iv), it is evident that the average value of the output voltage v_0 , is the same irrespective of whether one of the input voltages v_2 , say, lags or leads the other voltage v_1 , by a certain angle. Thus, the indicating meter M, normally cannot discriminate between the lagging or leading phase angle of v_2 with respect to v_1 . This is determined as below.

At first, the magnitude of the phase angle between v_1 and v_2 is noted from meter deflection. The sign of the phase angle, i.e., whether v_2 lags or leads v_1 , is then determined by injecting an auxiliary voltage v_i in series with v_2 . When the auxiliary voltage v_i , which leads v_2 by a certain angle is gradually increased in magnitude from zero by potentiometer P, the meter indication of the angle progressively decreases from its previously noted value if v_2 lags v_1 , whereas the indication increases if v_2 leads v_1 . As seen from Fig. 2, the leading phase angle of v_i with respect of v_2 is obtained by the CR-network across a tertiary winding of the potential transformer t_2 , which normally yields v_2 . The switches s_3 and s_4 , are normally kept open; these two switches are closed only during the determination of polarity of phase angle between two input voltages.

4. Circuit for measurement of power factor angle

(i) Single-phase load

For the measurement of power factor angle of a single-phase load, the circuit shown in Fig. 3 can be used. A low resistance non-inductive shunt S, is connected in series with the load circuit so that the voltage drop across it is in-phase with and proportional in magnitude to load current, i_L . The voltage v_1 , obtained from the secondary of transformer t_1 , has negligible phase angle error because of the use of mu-metal core. The voltage v_1 , is thus in-phase with and proportional to the load supply voltage. It is evident that the indication in meter M, corresponds to the phase angle between v_1 and v_2 , i.e., between the supply voltage and the load current. This arrangement can thus be utilized as a power factor meter suitable for use in a single-phase circuit. However with this arrangement, the deflection on the scale of meter M, range between full scale to mid-scale (i.e., between 0° to 90° of the previous calibration) as the power factor angle of the load changes from 0° to 90° . Thus only one-half of the scale of meter M, is utilized if the circuit of Fig. 3 is considered. In the equipment developed by the authors, improvement as shown in Fig. 4 is made over the circuit of Fig. 3, so that the complete scale calibration of M is utilized for the measurement of power factor angle in a single-phase circuit with the pointer indicating at the centre of the scale for 0° , and at the extreme left and right sides for 90° lagging and 90° leading power factor angles respectively.

From Fig. 1, it is seen that if any one of the two voltages, v_2 , say, is given an angular phase shift of 90° lagging with respect to its original phase and then connected to transistor T, the output voltage v_0 is zero when v_2 originally lags v_1 by 90° . Under this condition, the average value of v_0 increases linearly from zero to maximum as the

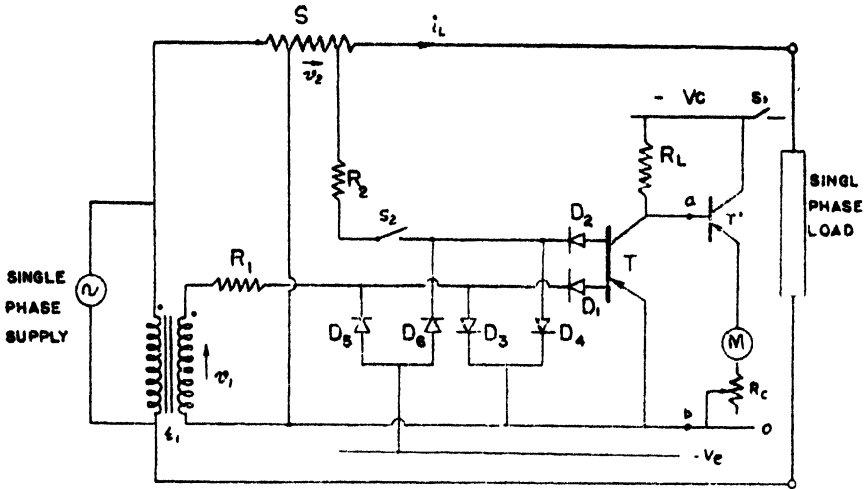


Fig. 3

Circuit for measurement of power factor angle of a single-phase load

phase angle of v_2 changes from 90° lagging through 0° to 90° leading with respect to v_1 . Thus the deflection in meter M , can be used to indicate the power factor angle of a single-phase load provided voltage v_2 , is made proportional to load current i_L , in magnitude but to lag i_L by 90° in phase. This has been achieved by the arrangement shown in Fig. 4 where a current transformer t_3 , is energized by passing load current i_L , through its primary thereby yielding the secondary voltage, v_3 . The voltage v_3 , is made linear with load current i_L , by introducing an air gap in the core of t_3 . The voltage v_1 , is obtained from the load supply voltage by using the potential transformer, t_1 . A separate scale is provided in meter M , for this purpose. This scale graduated from 90° lagging through 0° to 90° leading corresponding to zero, centre and full scale

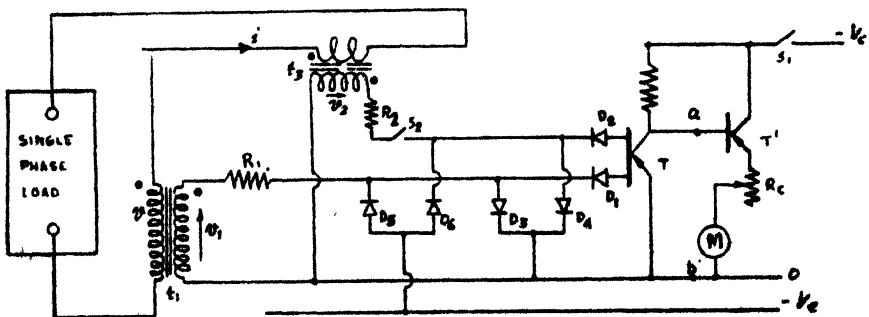


Fig. 4

Circuit for measurement of power factor angle of a single-phase load

deflection respectively of meter M, serves the purpose of measuring the power factor angle. The nature of calibration of the graduations of meter M, for use as a phase angle meter and a power factor meter is shown in Fig. 5. In both the cases, the same graduations are used but separate calibrations are provided in either case. For measurements in single-phase load circuits, transformers t_1 and t_3 are utilized and potential transformer t_2 , has no function. Connections of the primaries of t_1 and t_3 should be made in the test circuit with proper polarities so that there is no reversal of any of the voltages v_1 and v_2 , in their secondaries which are permanently connected with the transistor and the meter circuits. These polarities are shown in Fig. 3 by dots. It is clear that the method of checking up of leading/lagging conditions as necessitated for phase angle measurement becomes redundant.

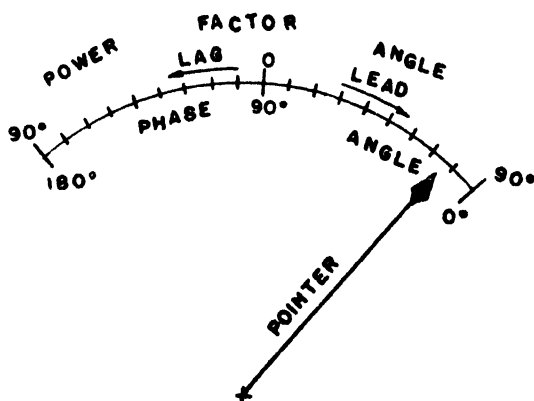


Fig. 5

Scale of the phase angle meter

(ii) Three-phase load

The circuit modifications shown in Fig. 6 are introduced for adapting the same equipment for the measurement of power factor angle in a balanced three-phase circuit. In Fig. 6, potential transformer t_2 , which is identical to potential transformer t_1 , is utilized. For the measurement in a three-phase circuit, t_1 and t_2 are in Scott connection with the three supply lines R, Y, and B of a balanced three-phase system. From the vector diagram (Fig. 7) for the circuit shown in Fig. 6, it is evident that voltage v_1 is proportional to and in-phase with the neutral-to-line voltage of phase R, and v_2 is proportional to the line current of phase R, lagging it by 90° . This results in an indication in meter M, which corresponds to the power factor angle of the load connected to phase R, the principle of operation remaining exactly the same as in a single-phase circuit. The system being balanced, the power factor angle in the other phases, Y and B, are the same as that in phase R.

5. Complete circuit diagram

Fig. 8 shows the complete circuit diagram of the instrument which can be used as :

- (i) a phase angle meter ; (ii) a power factor meter for a single-phase load ; and
- (iii) a power factor meter for a balanced three-phase load.

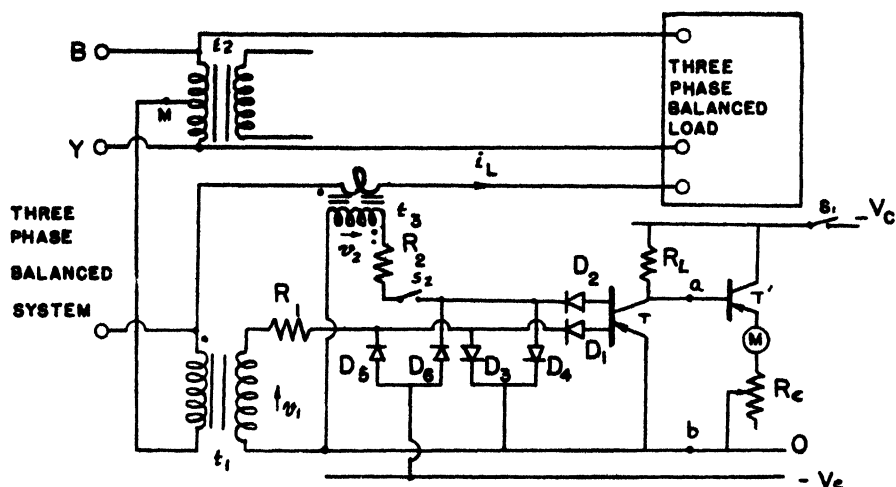
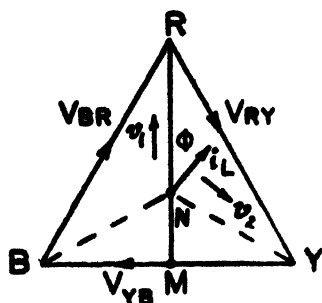


Fig. 6

Circuit for measurement of power factor angle of a balanced three-phase load



◆ IS THE POWER FACTOR ANGLE
VECTOR NR IS THE R-PHASE TO NEUTRAL VOLTAGE

Fig. 7

Vector diagram of the circuit in Fig. 6

Initial adjustment of the meter deflection is essential before any measurement is made. For this purpose, the supply source which yields voltage v_1 , across terminals 1 and 2, is connected to the transistor circuit, keeping switch s_2 in the off position.

For the measurement of phase angle between two sinusoidal voltages, the test voltages are connected to the terminals 1-2 and 5-7 of potential transformers t_1 and t_2 ; switch s_2 should be connected to position 1 during this measurement.

For the determination of power factor angle of a single-phase load, terminals 2 and 3 should be connected together; the supply voltage has to be connected across the terminals 1-2, while the load should be connected across terminals 1-4 with switch s_1 kept at position 2.

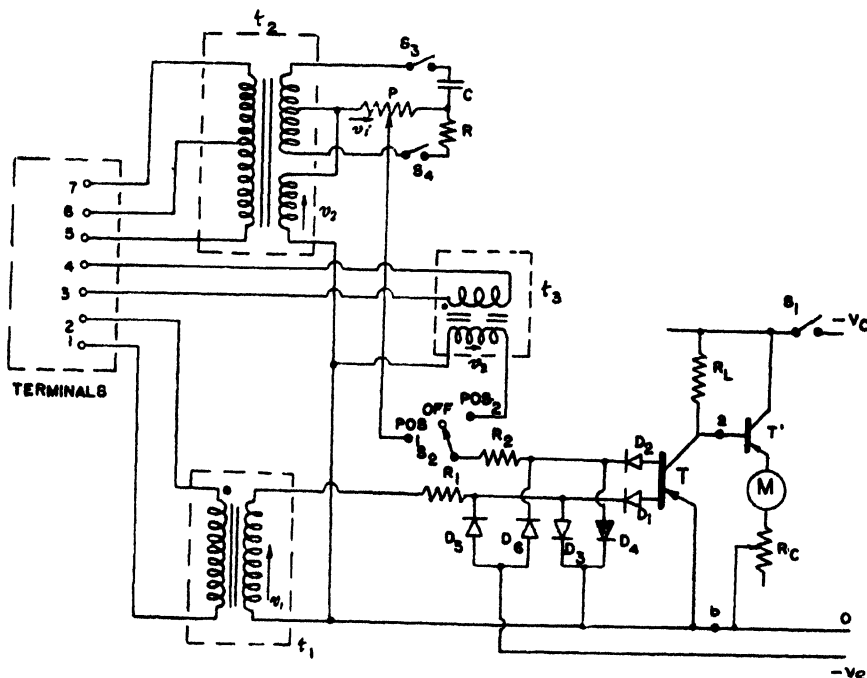


Fig. 8

Complete circuit diagram of the phase angle meter

T, T' : Transistor OC71 ; t_1 , t_2 : Potential transformer ; t_3 : Current transformer ; M : Micro-ammeter ; and D_1 to D_4 : Selenium diodes

Resistances in kilohm : $R = 7$; $R_1 = 2.5$; $R_2 = 2.5$ and $R_L = 2$

Potentiometers : $P_c = 100$ megohm ; and $P = 50$ kilohm

Capacitance : $C = 0.3$ microfarad

Volts : $-V_c = -12$ volts ; and $-V_e = -2$ volts

The power factor angle of a balanced three-phase load can be measured by connecting terminal 1 of transformer t_1 to the middle tap terminal 6 of transformer t_2 (Scott method) and connecting the three lines of a balanced three-phase supply to terminals 2, 5 and 7. During this measurement, terminals 2 and 3 are connected together and terminals 4, 5 and 7 connected to the three-phase load. The switch s_2 is to be kept in position 2 as in the single-phase power factor measurement.

6. Calibration and performance tests

Calibration of the scale of meter M, from zero to full scale for the measurement of phase angle between two alternating voltages was made at 50 cycles per sec. by keeping each of the voltages v_1 and v_3 , at 100 volts. The phase shift of one of the voltages was effected by a phase shifting device consisting of standard condensers and resistances of known values. The meter was tested at different frequencies ranging from 30 to 1,000 cycles per sec. Variations in the readings were within 2° between these extreme

limits. The meter was also tested for effects of voltage fluctuations at 50 cycles per sec. The test voltages were varied between 50 to 110% of the rated value and maximum deviation in the meter reading was noted to be within 3°.

For the measurement of power factor angle of single-phase and three-phase loads (balanced), load circuits were built up with standard condensers and resistances of known values.

7. Conclusions

The most outstanding feature of the transistorized phase angle meter is that it combines in a single equipment the functions of three separate instruments, *e.g.*, (i) phase angle meter for the measurement of phase angle between two separate sources of supply ; (ii) power factor meter for a single-phase load ; and (iii) power factor meter for a balanced three-phase load.

In this sense, it can be claimed to be unique of its kind. The frequency range of a transistorized phase angle meter is however lower than the conventional electronic phase angle meter, though it is immensely superior to the electrodynamic and moving iron type power factor meters by virtue of its greater frequency range and higher input impedance. It can be very conveniently used as an inexpensive laboratory instrument as a phase angle meter cum power factor meter.

8. Acknowledgment

The authors thank the authorities of the Jadavpur University, Calcutta, for providing the facilities for carrying out the work presented in this paper. They also thank Sarvashri N. C. Dey and U. N. Chowdhury of the Electrical Engineering Department, Jadavpur University, Calcutta, for their assistance in the preparation of the paper.

9. References

1. I. F. Kinnard. 'Applied Electrical Measurements'. *John Wiley & Sons, Inc.*, 1962.
2. N. P. Miller. 'Crossed Coil Power Factor Meters'. *Transactions of the American Institute of Electrical and Electronics Engineers*, vol. 63, 1944, p. 294.
3. A. T. Dover. 'Theory and Practice of Alternating Currents'. *Sir Isaac Pitman & Sons, Ltd.*, 1961.
4. E. F. Flormon and A. Tait. 'Electronic Phase Meter'. *Proceedings of the Institution of Radio Engineers*, vol. 37, 1949, p. 207.
5. E. O. Vandeven. 'Phase Meter'. *Proceedings of the Institution of Radio Engineers*, vol. 21, June 1948, p. 142.
6. E. R. Krentzmer. 'Measuring Phase Angle at Audio and Ultrasonic Frequencies'. *Electronics*, vol. 22, October 1949, p. 114.

PARTY LINE TELEPHONE WORKING USING A NEW DEVICE***P. N. Das***Non-member**Electrical Engineering Department, University of Roorkee, Roorkee***Summary**

A new transistorized device is used in party line telephone working by which different subscribers can be separately and selectively called unlike the party line working in a C. B. system. In this method, the bell of the called subscriber only rings during calling and as many as twenty different subscribers may be included in the same party using the same pair of lines.

Introduction

In manual rural telephone systems, some subscribers usually share a pair of telephone lines, A and B, say, as the traffic per subscriber is not heavy. Different subscribers are called by sending selective number of rings through A or B wire; in this case a maximum number of six subscribers can be included in one party. A new transistorized selective method is described in this paper by means of which as many as twenty subscribers can be included in a party and in which it is not necessary to send different trains of ringing current. The different subscribers are provided with different voltage operated transistorized selectors and D.C. bells; and these are operated by sending definite values of D.C. voltages from the operator. The system is suitable for 22-volt C.B. operation and not for magneto systems.

Theory of selecting device

With two complementary transistors, P-N-P and N-P-N, a circuit is possible which can select a particular range of D.C. voltage just as a band-pass filter can pass only a particular band of frequencies. Such a circuit is shown in Fig. 1.

When both the transistors are non-conducting the output voltage is zero; also when both of them are conducting, the output voltage is zero. If, however, P-N-P transistor conducts only and N-P-N transistor remains non-conducting, the output voltage becomes positive. Initially both the transistors are kept non-conducting by giving a positive bias voltage on the emitter of N-P-N by R_1 and a negative bias voltage on the emitter of P-N-P by R_2 . If an input voltage is applied with the polarities as shown in Fig. 1 having its centre point earthed, the base of N-P-N is given some positive voltage and if it exceeds the bias voltage of the emitter, it starts conducting; similarly the base of P-N-P is given some negative voltage and when it exceeds the bias voltage on its emitter, it also starts to conduct. Now, if the bias voltage on P-N-P is less than that on N-P-N, the P-N-P transistor starts conducting at a lesser input voltage than the N-P-N transistor. For the input voltage at which P-N-P conducts only, an output voltage is obtained. Thus, by applying suitable bias voltages

* Written discussion on this paper will be received until July 31, 1965.

This paper was received on March 25, 1964.

to the two transistors, output voltages can be obtained at different definite values of input voltages only. By having such voltage selecting devices at the different way stations and by sending different voltages from the control station, the required selection can be effected.

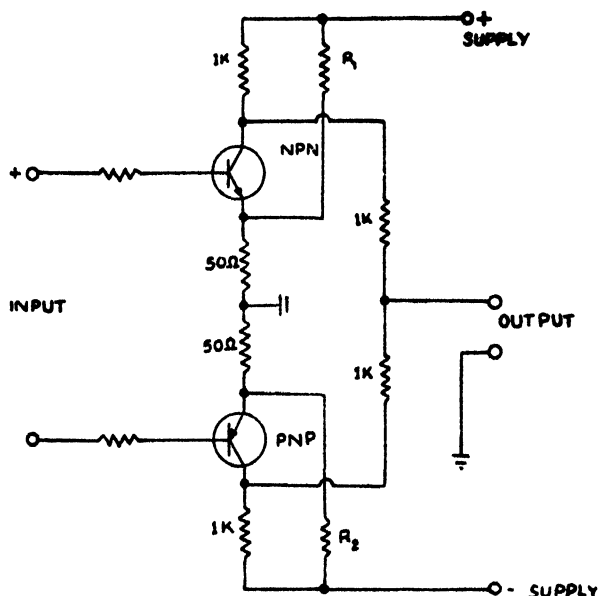


Fig. 1

A selecting circuit with two complementary transistors

Operator's cord circuit

The operator's cord circuit is provided with additional double-pole single-throw switches connected at one end across suitable different tapped points of a resistor as shown in Fig. 2. The resistor having its middle point earthed, is connected across a battery. The other ends of the switches are connected to the ring key as shown in Fig. 2. When calling any particular subscriber, the operator inserts the calling plug into the jack of the required party line and after operating the ring key, presses the appropriate switch corresponding to the subscriber number in the party. Thus, the required equal positive and negative voltages are connected to the lines of the party and the selector unit of the required subscriber only is operated and his bell starts ringing.

Subscriber's apparatus

The circuit of the selecting unit in the subscriber's set for ringing is shown in Fig. 3. A separate D.C. bell is provided and it works from the local battery when the station is called. When the subscriber takes up his receiver, the cradle switch contacts disconnect the selector unit from the lines; simultaneously, the telephone set is connected to the lines and conversation carried out. The selector units at the different

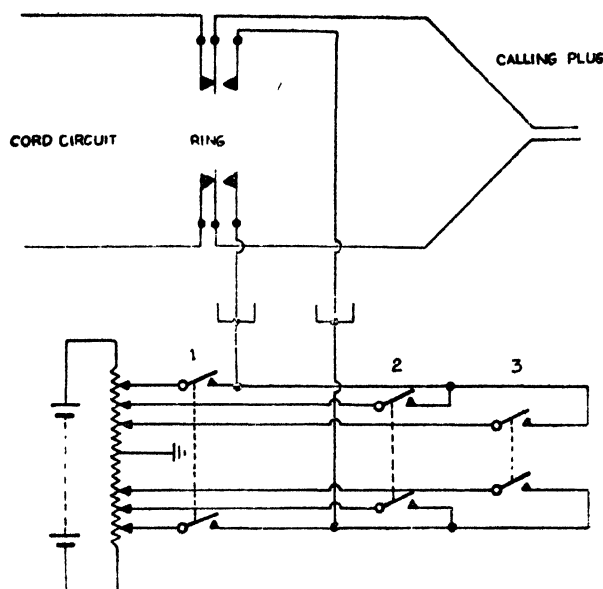


Fig. 2
Operator's cord circuit

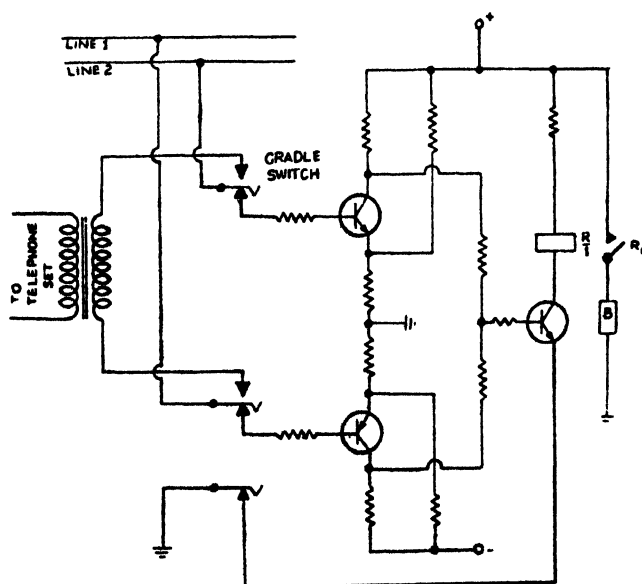


Fig 3
Circuit of a selecting unit in subscriber's set for ringing

subscriber sets are given such values of R_1 and R_2 that they are operated by the application of different distinct values of D.C. voltages. When any subscriber takes up his telephone set for calling, the lines are looped and the calling lamp indicator glows at the exchange. With the help of the operator, any subscriber can get connection with any other subscriber within his own group. The exchange voltage of 22 volts exceeds the operating voltage of any of the subscribers and so when speech transmission takes place, there is no possibility of any of the selectors being operated.

Merits of the system

The system has the following advantages over the usual party line telephone working :

- (i) In each party using the same pair of lines, there may be as many as twenty subscribers against the maximum number of six or so in the usual system;
- (ii) When any subscriber is called, the bells of the other subscribers are not affected ; and hence the uncalled subscribers are not disturbed;
- (iii) The subscriber is not required to be sufficiently alert for distinguishing the particular type of ring for his call;
- (iv) The operator is not required to send different numbers of ringing current and hence he is not required to be very careful when calling; and
- (v) As all the bells are not connected across the lines and all of them do not ring simultaneously, and also, as the selecting units draw either no current or very small currents, the lines are not overloaded during calling and a high ringing current is not required to be sent. Also, a small D.C. power is necessary during calling.

Conclusions

It is true that additional transistor selecting units are required in a system and this involves additional cost, but the price of transistors is likely to come down and it may not be so costly to have additional selecting units. As the advantages of the system described are many they may be used with advantage in all party line telephones working in a C.B. system.

Acknowledgments

The author thanks Prof. C. S. Ghosh, Head of the Electrical Engineering Department, University of Roorkee, Roorkee, for the encouragement given by him in carrying out the work presented in this paper.

References

1. J. Atkinson. 'Telephony—Vol. 1: General Principles and Manual Exchange Systems'. *Sir Isaac Pitman & Sons, Ltd.*, 1961.
2. P. N. Das. 'Gate Circuits with Semiconductor Devices'. *Journal of the Institution of Telecommunication Engineers*, vol. 9, no. 12, December 1963.

NEAR END INFRA-RED FILTERS FOR I. R. COMMUNICATION SYSTEMS*

K. R. Wadhera

Non-member

Defence Science Laboratory, Delhi

Summary

This paper relates to design and development of infra-red filters to transmit the near end infra-red band and attenuate the visible as well as the far end infra-red bands. Filters of this type designed and developed are: (i) plastic films of polyvinyl alcohol with two different dyes on glass plates, and (ii) plastic films of polyvinyl alcohol with two different dyes laminated between two glass plates and are characterized by the transmission band from 0.8 micron to 2.8 microns with transmittance percentage from 70 to 80 over the above transmission band, and with transmittance percentage from 3 to 10 over the attenuation bands. The effect of 'concentration of dyes' and 'thickness of film' on transmission characteristics has been studied. The effect of different dyes on sharpness of cut-off has been examined. These filters have their application in infra-red communication system terminal equipment.

1. Introduction

The near end and far end infra-red waves can be utilized for communication and guidance respectively. The near end infra-red waves were used for the purposes of communication during the Second World War mainly as a result of experiments carried out in Germany, the U.K. and the U.S.A., much of which is unknown. No systematic study on this subject has been made so far in this country.

Infra-red communications which can be established generally over a distance of 10 to 20 miles have the following advantages :

- (i) Privacy of communication as a result of narrow band width, lack of side lobes and forward scatter as well as easy removal of visible band by optical filter ;
- (ii) Freedom from interference as a result of narrow band width ;
- (iii) Securing of additional channels over and above radio channels in use ;
- (iv) Simplicity and low cost of equipment ; and
- (v) Long range capability both for day and night operation.

To establish reliable infra-red communication systems, it is necessary to make intensive studies on terminal equipment and devices like infra-red sources, modulators and detectors, infra-red filters of all types, and propagation of infra-red waves.

* Written discussion on this paper will be received until July 31, 1965.

This paper was received on March 15, 1965.

2. Earlier works on infra-red filters

Scientists in foreign countries have worked on a variety of infra-red filters for different wave bands.

Banning¹ has worked on the practical methods of making and using multilayer filters. This type of filters is prominent for the band between 0.3 to 1.5 microns. There are also a few filters of this type in 1.5 micron range, but most of them are in the 0.3 to 0.8 micron band. As the constituents required for the preparation of such filters are not available and also the range required by the author is different, this type has not been considered.

Blout, *et al*² have described the method of preparing infra-red filters using polyvinyl chloride and polyvinylidene chloride. These filters are of the absorption type and consist of organic dyes dissolved in plastics. The author of this paper has made infra-red transmitting filters by the conversion of the plastic supporting medium itself to a light absorbing structure rather than by the addition of extrinsic absorbing substances. Due to non-availability of the constituents, it has not been possible to try this type of filter.

Further, Blout, *et al*⁴ and also Shenk, *et al*³ have published works on infra-red filters.

3. Present work

The work presented in this paper relates to the development of near end infra-red filters from films of polyvinyl alcohol with different dyes either on glass plates or laminated between two glass plates. Three types of filters have been developed: (i) filters in which the plastic itself has been used as the supporting material; (ii) filters in which the plastic film has been deposited on a glass plate and baked after it has dried up; and (iii) filters in which a very thin plastic film has been laminated between two glass plates of equal dimensions and thickness.

4. Design considerations

Infra-red filters are designed to transmit the maximum of infra-red and the minimum of usual radiation for a particular system. The infra-red filters evolved and discussed in this paper have been designed to be used with a tungsten filament lamp source.

The effectiveness of a filter for the near end infra-red region can be described by comparing the transmission of radiation affecting the eye with the transmission of radiation which will actuate the receiver.³ The effective visual transmission of a filter, T_v , is given by

$$T_v = \frac{\int \psi_\lambda T_\lambda I_\lambda d\lambda}{\int \psi_\lambda I_\lambda d\lambda} \quad (1)$$

where λ is the wavelength, ψ_λ the relative luminosity function for the eye, T_λ the transmission of the filter and I_λ the spectral intensity of the source.*

*When λ is used with ψ , T and I , it is to be treated as a suffix.

The effective infra-red transmission T_r , is given by

$$T_r = \frac{\int R_\lambda T_\lambda I_\lambda d\lambda}{\int R_\lambda I_\lambda d\lambda} \quad (2)$$

Theoretically, the integrals are to be taken from $\lambda = 0$ to $\lambda = \infty$, but actually, the integration needs only to extend over the limited wavelength range in which the increment makes a significant contribution. The values of T_λ , I_λ , R_λ and ψ_λ have been taken from another paper.³

It will be noted that T_r differs for different filters when used with different receivers.

For a particular receiver, the figure of merit M , of an infra-red filter can be expressed by the ratio $\frac{T_r}{T_v}$. The merit ratings increase as the transmission curve is moved to longer wavelengths, since the visible transmission decreases at a greater rate than the infra-red transmission.

5. Fabrication technique employed

The glassware used for the preparation of the solution were first thoroughly cleaned with distilled water. A weighed quantity of polyvinyl alcohol was dissolved in a measured quantity of distilled water. In order to dissolve the polyvinyl alcohol powder completely in water, the above solution was stirred by a mechanical stirrer for about 7 hours. This solution and a weighed quantity of dye, also dissolved in distilled water, were then allowed to stand at rest for one night, so that the air bubbles formed in the solution during the process of dissolving may disappear. For one trial, the dye used was naphthol green B and for the second trial, the dye was calcomine diazo blue B₂RD.

Next day a measured quantity of the solution was poured over plates of methyl methacrylate sheet and these plates were dried up at room temperature. It took about 38 hours for the film to dry. Since polyvinyl alcohol is a hygroscopic material, it takes a long time for the film to dry. Also, the humidity of the atmosphere was high. The dimensions of the film were selected as 7.7 cm. \times 4.8 cm. to enable this to be used with Perkin Elmers infra-red spectrophotometer no. 221. With this particular spectrophotometer, only rectangular films of 7.7 cm. \times 4.8 cm. size could be used satisfactorily for accurate measurements. After the film was dry, it was kept in an oven maintained at 100°C. for about 6 hours for baking. Next the films were stripped off from the methyl methacrylate sheet plates. It is only with this particular sheet that the films could be stripped off. The thickness of the film thus obtained was 0.05 mm. The spectral characteristics of this film framed in a cardboard frame are shown in Fig. 1.

For the second trial, glass plates of 7.7 cm. \times 4.8 cm. were procured and another solution, prepared in the same manner as explained earlier, was poured over the glass plates. The same process was adopted for drying and baking the coated glass plates. In this case, the baked film could not be stripped off from the glass plate. The thickness of the film was found to be 0.05 mm. The spectral characteristics of these filters are shown in Fig. 2. This plastic film, if necessary, can be polished to restore its mirror-like finish.

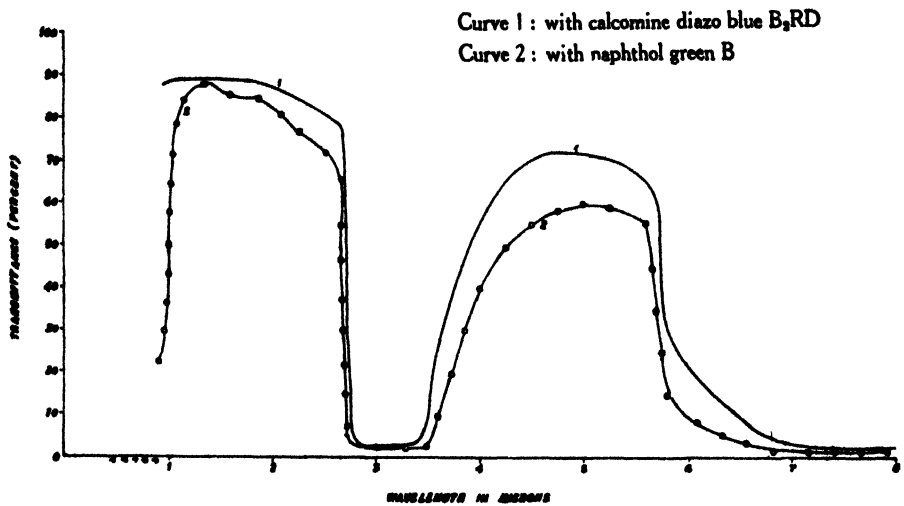


Fig. 1

Transmission curves of self-supported plastic filter for near infra-red band

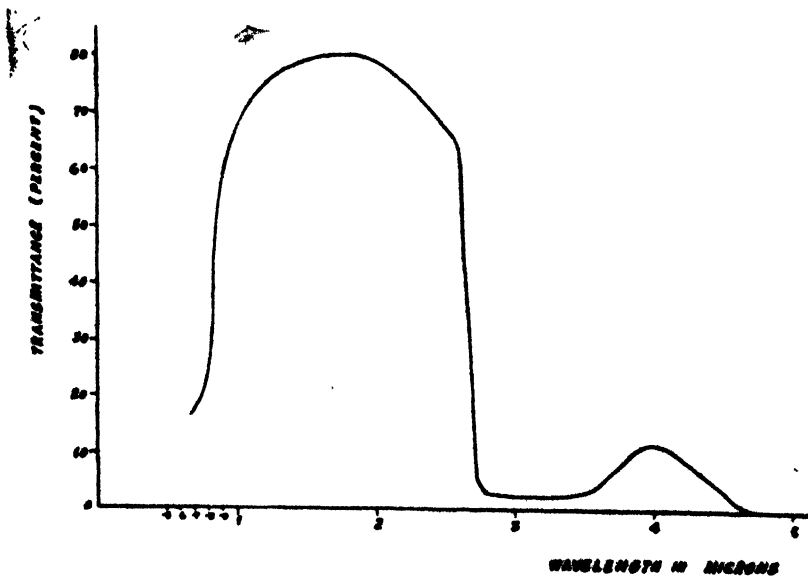


Fig. 2

Transmission curve of a filter for near infra-red band

For the third trial, a thin film of dyed polyvinyl alcohol solution, obtained as explained in the first two trials, was laminated between two glass plates of 7.7 cm. \times 4.8 cm. \times 0.285 cm. These laminated films were dried and baked in the same way as in the previous two cases. In this case, the thickness of the film was very small. The spectral characteristics of this type of filter are shown in Fig. 3.

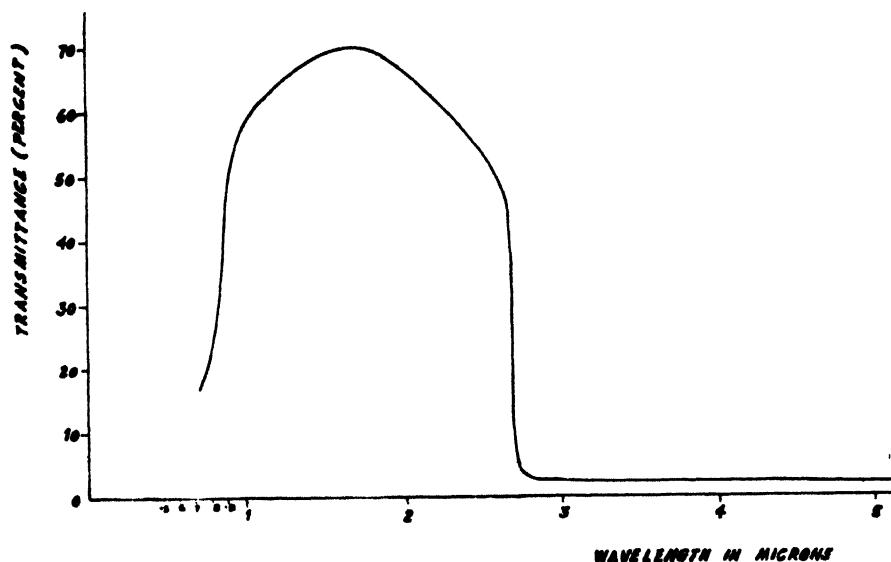


Fig. 3

Transmission curve of a filter for near infra-red band

All the three trials were repeated with both the dyes separately many times with different concentrations of constituents and different thicknesses of film.

6. Stability of filters

The stability of the above types of filter has been found to be good up to 100°C., but if heated beyond this, the films get charred. Both the plastic film and the glass laminated types of filters are essentially inert at room temperature and in humidity. At present, they can be used continually at temperatures up to 100°C.

The strength of the filters depends upon the relative humidity of the surrounding atmosphere. The film is water soluble, but its sensitivity to water can be decreased by formaldehyde, chromium components, certain dyestuffs, dibasic acids, and copper, zinc and ammonium compounds. These filters are also mechanically strong and hard, and can be easily moulded and bounded. These types of filters are effective over the wavelength range of 0.8 to 2.6 microns in the near infra-red band. The filters should be

as small in volume as possible *i.e.*, very thin and as large in area as possible, for cooling.

7. Transmission characteristics of filters

The transmission characteristics of the filters were measured with Perkin Elmers infra-red spectrophotometer no. 221, under the following conditions :

- (i) The source of light was a Nernst glower ;
- (ii) The prism used was of sodium chloride ;
- (iii) The range of the spectrophotometer with a sodium chloride prism was 1 to 15 microns ;
- (iv) The speed of the instrument was maintained at $2/4$;
- (v) Resolution of the instrument was 927 ;
- (vi) Response was 1,100 ;
- (vii) Gain of the instrument was 2 ;
- (viii) Suppression of the instrument was nil ; and
- (ix) The scale was 1:1.

The characteristics of the filters taken under the above settings are shown in Figs. 1, 2 and 3 for each sample prepared. The effects of : (i) the concentration of the dye ; and (ii) the thickness of the film on transmission characteristics have been studied in Figs. 4 and 5. From a study of Figs. 1 to 5, the following observations can be made :

- (i) From Figs. 1, 2 and 3, it can be said that the spectral characteristics of Fig. 3 are more suitable for use in a communication system than those of Figs. 1 and 2. The percentage of transmission in the case of unsupported and dyed polyvinyl alcohol film (Fig. 1) is higher than that in the other two cases (Figs. 2 and 3). That is, if the transmission in the case of Fig. 1 is 90%, the transmission in the other two cases will be 75 to 80%. In the case of unsupported PVA film, there are two points at which the percentage transmission decreases and then increases. In the other two cases, after the cut-off point is reached at 2.65 microns, the percentage transmission does not generally increase up to 15 microns which can be scanned with the available spectrophotometer. The effects of concentration and thickness of film have been studied with reference to a plastic filter of PVA with two different dyes on glass plates ;
- (ii) The effect of concentration of naphthol green B dye can be seen from Fig. 4 while the thickness has remained the same. It is observed that with increase in the concentration of the dye, the transmittance percentage in the pass band just decreases by a very small amount, but the sharpness of the rise and cut-off get improved. In the case of calcomine

diazo blue B₂RD, the effect of concentration of the dye is to decrease the transmittance percentage and the sharpness of the cut-off also gets affected ; and

- (iii) The effect of the thickness of the film dyed with naphthol green B (the concentration of the dye remaining the same) can be seen from Fig. 5. With an increase in the thickness of the film, the transmittance percentage in the pass band decreases by a small amount but the sharpness of cut-off remains almost the same. Also, with smaller thickness, the transmittance does not change beyond the cut-off point.

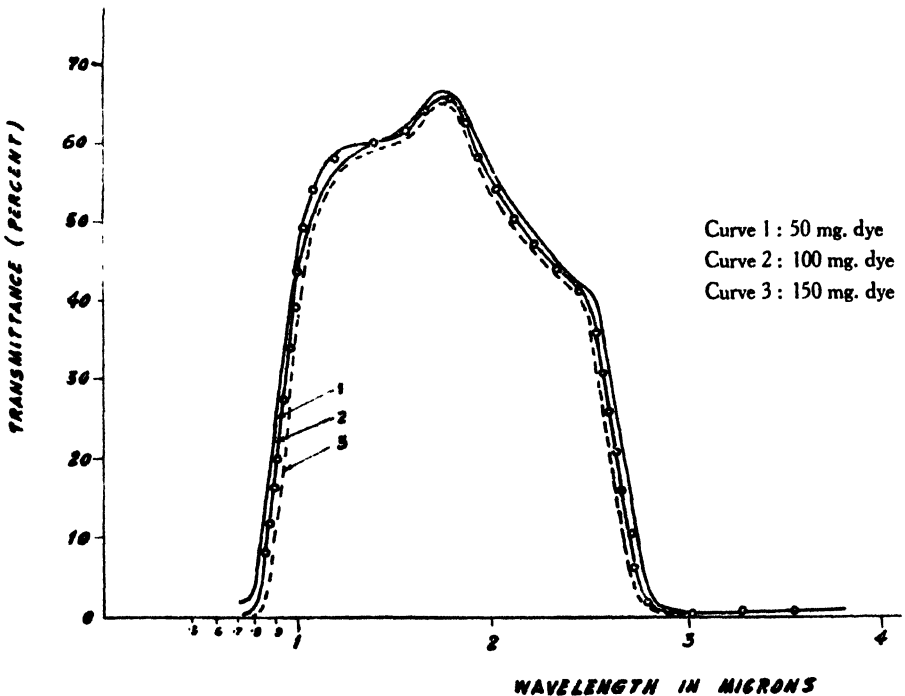


Fig. 4
Transmission curves of filters for near infra-red band

The effect of increase in the thickness of the film dyed with calcomine diazo blue B₂RD, is also to decrease the transmittance percentage ; but the decrease in this case is much greater than in the previous case. In this case, the cut-off is also affected, as can be seen from Fig. 6.

8. Discussion

The plastic filters under discussion are directly dyed polyvinyl alcohol films on glass plate as well as thin plastic films laminated between two glass plates. The advantages of these types of filter are that direct dyes generally have sharper cut-offs.

The efficiency of such filters for a particular wavelength cut-off depends upon the shape of the absorption characteristic which in turn depends upon the molecular structure of the dye used. For satisfactory suppression of side bands, an auxiliary broad band filter may be used to eliminate the unwanted wavelengths. In the near infra-red end, it is

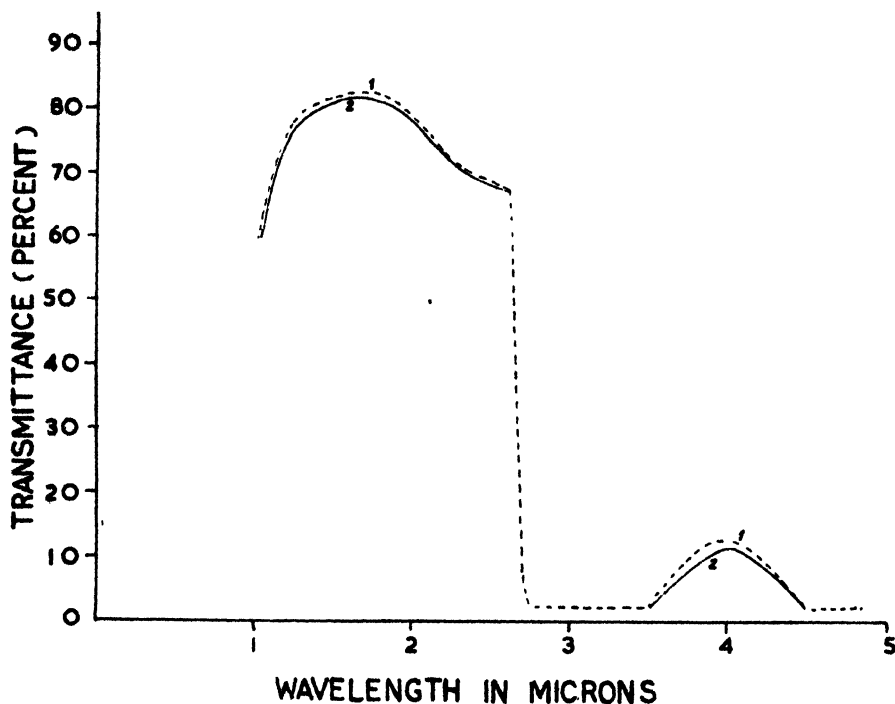


Fig. 5

Transmission curves of filters for near infra-red band

difficult to find suitable auxiliary filter for some wavelengths and these may have to be made of a crystalline semiconducting material such as germanium or silicon. In some cases, the use of auxiliary filter results in an appreciable reduction in peak transmission in the composite filter. When the two are used in conjunction, the transmission of the combined filter differs considerably.

Dyes suitable for infra-red filters produce a gradual sloping of the absorption characteristics on the long wavelength side. Addition of dyes and filters can be made readily, since polyvinyl alcohol has got excellent compatibility characteristics. Dyes in plastic filter is necessary because they absorb all the visible band.

Good self-supporting filters of dyed polyvinyl alcohol could be fabricated without the addition of a plasticizer, since the film contain 2 to 3% water at 35% relative humidity, and water has a plasticizing action. Plastic filters absorb a large percentage of visible light and transmit the near infra-red wavelengths satisfactorily.

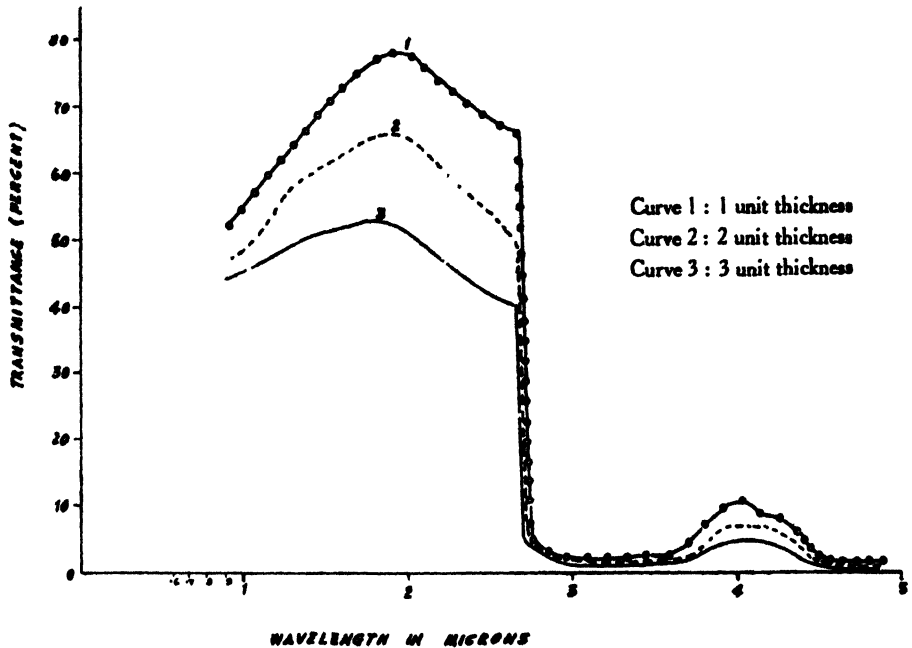


Fig. 6
Transmission curves of filters for near infra-red band

9. Conclusions

From the discussion, the following conclusions can be arrived at :

- (i) Near end infra-red filters suitable for infra-red communication system have been developed from : (a) plastic films of polyvinyl alcohol with two different dyes on glass plates ; and (b) plastic films of PVA with two different dyes laminated between two glass plates.

The transmission band is from 0.75 to 2.6 microns in the case of naphthol green B dye and from 0.65 to 2.65 microns in the case of calcomine diazo blue B₂RD ;

- (ii) The effect of concentration of dyes is to increase or decrease the transmittance percentage depending upon the nature of the dye and its concentration. In the case of naphthol green B dye, the higher the concentration the better is the cut-off on either side, and the effect on the transmittance percentage very little, whereas in the case of calcomine diazo blue B₂RD, its higher concentration affects the transmittance percentage and also the cut-off ;
- (iii) The effect of thickness of the film is to affect the transmittance percentage depending upon the nature of the dye as well as the thickness ; and

- (iv) The effect of different dyes on the sharpness of cut-off is evident in the case of naphthol green B, whereas this effect is not much pronounced in the case of calcomine diazo blue B₂RD. This effect may be due to the molecular structure of the dye.

10. Acknowledgments

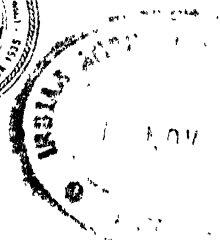
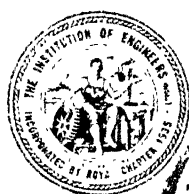
The author expresses his grateful thanks to Prof. S. P. Chakravarti, Director, Defence Science Laboratory, Delhi, for guiding him in the work undertaken and for his frequent discussion on the various points as well as for giving permission to publish the paper. Thanks are also due to Sarvashri Santokh Singh, Officer-in-charge (Electronics) and G. J. Chaturvedi for the help in making filters and to Shri V. Krishna Murty for assistance in taking measurements.

11. References

1. M. Banning. 'Practical Methods of Making and Using Multilayer Filters'. *Journal of the Optical Society of America*, vol. 37, no. 10, October 1947, p. 792.
2. E. R. Blout, W. F. Amon (Jr.), R. C. Shepherd (Jr.), A. Thomas, C. D. West and E. H. Land. 'Near Infra-red Transmitting Filters'. *Journal of the Optical Society of America*, vol. 36, no. 8, August 1946, p. 460.
3. J. H. Shenk, A. S. Hodge, R. J. Morris, E. E. Pickett and W. R. Brode. 'Plastic Filters for the Visible and Near Infra-red Regions'. *Journal of the Optical Society of America*, vol. 36, no. 10, October 1946, p. 569.
4. E. R. Blout, R. S. Corley and P. L. Snow. 'Infra-red Transmitting Filters—2: For the Region 1 to 6 Micron'. *Journal of the Optical Society of America*, vol. 40, no. 7, July 1950, p. 415.
5. W. R. Sorenson and T. W. Campbell. 'Preparative Methods of Polymer Chemistry'. *John Wiley & Sons, Inc.*, 1961.
6. L. W. Nichols. 'Optical Filtering'. *Proceedings of the Institute of Radio Engineers*, vol. 47, no. 9, September 1959, p. 1569.
7. W. Summer. 'Ultra-violet and Infra-red Engineering'. *Sir Isaac Pitman & Sons, Ltd.*, 1962.

E
L
E
C
T
R
O
N
I
C
S
&
T
E
L
E
C
O
M
M
U
N
I
C
A
T
I
O
N
E
N
G
I
N
E
E
R
I
N
G
D
I
V
I
S
I
O
N

JOURNAL OF THE INSTITUTION OF ENGINEERS (INDIA)



VOLUME 46

NUMBER 1

PART ET 1

SEPTEMBER 1965



PUBLISHED BY THE INSTITUTION

8 GOKHALE ROAD

CALCUTTA

Rs. 2.50



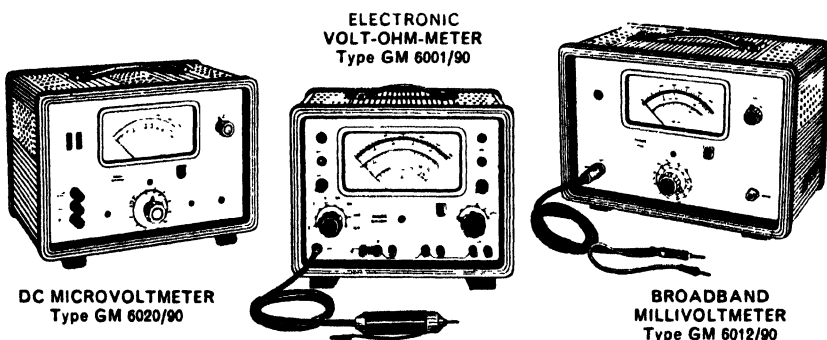
PHILIPS

Electronic Instruments

for Technical Institutes and Scientific Laboratories

Philips manufacture in India a wide range of electronic measuring instruments—Multimeters, Oscilloscopes, Electronic Test Instruments, Vacuum Tube Voltmeters and Industrial Instruments—to meet the growing needs of industries, technical institutes, scientific laboratories and service shops.

Illustrated here are a few Electronic Test Instruments for technical institutes and scientific laboratories:



DC MICROVOLTMETER
Type GM 6020/90

ELECTRONIC
VOLT-OHM-METER
Type GM 6001/90

BROADBAND
MILLIVOLTMETER
Type GM 6012/90

Other Philips Electronic Instruments for Technical Institutes and Scientific Laboratories
Multimeters
Vacuum Tube Voltmeters
Oscillators LF/RF
Oscilloscopes
LCR Bridges
Electronic Service Instruments
Conductivity Bridges, etc.

These instruments incorporate the famous Philips international know-how, and conform to rigid standards of performance.

Philips' qualified electronic engineers are always available for consultation on your particular requirements and problems. And Philips' *after-sales service is guaranteed.*



PHILIPS

for science and industry

PHILIPS INDIA LIMITED Calcutta • Bombay • Madras • New Delhi

THE JOURNAL

OF

The Institution of Engineers (India)

INDEX

ELECTRONICS AND TELECOMMUNICATION ENGINEERING DIVISION

VOL. 46, PTS. ET 1 to ET, 2, 1965-66

	Page
Address of Dr. A.K. Chatterjee, Retiring Chairman	1
Address of Brig. M.K. Rao, Chairman, Electronics and Telecommuni- cation Engineering Division	55
Advani, J.G. and Gupta, O.P.: Network Structures for a Special Class of Minimum Biquartic <i>PR</i> -Functions	31
Advani, J.G., and Kesavan, B.: Synthesis of an A.C. Lead Transfer Function for Minimum Sensitivity by Parallel Ladder Procedure ..	39
Aggarwal, G.K.: One Amplifier Simulation of Third Order Systems ..	6
Chatterjee, S.K.: Classification of Modes in Electromagnetic Waveguides	13
Classification of Modes in Electromagnetic Waveguides	13
Gupta, O.P., and Advani, J.G.: Network Structures for a Special Class of Minimum Biquartic <i>PR</i> -Functions	31
Harbans Lal, Mehrotra, R.R., and Tyagi, B.K.: Transistor Rectangular Pulse Generator	49
Kesavan, B. and Advani, J.G.: Synthesis of an A.C. Lead Transfer Function for Minimum Sensitivity by Parallel Ladder Procedure ..	39
Mehrotra, R.R., Tyagi, B.K., and Harbans Lal: Transistor Rectangular Pulse Generator	49
Network Structures for a Special Class of Minimum Biquartic <i>PR</i> -Functions	31
Nityanandan, B.N.: Wave form Analysis of E.D.A. Solutions and De- termination of Describing Functions with the Vectrometer ..	60
One Amplifier Simulation of Third Order Systems	6

THE INSTITUTION OF ENGINEERS (INDIA)

	Page
Synthesis of an A.C. Lead Transfer Function for Minimum Sensitivity by Parallel Ladder Procedure 	39
Transistor Rectangular Pulse Generator 	49
Tyagi, B.K., Harbans Lal, and Mehrotra, R.R. : Transistor Rectangular Pulse Generator 	49
Waveform Analysis of E.D.A. Solutions and Determination of Describ- ing Functions with the Vectrometer 	60

THE JOURNAL

OF

The Institution of Engineers (India)

SECRETARY & EDITOR : B. Seshadri, B.Sc., A.I.I.Sc., D.I.C. M.Sc.(Eng.), M.I.E.

TECHNICAL EDITOR : B. R. Subramanyam, B.Sc., B.E., A.M.I.E.

The Institution of Engineers (India) as a body accepts no responsibility for the statements made by the individual authors.

The Institution of Engineers (India) subscribes to the Fair Copying Declaration of the Royal Society and reprints of any portion of this publication may be made provided that reference thereto be quoted.

Vol. XLVI

SEPTEMBER 1965

No. 1, Pt. ET 1

CONTENTS

Page

ELECTRONICS AND TELECOMMUNICATION ENGINEERING DIVISION

Report of the Paper Meetings in the Electronics and Telecommunication Engineering Division at the Forty-Fifth Annual General Meeting, Lucknow, February 19-26, 1965

Address of Dr. A. K. Chatterjee, (M.) Retiring Chairman **1**

1. One Amplifier Simulation of Third Order Systems. G. K. Aggarwal.
Non-member **6**

2. Classification of Modes in Electromagnetic Waveguides. S. K. Chatterjee,
Non-member **13**

Electronics and Telecommunication Engineering Division Board

The President (*Ex-officio*)

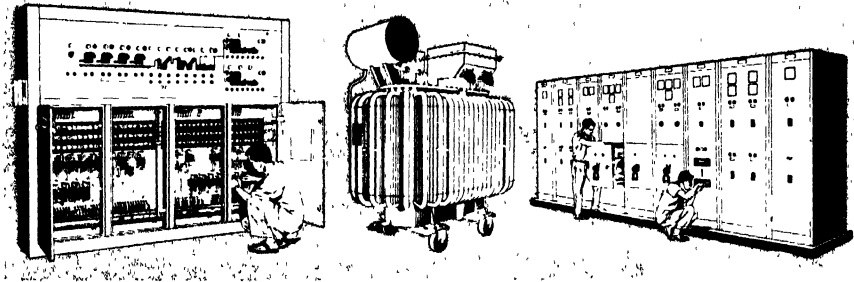
Brig. M. K. Rao (*M.*) Chairman

Prof. S. P. Chakravarti (*M.*)

Lt.-Col. S. Mishra (*M.*) (*Co-opted*)

Automatic Control Group

Prof. V. V. Sarwate, Chairman



**YOU CAN GET
ALL YOUR ELECTRICAL REQUIREMENTS
FROM ONE SOURCE**

■ Siemens make a comprehensive range of electrical equipment... whose high standards are internationally well-known. Whatever your needs, Siemens can meet them—whether individual units or complete plants.

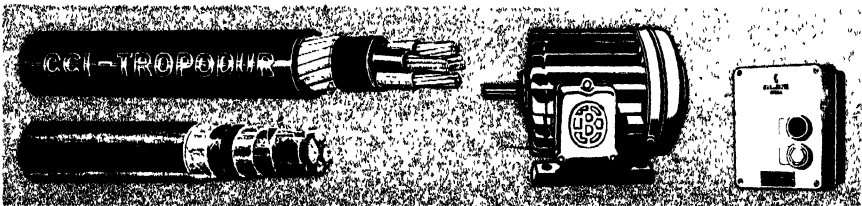
■ Siemens engineers are specialists. They are thoroughly trained to deal with the special problems of particular industries—and to advise on the diverse applications of electrical equipment.

■ Siemens have a wide network of dealers. As a result, products reach customers promptly in any part of the country

SIEMENS vast technological resources are behind every item of Siemens equipment... behind every aspect of Siemens service, whether planning, designing, supplying, installation, or After Sales Service.

For your specific requirements contact any Siemens branch office, or your nearest Siemens dealer.

POWER FOR PROGRESS—THROUGH SIEMENS



Licences: Bharat Bijlee Ltd.
for Motors and transformers
Cable Corporation of India Ltd.
for cables

**SIEMENS ENGINEERING & MANUFACTURING CO.
OF INDIA LTD.**
Bombay • Calcutta • New Delhi • Madras • Bangalore
Visakhapatnam • Ahmedabad • Lucknow • Nagpur
Hyderabad • Trivandrum • Rourkela • Patna

**REPORT OF THE PAPER MEETINGS IN THE ELECTRONICS AND
TELECOMMUNICATION ENGINEERING DIVISION AT THE FORTY-
FIFTH ANNUAL GENERAL MEETING, LUCKNOW,
FEBRUARY 19-26, 1965**

Dr. A. K. Chatterjee, A.M.I.E.E., M.S., Ph.D., M.I.E., Retiring Chairman, Electronics and Telecommunication Engineering Division, opened the proceedings by delivering the Divisional Address, and also presided over the proceedings.*

**DR. A. K. CHATTERJEE (M.), RETIRING CHAIRMAN,
ELECTRONICS AND TELECOMMUNICATION ENGINEERING DIVISION**

I have great pleasure in extending a very cordial welcome to all the members and guests who have taken all the trouble to attend the 45th Annual Convention of the *Institution* and, in particular, this Paper Meeting of the Electronics and Telecommunication Engineering Division. I hope you will be able to gainfully utilize your time in discussions and exchange of technical knowledge. I also hope that your stay at this beautiful city of Lucknow will be enjoyable.

It is customary for the Chairman to review the progress in a field of engineering related to the Division at the Annual Convention. Last year, in my Address, I referred briefly to the progress in 'control engineering' and some significant developments, such as adaptive and optimal control systems. It seems worthwhile to look into the field of computers, and consider our own problems *vis-a-vis* computer applications.

Computing machines, though made as early as the 17th century, have undergone fantastic developments only during the last decade and a half. These developments have been on two separate lines, differing mainly on the components and principle of operation involved. The two broad classifications are thus the analogue and the digital computers. The review that follows will mainly be in terms of these two broad classifications. However, it must be mentioned that of late the hybrid techniques involving both analogue and digital computer principles are finding increased applications.

Progress in analogue computer technology

Broadly speaking, analogue computer is a device in which the variables are analogous to those of the problem to be solved. A simple example of an analogue computing equipment is the common slide rule. In the 1920s, efforts were made to speed up the process of more complex mathematics putting the electrons to work and the electrical analogue computer was born. Such computers perform a direct simulation of a physical system. A good example is the A.C. network analyzer used by the power industry for planning the electrical system operation and growth. This direct analogue device is less versatile, however, than the mathematical analogue computer in which the individual parts are the analogues of the terms in the equations describing the system under study. The mathematical analogue computer contains devices that perform

* The Paper Meetings in the Electronics and Telecommunication Engineering Division commenced at 2.00 p.m. on February 22, 1965.

various mathematical operations such as addition, subtraction, multiplication and integration. The majority of the analogue computers in use are of this type, and have come to be known as 'differential analyzers'. A mechanical device was first built in 1931 at the Massachusetts Institute of Technology, U.S.A., by Dr. Vannevar Bush.

These analogue computers have since been developed and the majority of them incorporate electronic devices such as operational amplifiers, etc. The electronic differential analyzer has been an extremely useful tool in solving the mathematical equations of physical systems. Thus, any complex system whose performance may be written down in terms of differential equations could be studied by setting up on a computer in the laboratory. A unique and important feature of the simulation of the system in the laboratory is the ability to give the operator a physical 'feel' for the problem being solved, since the computer behaves, in a very real sense, just as the dynamic system under investigation. In the area of nonlinear system analysis and design, the use of analogue computer became almost indispensable. A large number of problems encountered in engineering practice are inherently nonlinear, and analogue computers are invaluable aids in the study of such systems. Besides this, the accuracy and speed obtainable with analogue computers are sufficient for a wide variety of application in simulation and control.

Apart from the study of complex systems, analogue computers have been used as parts of the control loop for mechanization. Examples of such use are radar tracking systems of an aircraft, interceptor and fire control. Other examples of the systems in operation today which use analogue computers for actuation are intercontinental ballistic missiles, training simulation devices of various types such as flight trainers, steel mill tandem cold rolling mill controls, economic dispatch computers for the automatic control of electrical power systems and many others. These examples of use need a special kind of job and hence they are known as special purpose analogue computers to distinguish them from the general purpose analogue computer used in the laboratory for study of any kind of problem. Although this kind of computer does not have the broad programming flexibility of a general purpose computer, this is an advantage rather than a limitation. For example, great precision and accuracy can be designed into the special purpose computer and the cost can be relatively low since the computer contains only those components needed for a given application. During the past decade, the use of such special purpose analogue computers in the field of industrial process control has increased by leaps and bounds. Petrochemical industries, iron and steel, power and many others have used such computers for optimization of process operations.

Progress in digital computers

In 1940, the digital computer was born. This was another electronic approach to solve complex mathematical equation. The first ones used relays or vacuum tubes to apply the very simple system of recognizing two states of an object; yes or no, true or false, 0 or 1. This method of recognizing 0 or 1, called the binary system, is the basic tool of all digital computers. In the early 1950's, only a few digital computers were built by the universities in the U.S.A. Most of the educational institutions possessing a computer initiated computer courses for the faculty and the post-graduate students. The proliferation of computer was rapid and during the last decade computers were to

be found in almost every sector of economy in technically advanced countries like the U.S.A., U.K. and West Germany.

The digital computer may be defined 'as a device that does arithmetic.' Actually, all a digital computer can do is to add, subtract, multiply and divide, along with such other operations as simple decisions, etc. Strictly speaking, it does only one operation and that is, just add. The other arithmetic manipulations follow from this basic operation. But the power of digital computer lies in carrying out this operation at fantastic speeds. Thus, some of the modern computers does the addition operation in a few microseconds. The Control Data 6600 system, the fastest computer at present, takes only 0.4 microsecond for addition.

The application of digital computers can be divided into three broad classifications; data processing, science and engineering application and lastly real-time control or, as sometimes called, on-line control. The electronic data processing or E.D.P., as it is usually called, refers to the application of computers for business and commercial purposes. The military system market in the U.S.A. has always been a keystone of the data processing industry's technological development. A major trend which has occurred in the last decade has been the rapid rise in the development of computer services. Establishment of computing centres by the manufacturers of computer equipment has resulted in the application of the data processing techniques by many smaller firms in their operations using the local E.D.P. service centre. This avoids a major investment in a machine installation.

The Federal Government and the manufacturing sector of the economy in the U.S.A. are the largest users of data processing equipment. In this sector, computers are utilized in a wide range of standard functional areas such as production planning, financial and accounts processing, warehouse and inventory control of research and development data analysis and calculations. The transport industry such as railroads, installed computers for accounting and financial operations as well as for processing the freight traffic and rate calculation. The communications industry, public utilities, wholesale and retail trade, the financial institutions such as banks and even service organizations like hotels, hospitals and law associations have also used E.D.P. for their normal operations.

In the field of scientific and engineering applications, digital computers have been used for a variety of uses, purposes numerous to enumerate. These include the calculation involved in plant designing, construction operation and other engineering activities.

Today there is considerable activity in the field of real-time controls or on-line computer control. Earlier applications of this technique were in the form of computer-assisted numerical machine tool control systems in the manufacturing industry. The power industry installed real-time control of load assignment and dispatching. One of the most significant computer applications in recent time is in the field of process control. Process control system performs one or more of the following functions in the operation of a complete process : data reduction, data logging and complete data control. If the system performs all the three functions, it is termed a 'closed loop' operation. More than 50 closed loop systems have been installed in the process industries, primarily

for petrochemical applications. The use of the digital computer for process control is very recent, and dates back to March 1959, when the first chemical plant was put under the direct control computer. By 1963, about 310 process control computers have come into existence in various industries as shown¹ in Table 1.

Table 1
Data of process control computers in industry

Industry	U.S.A. and Canada	France	U.K.	Japan	Germany	Italy	Other countries	Total
Power	61	17	5	9	1	4	2	99
Chemical	36	5	1	3	1	—	3	49
Steel	31	4	10	2	5	2	5	59
Petrol	21	1	1	—	—	—	1	24
Paper	18	11	—	1	1	1	—	22
Gas	7	—	—	—	1	—	1	9
Cement	3	—	—	2	—	—	—	5
Television	4	—	—	—	—	—	—	4
Miscellaneous	27	8	2	—	—	—	1	38
Total	208	36	19	17	9	7	13	309

Rapid improvement in digital computer technology has made this class of computers faster, more versatile and accurate; and placed the analogue computer to an inferior position. But to the system designer, the mathematical model offered by the analogue type still remains indispensable. Hybrid computing elements combining both analogue and digital techniques are being employed and analogue computers are becoming faster. We thus have the operational digital integrators, multipliers and resolvers replacing the corresponding conventional components, which not only speed up solutions and increase accuracy, but also maintain the direct model of computation.

Computers and their use in India

The A.C. network calculator at the Indian Institute of Science, Bangalore, was installed in 1950, and has since then been the workhorse of power industry in the country. The electronic differential analyzer, *i.e.*, the mathematical analogue computer, has found its application only in a few organizations in the country, and the total number in use at present may not be more than 10.

The applications of E.D.P. are to be found in TISCO, the Life Insurance Corporation of India, Hindustan Steel Ltd., Delhi Cloth Mills Ltd., and a few such organizations. The total computer installations which are used for this purpose is expected to be of the order of 25 or so in the near future. The scientific and engineering digital computer

installations are at the Tata Institute of Fundamental Research, Bombay ; the Delhi University; the Indian Institute of Technology, Kanpur; the Guindy Engineering College, Madras ; the University of Roorkee; and the Defence Laboratories, Hyderabad. About a dozen organizations like the Central Mechanical Engineering Institute, Durgapur, the A.I.T.R.A., etc., have placed orders for such computers.

The above review indicates clearly that our use of these modern tools is rather very meagre. The use of these devices is often erroneously related to the standard of living and a conclusion is drawn that computers will bring in a new unemployment threat. It is, however, undeniable that computers can contribute to increase productivity by a marked increase in material wealth. A country like ours requires rapid rise in productivity in order to offer a decent standard, of living. To this end, automation will undoubtedly play an important part and help in bringing the vast production of goods that we need in future. The increase in production will naturally create new jobs in the distribution of goods, such as transport, shipping, etc., which will compensate for the corresponding reduction of employment in industry through automation. Thus, the problem is to fully exploit the economic potential available in the country with only a few working in the industry, and this calls for good management with the help of computers.

Computers can aid the planner in making a thorough investigation of the various alternatives for action at a rapid rate, and it must be admitted that we are guilty of not utilizing fully the potentialities of a valuable tool like the computer in the various sections of our economy. It has been claimed that electronic digital computers are being made in China since 1958 and are now serving many branches of their national economy. Computers have been used for designing and building more than a dozen huge dams. As against these, our present method of approach is outdated and ineffective. That the qualitative evaluation of the various alternatives involved in a complex decision in matters of vital importance, like food production, requires the use of computers need hardly be emphasized. Let us hope that in the years to come, this vital tool for working out our Five Year Plans and implementing them will be utilized at all levels and in various sectors of our country to raise the standard of living of our people in the quickest possible time.

Reference

1. D. N. Truscott. 'Computers in Control of Processes'. *Electronics and Power*, June 1964.

ONE AMPLIFIER SIMULATION OF THIRD ORDER SYSTEMS***G. K. Aggarwal***Non-member***Summary**

This paper gives a set of six tables which are found to be useful in synthesizing various forms of third order linear transfer functions, using a chain of inverted L-sections of passive resistor-capacitor elements in conjunction with a single operational amplifier. The actual procedure for synthesizing such transfer functions using this technique is illustrated.

Introduction

In his earlier communications, the author has discussed a most general network configuration which, in conjunction with a single operational amplifier, can simulate any order of linear transfer functions. The network, shown in Fig. 1, consists of a chain of inverted L-sections comprising resistor-capacitor combinations and one operational amplifier to which this chain of L-sections forms a multi-path input-feed passive network.

An impedance-admittance (Z - Y) table, first developed by the author, enables the voltage transfer function of this chain of L-sections (and including the operational amplifier) to be written straightaway without performing actually the usual nodal or star-delta transformation analysis. A thorough treatment of the network has been given for a general form of third order linear systems.¹ The design analysis of the network has also been performed for simulating ten forms of fourth order linear systems.² Also, a very generalized treatment of the network for fourth order linear systems has been presented.³

Contrary to what many authors^{4,5} have apprehended, the above network has yielded itself to a manageable design analysis up to, at least, fourth order linear transfer functions.

In favour of using this technique for special problems where economy of equipment is of paramount importance, it is a suggestion from the author that one would probably fear the imperfections of passive circuit elements less than those of the operational amplifiers which, if used in larger number, introduce errors at every step owing to their departure from the ideal. In all the circuits discussed by the author, the number of passive circuit elements has been kept to the minimum.

The network, shown in Fig. 2, can simulate a large class of third order linear transfer functions, the admittances (Y 's) comprising parallel resistor-capacitor combinations, in general. The purpose of this paper is to enlist a number of alternative combinations of the resistors and the capacitors for the Y 's in this network to simulate various forms of third order linear transfer functions. In selecting these alternatives, an attempt is made to keep the number of circuit elements to the minimum.

* Presented at the Paper Meeting in the Electronics and Telecommunication Engineering Division at the 45th Annual Convention at Lucknow, February, 19-26, 1965.

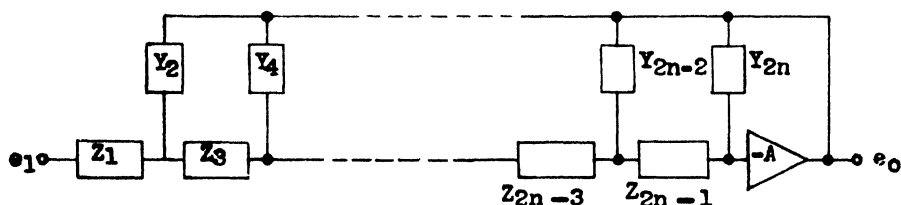


Fig. 1

Network comprising a chain of inverted L-sections

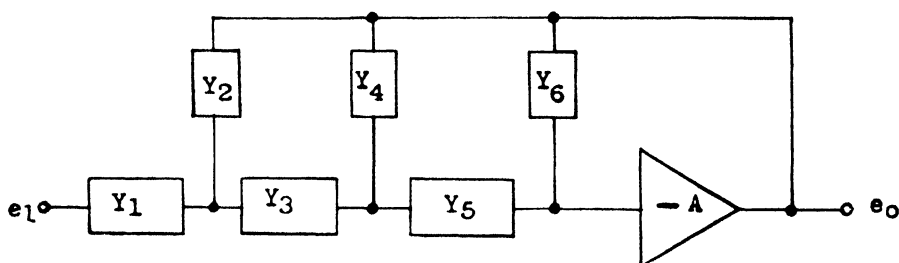


Fig. 2

Network for simulating third order linear transfer functions

Theory

In Tables 1 to 6, the a 's and the b 's are all real, positive, non-zero constants. The range of values of the a 's and b 's for which simulation is possible by choosing any of these alternatives is limited by the fact that the resistor-capacitor values have to be all real and positive.

The transfer function, $\frac{e_o}{e_1}$, of the network in Fig. 2, to which Tables 1 to 6 refer, can be shown to be¹

$$\frac{-Y_1 Y_3 Y_5}{Y_2 Y_3 Y_5 + (Y_1 + Y_2)(Y_3 + Y_4 + Y_5) Y_6 + (Y_1 + Y_2 + Y_3) Y_4 Y_5 + Y_3 Y_6 (Y_4 + Y_5)} \quad (1)$$

The analysis procedure will be to take any possible choice of Y 's suited for simulating the given form of the third order linear transfer function and substitute the chosen values of Y 's in equation (1). Then we need to determine the values of the resistors and the capacitors equating the corresponding terms in equation (1) and in the given transfer function. This analysis will also bring out the restrictions on the system constants, i.e., the a 's and b 's under which that particular alternative can simulate the given form of the linear transfer functions. In general, all these constraints are not common to all the alternatives so that the overall range of applicability of the network as a whole is quite wide. The entire set of alternatives contained in Table 6 has been worked out in an earlier communication.² A simple example taken from Table 2 is worked out here for illustration.

Table 1

$$F(s) = \frac{-b_0}{a_3 s^3 + a_2 s^2 + a_1 s + 1}$$

Resistor	Capacitor	Parallel resistor-capacitor combination	Zero admittance
Y_1, Y_3, Y_5	Y_4, Y_6	Y_2	—
Y_1, Y_3, Y_5	Y_2, Y_4	Y_6	—
Y_1, Y_3, Y_5	Y_2, Y_6	Y_4	—

Table 2

$$F(s) = \frac{-b_1 s}{a_3 s^3 + a_2 s^2 + a_1 s + 1}$$

Resistor	Capacitor	Parallel resistor-capacitor combination	Zero admittance
Y_2, Y_3, Y_5	Y_1, Y_4, Y_6	—	—
Y_3, Y_5	Y_1, Y_6	Y_4	Y_2
Y_3, Y_5	Y_1, Y_4	Y_6	Y_2
Y_1, Y_5	Y_2, Y_3	Y_6	Y_4
Y_1, Y_4, Y_5	Y_2, Y_3, Y_6	—	—
Y_1, Y_5	Y_3, Y_4	Y_6	Y_2
Y_1, Y_5	Y_3, Y_6	Y_4	Y_2
Y_1, Y_3	Y_2, Y_5	Y_6	Y_4
Y_1, Y_3, Y_6	Y_2, Y_4, Y_5	—	—

Table 3

$$F(s) = \frac{-b_2 s^2}{a_3 s^3 + a_2 s^2 + a_1 s + 1}$$

Resistor	Capacitor	Parallel resistor-capacitor combination	Zero admittance
Y_2, Y_5	Y_1, Y_3	Y_6	Y_4
Y_2, Y_4, Y_5	Y_1, Y_3, Y_6	—	—
Y_2, Y_3	Y_1, Y_5	Y_6	Y_4
Y_3, Y_4	Y_1, Y_5	Y_6	Y_2
Y_2, Y_3, Y_6	Y_1, Y_4, Y_6	—	—
Y_3, Y_6	Y_1, Y_5	Y_4	Y_2
Y_1, Y_4, Y_6	Y_2, Y_3, Y_5	—	—
Y_1, Y_4	Y_3, Y_6	Y_6	Y_2
Y_1, Y_6	Y_3, Y_5	Y_4	Y_2

Table 4

$$F(s) = \frac{b_0 (b_1 s + 1)}{a_3 s^3 + a_2 s^2 + a_1 s + 1}$$

Resistor	Capacitor	Parallel resistor-capacitor combination	Zero admittance
Y_3, Y_5	Y_4	Y_1, Y_6	Y_2
Y_3, Y_5, Y_2	Y_4, Y_6	Y_1	—
Y_3, Y_5	Y_6	Y_1, Y_4	Y_2
Y_3, Y_5	Y_4	Y_1, Y_6	Y_2
Y_1, Y_5	Y_2	Y_3, Y_6	Y_1
Y_1, Y_5	Y_6	Y_2, Y_3	Y_4
Y_1, Y_5, Y_4	Y_2, Y_6	Y_3	—
Y_1, Y_5	Y_2	Y_3, Y_6	Y_1
Y_1, Y_5	Y_4	Y_3, Y_6	Y_2
Y_1, Y_5, Y_2	Y_4, Y_6	Y_3	—
Y_1, Y_5	Y_4	Y_3, Y_6	Y_2
Y_1, Y_5	Y_6	Y_3, Y_4	Y_2
Y_1, Y_3	Y_2	Y_5, Y_6	Y_4
Y_1, Y_3	Y_6	Y_5, Y_2	Y_4
Y_1, Y_3	Y_2	Y_5, Y_6	Y_4
Y_1, Y_3, Y_4	Y_2, Y_6	Y_5	—
Y_1, Y_3, Y_6	Y_2, Y_4	Y_5	—

Table 5

$$F(s) = \frac{-b_1 s (b_2 s + 1)}{a_3 s^3 + a_2 s^2 + a_1 s + 1}$$

Resistor	Capacitor	Parallel resistor-capacitor combination	Zero admittance
Y_5, Y_2	Y_1, Y_6	Y_3	Y_4
Y_5	Y_1	Y_3, Y_6	Y_3, Y_4
Y_5, Y_4	Y_1, Y_6	Y_3	Y_2
Y_3, Y_2	Y_1, Y_6	Y_5	Y_4
Y_3	Y_1	Y_5, Y_6	Y_3, Y_4
Y_3, Y_4	Y_1, Y_6	Y_5	Y_2
Y_3, Y_6	Y_1, Y_4	Y_5	Y_3
Y_5	Y_3	Y_1, Y_6	Y_2, Y_4
Y_5, Y_4	Y_3, Y_6	Y_1	Y_2
Y_1, Y_6	Y_3, Y_2	Y_5	Y_4
Y_1	Y_3	Y_5, Y_6	Y_2, Y_4
Y_1, Y_4	Y_3, Y_6	Y_5	Y_2
Y_1, Y_6	Y_3, Y_4	Y_5	Y_2
Y_3	Y_5	Y_1, Y_6	Y_2, Y_4
Y_3, Y_6	Y_5, Y_4	Y_1	Y_2
Y_1, Y_6	Y_5, Y_2	Y_3	Y_4
Y_1	Y_5	Y_3, Y_6	Y_2, Y_4
Y_1, Y_6	Y_5, Y_4	Y_3	Y_2

Table 6

$$F(s) = \frac{-b_0(b_3 s^2 + b_1 s + 1)}{a_3 s^3 + a_2 s^2 + a_1 s + 1}$$

Resistor	Capacitors	Parallel resistor-capacitor combination	Zero admittance
Y_5, Y_4 Y_5, Y_2 Y_3, Y_6 Y_3, Y_4 Y_3, Y_2 Y_1, Y_6 Y_1, Y_6 Y_1, Y_4 Y_1, Y_2	Y_6 Y_6 Y_4 Y_6 Y_6 Y_2 Y_4 Y_6 Y_6	Y_1, Y_3 Y_1, Y_3 Y_1, Y_5 Y_1, Y_5 Y_1, Y_5 Y_3, Y_5 Y_3, Y_5 Y_3, Y_5 Y_3, Y_5	Y_3 Y_4 Y_2 Y_2 Y_4 Y_4 Y_2 Y_2 Y_4

Example

Consider the transfer function given by

$$-\frac{e_0}{e_1} = \frac{b_1 s}{a_3 s^3 + a_2 s^2 + a_1 s + 1} \quad (2)$$

where b_1 and the a 's are all real, positive and non-zero constants. Let us choose alternative 2 (Table 2) since its analysis is quite simple, requiring the solution of only linear equations. Thus, we choose

$$Y_1 = S C_1, Y_2 = 0, Y_3 = \frac{1}{R}, Y_4 = S C_4 + \frac{1}{\alpha_4 R}, Y_5 = \frac{1}{\alpha_5 R}, \text{ and } Y_6 = S C_6 \quad (3)$$

The resulting configuration is shown in Fig. 3. Substituting equation (3) in equation (1), we get

$$-\frac{e_0}{e_1} = \frac{(T_1 \alpha_4) S}{(T_1 T_4 T_6 \alpha_4 \alpha_5) S^3 + \{(\alpha_4 \alpha_5 + \alpha_4 + \alpha_5) T_1 T_6 + T_4 \alpha_4 (T_6 \alpha_5 + T_1)\} S^2 + \{T_6 (\alpha_4 + \alpha_5) + T_4 \alpha_4 + T_1\} S + 1} \quad (4)$$

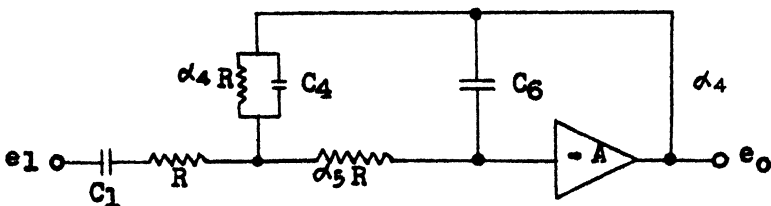


Fig. 3

Resultant configuration of the network in the example

Comparing the coefficients of the various powers of S in equations (4) and (2), we get

$$b_1 = T_1 \alpha_4 \quad (5)$$

$$a_3 = (T_1 \alpha_4) T_4 T_6 \alpha_5 \quad (6)$$

$$a_2 = (\alpha_4 \alpha_5 + \alpha_4 + \alpha_5) T_1 T_6 + T_4 T_6 \alpha_4 \alpha_5 + (T_1 \alpha_4) T_4 \quad (7)$$

$$a_1 = T_6 (\alpha_4 + \alpha_5) + T_4 \alpha_4 + T_1 \quad (8)$$

The α 's and T 's have to be determined in terms of the a 's and b_1 , and the restrictions, if any, on the a 's and b_1 to be found out so that all the α 's and the T 's are real and positive. These are the restrictions on the range of applicability of this particular choice of resistor-capacitor combination. If some other alternatives were chosen, these restrictions would have worked out to be different.

Since there are five unknowns, viz., T_1 , T_4 , T_6 , α_4 and α_5 , and only four equations, one of these unknowns, T_1 , say, may be kept as arbitrary to begin with and determine the other four unknowns in terms of T_1 , the a 's and b_1 . Then, a positive real value of T_1 is to be chosen so that the other four variables are all ensured a real positive character.

Equation (5) gives the value of α_4 as

$$\alpha_4 = \frac{b_1}{T_1} \quad (9)$$

Using this value of α_4 and putting α_5 from equation (6) in equation (7), we get

$$b_1^2 T_1 T_4 T_6 = -b_1^2 T_1 T_4^2 + (a_2 b_1 T_1 - b_1 a_3) T_4 - a_3 (T_1 + b_1) T_1 \quad (10)$$

Using this value of α_4 , putting α_5 from equation (6) in equation (8), and multiplying with T_1 , we get

$$b_1^2 T_1 T_4 T_6 = -b_1^2 T_1 T_4^2 + b_1 (a_1 - T_1) T_4 T_1^2 - a_3 T_1^2 \quad (11)$$

From equations (10) and (11), we get

$$T_4 = \frac{a_3 T_1}{(a_2 T_1 - a_3) - (a_1 - T_1) T_1^2} \quad (12)$$

Equation (11) then gives the value of T_6 as

$$T_6 = a_3 + (a_1 b_2 - a_2) T_1 + (a_1 - b_1) T_1^2 - T_1^3 - \frac{a_3 T_1}{(a_2 T_1 - a_3) - (a_1 - T_1) T_1^2} \quad (13)$$

Equations (9), (12), (13) and (6) give the values of α_4 , T_4 , T_6 and α_5 . A real positive value of T_1 is chosen, so that

$$T_1^3 - a_1 T_1^2 + a_2 T_1 - a_3 > 0 \quad (14)$$

$$a_3 + (a_1 b_2 - a_2) T_1 + (a_1 - b_1) T_1^2 - T_1^3 - \frac{a_3 T_1}{(a_2 T_1 - a_3) - T_1^2 (a_1 - T_1)} > 0 \quad (15)$$

to ensure a real positive character for T_4 and T_6 . Once T_1 , T_4 and T_6 are real and positive, α_4 and α_5 will be real and positive also, since the a 's and b_1 are all real, positive and non-zero.

Then the design procedure will be to choose a suitable value of T_1 and work out the values of the other circuit elements using the above equations.

Conclusions

The technique described above is specially useful in simulating linear transfer functions which do not involve frequent change of parameters. It effects considerable economy in equipment. In a large number of cases, the labour of computing the values of the resistors and capacitors is not excessive. It is hoped that with the recent developments in producing precision passive components, the accuracy obtained by this technique will be acceptable for many applications.

Acknowledgments

The author thanks Col. Pritampal Singh, Director, Weapons Evaluation Group, Ministry of Defence, New Delhi, for his encouragement and kind permission to publish this paper. He is also grateful to Prof. S. P. Chakravarti, Director, Liaison, R & D Council, Ministry of Defence, New Delhi, for his comments on the work presented in the paper.

References

1. G. K. Aggarwal. 'A Single Operational Amplifier Simulates General Third Order Linear Systems'. *Proceedings of the Indian Academy of Sciences*, vol. 40, November 1963.
2. G. K. Aggarwal. 'A Single Operational Amplifier Simulates Fourth Order Linear Systems'. *Instruments and Control Systems*, 1965.
3. G. K. Aggarwal. 'On Fourth Order Simulation with One Amplifier'. *Journal of Electronics and Control Systems*, November 1963.
4. W. J. Karplus and W. W. Soroka. 'Analogue Methods'. *McGraw-Hill Book Co. Inc.*, 1959.
5. F. Stanley. 'Analogue Computation, Vol. 2'. *McGraw-Hill Book Co., Inc.*, 1961.
6. S. Godet. 'Synthesis of Input and Output Network for Feedback Amplifiers'. *B.E.A.C. Information Bulletin*, no. 4, 1960.
7. F. R. Bradley and R. P. McCoy. 'Driftless D.C. Amplifier'. *Electronics*, vol. 25, no. 4, April 1952, p. 144.
8. A. Bridgeman and R. Brennen. 'Simulation of Transfer Functions Using Only One Amplifier'. *Wescon Convention Record*, pt. 4, August 1957, p. 273.
9. G. K. Aggarwal and L. K. Wadhwa. 'Simulation of Third Order Systems with One Operational Amplifier'. *Journal of the Institution of Engineers (India)*, vol. 43, no. 5, pt. ET 2, January 1963, p. 42.

CLASSIFICATION OF MODES IN ELECTROMAGNETIC WAVEGUIDES***S. K. Chatterjee***Non-member**Indian Institute of Science, Bangalore***Summary**

The classification of modes in electromagnetic waveguides based on the model solutions of the source-free homogeneous wave equation and the limitations of such classification are discussed. The concept of the existence of pole waves and branch-cut waves in waveguides is explained. It is shown that guided waves, surface waves and leaky waves arise as special cases of pole waves associated with the residues evaluated at the poles and the radiation field is associated with the branch-cut integration of a contour integral, in terms of which the field is expressed as a waveguide containing an exciting source.

1. Introduction

A system in which all boundary surfaces are parallel to a given straight line may be considered as a waveguide. The boundary surfaces may assume any form as long as they can be generated by a straight line which extends always parallel to the direction of wave propagation. Systems having different shapes are possible, but cylinders of rectangular and circular cross-sections are more frequently used. In order that a system may act as a waveguide, it is necessary that there must be, at least, one surface dividing any two different media. A waveguide can have also more than one surface such as 'Harms-Goubau line', a hollow metal cylinder containing one or two dielectrics, ferrites or plasma. A waveguide may also contain both dielectric and ferrite as in phase shifters. The boundary surface may be closed which indicates that no energy can escape or enter the bounded region. The surface may, also, be open which signifies that energy can be radiated into space in all possible directions or, in a particular direction or can enter the bounded region. Hollow metal waveguides belong to the first category, whereas a dielectric rod waveguide and other surface wave structures may be termed as 'open' type waveguides.

The media enclosed within the bounding surfaces may be metallic, dielectric, magnetic or plasma. The physical constituents such as permittivity or permeability of the media may be real, imaginary, complex, scalar or tensors. The conventional waveguide, which is extensively used in practice, comprises a single boundary surface described by a perfect ($\sigma = \infty$) conductor and enclose within it a homogeneous, loss-free ($\epsilon'' = 0$), perfect ($\sigma = 0$) isotropic dielectric medium. The conventional hollow metal waveguide approaches very closely the mathematically idealized homogeneous,

* Written discussion on this paper will be received until November 30, 1965.

This paper was received on August 30, 1965.

simple and perfect (H.S.P.) guide,¹ where homogeneity means that the energy of the propagating electromagnetic wave is restricted only to a simple homogeneous medium; simplicity means that the guide contains scalar media; and perfection means that all the concerned media are loss-free.

From the topological point of view, a conventional waveguide may be regarded as a simply connected region,² because it satisfies the properties of reconcilability, reducibility and because an infinite number of paths lying completely inside the region may be described to pass from one point to another within the region.

2. Solution of Maxwell's field equations

The study of all waveguide problems depend on the solution of Maxwell's field equations in appropriate coordinate systems, subject to proper boundary condition, viz., specification of the value of the field at any point on the boundary surface (Dirichlet condition), or specification of the normal gradient of the field to the surface at the surface (Neumann condition), or specification of both value and normal gradient of the field on the surface (Cauchy condition). Since all the well behaved time functions can be synthesized from a Fourier spectrum of simple harmonic eigenvalues, the solution of Maxwell's equations in orthogonal curvilinear coordinates (u_1, u_2, u_3) can be obtained assuming the time variation of the field vectors \vec{E} and \vec{H} of the form

$$\left. \begin{aligned} \vec{E}(u_1, u_2, u_3) &= |\vec{E}(u_1, u_2, u_3)| \exp. (\pm i \omega t) \\ \vec{H}(u_1, u_2, u_3) &= |\vec{H}(u_1, u_2, u_3)| \exp. (\pm i \omega t) \end{aligned} \right\} \quad (1)$$

Most physical problems are conveniently treated by orthogonal curvilinear coordinates. The condition that the coordinates should form an orthogonal system is

$$\nabla u_i \cdot \nabla u_r = 0, \quad r \neq i \quad (2)$$

It is sometimes convenient to work with a coordinate system which is related to the symmetry of the system under consideration. The study any problem in a waveguide of a particular geometry becomes simpler if the cylindrical surfaces of the system are described by equations of the form, $u_1 = \text{constant}$ and $u_2 = \text{constant}$. Source-free ($\vec{J} = 0, \rho = 0$) solution of Maxwell's equations are obtained from two scalar functions Φ and Ψ , which can be obtained in different ways³ and which satisfy the scalar Helmholtz equations.

The cylindrical symmetry in the case of a conventional waveguide suggests the use of the axial components of the electric Hertz vector $\vec{\pi}_e$ and magnetic Hertz vector $\vec{\pi}_h$, where Φ and Ψ are related to $\vec{\pi}$ as follows, when the cartesian system of coordinates (x, y, z) is considered and the direction of propagation is assumed to be along the z -axis.

$$\left. \begin{aligned} \vec{\pi}_e(x, y, z) &= \vec{i}_z \pi_e^z(x, y, z) = \vec{i}_z \Phi(x, y) \exp. (\pm i^e h z) \\ \vec{\pi}_h(x, y, z) &= \vec{i}_z \pi_h^z(x, y, z) = \vec{i}_z \Psi(x, y) \exp. (\pm i^h h z) \end{aligned} \right\} \quad (3)$$

The field vectors, \vec{E} and \vec{H} , are related to $\vec{\pi}$ as follows :

$$\left. \begin{aligned} \vec{E}_e &= \nabla \times \nabla \times \vec{\pi}_e \\ \vec{H}_e &= -i \omega \epsilon \nabla \times \vec{\pi}_e \\ \vec{E}_h &= i \omega \mu \nabla \times \vec{\pi}_h \\ \vec{H}_h &= \nabla \times \nabla \times \vec{\pi}_h \end{aligned} \right\} \quad (4)$$

where $\vec{\pi}_e$ and $\vec{\pi}_h$ satisfy the following vector wave equations respectively :

$$\left. \begin{aligned} (\nabla^2 + k^2) \vec{\pi}_e &= 0 \\ (\nabla^2 + k^2) \vec{\pi}_h &= 0 \end{aligned} \right\} \quad (5)$$

where

$$k^2 = \omega^2 \mu_0 \epsilon_0 = \frac{\omega^2}{c^2}$$

is the free space wave number. Calculating $\nabla \times \nabla \times \vec{i}_z \pi_e^*$, the solution for a plane inhomogeneous wave with $H_z = 0$, $E_z \neq 0$ is obtained. This is termed E wave. Similarly, calculating $\nabla \times \nabla \times \vec{i}_z \pi_h^*$ one obtains a plane inhomogeneous wave with $H_z \neq 0$ and $E_z = 0$. This is called H wave. The field components of the two waves are then calculated from equation (4). These two solutions are independent of each other and so the general solution of Maxwell's equations can be obtained by a superposition of the two solutions. The above method of solution is also applicable in any other orthogonal coordinate system.

3. Model solution

In the case of conventional waveguides, having perfectly conducting walls and enclosing a perfect dielectric, it is usual to assume that in the waveguide the fields, which have harmonic time dependence, can be expressed in terms of an infinite series of partial waves, called 'normal modes', each of which satisfies the wave equation and proper boundary conditions. The normal modes are considered to be waves having z -dependence as $[\exp. (i h z)]$ for the six components of vectors, \vec{E} and \vec{H} . The boundary conditions in the case of conventional waveguides are $\vec{n} \times \vec{E}_e = 0$ and $\vec{n} \times \vec{E}_h = 0$ on the guide walls in the case of E and H waves respectively. This leads to $\Phi = 0$ and $\frac{\partial \Psi}{\partial n} = 0$ on the guide wall surface. The wave equations are then scalar,

$$\nabla^2 \Phi + k^2 \Phi = 0 \quad [6(a)]$$

with $\Phi = 0$ on the guide walls, and

$$\nabla^2 \Psi + k^2 \Psi = 0 \quad [6(b)]$$

with $\frac{\partial \Psi}{\partial n} = 0$ on the guide walls. These two equations are eigenvalue equations and permit an infinite discrete set of values for γ^2 , producing thereby a discrete spectrum of waves. The values of h^2 corresponding to γ^2 are determined from equation (7). The functions, Φ_p and Ψ_p , are eigenfunctions of the equations and are associated with the eigenvalues ${}^e\gamma_n$ and ${}^h\gamma_m$ respectively

$$\left. \begin{aligned} {}^e\gamma_n^2 &= k^2 - {}^e h_n^2 \\ {}^h\gamma_m^2 &= k^2 - {}^h h_m^2 \end{aligned} \right\} m = n = 0, 1, 2, \text{ etc.} \quad (7)$$

It may be pointed out that ${}^h\gamma_0^2 = 0$, but ${}^e\gamma_0^2 \geq 0$ and ${}^h\gamma_0^2 \leq {}^h\gamma_{q+1}^2$, ${}^e\gamma_0^2 \leq {}^e\gamma_{p+1}^2$. It can also be shown that ${}^h\gamma_{p+2}^2 < {}^e\gamma_p^2$, where, $p = 0, 1, 2$, etc. This signifies that H mode is the dominant mode in a conventional waveguide having a simply connected dielectric medium.

Each mode is characterized by a certain eigenvalue and has a cutoff frequency f_c , which can be derived from the eigenvalues. The cutoff condition in a conventional guide is attained when the phase constant $\beta = 0$. Below f_c , h is imaginary and the mode is damped, and above f_c , h is real and the mode is propagated, when the time dependence is assumed to be $[\exp. (-i \omega t)]$. At any given frequency, only a given number of modes are propagated and the rest are damped. The mode which has the lowest f_c is called the dominant mode. This classical classification of modal analysis of waveguide field into E and H modes is useful, as it helps a physical interpretation of the cutoff phenomenon, and justifies Brillouin's concept of elementary waves travelling in a zigzag fashion by multiple reflections from the walls of a guide. This mode concept also helps to explain the concept of impedance and Poynting vector.

The E mode comprises vectors \vec{E}_n and \vec{H}_n , the components of which are expressed as functions of ${}^eE_{zn}$, whereas the H mode comprises vectors \vec{E}_m and \vec{H}_m and are expressed as functions of ${}^hH_{zm}$. The order of E and H modes is defined by a discrete set of values of ${}^e h_n^2$ and ${}^h h_m^2$ respectively. The set of functions, E_{zn} and H_{zm} , are closed and complete in the sense that it permits a properly well behaved arbitrary field, E or H , within the guide to be expanded in terms of these functions as follows:⁴

$$\left. \begin{aligned} E &= \vec{E}_s + \sum_n C_n \vec{E}_n + \sum_m D_m \vec{E}_m \\ H &= \vec{H}_s + \sum_n C_n \vec{H}_n + \sum_m D_m \vec{H}_m \end{aligned} \right\} \quad (8)$$

when the dielectric region enclosed by the boundary surface of the guide is simply connected. The vectors, \vec{E}_s and \vec{H}_s , represent the source field and vanish when the source is absent or moved to $Z = \pm \infty$. The expansion coefficients, C and D , are obtained from the relationships :

$$\left. \begin{aligned} C_n &= \int_A \vec{E} \cdot \vec{E}_n^* dA \\ &= \int_A \epsilon \vec{E}_n \cdot \vec{E}_n^* dA \\ D_m &= \int_A \vec{E} \cdot \epsilon \vec{E}_m^* dA \\ &= \int_A \epsilon \vec{E}_m \cdot \epsilon \vec{E}_m^* dA \end{aligned} \right\} \quad (9)$$

in which the integration is performed over cross-section A of the guide.

When the dielectric region inside a guide is simply connected, only E or H wave or their linear combination, EH or HE , but not T wave ($E_z = 0, H_z = 0$) can be physically supported since the eigenvalue equations for T wave is given by

$$\begin{aligned} \Delta_t^2 \Phi &= 0 \\ \Delta_t^2 \Psi &= 0 \end{aligned} \quad (10)$$

with boundary conditions $\Phi = \text{constant}$; the conditions $\Phi_o = 0$ and $\frac{\delta \Psi}{\delta n} = 0$ on the boundary wall lead to the solutions

$$\begin{aligned} \Phi(x, y) &= \Phi \\ \Psi(x, y) &= \text{constant} \end{aligned} \quad (11)$$

which yield the transverse components of the field vectors as $\vec{E}_t = 0$ and $\vec{H}_t = 0$. This proves the non-existence of the T wave in a conventional waveguide which is simply connected. But T wave can exist inside a guide whose boundary surface encloses a multiple connected dielectric region, such as an inhomogeneous guide, viz., coaxial guide, guide containing more than one concentric dielectric rod, etc. In the case of such guides, an arbitrary field can be expanded in the following form:⁴

$$\begin{aligned} \vec{E} &= \vec{E}_o + \sum_n C_n \vec{E}_n + \sum_m D_m \vec{E}_m + C_o \vec{E}_o \\ \vec{H} &= \vec{H}_o + \sum_n C_n \vec{H}_n + \sum_m D_m \vec{H}_m + C_o \vec{H}_o \end{aligned} \quad (12)$$

where \vec{E}_o and \vec{H}_o represent the field due to T waves.

4. Orthogonality of field vectors

The orthogonality properties of the field components are the direct consequences of the orthogonality properties of the eigenfunctions. Any two functions, $f(x)$ and $g(x)$, for which the inner product (f, g) vanishes, are said to be orthogonal. The integral

$$(f, g) = \int f(x) g(x) dx$$

taken over the finite domain is called the inner product of the two functions f and g . The limits are omitted for convenience. It satisfies the Schwarz inequality $(f, g)^2 \leq (f, f)(g, g)$, where the equality holds if f and g are proportional.

The norm of a function, denoted by Nf , is the inner product of function $f(x)$ with itself *i.e.*,

$$Nf = \int f^2 dx \quad (13)$$

When $Nf = 1$, function $f(x)$ is said to be normalized. If any two members of a system of normalized functions $\Psi_1(x), \Psi_2(x), \dots, \Psi_n(x)$ are orthogonal, the system is said to be an 'orthonormal' system. The orthogonality relationships are expressed as

$$(\Psi_m, \Psi_n) = \delta_{mn}$$

where

$$\delta_{mn} = \begin{cases} 1 & \text{for } m = n \\ 0 & \text{for } m \neq n \end{cases} \quad (14)$$

For the functions of a real variable which can have complex values, the concept of orthogonality can be applied in the following way. Two complex functions, $f(x)$ and $g(x)$, are said to be 'orthogonal', if the following relationships are satisfied :

$$(f, g^*) = (f^*, g) = 0 \quad (15)$$

where f^* and g^* indicate complex conjugate of f and g respectively. The function $f(x)$ is said to be 'normalized', if

$$Nf = \int |f|^2 dx = 1 \quad (16)$$

It may be useful to mention that the functions of an orthogonal system are always linearly independent. Equation (9) is obtained by the normalization procedure. It may be remarked that the property of orthogonality is important and useful but the property of normalization is only of formal utility. The orthogonality properties permit a given arbitrary field represented by a general solution to be expanded [*vide* equations (8) and (12)] as a sum of solutions for the various normal modes. The E and H modes have several useful orthogonality properties.^{6,7}

If in a waveguide bounded by infinitely conducting walls, Ψ_i and Ψ_j represent the solutions for the i th and j th E or H modes, the following orthogonality relationships hold :

$$\iint_A \Psi_i \Psi_j da = 0, \quad i \neq j \quad (17)$$

which states that the axial components of the field for the two different modes (i and j) are orthogonal, *i.e.*, the integral over cross-section A of the guide of the product, $E_{zn} E_{zm}$ or $H_{zn} H_{zm}$, vanishes when $n \neq m$.

For two different E or H modes, the transverse electric fields are also orthogonal, *i.e.*,

$$\iint_A \nabla_t \Psi_i \nabla_t \Psi_j da = 0 \quad (18)$$

or, in other words, the integral over cross-section A of the scalar product, $\vec{E}_{in} \vec{E}_{im}$ or $\vec{H}_{in} \vec{H}_{im}$, vanishes when $n \neq m$. The functions, ψ_i and ψ_j , are two different eigenfunctions from which the E or H modes may be derived. The orthogonality relationships hold also for the transverse magnetic fields for any two E or H modes.

The transverse electric fields for one E mode and one H mode also obey the orthogonality relationship

$$\iint_A (\vec{i}_z \times \nabla_t \psi_{hi}) \nabla_t \psi_{ej} da = 0 \quad (19)$$

i.e., the integral over cross-section A of the guide of $\vec{i}_z (\vec{E}_{in} \times \vec{H}_{im})$ vanishes when $n \neq m$. The functions, ψ_{hi} and ψ_{ej} , represent the two eigenfunctions which give rise to H and E waves respectively. The field \vec{E}_{in} is the transverse electric field for the n th mode and \vec{H}_{im} is the transverse magnetic field for the m th mode. Similar orthogonality relationship is also obtained for the transverse magnetic fields of E and H waves.

In the case of a waveguide with walls of finite conductivity, the eigenfunctions, ψ_e and ψ_h , do not satisfy the conditions $\psi_e = 0$ and $\frac{\partial \psi_h}{\partial n} = 0$ respectively on the guide boundary, assumed in deriving the above orthogonality relationships. The presence of finite conductivity results in a cross-coupling between the various E and H modes. However, the more general relationship

$$\iint_A (\vec{E}_{in} \times \vec{H}_{im}) \vec{i}_z da = 0 \quad (20)$$

holds when $n \neq m$. The fields, \vec{E}_{in} and \vec{H}_{im} , represent the transverse electric fields for n th mode and m th mode respectively.

In the case of degeneracy ($n=m$), the above relationship is not valid. It is however possible to secure orthogonality in the following way. If ψ_1 and ψ_2 are two degenerate modes such that

$$\iint_A \psi_i \psi_j da = P_{ij} \quad (21)$$

where, $i, j = 1, 2$, and $\psi_1' = \psi_1$ and $\psi_2' = \psi_2 + \alpha \psi_1$ represent two subsets, where the constant α is so determined that

$$\iint_A \psi_1' \psi_2' da = 0$$

then the two modes are orthogonal, when $\alpha = -\frac{P_{12}}{P_{11}}$. It may be said, in general, that any subset of n degenerate modes may be converted into a new subset of n mutually orthogonal modes.

5. *LSE* and *LSM* modes

In the case of inhomogeneously filled waveguides such as guides containing dielectrics, the normal modes of propagation are, in general, not pure *E* or *H* modes, but *EH* or *HE* modes except in the case of H_{m0} modes.⁵ Where E_{mn} and H_{mn} have the same order in the ordinal numbers m and n and where $m, n \geq 1$, they have the same propagation factor and so they can be superposed. The superposition can be done in such a way that one of the transverse component of *E* or *H* is zero. The wave then lies in the longitudinal section. In this case, the waves are designated as

$$(LSE)_{mn \perp x}: E_x = 0, E_y, E_z, H_x, H_y, H_z \neq 0$$

$$(LSM)_{mn \perp x}: H_x = 0, E_x, E_y, E_z, H_y, H_z \neq 0$$

Similarly, $E_y = 0$ and $H_y = 0$ for $(LSE)_{mn \perp y}$ and $(LSM)_{mn \perp y}$ respectively. This mode designation is convenient in dealing with dielectric slab loaded waveguides. The waves $(LSM)_{om}$ and $(LSE)_{no}$ are similar to H_{om} and E_{no} waves in a homogeneous guide.

6. Applications of mode concept

The ordinal designations, p and q , in the eigenvalue equations⁶ may be replaced by m and n , which represent the number of half-cycle variations in the direction transverse, to the direction of propagation. Some of the significant facts which arise as a consequence of modal analysis in the case of conventional guides of different shapes are as follows :

- (i) In the case of a rectangular guide, H_{01} is the dominant mode, i.e., f_c is the lowest of all modes or the cutoff wavelength λ_c is the longest; and
- (ii) In the case of a circular cylindrical guide, E_{mn}^0 and H_{mn}^0 modes are doubly degenerate since the ϕ (azimuthal coordinate) dependence can be either $\sin m\phi$ or $\cos m\phi$. For E_{mn} modes, $m=0$ and $n=0$ are not allowed. For H_{mn} modes, $m=0, n \neq 0$ and $n=0, m \neq 0$ are allowed, but not $m=0, n=0$. The eigenvalues of E_{mn} and H_{mn} modes are determined respectively from the roots of the following Bessel equations :

$$\left. \begin{aligned} J_\nu(\gamma_{mn} a) &= 0 \\ J'_\nu(\gamma_{mn} a) &= 0 \end{aligned} \right\} \quad (22)$$

where a represents the radius of the circular guide. It is evident from equation (22) that H_{01}^0 and E_{11}^0 are companion modes having $\lambda_c = 1.64 a$. It has to be noted that H_{01}^0 mode is not dominant, but from the practical point of view, it is an important mode, since it is the only mode, in the case of which the attenuation constant decreases as $\omega^{-3/2}$ monotonically. It may however be emphasized that particular care is needed in maintaining the cross-section of the guide as perfectly circular as possible, as the purity of the mode depends on the cross-section. For slight deformation, H_{01} mode is coupled with E_{11} mode and exchange of energy occurs between the two companion modes. This mode instability, in the extreme case of deformation, may lead to the complete transfer of energy to E_{11} mode.

For a coaxial guide, the cutoff wavelength for E_{01} mode is $\lambda_c \simeq 2(a - b)$; and for H_{01} mode, $\lambda_c \sim \pi(a + b)$, where a and b represent the radius of the inner and outer conductors respectively. For E_{01} mode, λ_c varies as the spacing between the two conductors which is very small and $\lambda_c (H_{01})$ exceeds the outer perimeter of the guide. So, these two waves are not suitable for practical purposes. The T wave which has no cutoff is the convenient mode to be used for a coaxial guide.

In the case of an elliptical guide, mode vectors are expressed in terms of even and odd Mathieu functions of the first kind and integral order. The dominant mode is H_{11} . When the eccentricity of the ellipse approaches zero, λ_c for some of the modes in an elliptical guide approaches that of a circular guide, e.g.,

$$\lambda_c ({}_0H_{11}^0, {}_eH_{11}^0) \rightarrow \lambda_c (H_{11}^0)$$

$$\lambda_c ({}_0E_{11}^0, {}_eE_{11}^0) \rightarrow \lambda_c (E_{11}^0)$$

$$\lambda_c ({}_eE_{01}^0) \rightarrow \lambda_c (E_{01}^0)$$

$$\lambda_c ({}_eH_{01}^0) \rightarrow \lambda_c (H_{01}^0)$$

If a circular guide is deformed, the modes H_{11}^0 and E_{11}^0 may be considered as split up into two even and odd modes. The splitting occurs as the above two modes are degenerate. For non-degenerate modes such as E_{01}^0 and H_{01}^0 , no such instability appears.

7. Excitation of waveguides

The modal solution for an electromagnetic structure is derived from the source-free wave equation. In any finite region bounded by electromagnetically opaque walls, the modal solution gives discrete spectrum which is finite everywhere and individually satisfies the boundary conditions and field equations. But a dynamic electromagnetic field emanates from a physical source. In this sense, a source-free field may be regarded as being originated from a source placed at $z = \pm \infty$, where the direction of propagation is along the z -axis. The physical reality of all electromagnetic waves depends, therefore, on launching conditions, in addition to their being the solutions of Maxwell's equations subject to the boundary conditions and or radiation condition at infinity. So, the entire field as a solution to Maxwell's equations is obtained by superposing discrete spectrum and continuous spectrum solutions. If a source placed in a metallic waveguide is represented by an electric current distribution, $\vec{J}_e(\vec{r}_0)$, throughout a finite volume v of the guide, then the electric field, $\vec{E}(\vec{r})$, at any point \vec{r} in the guide is given by equation (8) as

$$\vec{E}(\vec{r}) = \int_u \vec{\Gamma}^{(1)}(\vec{r} | \vec{r}_0) \vec{J}_e(\vec{r}_0) dv_0 \quad (23)$$

But if the source is represented by a magnetic current distribution, $\vec{J}_m(\vec{r}_0)$, the field is given by

$$\vec{H}(\vec{r}) = \int \vec{\Gamma}^{(2)}(\vec{r} | \vec{r}_0) \vec{J}_m(\vec{r}_0) dv_0 \quad (24)$$

where \vec{r} and \vec{r}_0 indicate the observation and source points' coordinates, $\vec{\Gamma}^{(1)}(\vec{r} | \vec{r}_0)$ and $\vec{\Gamma}^{(2)}(\vec{r} | \vec{r}_0)$ are the dyadic Green's function of the first and second kind respectively and are related^{8,9} to the scalar Green's functions of the first kind, $G^{(1)}(\vec{r} | \vec{r}_0)$, and the second kind, $G^{(2)}(\vec{r} | \vec{r}_0)$, respectively. The scalar Green's functions, $G^{(1)}$ and $G^{(2)}$, obey the inhomogeneous wave equations :

$$\left. \begin{aligned} (\nabla^2 + k^2) G^{(1)}(\vec{r} | \vec{r}_0) &= -\delta(\vec{r} - \vec{r}_0) \\ (\nabla^2 + k^2) G^{(2)}(\vec{r} | \vec{r}_0) &= -\delta(\vec{r} - \vec{r}_0) \end{aligned} \right\} \quad (25)$$

subject to the boundary conditions, $G^{(1)}(\vec{r} | \vec{r}_0) = 0$ and $\frac{\partial}{\partial n} G^{(2)}(\vec{r} | \vec{r}_0)$ on the wall of the guide. The Dirac delta function δ , is defined to be zero everywhere except at the source $\vec{r} = \vec{r}_0$, i.e., where it is discontinuous in such a way that

$$\int_v \delta(\vec{r} - \vec{r}_0) dv_0 = \begin{cases} 0 & \vec{r} \text{ not in } v \\ 1 & \vec{r} \text{ in } v \end{cases} \quad (26)$$

when the source is of unit strength and is taken for convenience as $\frac{1}{i\omega\mu}$ and located at \vec{r}_0 . The Green's function G , is a solution to a given differential equation subject to specified boundary conditions, with the excitation function of unit strength located at \vec{r}_0 in space. The Green's function is a function of both source and field point and is symmetrical in the variables \vec{r}_0 and \vec{r} , i.e.,

$$G(\vec{r} | \vec{r}_0) = G(\vec{r}_0 | \vec{r}) \quad (27)$$

Knowing the solution when the source function is represented by a delta function, the solution for any given arbitrary source distribution is found by the superposition of elementary solutions. The inhomogeneous wave equations (25) are solved using the Fourier transform technique.

8. Pole waves and branch-cut waves

To determine the E field or H field in a waveguide containing a source, the Green's function is determined by solving the inhomogeneous equation. The solution is set up as a Fourier integral which is then expressed in the form of a contour integral. The integrand, in general, contains branch points and an infinite number of poles. The contour integral may be evaluated in either of the following ways. The first method comprises the deformation of the contour, so that the resultant integral consists of a branch-cut integral and a residue integral around the poles. If there is no pole, the deformation may result in two branch-cut integrations. The deformation of the contour with regard to the location of the poles in relationship with the branch-cut is done in such a manner so that they lie on the correct leaf of the Riemannian plane.² The second method consists in employing the saddle-point method of integration,^{10 to 12}

or the method of steepest descent, in which the path of integration is deformed in such a manner that the principal part of the integral can be evaluated along the deformed path.

The saddle-point method will yield correct result, if the integral can be expressed in the form

$$I(z) = \int_C \exp. [z f(t)] dt \quad (28)$$

where the contour C is such that the integrand is zero at the ends of the contour. The best form of the contour comprises loops around the branch points and poles and come from $+\infty$ in straight line and recede to $+\infty$ parallel to the incoming straight line. In the case of a branch point, the straight parts of the loop lie on opposite sides of the branch-cut. In the case of a pole not coinciding with a branch point, the integrals over the two straight parts cancel and the result is only the residue at the pole. The integral (28) may be split up as

$$I(z) = \exp. [i I_m \{z f(t)\}] \int_C \exp. [R_e \{z f(t)\}] dt \quad (29)$$

As $|z| \rightarrow \infty$, the exponential factor with imaginary argument oscillates rapidly. To reduce such oscillatory effects, the contour is deformed such that $I_m [z f(t)]$ remains constant, where $R_e [z f(t)]$ is maximum. The point $t = t_0$, where $R_e [z f(t)]$ is maximum, is such that $f'(t) = 0$. The contour near $t = t_0$ is deformed such that $I_m [z f(t)] = I_m [z f(t_0)]$. The surface of the contour at the stationary point $t = t_0$, must be flat, as the real part of a function of a complex variable cannot have a maximum or a minimum. The point $t = t_0$ is the saddle-point.

In order to obtain the solution of the branch-cut integral, the integrand is expanded in asymptotic series, and then integrated term by term, provided none of the poles is in the immediate vicinity of the branch point, in which case, the expansions do not converge.

The solution of the contour integral give the total field which is composed of the sum of the fields contributed by the residues evaluated at the poles, Ψ_i , and that contributed by the branch-cut, Ψ_B . So, the total field in a waveguide may be said to comprise pole waves; and this field is associated with the existence of individual poles and branch-cut waves which is a consequence of the integration around the branch-cut. Hence, the field in a waveguide may be represented as

$$\Psi = \sum_{i=0}^n \Psi_i + \Psi_B \quad (30)$$

where n represents the number of poles on the right leaf of the Riemannian plane. The poles may lie on the real axis, or on the imaginary axis or on both the h -complex planes, or the poles may be shifted from the axis in the first quadrant of the Argand diagram, depending on the properties of the waveguide. The poles on the real axis give rise to evanescent waves in z -direction, as the amplitude of these pole waves vary as $[\exp. (-h_n z)]$, when the time variation of the harmonic field is taken as

[exp. $(-i \omega t)$], whereas the poles distributed on the imaginary axis give rise to propagating waves. The distribution of the poles and their positions with regard to the branch-cut are functions of the physical properties of the waveguide. The physical properties of the waveguide in relationship with that of the medium in which it is immersed decide which of the two waves, due to the poles or the branch-cut, will predominate. In a physical waveguide, the pole waves are of the form¹³

$$\Psi_i = a_i f_i(x) \wedge_i \exp. (-h_i z) \quad (31)$$

where a_i represents the product of the sum of the residues at the poles and the intensity of the source and

$$\wedge_i = \exp. (-b^2 z) \operatorname{erfc} \left(j b \sqrt{\frac{z}{\pi}} \right) \quad (32)$$

which depends on z and on the distance between the pole and the branch-cut. The value of \wedge_i is unity or zero in the far field depending on whether the pole is above or below the branch-cut respectively. Pole waves, as defined above, are the proper modes and pole waves with $\wedge_i = 1$ are defined as 'quasi-modes'.

The branch-cut integration does not give a modal type of solution, because the branch-cut wave originates from the integration over a continuous range of h unlike the pole waves which originate from a pole at a single value of h . In the case of a conventional metal waveguide, the pole wave is a consequence of the modal solution. In the case of open guides such as a dielectric rod guide, the poles in the integrand lying on the correct leaf of the Riemannian plane will give rise to surface waves. There may be some poles which lie on the wrong leaf of the Riemannian plane and may give rise to leaky waves. In evaluating the contour integral, the contour is deformed into a contour of steepest descent and in this process, a part of the contour may lie on the wrong leaf, which will cause a contribution from the leaky modes to add to the resultant field. In the case of an open guide, the contribution of the integration round the branch-cut will give rise to a radiation field and the poles enclosed within the contour give rise to surface wave modes. The leaky modes have the space dependence of the form $\{\exp. [(ip - q)x + (ir - s)z]\}$ with p, q, r and s each positive for $x, z > 0$, when the unit current filament is located parallel to y -direction.

In order to explain the concept of surface and leaky waves in some more detail, let us consider a delta function source located at $x = a, z = 0$ (Fig. 1) over a grounded loss-less dielectric slab.¹⁴ The wave equations in the two media, 1 and 2, are respectively

$$\begin{aligned} (\nabla_t^2 + k_0^2) E_0(x, z) &= -\delta(x - a) \delta(z), x \geq 0 \\ (\nabla_t^2 + k^2) E_1(x, z) &= 0 \end{aligned} \quad (33)$$

where Δ_t^2 is the two-dimensional Laplacian transverse to y , k_0 and k_1 are the transverse wave numbers in media 1 and 2 respectively. Then E_0 and E_1 can be expressed as Fourier integrals in terms of modal amplitudes, $e_0 \left(\frac{x}{\beta_z} \right)$ and $e_1 \left(\frac{x}{\beta_z} \right)$ where β_z represents the eigenvalue specifying the mode

$$E_0(x, z) = \int_0^\infty e_0 \left(\frac{x}{\beta_z} \right) \exp. (i \beta_z z) d\beta_z \quad (34)$$

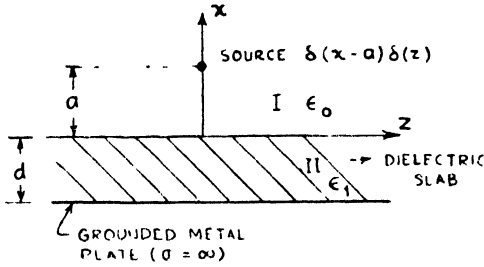


Fig. 1
Location of the delta function source
on a lossless dielectric slab

The inverse of the above integral is given by

$$e_0 \left(\frac{x}{\beta_z} \right) = \int_{-\infty}^{\infty} E_0(x, z) \exp. (-i \beta_z z) dz \quad (35)$$

Using the usual Fourier transform technique, separating the x -dependent terms, imposing proper boundary conditions and the radiation condition at infinity, the expression for the field in medium 1 is obtained as :

$$E_0(x, z) = -\frac{i}{4\pi} \int_{-\infty}^{\infty} \frac{1}{k_{x0}} [\exp. \{i k_{x0} |x - a|\} + \Gamma(\beta_z) \exp. \{i k_{x0} |x + a|\}] \exp. (i \beta_z z) d\beta_z \quad (36)$$

which represents the superposition of a downward and an upward wave, and

$$k_{x0}^2 = k_0^2 - \beta_z^2; k_{x1}^2 = k_1^2 - \beta_z^2 \quad (37)$$

and

$$\Gamma(\beta_z') = \Gamma(k_{x0}, k_{x1}) = \frac{-i k_{x0} - k_{x1} \cot k_{x1} d}{-i k_{x0} + k_{x1} \cot k_{x1} d} \quad (38)$$

which is the reflection coefficient at the interface of the dielectric slab and the grounded metal plate.

The existence of surface waves or leaky waves can be studied by exploring the effect of β_z on k_{x0} as β_z changes continuously from $-\infty$ to $+\infty$. From the propagation factor, $\{\exp. [i k_{x0} x + i \beta_z z]\}$, the following significant results are obtained :

- (i) If $\beta_z = 0$, then $k_{x0} = k_0$, which gives rise to waves travelling in x -direction, i.e., broadside to the surface of the structure ;
- (ii) If $\beta_z = \pm k_0$, $k_{x0} = 0$, which gives rise to waves in the $\pm z$ -directions, i.e., parallel to the surface of the structure;
- (iii) If $|\beta_z| < k_0$, then k_{x0} is real. If β_z is positive, the wave is propagated toward the upper z -direction. If β_z is negative, the wave is propagated toward the upper $-z$ -direction;
- (iv) If $|\beta_z| > k_0$, then k_{x0} is imaginary, which gives rise to an evanescent wave, i.e., a wave is propagated toward $+z$ - or $-z$ -direction undergoing at the same time an exponential decay in the broadside x -direction;
- (v) The sum of these modes as β_z changes from $-\infty$ to $+\infty$ gives the entire field which satisfies the boundary condition; and

- (vi) If the evanescent mode satisfies the boundary condition, then the mode is a surface wave.

The integrand in equation (36) possesses branch points at $\beta_z = \pm k_0$ and poles corresponding to the zeros of the denominator of equation (38). The poles are given by the roots of the equation

$$k_{x1} \cot k_{x1} d - i k_{x0} = 0 \quad (39)$$

which reduces to

$$\alpha_{x0} d + \beta_{x1} d \cot \beta_{x1} d = 0$$

When $k_{x0} = i \alpha_{x0}$ and $k_{x1} = \beta_{x1}$, equation (37) reduces to

$$k_0^2 K_r d^2 - (\beta_{x1} d)^2 - (\alpha_{x0} d)^2 = 0 \quad (40)$$

where $\epsilon_r = \frac{\epsilon_1}{\epsilon_0}$ is the relative permittivity of the dielectric slab and $k_r = \epsilon_r - 1$. Equations (39) and (40) give the surface wave poles β_z , which account for the existence of the surface wave. The surface wave pole lies between $|k_0|$ and $|k_1|$.

If k_z is complex, then α_{x0} is negative. If β_{x0} is positive, then equating the imaginary parts in equation (37),

$$\alpha_{x0} \beta_{x0} = -\alpha_z \beta_z \quad (41)$$

where α_z and β_z must be of the same sign.

- (i) If α_z and β_z are positive, the propagation factor is $\{\exp.[-\alpha_z z + i \beta_z z]\}$ which indicates a travelling wave in $+z$ -direction; and
- (ii) If α_z and β_z are negative, the propagation factor is $\{\exp.[\alpha_z z - i \beta_z z]\}$ which signifies a wave travelling in $-z$ -direction.

The above two modes are leaky waves which travel in $+z$ - or $-z$ -direction undergoing attenuation as it progresses and increasing exponentially in the broadside direction as α_{x0} is negative. The leaky wave is associated with the existence of the pole k_z , which lies on the wrong leaf of the Riemannian plane and hence does not contribute any residue, if the contour is properly chosen. The position of the surface wave pole and the leaky wave pole in relationship with the branch-cut and the contour is shown in Fig. 2. But, in following the saddle-point method, if the line of steepest descent is so deformed as to include the leaky wave pole k_z , then it will contribute to the residue and hence to the total field. In the case of a surface wave antenna or plasma sheath, leaky wave contribution forms the dominant part of the field.

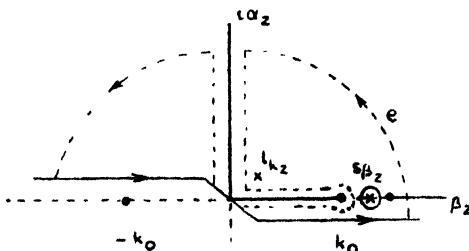


Fig. 2
Positions of wave poles

The nature of the surface wave and the leaky wave are best illustrated in Figs. 3 and 4. It is evident that leaky wave is a non-modal solution, as it does not satisfy the condition at infinity in the broadside direction ($x = +\infty$). The surface wave mode also does not satisfy the condition at infinity ($x = 0, z = \pm\infty$). But in the case of a surface wave mode, the small losses in the structure introduce an imaginary part in the surface wave pole k_x , and hence the condition at infinity ($z = \pm\infty, x = 0$) is not violated in practice. So, the surface wave mode may be regarded, in this sense, as a consequence of modal solution.

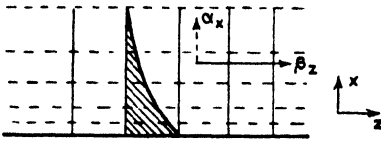


Fig. 3
Nature of surface wave

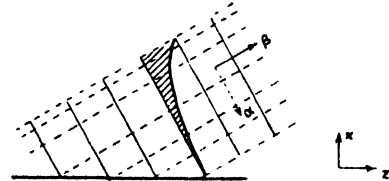


Fig. 4
Nature of leaky wave

9. Inhomogeneous guide

In the case of an inhomogeneous guide, the constitutive parameters ϵ and μ are the functions of coordinates, $\epsilon, \mu = f(x, y)$, say.

Let

$$\gamma^2 = -(h^2 + k^2) \quad (42)$$

where

$$k^2 = \omega^2 \mu \epsilon$$

which indicates that $\gamma^2 = f(x, y)$. So, γ^2 does not have the usual significance of an eigenvalue characterizing a mode as in the case of a homogeneous guide. Since, $k^2 = f(x, y, \omega)$ and $h^2 = f(\omega)$, therefore, $\gamma^2 = f(x, y, \omega)$. Hence, in an inhomogeneous guide, the field distribution for each mode will change with the angular frequency of excitation of the wave, ω , unlike that in a homogeneous guide, where γ^2 is independent of ω for each mode, and the wave equation in E_x or H_x does not contain coefficients $f(\omega)$. So, in the case of an inhomogeneous guide, the identification of modes in terms of E or H becomes difficult as the field distribution is not invariant with ω .

Whereas modal classification into E or H waves is possible in the case of a homogeneous guide as the field distribution remains invariant with change in ω over the range $0 < \omega < \infty$, in the case of inhomogeneous guides, E_x and H_x coexist with each other by the variation in ϵ and μ with x, y and as such, a complete set of modes, if it exists, must be composed of E, H or HE modes.

10. Conclusions

From the foregoing discussion on the classification of modes, the conclusions that may be drawn are :

- (i) The problem of finding the modes in a waveguide is equivalent to determining the eigenvalues of a differential equation. In waveguide

problems, if the coefficients of the differential equation are real, the eigenfunctions and eigenvalues are also real and unique modal classifications and ordering of modes are possible. But if the coefficients, eigenfunctions and eigenvalues are complex, an unique ordering of modes is not possible ;

- (ii) In general, except in the case of H.S.P. guides, no mode can exist on its own ; but it can exist in conjunction with other modes ;
- (iii) In the regions of finite extent and completely bounded electromagnetically opaque walls, the source-free solutions possess a discrete spectrum, everywhere finite, and individually satisfy the field equations and boundary conditions ;
- (iv) In the case of open guides, there may exist a discrete spectrum of modes but these must be supplemented, in general, by a continuous spectrum of modes ;
- (v) The continuous modes are improper in that they are not square integrable (finite energy), and they do not satisfy the boundary conditions at the singular point, *i.e.*, infinity ;
- (vi) In addition to a continuous spectrum, there may exist a set of non-modal solutions which may become infinite in the infinitely remote region of space. To this category belong the leaky modes ;
- (vii) The entire field in a waveguide may be expressed as the sum of pole waves and branch-cut waves. The subdivision of a dynamic electromagnetic field into guided waves, surface waves, leaky waves and a radiation field depends on the nature of the integrand in the contour integral, in terms of which the total field at a point is expressed ; and
- (viii) The existence of guided waves, surface waves or leaky waves depends on the nature of the poles in the integrand of the contour integral and is associated with the residues evaluated at the respective poles. The radiation field arises as a consequence of the branch-cut integration.

11. Acknowledgment

The author acknowledges with thanks the encouragement given by Prof. S. V. C. Aiya, Professor of Electrical Communication Engineering, Indian Institute of Science, Bangalore.

12. References

1. R. A. Waldron. 'The Theory of Waveguides and Cavities'. *Electronic Technology*, vol. 38, no. 4, 1961, p. 140.
2. A. R. Forsyth. 'Theory of Functions of a Complex Variable'. *Cambridge University Press*, 3rd ed., 1918.
3. A. Nisbet. 'Hertzian Electromagnetic Potentials and Associate Gauge Transformation'. *Proceedings of the Royal Society*, vol. A 231, no. 1185, 1955, p. 250.

4. J. Van Bladel. 'Field Expandability in Normal Modes for a Multilayered Rectangular or Circular Waveguide'. *Journal of the Franklin Institute*, vol. 253, 1952, p. 313.
5. S. K. Chatterjee. 'Propagation of Microwaves through a Cylindrical Metallic Guide Filled Coaxially with Two Different Dielectrics, Pts. 1-5'. *Journal of the Indian Institute of Science*, vol. 35, 1953, p. 1 ; vol. 35, 1953, p. 103 ; and vol. 36, 1954, p. 1.
6. A. D. Bresler, G. H. Joshi and N. Marcuvitz. 'Orthogonality Properties for Modes in Passive and Active Uniform Waveguides'. *Journal of Applied Physics*, vol. 29, 1958, p. 794.
7. H. Levine and J. Schwinger. 'On the Theory of Electromagnetic Wave Diffraction by an Aperture in an Infinite Plane Conducting Screen'. *Communications on Pure and Applied Mathematics*, vol. 3, no. 4, 1950, p. 355.
8. F. E. Borgnis and C. H. Papas. 'Randwerte Probleme der Mikrowellenphysik'. *Springer Verlag*, Berlin, 1955.
9. B. L. Van der Warden. 'On the Method of Saddle Points'. *Applied Science Research*, vol. 2B, 1950, p. 33.
10. P. C. Clemow. 'Some Extension to the Method of Integration by Steepest Descents'. *Quarterly Journal of Mechanical and Applied Mathematics*, vol. 3, 1950, p. 241.
11. H. Ott. 'Die Sattelpunktes Methode in der Umgebung eines Pols mit Anwendungen und die Wellenoptik und Akustik'. *Annalen der Physik*, vol. 43, 1943, p. 393.
12. A. E. Karbowiak. 'Radiation and Guided Waves'. *Transactions of the Institute of Radio Engineers*, vol. AP-7, 1959, p. 191.
13. C. T. Tai. 'The Effect of a Grounded Slab on the Radiation from a Line Source'. *Journal of Applied Physics*, vol. 22, no. 4, 1951, p. 405.



THE HOME OF ELECTRONICS

The modern, well-equipped BHARAT ELECTRONICS' Plant in Bangalore, with its comprehensive production and development facilities, has harnessed the new medium of Electronics.

BHARAT ELECTRONICS produces and supplies a broad range of Electronic Equipment and Components which are used by the Defence Services, the Railways, the Overseas Communications Services, Police departments, All India Radio, Transport undertakings, Meteorological department, Radio manufacturers and a host of other designers and professional users.

BHARAT ELECTRONICS LTD.

Regd. Office: JALAHALLI — BANGALORE - 13



..... *Going forward with the Nation*

EP-BEL-14

THE JOURNAL

OF

The Institution of Engineers (India)

DEPUTY SECRETARY & ACTING EDITOR : D. K. Ghosh, B.E., C.E.,
D.T.R.P., A.M.I.E.

The Institution of Engineers (India) as a body accepts no responsibility for the statements made by the individual authors.

The Institution of Engineers (India) subscribes to the Fair Copying Declaration of the Royal Society and reprints of any portion of this publication may be made provided that reference thereto be quoted.

Vol. XLVI

JANUARY 1966

No. 5, Pt. ET 2

CONTENTS

Page

ELECTRONICS AND TELECOMMUNICATION ENGINEERING DIVISION

1. **Network Structures for a Special Class of Minimum Biquartic PR-Functions.** J. G. Advani, *Non-member*, and O. P. Gupta, *Non-member* .. 31
2. **Synthesis of an A.C. Lead Transfer Function for Minimum Sensitivity by Parallel Ladder Procedure.** J. G. Advani, *Non-member*, and B. Kesavan, *Non-member* .. 39
3. **Transistor Rectangular Pulse Generator.** R. R. Mehrotra, *Non-member*, Harbans Lal, *Non-member*, and B. K. Tyagi, *Non-member* .. 49

Electronics and Telecommunication Engineering Division Board

The President (*Ex-officio*)

Brig. M. K. Rao (*M.*), *Chairman*

Prof. S. P. Chakravarti (*M.*)

Lt.-Col. S. Mishra (*M.*) (*Co-opted*)

Automatic Control Group

Prof. V. V. Sarwate, *Chairman*

HIVELM

**HIGH VOLTAGE EQUIPMENT &
LINE MATERIAL**

**ISOLATORS &
AIR BREAK
SWITCHES**

**ROBUST DESIGN FOR
ENDURING SERVICE**

**FROM 11 KV TO 220 KV
RATINGS UP TO 1200 AMPS**

- Mechanical Interlocks • Electrical Interlocks
- Motor Operation • Auxiliary Switches
- Interlocked Grounding Blades
- Heavy Duty Busbar Connectors and Clamps, etc.

Manufactured by:

HIVELM INDUSTRIES PRIVATE LTD.

Works: A-5/6, Industrial Estate, Guindy, Madras-32

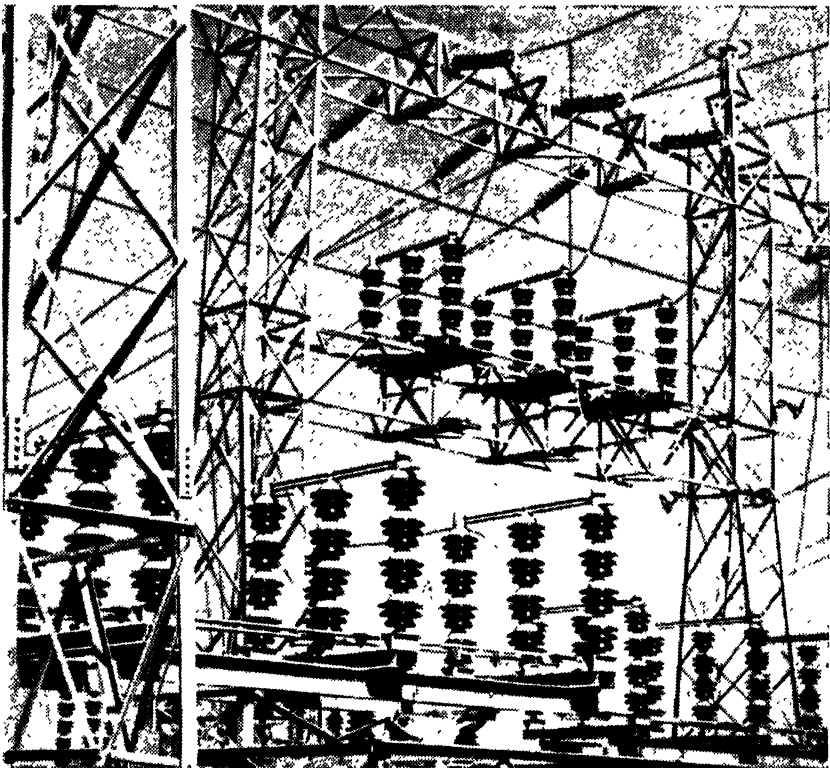
Phone: 80504; 80939 Grams: 'HIVELM'

Administrative Office: 8, 1st Main Road,

Kasturba Nagar, Adyar, Madras-20

Phone: 74461 Grams: 'HIVELM'

EP-HI-3



NETWORK STRUCTURES FOR A SPECIAL CLASS OF MINIMUM BIQUARTIC PR-FUNCTIONS*

J. G. Advani

Non-member

and

O. P. Gupta

Non-member

Summary

Network structures to realize the minimum pr-impedance functions were discussed by Valkenburg, Foster, Kim and Seshu. The networks were derived mostly for the simplest form of minimum pr-functions, i.e., the minimum functions having zero real part at one frequency. This paper attempts to obtain the network configurations realizing a sub-class of minimum pr-functions having zero real part at two frequencies, which are biquartic functions. The basic five-element networks (realizing the minimum biquadratic functions) discussed by Valkenburg are modified to yield the minimum biquartic pr-functions having zero real part at two frequencies. Some theorems from the graph theory are used in deriving the modified structures. The networks obtained in this fashion are two 7-element, two 8-element and six 9-element networks. The conditions on the coefficients of a given biquartic function so that it is realizable by the above networks, and the values of the network elements in terms of the coefficients are derived and tabulated.

1. Introduction

A biquartic function given by

$$Z(s) = K \frac{s^4 + a_3 s^3 + a_2 s^2 + a_1 s + a_0}{s^4 + b_3 s^3 + b_2 s^2 + b_1 s + b_0} \quad (1)$$

will be the minimum pr-function having $\text{Re. } Z(j\omega) = 0$ at two positive real and distinct frequencies if the following six conditions, in addition to the requirement that all the coefficients are positive, are satisfied by the coefficients of $Z(s)$.

$$a_2 > \frac{a_1}{a_3} + a_0 \frac{a_3}{a_1} \quad (2)$$

$$b_2 > \frac{b_1}{b_3} + b_0 \frac{b_3}{b_1} \quad (3)$$

$$\sqrt{a_0 b_0} (a_2 + b_2 - a_3 b_3) = a_2 b_0 + a_0 b_2 - a_1 b_1 \quad (4)$$

$$\left(\frac{a_3 + b_3 - a_3 b_3}{2} \right)^2 = (\sqrt{a_0} - \sqrt{b_0})^2 + a_2 b_2 - (a_1 b_3 + a_3 b_1) \quad (5)$$

* Written discussion on this paper will be received until March 31, 1966.

This paper was received on February 23, 1965.

$$a_2 + b_2 > a_3 b_3 \quad (6)$$

$$\left(\frac{a_2 + b_2 - a_3 b_3}{2} \right)^2 > 4 \sqrt{a_0 b_0} \quad (7)$$

Conditions (2) and (3) ensure that the numerator and denominator of $Z(s)$ are strict Hurwitz polynomials, conditions (4) and (5) ensure that $\text{Re. } Z(j\omega) = 0$ at two frequencies, ω_1 and ω_2 , and conditions (6) and (7) ensure that ω_1 and ω_2 are positive real and distinct.

The further conditions on the coefficients of $Z(s)$, so that it may be realizable by the networks, derived in section 2, are obtained in section 3.

2. Derivation of network structures

For any biquartic pr -function with $Z(0) = Z(\infty)$, at least one resistor and four reactive elements shall be required. The only two possible networks with five elements and satisfying path and cut-set requirements are discussed elsewhere.⁶

For any biquartic pr -function with $Z(0) \neq Z(\infty)$, at least two resistive and four reactive elements shall be required. All the possible six element networks realizing the minimum pr -functions, with $Z(0) \neq Z(\infty)$, discussed by Foster,² Kim,³ Seshu⁴ and Reed⁵ can realize pr -functions having real part zero at one frequency only.

Network configurations having 2 resistive and 5 (also 6 and 7) reactive elements for the realization of some of the minimum pr -functions having $\text{Re. } Z(j\omega) = 0$ at two frequencies, are derived below.

The Valkenburg¹ network, shown in Fig. 1, for a minimum biquadratic function is considered. This gives one real frequency transmission zero through R_2 when R_1 is open-circuited or short-circuited, or *vice versa*, and hence $\text{Re. } Z(j\omega) = 0$ at one frequency only. To achieve two real frequency transmission zeros for $\text{Re. } Z(j\omega) = 0$ at two frequencies, the network of Fig. 1 is modified to the network structures shown in Figs. 2 and 3.

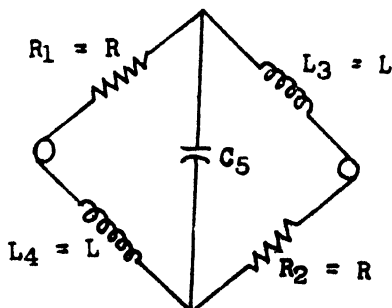


Fig. 1
The Valkenburg network

In the network of Fig. 2, Z_3 and Z_4 are reactive circuits and are of such form that the path and cut-set conditions are satisfied, for this network to yield the minimum pr -function. To get the zero of transmission through R_2 at two frequencies, when

R_1 is open-circuited, $(Z_3 + Z_4)$ should have two pairs of zeros on the real frequency axis. The minimum number of reactive elements to give two pairs of finite zeros are four and the various combinations of $(Z_3 + Z_4)$ are given in Fig. 4. These combinations are divided into two parts (shown by dotted lines) and any one part may be used as Z_3 and the other as Z_4 . Actually, the network structures obtained from Z_3 and Z_4 of Fig. 4(iii) shall realize the same special class of biquartic pr -functions as those obtained from Fig. 4(i) and the same is true for the structures obtained from Figs. 4(ii) and (iv). Thus, there will be only six network structures, shown in Fig. 5, which can realize special class of the minimum biquartic pr -functions.

In the network structures of Fig. 3, one transmission zero is the same as in the case of Valkenburg while the other transmission zero is obtained by (i) introducing anti-resonant circuit in series with the resistances, or (ii) by introducing a series resonant circuit in parallel with the resistances. This way, there shall be another four networks, shown in Fig. 6, which can realize special class of minimum biquartic pr -functions.

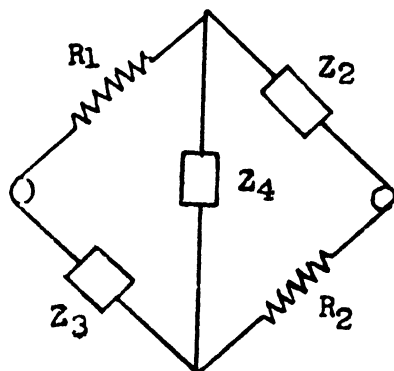
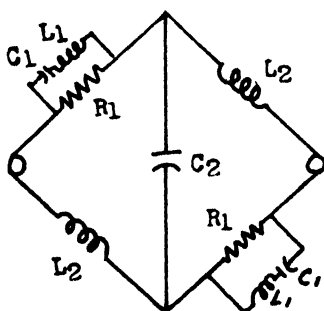
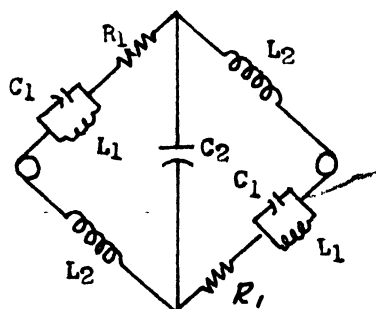


Fig. 2
 Modified network



(1)



(ii)

Fig. 3
 Modified networks

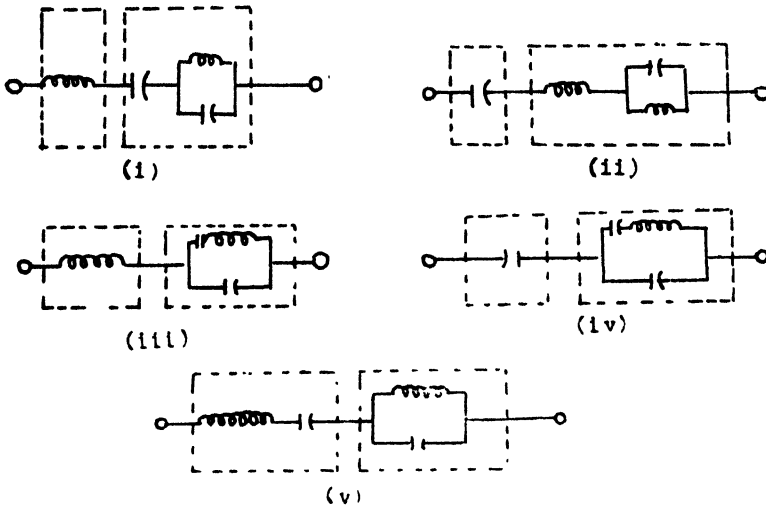


Fig. 4

Various combinations of $(Z_3 + Z_4)$

3. Restrictions on minimum biquartic *pr*-functions

The driving-point impedance function of the network of Fig. 5(i) is given by

$$Z(s) = 2R \frac{s^4 + \frac{S_1 + S_2}{2R} s^3 + \left(\frac{S_1 + S_2}{2L_1} + \frac{S_3}{L_2} \right) s^2 + \frac{S_1 S_2}{2R L_2} s + \frac{S_1 S_1}{2L_1 L_2}}{s^4 + \frac{R}{L_1} s^3 + \left(\frac{S_2}{L_2} + \frac{2S_1 + 2S_2}{L_1} \right) s^2 + \frac{R S_2}{L_1 L_2} s + \frac{2S_1 S_2}{L_1 L_2}} \quad (8)$$

A given function, $Z(s)$, of equation (1) will be realizable by the network of Fig. 5(i), if $Z(s)$ given by equations (1) and (8) are the same, i.e., the corresponding coefficients of the functions of equations (1) and (8) are equal.

Comparing the coefficients, nine equations are obtained. All the nine equations should be satisfied simultaneously for $Z(s)$ of equation (1) to be realizable by the network of Fig. 5(i). In these nine equations, five unknowns (R_1 , L_1 , L_2 , S_1 and S_2) are present. Eliminating these, four conditions on the coefficients of $Z(s)$ of equation (1) should be satisfied. The element values and the conditions are given below.

Element values

$$R = \frac{K}{2}, L_1 = \frac{K}{2b_3}, L_2 = \frac{K b_3}{b_1} \left(a_3 - \frac{a_0}{b_1} \right)$$

$$S_1 = \frac{K a_0}{b_1}, S_2 = K \left(a_3 - \frac{a_0}{b_1} \right)$$

Conditions

$$4a_0 = b_0 \quad (9)$$

$$a_0 = a_1 b_3 \quad (10)$$

$$b_1 = b_3 (a_2 - a_3 b_3) \quad (11)$$

$$b_3 = a_3 + 3a_3 b_3 \quad (12)$$

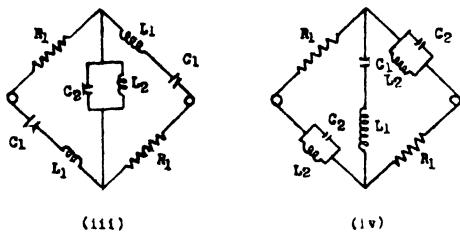
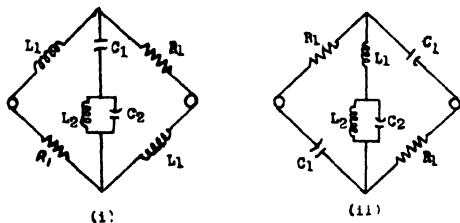


Fig. 5
Networks for realizing special
class of minimum biquartic
 pr -functions

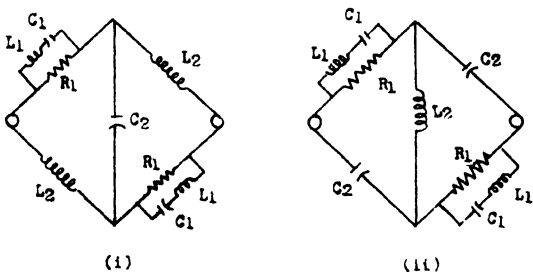
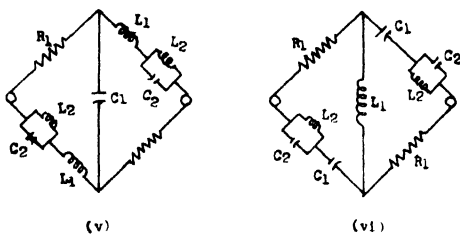
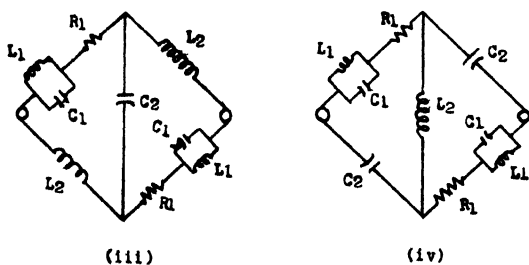


Fig. 6
Additional networks for
realizing special class of
minimum biquartic
 pr -functions



For the elements to have positive values, one more condition (inequality), given by equation (13), should be satisfied :

$$a_3 b_1 > a_0 \tag{13}$$

The five conditions given by equations (9) to (13) satisfy the conditions given by equations (2) to (7). Thus, the above-mentioned five conditions are the necessary conditions on the coefficients of a given biquartic function $Z(s)$, for $Z(s)$ to be the minimum *pr*-function having $\text{Re. } Z(j\omega) = 0$ at two positive real and distinct frequencies and as well be realizable by the network configuraton of Fig. 5(i). The four conditions in equations (9) to (12) satisfy the two conditions of equations (4) and (5) and hence this set of four conditions can be said to be equivalent to the set of four conditions of equations (4), (5), (9) and (10). Thus, the set of five conditions of equations (9) to (13) is the same as the set of five equations (4), (5), (9), (10) and (13). The conditions on the coefficients of $Z(s)$ for it to be a minimum *pr*-function having $\text{Re. } Z(j\omega) = 0$ at two positive real and distinct frequencies and as well be realizable by the various networks of Figs. 5 and 6 are given in Table 2.

If it is known that the given function, $Z(s)$, is a minimum *pr*-function having $\text{Re. } Z(j\omega) = 0$ at two positive real and distinct frequencies, *i.e.*, it satisfies the conditions of equations (2) to (7), then the coefficients of $Z(s)$ should satisfy fewer conditions than mentioned in Table 2, for it to be realizable by the various networks of Figs. (5) and (6).

For such $Z(s)$ to be realizable by network of Fig. 5(i), only two conditions, given by equations (9) and (10) should be satisfied, because the conditions (4) and (5) are automatically satisfied and condition (13) can be derived from condition (3). The necessary conditions on the coefficients of $Z(s)$ for it to be realizable by the other networks of Figs. 5 and 6 are given in Table 1.

The element values for networks of Figs. 5(i), 5(iii) and 6(i) in terms of the coefficients of $Z(s)$ are given in Table 3. The element values for the other networks can be simply manipulated by the principle of duality or by the substitution, $s = \frac{1}{p}$.

Table 1
Conditions on $Z(s)$ to be the minimum *pr*-function having $\text{Re. } Z(j\omega) = 0$
at two positive real and distinct frequencies, to be realizable
by various networks

Network	Conditions
Fig. 5(i)	(1) $4 a_0 = b_0$ and (2) $a_0 = a_1 b_3$
Fig. 5(ii)	(3) $a_0 = 4 b_0$ and (4) $b_0 = a_3 b_1$
Fig. 5(iii)	(5) $a_0 = b_0$ and (6) $b_2 = a_2 + 3 a_3 b_3$
Fig. 5(iv)	(7) $a_0 = b_0$ and (8) $a_2 = b_2 + 3 a_3 b_3$

Table 1 (*Contd.*)

Fig. 5(v)	(9) $4 a_0 = b_0$	and	(10) $a_0 = a_3 b_1$
Fig. 5(vi)	(11) $a_0 = 4 b_0$	and	(12) $b_0 = a_1 b_3$
Fig. 6(i)	(13) $4 a_0 = b_0$	and	(14) $a_1 = a_3 (a_2 - a_3 b_3)$
Fig. 6(ii)	(15) $a_0 = 4 b_0$	and	(16) $a_1 a_3 b_2 = a_1^2 + a_3^2 b_0$
Fig. 6(iii)	(17) $4 a_0 = b_0$	and	(18) $a_2 b_1 b_3 = a_0 b_3^2 + b_1^2$
Fig. 6(iv)	(19) $a_0 = 4 b_0$	and	(20) $a_2 b_1 b_3 = a_0 b_3^2 + b_1^2$

Table 2

Conditions on $Z(s)$ to be the minimum *pr*-function having $\text{Re. } Z(j\omega) = 0$
at two positive real and distinct frequencies and also realizable by
the varicus networks

Network	Conditions
Fig. 5(i)	Equations (4), (5) ; conditions (1), (2) in Table 1 and $a_3 b_1 > c_0$
Fig. 5(ii)	Equations (4), (5); conditions (3), (4) in Table 1 and $a_1 b_3 > b_0$
Fig. 5(iii)	Equations (4), (5); and conditions (5), (6) in Table 1
Fig. 5(iv)	Equations (4), (5); and conditions (7), (8) in Table 1
Fig. 5(v)	Equations (4), (5); conditions (9), (10) in Table 1 and $a_1 b_3 > c_0$
Fig. 5(vi)	Equations (4), (5); conditions (11), (12) in Table 1 and $a_3 b_1 > b_0$
Fig. 6(i)	Equations (3), (4), (5), (7); conditions (13), (14) in Table 1 and $a_3 b_1 > c_0$
Fig. 6(ii)	Equations (3), (4), (5), (7); conditions (15), (16) in Table 1 and $a_1 b_3 > b_0$
Fig. 6(iii)	Equations (2), (4), (5), (7); conditions (17), (18) in Table 1 and $a_3 b_1 > c_0$
Fig. 6(iv)	Equations (2), (4), (5), (7); conditions (19), (20) in Table 1 and $a_3 b_1 > b_0$

Table 3

Element values in terms of coefficients of $Z(s)$

Network	Element values
Fig. 6(i)	$R_1 = \frac{K}{2}, L_1 = \frac{2 K a_0 a_3^2}{a_1 (a_3 b_1 - a_0)}, L_2 = \frac{K a_1}{2 a_0}, S_1 = \frac{2 K a_0 a_3}{a_3 b_1 - a_0}, S_2 = K a_3$
Fig. 5(i)	$R_1 = \frac{K}{2}, L_1 = \frac{K}{2 b_3}, L_2 = \frac{K b_3 (a_3 b_1 - a_0)}{b_1^2}, S_1 = \frac{K a_0}{b_1}, S_2 = \frac{K (a_3 b_1 - a_0)}{b_1}$
Fig. 5(iii)	$R_1 = \frac{K}{2}, L_1 = \frac{K}{2 b_3}, L_2 = \frac{K a_1}{b_0}, S_1 = \frac{K b_0}{2 b_1}, S_2 = K a_3$

4. Conclusions

The calculations presented in this paper gives more familiarity and insight on an aspect of passive network synthesis techniques using the basic ideas from graph theory. Network structures yielding a special class of minimum pr -functions having $\text{Re. } Z(j\omega) = 0$ at three or more frequencies can be developed by following the methods presented herein. The special class of $Z(s)$ realized here requires 7, 8 or 9 elements which by Bott-Daffin procedure would require 19 elements. It is of some interest to note that the networks of Fig. 6 realize $Z(s)$ having $\text{Re. } Z(j\omega) = 0$ at two frequencies $\omega_1 = \frac{1}{\sqrt{L_1 C_1}}$ and $\omega_2 = \frac{1}{\sqrt{L_2 C_2}}$. So if $L_1 C_1 = L_2 C_2$, the networks of Fig. 6 can realize impedance functions having real part of the form $\frac{(\omega^2 - \omega_0^2)^4}{\text{Denominator}}$ (i.e., it is zero at only one frequency but the zero is of fourth order instead of second order).

5. References

1. M. F. Van Valkenburg. 'Special Case of a Bridge Equivalent of Brune Networks'. *Proceedings of the Institution of Radio Engineers*, vol. 44, November 1956, p. 1621.
2. R. M. Foster. 'Minimum Biquadratic Impedances'. *I.E.E.E. Transactions on Circuit Theory*, vol. CT-10, December 1963, p. 527.
3. W. H. Kim. 'On Non-Series-Parallel Realization of Driving-Point Functions'. *I.R.E. National Convention Record*, pt. 2, 1958, p. 76.
4. S. Seshu. 'Minimal Realizations of the Biquadratic Minimum Functions'. *I.R.E. Transactions on Circuit Theory*, vol. CT-6, December 1959, p. 345.
5. S. Seshu and M. B. Reed. 'Linear Graphs and Electrical Networks'. *Addison-Wesley Publishing Co., Inc.*, 1961.
6. O. P. Gupta. 'Realization Techniques for Some Classes of Minimum pr -Functions'. Thesis submitted to the Rajasthan University for M.E. (Electronics) Degree, 1964.

SYNTHESIS OF AN A.C. LEAD TRANSFER FUNCTION FOR MINIMUM SENSITIVITY BY PARALLEL LADDER PROCEDURE*

J. G. Advani

Non-member

and

B. Kesavan

Non-member

Summary

The performance of an A.C. system is adversely affected by the changes in either carrier frequency or the notch frequency of the A.C. compensating network. This paper presents a procedure for synthesis that minimizes the changes in the notch frequency ω_0 , and defines the overall sensitivity, S_0 , with respect to the variations in the various elements of the network. The transfer function of a T-network is synthesized by Guillemin's procedure. The values of the elements of networks realized are in terms of a and b . The overall sensitivity, W_0 , is found in terms of a and b for two cases. It is observed that for case 1, $a = 0.293$ and 1.707 give the minimum sensitivity of 0.935 and for case 2, $a = 0.27$ and $b = 3.75$ give the minimum sensitivity of 0.371 . The overall sensitivity of the twin T-network is found to be 1.414 .

1. Introduction

The A.C. lead compensating networks (twin-T and bridge-T), containing resistances and capacitances are widely used to satisfy simultaneously the performance specifications given for steady state and transient response in an A.C. servo system.

The performance of an A.C. control system is adversely affected due to changes in carrier frequency or notch frequency. Many authors^{1,2,3} have worked on the design of A.C. compensating networks (bridge-T and twin-T), which would provide satisfactory compensation for changes/predetermined changes in the carrier frequency. Networks designed this way are effective even if there are changes in the notch frequency instead of carrier frequency. These networks though give satisfactory performance for changes in the notch frequency, the change in the notch frequency gives some quadrature component and thus would affect the performance of the control system to some extent.

In this paper, A.C. compensating networks are synthesized for the minimum variation in notch frequency, ω_0 , due to changes in the various elements of the network. The synthesis is carried out by parallel ladder method for the transfer function of a twin T-network.

*Written discussion on this paper will be received until March 31, 1966.

This paper was received on September 17, 1965.

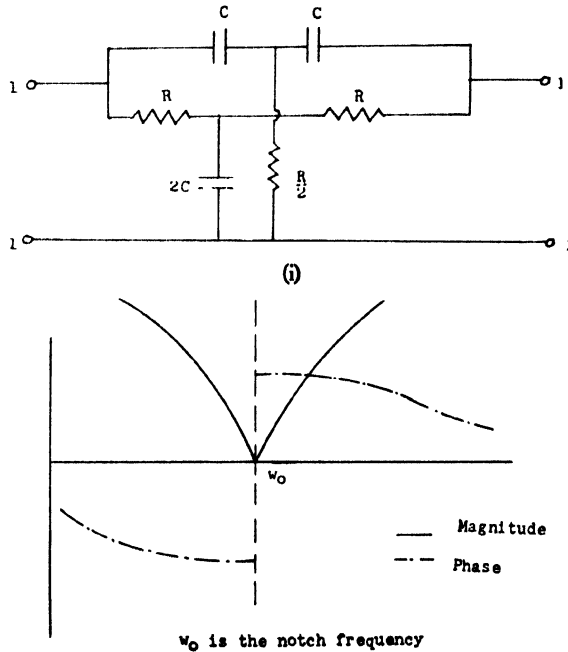
2. Sensitivity of a twin T-network

2.1. Transfer function

For the twin T-network shown in Fig. 1(i), the transfer function is found to be

$$T(s) = \frac{s^2 + \frac{1}{\tau^2}}{s^2 + \frac{4s}{\tau} + \frac{1}{\tau^2}} \quad (1)$$

where $\tau = RC$.



(ii)

Fig. 1

Twin T-network and its performance curves

The magnitude and phase shift of $T(j\omega)$ is plotted against ω_0 in Fig. 1(ii). The notch frequency ω_0 , for this network is given by

$$\omega_0 = \frac{1}{\tau}$$

or,

$$\omega_0 = \frac{1}{RC} \quad (2)$$

2.2. Overall sensitivity

The sensitivity of notch frequency ω_0 , with respect to any element e_k is defined as

$$S_k = \frac{\ln \omega_0}{\ln e_k}$$

or,

$$S_k = \frac{e_k}{w_0} \frac{\partial w_0}{\partial e_k} \quad (3)$$

The overall sensitivity of w_0 with respect to all the n elements of the network is defined as

$$S = \sqrt{\sum_{k=1}^n S_k^2} \quad (4)$$

From equation (2), it is observed that w_0 depends on R and C . The total sensitivity of w_0 , as defined by equation (4), is calculated to be

$$S = 1.414 \quad (5)$$

3. Synthesis of $T(s)$ by parallel ladder procedure

The transfer function $T(s)$, of equation (1) is synthesized by Guillemin's procedure in two ways for the two cases given below.

Case 1

In this case, one finite pole is at $s = -\frac{a}{\tau}$ of y_{22} . Transfer function $T(s)$, of equation (1) can be written as

$$T(s) = \frac{\left(s^2 + \frac{1}{\tau^2}\right) \left(s + \frac{a}{\tau}\right)}{\left(s^2 + \frac{4s}{\tau} + \frac{1}{\tau^2}\right) \left(s + \frac{a}{\tau}\right)} \quad (6)$$

Using the y -parameters of a two-port network, $T(s)$ can be written as

$$T(s) = -\frac{y_{12}}{y_{22}} \quad (7)$$

From equations (6) and (7), $-y_{12}$ and y_{22} can be recognized as

$$-y_{12} = \frac{\left(s^2 + \frac{1}{\tau^2}\right) \left(s + \frac{a}{\tau}\right)}{\left(s + \frac{a}{\tau}\right)}$$

and

$$y_{22} = \frac{\left(s^2 + \frac{4s}{\tau} + \frac{1}{\tau^2}\right) \left(s + \frac{a}{\tau}\right)}{\left(s + \frac{a}{\tau}\right)} \quad (8)$$

For y_{22} to be an R - C admittance, $2 - \sqrt{3} < a < 2 + \sqrt{3}$. Guillemin's procedure⁴ is adopted to synthesize a network from the y -parameters of equation (8) and the network realized is shown in Fig. 2. The values of the various elements of the network are :

$$R_1 = \frac{2(4a - a^2 - 1)\tau}{(4 - a)}$$

$$R_2 = \frac{2\tau}{4 - a}$$

$$R_3 = \frac{2a(4a - a^2 - 1)\tau}{(4a - 1)^2}$$

$$R_4 = 2a\tau$$

$$C_1 = \frac{(4 - a)^2}{2(4a - a^2 - 1)}$$

$$C_2 = \frac{1}{2}$$

$$C_3 = \frac{(4a - 1)}{2(4a - a^2 - 1)}$$

$$C_4 = \frac{4a - 1}{2a^2} \quad (9)$$

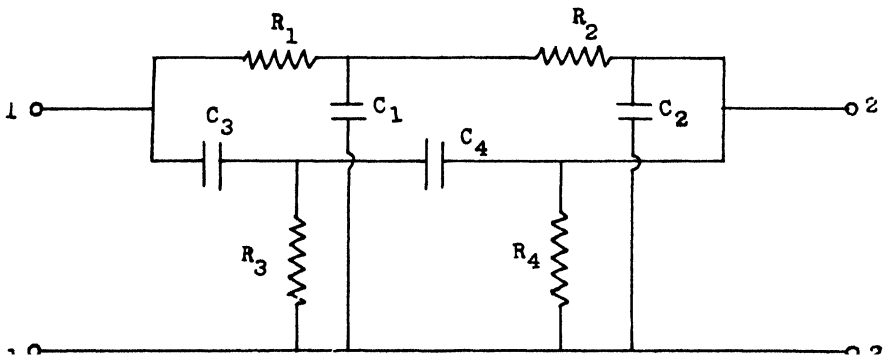


Fig. 2

Network realized by synthesis

The transfer function of the network of Fig. 2, in terms of its elements, is found to be

$$T(s) = \frac{s^3 R_4 R_1 R_2 R_3 C_1 C_3 C_4 + s^2 R_4 R_3 C_3 C_4 (R_1 + R_2) + s R_4 (R_3 C_3 + R_3 C_4) + R_4}{\text{Denominator}} \quad (10)$$

The denominator polynomial of equation (10) is also of third order. The transfer functions of equations (10) and (1) refer to the same network of Fig. 2. So the numerator and denominator polynomials of equation (10) must be quadratic expressions

in s and must have a factor $(s + p)$ in common. Hence, equation (10) can be re-written as

$$T(s) = \frac{(s + p)(s^2 + d)}{(s + p)(\text{Remainder of the denominator})} \quad (11)$$

or,

$$T(s) = \frac{(s^2 + d)}{\text{Remainder of the denominator}} \quad (12)$$

Comparing the coefficients of the numerator polynomials of equation (11) and (10), d is found to be

$$d = \frac{C_3 + C_4}{R_1 R_2 C_1 C_3 C_4}$$

From equations (12) and (1), it is observed that $d = \frac{1}{\tau^2}$ and knowing that $w_0 = \frac{1}{\tau}$, the value of w_0 would be

$$W_0 = \sqrt{\frac{C_3 + C_4}{R_1 R_2 C_1 C_3 C_4}} \quad (13)$$

The sensitivities of w_0 with respect to R_1 , R_2 , C_1 , C_3 and C_4 are found out from the definition of equation (3). The overall sensitivity w_0 , as defined in equation (4) is found to be

$$S = \frac{1}{2 w_0} \left[3 \frac{C_3 + C_4}{R_1 R_2 C_1 C_3 C_4} + \left(\frac{1}{C_3^2} + \frac{1}{C_4^2} \right) \frac{C_3 C_4}{R_1 R_2 C_1 (C_3 + C_4)} \right]^{\frac{1}{2}} \quad (14)$$

Substituting the values of the various elements from equation (9),

$$S = \frac{1}{2} \left[3 + \frac{a^4 + (4a - a^2 - 1)^2}{(4a - 1)^2} \right]^{\frac{1}{2}} \quad (15)$$

The plot of S of equation (15) for different values of a is given in Fig. 3. From this plot, it is observed that the minimum value of S is 0.935 and it occurs for $a=0.293$ and also for $a = 1.707$. The element values of equation (9) for these two values of a are given in Table 1 and it is observed that the higher value of a ($= 1.707$) gives smaller capacitances in the network.

Case 2

In this case, two finite poles are at $s = -\frac{a}{\tau}$ and $s = -\frac{b}{\tau}$ of y_{22} .

Dividing the numerator and denominator of $T(s)$ of equation (1) by $\left(s + \frac{a}{\tau}\right)$ $\left(s + \frac{b}{\tau}\right)$, the two y -parameters are obtained as given below.

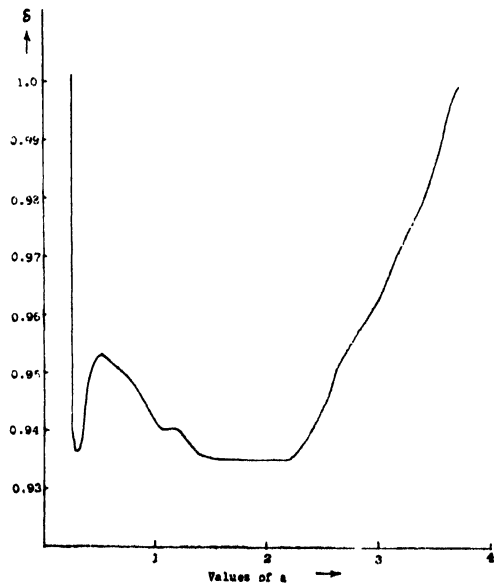


Fig 3
Plot of *S* for different values of *a*

Table 1
Element values of equation (9)

Elements	Element values	
	<i>a</i> =0.293	<i>a</i> =1.707
<i>R</i> ₁	0.0464 τ ohm	2.555 τ ohm
<i>R</i> ₂	0.5400 τ ohm	0.872 τ ohm
<i>R</i> ₃	1.7050 τ ohm	0.295 τ ohm
<i>R</i> ₄	0.8600 τ ohm	3.414 τ ohm
<i>C</i> ₁	80 farad	0.895 farad
<i>C</i> ₂	0.5 farad	0.500 farad
<i>C</i> ₃	1 farad	0.995 farad
<i>C</i> ₄	1 farad	1.002 farad

$$\left. \begin{aligned} -y_{12} &= \frac{s^2 + \frac{1}{\tau^2}}{\left(s + \frac{a}{\tau}\right)\left(s + \frac{b}{\tau}\right)} \\ y_{22} &= \frac{s^2 + \frac{4s}{\tau} + \frac{1}{\tau^2}}{\left(s + \frac{a}{\tau}\right)\left(s + \frac{b}{\tau}\right)} \end{aligned} \right\} \quad (16)$$

and

For y_{22} to be an R - C admittance,

$$2 - \sqrt{3} < a < 2 + \sqrt{3}$$

and

$$b > 2 + \sqrt{3} \quad (17)$$

Following Guillemin's procedure, the network is synthesized from y -parameters of equation (16) and the network thus realized is shown in Fig. 4. The values of the various elements of the network are as below.

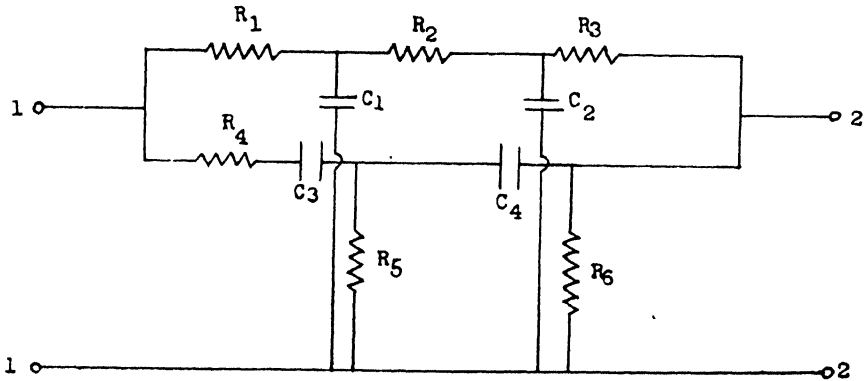


Fig. 4

Network realized by synthesis

$$\begin{aligned} R_1 &= \frac{\frac{P}{L\beta}}{(15 + ab - 4a - 4b)} \\ R_2 &= \frac{\left(\frac{a+b-4}{L\beta}\right)^2}{(4a + 4b - 15 - ab)} \\ R_3 &= \frac{1}{L\beta} \\ R_4 &= \frac{\frac{X}{L\alpha}}{(4ab - a - b)(a + b - 4) - (ab - 1)^2} \end{aligned}$$

$$\begin{aligned}
 R_5 &= \frac{\frac{a b X}{L_\alpha}}{(4 a b - a - b)^2} \\
 R_6 &= \frac{L_\alpha}{a b} \\
 C_1 &= \frac{(15 + a b - 4 a - 4 b)^2 \tau L_\beta}{(4 - a - b)} \\
 C_2 &= \frac{\tau L_\beta}{(4 a b - a - b) P} \\
 C_3 &= \frac{(4 a b - a - b) \{(4 a b - a - b)(a + b - 4) - (a b - 1)^2\} \tau L_\alpha}{X^2} \\
 C_4 &= \frac{(4 a b - a - b) \tau L_\alpha}{a^2 b^2}
 \end{aligned} \tag{18}$$

where

$$\begin{aligned}
 X &= 4 a b (a + b) - (a + b)^2 - a b (a b - 1) \\
 P &= (a + b)^2 + a b (a b + 14) - 4 (a + b) (a b + 1) + 1 \\
 L_\alpha &= \frac{X}{(4 a b - a - b)(a + b - 4) - (a b - 1)^2 + X} \\
 L_\beta &= \frac{(4 a b - a - b)(a + b - 4) - (a b - 1)^2}{(4 a b - a - b)(a + b - 4) - (a b - 1)^2 + X}
 \end{aligned}$$

The transfer function of the network of Fig. 4 is found to be

$$T(s) = \frac{s^4 (R_1 R_2 R_3 R_6 C_1 C_2 C_3 C_4) + s^3 R_5 C_4 C_3 (R_2 R_3 C_2 + R_1 R_3 C_2 + R_1 R_3 C_1 + R_1 R_2 C_1) + s^2 (R_6 C_4 C_3) (R_1 + R_2 + R_3 + R_4) + s (R_5 C_3 + R_5 C_4 + R_4 C_3) + 1}{\text{Denominator}} \tag{19}$$

where the denominator polynomial is of 4th order in s .

The numerator and denominator polynomials of equation (19) are quartic in s . Since the transfer functions of equations (19) and (1) refer to the same network of Fig. 4, the numerator and denominator polynomials of equation (19) should be quadratic in s and so they have a factor of the form $(s^2 + p s + q)$ in common. Thus, transfer function $T(s)$ can be written as

$$T(s) = \frac{(s^2 + p s + q)(s^2 + d)}{(s^2 + p s + q)(\text{Remainder of denominator})} \tag{20}$$

or,

$$T(s) = \frac{(s^2 + d)}{(\text{Remainder of denominator})} \tag{21}$$

Comparing the coefficients of the numerator polynomials of equations (20) and (19), d is found to be

$$d = \frac{(R_5 C_3 + R_5 C_4 + R_4 C_3)}{R_6 C_3 C_4 (R_2 R_3 C_2 + R_1 R_3 C_2 + R_1 R_3 C_1 + R_1 R_2 C_1)} \tag{22}$$

Comparing the numerator polynomials of equations (21) and (1), the notch frequency $w_0 \left(= \frac{1}{\tau} \right)$ is found to be

$$w_0 = \left[\frac{(R_5 C_3 + R_5 C_4 + R_4 C_3)}{R_5 C_3 C_4 (R_2 R_3 C_3 + R_1 R_3 C_2 + R_1 R_3 C_1 + R_1 R_3 C_1)} \right]^{\frac{1}{2}} \quad (23)$$

The overall sensitivity of the notch frequency w_0 , with respect to the elements in equation (23) is found to be

$$S = \frac{1}{2 w_0} \left(\frac{\left[\left(\frac{1}{C_4} + \frac{1}{C_3} + \frac{R_4}{R_5 C_4} \right) \{ R_1^2 (R_3 C_2 + R_3 C_1 + R_2 C_1)^2 + R_2^2 (R_3 C_2 + R_1 C_1)^2 + R_3^2 (R_2 C_2 + R_1 C_1 + R_1 C_1)^2 + C_1^2 (R_1 R_3 + R_1 R_2)^2 + C_3^2 (R_2 R_3 + R_1 R_3)^2 \} \right]}{[(R_2 R_3 C_3 + R_1 R_3 C_2 + R_1 R_3 C_1 + R_1 R_3 C_1)]} \right. \\ \left. + \frac{\left[\frac{1}{C_3^2} + \frac{1}{C_4^2} \left(1 + \frac{R_4}{R_5} \right)^2 + 2 \left(\frac{R_4}{R_5 C_4} \right)^2 \right]}{\left[\left(\frac{1}{C_3} + \frac{1}{C_4} + \frac{R_4}{R_5 C_4} \right) (R_3 R_2 C_2 + R_3 R_1 C_2 + R_1 R_3 C_1 + R_1 R_2 C_1) \right]} \right)^{\frac{1}{2}} \quad (24)$$

The values of the various elements from equation (18) can be substituted in equation (24) and the expression for the (overall sensitivity)² be obtained in terms of a and b .

For various values of a and b , the values of S are found out and the results are given in Table 2.

From Table 2, it is observed that the minimum value of S occurs for $a = 0.27$ and $b = 3.75$ and its value is 0.371.

Table 2
Calculated values

$a=0.3$		$a=0.27$	
b	S	b	S
10	0.870	10	0.740
6	0.751	6	0.770
4	0.675	4	0.392
3.75	0.372	3.75	0.371

4. Conclusions

It is observed that the overall sensitivity of the network realized in case 2 is much better than that realized in case 1. The overall sensitivity of network given in Fig. 4 is improved by a factor of 3.81 as compared to the original twin T-network of Fig. 1(i). This network, of course, contains four more elements but since the resistance and capacitances are fairly small in size, the additional four elements give negligibly small increase in weight, also the increase in the cost would be very small since these components are fairly cheap.

There is a good scope of further work on this topic. A couple of other synthesis procedures could be followed and still lesser values of overall sensitivity could be found. Even the general procedure, as presented by Schoeffler,⁵ for obtaining equivalent networks could be followed for obtaining the minimum sensitivity.

5. Acknowledgments

The authors thank Prof. L. B. Shah, Dean, and Dr. S. M. Sen, Vice-Dean and Head of Electrical Engineering Department, Faculty of Technology and Engineering, M. S. University, Baroda, for the facilities to carry out the work presented in this paper.

6. References

1. A. Sobczyk. 'Stabilization of Carrier Frequency Servomechanisms'. *Journal of the Franklin Institute*, vol. 246, July 1948, p. 21; vol. 246, August 1948, p. 95; and vol. 246, September 1948, p. 187.
2. P. Notthof (Jr.). 'Phase Load for A.C. Servo Systems with Compensation for Carrier Frequency Changes'. *Transactions of the American Institute of Electrical Engineers*, vol. 69, pt. 1, 1950, p. 285.
3. I. J. Nagrath and V. K. Arya. 'Design of Lead Networks for A.C. Servo with Carrier Frequency Drift'. *Application and Industry*, November 1962.
4. N. Balbian. 'Network Synthesis'. *Prentice Hall, Inc.*, 1962.
5. J. D. Schoeffler. 'The Synthesis of Minimum Sensitivity Networks'. *Transactions of the Institute of Electrical and Electronics Engineers*, 1964.

TRANSISTOR RECTANGULAR PULSE GENERATOR***R. R. Mehrotra***Non-member***Harbans Lal***Non-member*

and

B. K. Tyagi*Non-member**Department of Physics, D. J. College, Meerut***Summary**

A new type of emitter-coupler multivibrator, having simply a condenser in the base circuit, has been designed and the performance behaviour discussed on the basis of the circuit conditions which make the two transistors alternately conducting and non-conducting. The expressions for the time period for quasi-stable states in which transistor X_1 , conducts and transistor X_2 , is cut off and vice versa, have been developed by taking the charging of the base capacitor due to forward base current and its discharge due to the reverse base current. The circuit is capable of generating fairly suitable symmetrical and asymmetrical rectangular waveforms of quite small rise and fall times, as the signal at the collector of one transistor is not directly involved in the regenerative loop and hence, no integrating effect is present in the collector.

1. Introduction

The use of satisfactorily shaped rectangular waveforms is well known. Conventional type of multivibrators^{1-6, 12-14} do not give rectangular waveforms of good shapes due to the influence of cross-coupling capacitors. The integrating effect of the cross-coupling condensers lengthens the rise and fall time of the waveforms. There are, however, several methods of reducing the integrating effects;⁷⁻¹¹ but in all these cases, improvement can be achieved at the cost of the simplicity of the circuit. Rokavich¹¹ realized the importance of the design and study of simple transistorized multivibrator giving fairly suitable rectangular pulses. He used an emitter-coupled multivibrator having in the base circuit a R - C combination in parallel. In this type of multivibrator, the charging of the condenser takes place due to forward base current during conduction period of the transistor. The discharge of the condenser, however, mainly takes place through the resistance connected across it.

The purpose of this paper is to describe a simple type of multivibrator, having in the base a condenser for the generation of rectangular waveforms having sharp rise and

* Written discussion on this paper will be received until March 31, 1966.

This paper was received on May 11, 1966.

fall times. Moreover, in this circuit, the integration effect is absent, because the signal at the collector of one transistor is not directly involved in the regenerative loop.

2. Description and performance

The multivibrator circuit is shown in Fig. 1. The emitters of the two transistors are connected to the positive terminal of a battery through a resistance, R_e . The base of transistor X_1 , is connected through a condenser C_1 , to the negative of the battery. The base of transistor X_2 , is connected to the collector of transistor X_1 , through a condenser, C_2 . The collectors of the two transistors are connected to the negative of the battery through resistances, R_1 and R_2 .

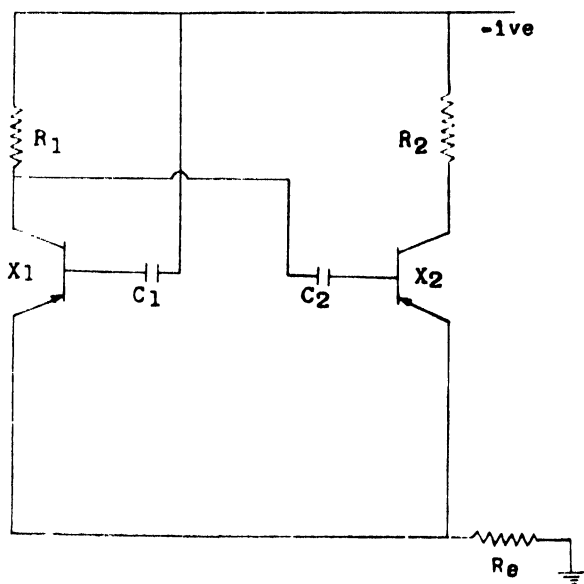


Fig. 1

Circuit diagram of the multivibrator

The performance behaviour may be understood by taking any one transistor, X_1 , say, conducting. In this quasi-stable state when X_1 conducts, its base current charges C_1 , and during this period X_2 remains cut off. The condenser C_2 , discharges due to reverse current through R_1 and R_2 . The moment the base voltage of X_2 becomes equal to the common emitter voltage, it starts conducting. If the emitter current of the second transistor is greater than the first transistor at $t = T_1$, the common emitter voltage will drop and will therefore instantaneously render the first transistor non-conducting. This termination will result in the removal of the voltage across R_1 due to the collector current of X_1 and as a result of this, the base voltage of X_2 will fall instantaneously. During the conduction period of X_2 , condenser C_1 discharges through R_1 due to the reverse current of X_1 and when its base voltage becomes equal to the common emitter voltage, transistor X_1 starts conducting. The voltage fall across R_1 increases the base voltage of X_2 , rendering it non-conducting.

The circuit is designed such that the transistors do not saturate when conducting. Otherwise, a noticeable distortion in the flat tops of rectangular output pulses will result.

3. Determination of frequency

In the quasi-stable state when transistor X_1 conducts and transistor X_2 is cut off, the following equations can be written in connection with the charging of capacitor C_1 , through the forward base current.

$$-E + R_e i_{e1} + \frac{1}{C_1} \int i_1 dt + V_1 = 0 \quad (1)$$

$$i_1 = (1 - \alpha) i_{e1} - I_{co1} \quad (2)$$

where i_{e1} is the emitter current of X_1 , i_1 the base current of X_1 , α the current gain, I_{co1} the reverse base current of X_1 , and V_1 the voltage across C_1 at the instant X_1 starts conducting.

Eliminating i_1 from equations (1) and (2), we get

$$\frac{di_{e1}}{dt} + \frac{(1 - \alpha)}{C_1 R_e} i_{e1} - \frac{I_{co1}}{C_1 R_e} = 0 \quad (3)$$

The solution gives

$$i_{e1} = \frac{I_{co1}}{1 - \alpha} + K e^{-\frac{t}{\tau_1}} \quad (4)$$

where

$$\tau_1 = \frac{C_1 R_e}{1 - \alpha} \quad (5)$$

The value of the integrating constant K , can be found from the following conditions :

$$(-E + V_1) = \text{Voltage at the base of transistor } X_1 \text{ at } t = 0$$

At $t = 0$,

$$i_{e1} = \frac{-E + V_1}{R_e}$$

neglecting the emitter base resistance in comparison with R_e during the conduction of X_1 . Just at the instant of the start of conduction of X_1 , when the base voltage becomes equal to the emitter voltage, the potential fall across R_e may be given by $(-E + V_1)$ and

$$I_{e2} = \frac{-E + V_1}{R_e}$$

Therefore,

$$(i_{e1})_{t=0} = I_{e2} \quad (6)$$

where I_{e2} is the emitter current of transistor X_2 when this transistor is conducting.

Substituting this condition in equation (4), we get

$$K = I_{e2} - \frac{I_{co1}}{1 - \alpha}$$

Hence,

$$i_{e1} = \frac{I_{co1}}{1-\alpha} + \left(I_{e2} - \frac{I_{co1}}{1-\alpha} \right) e^{-\frac{t}{\tau_1}} \quad (7)$$

During the conducting period, the collector voltage of transistor X_1 , may be written as

$$V_{K1} = -E + (\alpha i_{e1} - I_{co2}) R_1 = -E + \alpha R_1 \left\{ \left(\frac{I_{co1}}{1-\alpha} \right) + \left(I_{e2} - \frac{I_{co1}}{1-\alpha} \right) e^{-\frac{t}{\tau_1}} \right\} - I_{co2} R_1 \quad (8)$$

The voltage at the base of X_2 may be given as

$$V_{B2} = V_{K1} + \left(V_4 - I_{co2} \frac{t}{C_2} \right) \quad (9)$$

where V_4 is the voltage across C_2 at the instant transistor X_2 stops conducting.

The charging of C_1 (or, conduction of X_1) will terminate at the instant, $t = T_1$, when V_{B2} becomes equal to the common emitter voltage $R_{e1} (i_{e1})_{t=T_1}$, where T_1 is the time during which X_1 conducts, or,

$$-E + \alpha R_1 \left\{ \frac{I_{co1}}{1-\alpha} + \left(I_{e2} - \frac{I_{co1}}{1-\alpha} \right) e^{-\frac{T_1}{\tau_1}} \right\} - I_{co2} R_1 + V_3 = -R_e (i_{e1})_{t=T_1} \quad (10)$$

where V_3 is the voltage across C_2 at the instant when transistor X_2 starts conducting and may be given by

$$-E + I_{co1} R_1 + R_e I_{e2} = -V_3 \quad (11)$$

Simplifying equation (10), we get

$$T_1 = \tau_1 \log \frac{\left(I_{e2} - \frac{I_{co1}}{1-\alpha} \right) \left(\alpha R_1 + R_e \right)}{E - R_e \frac{I_{co1}}{1-\alpha} + R_1 I_{co2} - V_3 - R_1 \alpha \frac{I_{co1}}{1-\alpha}} \quad (12)$$

For T_1 to be positive, the numerator of equation (12) has to be positive and hence, the necessary condition for oscillation is given by

$$I_{e2} > \frac{I_{co1}}{1-\alpha}$$

In the second quasi-stable state, when transistor X_2 conducts and transistor X_1 is cut off, condenser C_1 discharges due to reverse base current of transistor X_1 . The voltage at the base of transistor X_1 (during the discharge of C_1) at any instant is given by

$$V_{B1} = -E + V_2 - \frac{I_{co1} t}{C_1} \quad (13)$$

where V_2 is the voltage across C_1 at the instant when X_1 stops conducting and is given by

$$-V_2 = -E - (V_{B1})_{t=T_1}$$

or,

$$-V_2 = -E + R_e (i_{e1})_{t=T_1} \quad (14)$$

The moment the voltage at the base of transistor X_1 becomes equal to the common emitter voltage, the discharge of C_1 will terminate, after time T_2 , say i.e.,

$$-E + V_2 - \frac{I_{co1} T_2}{C_1} = -R_e I_{e2} \quad (15)$$

From equation (14), we get

$$T_2 = \frac{C_1 R_e}{I_{co1}} \left\{ I_{e2} - (i_{e1})_{t=T_1} \right\} \quad (16)$$

Hence, the frequency of oscillation is given by

$$f = \frac{1}{T_1 + T_2}$$

or,

$$f = \frac{1}{\tau_1 \log \frac{\left(I_{e2} - \frac{I_{co1}}{1-\alpha} \right) (\alpha R_1 + R_e)}{E - \frac{R_e I_{co1}}{1-\alpha} + R_1 I_{co2} - V_3 - \frac{R_1 \alpha I_{co1}}{1-\alpha}} + \frac{C_1 R_e}{I_{co1}} \{ I_{e2} - (i_{e1})_{t=T_1} \}} \quad (17)$$

4. Experimental results

For illustration, the results obtained with the designed multivibrator using transistors 2SA15 (OC 44 type) and having the component values as given below, are described.

$$R_1 = 32 \text{ kilohm}, R_e = 22 \text{ kilohm}, R_2 = 10 \text{ kilohm}$$

$$C_1 = 75 \text{ picofarad}, C_2 = 0.1 \text{ microfarad}$$

$$E = -15 \text{ volts}$$

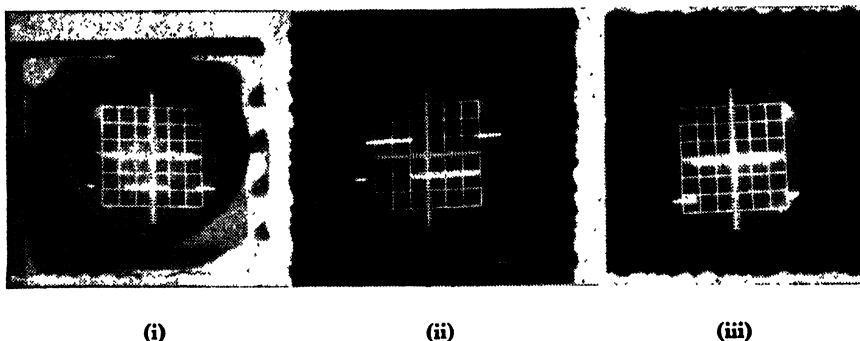
The transistor parameters used are :

$$\alpha' = 100, f_\alpha = 15 \text{ megacycles per sec.}, I_{co} = 0.7 \text{ micro-amp.}$$

Fig. 2 gives the waveshapes of the multivibrator at different points. The waveshape obtained across R_2 is of special interest, as a rectangular waveform is obtained. The frequency of oscillation, as calculated with the help of the derived equation (17), using the transistor parameters, comes out to be 1.5 kilocycles per sec. The transistor parameters listed above give the rise time for the transistor to be 2.8 micro-sec. The photographs of the waveform taken with the help of a high speed cathode ray oscilloscope gives the rise time as 2 micro-sec.

The experimentally observed and calculated values of T_1 and T_2 , for different values of C , are given in the table and the corresponding waveforms are given in Fig. 2.

A comparison of the values indicate that the calculation of T_1 and T_2 with the help of the derived equation is in close agreement with the observed values.

**Fig. 2**

Waveforms across R_2 for different values of C_1

Calculated and observed values of T_1 and T_2 in milli-sec. for different values of C_1

R_e , kilohm	R_1 , kilohm	C_1 , pico-farad	T_1 , milli-sec. (calculated)	T_2 , milli-sec. (calculated)	T_1 , milli-sec. (observed)	T_2 , milli-sec. (observed)
22	32	75	0.379	0.280	0.380	0.270
22	32	100	0.505	0.373	0.500	0.360
22	32	150	0.758	0.560	0.760	0.540
22	32	300	1.516	1.120	1.520	1.060

5. Acknowledgment

The authors thank Shri A. B. Malkani, Principal, D. J. College, Meerut, for his interest in the work presented in this paper.

THE JOURNAL OF The Institution of Engineers (India)

DEPUTY SECRETARY & ACTING EDITOR: D K Ghosh, B.E., C.E.,
D.T.R.P., A.M.I.E.

The Institution of Engineers (India) as a body accepts no responsibility for the statements made by the individual authors.

The Institution of Engineers (India) subscribes to the Fair Copying Declaration of the Royal Society and reprints of any portion of this publication may be made provided that reference thereto be quoted.

Vol. XLVI

MAY 1966

No. 9, Pt. ET 3

CONTENTS

Page

ELECTRONICS AND TELECOMMUNICATION ENGINEERING DIVISION

Report of the Paper Meetings in the Electronics and Telecommunication Engineering Division at the Forty-Sixth Annual General Meeting, Patna, January 30-February 6, 1966

Address of Brig. M. K. Rao, Chairman, Electronics and Telecommunication Engineering Division 55

- 1. Waveform Analysis of E.D.A. Solutions and Determination of Describing Functions with the Vectormeter. B. N. Nityanandan, Non-member** .. 60

Electronics and Telecommunication Engineering Division Board

The President (*Ex-officio*)

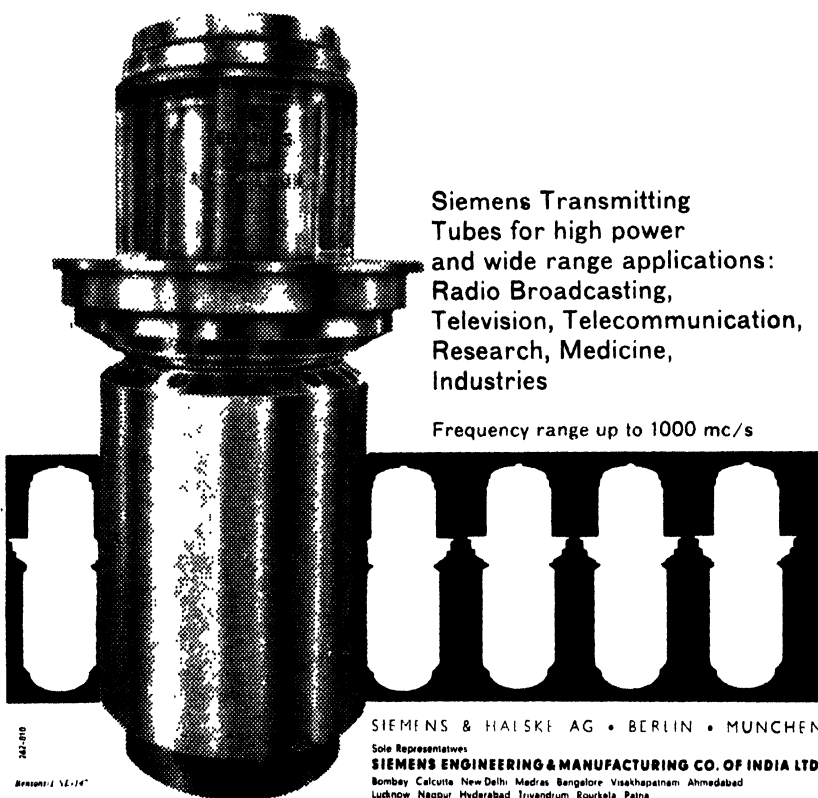
Brig. M. K. Rao (*M.*), Chairman

Prof. S. P. Chakravarti (*M.*)

Lt.-Col. S. Mishra (*M.*) (*Co-opted*)

Automatic Control Group

Prof. V. V. Sarwate (*M.*), Chairman



Siemens Transmitting
Tubes for high power
and wide range applications:
Radio Broadcasting,
Television, Telecommunication,
Research, Medicine,
Industries

Frequency range up to 1000 mc/s

242-010

Broschüre 1. 12. 1967

SIEMENS & HANSKE AG • BERLIN • MÜNCHEN

Sole Representatives

SIEMENS ENGINEERING & MANUFACTURING CO. OF INDIA LTD.

Bombay Calcutta New Delhi Madras Bangalore Visakhapatnam Ahmedabad
Lucknow Nagpur Hyderabad Trivandrum Rourkela Patna

**REPORT OF THE PAPER MEETINGS IN THE ELECTRONICS AND
TELECOMMUNICATION ENGINEERING DIVISION AT THE
FORTY-SIXTH ANNUAL GENERAL MEETING, PATNA,
JANUARY 30-FEBRUARY 6, 1966.**

Brig. M. K. Rao, B.Sc., B.Sc. (Eng.), M.A., A.C.G.I., M.I.E., Chairman of Electronics and Telecommunication Engineering Division opened the proceedings by delivering the Divisional address, and also presided over the proceedings.*

**ADDRESS OF BRIG. M. K. RAO (M.),
CHAIRMAN, ELECTRONICS AND TELECOMMUNICATION ENGINEERING DIVISION**

'I welcome you to this meeting of the Electronics and Telecommunication Engineering Division.

I would like to speak on 'Satellite Communication' which has been playing a sensational role in the long distance communication. It has a tremendous future in the years to come.

Historical background

Microwave has helped a great deal in the communication of signal. In a recent Bell system microwave relay, 11,000 simultaneous two-way telephone conversation in a 500 megacycles per sec. band has been possible. But for the transmission of microwave signal, a large number of relay stations are needed. Long distance communication, particularly over oceans, becomes, therefore, difficult. Transoceanic communication, has, therefore, been restricted to cables. For television broadcasting, an equivalent of 600 voice-circuits is required which is almost the same as the radio and cable facilities available across the Atlantic now. Arthur C. Clark was the first to express his ideas on satellite communication in 1945. Satellites will enable microwave signals to be communicated over long distances and provide large capacity for television transmission.

The first effort to use a satellite for communication was the use of the Moon. This was achieved in 1960 between Hawaii and Maryland in the U.S.A. The next attempt was to place a passive reflector satellite and use it for communication. Echo 1, launched on August 12, 1960, was a 100-ft. balloon, made of aluminized 'Mylar Polyester'. It had 98% reflectivity and could reflect energy at frequencies up to 20,000 megacycles per sec. Using Echo 1, communication was established between New Jersey and California. Other passive reflector satellites have also been used. The first satellite using a relay equipment was launched on December 18, 1958. It relayed the Christmas message from President Eisenhower. Many attempts have been made by various agencies to put satellites on orbit for communication purposes. All these fall into two categories: some relay signal directly, others are delayed action repeaters. The latter type receive messages transmitted from a ground station, store it on tape and re-broadcast when passing over a second ground station.

So promising was the use of satellite for communication of information that the American Telephone and Telegraph Co. spent 50 million dollars to put Telstar 1 in

*The Paper Meetings in the Electronics and Telecommunication Engineering Division commenced at 12.00 noon on February 1, 1966.

orbit on July 18, 1962. It was a 34.5 in. diameter electronic pack that connected the Western Europe and the U.S.A. by television for the first time. A similar satellite, called 'Relay', designed by N.A.S.A. and R.C.A., was sent up on December 13, 1962. Both Telstar and Relay operated in real time.

Satellite orbits

We know Earth satellites take near about 100 min. to go round the Earth once. The Moon takes 23 days. So, in between, it is possible to find an orbit where a satellite can orbit in a day. This orbit is at 22,300 miles above the equator. Such an orbit is called a '24-hr. orbit', 'stationary orbit' or 'synchronous orbit'. Three satellites are required for global coverage. The ideal launching sites for the synchronous orbit is a place on the equator. Such convenient sites are not available for the U.S.A. If launched at 30°N., the plane of the orbit has to be turned 30° when the satellite crosses the equatorial plane. Other techniques also exist, but all these are complicated. Again, much larger power is required to boost a particular size of satellite to a height of 22,300 miles than to the orbits at smaller heights.

Equatorial circular orbits of lower altitude have been suggested at heights giving 6 hr. and 8-hr. orbits. The launching of satellites on such orbits require less power and thus are less costly. In such a case, however, a large number of satellites are required for continuous communication. These orbits are of many types :

- (i) Equatorial circular orbit ;
- (ii) Polar circular orbit ;
- (iii) Inclined circles ;
- (iv) Equatorial elliptical orbit ; and
- (v) Inclined elliptical orbit.

Elliptic orbits are advantageous when particular parts of the earth are required to be covered. The orbit has to be such that at perigee it is nearest to the region to be covered. The main disadvantage of an elliptic orbit is to achieve altitude stabilization. It is necessary that the satellite is aligned with respect to the radius vector of the earth and stay aligned so that the radio energy can be directed towards earth and not wasted in space. With a circular orbit, this condition once established will be maintained.

Choice of frequency

The choice of frequency is a complex problem. The transmission should be capable of penetrating atmosphere, ionosphere and plasma round the earth in its two-way journey and still should have good signal-to-noise ratio. It is well known that absorption of electromagnetic energy by atmospheric gases increases at frequencies greater than 5,000 megacycles per sec. The lower end of frequency spectrum will be the minimum frequency that can penetrate the ionosphere. The lowest frequency has to be greater than 100 megacycles per sec.

Noise plays a very important part in receiving information. These are of two types :

- (i) Receiver noise ; and
- (ii) External noise.

The effects of receiver noise can be reduced, using microwave amplifiers like parametric amplifiers, masers, etc. External noise is mostly galactic and cosmic that vary in the different parts of the sky. The noise from the sky varies, at 10°K. to 110°K. , in the range of 1,000-10,000 megacycles per sec. The noise from the Sun is excessive and should be avoided.

Power supplies

Provision of power to equipment inside a satellite is a major problem. The criteria which is often used to specify the suitability of a particular type of power supply is the 'weight-power ratio'. Further, the power supply should withstand launching shock, radiations and other space conditions.

It is desirable to use direct methods of energy conversion. Some of these are given below.

- (i) Seebeck effect : this can be used for generating power. Recent advances in semiconductor materials has considerably improved the efficiency of the system. It is possible to get 200 volts per degree at an efficiency of 14% ; and
- (ii) Fuel cell : in the fuel cell method, hydrogen atom is made to react with oxygen to give power. This is the reverse process of electrolysis of water. To get useful power and efficiency, steps must be taken to speed up the reaction at each interfacc and remove water which is the product of reaction in order to prevent dilution of electrolyte. A single fuel cell produces 1 volt open-circuit power at $60\text{-}70\%$ efficiency. Connecting fuel cells in series, a battery to produce sufficient power can be made. In this case fuel and oxidant have to be carried, thus consuming a lot of space. A regenerative fuel cell, which is a closed cycle system where fuel is regenerated, will make this system more effective.

Solar energy

Photo-voltaic effect can be used to generate power. With the advent of semi-conductors, a higher efficiency of power generation is possible to be attained. GaAs (Gallium assinide) gives an efficiency of 15% . About 20,000 cells are necessary to produce the required power in a satellite.

Nuclear energy

The nuclear reaction produced by unstable nuclei have the advantage of a long operational life. The reaction generates heat which is used as primary energy for generating power through thermo-electric generators, mercury turbines and various other methods. The main disadvantage is the fouling of the space by the products of reaction. Since all the power sources generate D.C., inverters for generating A.C. are necessary. Inverters to give 400 cycles per sec. at 115 volts providing 500 watts from a 22-29 volts D.C. have been made that work at an efficiency of 70% .

Reliability

Reliability of components and systems is a very important requirement in a satellite. The components are, therefore, specially made. The worst hazard is the effect of

radiations and particles in the space. The Van Allen belt is the source of worst hazard. This layer stretches between 500-600 km. with a maximum penetration up to 3,000 km. It consists of very high energy particles that can cause damage to electronic components, solar cells, etc. These particles also produce secondary radiations such as hard X-rays and rays that have a great damaging effect.

Economics

It is well known that putting satellites into orbit and establishing communication through them is a very costly project. So, any attempt made in this direction has to be looked carefully into the economics of the system. The growth of transatlantic telephone and telegraph traffic has been so good (four-fold in 10 years) that there is a promising scope, but one cannot be over-optimistic. There is also the additional requirement of capacity for television, facsimile, etc. But here a warning is worth giving. Unless the transmission is required to be done in real time, satellites do not provide any advantage because within a few hours jet aircraft can transmit on tape at a much cheaper cost. However, on a long term view, a closed circuit telephone-vision may prove as a rival to personal visits. Then satellite communication will play a big role.

The American Telephone and Telegraph Co. has put a cable in 1963 which costs 27,000 dollars per year per voice channel. According to estimates of Mueller, the cost per voice channel per year with an active satellite system on a 24-hr. orbit is about 13,000 dollars. The present estimates are that about 100 million dollars will have to be spent on transatlantic cable. The development cost of launching of satellite will cost about the same. So, satellite system cannot be justified on lower cost in establishing higher capacity. The case is founded rather on the greater growth potential, flexibility of expansion in area of greatest requirement and on the wider social facility which satellites will provide.

Future trends

It is fairly certain that by the end of this decade, a satellite communication system will operate. If the satellite transmitter power is of the order of 10 watts, it will be able to handle 600 telephone channels or one television channel. Extension of life of satellite will ensure lower launching cost. A life of 5-10 years will reduce the system cost to one-half.

Two possible sources of higher power are solar and nuclear; the SNAP 8 nuclear system can provide 60 kW. The dissipation of heat produced by this power system puts very exacting requirements in the design of the satellite.

By 1970, high power satellites are possible. The capacity then can be increased to 27,000 two-way voice channels. By 1970, the requirement will be about 6,000 voice channels. Thus, there remains sufficient extra capacity for expansion.

It takes 75 days to place a satellite in operating position. To maintain a sufficiently high probability of uninterrupted service a higher order of redundancy in satellite and repeaters must be provided for.

With technological advance, it is possible to get radiated power of megawatts from satellites thus giving a greater channel capacity. Because of limitation of antenna size, the area covered now is large. It is possible in future to service smaller areas with greater signal intensities.

At present, only industrially advanced areas around the Atlantic can economically be served by satellite communication. By 1980, it is hoped that even smaller nations can use this service.'

WAVEFORM ANALYSIS OF E.D.A. SOLUTIONS AND DETERMINATION OF DESCRIBING FUNCTIONS WITH THE VECTORMETER*

B. N. Nityanandan

Non-member

Electrical Engineering Department, Thiagarajar College of Engineering, Madurai

Summary

This paper presents an experimental method for accurate analysis of waveforms representing solutions of linear and non-linear systems obtained on a repetitive differential analyzer. The method proposed is also shown to be useful for the direct evaluation of 'describing functions' for non-linear characteristics, commonly encountered in control systems. The method proposed envisages the use of a less-used instrument designed by Koppelman (1948). The design considerations for the circuitry needed to adopt this equipment in the present case, are also discussed.

1. Introduction

In a repetitive type electronic differential analyzer, the solutions of linear or non-linear equations are repeated at a frequency determined by the signal repetition rate. In typical cases, the solutions come out in the form of unsymmetrical periodic waves.

There exist many methods for measuring and recording such waveforms. Servo-driven pen recorders and cathode-ray oscilloscopes with photographic arrangements may be cited as typical examples.

This paper proposes an alternative method for recording and analyzing such waveforms. The method is based upon an extension of the range of applicability of an instrument, termed 'vectormeter', first designed by Koppelman (1948).

For servo-driven or mechanically driven recorders, the effective bandwidth is extremely small, usually up to 5 cycles per sec., and is, therefore, of limited usefulness in such applications where higher frequencies are encountered.

Photographing of a waveform from an oscilloscope and its subsequent analysis is a time consuming process. Errors can enter in the recording of the wave, for example, through optical errors or on account of changes in photographic material during development. These errors are troublesome since it is difficult to control them.

The vectormeter is a precision universal measuring instrument of the moving coil type combined with a contact rectifier driven by a synchronous motor. The mechanical arrangements in the vectormeter enable the contact period to be varied to any value between 0° and 360° . Also, the instant at which the contact is made can be adjusted arbitrarily with respect to the phase position of the measured quantity over the range

* Written discussion on this paper will be received until July 31, 1968.

This paper was received on April 1, 1966.

from 0° to 360° . These basic properties of the vectormeter are made use of in obtaining the waveforms of the solutions of differential analyzers. The non-linear component's output generally contains the fundamental and a few harmonics. By a proper choice of the contact period, the effect of the predominant harmonic of the output of the non-linear device is eliminated and the describing function of the non-linear device easily determined with the vectormeter.

Errors caused by the inherent limitations of the vectormeter, are predictable and can be compensated for. The major disadvantage, however, lies in not having any visual presentation of the solutions which have to be obtained, instant by instant, in a tabulated form. Yet another advantage of the vectormeter is that the harmonic contents of waveform may be obtained directly from instrument readings, although this is restricted to cases where the other harmonics are considered negligible.

2. Adaptation of the vectormeter

2.1. General remarks

In this past, the instrument has been used for the measurement of waveforms of voltages obtained from relatively high-power sources. For analysis of periodic waveforms obtained from networks at low-power level, as in the present case, it becomes necessary to adopt a circuit arrangement as shown in the block diagram of Fig. 1.

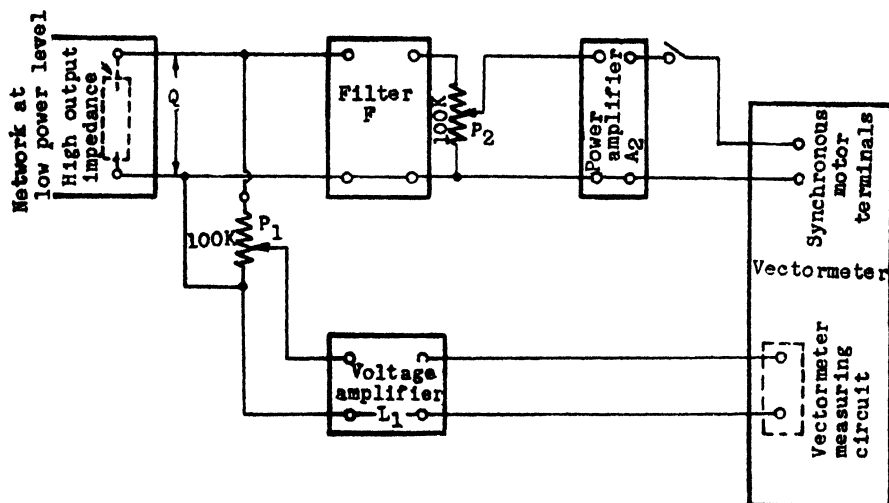


Fig. 1

Circuit arrangement of a vectormeter

The frequency range for which the synchronous motor of the vectormeter is operative is 15-80 cycles per sec. For correct measurement of waveforms, the frequency of the quantity to be measured must be equal to or an exact multiple of the frequency of the voltage driving the synchronous motor. When the fundamental frequency of the measured quantity is within the operative frequency range of the motor, it is advantageous to drive the synchronous motor from the same source, instead of having a separate

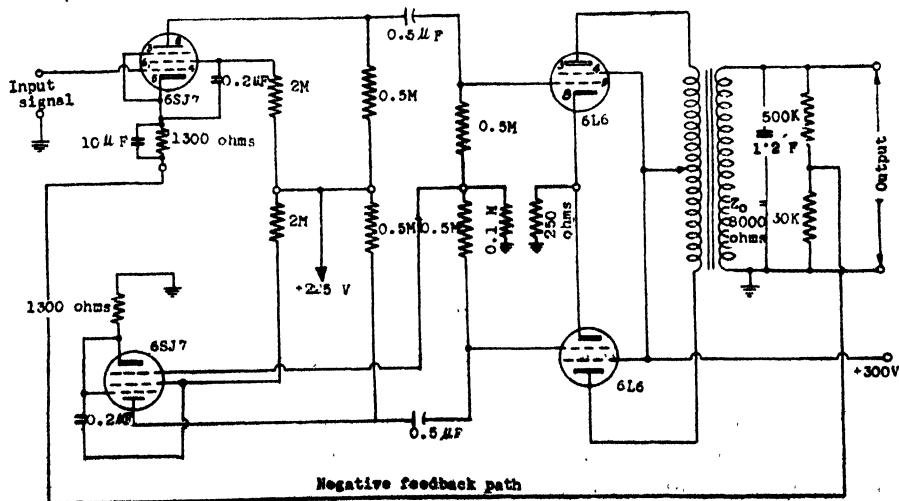
variable frequency supply for driving the synchronous motor. If, however, the frequency of the measured quantity exceeds this range, then this arrangement does not hold good and a variable frequency supply for driving the motor becomes essential.

The power amplifier A_2 (Fig. 1) provides the voltage and power amplifications necessary for driving the synchronous motor (90 milli-amp. at 230 volts, 50 cycles per sec., 8 watts) from the usual low-power source of the differential analyzer (3 milli-amp. at ± 100 volts). The potentiometer P_2 , helps adjustment of the desired voltage at the output terminals of A_2 . The filter has to be incorporated for the obvious reason of passing only the fundamental wave to the driving circuit.

The amplifier A_1 in the measuring branch serves to isolate the vectormeter measuring circuit from the low-power network, in addition to providing amplification when necessary.

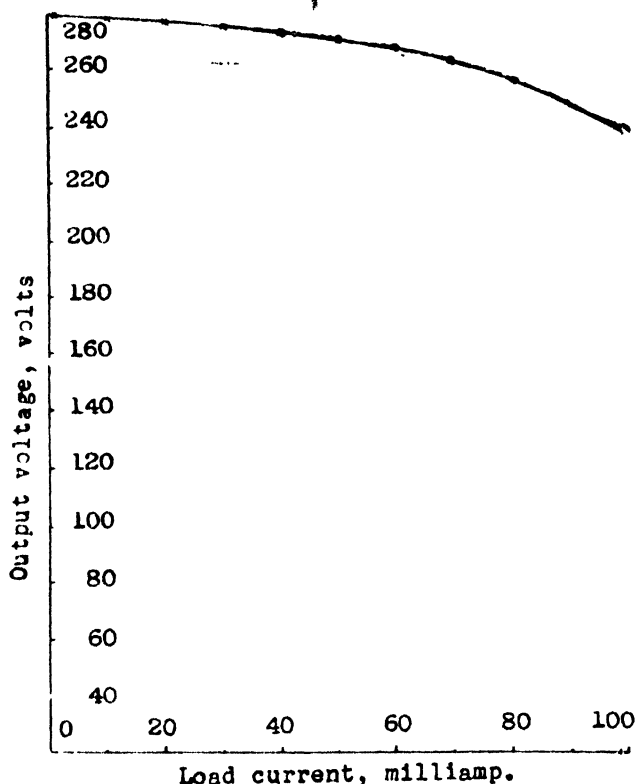
2.2. Design of circuits

Circuit diagram for amplifier A_2 is shown in Fig. 2(i). The amplifier is designed to have low-pass characteristics (0-1,000 cycles per sec.). It is a two-stage degenerative amplifier with 6L6 tubes used in the push-pull power stage. For the 6L6 push-pull output transformer, the output impedance has to be as high as 8,000 ohms to give 230 volts output. But the impedance of the vectormeter motor is about 2,600 ohms at 50 cycles per sec. Hence, when the synchronous motor is switched on to the amplifier, despite negative feedback, there is considerable drop in the output voltage. It is observed that when a condenser of suitable value (1-2 microfarad) is used across the output of A_2 as shown, the drop is considerably reduced and it is easy to obtain 230 volts at the output with the synchronous motor load on [Fig. 2(ii)].



(i)

Fig. 2 (contd.)



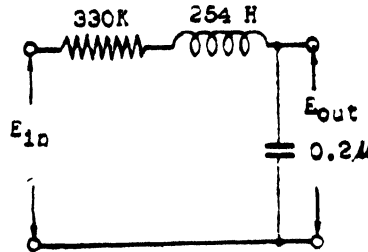
(ii)

Fig. 2

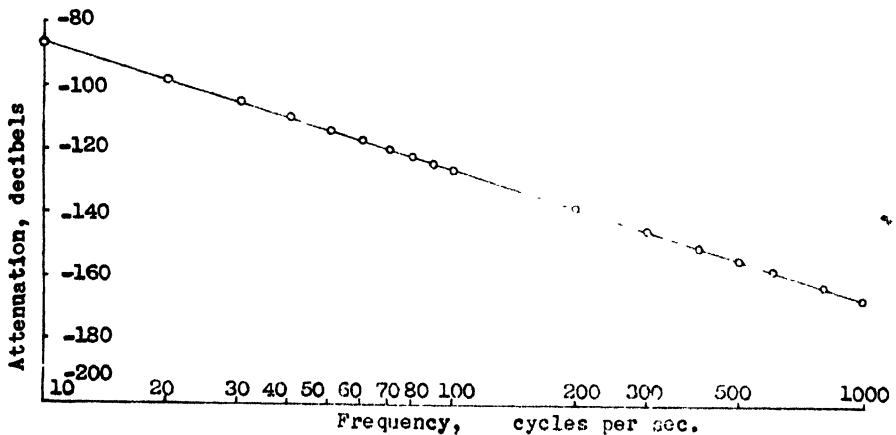
Circuit diagram and load characteristic at 50 cycles of amplifier A_2

The filter which has to be designed to have a passband of 15-80 cycles requires a high impedance choke in the L - R - C circuit shown in Fig. 3(i). The frequency response characteristic of the filter is shown in Fig. 3 (ii).

The measuring circuit amplifier A_1 has to be a wideband audio frequency amplifier, with a bandwidth of 0-1,500 cycles per sec. and having almost the same phase-shift within this bandwidth (Fig. 4). Proper impedance matching at the input and output stages has had to be realized. Although a cathode follower could have been used for this purpose, the output of the cathode follower would be too small to enable effective measurement. The circuit of A_1 is similar to that of A_2 and differs from it in two ways : (i) the output transformer in A_1 has very low output impedance, (ii) the amplifier A_1 is essentially an R - C coupled amplifier. A square wave input would be distorted to the extent that its flat top would become exponentially drooping. For this reason, the coupling capacitors are made large in value, so that the time constant of the R - C coupling (more than 5 sec.) is made large enough compared to the time period (50 milli-sec.) of the minimum frequency encountered.



(i)



(ii)

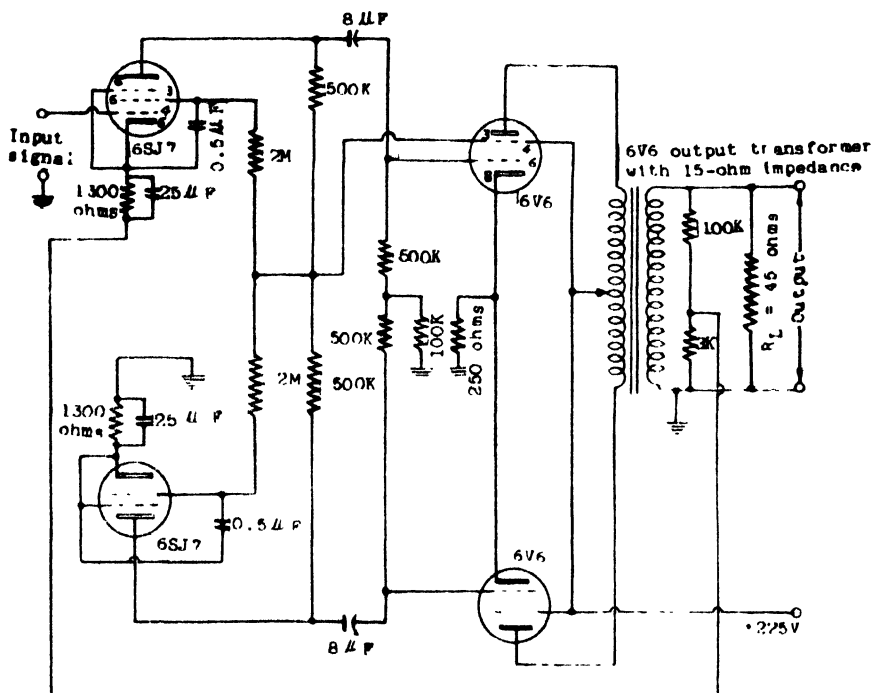
Fig. 3

Circuit diagram and frequency response characteristic of *L-R-C* filter

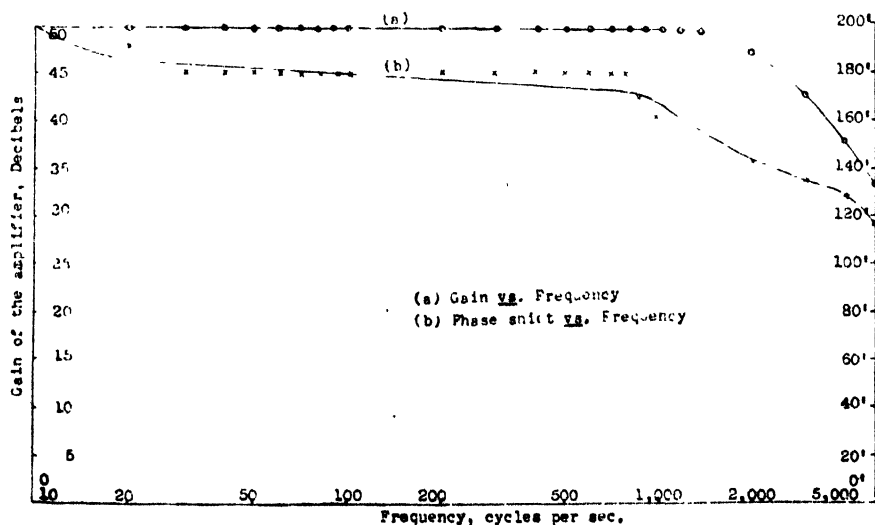
3. Waveform analysis of repetitive differential analyzer solutions

Typical set-up for a second order differential equation on a differential analyzer, built in the Bengal Engineering College, Howrah, is given in Fig. 5(i).^{6,10} Fig. 5(ii) gives a photographic record of the solution of the system with rectangular repetitive pulses for its input. The pulse width is chosen to be greater than the solution time of the differential equation. In many applications, such as in synthesis of control systems and networks, it is important to be able to have a quick knowledge of the magnitude of the peak overshoot and time to peak overshoot, and the zeros of the solution. The vectormeter affords a ready means for accurate ascertainment of these quantities. The details of obtaining the point-by-point plot is outlined in Appendix 1.

A comparison of the waveform obtained with the vectormeter and the photographic record of the oscillographic solution is shown in Fig. 5(iii). An analysis of error is given in section 5.



(i)



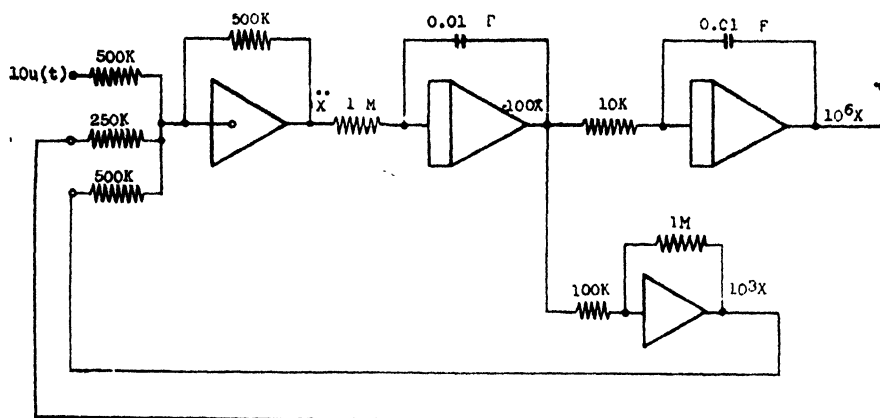
(ii)

Fig. 4

Circuit diagram and frequency response characteristics of amplifier A₁

4. Evaluation of describing functions

In control system analysis, frequently, components having non-linear transfer characteristics are encountered. A widely used technique known as the 'describing function' method¹³ takes account of the effect of presence of such non-linearities by replacing the non-linear characteristics with an equivalent quasilinear model. In short, this concept assumes sinusoidal input to the non-linearity and considers only the fundamental component of the output. The neglect of harmonics is justified on the grounds of low-pass characteristics that usually follow the non-linearities in such systems. The describing function which is defined as the ratio of the fundamental amplitude of the output to the input amplitude, is a complex quantity and is, in general, a function of both the frequency and the amplitude of the input. The describing function values for the non-linearity are then used for the study of stability of such systems. Determination of describing function then necessitates simultaneous measurement of the amplitude and relative phase shift of the fundamental output and the input for different amplitudes of the input sinusoid.



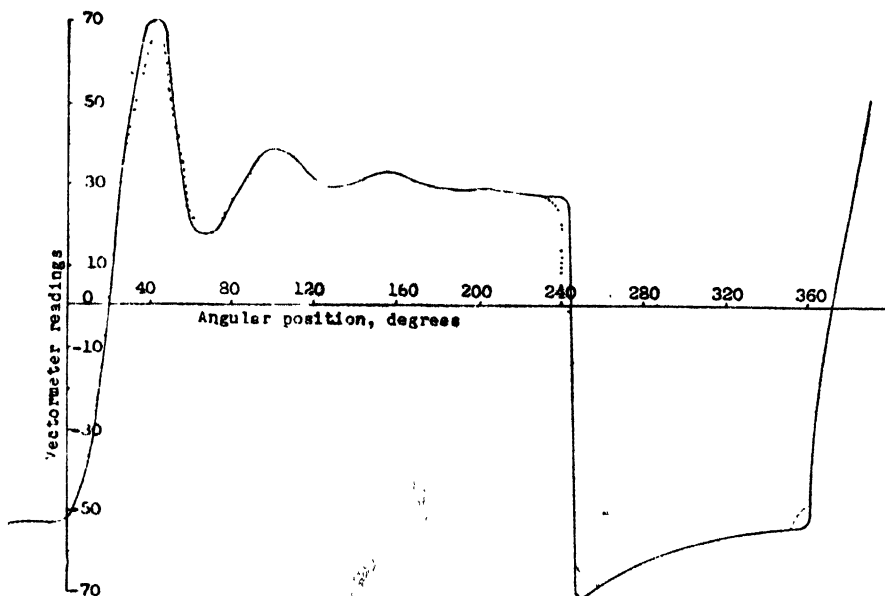
(i)



(ii)

Photographic record of solution for second order differential equation

Fig. 5 (contd.)



(iii)

Fig. 5

Waveform analysis with differential analyzer

The vectormeter offers an excellent method of rapid determination of the describing functions experimentally. For most commonly encountered non-linearities such as saturation, hysteresis and backlash, for which analytical determination is relatively simple, the vectormeter does not seem to offer any special advantage. But, for non-linear characteristics which are expressed in terms of implicit or regular functions^{1,7} such as multiplicative non-linearities and others or are specified graphically, the analytical determination may be difficult. In such cases, the non-linearity may be simulated with the help of function generators and computer elements and the waveforms and the harmonic contents may be analyzed with the help of the vectormeter. Although the above remarks refer to cases where the vectormeter may be used to advantage we shall illustrate the technique by using a non-linearity for which the analytic method of finding the describing function may be referred to for comparison.

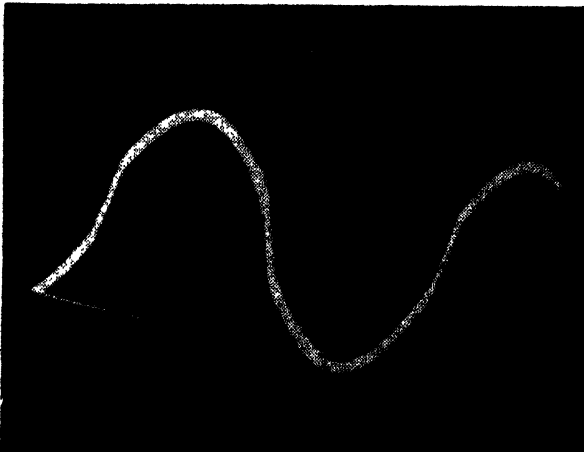
Fig. 6(i) shows photographic record of a soft spring type non-linearity, simulated on a diode function generator. The output of non-linearity for a sinusoidal input, is shown in Fig. 6(ii). The waveform of the output of the soft spring non-linearity, one obtained analytically and the other by point-by-point method using the vectormeter are given in Fig. 6(iii). The effect of the finite contact period is to round off the curve at places where comparatively abrupt changes take place. The abrupt changes correspond to high frequency components and as far as the describing function determination

is concerned the high frequency components can be neglected since that is the very essence of the describing function technique. This apart, the experimentally determined describing functions are compared with analytical values in Fig. 6(iv). Details of the experimental method for determining the fundamental and third harmonic of the output are outlined in Appendix 2. The method for determining the phase shift of the output wave is also explained in Appendix 2.



(i)

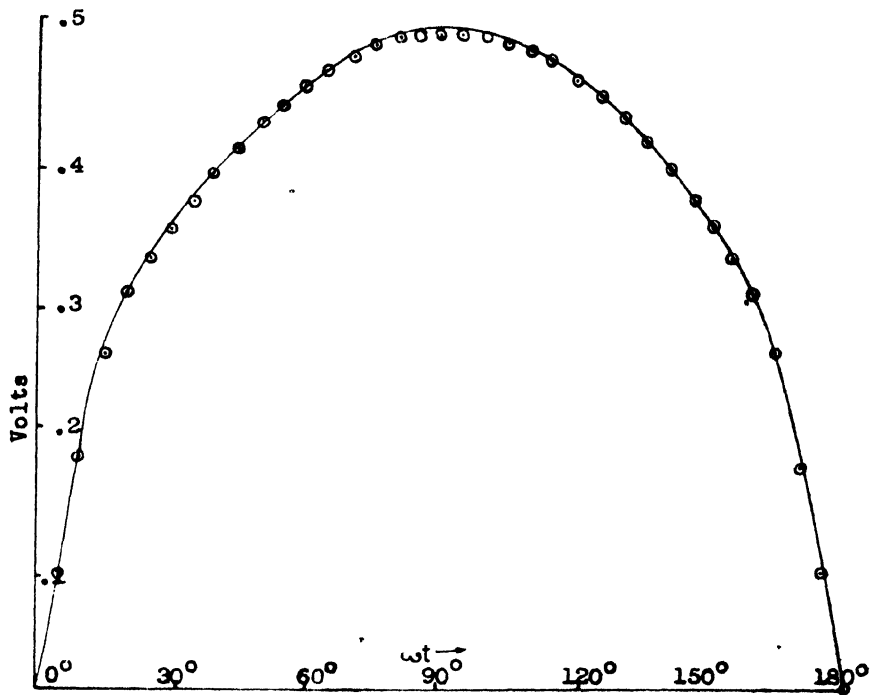
Soft spring type non-linearity



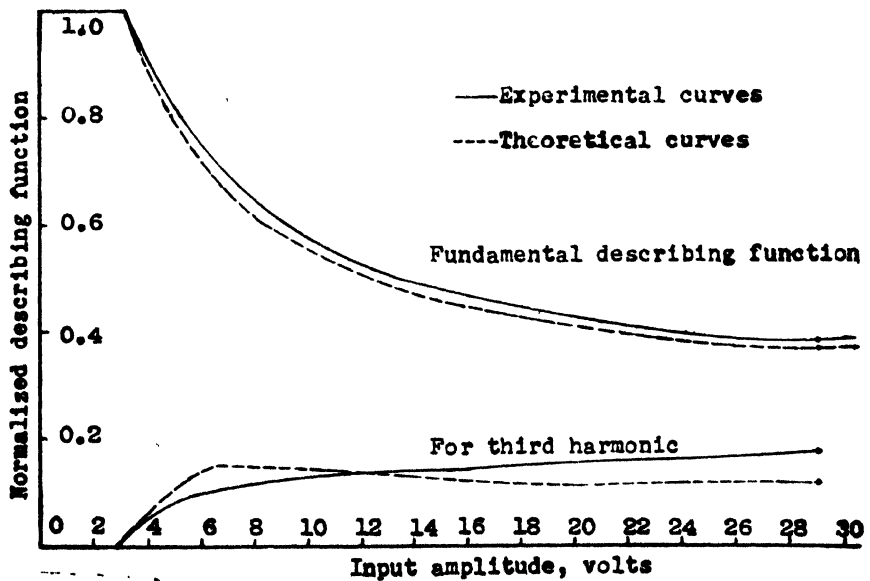
(ii)

Output of non-linearity for
a sinusoidal input

Fig. 6 (contd.)



(iii)



(iv)

Fig. 6

Photographs and curves for determining soft spring non-linearity waveform by vectormeter

5. Error analysis^{8,9,14}

In the vectormeter method of measuring an unsymmetrical waveform with short contact period, a small area of the waveform is integrated in the neighbourhood of an instant and this is assumed to give the value of the function at the particular instant. If the contact period could be reduced to very small values, then, the measurement would be accurate. In practice, however, the contact period cannot be reduced to be, say, less than 10° and this finite contact period would cause error in the measurement. The peaks would not be sincerely reproduced by the vectormeter. A knowledge of the error caused by the finite contact period for various harmonics will enable us to specify the utility of the method of measurement of waveforms with predominant higher harmonics. In this section, the error in the measurement of various harmonics for a general function is discussed, and an expression for the r.m.s. error, an important index for specification of accuracy, is given in terms of harmonic coefficients and the contact time.

Any complex function can be split up into a Fourier series of the form and can be represented as $F(\theta) = \sum_{r=0}^{\infty} a_r \sin(r\theta + \sigma_r)$; $r = 0$ represents the D.C. component and it can be shown that the error in the D.C. component is zero. Hence, taking values $r = 1$ to ∞ , if $F(\theta) = \sum_{r=1}^{\infty} a_r \sin(r\theta + \sigma_r)$, the instantaneous value as measured by the vectormeter at any instant θ_1 [Fig. 7(i)] is given by

$$F(\theta_1) = \frac{1}{2\beta} \int_{\theta_1 - \beta}^{\theta_1 + \beta} \sum_{r=1}^{\infty} a_r \sin(r\theta + \sigma_r) d\theta$$

where θ_1 can take any value from 0 to 2π . The coefficient of n th harmonic, calculated from vectormeter readings, is then given by

$$b_n = \frac{j}{\pi} \int_0^{2\pi} e^{-jn\theta} \frac{1}{2\beta} \int_{\theta - \beta}^{\theta + \beta} \sum_{r=1}^{\infty} a_r \sin(r\theta + \sigma_r) d\theta d\theta$$

which simplifies to

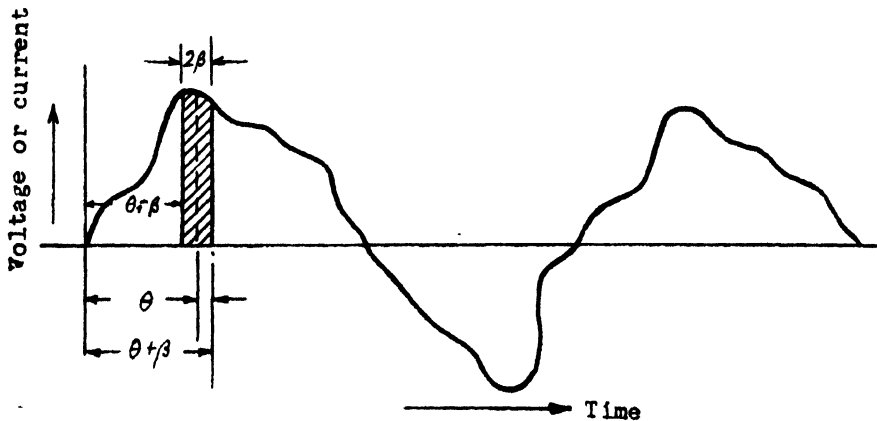
$$b_n = \frac{a_n \sin \beta}{n \beta} (\cos \sigma_n + j \sin \sigma_n)$$

$$|b_n| = \frac{a_n \sin \beta}{\beta n}$$

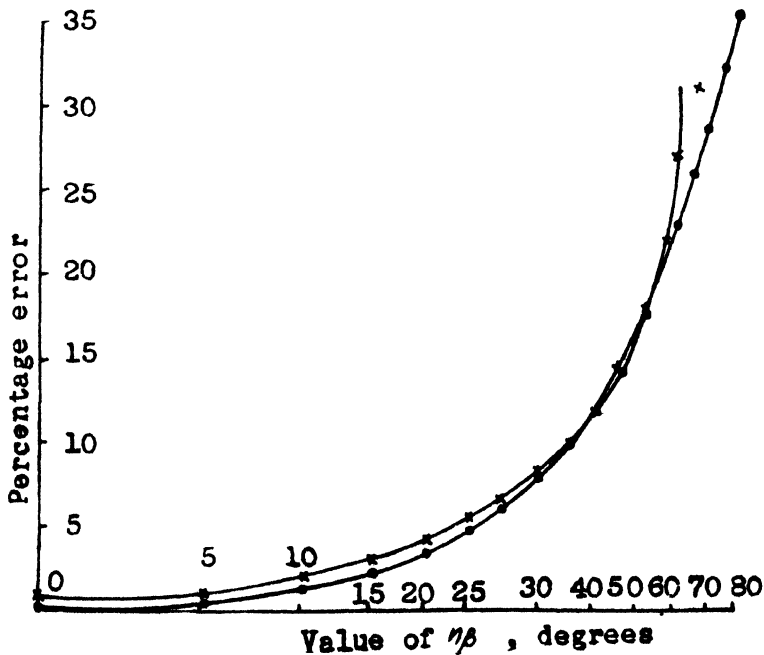
$$\text{Percentage error in magnitude} = \left(1 - \frac{\sin \beta}{\beta n}\right) \times 100$$

where a_n is the true coefficient of the n th harmonic, and b_n the n th harmonic coefficient as determined by vectormeter.

This analysis shows that the error is small, if the contact period, 2β , is kept small [Fig. 7(i)]. Fig. 7(ii) shows the variation of error with $n\beta$ calculated theoretically. The variation of error with $n\beta$ calculated from vectormeter readings for the solution of second order differential equation is also shown for comparison.



(i)



(ii)

Fig. 7

Curves for error analysis

For a finite value of contact period, 2β , the error in the value at any instant, $t = \frac{\theta}{\omega}$, is given by

$$\sum_{n=1}^{\infty} a_n \sin n\theta \left(1 - \frac{\sin n\beta}{n\beta}\right)$$

The root-mean-square error is

$$\left[\frac{1}{2\pi} \int_0^{2\pi} \left\{ \sum_{n=1}^{\infty} a_n \sin n\theta \left(1 - \frac{\sin n\beta}{n\beta}\right) \right\}^2 d\theta \right]^{\frac{1}{2}}$$

which simplifies to

$$\left[\sum_{n=1}^{\infty} \frac{a_n^2}{2} \left(1 - \frac{\sin n\beta}{n\beta}\right)^2 \right]^{\frac{1}{2}}$$

The r.m.s. value of the function is

$$\left[\sum_{n=1}^{\infty} \frac{a_n^2}{2} \right]^{\frac{1}{2}}$$

Hence, the percentage r.m.s. error is

$$\left[\frac{a_1^2 \left(1 - \frac{\sin \beta}{\beta}\right)^2 + a_2^2 \left(1 - \frac{\sin 2\beta}{2\beta}\right)^2 + a_3^2 \left(1 - \frac{\sin 3\beta}{3\beta}\right)^2 + \dots}{a_1^2 + a_2^2 + a_3^2 + \dots} \right]^{\frac{1}{2}} \times 100$$

This also leads us to the conclusion that the overall error is small, if the contact period is kept small.

6. Conclusions

Koppelman, Hollufer and Funk had previously used the vectormeter for measurement of current, voltage, power and measurement of waveforms in the high power levels only. In the present paper, it has been shown that with certain modifications in its method of use, the vectormeter serves as a powerful instrument for rapid analysis of repetitive differential analyzer solutions of linear and non-linear systems. Further, it is indicated that the describing functions for non-analytic or implicit functional non-linearities can be readily evaluated. This aspect becomes important in cases where non-linear functions are simulated from a knowledge of the actual non-linear characteristics, for which theoretical evaluation may be difficult. Finally, the measures of absolute errors in using this instrument for such applications have been discussed.

7. Acknowledgments

The author is deeply indebted to Dr. S. Dasgupta, Reader of Electrical Engineering, Jadavpur University, Calcutta, India who first suggested the approach and helped in many ways towards completion of the work. The author is also deeply indebted to Prof. B. P. Bhattacharya of the Electrical Engineering Department, Bengal Engineering College, Howrah, who later guided him in the present work, especially in connection with the work on describing functions.

The author expresses his indebtedness to Prof. A. K. Chowdhuri, Reader, Institute of Radiophysics and Electronics, Calcutta, and Prof. R. R. Benedict, Professor of Elec-

trical Engineering, University of Wisconsin, U.S.A., who was in India as a Guest Professor at Bengal Engineering College, Howrah, for providing stimulating discussions. Finally, the author acknowledges the help rendered by his colleague Mr. N. K. Gupta, in the development of the function generator and Prof. M. L. Dasgupta, Head of the Department of Electrical Engineering, Bengal Engineering College, Howrah, India (presently the Principal, Tripura Engineering College, Tripura) for his constant encouragement during the progress of the work.

8. References

1. B. P. Bhattacharyya. 'Describing Function Expressions for Sine Type Functional Non-linearity in Feedback Control Systems'. *Proceedings of the Institution of Electrical Engineers*, vol. 108, pt. B, no. 41, 1961, p. 529.
2. W. Brauer. 'Die Bestimmung der Kurvenform des Weshsel Stroms durch den AEG Vektormesser'. *Die Elektropost*, vol. 24, 1950, p. 373.
3. W. Hollefuer. 'Bestimmung der Kurvenform Elektrischer Wechselgrossen mit den Vektormesser'. *Elektrotechnische Zeitschrift*, vol. 72, 1951, p. 199.
4. F. Koppelman. 'Vektormesser, ein Neuer Mechanischer Messgliedrichte'. *Elektrotechnik*, vol. 2, 1948, p. 11.
5. F. Koppelman. 'Grundwellenmessung mit Drehspulinstrument und Präzisionsmesskontakt'. *Elektrotechnische Zeitschrift*, vol. 70, 1949, p. 125.
6. A. A. Korn and T. M. Korn. 'Electronic Analogue Computers'. *McGraw-Hill Book Co., Inc.*, 1956.
7. Y. H. Ku and C. F. Chen. 'Stability Study of Third Order Servomechanism with Multiplicative Feedback Control'. *Transactions of the American Institute of Electrical Engineers*, vol. 77, pt. 2, 1958, p. 131.
8. P. Madich, J. Petrich and N. Pareznovich. 'The Use of a Repetitive Differential Analyzer for Finding Roots of Polynominal Equations'. *Transactions of the Institution of Radio Engineers*, vol. Ec.-8, no. 2, 1959, p. 182.
9. W. H. Middendorf. 'Graphical Determination of Fourier Series Coefficients'. *Transactions of the American Institute of Electrical Engineers*, vol. 76, pt. 1, 1956, p. 478.
10. Ravish Chandra. 'An Analogue Computer Approach to Mitrovics Method'. M. E. thesis submitted to the University of Calcutta, 1961.
11. R. K. Swank and E. A. Mroz. 'New Method for Graphical Reproduction of Cathode-ray Oscillograms'. *Review of Scientific Instruments*, vol. 30, no. 10, 1959, p. 880.
12. D. D. Trautner. 'A New Concept of Analogue Recording'. A.I.E.E. Analogue and Digital Instrumentation Conference Paper, p. 37.
13. J. G. Truxal. 'Automatic Feedback Control System Synthesis'. *McGraw-Hill Book Co., Inc.*, 1955.
14. A. Willers. 'Practical Analysis'. *Dover Publications, Inc.*, 1948.
15. R. C. Wood and G. W. Smith. 'Principles of Analogue Computation'. 1959.

Appendix 1

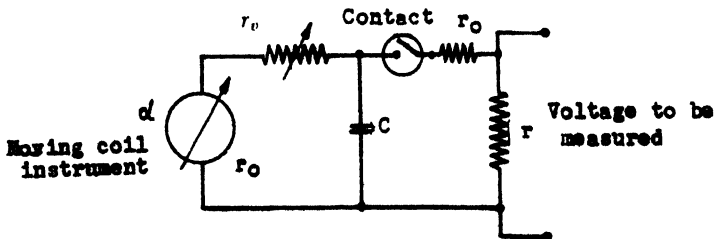
Operating principles of vectormeter

The vectormeter is a precision universal measuring instrument of the moving coil type combined with a contact rectifier driven by a synchronous motor. The mechanical arrangements in the vectormeter, enable the contact period to be varied to any value between 0° and 360° . Also, the instant at which the contact is made can be adjusted arbitrarily with respect to the phase position of the measured quantity over the range from 0° to 360° . The fundamental frequency of the measured quantity should be accurately the same as the frequency of the voltage applied to the synchronous motor.

Generally, the moving coil instrument is connected in series with the contact and current flows through it only whenever the contact remains closed. The deflection of the instrument is a measure of the integral of the current or voltage over the contact period.

In case of symmetrical waveforms, by using 180° contact time and varying the instants of contact, instrument readings can be obtained to plot the waveform as accurately as required. Using the contact periods as low as 10° , unsymmetrical waveforms can also be plotted. Unsymmetrical waveforms can be analyzed more accurately by use of an arrangement as shown in Fig. 8. The circuit reduces the effects of fluctuations of the contact time and enables sensitive measurement. During the contact time, C is charged to a potential difference U_1 , at the instant T_{out} of opening the circuit. During the open contact time, C discharges through r_o and the D.C. motor, gradually to a potential difference U_2 , at which a new contact is made at T_{in} to allow C to re-charge. To keep $U_1 - U_2$ small and to charge C to the potential U_1 , during the contact time, the conditions to be satisfied are :

$$(r_o + r_v) C \gg T \gg T_k \gg r_D C$$



$$\text{Contact period} = 10^\circ = T_k$$

Fig. 8

Circuit for analyzing unsymmetrical waveform

The circuit is calibrated by use of a known D.C. potential and r_v is adjusted to give a convenient direct scale on the instrument.

The instantaneous value of the waveform at time T_1 is obtained (Fig. 9) for the case shown in Fig. 8. Since it is possible to change the instant at which the contact is first

made, (keeping the contact period constant) the instantaneous values of the waveform for all instants can be accurately measured by this method and hence the entire waveform can be easily obtained.

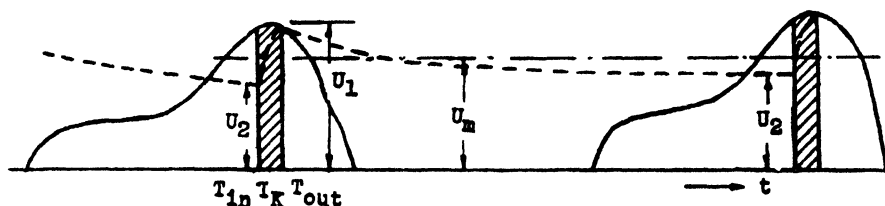


Fig. 9

Instantaneous value of waveform

Appendix 2

Measurement of selective harmonic components

The effect of individual harmonics on the measurement of a complex waveform (Fig. 10) can be removed by proper choice of the contact time. If instead of the usually employed contact period of 180° , a value of $180 \times \frac{2}{3} = 120^\circ$, or $180 \times \frac{4}{3} = 240^\circ$ is set on the vectormeter, then the half-waves of the third harmonic cancel out and have no effect on the meter reading. For a contact period of 120° , the meter deflection is reduced by a factor 0.866. Since this is a fixed correction factor, this has no effect on the measurement.

Similarly, the measurement of an individual harmonic is also rendered very simple with the vectormeter. It is necessary to take three readings for the third harmonic, five readings for the fifth harmonic, etc. With reference to Fig. 11, if we desire measurement of the third harmonic of the fundamental wave shown, we determine the instantaneous values a_{30}, a_{90}, a_{150} for the three phase angles $30^\circ, 90^\circ, 150^\circ$ and combine the readings by Fischer-Hinnen formula. The summation for the third harmonic is $a_{30} - a_{90} + a_{150}$. The fundamental has no effect, since the sum, $0.5 - 1.0 + 0.5 = 0$. However, the third harmonic gives, $1 - (-1) + 1 = 3$, thus enabling the determination of third harmonic amplitude.

The determination of describing function for fundamental and the third harmonic requires that both the input and output of the non-linear element be connected to the vectormeter for measurement. If a_m is the maximum reading for output with 120° contact time, a_{30}, a_{90}, a_{150} are readings at phase positions of $30^\circ, 90^\circ$ and 150° for the output wave with 20° contact time, and A_{m1} is the maximum reading for the input wave with 120° contact time and A_{m3} for 20° contact time, then the describing function for the fundamental is given by $G_{D1} = \frac{a_m}{A_{m1}}$; the describing function for the third harmonic is given by

$$G_{D3} = \frac{(a_{30} + a_{150} - a_{90})}{3 A_{m3}}$$

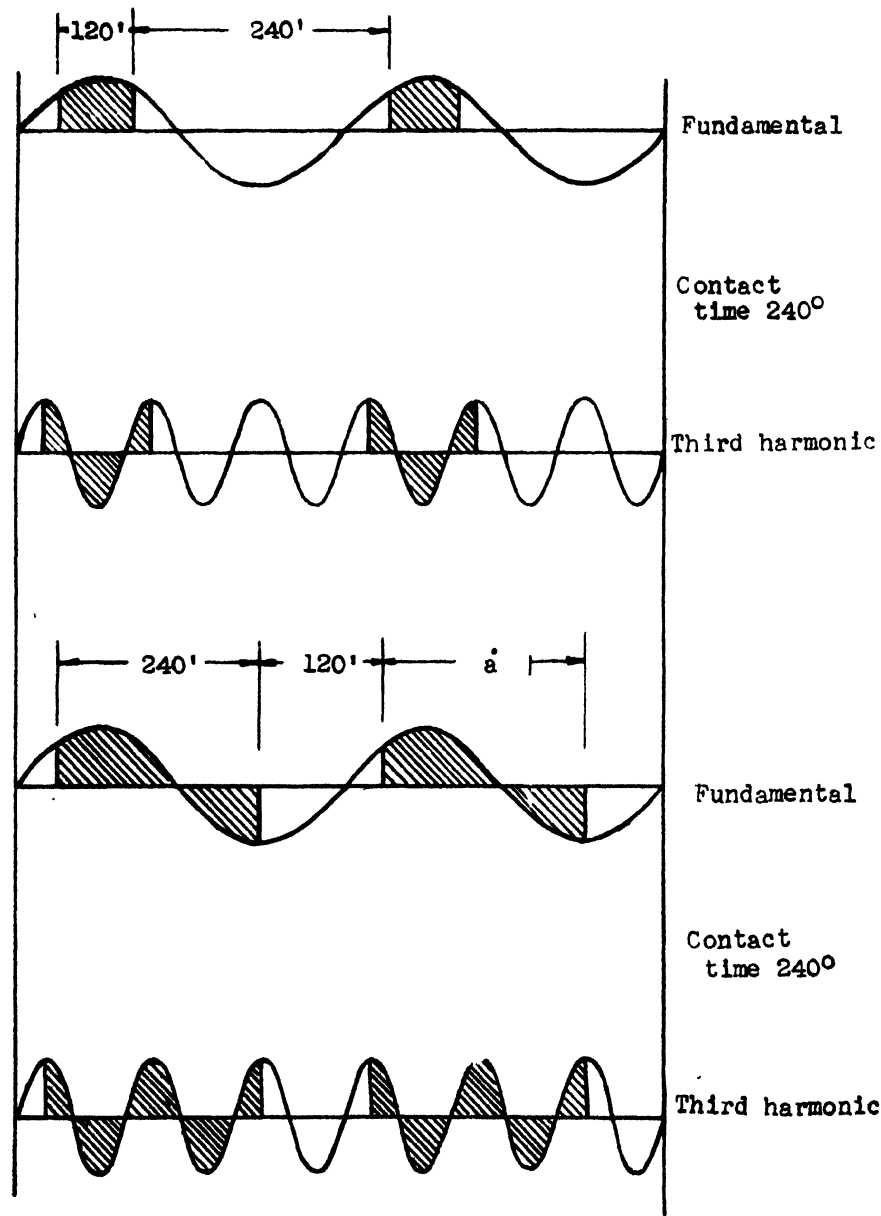
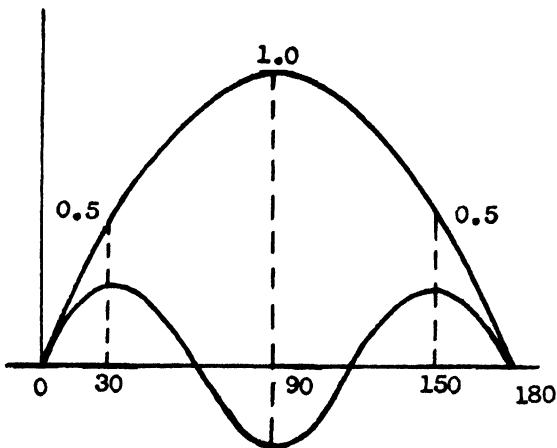


Fig. 10

Curves showing effect of individual harmonics on measurement of a complex waveform

**Fig. 11****Measurement of third harmonic with vectormeter**

This method for evaluating the describing function is simple and quick and is accurate only if the higher harmonics are negligible and has been used in obtaining the describing function of the soft spring non-linear device described in section 4.

INDEX TO ADVERTISERS

JOURNAL

Civil Engineering Division

1. Burmah-Shell	556
2. Cement Marketing Co. of India Ltd.	Cover (ii)
3. Gannon, Dunkerley & Co. (Madras) Ltd.	ii
4. Grindwell Abrasives Ltd.	i
5. Killick Nixon & Co. Ltd.	Cover (iii)
6. Madras Pencil Factory	v
7. Martin Burn Ltd.	ii
8. Statesman Ltd.	Cover (iv)

Mechanical Engineering Division

1. Aluminium Industries Ltd.	iv
2. Bird & Co. (P) Ltd.	vi
3. Cement Marketing Co. of India Ltd.	Cover (ii)
4. Cooper Engineering Ltd.	ii
5. Coventry Spring & Engineering Co. (P) Ltd.	viii
6. Electrical Manufacturing Co. Ltd.	Cover (iv)
7. Garlick & Co. (P) Ltd.	iii
8. National Tannery Co. Ltd.	xiii
9. Precision Bearings India Ltd.	x
10. Trade Representation of the Rumanian People's Republic	vii
11. Vinar Ltd.	xii
12. Voltas Ltd.	i
13. Welding Electrodes & Metallic Alloys Ltd.	v
14. William Jacks & Co. Ltd.	Cover (iii)

Electronics and Telecommunication Engineering Division

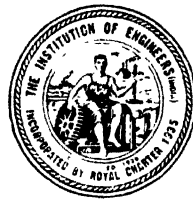
1. Electronics Ltd.	Cover (iii)
2. English Electric Co. Ltd.	ii
3. Indian Oxygen Ltd.	Cover (ii)
4. Jyoti Calor-Emag Ltd.	i
5. Mysore Kirloskar Ltd.	Cover (iv)
6. Siemens Engineering & Manufacturing Co. of India Ltd	iv

BULLETIN

1. S. Chand & Co.	37
2. Greaves Cotton & Crompton Parkinson Ltd.	iii
3. Kaycee Industries Ltd.	iv
4. Sir Isaac Pitman & Sons Ltd.	ii
5. Statesman Ltd.	Cover (iv)

TELECOMMUNICATIONS
ENGINEERING
DIVISION

JOURNAL OF THE INSTITUTION OF ENGINEERS (INDIA)



VOLUME 47

NUMBER 1

PART ET 1

SEPTEMBER 1966



PUBLISHED BY THE INSTITUTION

8 GOKHALE ROAD

CALCUTTA

Rs. 2.50

THE JOURNAL

OF

The Institution of Engineers (India)

SECRETARY & EDITOR. Prof. R. N. Banerjee, B.E. (Elec.), M.S. (Mech.) (U.S.A.),
M. Tex. A. (India), M.I.E. (India)

The Institution of Engineers (India) as a body accepts no responsibility for the statements made by the individual authors.

The Institution of Engineers (India) subscribes to the Fair Copying Declaration of the Royal Society and reprints of any portion of this publication may be made provided that reference thereto be quoted.

Vol. XLVII

SEPTEMBER 1966

No. 1, Pt. ET 1

CONTENTS

Page

ELECTRONICS AND TELECOMMUNICATION ENGINEERING DIVISION

1. **Single Transistor Voltage Controlled Oscillator and Its Application.**
K. G. Nadar, *Associate Member* 1
2. **Fluctuation Theory of Luminance Discrimination for the Light-Adapted Eye and Its Particular Application to the Television Case.** P. S. Moharir, *Non-member* 17
3. **About the Gray Scale Properties of the Eye.** P. S. Moharir, *Non-member*,
and K. V. Saprykin, *Non-member* 26

AUTOMATIC CONTROL GROUP

4. **A Technique of Characterization and Equivalent Model Construction of a Class of Non-linear Systems.** D. N. Khandelwal, *Non-member* 37
- About the Authors** 45

Electronics and Telecommunication Engineering Division Board

The President (*Ex-officio*)

Brig. M. K. Rao (*M.*), *Chairman*

Prof. S. P. Chakravarti (*M.*)

Lt.-Col. S. Mishra (*M.*) (*Co-opted*)

Automatic Control Group

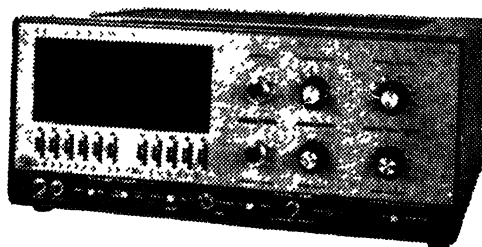
Prof. V. V. Sarwate (*M.*), *Chairman*

COUNT THE ONES THAT COUNT

SCINTILLATION

S | P | E | C | T | R | O | M | E | T | E | R

UNIVERSITY II SERIES MODEL 530



Featuring Automatic Background Subtract

Control the condition...establish the authority of your research...and organize the counting logic of your investigation.

COUNT THE ONES THAT COUNT in scintillation studies. Define the conditions by simple control settings on the University II Scintillation Spectrometer Model 530. Set the predetermined background rate you wish to subtract. Set the upper and lower levels of the window to admit "the ones that count".

Set the all-electronic automatic baseline advance, if desired, to create 100 channels (in 1% steps) over the full scale. Take advantage of a choice of either voltage or current inputs to the high-gain amplifier for different detector arrangements or for long-cable applications. Manual and automatic operation, visual and printer readout, and solid state circuit reliability in the University II Spectrometer Model 530 assure you controlled conditions—you COUNT THE ONES THAT COUNT.

**BAIRD-ATOMIC,
INC. U.S.A.**

**B
A**

Sales Distributors:

**MOTWANE
PRIVATE LIMITED**

127 Mahatma Gandhi Road, Post Box No. 1312 Bombay-1
Phone 292331 Grams. 'CHIPPHONE' all offices • Branches at:
New Delhi, Calcutta, Lucknow, Kanpur, Madras and Bangalore.

CBML-45

THE JOURNAL

OF

The Institution of Engineers (India)

SECRETARY & EDITOR · Prof R N Banerjee, B.E. (Elec.), M.S. (Mech.) (U.S.A.),
M. Tex. A. (India), M.I.E. (India)

The Institution of Engineers (India) as a body accepts no responsibility for the statements made by the individual authors

The Institution of Engineers (India) subscribes to the Fair Copying Declaration of the Royal Society and reprints of any portion of this publication may be made provided that reference thereto be quoted.

Vol. XLVII

JANUARY 1967

No. 5, Pt. ET 2

CONTENTS

Page

ELECTRONICS AND TELECOMMUNICATION ENGINEERING DIVISION

- | | | |
|-----------|---|-----------|
| 1. | Infra Red Radiation and its Applications. S. K. Chatterjee, <i>Non-member</i> .. | 47 |
| 2. | A Direct Discrete Analogue for Flood Routing. K. V. Ramana Murthy, <i>Non-member</i> | 66 |

AUTOMATIC CONTROL GROUP

- | | | |
|-----------|---|-----------|
| 3. | A Temperature Regulator for Low Capacity Baths. J. S. Gupta, <i>Associate Member</i> | 81 |
| 4. | Transient Descriptors Determining the Performance of Linear and Non-linear Systems. T. R. Natesan, <i>Non-member</i> | 88 |
| | About the Authors | 97 |

Electronics and Telecommunication Engineering Division Board

The President (*Ex-officio*)

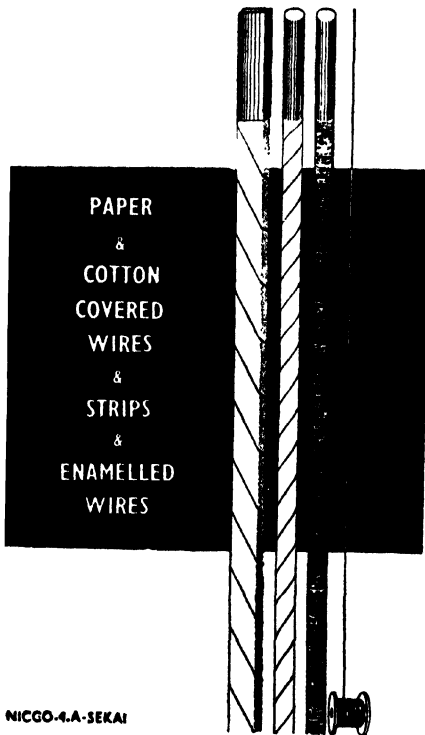
Brig. M. K. Rao (M.), *Chairman*

Prof. S. P. Chakrabarti (M.)

Lt-Col S. Mishra (M.) (*Co-opted*)

Automatic Control Group

Prof V V Sarwate (M.), *Chairman*



WHEN QUALITY COUNTS NICCO

For all electrical motors,
fans, transformers and
Tele-communication
requirements.

Manufactured in accordance
with appropriate BSS & ISS



THE NATIONAL INSULATED CABLE CO. OF INDIA LTD.

NICCO HOUSE, 2, HARE STREET, CALCUTTA-1

BRANCH: KASHMERE GATE
POST BOX NO 1644, DELHI

Agents at Bombay • Madras
Cauhati • Patna • Lucknow
Kanpur • Cuttack • Rourkela
Jabalpur • Nagpur • Secunderabad
Bangalore • Kozhikode • Ernakulam
Kottayam • Trivandrum

THE JOURNAL

OF

The Institution of Engineers (India)

SECRETARY & EDITOR : Prof R. N. Banerjee B.E. (Elec.),
M.S. (Mech.) (U.S.A.), M. Tex. A. (India), M.I.E. (India)

The Institution of Engineers (India) as a body accepts no responsibility for the statements made by the individual authors.

The Institution of Engineers (India) subscribes to the Fair Copying Declaration of the Royal Society and reprints of any portion of this publication may be made provided that reference thereto be quoted.

Vol. XLVII

MAY 1967

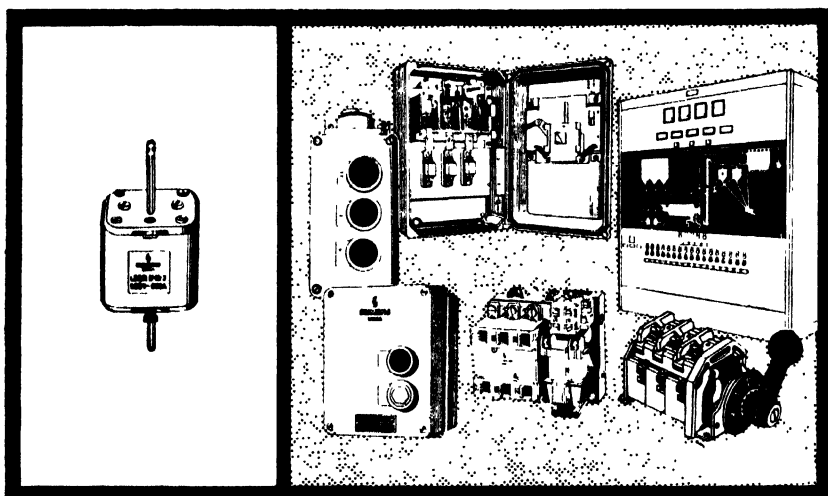
No. 9, Pt. ET 3

CONTENTS

Page

ELECTRONICS AND TELECOMMUNICATION ENGINEERING DIVISION

1. Networks Realizing Bisextic Minimum Positive Real Functions.	99
<i>J. G. Advani, Non-member, and P. K. Baokar, Non-member</i>	
2. Stereophonic Sound Reproduction.	118
<i>Lt.-Col. R. S. Attre, Member</i>	
3. A Direct-Coupled Low-Frequency Phase Meter.	158
<i>A. K. Mohanty, Non-member, and T. Natarajan, Non-member</i>	
4. Limitations on the Performance of a Television System due to Phosphor Decay.	169
<i>P. S. Moharir, Non-member, and Prof. K. V. Saprykin, Non-member</i>	
5. On Nonequi-Ripple Approximation,	181
<i>Dr. S. N. Rao, Non-member</i>	
About the Authors	189
Corrigenda	190



A fuse...

or a complete switchgear
range for any application

SIEMENS SWITCHGEAR

The Siemens range of Switchgear is noted for certain distinctive qualities. First, design—years of research and experimentation and practical application lie behind the design of every item of Siemens Switchgear. Second, quality control—with Siemens quality control is a concept that extends all the way from raw material to the finished product. Third, versatility—the Siemens range of Switchgear extends from an HRC fuse to complicated control boards. And lastly, extreme flexibility—Siemens can provide Switchgear combinations to meet any industrial requirements.

Please fill in and post this coupon to: SIEMENS, 134A, Dr. Annie Besant Road, Worli, Bombay 18.

Please send me details on the range of Siemens Switchgear

Name

Company

Address

Sole Representatives

SIEMENS ENGINEERING & MANUFACTURING CO. OF INDIA LTD.

Ahmedabad • Bangalore • Bombay • Calcutta • Hyderabad • Lucknow • Madras
Nagpur • New Delhi • Patna • Rourkela • Trivandrum • Visakhapatnam

THE JOURNAL

OF

The Institution of Engineers (India)

SECRETARY & EDITOR — Prof. R. N. BANERJEE, B.E. (Elec.),
M.S. (Mech.), U.S.A., M. Tech. A. (India), M.I.E. (India)
Assistant Editor — S. MEENAKSHY, B.E. (Hons.), M.S.E.I., A.M.I.E. (India)
Sub-Editor — D. GUHA, M. Sc.

Vol. XLVII AUGUST 1967 Special No. 12, Pt. ET 3 (SP)

CONTENTS	Page
<i>ELECTRONICS AND TELECOMMUNICATION ENGINEERING DIVISION</i>	
Inaugural Address of Major General S.P. Vohra (M) — President . . .	191
Welcome Address of Shri O. Thimmaiah (M) , <i>Chairman, Andhra Pradesh Council</i> . . .	193
Opening Address of Prof. S.P. Chakravarti (M) , <i>Chairman, Federation of Technicians, Engineers and Scientists</i> . . .	195
 Session I <i>Chairman — Prof. S.P. Chakravarti (M)</i>	
1. Unidigit PCM System. — Dr. M.N. Faruqi, Non-member . . .	204
2. Survey of Developments in Digital Communication Systems. V. Narayana Rao, Non-member and C.R. Chakravorthy, Non-member . . .	218
3. Digital Filters. — A. Prabhakar, Non-member . . .	231
4. Shift Register Sequences. — G. Satvanarayana, Non-member . . .	237
5. Satellite Communications. — Major R K. Joshi, Non-member . . .	245
6. Decoding of Pseudo-Random Coded Sequences. — A. Mukherjee, Non-member . . .	262
 Session II <i>Chairman — Brig. M K. Rao (M)</i>	
7. Microwave Communication along Railway Routes and Radio Patching of Train Traffic Control System with 400 megacycles per sec. Equipment in the U.H.F. Band. — S.A. Srinivasan, Non-member . . .	269
8. Speech Compression and Expansion. — S.V.R. Naidu, Non-member . . .	277
9. Speech Bandwidth Compression. — G. Kanttaiah, Non-member . . .	291

CONTENTS (Contd.)

Other papers Received for Symposium

10. Tropospheric Scatter Communication. Major P.P. Chawla, <i>Associate Member</i>	300
11. Cassegrain Aerial. C.R. Ramachandran Nair, Non-member	...				310
12. Frequency Synthesis in Communication Equipment. P.R. Santhanam, Non-member	317
13. A Pitch Finder Circuit for Use in Vocoders. P. Baskaran, Non-member	323
14. Tropospheric Scatter Communication Systems. M.S.V. Gopal Rao, Non-member	329
15. Satellite Communication System. Wing. Cdr. R. Nagaraja Rao, Non-member	336
16. Delta Modulation. G.V. Subba Rao, Non-member	...				354
Proceedings	363
About the Authors	365

Electronics and Telecommunication Engineering Division Board

Major General S. P. Vohra (M), President (*Ex-officio*)

Prof. S. P. Chakravarti (M), *Chairman*

Brig. M. K. Rao (M) Prof. V. V. L. Rao (*Co-opted*)

Automatic Control Group

V. V. Sarwate (M), *Chairman*

The Institution of Engineers (India) as a body accepts no responsibility for the statements made by the individual authors.

The Institution of Engineers (India) subscribes to the Fair Copying Declaration of the Royal Society and reprints of any portion of this publication may be made provided that reference thereto be quoted.

SINGLE-TRANSISTOR VOLTAGE-CONTROLLED OSCILLATOR AND ITS APPLICATION*

K. G. Nadar

Associate Member

National Aeronautical Laboratory, Bangalore

Summary

This paper discusses the theory and performance considerations pertinent to a single-transistor voltage-controlled oscillator. The performance characteristics of such a circuit and also its application is dealt with in detail. The wide range of design flexibility and usefulness are demonstrated by a block of device fabrication. A comparison is made with conventional circuits and also their shortcomings are pointed out.

1. Introduction

The circuit described here is a single-transistor oscillator and the effect of bias voltage on frequency is discovered with a view to use in instrumentation and data handling devices. Performance requirements imposed in these applications dictate unique device considerations and that results in an oscillator with extended performance characteristics. It is the purpose of this paper to discuss the theory and application pertinent to this circuit and to present an experimental data which describes the performance characteristics.

Discovery of this effect in the circuit excited a considerable theoretical interest and only a few aspects of circuit are dealt with in this paper. To establish its extensive use on practical aspects require a more detailed investigation and this has not yet been attempted. Meanwhile it is hoped that the following account of preliminary work will stimulate the future interest in both theoretical and practical aspects.

2. Characteristics

Some of the important characteristics are as given below.

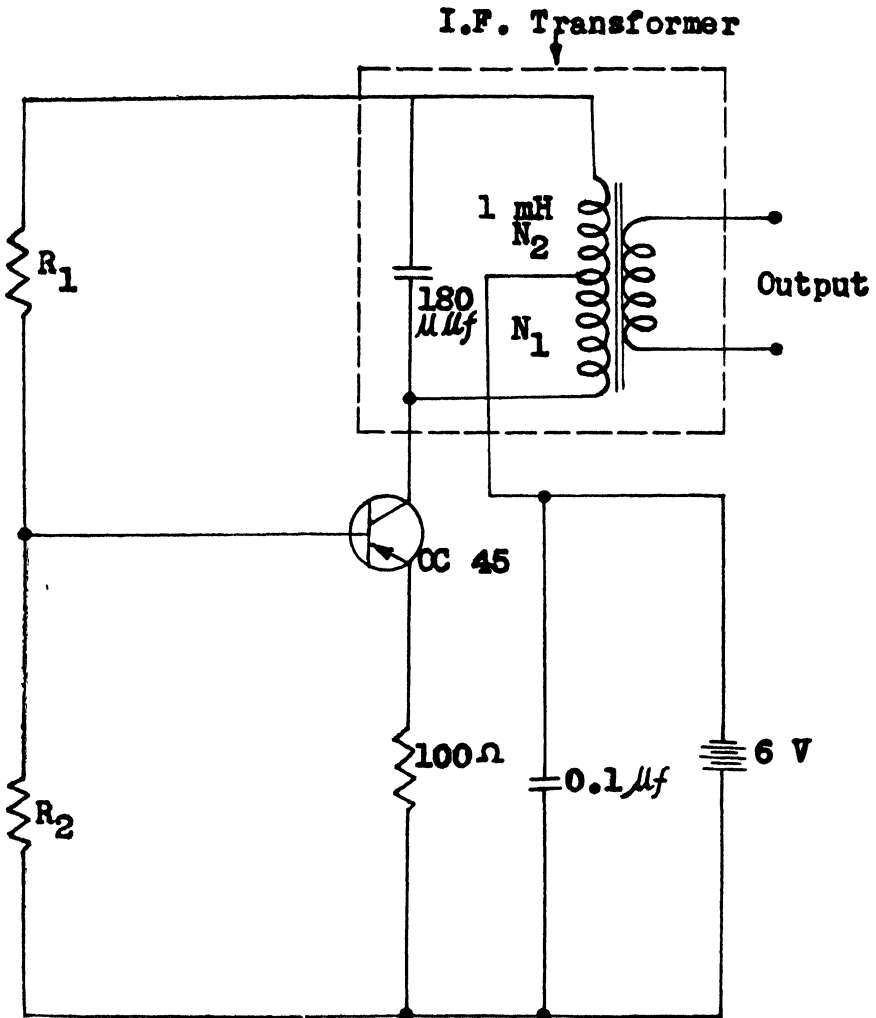
- (i) Operating frequency is a linear function of D.C. input voltage.
- (ii) Input impedance can be adjusted from 100 ohms to 2 kilohm.
- (iii) Overall linearity of voltage to frequency characteristic is expressed as percentage deviation of incremental slope, not exceeding 1%, but it is possible to select a limited frequency range of about 25 kilocycles per sec. within an accuracy of 0.1%.
- (iv) The overall system can be designed in such a way that the temperature, voltage variation, etc. can be compensated as cited in the device fabrication.
- (v) Power consumption is less than 20 milliwatt.

* Written discussion on this paper will be received until January 31, 1967.

This paper (re-drafted) was received on May 11, 1966.

3. Circuit operation

The schematic circuit diagram of the oscillator configuration with the characteristics mentioned is shown in Fig. 1. The circuit function is now briefly described.



$R_1 + R_2 \gg 250$ ohms but not exceeding 5 kilohm

$R_1 : R_2$ determines the frequency of oscillation

Fig. 1

Schematic circuit diagram of the oscillator

The circuit is a simple conventional type Hartley oscillator. Feedback for oscillations is obtained from the part of the inductance; hence, the amplitude of oscillation is always determined by the amount of flux linkage between N_1 and N_2 turns of the tuned circuit windings.

The two series-connected windings on one core constitute the oscillatory winding and a portion of it acts as a feedback winding. The circuit is considered to be in steady condition and executing the frequency of oscillation within the range. One complete cycle consists of conducting and non-conducting states. The analysis will be restricted to the case in which the conducting and non-conducting stages are not identical for constant bias conditions.

The time is denoted by y_1 during conducting state and by t during non-conducting state. During the transitional period, the limiting threshold is proportional to the D.C. input voltage and also to the biasing condition. The normal operating range can be either positive or negative or both in the operating range; beyond this limit the oscillation ceases as the conditions are not satisfied to maintain the oscillation. This results in an upper voltage limit on the core winding and a constant core reversal flux irrespective of frequency. Considering the boundary conditions of current in the inductor, the boundary condition cannot change instantaneously and the current in the inductance is continuous during switching operation.

The voltage across the tuned circuit is assumed to be constant for the whole range of frequencies irrespective of small variations due to feedback.

Switching occurs when collector voltage is sufficiently high. This is determined by the algebraic sum of the base voltage and the voltage across the condenser.

Consider the case in which the voltage across the condenser is zero and the base voltage is in the operating range. Then, the transistor starts conducting and the current in coil N_1 will induce an electromotive force (e.m.f.) in coil N_2 .

Let the voltage across the coils N_1 and N_2 , due to the collector current be E_1 and E_2 respectively. Therefore,

$$\text{Voltage across the tuned circuit} = E_1 \frac{N_1 + N_2}{N_1} = E_1 + E_1 \frac{N_2}{N_1} \quad (1)$$

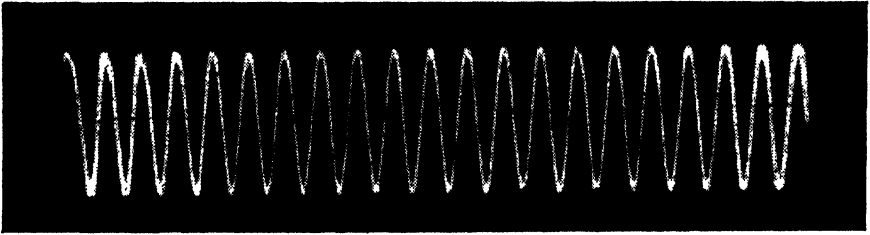
The voltage E_2 , will only exist when the flux changes. It performs the following two functions :

- (i) It accelerates the growth of current and brings I_c to the maximum value ; and
- (ii) It introduces an unbalance when the current is steady.

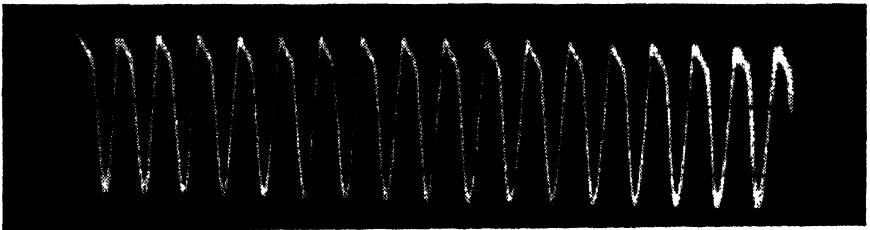
Now, the condenser starts discharging through the coil. The voltage across the condenser is always floated across the transistor base and the collector. The condenser will be discharged to the extent as determined by the instantaneous bias. This discharge current will induce an e.m.f. in the feedback winding that will provide a negative feedback.

It is interesting to note that even though the current through the transistor is very small, the voltage across the transistor is only a fraction of a volt because of the accumulation of charges in the condenser which raises the potential to almost equal to the emitter voltage. The transistor is now floated between the two positive potentials differing by a fraction of a volt. When the condenser discharges, the voltage across the transistor increases, and induced voltage on N_2 will provide a negative feedback which will maintain the transistor at cut-off position till such time the collector voltage is

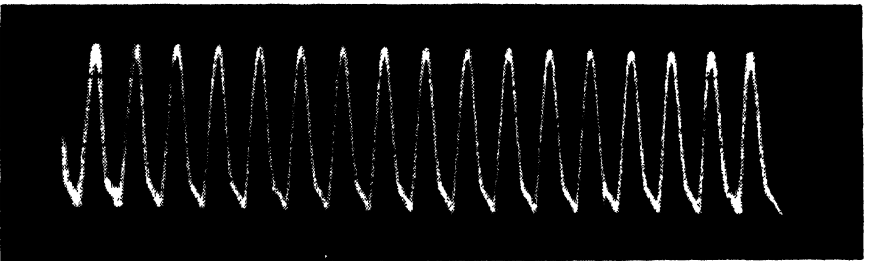
sufficiently high to conduct. Fig. 2(i) to (vii) show the waveforms at different frequencies.



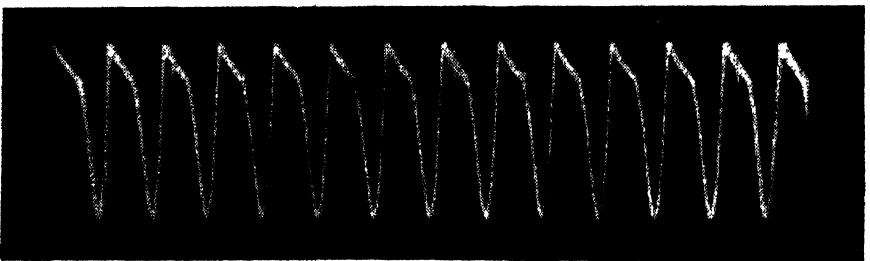
(i)



(ii)

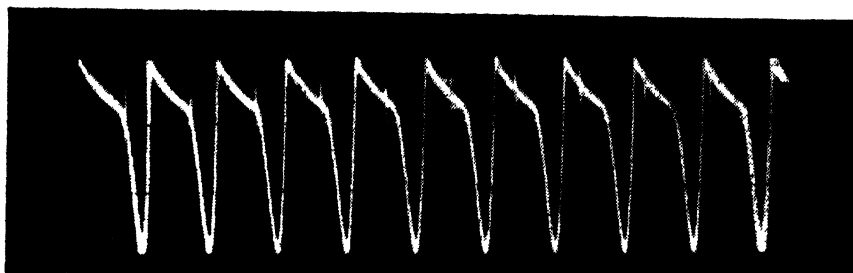


(iii)

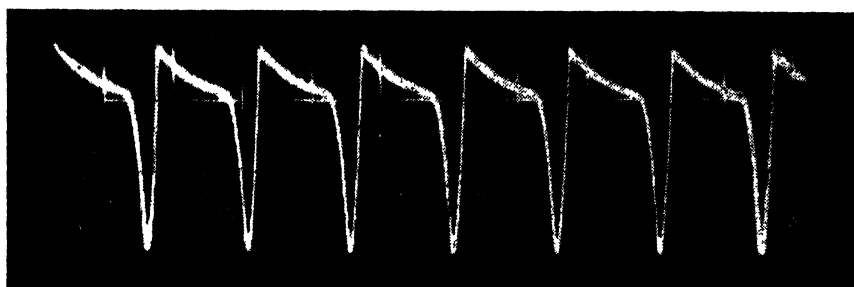


(iv)

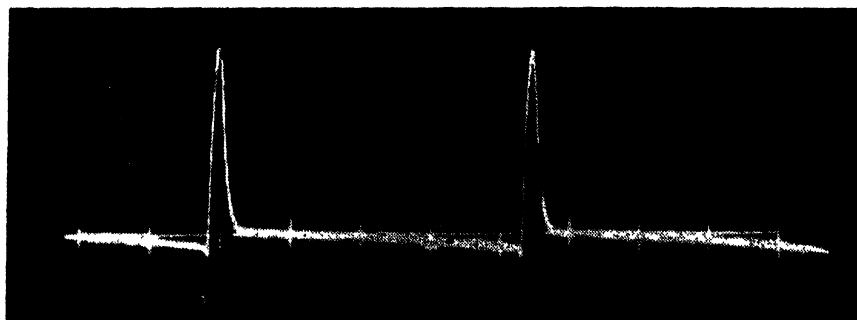
Fig. 2 (contd.)



(v)



(vi)



(vii)

Fig. 2

Oscillographs showing waveforms at different frequencies

The frequency of oscillation is determined by the following factors. Let us consider the circuit in operation during complete flux reversal. The time required for this remains constant throughout the range and is denoted by t_1 . It is experimentally found that,

$$t_1 = \frac{3\pi\sqrt{LC}}{2}$$

where L is the inductance of the coil in henry and C the capacitance of the condenser in farads.

In order to relate the frequency with other parameters, it is necessary to consider the transient voltage across the tuned circuit.

$$\text{Voltage across the tuned circuit} = E_1 \frac{N_1 + N_2}{N_1}$$

The voltage E_1 , is determined by the final value of the collector current and also the rate of change of current. The voltage swing at the collector of the oscillator at different frequencies is given in Fig. 3.

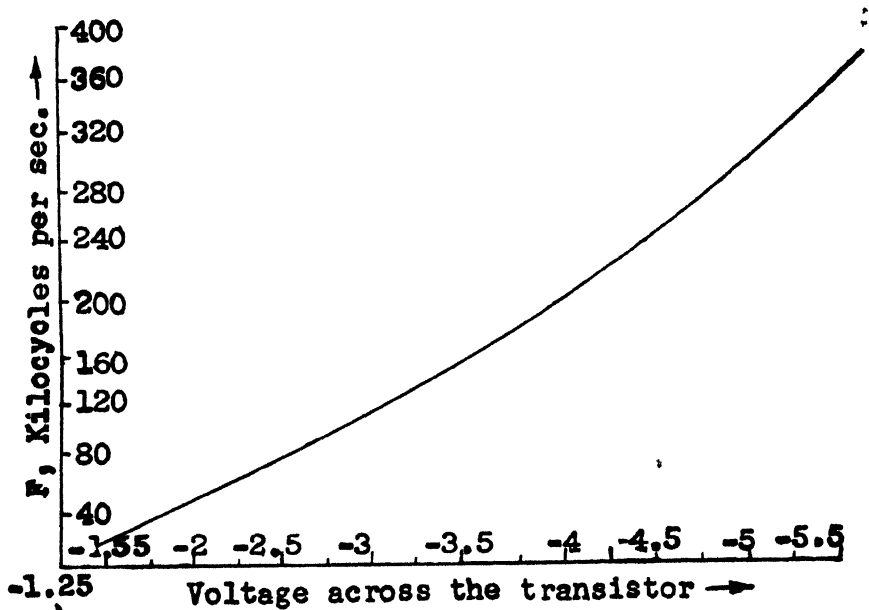


Fig. 3

Voltage swing at the collector of oscillator at different frequencies

Fig. 4 shows the level at which the condenser discharges at different frequencies.

The voltage across the condenser undergoes a change due to the discharge and the maximum variation is about 5 volts, *i.e.*, from 19.5-24.5 volts; but the subsequent changes in collector voltage are as shown in Fig. 3. The effect of feedback within the transistor is extremely important and not directly comparable with anything that occurs in a valve. A typical characteristic of a transistor with feedback is reproduced in Fig. 7. Therefore, for finding out the time t , only the voltage change across the tuned circuit is considered. It is obvious from Fig. 2 that the waveform departs from the sine-wave as frequency decreases. Therefore, transient condition can be easily obtained by assuming that the input to the tuned circuit is sinusoidal and that the condenser is charged to a peak value of E_c .

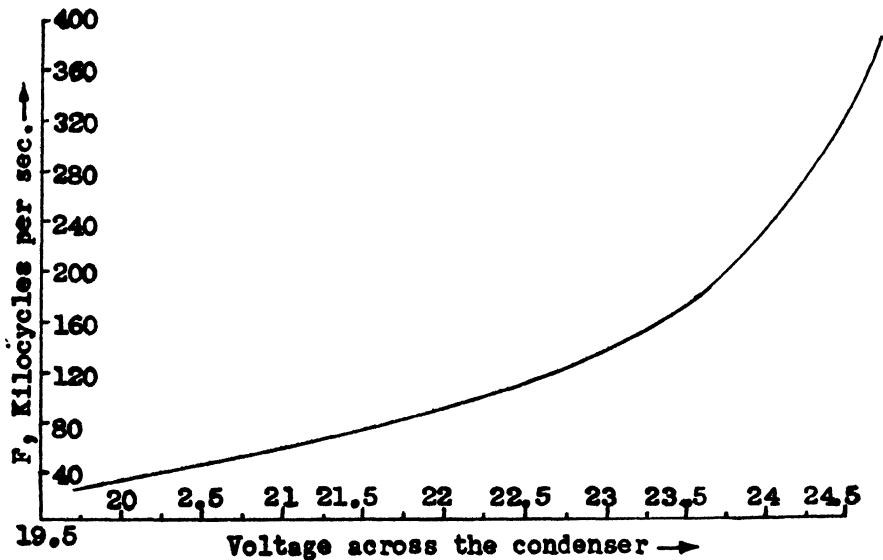


Fig. 4

Curve showing voltage level at which condenser discharges at different frequencies

Therefore,

$$e = E_c \sin(\omega t + \phi)$$

Then, the fundamental equation connecting the current and voltage is

$$E_c \sin(\omega t + \phi) = L R + L \frac{di}{dt}$$

where i is the value of the current at time t , and is given by

$$i = C_1 e^{\lambda t} + \frac{e^{\lambda t}}{L} \int e^{-\lambda t} E_c \sin(\omega t + \phi) dt \quad (3)$$

where $\lambda = -\frac{L}{R}$ and C_1 is an arbitrary constant.

From equations (3) and (4), we get

$$i = C_1 e^{\lambda t} \frac{E_c}{L \sqrt{\lambda^2 + \omega^2}} \sin(\omega t + \phi + \alpha)$$

when

$$\alpha = \tan^{-1} \frac{\omega}{\lambda}, t=0, i=0$$

$$0 = C_1 - \frac{E_c}{\sqrt{R^2 + \omega^2 L^2}} \sin \left\{ \phi - \tan^{-1} \left(\frac{\omega L}{R} \right) \right\}$$

$$C_1 = \frac{E_c}{\sqrt{R^2 + \omega^2 L^2}} \sin \left\{ \phi - \tan^{-1} \left(\frac{\omega L}{R} \right) \right\}$$

$$i = \frac{E_c e^{-\frac{R}{L}t}}{\sqrt{R^2 + \omega^2 L^2}} \sin \left\{ \phi - \tan^{-1} \left(\frac{\omega L}{R} \right) \right\} - \frac{E_c}{\sqrt{R^2 + \omega^2 L^2}} \sin \left\{ \omega t + \phi \tan^{-1} \left(\frac{\omega L}{R} \right) \right\}$$

The first term is the transient component and the second is the A.C. component of constant amplitude. It is to be noted that the rate at which the transient component dies away, is again determined by the value of $e^{-\frac{R}{L}t}$ and thus, this rate is proportional to $\frac{R}{L}$.

In this particular example, t is small as compared with $\frac{R}{L}$ and the transient component will be of importance in determining the value of i . The voltage induced in the feedback coil during the discharge of the condenser is negative and mainly depends on the current i , and the A.C. component is suppressed as the transistor is not allowed to conduct. Thus, the restoration of collector voltage to a value is determined by the bias voltage only.

The term, $\sin \left\{ \phi \tan^{-1} \left(\frac{\omega L}{R} \right) \right\}$ tends to be equal to 1.

$$\epsilon = i \sqrt{R^2 + \omega^2 L^2}$$

$$\epsilon = E_c e^{-\frac{R}{L}t}$$

$$t = \frac{R}{L} \log_e \frac{E_c}{\epsilon}$$

$$f = \frac{1}{t_1 + t} = \frac{2}{3 \pi \sqrt{LC} + \frac{2L}{R} \log_e \frac{E_c}{\epsilon}} \quad (5)$$

The ratio $\frac{E_c}{\epsilon}$, varies from 1.00-1.28 and corresponding frequency variation is 400 to 20 kilocycles per sec. The level at which the condenser is allowed to discharge is determined by the instantaneous bias of the transistor. The ratio $\frac{E_c}{\epsilon}$, is the decisive factor that determines the frequency of oscillation. This ratio is varied

according to the instantaneous value of the base voltage and $\frac{L}{R}$ is the time constant of the inductive branch of the tuned circuit. The relationship between V_{bc} and the collector current is shown in Fig. 5. The condenser will discharge to such an extent as to restore the collector voltage to a sufficient value to conduct the transistor. The induced voltage in the feedback winding due to the discharge of the condenser will provide a negative feedback, thus maintaining the transistor at cut-off position; whereas during conduction, the induced voltage in the feedback winding will be such that the feedback is positive. Hence, the action is accelerated.

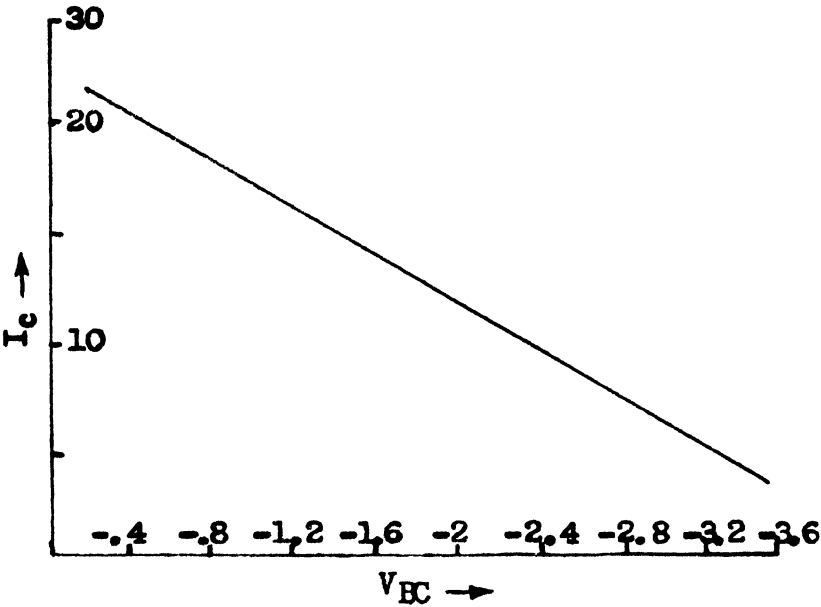


Fig. 5

Variation of collector current with voltage

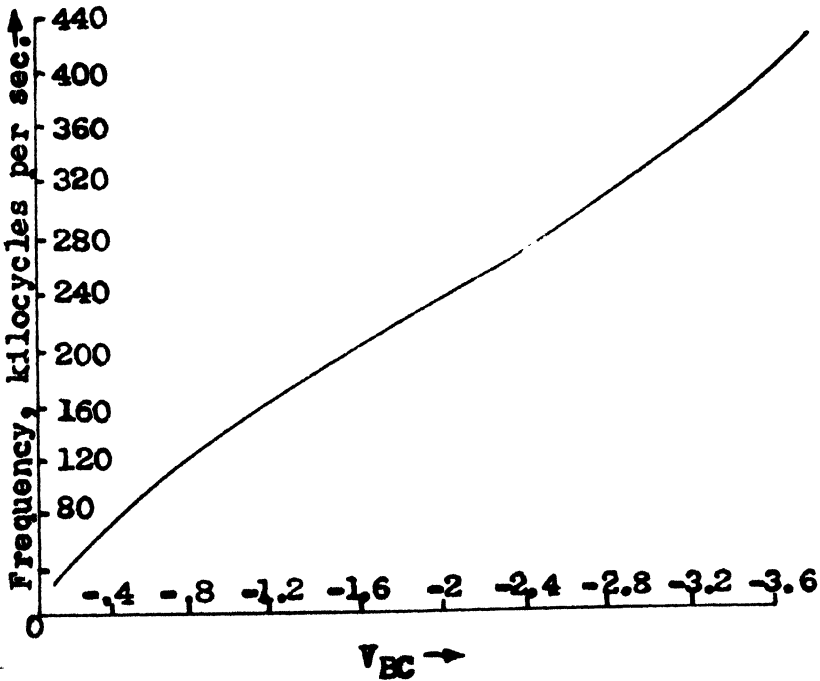


Fig. 6

Variation of voltage with frequency

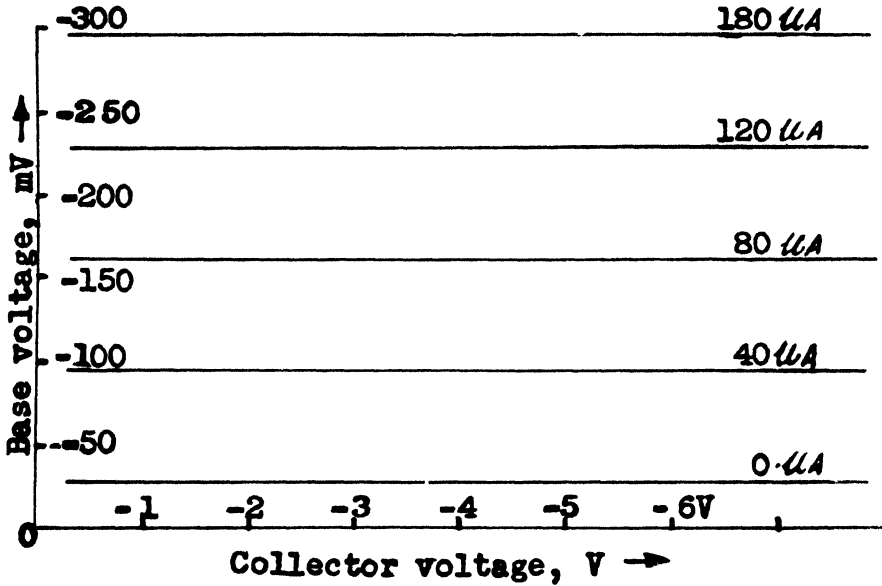


Fig. 7

Typical characteristic of a transistor with feedback

4. Operating frequency range

The highest possible frequency f_h , is obtained when the bias is such that the transistor current is at the minimum so as to maintain oscillations. The lowest possible frequency is obtained when the ratio $\frac{E_c}{\epsilon}$, is the maximum. As V_{eb} is allowed to decrease, V_{bc} increases and frequency becomes progressively higher and *vice versa*.

Therefore, at the maximum frequency, the quantity $\frac{L}{R} \log_e \frac{E_c}{\epsilon}$ tends to zero.

$$f_h = \frac{2}{3 \pi \sqrt{L C}} \quad (6)$$

From equations (5) and (6),

$$\frac{f_h}{f_l} = 1 + \frac{2}{3 \pi R} \sqrt{\frac{L}{C} \log_e \frac{E_c}{\epsilon}} \quad (7)$$

The voltage-controlled oscillator operates between the frequencies f_o and f_l , where f_o is the resonant frequency of the tuned circuit, and

$$f_l > \frac{2 R}{2 L + 3 \pi R \sqrt{L C}} \quad (8)$$

Therefore, the maximum frequency variation can be obtained from equation (9).

From equations (6) and (8),

$$\text{Maximum frequency} = \frac{4 L}{3 \pi \sqrt{L C} (2 L + 3 \pi R \sqrt{L C})} \quad (9)$$

The equations for upper and lower limits of frequencies do not contain any voltage as a function of the frequency. The maximum ratio of the frequency that can be obtained theoretically is given by equation (10).

From equations (6) and (8),

$$\text{Maximum ratio of frequency} = 1 + \frac{2\sqrt{L}}{3\pi R\sqrt{C}} \quad (10)$$

The frequency is being controlled by a factor $\log_e \frac{E_c}{\epsilon}$. Even though the frequency is a function of the reciprocal of $\log_e \frac{E_c}{\epsilon}$, the linearity is being maintained due to feedback.

5. Input control

Equation (5) shows that the frequency of the oscillator is a function of voltages which is purely determined by the instantaneous bias. In order to relate the frequency to the instantaneous bias voltage, it is necessary to consider V_b and V_{bc} . Any change in V_b will bring the corresponding change in V_{bc} also.

The level at which the condenser is allowed to discharge is determined by V_{bc} and other circuit parameters. The analysis is further simplified by assuming that,

$$\begin{aligned} \epsilon &= K_1 V_{cb} \\ V_{cb} &= V_b - I_e R_e \end{aligned}$$

Therefore,

$$\begin{aligned} f &= \frac{1}{\frac{3\pi\sqrt{L}C}{2} + \frac{L}{2R} \log_e \frac{E_c}{\epsilon}} \\ t &= \frac{3\pi\sqrt{L}C}{2} + \frac{L}{2R} \log_e \frac{E_c}{K_1 V_{cb}} \end{aligned} \quad (11)$$

$$t = C + |m| \log_e \frac{E_c}{K_1 V_{cb}} \quad (12)$$

The linear equation (12) relates the periodic time of the oscillator frequency to the voltage V_{cb} , as all other parameters are constant. The voltage V_{cb} , is directly proportional to the input voltage. Fig 8 is a schematic circuit showing the different voltages. A simplification of equation (12) expresses f as the function of V_{cb} in the slope intercept form of a straight line equation,

$$\frac{1}{f} = \frac{1}{f_h} + |m| \log_e \frac{E_c}{K_1 V_{cb}} \quad (13)$$

where $|m|$ is the slope of t to $\log_e \frac{E_c}{K_1 V_{cb}}$ characteristic curve and is given by

$$|m| = \frac{f_h - f}{f_h f \log_e \frac{E_c}{K_1 V_{cb}}} \quad (14)$$

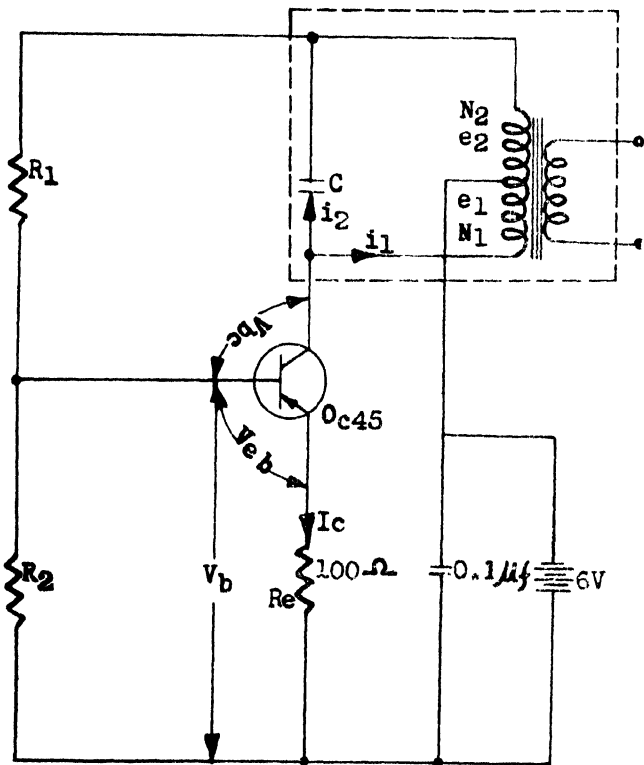


Fig. 8
Schematic circuit
showing the different
voltages

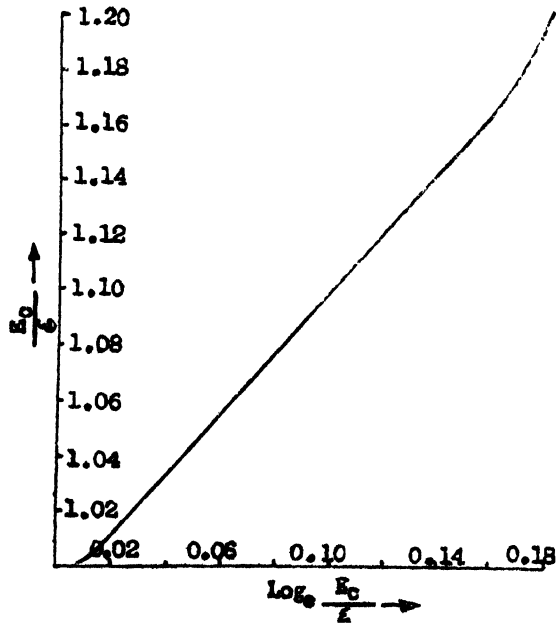


Fig. 9
Variation of circuit
parameters

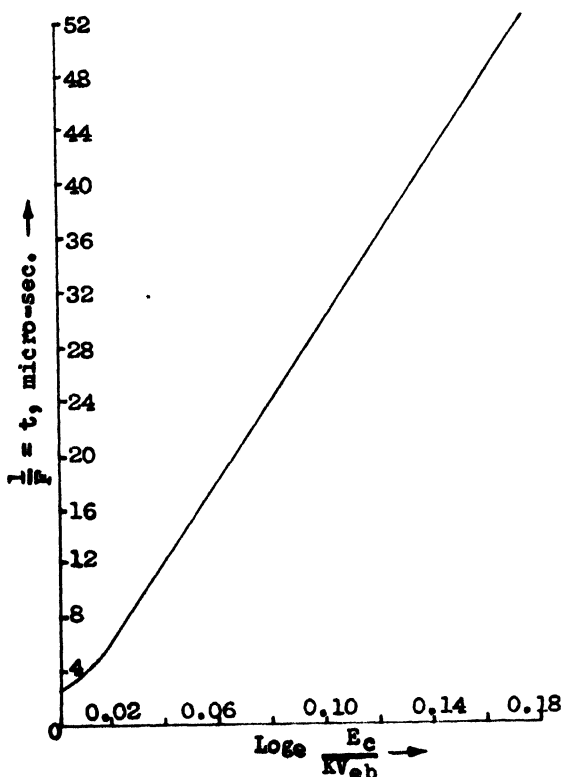


Fig. 10

The characteristic curve

The effect of increasing the control voltage is to decrease the frequency. The required slope $|m|$ can be obtained by selecting proper components and accurate adjustments can be done by including a trimming pot in the inductive branch of the tuned circuit.

6. Design considerations

Design of the voltage controlled oscillator for a specific requirement involves the application of equations (1) to (14) which have been established on desired operation. Due to the fact that there are certain practical limitations, such as, the type of the transistor, its current rating and junction capacitance and tuned circuit load-current ratio, etc., it is expected that some modification of the results obtained may be necessary.

7. Device fabrication

A detailed discussion of the construction of fabrication devices is not needed here. Fig. 11 shows a general layout and some important physical features of the devices which can be made utilizing this circuit technique.

In addition to the recording and indicating of the digital quantities, it is also possible to expand the time-scale and any transient phenomena recorded in a tape recorder can be displayed in an ordinary strip chart recorder or similar devices—a feature which may not be easy to obtain by other means.

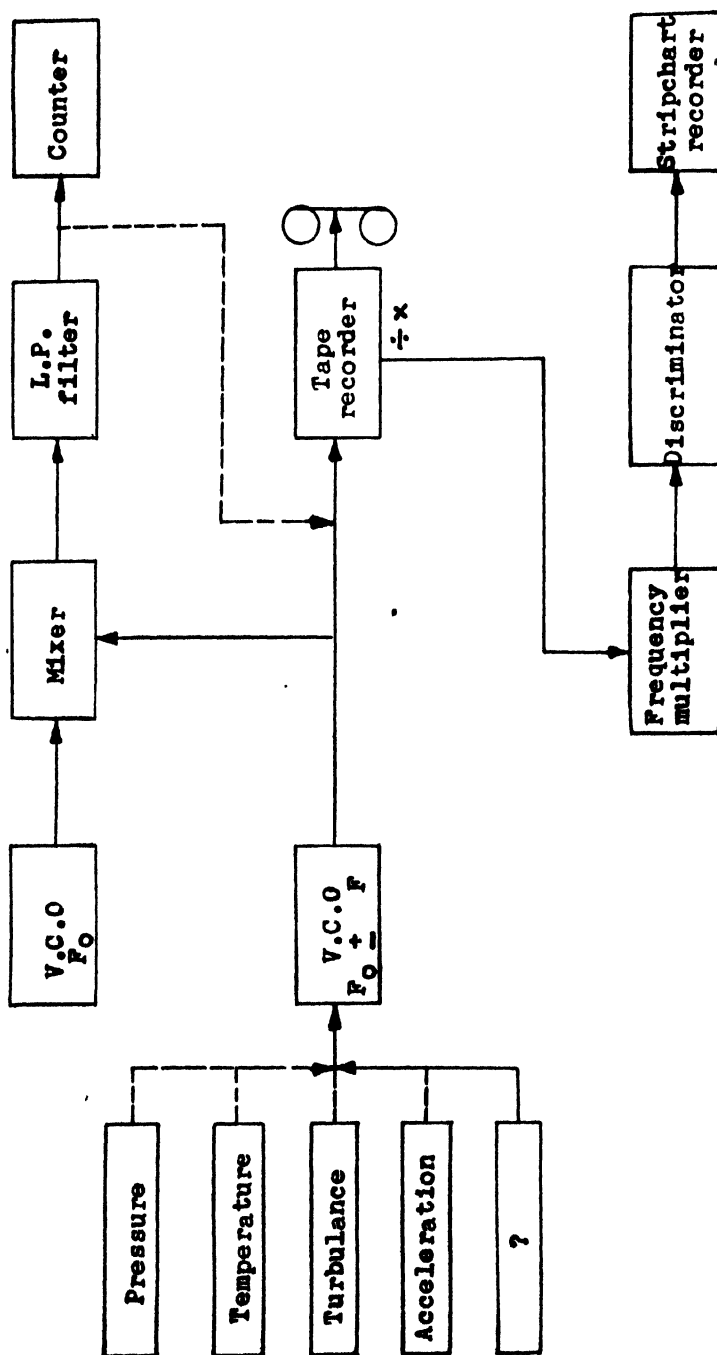


Fig. 11
General layout and important features of devices

One of the important features of this design is that the temperature and other parameters can be compensated as it will affect both voltage-controlled oscillators at a time and the difference is maintained constant. The second advantage is that, after the data leave the instrumentation system, these are subjected to a number of operations including recording, reducing and plotting. Each of these operations can introduce additional error into the data. In order to reduce these errors, the digital system is preferred. In general, the errors introduced by the data handling and processing can be made negligible compared with basic instrumentation errors. Random noise and dynamic lag introduced by the filter is reduced to the minimum.

8. Conclusions

To sum up, the various factors dealt with in this paper are important in the application of the single-transistor voltage-controlled oscillator. Fig. 11 shows the main results of this circuit and from these the pertinent conclusion can be drawn. The design binds itself to high speed measurements. This system is capable of being implemented with strain gauge output, the details of which will be dealt with in another paper, 'High Speed Data Handling', by the author. The opinions expressed in device fabrication are exclusively of the author and not those of any group or organization.

9. Acknowledgments

The author thanks the Director of the National Aeronautical Laboratory, Bangalore, for providing facilities for carrying out the work presented in this paper. He also thanks the members of the Electronics Division of the Laboratory for their assistance in the preparation of this paper.

10. References

1. S. Paul. 'A Magnetic Core Voltage to Frequency Converter'. *IRE Transactions of Space Electronics and Telemetry*, vol. 9, 1963, p. 13.
2. J. P. Frazier and J. Page. 'Phase Lock Loop Frequency Acquisition Study'. *IRE Transaction on Space Electronics and Telemetry*, September 1962, p. 210.
3. Herbert and J. Reigh. 'Functional Circuits and Oscillators'.
4. B. G. Kuhn, K. H. Morey and W. B. Smith. 'The Orthomatch Data Transmission System'. *IEEE Transaction on Space Electronics and Telemetry*, vol. 9, 1963, p. 63.
5. M. K. Stark. 'Short Range Telemetry'. *IEEE Transaction on Industrial Electronics and Control Instrumentation*, vol. IECI 12, no. 1, March 1965, p. 29.
6. R. Lee Price. 'A Magnetic Feed Back Modulator for Improved F.M. Carrier Recording'. *IEEE Transactions on Magnetic Systems*, vol. CT-12, no. 1, June 1965.
7. R. W. Mann. 'Electronics for a Low Cost Orbiting Vehicle'. *IEEE Transactions on Aero Space and Electronic Systems*, vol. AES-2, no. 3, January 1966, p. 103.

8. R. C. Mackey. 'Clock Sources for Synchronized Communications System'. *IRE Transactions on Space Electronics and Telemetry*, vol. 8, 1962, p. 23.
9. S. C. Gupta and R. J. Solem. 'Optimum Filters for Second and Third Order Phase Locked Loops by an Error Function Criterion'. *IEEE Transactions on Space Electronics and Telemetry*, vol. 11, no. 2, June 1965, p. 54.
10. C. S. Weaver. 'Threshold and Tracking Ranges in Phase Locked Loops'. *IRE Transactions on Space Electronics and Telemetry*, vol. 7, no. 3, September 1961, p. 6.
11. R. M. Glorioso and E. H. Grazeal. 'Experiments in SSB. F.M. Communication Systems'. *IEEE Transactions on Communication Technology*, vol. 13, no. 1, March 1965, p. 108.

FLUCTUATION THEORY OF LUMINANCE DISCRIMINATION FOR THE LIGHT-ADAPTED EYE AND ITS PARTICULAR APPLICATION TO THE TELEVISION CASE*

P. S. Moharir

Non-member

*Research Scholar, Electrical Engineering Department,
Indian Institute of Technology, Kanpur*

Summary

The fluctuation theory of luminance discrimination was developed for the dark-adapted eye by Bouman, Vos and Walraven. It has been extended in this paper to the case of light-adapted eye. It has also been shown that the required data for the light-adapted eye, can be calculated using the data for the dark-adapted eye, if one knows the adaptation level. It is further shown that if the human eye is considered as a sufficiently fast device, then the solution for the television case can be obtained very easily.

1. De Vries-Rose (V.R.) region

When the eye is viewing a scene of luminance B , the number of photons that enter the eye per unit area per unit time is

$$n = f B \quad (1)$$

The number of photons entering the eye over a time T , from the area A , would be

$$N = n A T \quad (2)$$

This number is subject to the statistical fluctuations whose r.m.s. value is

$$\Delta N = \pm (n A T)^{1/2} \quad (3)$$

Now the two luminance levels, B_1 and B_2 , can be told apart when the corresponding difference, $N_1 - N_2$, exceeds the noise by a suitable safety factor. For the dark-adapted eye, this noise is given by equation (3). But for the light-adapted eye, the noise of interest would be different. For the adaptation level B_0 , the number of photons that enter the eye would be given by

$$N_0 = n_0 A T \quad (4)$$

and the associated r.m.s. fluctuation would be

$$\Delta N_0 = \pm (n_0 A T)^{1/2} \quad (5)$$

Next, we make an important assumption that as one sees the luminance level B , the adaptation level B_0 acts as a comparison level or as a background level. This means that the eye is sensitive to the difference, $B - B_0$, rather than to B . As both N and N_0 are subject to independent statistical fluctuations, as long as we are interested in $B - B_0$,

* Written discussion on this paper will be received until January 31, 1967.

This paper was received on January 15, 1966.

the resultant noise would be given by the quadratic addition of the two noises given by equations (3) and (5). Thus, the resultant noise is

$$\Delta N_r = \pm [(\bar{n} + n_0) A T]^{\frac{1}{2}} \quad (6)$$

So for the discrimination between the levels, B_1 and B_2 , to be possible, we must have

$$N_1 - N_2 = K [(\bar{n} + n_0) A T]^{\frac{1}{2}} \quad (7)$$

i.e.,

$$f A T (B_1 - B_2) = K [f (B + B_0) A T]^{\frac{1}{2}} \quad (8)$$

or,

$$\left[\left(\frac{\Delta B}{B} \right)_L \right]_{V.R.} = K (f A T)^{-\frac{1}{2}} \left[\frac{B + B_0}{B^2} \right]^{\frac{1}{2}}$$

or,

$$\left[\left(\frac{\Delta B}{B} \right)_L \right]_{V.R.} = K (f A T)^{-\frac{1}{2}} \left[\frac{1}{B} \left(1 + \frac{B_0}{B} \right) \right]^{\frac{1}{2}} \quad (9)$$

Similar calculations for the dark-adapted eye would give

$$\left[\left(\frac{\Delta B}{B} \right) \right]_{V.R.} = K (f A T)^{-\frac{1}{2}} \left[\frac{1}{B} \right]^{\frac{1}{2}} \quad (10)$$

The subscripts L and d refer to the light-adapted and dark adapted cases.

These calculations describe the behaviour in the de Vries-Rose region. Therefore, in this region

$$\left[\frac{\left(\frac{\Delta B}{B} \right)_L}{\left(\frac{\Delta B}{B} \right)_d} \right]_{V.R.} = \left(1 + \frac{B_0}{B} \right)^{\frac{1}{2}} \quad (11)$$

Thus, knowing the Weber-function, i.e., the contrast sensitivity for the dark-adapted eye, the contrast sensitivity for any level of adaptation can be calculated for the de Vries-Rose region.

2. Weber-Fechner region

For the Weber-Fechner region, the statistics should be applied on the neural coding rather than on the quantum incidence following Bouman, Vos and Walraven.¹ Although, the nervous system has a discrete and statistical nature just as the emission of photons, the nervous transmission channels have the refractory period t_0 , such the chance C_t , between two successive spikes in one channel is

$$C_t = 0 \text{ when } t < t_0 \quad (12)$$

and

$$C_t \simeq n \exp. [-n(t - t_0)] \text{ } t \geq t_0 \quad (13)$$

* In the text and mathematical expressions, $N, N_0, N_1, N_2, n, n_0, n_1, n_2, t$, etc. stand for $\bar{N}, \bar{N}_0, \bar{N}_1, \bar{N}_2$, etc.

where n is the number of spikes evoked by the neural system. The average time t , between the two successive spikes on the same channel is then given by

$$t = t_0 + \frac{1}{n} \quad (14)$$

The standard deviation of t around t is

$$\Delta t = \pm \frac{1}{n} \quad (15)$$

or,

$$t = t_0 + \frac{1}{n} \pm \frac{1}{n} \quad (16)$$

The number of spikes v , counted over T and A is now given by

$$v = \bar{v} \pm \Delta v = \frac{TA}{t_0 + \frac{1}{n} \pm \left(\frac{1}{n}\right)} \quad (17)$$

i.e.,

$$v = \frac{TA}{t_0 + \frac{1}{n} \pm \frac{1}{n} \left[t_0 + \frac{1}{n} \right]^{\frac{1}{2}}} \quad (18)$$

or,

$$v = \frac{TA}{t_0 + \frac{1}{n}} \pm \frac{1}{n} \left[\frac{TA}{\left(t_0 + \frac{1}{n}\right)^3} \right]^{\frac{1}{2}} \quad (19)$$

Thus, we have

$$\bar{v} = \frac{TA}{t_0 + \frac{1}{n}} \quad (20)$$

and the associated r.m.s. fluctuation

$$\Delta v = \pm \frac{1}{n} \left[\frac{TA}{\left(t_0 + \frac{1}{n}\right)^3} \right]^{\frac{1}{2}} \quad (21)$$

Using equation (20), we get

$$\Delta v = \frac{\bar{v}^2}{n^{\frac{3}{2}}} \times \frac{1}{TA} \times \Delta n \quad (22)$$

Therefore,

$$\Delta n = \pm \frac{n}{\bar{v}^2} (TA)^{\frac{3}{2}} \left[\left(t_0 + \frac{1}{n} \right)^3 \right]^{\frac{1}{2}} \quad (23)$$

or,

$$\Delta n = \pm n \left[t_0 + \frac{1}{n} \right]^{\frac{1}{2}} \quad (24)$$

For the adaptation level, similar calculations would yield

$$\Delta n_0 = \pm n_0 \left[t_0 + \frac{1}{n_0} \right]^{\frac{1}{2}} \quad (25)$$

Again using the same principle of comparison level, the resultant noise of interest to us would be the quadratic addition of individual noises given in equations (24) and (25). So, the resultant noise is

$$\Delta n_r = \pm [(\Delta n)^2 + (\Delta n_0)^2]^{\frac{1}{2}} \quad (26)$$

or,

$$\Delta n_r = \pm \left[n \left(1 + t_0 n \right) + \frac{n_0 \left(1 + t_0 n_0 \right)}{TA} \right]^{\frac{1}{2}} \quad (27)$$

Now, the two luminance levels B_1 and B_2 can be told apart only if

$$n_1 - n_2 = K \left[\frac{n \left(1 + t_0 n \right) + n_0 \left(1 + t_0 n_0 \right)}{TA} \right]^{\frac{1}{2}} \quad (28)$$

Using equation (1)

$$f(B_1 - B_2) = K \left[\frac{fB \left(1 + t_0 fB \right) + fB_0 \left(1 + t_0 fB_0 \right)}{TA} \right]^{\frac{1}{2}} \quad (29)$$

or,

$$\left(\frac{\Delta B}{B} \right)_L = K (fTA)^{-\frac{1}{2}} \left[\frac{1}{B} \left(1 + \frac{B_0}{B} \right) + t_0 f \left(1 + \frac{B_0^2}{B^2} \right) \right]^{\frac{1}{2}} \quad (30)$$

For the dark-adapted eye we would get

$$\left(\frac{\Delta B}{B} \right)_d = K (fTA)^{-\frac{1}{2}} \left[\frac{1}{B} + t_0 f \right]^{\frac{1}{2}} \quad (31)$$

For the low values of the luminance level B , the terms involving t_0 are insignificant and so the equations (30) and (31) become identical to the equations (9) and (10).

For higher values of B , i.e., in the Weber-Fechner region, only the terms involving t_0 are significant and so the equation for the Weber-Fechner (W.F.) region are

$$\left[\left(\frac{\Delta B}{B} \right)_L \right]_{W.F.} = K (fTA)^{-\frac{1}{2}} \left[t_0 f \left(1 + \frac{B_0^2}{B^2} \right) \right]^{\frac{1}{2}} \quad (32)$$

and,

$$\left[\left(\frac{\Delta B}{B} \right)_d \right]_{W.F.} = K (fTA)^{-\frac{1}{2}} (t_0 f)^{\frac{1}{2}} \quad (33)$$

Therefore,

$$\left[\frac{\left(\frac{\Delta B}{B} \right)_L}{\left(\frac{\Delta B}{B} \right)_d} \right]_{W.F.} = \left(1 + \frac{B_o^2}{B^2} \right)^{\frac{1}{2}} \quad (34)$$

Thus, in the Weber-Fechner region also if the Weber function is known the contrast sensitivity for any other adaptation level can be calculated. But for the transition region, we must use the exact equations (30) and (31). Thus, in this region, in order to be able to calculate the contrast sensitivity of the light-adapted eye, in addition to the Weber function and the adaptation level we must know the factor $t_o f$.

3. Breakdown region

For still higher values of the luminance level B the Weber-Fechner law breaks down. To explain this Bouman, Vos and Walraven¹ assumed that the refractory period t_o itself is subject to statistical fluctuations. The effect of this fluctuation can be expressed as¹

$$\Delta v = \pm \frac{\Delta t_o}{t_o + \left(\frac{1}{n} \right)^2} (t_o T A)^{\frac{1}{2}} \quad (35)$$

As the neural statistics and the statistical fluctuations in t_o are both parallel effects each of which can separately result in contrast threshold phenomenon, the result due to both of them can be calculated by quadratically adding equations (21) and (35). This gives¹

$$\Delta n = \pm \left[\frac{n(1 + t_o n) + (\Delta t_o)^2 n^4 t_o}{T A} \right]^{\frac{1}{2}} \quad (36)$$

Similarly for the adaptation level B_o , we would get

$$\Delta n_o = \pm \left[\frac{n_o(1 + t_o n_o) + (\Delta t_o)^2 n_o^4 t_o}{T A} \right]^{\frac{1}{2}} \quad (37)$$

Again using the same principle of comparison level, the resultant noise of interest to us would be the quadratic addition of individual noises given in equations (36) and (37). So the resultant noise is

$$\Delta n_r = \pm \left[\frac{(n + n_o) + t_o(n^2 + n_o^2) + (\Delta t_o)^2 t_o(n^4 + n_o^4)}{T A} \right]^{\frac{1}{2}} \quad (38)$$

For the discrimination to be possible in the two luminance levels B_1 and B_2 , we must have

$$n_1 - n_2 = K \Delta n_r \quad (39)$$

or,

$$\frac{n_1 - n_2}{n} = \frac{K \Delta n_r}{n} \quad (40)$$

i.e.,

$$\left(\frac{\Delta B}{B}\right)_L = K \left[\frac{\frac{1}{fB} \left(1 + \frac{B_0}{B}\right) + t_0 \left(\frac{B_0^3}{B^2}\right) + (\Delta t_0)^2 t_0 f^2 B^2 \left(1 + \frac{B_0^4}{B^4}\right)}{TA} \right] \quad (41)$$

For the dark-adapted eye, we would get

$$\left(\frac{\Delta B}{B}\right)_d = K \left[\frac{\frac{1}{fB} + t_0 + (\Delta t_0)^2 t_0 f^2 B^2}{TA} \right] \quad (42)$$

For small values of B the last terms are insignificant and the equations (41) and (42) are again reduced to the equations (30) and (31). But for large values of B , only the last terms are significant and we get for this break-down (b.d.) (of Weber-Fechner law) region

$$\left[\left(\frac{\Delta B}{B}\right)_L \right]_{b.d.} = K (\Delta t_0) f B \left[\frac{t_0}{TA} \left(1 + \frac{B_0^4}{B^4}\right) \right] \quad (43)$$

and

$$\left[\left(\frac{\Delta B}{B}\right)_d \right]_{b.d.} = K (\Delta t_0) f B \left[\frac{t_0}{TA} \right] \quad (44)$$

Therefore,

$$\left[\frac{\left(\frac{\Delta B}{B}\right)_L}{\left(\frac{\Delta B}{B}\right)_d} \right]_{b.d.} = \left(1 + \frac{B_0^4}{B^4}\right) \quad (45)$$

Thus, in this region also, we can calculate the contrast sensitivity for the light-adapted eye from the knowledge of only the Weber-function and the adaptation field. But for the general case including the transition regions and also the case when the same approximations cannot be applied to the two equations because of the large value of the ratio $\frac{B_0}{B}$, we must make use of the most general equations (41) and (42). Thus,

$$\frac{\left(\frac{\Delta B}{B}\right)_L}{\left(\frac{\Delta B}{B}\right)_d} = \left[\frac{\frac{1}{fB} \left(1 + \frac{B_0}{B}\right) + t_0 \left(1 + \frac{B_0^3}{B^2}\right) + (\Delta t_0)^2 t_0 f^2 B^2 \left(1 + \frac{B_0^4}{B^4}\right)}{\frac{1}{fB} + t_0 + (\Delta t_0)^2 t_0 f^2 B^2} \right] \quad (46)$$

Thus, to calculate the contrast sensitivity of the light-adapted eye, in addition to the Weber function and adaptation level, we must know f , t_0 and Δt_0 .

4. Derivation of the data for the light-adapted eye

Now, in theory at least there appears a possibility of getting the required information about the parameters f , t_0 and Δt_0 from the data for the dark-adapted eye alone. For this, we consider the three luminance levels: (i) the lowest possible, so that only equation (10) need be considered; (ii) the middle value that gives the lowest value for the Weber function such that only equation (33) need be considered; and (iii) the

highest possible, so that only equation (44) need be considered. Rearranging the abovementioned equations, we get

$$K(fAT)^{-\frac{1}{2}} = \left[\left(\frac{\Delta B}{B} \right)_d \right]_{\text{v.R.}} B^{\frac{1}{2}} = a \quad (47)$$

$$K(AT)^{-\frac{1}{2}} t_o^{\frac{1}{2}} = \left[\left(\frac{\Delta B}{B} \right)_d \right]_{\text{w.F.}} = b \quad (48)$$

$$K(AT)^{-\frac{1}{2}} (\Delta t_o) f t_o^{\frac{1}{2}} = \frac{1}{B} \left[\left(\frac{\Delta B}{B} \right)_d \right]_{\text{b.d.}} = c \quad (49)$$

$$f t_o = \frac{b^2}{a^2} \quad (50)$$

$$\frac{\Delta t_o}{t_o} = \frac{ca^2}{b^3} \quad (51)$$

$$(\Delta t_o)^2 t_o f^3 = \frac{c^2}{a^3} \quad (52)$$

Now, we can rewrite equation (46) as

$$\left(\frac{\Delta B}{B} \right)_L = \left(\frac{\Delta B}{B} \right)_d \left[1 + \frac{F(B_o)}{F(B)} \right]^{\frac{1}{2}} \quad (53)$$

where

$$F(B) = B + f t_o B^2 + (\Delta t_o)^2 t_o f^3 B^4 \quad (54)$$

Thus, using equations (50) and (52), we can plot $F(B)$ as a function of B . Then, using this curve together with the luminance discrimination data for the dark-adapted eye, we can construct the luminance discrimination data for the light-adapted eye for any value of the adaptation level B_o .

The calculations as indicated above were done using Hecht's curve,² wherein $\left(\frac{\Delta B}{B} \right)_d$ has been plotted as a function of B . It should be remembered that the calculations have been done using three extreme isolated points of the curve and, therefore, serve only to indicate the rough magnitudes involved. The results of calculations are

$$f t_o = 22.25 \text{ (milli-lambert)}^{-1} \quad (55)$$

$$\frac{\Delta t_o}{t_o} = 1.617 \times 10^{-5} \quad (56)$$

$$(\Delta t_o)^2 t_o f^3 = 2.88 \times 10^{-8} \text{ (milli-lambert)}^{-3} \quad (57)$$

$\left(\frac{\Delta B}{B} \right)_L$ has been calculated as a function of B for three particular cases: (i) $B_o = 1$ milli-lambert; (ii) $B_o = 10$ milli-lambert; and (iii) $B_o = B$.

Case (iii) will be considered further. The results are shown in the figure.

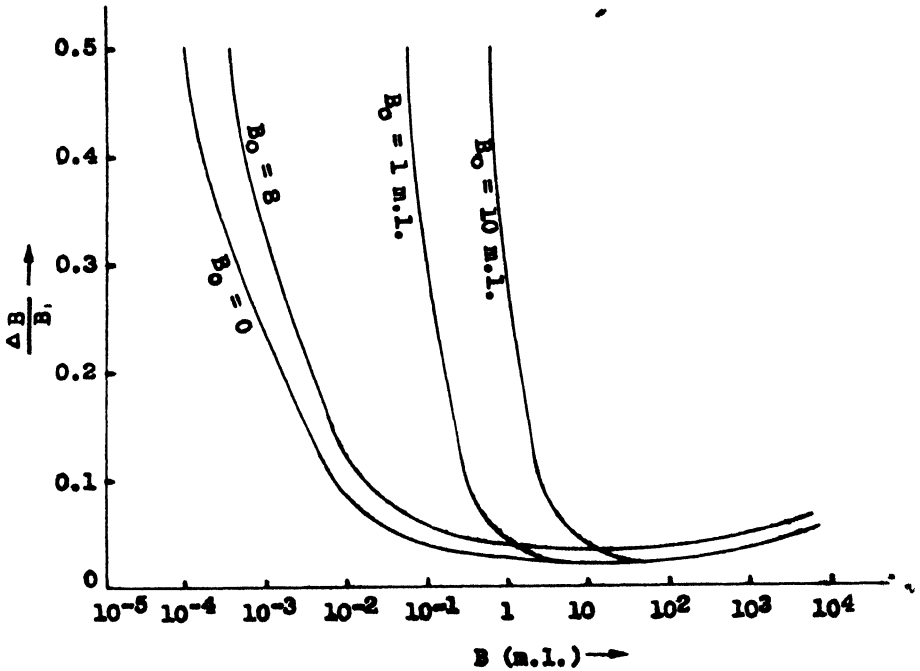


Fig. 1

Curves showing the results

5. Calculations for television case

As a first approximation, we might assume that the adaptation level of the eye viewing a television picture is equal to the mean luminance of the picture. Such an assumption implies that the eye is an extremely slow device which does not respond to the continuous changes of luminance. Such an assumption is of course not true. In fact, while studying the contrast sensitivity of the eye at any adaptation level, the eye is subjected to see that adaptation level for a long time and then is suddenly shown for a short duration, the two luminances that it is supposed to distinguish apart. This particular procedure is adopted to minimize the effect of test field on the adaptation of the eye. As in case of the eye viewing a television picture such a precaution is redundant, we must assume that to some extent the eye is capable of responding to the continuous changes of luminance. We might assume that the instantaneous luminance value B serves as the adaptation level B_0 . This assumption implies that the eye is a very fast device, capable of changing its state of adaptation in a negligible time. This also is not a correct state of affairs.

But we must for the sake of calculations stick to one of these assumptions. The first assumption would involve the knowledge of the average luminance level of a television scene and also of $f t_0$ and $(\Delta t_0)^2 t_0 f^2$. The second assumption leads itself

to the correct mathematical analysis without the knowledge of the average luminance level of $f t_0$ and $(\Delta t_0)^2 t_0 f^3$. Because by putting $B_0 = B$ in equation (53), we get

$$\left(\frac{\Delta B}{B}\right)_L = 2^{\frac{1}{2}} \left(\frac{\Delta B}{B}\right)_d \quad (58)$$

Thus, it is seen that with the assumption of eye being the fast device any data about the number of gray shades that can be told apart by the dark-adapted eye can be used also for the television case provided the number of gray shades is multiplied by 0.707.

6. Acknowledgment

The author wishes to acknowledge the keen interest taken by Prof. K. V. Saprykin, Unesco Expert at Indian Institute of Technology, Bombay, in this work.

7. References

1. M. A. Bouman, J. J. Vos and P. L. Walraven. 'Fluctuation Theory of Luminance and Chromaticity Discrimination'. *Journal of the Optical Society of America*, vol. 53, no. 1, January 1963, p. 121.
2. S. Hecht. 'The Visual Discrimination of Intensity and the Weber-Fechner Law'. *Journal of General Physiology*, vol. 7, 1924, p. 241.

ABOUT THE GRAY SCALE PROPERTIES OF THE EYE***P. S. Moharir***Non-member**Research Scholar, Electrical Engineering Department,
Indian Institute of Technology, Kanpur*

and

K. V. Saprykin*Non-member**Unesco Expert, Indian Institute of Technology, Bombay***Summary**

In view of estimating the upper limit on the number of shades of gray that a television system should reproduce, the number of shades of gray that the dark-adapted eye can resolve over about a contrast range of 1.5×10^7 has been calculated. The maximum number of shades of gray that the eye can distinguish apart is also studied as a function of restricted contrast range and the empirical relationship has been fitted to the data. Some calculations over a narrow contrast range have been done for the light-adapted eye.

1. Eye—the ultimate critic

Human eye is the ultimate critic of any television display. This important fact governs the minimum requisites to be demanded of a television system as well as the upper limit of a performance of the television system, the betterment of the performance above which would draw no extra credit from the ultimate critic and hence this betterment would be redundant.

The property of a television system of concern to us here is the number of gray shades that it should be able to resolve in a given contrast range that it accommodates. The lower limit of this number is determined by the desirability of having as close a relationship between the natural scene and its television counterpart as can be allowed by the television system without imposing on it the standards that may be difficult to accomplish. The upper limit, of course, is set up by the number of gray shades that the eye can resolve in a contrast range which it can usually accommodate while viewing a single scene. Thus, it is necessary to determine the number of shades that the eye can recognize as separate ones.

2. Usual method of the presentation of data

One of the important properties of the eye that are studied is its luminance discrimination or contrast sensitivity. If the two areas are simultaneously viewed by the eye, one with luminance B and the other with luminance, $B + \Delta B$, there exists a minimum value of ΔB , necessary for the eye to be able to recognize the two luminances as distinct ones. The ratio $\frac{\Delta B}{B}$ has come to be known as Weber's fraction. Weber's

* Written discussion on this paper will be received until January 31, 1967.

This paper was received on July 17, 1966.

fraction is usually plotted as a function of B . The value of this fraction depends considerably on the state of adaptation of the viewer's eye, *i.e.*, on the luminance level to which the viewer is accustomed before trying to resolve the two luminance levels. As the adaptation level increases the contrast sensitivity of the eye, *i.e.*, the power of luminance discrimination decreases.

Thus, for the dark-adapted eye the Weber's fraction has got the least value. When $\frac{\Delta B}{B}$ is plotted as a function of B for the dark-adapted eye, it is found that at very low luminances the value of $\frac{\Delta B}{B}$ is relatively large, *i.e.*, the discriminating power of the eye is poor. As the luminance increases, the value of $\frac{\Delta B}{B}$ decreases, and when it attains a minimum value, it remains constant over a considerable range of luminance. Then, at higher luminances, the value of $\frac{\Delta B}{B}$ again increases with B . The total luminance range that the human eye can accommodate is very large. Its lower limit can be set at that luminance for which $\frac{\Delta B}{B}$ is unity. On the high luminance side there would be yet another value of luminance which yields $\frac{\Delta B}{B} = 1$. But the upper limit of the luminance range of the human eye is set by the maximum luminance that the eye can tolerate and it comes much earlier. In fact, it comes soon after the $\frac{\Delta B}{B}$ curve starts rising after the minimum.

It would be interesting to estimate the total number of shades of gray that the human eye can distinguish between these two limits of the luminance range.

3. Various factors affecting $\frac{\Delta B}{B}$

Before attempting this, it is necessary to emphasize that the value of $\frac{\Delta B}{B}$ depends on a multitude of factors.

Piper's law of absolute threshold reads¹

$$\Delta B \sim A^{-1} \quad (1)$$

where A is the area of the aperture of the viewer's eye at a distance at which the two luminances are to be told apart.

Pieron's quadratic law states that¹

$$\Delta B \sim T^{-1} \quad (2)$$

where T is the time of exposure of the two luminances. But the fact remains that A and T affect $\frac{\Delta B}{B}$.

The problem of the effect of the pupillary movement on the Weber's fraction was studied by Krauskopf.² His results indicated that while some components of the

pupillary movement aggravate the brightness discrimination properties of the eye, the others are detrimental. Low frequency (1-5 cycles per sec.) motions reduce the contrast thresholds and high frequency (10-50 cycles per sec.) motions elevate them.

De Palma and Lowry³ have studied the effect of some other factors on the Weber's fraction. They have established that the Weber's fraction depends on the spatial frequency of the two luminances to be distinguished apart and also, that its value is different for sine-wave and squarewave recurrences. The maximum contrast sensitivity, *i.e.*, the minimum value of the Weber's fraction was found to occur at spatial frequencies in the neighbourhood of 10 lines per mm. on the retina. On lower as well as upper side of this spatial frequency the contrast sensitivity of the human eye decreases. Increased viewing distance results in increased contrast sensitivity at higher spatial frequencies. But at the lower spatial frequencies, increased viewing distance results in decreased contrast sensitivity.

A similar behaviour was observed for square-wave contrast sensitivity. But the square-wave test objects need lower contrast thresholds for perceptibility compared to sine-wave test objects in the low spatial frequency range. But in the higher spatial frequency range, sine-wave test objects need lower contrast thresholds for perceptibility compared to square-wave test objects.

Again, the luminance discrimination properties of the human eye depend on the colour⁶ under investigation. Luminance discrimination sensitivity of the eye is maximum for the blue colour, intermediate for the green colour and the least for the red colour. The luminance discrimination sensitivity for the white light is intermediate between blue and green colours.

4. Method of calculations

Our interest lies in calculating the number of shades of gray that the eye can resolve in a given luminance range. The luminance range of interest may be anywhere in the total luminance range that the eye can accommodate. Therefore, we must study the entire luminance range that the eye accommodates. The method of calculations, although laborious, is very simple in principle. If we know the Weber's fraction,

$$W(B) = \frac{\Delta B}{B} \quad (3)$$

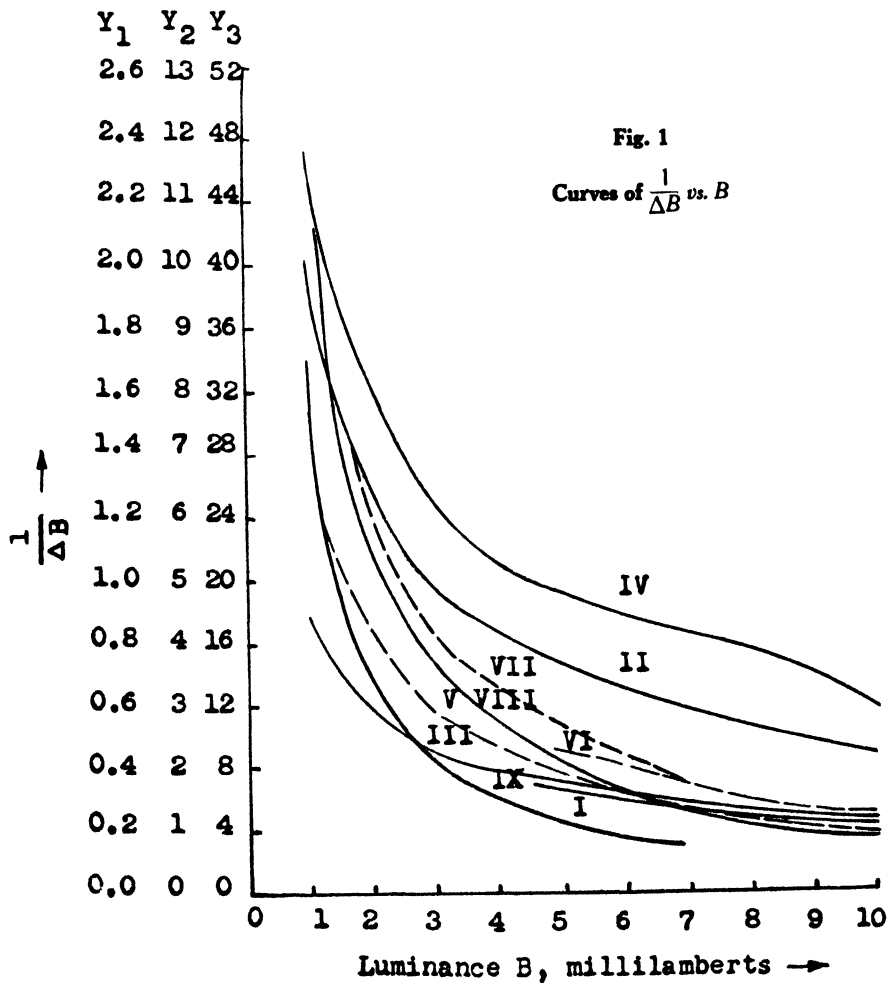
we can calculate

$$\frac{1}{\Delta B} = \frac{1}{B W(B)} \quad (4)$$

Now the number of gray shades that the eye can tell apart in a luminance range between B_1 and B_2 is

$$N = \int_{B_1}^{B_2} \frac{dB}{\Delta B} = \int_{B_1}^{B_2} \frac{dB}{B W(B)} \quad (5)$$

Now the Weber's fraction is determined experimentally as a function of B and no single formula can be fitted to it. Hence the above integration is to be performed graphically. For this, $\frac{1}{\Delta B}$ is plotted as a function of B on the linear scale and the area under the curve is measured. As the range of B to be covered is very vast, the range is broken into several parts in each of which a linear scale can be used. Hecht⁴ has studied Weber's fraction $\frac{\Delta B}{B}$ as a function of B . His data are used to get $\frac{1}{\Delta B}$ as a function of B . The curves are shown in Fig. 1.



5. Calculations for the dark-adapted eye

The data for the Weber's fraction as a function of B were taken from the work of Hecht⁴ which refer to dark-adapted eye. This particular source for the data was

chosen because it covers the largest range of luminance and includes all the three important regions of the behaviour of the eye; the De-Vries-Rose region, the Weber-Fechner region and the region in which Weber's law again breaks down. All these regions are experimentally established and theoretically explained.^{1,5} It was thought necessary to do these calculations using these data, although, similar calculations have been quoted earlier by Schade⁶ because these earlier calculations cover a smaller luminance range. Moreover, although the earlier calculations start right from the lower limit $\frac{\Delta B}{B} = 1$ which unfortunately is not included in our calculations, they exclude the region in which Weber-Fechner law breaks down. As will be seen, this latter region excluded in the earlier calculations is much more important than the region just near the threshold of vision and leads to some interesting results.

In Table 1, the number of gray shades N_B that can be distinguished apart by the human eye upto the luminance B starting from the luminance 5×10^{-5} milli-lamberts is indicated.

Table 1
Number of gray shades N_B that can be told apart by the
dark-adapted human eye up to the luminance level B

B , milli-lamberts	N_B	B , milli-lamberts	N_B
5×10^{-5}	0	1×10^{-4}	1.23
5×10^{-4}	5.49	1×10^{-3}	8.12
5×10^{-3}	17.99	1×10^{-2}	24.74
5×10^{-2}	51.80	1×10^{-1}	71.20
5×10^{-1}	124.3	1	149.20
2	175.4	5	214.00
8	235.6	10	245.60
15	265.5	20	279.20
30	298.8	50	324.70
80	348.2	100	358.20
200	388.5	500	427.70
1,000	452.5	2,000	472.30
5,000	494.2	6,500	499.50

The upper limit of visual tolerance for the human eye is little less than 14,000 millilamberts.⁶ Thus, our calculations extend right upto one octave below this upper limit. In the region near the upper limit of visual operation the eye would be put to strain. Television programmes generally aim at entertainment and education of viewers. Therefore, they should allow casual attention in a relaxed mood. In any case, those very high luminance levels which strain the eye, cannot form a part of any television programme. Therefore, the luminance region right below the upper limit of visual tolerance is not of any interest to engineers and hence this region would not be of much interest. Thus, our calculations cover the entire range of our interest.

Although the total contrast range covered by our calculations is about 1.5×10^7 and the total contrast range that the eye can accommodate is about 10^6 , these enormous capabilities of the eye are never utilized while viewing a single scene. It has been estimated⁶ that the upper limit of a contrast range that the eye can accommodate while viewing any single scene is about 1,000, the usual order being about 100, whereas the contrast ranges of interest to us in case of television are usually less than 20. This limit in case of television is set by the contrast range that can be accommodated by a receiver tube in the present state of technology. So now we would like to calculate the number of gray shades that the eye can distinguish apart in a given contrast range. The contrast, C , accommodated would be taken as a parameter for a particular set and the number of gray shades would be plotted as a function of the maximum luminance B seen.*

The contrast C is defined as

$$C = \frac{B_{\max.}}{B_{\min.}} \quad (6)$$

where $B_{\max.}$ and $B_{\min.}$ are maximum and minimum luminance values in a scene.

With the contrast C accommodated and the maximum luminance B seen, the number of gray shades N that can be seen would be the number that the eye can tell apart in a luminance range from $\frac{B}{C}$ to B . The data is presented in Fig. 2.

Thus, it is seen that as B increases the number of shades N that can be distinguished apart increases, then reaches a maximum $N_{\max.}$ at a particular value of B and then decreases again. This is the general behaviour of the curves for all values of C . But in some respects the value of C marks a difference between the behaviour of the curves. Thus, as the value of C increases the value of B at which we get $N_{\max.}$ also increases. Again, the region in which the curves remain sensibly flat, shrinks as the value of C increases. This can be very easily explained. Consider a region in which Weber—Fechner relationship holds good. Now as in this region the Weber's fraction W is a constant, from equation (5), we get

$$N = \frac{1}{W} \int_{\frac{B_1}{C}}^{\frac{B_2}{C}} \frac{dB}{B} = \frac{1}{W} \log_e B \Big|_{\frac{B_1}{C}}^{\frac{B_2}{C}} \quad (7)$$

* In the subsequent text, B stands for B .

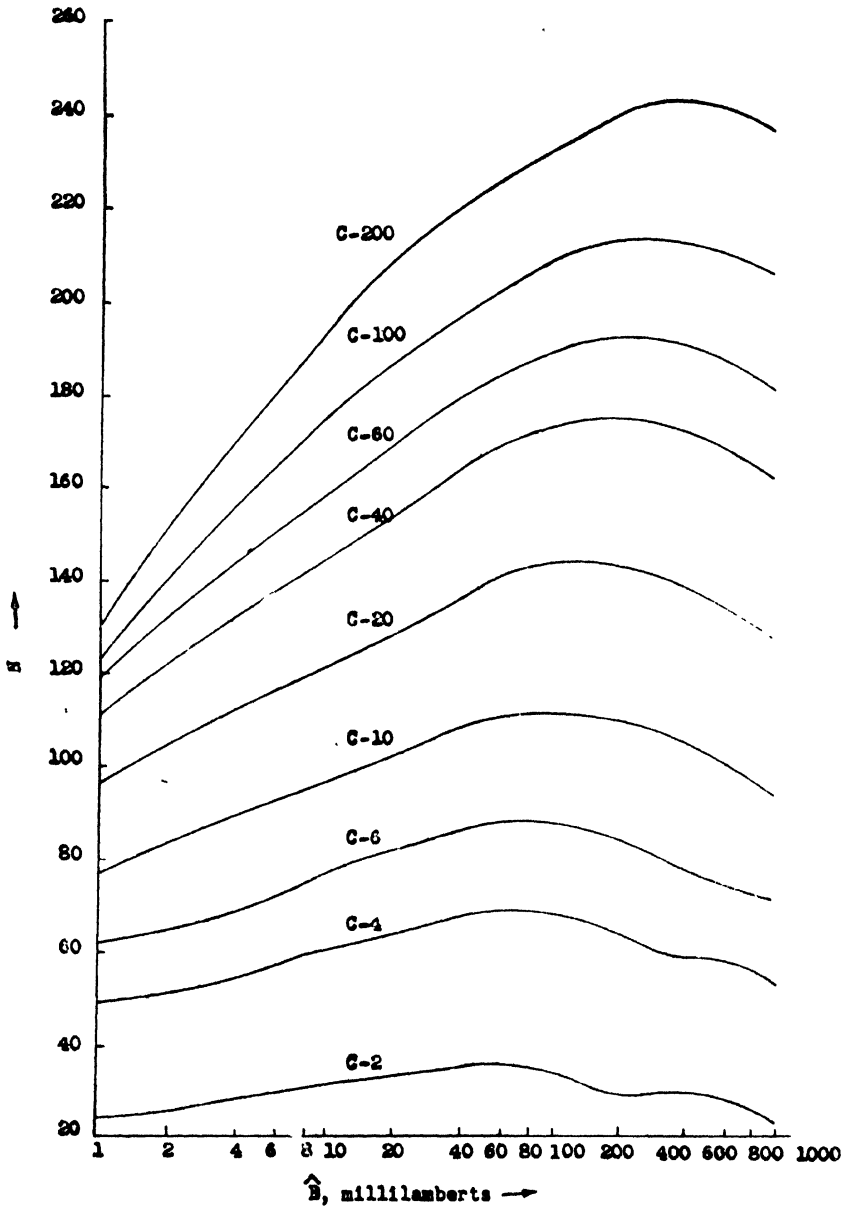


Fig. 2
Curves showing the data

For a contrast range C , we get

$$\frac{B_2}{B_1} = C \quad (8)$$

$$N = \frac{1}{W} \log_e C \quad (9)$$

Thus, in the Weber-Fechner region, the curves in Fig. 2 should be flat for a given value of C . Here, we have assumed that both the limits of luminance values within which the integration is carried out lie in a Weber-Fechner region. But as the value of C increases the range of B for which these limits of integration can stay in Weber-Fechner region shrinks, and hence the region of flatness of the curves in Fig. 2 also shrinks. Again, as the value of C increases, the lower limit of integration enters the Weber-Fechner region at a greater value of B and hence for the larger values of C the values of B that give N_{\max} are also larger.

6. Empirical relationship between N_{\max} and C for the dark-adapted eye

Introduce the parameters,

$$y = \log \log C \quad (10)$$

$$x = \log N_{\max} \quad (11)$$

Taking clue from some preliminary calculations, it was found that a relationship,

$$y = ax^2 + bx + c \quad (12)$$

can be fitted satisfactorily to the data. To calculate the values of the constants a , b and c , the principle of least squares from the theory of errors was used to get the best fit to the data.

Thus, we get for the range of C equal to 2-100,000,

$$a = 0.1527 \quad (13)$$

$$b = 0.397 \quad (14)$$

$$c = -1.4525 \quad (15)$$

Therefore, the empirical relationship between N_{\max} and C becomes

$$\log \log C = 0.1527 (\log N_{\max})^2 + 0.397 \log N_{\max} - 1.4525 \quad (16)$$

To get the idea of the closeness of the fit, the actual values of

$$\log \log C = y$$

are compared with those calculated from the above empirical relationship.

Taking into account the contrast range covered by the empirical relationship, the fit is quite good.

For $C < 10$, Deviation $\approx 10\%$

For $10 < C < 1,000$, Deviation $< 1\%$

For $1,000 < C < 100,000$, Deviation $< 5\%$

Thus, the fit is very good in the central contrast range, satisfactory for the high contrast values and not so good for the low contrast values.

Usually, our interest would be to calculate the value of N_{\max} for a given value of C . Therefore, equation (16) is re-arranged in the form,

$$\log N_{\max} = -1.3 + \sqrt{11.28 + 6.555 \log \log C} \quad (17)$$

The data calculated by using this empirical relationship is shown graphically in Fig. 3.

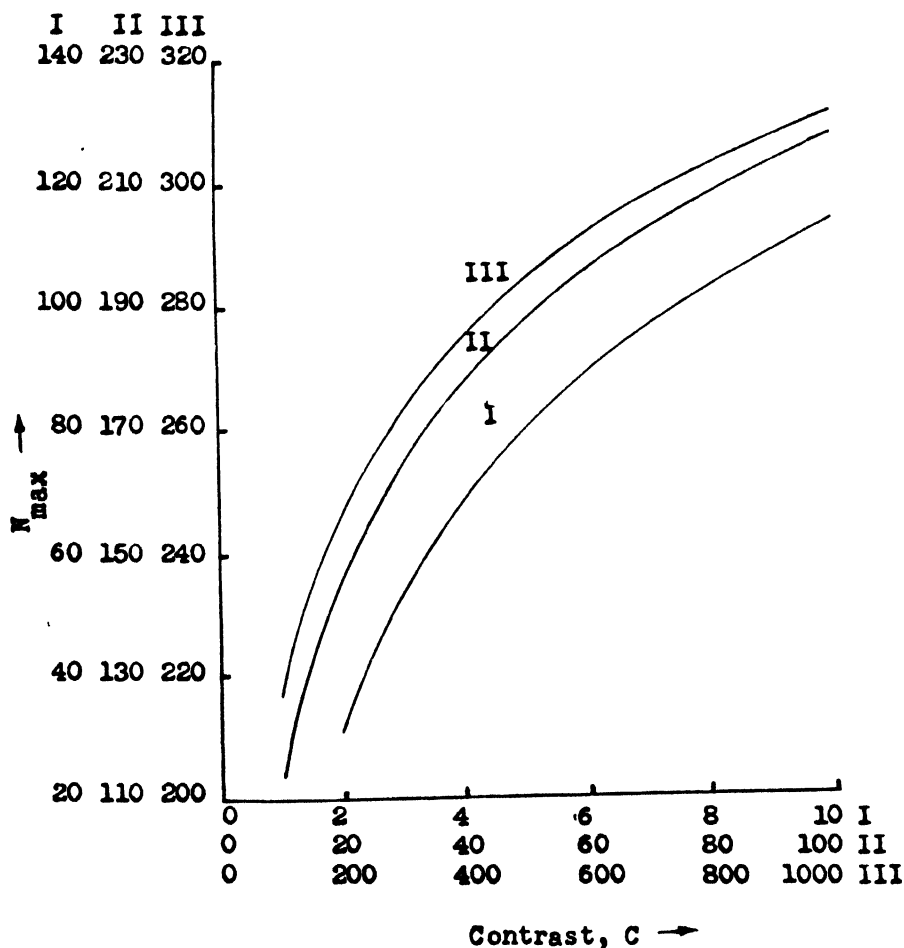


Fig. 3

Curves showing the data calculated using empirical relationship

7. Calculations for the bright-adapted eye

Contrast sensitivity of the human eye in the test field with a bright surrounding was studied by Schreuder.⁷ The result of his investigation is expressed by an empirical relationship,

$$\log B_2 = -0.97 + 0.51 B_1^{\frac{1}{2}} + 39.1 \left(\frac{B_2 - B_3}{B_2} \times 100 \right)^{-\frac{5}{4}} \quad (18)$$

where B_1 is the adaptation level in nits, B_2 the test field luminance in nits, B_3 the test object luminance in nits, and $(B_2 - B_3)$ the smallest luminance difference that can be told apart.

This can be re-written as

$$\frac{1}{\Delta B} = \frac{100 (39.1)^{-\frac{1}{2}} (\log B + 0.97 - 0.51 B_0^{\frac{1}{2}})^{\frac{1}{2}}}{B} \quad (19)$$

where B_0 is the adaptation level in nits.

This relationship is valid between the limits,⁷

$$300 < B_0 < 10,000 \quad (20)$$

$$0.15 < \frac{\Delta B}{B} < 0.968 \quad (21)$$

Using the above relationship, the results shown in Table 2 were arrived at.

Table 2

Number of gray shades N_B that can be seen by the light-adapted eye in the luminance range from 40-120 nits

B_0 , nits	N_B
500	6.085
800	5.244
1,000	4.952
1,500	3.929
2,000	3.199

Thus, it is seen that when the adaptation level of the eye is above the test field luminance, the number of gray shades that the eye can tell apart in a given luminance range is poor and becomes poorer and poorer as the adaptation level is raised higher and higher above the test field level.

8. Calculations for the television case

So far we have studied two cases. One, studied quite thoroughly that when the dark-adapted eye is seeing the lighter field. The second one, studied only over a narrow luminance range, is one when the light-adapted eye is seeing comparatively darker field. The television case lies in between these two. Here, the mean luminance level of the test field forms the adaptation level. The correct calculations for this case can be done only if the experimental data is available. But the rough estimate can be made from the two extreme cases with some plausible assumptions. This would be the estimate of the higher limit of the number of shades set by the properties of the eye. There are certain properties of the television system too, that set the maximum limit on the number of shades that can be seen. The derivation of the data for the light-adapted eye starting with the data for the dark-adapted eye would be considered later in a paper entitled 'Fluctuation Theory of Luminance Discrimination for the Light-adapted Eye and its Particular Application to the Television Case'. It is also proposed to discuss the limitations of the television system at some later stage.

9. Acknowledgment

The junior author takes this opportunity to acknowledge the able guidance and the kind appreciation of the work by Prof. K. V. Saprykin, Unesco Expert at Indian Institute of Technology, Bombay. The work was persued as a part of the Project assignment for M. Tech. degree.

10. References

1. M. A. Bouman., J. J. Vos and P. L. Walraven. 'Fluctuation Theory of Luminance and Chromaticity Discrimination'. *Journal of the Optical Society of America*, vol. 53, no. 1, January 1963, p. 121.
2. J. Krauskopf. 'Effect of Target Oscillation on Contrast Resolution'. *Journal of the Optical Society of America*, vol. 52, no. 11, November 1962, p. 1306.
3. J. J. De Palma and E. E. Lowry. 'Sine-Wave Response of the Visual System': Sine-Wave and Square Wave Contrast Sensitivity'. *Journal of the Optical Society of America*, vol. 52, no. 3, March 1962, p. 328.
4. S. Hecht. 'The Visual Discrimination of Intensity and the Weber-Fechner Law'. *Journal of General Physiology*, vol. 7, 1924, p. 241.
5. V. K. Zworykin and G. A. Morton. 'Television : The Electronics of Image Transmission in Colour and Monochrome'. *John Wiley and Sons., Inc.*, 2nd edition, 1954.
6. O. H. Schade. 'Electro-Optical Characteristics of Television Systems'. *R.C.A. Review*, vol. 9, no. 1, March 1948.
7. D. A. Schreuder. 'Contrast Sensitivity in Test Field with Bright Surround'. *Journal of the Optical Society of America*, vol. 55, no. 6, June 1965, p. 729.

A TECHNIQUE OF CHARACTERIZATION AND EQUIVALENT MODEL CONSTRUCTION OF A CLASS OF NON-LINEAR SYSTEMS*

D. N. Khandelwal

Non-member

*Reader in Electrical Engineering,
Government College of Engineering & Technology, Raipur*

Summary

The rapid increase in the complexity of modern technology—whether industrial, military applications or space research programmes—has placed severe strains on the control systems which invariably form the central core. The need for an insight into the controlled processes in all possible parameteric changes during operation and subsequent adaptation has led to the use and development of self-adaptive control systems. The crucial problem in non-linear as well as linear control system is the identification of process characteristics. The solution to the problem of identification of non-linear systems belonging to the class η_1 , of Zadeh by constructing an equivalent model has been presented in this paper. The models of the zero-memory systems and of the systems with memory have been constructed. The modified Hermite polynomials have been used to represent the orthonormal polynomials $\phi_n(x)$. In each path of the multi-path model, the Hermite function generators are followed by realizable linear networks containing adjustable parameters. This investigation considered a class of non-linear systems belonging to Zadeh's class η_1 . However, a large number of non-linear processes fall in this category and the present study, therefore, is not unduly restricted.

1. Introduction

Physical systems, strictly speaking, are non-linear. However, exact solutions of problems associated with the non-linear systems have been far from satisfactory due to the lack of a unified analytical non-linear theory. Mathematical solutions of the simpler cases have been obtained and Van der Pol's equation for the relaxation oscillators is one of the early attempts. But such examples are few and in general, so far, no unified theory has been developed to solve the non-linear problems completely. Most of these, however, have been reduced to linear problems and satisfactory solutions have been obtained. The high degree of accuracy required in the space research programmes and other sophisticated military applications, could no longer be achieved by the linearization techniques. Exact and explicit solutions are needed in such cases.

* Written discussion on this paper will be received until January 31, 1967.

This paper was received on April 20, 1966,

In the field of automatic control systems and allied applications, certain techniques have been evolved for solving the problems of non-linear systems. Notable among them are :

- (i) The describing-function analysis ;
- (ii) The phase-plane technique of Poincare ;
- (iii) The series approximation methods including perturbation technique ; and
- (iv) Liapunov's methods.

During the late 1950's an entirely novel technique was proposed by Norbert Wiener. For analysis and synthesis of the non-linear systems, a Gaussian input was suggested as the investigating probe. It was argued by Wiener that there is always a finite probability that the white noise will, at some time, approximate any time-function arbitrarily closely over any finite time interval.

Although, the Wiener characterization of the non-linear systems is unique, having a wide scope, its practical realization has not been probably achieved so far.

2. Problems of identification and self-optimization

While the research in the non-linear control field is progressing, its two related problems have assumed great importance. These are :

- (i) The identification of a non-linear process dynamics ; and
- (ii) The self-adaptive systems.

An adaptive control system has two important aspects, *viz.*, (i) identification; and (ii) actuation. The problem of identification refers to the continuous measurement of dynamic characteristics of the controlled process. An adaptive control system has to measure automatically and frequently its process dynamics during wide range of operation. The identification problem is, therefore, of very great importance.

The measurement of dynamic transfer characteristics in the case of linear systems is relatively easy and a large variety of techniques exist. A novel, yet, simple procedure for the continuous evaluation of process transfer characteristics of linear systems has been given by Kitamori.² His work further extends to the design of the self-optimizing systems.

The identification problem is, however, much more difficult in the case of non-linear systems. All the existing techniques either fail mathematically or are reduced to approximation methods. The only available explicit analytical approach is that of Wiener.

The self-optimizing systems have been studied extensively in the linear systems.³ The mathematical and graphical tools available are easy to handle and variety of design techniques exist. For the non-linear systems, however, the progress in this direction is far from satisfactory. Practically no significant work has been done.

3. Characterization of a non-linear process and equivalent model construction

A class of non-linear systems has been defined by Zadeh⁴ in the manner given below.

The class η_1 , is defined by the input-output relationship for a two-terminal system :

$$y(t) = \int_0^{\infty} K [x(t - \tau), \tau] d\tau \quad (1)$$

where $x(t)$ is the input function of time, $y(t)$ the output function of time, τ the variable of integration and $K [x(t - \tau), \tau]$ is any real function of $x(t - \tau)$ and τ .

The generalization of equation (1) leads to the equation,

$$y(t) = \int_0^{\infty} \int_0^{\infty} \dots \int_0^{\infty} K [x(t - \tau_1), x(t - \tau_2), \dots, x(t - \tau_n); \tau_1, \tau_2, \dots, \tau_n] d\tau_1, d\tau_2, \dots, d\tau_n$$

defining the class η_n .

It is readily seen from equation (1) that the following classes of systems are the sub-classes of the general class η_1 .

(i) *Attenuators* :

$$y(t) = \int_0^{\infty} K \delta(\tau) x(t - \tau) d\tau = K x(t)$$

(ii) *Linear memory systems* :

$$y(t) = \int_0^{\infty} x(t - \tau) h(\tau) d\tau$$

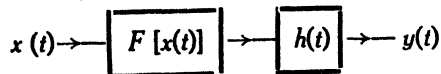
(iii) *Non-linear systems with zero-memory* :

$$y(t) = \int_0^{\infty} F[x(t - \tau)] \delta\tau = F[x(t)]$$

(iv) *Non-linear systems with memory* :

$$y(t) = \int_0^{\infty} F[x(t - \tau)] h(\tau) d\tau$$

The last sub-class can be represented by a zero-memory system described by the functional $F[x(t)]$, followed by a linear network as shown below.



A slightly different representation⁵ of the class η_1 , is given by the following equation :

$$y(t) = \sum_{n=0}^N \int_0^{\infty} \phi_n [x(t - \tau)] h_n(\tau) d\tau \quad (2)$$

where $x(t)$ and $y(t)$ are the input and output time functions and $\phi_n [x(t)]$ are linearly

independent n th orthonormal polynomial with respect to the first probability density of the input $x(t)$, and $h(t)$ the linear network weighting function.

4. Theory of equivalent multi-path systems

Zadeh⁴ has shown that a two-pole non-linear system of class γ_1 , can be canonically realized by a parallel combination of pairs of two poles in tandem, the n th pair being made up of a zero-memory non-linear two-pole system having the input-output relationship given by

$$y(t) = f_n [x(t)]$$

and a linear two-terminal network with impulse response, $h_n(t)$. Thus, any non-linear two-pole of class γ_1 can be realized approximately in the form shown in Fig. 1.

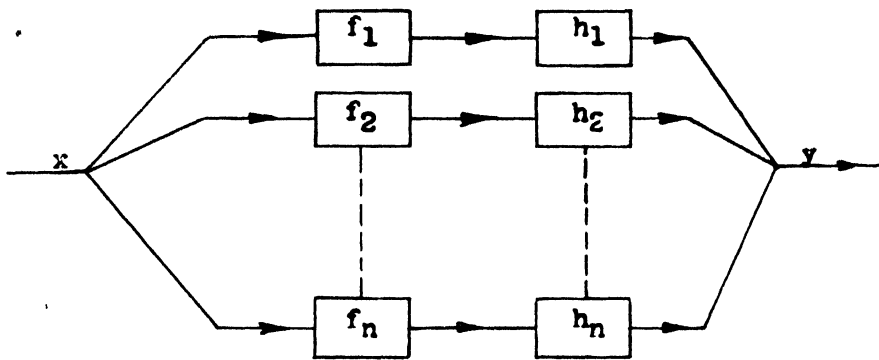


Fig. 1

A non-linear two-pole system

It has been shown⁶ that the defining equation (2) of the class γ_1 , leads to the practical realization of a given non-linear system belonging to this class in the form of a number of parallel paths based on Zadeh's realization technique, each path containing a zero-memory non-linearity followed by linear memory network, the summation sign extending over N paths.

If the given non-linear system is having no memory, equation (2) can be written as

$$y(t) = \sum_{n=0}^N \int_0^{\infty} \phi_n [x(t - \tau)] C_n \delta \tau d\tau$$

Since,

$$h_n(\tau) = C_n \delta \tau$$

i.e.,

$$y(t) = \sum_{n=0}^N C_n \phi_n[x] \quad (3)$$

where C_n are the constants and $\phi_n[x]$ the orthonormal polynomials with distribution $p(x)$ as the weighting function over the whole range of x .

Thus, a zero-memory non-linear system can be realized as a number of N parallel paths as shown in Fig. 2.

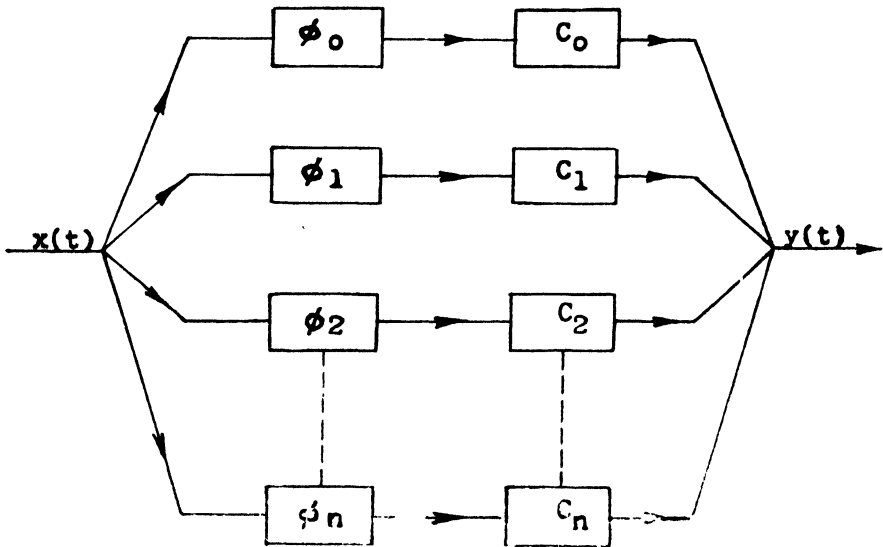


Fig. 2

A zero-memory non-linear system

Similarly a non-linear system defined by the equation (2) will lead to the configuration shown in Fig. 3.

Now, whenever a non-linear system is described, it will be assumed to belong to the class defined by the equation (2).

5. Procedure of equivalent model realization

As mentioned earlier, the characterization of controlled processes, whether linear or non-linear, is one of the most crucial and important problems in the self-adaptive control systems. The theory of realization of a given non-linear system presented in the previous sections immediately leads to the characterization of the given non-linear process. It also follows that the system, once characterized in terms of the equivalent multi-path system, will lend itself to adaptation in the self-adaptive control system.

The investigating probe for characterization of the given system will be the white noise. As Wiener has said that the white noise has always a finite probability to approximate any time-function arbitrarily closely over any finite time interval; it follows that if a given non-linear system is characterized by the white noise and its equivalent multi-path model is constructed, then this model will be identical to the given system for any input function of time.

It is difficult to obtain the white noise in practice. However, the output of a shot noise generator, having the frequency spectrum well beyond and well spread over the frequency range under consideration, closely approximates the white noise.

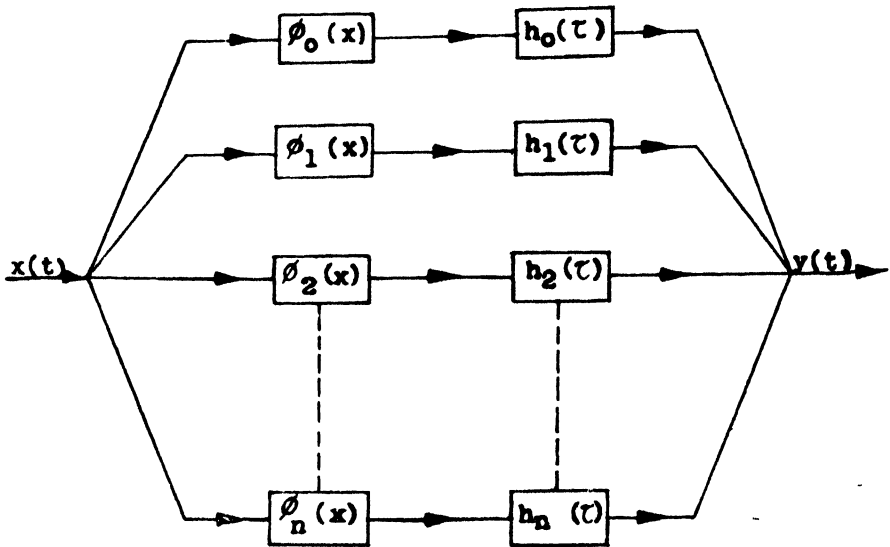


Fig. 3

Non-linear system given by equation (2)

For the white noise input, the first probability distribution is given by

$$p(x) = \frac{1}{\sqrt{2\pi}} e^{-\frac{x^2}{2}}$$

Now, the Hermite polynomials are orthonormal with the weighting function e^{-x^2} . Therefore, the $\phi_n[x]$ functions will be the modified Hermite polynomials having the weighting function,

$$w(x) = \frac{1}{\sqrt{2\pi}} e^{-\frac{x^2}{2}}, -\infty < x < +\infty$$

The procedure for characterization and equivalent model construction can now be explained with reference to Fig. 4.

The output of the shot noise generator is applied simultaneously both to the given system and the modified Hermite function generators arranged in N paths followed by the linear network. The latter may be of the forms

$$\frac{k}{1 + sT} \quad \frac{k_1 e^{-sk_2}}{1 + sT} \quad \frac{k w_n^3}{s^3 + 2\xi w_n s + w_n^2} \quad \frac{b_0 s^m + b_1 s^{m-1} + \dots + b_m}{a_0 s^n + a_1 s^{n-1} + \dots + a_n}$$

where $k, k_1, k_2, T, w_n, a_1',$ etc., are the adjustable parameters.

The output, $z(t)$, of the given system and $y(t)$ of the equivalent multi-path are compared and an error, ϵ , is obtained. The mean of the square of this error, i.e., $\bar{\epsilon}^2$, is minimized by adjusting the parameters $k, k_1, k_2, T,$ etc. of the linear networks.

Once the equivalent multi-path system is obtained for a desired mean square error, it will be the exact model of the given system for any input.

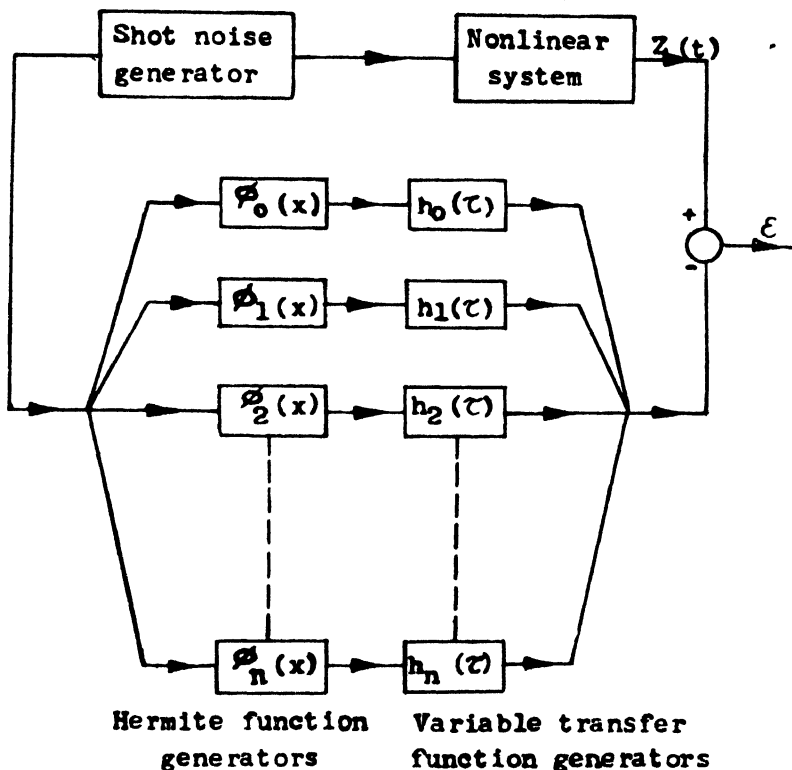


Fig. 4

Construction of an equivalent model

6. Remarks on the construction of the model

- (i) In practice, the mean square error may not be made entirely equal to zero. However, a practical limit on the minimum value of the error $\bar{\epsilon}^2$, can always be fixed. The number of parallel paths in the model then depends on the accuracy required to approach the minimum value of the mean square error. The minimization of the number of parallel paths and its exact dependence on the degree of accuracy needs a rather rigorous mathematical treatment.
- (ii) It has been explicitly shown⁶ that the weighting functions of the linear-networks depend exclusively on the actual output $z(t)$, of the non-linear system and the orthonormal polynomials, $\phi_n[x]$. A measurement technique is conceivable to correlate the output of the actual system with the polynomials $\phi_n[x]$ to evaluate $h_n(t)$.
- (iii) It is important, especially when the model is to be used in a parameter tracking servo, to consider the mutual interaction of the adjustable parameters. That is, once a parameter is adjusted to an optimum

value by minimizing the mean square error, it is quite probable that during the time the next parameter is adjusted to minimize the error, the first may not remain at the optimum position. This has been discussed in Reference 6.

7. Acknowledgment

The author wishes to thank Dr. M. Lal, Department of Electronics and Communication, University of Roorkee, for suggesting the problem and his interest and encouragement throughout the execution of this work at the University. Thanks are also due to Shri S. K. Gupta, University of Roorkee, for helpful discussion.

8. References

1. N. Wiener. 'Non-linear Problems in Random Theory'. *John Wiley & Sons, Inc.*, 1958.
2. T. Kitamori. 'Applications of Orthogonal Functions to the Determination of Process Dynamic Characteristics and to the Construction of Self-Optimizing Control Systems'. *Proceedings of the First International Congress of the I.F.A.C.*, Moscow, 1960.
3. E. Mishkin and L. Braun. 'Adaptive Control Systems'. *McGraw-Hill Book Co., Inc.*, 1961.
4. L. A. Jadh. 'A Contribution to the Theory of Non-Linear Systems'. *Journal of the Franklin Institute*, vol. 255, 1953, p. 387.
5. J. K. Lubbock. 'Optimization of a Class of Non-Linear Systems'. *Proceedings of the First International Congress of the I.F.A.C.*, Moscow, 1960.
6. D. N. Khandelwal. 'Non-Linear Systems—Identification and Optimization'. Thesis submitted to the University of Roorkee for M.E. Degree, 1965.

About the Authors

Shri K. G. Nadar

Shri K. G. Nadar received his early education from the Kerala University. During 1945-60 he completed numerous evening and correspondence courses from the Government Technical College, Hyderabad, and others in mathematics, physics, and electronics and telecommunication engineering. During this period he was trained as Armament Arts in communication engineering and, subsequently, he worked as Instructor in the Electronic Wing of the E.M.E. School, Secunderabad, where he was associated with a number of research projects. Since 1960 he has been employed at the National Aeronautical Laboratory (C.S.I.R.), Bangalore, where he is working as Scientist. In 1962 he was awarded a fellowship by the International Civil Aviation Organization for training in data processing equipment in the U.K.

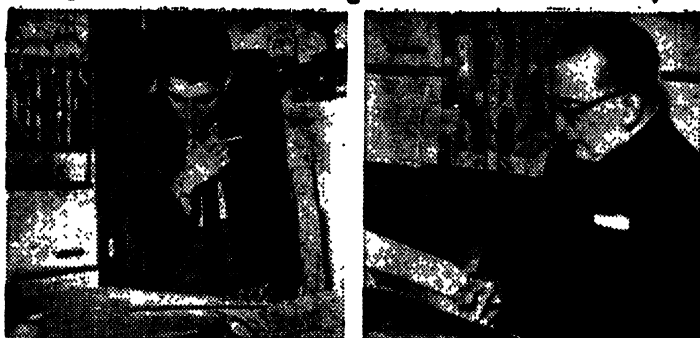
Shri P. S. Moharir

Shri P. S. Moharir took his M.Sc. degree in Physics with specialization in Electronics in 1964 from the Nagpur University. He got his M.Tech. degree in Television Engineering from the Indian Institute of Technology, Bombay, in 1966. He is at present a research scholar in Electrical Engineering at the Indian Institute of Technology, Kanpur. The work reported here was done for his Master's degree at the Indian Institute of Technology, Bombay.

(The particulars of Mr. K. V. Saprykin were not received).

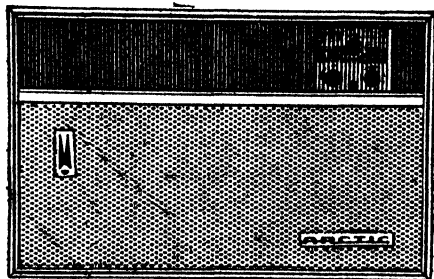
Shri D. N. Khandelwal

Shri D. N. Khandelwal obtained his B.Sc. degree from the Nagpur University in 1957, and B.E. (Hons.) from Jabalpur Engineering College in 1960. He joined the Government College of Engineering & Technology, Raipur, as Lecturer in Electrical Engineering. In 1963, he joined the Roorkee University as a student of M.E. (Applied Electronics and Servomechanism). There he worked under Dr. M. Lal on the problems pertaining to the nonlinear adaptive control systems. The present paper shows one of the results which were obtained during that period. In 1965, the author came back to the College of Engineering and Technology, and is now Reader in the Electrical Department.



People who matter

INSIST ON



ARCTIC

ROOM AIRCONDITIONERS

Why? Engineers, Housewives, Administrators know that the only way to judge a product is by its performance. And Arctic has proved itself an efficient airconditioner with a success record in export markets for over a decade.

Arctic does what other airconditioners claim to do...and does it better. Its new 50-cycle compressor, superb assembly of components and finely balanced mechanism make it the most effective airconditioner.

**Arctic carries a guarantee
and free service for one year.**



Electronics Limited

New Delhi Bombay Calcutta.

Sold and Serviced by :

W. A. BEARDSSELL & Co. (Pvt.) LTD. Calcutta Madras
BLUE STAR ENGG. CO. (BOMBAY) Pvt. LTD. Bombay. New Delhi

INFRA RED RADIATION AND ITS APPLICATIONS***S. K. Chatterjee***Non-member**Indian Institute of Science, Bangalore***Summary**

This paper discusses the fundamental principles of infra red radiation and detection. The transmission properties of infra red radiation through the atmosphere are briefly reviewed. The sensitivity of an infra red system and the maximum range that can be attained are also discussed on the basis of the existing theories.

1. Introduction

The discovery of infra red radiation, and its final evolution into a mature engineering operation have led to a complex combination of techniques unique to this field. The design of infra red communication systems require a basic understanding of the physical background of optics, optical materials, space filtering, small signal electronics, spectroscopy, mechanical subsystems, etc. It is also necessary to understand and employ analytical techniques which are somewhat more sophisticated than those involved in the design of conventional types of communication systems.

The electromagnetic spectrum is divided into different regions, such as, gamma rays, x-rays, ultraviolet, visible, infra red, microwaves and radio waves which are classified on the basis of the methods used to generate and detect the radiation. All objects which are not at absolute zero of temperature radiate energy in the form of electromagnetic waves. The infra red spectrum extends from $0.72\ \mu$ to $1,000\ \mu$ which is divided into three regions, viz., the near infra red ($0.72\ \mu$ to $1.5\ \mu$), the intermediate infra red ($1.5\ \mu$ to $20\ \mu$) and the far infra red ($20\ \mu$ to $1,000\ \mu$) on the basis of the response of different detectors. The object of the presentation of this paper is not meant to be encyclopedic or to be a mere catalogue of all the results obtained in a given field, but to discuss some of the already well known fundamental principles that will provide a basic understanding of the problems related to the development of infra red equipments, and, in particular, infra red communication equipments.

2. Blackbody radiation

The phenomenon of reflection, transmission or absorption of electromagnetic energy or a combination of the above phenomena may take place when a body is exposed to electromagnetic radiation. The body is called a blackbody when it absorbs all the incident radiation at any wave length. It has also been established that a good absorber is a good radiator. In terms of the total emissivity, ϵ , a body is said to be a blackbody when $\epsilon = 1$ and a grey body when $\epsilon < 1$. The following well established laws govern

*Written discussion on this paper will be received until April 30, 1967.

This paper was received on August 24, 1966.

the radiation characteristics as a function of temperature T , to which a solid body is heated.

$$\text{Stefan-Boltzmann : } E = \sigma T^4 \quad (1)$$

$$\text{Wien : } E_\lambda = C_1 \lambda^{-5} \exp. \left(\frac{-C_2}{\lambda T} \right) \quad (2)$$

$$\lambda_m T = 2,891 \mu^\circ\text{K.} = \text{constant} \quad (3)$$

$$\text{Rayleigh-Jeans : } \rho_\lambda d\lambda = 8 \pi K T \lambda^{-4} d\lambda = 8 \pi v^2 K \frac{T}{C^3} d\lambda \quad (4)$$

$$\text{Planck : } E_\lambda = C_1 \lambda^{-5} \left[\exp. \left(\frac{C_2}{\lambda T} \right) - 1 \right]^{-1} \quad (5)$$

where E is the radiant emittance, ρ_λ the radiant energy density within a range λ and $\lambda + d\lambda$, $K = \text{Boltzmann constant} = 1.38 \times 10^{-23} \text{ joules } ^\circ\text{K.}^{-1}$, $\sigma = \text{Stefan-Boltzmann constant} = 5.668 \times 10^{-8} \text{ watts m}^{-2} ^\circ\text{K.}^{-4}$, calculated from atomic constants appearing in the integration of Planck's equation, λ_m the wavelength at which maximum radiation takes place, $C_1 = (2\pi c^2 h) = 3.74 \times 10^8 \text{ watts } \mu^4 \text{ m}^{-2}$, $C_2 = \left(\frac{c h}{K} \right) = 1.4388 \times 10^4 \mu^\circ\text{K.}$, $c = \text{velocity of electromagnetic waves in free space}$, h the Planck's constant $= 6.62 \times 10^{-27} \text{ erg.-sec.}$, and E_λ the spectral emissive power.

The Wien's displacement law [equation (3)] is illustrated in Fig. 1. It is evident that the peak energy emission occurs at shorter wavelength as the temperature of a body is raised. The Rayleigh-Jeans law shows that the energy density of radiation varies directly as temperature T_1 and as square of the frequency v^2 . This conclusion leads to what is known as 'ultraviolet catastrophe'. Planck's law which is derived on the basis of quantum mechanics holds good for all wavelengths. The deviation of all other laws is illustrated in Fig. 2. Due to the complicated nature of Planck's radiation law, the calculation of quantities, such as, the total emissive power, emissive power within a given wave length range, the number of quanta in blackbody radiation, and combinations of these quantities is done with the help of slide rules, nomographs and Tables 1-4, evolved to reduce the labour of computations.

3. Spectrum of gases

The spectral emission of gases is a consequence of electron transition between allowed energy levels. In spectral emission, unlike the continuous spectrum from a blackbody, the radiation is a rapidly varying function of wavelength. The absorption characteristics of gases when exposed to electromagnetic radiation depends on the number of lines in a band, spacing, shape and half width of the lines. The shape of the lines determines how the absorption of radiation by gases depends on pressure and path length of transmission. The thermal motion of the molecules, natural lifetime of an excited state, interaction and collision between neighbouring molecules contribute to the finiteness of the width of the spectral lines. The line shape (Lorentz) due to collision broadening decreases at wave numbers away from the centre, whereas, the line

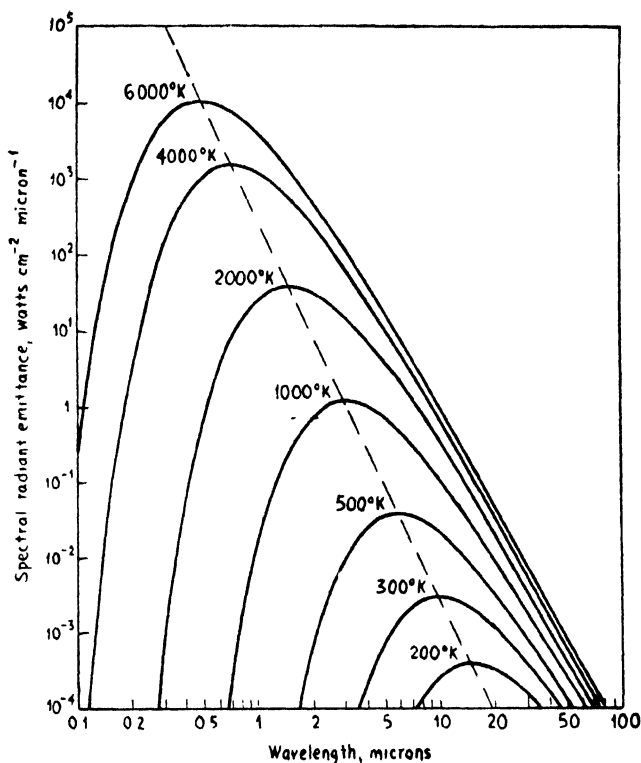


Fig. 1

Spectral emittance of blackbody

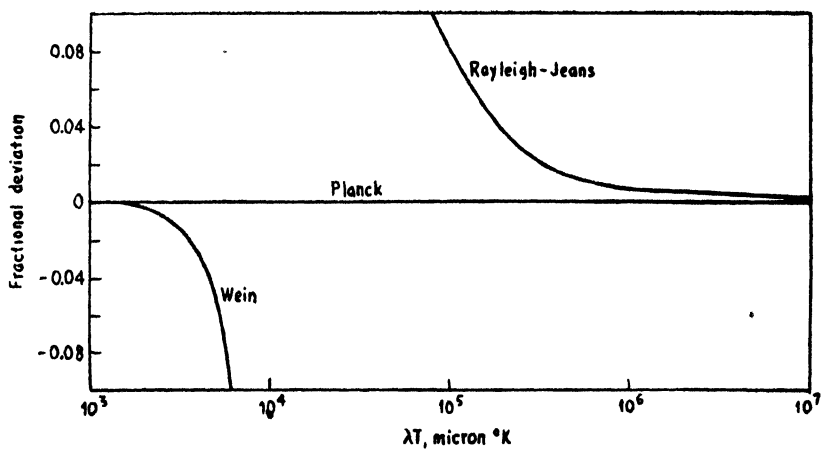


Fig. 2

Fractional deviation

shape (Doppler) due to the to and fro motion of the molecules with respect to an observer is concentrated near the centre and decreases exponentially at the wings. The uncertainty of our knowledge of the product of the energy and mean lifetime of an atomic state being equal to $\frac{h}{2\pi}$ (Heisenberg's uncertainty principle), where h is the Planck's constant, and the mean lifetime being definite, the exact measurement of energy is not possible. This also contributes to the broadening of the lines. It is shown by quantum mechanical calculation that the line half-width is proportional to pressure but its temperature dependence is a function of different molecular interactions.

4. Absorption

The atmospheric gases, such as CO_2 , H_2O , O_3 , N_2O , CO , CH_4 , A , N_2 , and O_2 give rise to attenuation depending on the wavelength of radiation. The first three gases have strong absorption lines compared to other gases and the peak of the absorption lines is given in Table 1.

Table 1
Absorption spectrum

Gases	Wavelength μ at which peak absorption takes place				
CO_2	2.70	4.30	15.0	—	—
O_3	4.80	9.60	14.2	—	—
H_2O	1.38	1.87	2.7	3.2	6.2

The attenuation is also produced due to scattering of radiation by gaseous molecules, particles and water droplets suspended in the atmosphere. If there is no overlapping of lines in a band, the fractional radiant absorption A for a mass u of absorbing gas per unit area and over a finite frequency interval, $\Delta\nu$, is given, in terms of, the absorption coefficient k_ν , by the following integral :

$$A = \frac{1}{\Delta\nu} \int_{\Delta\nu} \left[1 - \exp. (-k_\nu u) \right] d\nu \quad (6)$$

The absorption coefficient k_ν , is a rapidly varying function of frequency ν , which leads to some difficulty in evaluating A by integration. Several models (Fig. 3) known as Elasser,⁶ statistical, and random Elasser^{7,8} have been proposed which help fairly accurately the calculation of absorption of infra red radiation when transmitted through the atmosphere. The Elasser model holds good when the spacing and intensity of the lines are uniform. The statistical model is applicable when the spacing is random but the intensity of the lines is governed by a distribution function. The random Elasser model consists of several Elasser bands superimposed on each other. The models as represented analytically are given below.

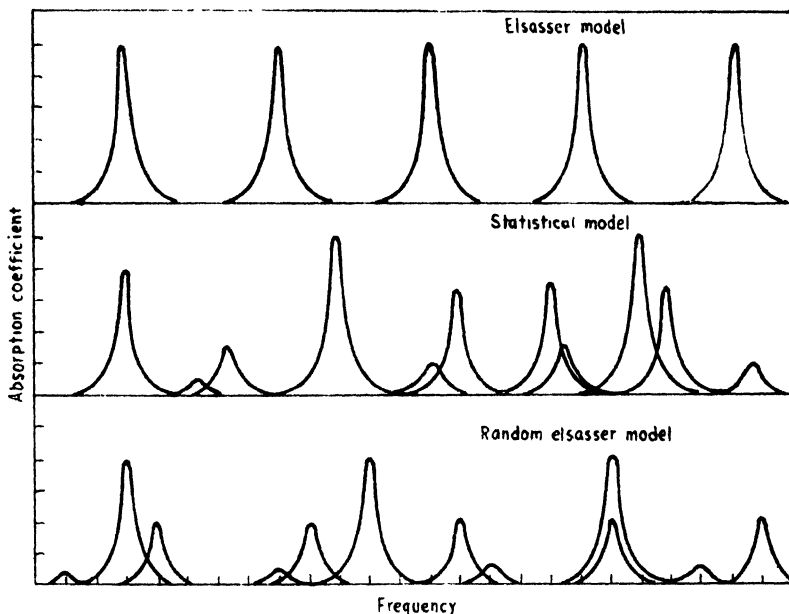


Fig. 3
Elsasser, statistical and random Elsasser models

$$A (\text{Elsasser model}) = 1 - \frac{1}{2\pi} \int_{-\infty}^{\infty} \exp. \left[\frac{-\beta x \sinh \beta}{(\cosh \beta - \cos z)} \right] dz \quad (7)$$

$$A (\text{Statistical model}) = 1 - \left[1 - \left(\frac{2 \beta^2 x}{\pi} \right)^{\frac{1}{2}} \right]^N \quad (8)$$

$$A (\text{Random Elsasser model}) = 1 - \prod_{i=1}^M \{1 - \phi [(\frac{1}{2} \beta_i^2 x_i)^{\frac{1}{2}}]\} \quad (9)$$

where the product is taken over the M superimposed Elsasser bands,

$$\beta = \left(\frac{2 \pi \alpha}{d} \right),$$

d = mean line spacing,

$$x = \frac{S u}{2 \pi \alpha},$$

α = line half-width,

S = line shape factor,

$$\left. \begin{aligned} \beta_i &= \frac{2 \pi \alpha_i}{d_i} \\ x_i &= \frac{S_i u}{2 \pi \alpha_i} \end{aligned} \right\} \text{ for the } i\text{th Elsasser band,}$$

$$\phi(z) = \left(\frac{2}{\pi^{\frac{1}{2}}}\right) \int_0^z \exp. (-z^2) dz,$$

N = number of Elasser bands which are randomly superposed.

The spectral regions between any two principal absorption lines can be utilized for transmission of infra red radiation. The transmission data as reviewed by Elder and Strong⁹ can be fitted approximately to equations of the form

$$T' = -K \log w + T_o \quad (10)$$

where T' is the selective window transmission in percentage, w represents the water vapour concentration of the absorption path, K and T_o are the empirical constants for each window. The following table represents the infra red windows in the atmosphere.

Table 2
Infra red windows

Window	Wavelength (μ) interval	K	T_o
I	0.72-0.92	15.1	106.3
II	0.92-1.10	16.5	106.3
III	1.10-1.40	17.1	96.3
IV	1.40-1.90	13.1	81.0
V	1.90-2.70	12.5	72.5
VI	2.70-4.30	21.2	72.3
VII	4.30-5.90	—	51.2

5. Background radiation

Any infra red system viewing a target which may be seaborne ground or airborne, receives radiation not only from the target but also from the background in which the target is situated. The radiation from the earth and ocean depends on the emissivity and temperature of the surface. The sky radiation depends on the molecular emission of the atmospheric gases and/or the scattering of sunlight by the molecules and suspended particles in the atmosphere. Since the effective temperature of the atmosphere lies between 200 °K. to 300 °K., the maximum emission of radiation occurs near 10 μ and has an approximate value of 3×10^{-3} watt cm.⁻² μ^{-1} . In the wavelength range of 3 μ to 4 μ , the molecular emission and scattered sunlight radiances are equal. Above 4 μ radiation due to scattered sunlight is very small and radiation due to molecular emission predominates. But at shorter wavelength radiation due to scattering predominates and that due to molecular emission is comparatively very small. The stars, aurora and other celestial bodies also radiate and in some cases, the radiation due to celestial background influences the operation of an infra red system. The visual magnitude (m) of the radiation flux of some of the celestial objects as measured by a lead sulphide detector is given in Table 3 which shows that sun is the brightest object.

Table 3
Visual magnitude of some celestial objects at maximum brightness

Sun	Moon	Venus	Mars	Jupiter
-26.8	-12.6	-4.4	-2.8	-2.5

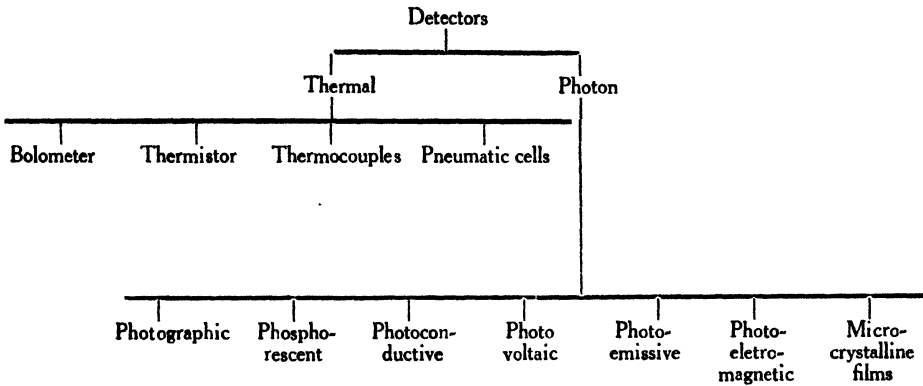
The visual magnitude m , is given by the relationship

$$m = -2.5 \log \left(\frac{I}{I_0} \right) \tag{11}$$

where I_0 is some reference irradiance and I the effective radiance in watt per cm^2 .

6. Infra red detectors

The detectors that are in use or may find wide applications in the infra red regions may be broadly classified as given below.



The process of stimulated emission as in optical maser may also be used for detection of infra red photons. The detection may also be achieved by utilizing the process of absorption and then excitation of electrons from a metastable level into a higher level and then decay into a lower level resulting in the emission of a photon. Many other types of detectors such as zinc doped germanium (ZIP), infra red vidicon show good promise of finding applications, due to their high directivity and rapid response characteristics.

As the radiation is quantized, both the types, thermal and photon are quantum detectors. From the thermodynamic point of view of classification of solids, the thermal detectors may be classified as lattice type composed of atoms and molecules, whereas, the photon detectors may be said to be of electronic type characterized by the consideration of energy levels such as valence band, forbidden band, impurity levels, conduction band.

When a thermal detector is exposed to infra red radiation, the absorption of photon leads to the heating of the lattice, which causes a change in the electronic system. Bolometer, and thermistor operate on the principle of change of resistance caused by heating, the difference being that the bolometer is characterized by positive temperature coefficient, whereas, the thermistor possesses negative temperature coefficient. In the case of thermocouple, the voltage, e , developed at a junction due to a change in temperature of ΔT is related to the thermoelectric power $P(T)$ as $e = P(T) \Delta T$. For example, $P(T)$ for Bi-Sb junction is 10^{-4} volts per $^{\circ}\text{C}$. The pneumatic cell operates on the principle that heating due to absorption of photons causes an expansion in the volume of gas, Golay cell^{13,14} (Fig. 4) operates on this principle. When a thermal detector is exposed to heat radiation, the net heat flow $W(t)$ into the detector is due to the combined effects of heat flow from surroundings (W_r), heat flow due to radiation from the source (W_a), heat flow due to change in the operating characteristics (W_{op}) such as Peltier effect, change in the biasing current, heat flow from the detector to the surroundings (W_r'), conduction flow between the detector and background (W_c). In order that the detector may be able to discriminate the target from the background, it is necessary that W_r , W_{op} , W_r' , W_c remain invariant. So the net heat flow equation

$$W(t) = W_r + W_a + W_{op} - W_r' - W_c \quad (12)$$

reduces to

$$W(t) = W_o (\text{constant}) + W_{\text{source}}(t) \quad (13)$$

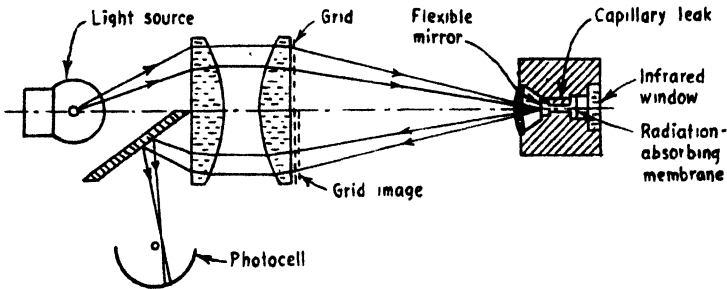


Fig. 4
Golay cell

Semiconductors which operate as detectors in the infra red region undergo a change in conductivity $\Delta\sigma$, under the influence of incident photon flux F_s according to the following relationship involving the carrier lifetime τ , equilibrium carrier concentration n_o and the effective reponsive quantum efficiency η_s

$$\frac{\Delta\sigma}{\sigma} = \frac{F_s \tau \eta_s}{\{n_o (1 + \omega^2 \tau^2)\}^{\frac{1}{2}}} \quad (14)$$

when the incident radiation flux F_s , is modulated with an angular frequency ω . In order that the semiconductor detector may be broadband, the long wavelength limit, λ_c , should be as large as possible which may be achieved according to the relationship, $\lambda_c = \frac{1.24}{E_s}$, by reducing the forbidden energy gap E_s (electron volts). For

semiconductors, E_g can be reduced by doping with impurities. For impurity type detectors, the absorption coefficient α depends on the density N and cross-section of impurity level atoms according to the relationship $\alpha = \sigma N$. As the absorption coefficient of impurity type semiconductor is small, the thickness of the crystal for maximum absorption of incident radiation should be large, whereas, intrinsic type of semiconductor possesses high absorption coefficient and hence a very thin intrinsic type semiconductors will be sufficient to absorb most of the incident photons. For example, for gold doped germanium $\alpha \cong 0.14 \text{ cm.}^{-1}$, whereas, for intrinsic type, near the main band region $\alpha \sim 10^4 \text{ cm.}^{-1}$. This makes it possible for intrinsic type to absorb most of the photons within 1μ of the surface, whereas, an impurity type would require a thickness of about 1 to 10 mm. for the absorption of most of the radiation energy.

The photographic type of detection at longer wavelength has been achieved by mixing certain dye compounds with colloid suspension of silver halides. Both silver bromide and silver iodide are used for infrared sensitive materials. If the only component in the gelatin is silver halide, the spectral response is limited to wavelength range less than 0.5μ . But the addition of dye compounds increases the range to about 1.4μ . The process of absorption of photons with consequent reradiation by phosphors¹⁵ has been utilized for the purpose of detection.

A photovoltaic detector is made of p - n junction semiconductor. The spectral response is determined by the forbidden energy gap (E_g). The space charge layer formed at the transition boundary of the junction creates a local electric field which is responsible for the movement in the opposite direction of the charge carriers which are generated due to the formation of the electron-hole pairs created by absorption of photons. This creates a voltage at the junction.

Certain semiconductors, *viz.*, Cs_3Sb , and $\text{Na}_2\text{K Sb : Cs}$ act as detector due to surface emission under the influence of photon excitation. The forbidden band energy, E_g , electron affinity E_a , and long wave limit, λ_c , of these materials are given in Table 4.

Table 4
 E_g , E_a and λ_c for photo emitters

	E_g , electron volts	E_a , electron volts	λ_c (μ)
Cs_3Sb	1.6	0.45	0.6
$\text{Na}_2\text{K Sb : Cs}$	1.0	0.55	0.8

The process of photo-emission may involve the following processes :¹⁶ (i) excitation of an electron by the absorption of a photon, (ii) transport of the electron from the point of excitation to the surface of the emitter, and (iii) the emission of the electron through the surface potential barrier at the inter-face between the emitter and vacuum.

In photo-electromagnetic detector¹⁷ the detection of the electron-hole pair created by incident photons, may be achieved by a magnetic field. The electron-hole

pairs produced at the front surface of a semiconductor by incident photons diffuse downward. When a magnetic field is applied perpendicular to this initial diffusion current, the charge carriers, electrons and holes move in the opposite direction, resulting in a photovoltage.

Certain intermetallic compounds such as PbS, Pb Te, Pbse, $Tl_2 S_3$ in the form of microcrystalline film exhibit detection properties.

The ultimate sensitivity of a system depends on the signal, S , to noise, N , ratio of the detector. The $\frac{S}{N}$ ratio is referred to the background limited condition (Blip) which takes into consideration both the lattice induced noise and noise due to background radiation. The noise figure, F , of a detector is defined as

$$F = \left(\frac{S}{N} \right)_{\text{Blip}}^2 \left(\frac{S}{N} \right)_{\text{actual}}^2 \quad (15)$$

and is unity for an ideal Blip detector and is greater than unity for a non-ideal detector. For an ideal Blip detector, noise is only due to the background, the lattice induced noise being zero. The lattice induced noise is reduced by cooling the detector with liquid nitrogen or liquid oxygen. Lead sulphide detectors work well at room temperature and PEM detectors work almost under Blip condition at room temperature without cooling. Table 5 gives the F value of Insb detectors worked under different conditions.

Table 5
Values of F for Insb detectors

T in °K.	Photoconductive	Photovoltaic	Photo-electromagnetic
90	10	5 at	300 at
292	300	$T = 78^\circ \text{ K.}$	$T = 292^\circ \text{ K.}$

7. Optics of infra red systems

Infra red optical systems such as reflecting (Fig. 5), dioptric (Fig. 6), catadioptric (Fig. 7) are similar in principle to the visual optics. The main differences between the two systems are (i) λ (infra red) $>$ λ (visual), (ii) many materials which are transparent in the visual range are not so in the infra red range, consequently, the construction of lenses and mirrors in the infrared requires the use of different materials. The limitations in imaging characteristics due to diffraction effects are function of λ . For example for a point source of wavelength λ , the image produced by an optical system of aperture D and effective focal length is a central image of diameter $d = \frac{Kf}{N}$ where $N = \frac{f}{D}$, and K is image size factor. Due to the refractive index $n = f(\lambda)$ and the fact that λ covers several octaves, an error similar to chromatic aberration in visual optics arises in infra red optics. Table 6 gives an idea¹⁰ of the image size of systems made of different material.

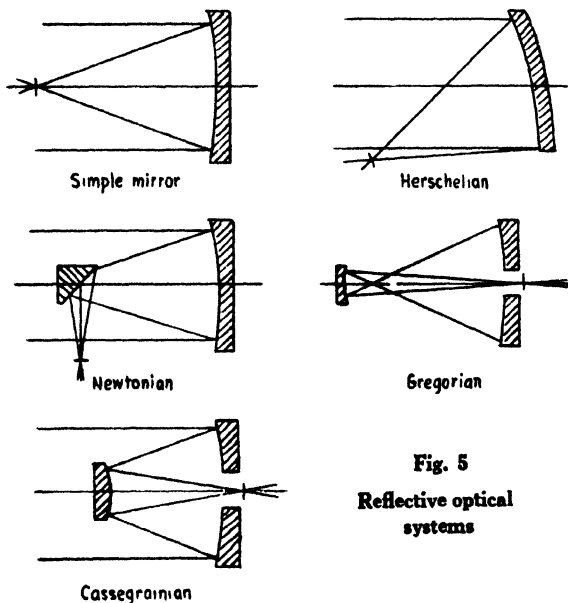


Fig. 5
Reflective optical
systems

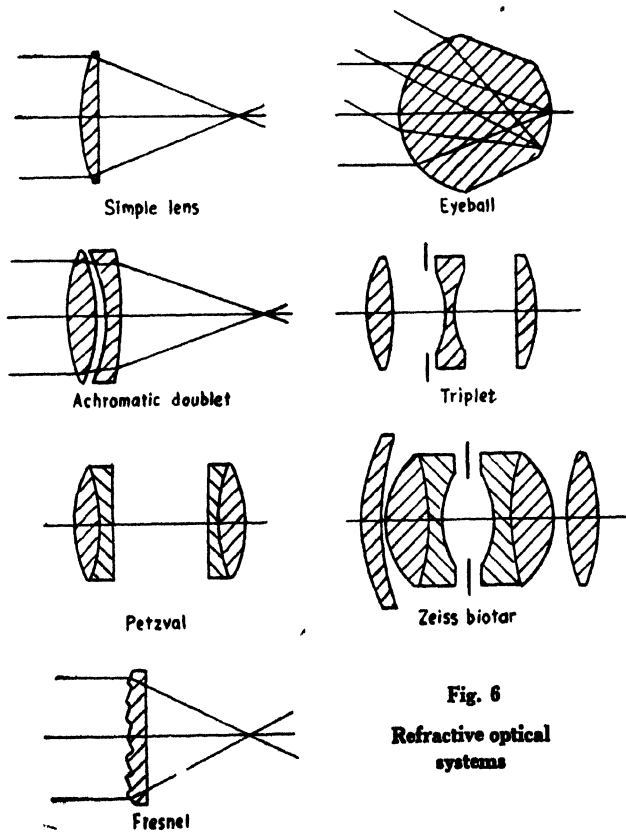


Fig. 6
Refractive optical
systems

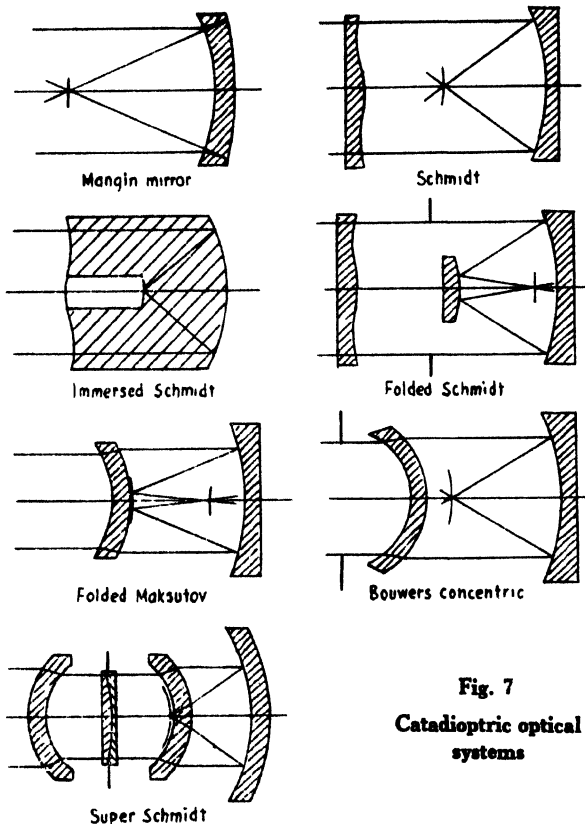


Fig. 7
Catadioptric optical
systems

Table 6
Image size as $f(\lambda)$

Material	Ge		Si	
$\lambda(\mu)$	2.5-7	2.5-9	3-7	3-9
K	0.010	0.011	0.0025	0.0030

The chromatic aberration can be reduced by using combination of two lenses with different refractive indices. The reflective system suffers from the disadvantage of reflectance loss and consequently low transmission efficiency, but it has the advantage that it is free from chromatic aberration. The catadioptric systems possess the advantages of both the dioptric and reflecting systems. The Maksutov and Bouwers systems are very suitable for wide angle operation. In order to, improve system sensitivity field lenses in addition to the above systems are used. The use of field lens enables to reduce the image size and hence the size of the detector.

8. Materials for optical systems

A lens made of material of refractive index n , will reflect a fraction of $\frac{(n-1)^2}{(n+1)^2}$ of the incident radiation. The system design requires a high infra red transmission and low visible transmission. The high transmission efficiency can be achieved by reducing the loss due to reflection by coating the surface of the lens with a material of refractive index, n_f , such that $n = n_f^2$. The material coating thickness d , should be such that the following condition in addition to the condition $n_f = \sqrt{n}$ is fulfilled.

$$n d \cos i = (2m + 1) \frac{\lambda}{4} \quad (15)$$

$m = 1, 2, 3, \dots$, when the incidence of the radiation takes place at an angle i , to the film normal. The materials used for antireflection coating are glasses, titanates, intermetallic compounds, halides, chalconides of lead, rare earth fluorides, etc.

9. Space filtering

An infra red system may receive radiation from a desired target, or from a source which is not a target or from combination of both. The problem of detecting the desired information from an irrelevant information is done by using a reticle in the telescope image plane. The reticle is given a suitable motion such that the resulting modulated flux function causes the target signal to stand out conspicuously from the background signal. This signal is then passed through an electronic filter which separates the signal of the target from that of the background. The recticle which is a mask composed of alternate opaque and translucent portions may be of several types, such as checkerboard type, picket fence type or slanted bar type (Fig. 8). The various types of scanning systems employed in the design of infra red system is shown in the Fig. 8.

10. Infra red source

The phenomenon of excitation of molecules electrically as in arc lamps has been utilized in making infrared sources with gases like helium, cesium, mercury, xenon. The observed radiation consists of the superposition of these random emissions which is responsible for making these sources incoherent. A tungsten filament lamp also acts as an infrared source. It is however a broadband device. When operated at $2,900^\circ\text{K}$., maximum portion (80%) of the radiated energy lie in the near infrared, 10.7% in the visible region, 0.1% in the ultraviolet region and the rest (9.2%) in the far infra red region. Cesium vapour lamp radiates strongly at 0.85μ and 0.89μ but only 22% of the total radiated energy is in these two lines. The detectors generally used with xenon are lead sulphide cells whose wavelength range of response is between 0.8μ to 3.5μ which corresponds to the frequency range of $37.5 \times 10^7 \text{ mc}$ and $8.57 \times 10^7 \text{ mc}$, i.e., a band width of $289.3 \times 10^6 \text{ mc}$. This may seem to be able to accommodate a large number of communication channels. But due to the incoherent nature of the source, only one channel is obtained.

11. Infra red systems

The function of an infra red system is to sense the source, process suitably the information and finally make a decision. The capability of a system to detect the

desired target will depend on the system noise and background noise. The physical mechanisms of the different types of system noise are well understood and are summarised in Table 7.

Table 7
System noise

Types of noise	Physical mechanisms giving rise to noise	Types of detectors concerned
Radiation noise	Bose-Einstein fluctuation of infra red photons	All detectors
Generation-recombination noise	Fermi-Dirac fluctuation of current carriers	Photoconductive, Bolometer
Shot noise	Random emission of electrons due to thermionic emission	Thermionic detector
Temperature noise	Temperature fluctuation	Thermal detectors
Thermal noise	Thermal agitation of current carriers	All detectors
Modulation noise	Resistance fluctuation in semiconductors	Photoconductive and Bolometer
Contact	Resistance fluctuation at contacts	Photoconductive, Bolometer
Flicker	Fluctuation of work function	Thermionic

The noise due to background radiation may be described by the two dimensional autocorrelation function or its Fourier transform called the Wiener spectrum. The system performance which is limited by the internal and background noise determines what and how far can it sense and detect. The following integral gives the relation between voltage $V(f)$ developed at the output of a detector of responsivity $R(\lambda, f)$ to the signal radiant power $W(\lambda)$,

$$V(f) = \int_0^{\infty} R(f, \lambda) W(\lambda) d\lambda \quad (17)$$

The response characteristic of the detector which is dependent on both frequency and wavelength can be separated into frequency dependent term $R_\lambda(f)$ and wavelength dependent term $R_{f_0}(\lambda)$, where both $R_\lambda(f)$ and $R_{f_0}(\lambda)$ are mutually exclusive. If the output of the detector is passed through a filter of characteristic $|F(f)|$ and if the noise power spectrum of the detector is denoted by $|N(f)|^2$, the signal, (v_s) , to noise, v_n , ratio of any detector system is then given by the relationship,

$$\frac{v_s}{v_n} = \frac{k_y \int_0^{\infty} R_{f_0}(\lambda) W(\lambda) d\lambda}{\left[\int_{-\infty}^{\infty} |N(f)|^2 |F(f)|^2 df \right]^{\frac{1}{2}}} \quad (18)$$

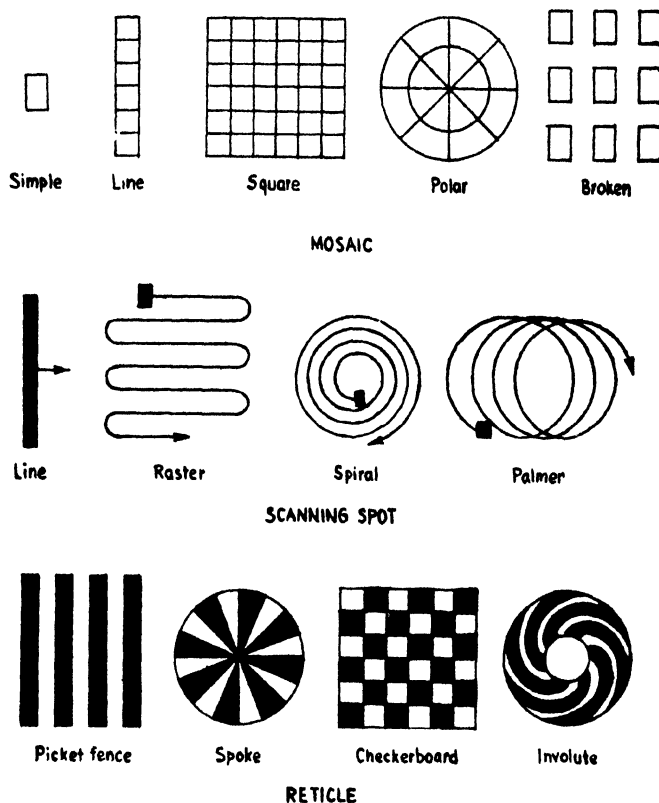


Fig. 8

Scanning classification

where k_v represents the encoding factor. The noise equivalent flux density (NEFD), which determines the figure of merit of a system and which is used to calculate the maximum range over which a system can usefully operate is related to the system detectivity $D_{sys.}$ and the area of the radiation collecting aperture A_0 , by the following relationship :

$$NEFD = \frac{1}{(A_0 D_{sys.})} \quad (19)$$

where,

$$D_{sys.} = \frac{\frac{\nu_s}{\nu_n}}{\int_0^\infty W'(\lambda) d\lambda} \quad (20)$$

$$W(\lambda) = k_t(\lambda) W'(\lambda) \quad (21)$$

The factor $k_t(\lambda)$ accounts for the transmission loss suffered by the radiation in passing from the optical system to the detector.

12. Range equation

The determination of maximum range, R , at which an infra red system can detect a target requires the detail analysis of the spectral radiance properties of the target, the spectral transmittance $k_a(\lambda, R)$ of the path between the target and the system, the response of the detector $D_{fo}^*(\lambda)$, the characteristics of the collector system, radiant intensity $J(\lambda)$ of the source and area of the detector, A_d . The range equations for a point source, i.e., a source which cannot be further resolved optically and an extended source are respectively given by the following expressions:⁵

$$R_{\text{(point source)}} = \left\{ \frac{k_y k_n A_o \int_0^\infty D_{fo}^*(\lambda) J(\lambda) k_a(\lambda) k_t(\lambda) d\lambda}{[A_d (\Delta f)_n]^{\frac{1}{2}}} \left(\frac{\nu_n}{\nu_s} \right) \right\}^{\frac{1}{2}} \quad (22)$$

$$R_{\text{(extended source)}} = \left[\frac{k_y \int_0^\infty k_t(\lambda) k_a(\lambda) D_{fo}^*(\lambda) J(\lambda) d\lambda}{\theta \int_0^\infty k_t(\lambda) D_{fo}^*(\lambda) B_n'(\lambda) d\lambda} \left(\frac{\nu_n}{\nu_s} \right) \right]^{\frac{1}{2}} \quad (23)$$

where $(\Delta f)_n$ is the equivalent noise band width at a centre frequency f_c , k_n the ratio of the noise at the test frequency to that at frequency f_c , $B_n'(\lambda)$ the background noise radiance level at the entrance aperture, and θ the total solid angular field of view seen by the single detector element.

Ratio $\frac{\nu_n}{\nu_s}$ in equation (23) indicates the noise-signal ratio for the extended source. Evidently, the range depends on atmospheric transmission, source area, flux, brightness, modulation, beam widths, responsivity of detector, focal lengths of receiver, noise, etc.

13. Communication system

In a communication system (Fig. 9) the intelligence is transmitted by encoding the radiating beam. In any communication system, the ratio $\frac{\nu_s}{\nu_n}$ which can be used to find the maximum useful range of transmission is given by the relationship (5).

$$\frac{\nu_s}{\nu_n} = \frac{K_7 B A_b D_\lambda^* D_o}{R^2 (N) [\theta (\Delta f)_n]^{\frac{1}{2}}} \quad (24)$$

where

$$K_7 = \frac{\pi}{4} k_t (k_d d)^{\frac{1}{2}} k_b$$

$$K_8 = k_y k_n k_s k_a k_m$$

where, k_m is the modulation efficiency, $k_b(\lambda)$ the beacon's optical efficiency, k_d is a factor which accounts for the mismatch between the detector and the exit operation,

N indicates the F -number of the objective or field lens, $k_g = (1 + g^2)^{-1/2}$, g is the ratio of electronic system r.m.s. noise voltage to the detector noise voltage over the band pass, θ is the total solid angular field of view seen by the single detector element, $B(\lambda)$ the source radiance, D_o the circular collector aperture diameter, A_b the beacon's lens or mirror aperture area, and $k_t(\lambda)$ the transmission factor that account for energy loss between the detector and the collecting aperture. It is observed that greater sensitivity can be achieved by reducing the field of view of the receiver and increasing the Beacon's diameter.

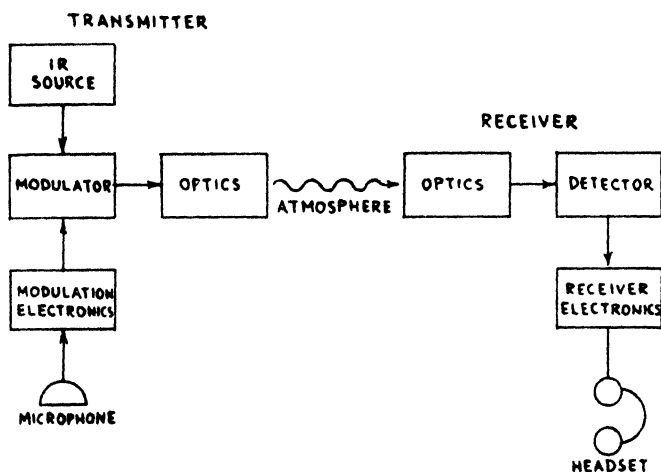


Fig. 9

Block diagram of infra red communication system

Advantages

The infra red system possesses the following advantages :

- (i) Privacy of communication due to narrow bandwidth, lack of side lobes and forward atmospheric scatter, and the ease with which the visible part can be removed by optical filter ;
- (ii) Freedom from interference ;
- (iii) Availability of extra channel for communication ; and
- (iv) Simplicity, smaller size and comparatively low cost.

14. Conclusions

Though infra red is finding extensive applications in medical and biological electronics, astronautical purposes such as satellite tracking, celestial probe, military programmes such as surveillance, early warning and detection, aerial mapping, search, acquisition and track, missile guidance, fire control, counter measures, etc. ; it is still, relatively, a new science, and extensive research and development work are under progress to advance the state-of-the-art. This is a field of basic science which has

blossomed and developed through the cooperative efforts made from several interdisciplinary fields and invariably needs further sustained work. The future trends of investigations seem to develop Blip detectors, improve quantum efficiency, anti-reflection coatings, optimising detector thickness relative to absorption coefficient, detectors which can work under Blip condition without the necessity of cooling. This would require further intense investigations on contact and surface phenomena, physics and chemistry of materials, electron-hole recombination process, etc.

15. References

1. M. Pivovonsky and M. R. Nagel. 'Tables of Blackbody Radiation Function'. *Macmillan Co.*, New York, 1961.
2. A. H. Canada. 'Simplified Calculation of Blackbody Radiation'. *General Electric Review*, vol. 51, 1948, p. 50.
3. R. S. Knox. 'Direct Reading Planck Distribution Sliderule'. *Journal of the Optical Society of America*, vol. 46, 1956, p. 879.
4. M. M. Fulk, M. M. Reynolds and R. M. Burley. 'American Institute of Physics Handbook'. *McGraw-Hill Book Co., Inc.*, 1957, p. 6-64-6-67.
5. J. A. Jamieson, *et al.* 'Infra Red Physics and Engineering'. *McGraw-Hill Book Co., Inc.*, 1963.
6. W. M. Elasser. 'Mean Absorption and Equivalent Absorption Coefficient of a Band Spectrum'. *Physics Review*, vol. 54, 1938, p. 126.
7. G. N. Plass. 'Useful Representations for Measurements of Spectral Band Absorption'. *Journal of the Optical Society of America*, vol. 50, 1960, p. 868.
8. G. N. Plass. 'Models for Spectral Band Absorption'. *Journal of the Optical Society of America*, vol. 48, 1958, p. 690.
9. T. Elder and J. Strong. 'The Infra Red Transmission of Atmospheric Windows'. *Journal of the Franklin Institute*, vol. 255, 1953, p. 189.
10. R. M. Scott. 'Optics for Infra Red Systems'. *Proceedings of the Institute of Radio Engineer*, vol. 47, 1959, p. 1,530.
11. W. L. Wolfe and S. S. Bullard. 'Optical Materials, Films and Filters for Infra Red Instrumentation'. *Proceedings of the Institute of Radio Engineer*, vol. 47, 1959, p. 1540.
12. S. S. Ballard and K. A. McCarthy. 'Optical Material for Infra Red Instrumentation'. *Nuovo Climento Supplement*, vol. 2, series 10, 1952, p. 648.
13. M. J. E. Golay. 'Pneumatic Infra Red Detector'. *Review of Scientific Instruments*, vol. 18, 1947, p. 357.
14. M. J. E. Golay. 'Theoretical Consideration in Heat and Infra Red Detection with Particular Reference to the Pneumatic Detector'. *Review of Scientific Instruments*, vol. 18, 1947, p. 347.

15. F. D. Urbach and D. Pearlman, *et al.* 'On Infra Red Sensitive Phosphorus'. *Journal of the Optical Society of America*, vol. 36, 1946, p. 372.
16. W. E. Spicer. 'Photoemissive, Photoconductive and Optical Absorption Studies of Alkali-Antimony Compounds'. *Physical Review*, vol. 112, 1958, p. 114.
17. S. W. Kurmick and R. N. Zitter. 'Photoconductive and Photoelectromagnetic Effects in Insb'. *Journal of Applied Physics*, vol. 27, 1956, p. 278.
18. C. Hilsum and I. M. Ross. 'An Infra Red Photocell Based on the Photo-Electromagnetic Effects in Indium Antimonide'. *Nature*, vol. 179, 1957, p. 146.

A DIRECT DISCRETE ANALOGUE FOR FLOOD ROUTING***K. V. Ramana Murthy***Non-member**Research Officer,**Central Water & Power Research Station, Khadakwasla (South), Poona***Summary**

A direct discrete analogue based on Muskingum storage equation, for flood routing, has been developed by the U.S. Weather Bureau in the year 1948. In this, consideration has not been given for the source resistance. This paper, gives the results of the investigation into the effect of the source resistance and describes a method to evaluate the correct value. The development of a practical circuit utilizing the correct value of the source resistance and the procedure for routing the outflow discharge hydrograph are given. It also gives the development of a discharge-stage converter, to obtain the results directly in terms of stages, for facilitating purposes like flood forecasting. The outflow in terms of stage is displayed on a digital voltmeter which gives directly in numbers either in ft. or in m. The applicability of the analogue is tested, for the reach of about 97 km. in length, between Baramul and Kaimundi on the River Mahanadi, by feeding to the analogue the discharge hydrographs at Baramul and obtaining the discharge as well as stage hydrographs at Kaimundi. For obtaining accurate results, a continuously recorded inflow discharge hydrograph was fed to the analogue. The analogue offers a quick and accurate method for routing flood waves for all those reaches, for which Muskingum storage equation holds good.

1. Introduction

Electrical analogues can be classified into two major categories, one direct and the other indirect. The direct electrical analogues can be subdivided into continuous and discrete types. The analogy between the flow of current in an electrical circuit and the flow of water in a permeable medium, in accordance with Darcy's Law, has long been recognized and has been used in the analysis of flow nets under dams and drainage systems. The continuous field analogues are mostly used for this purpose. The analogy between the electrical flow and water flow may be exploited much further, in the solution of stream flow routing problems. A direct discrete analogue for stream flow routing has been developed by U.S. Weather Bureau in the year 1948.¹⁻⁶ This provides a simple, fast and accurate method for routing flood waves. This analogue automatically produces the discharge hydrograph for the lower end of any selected river reach, when the discharge hydrograph of the inflow at the upper end of the reach

* Written discussion on this paper will be received until April 30, 1967.

This paper was received on June 8, 1966.

is traced by an operator. In this, consideration has not been given for the source resistance.

2. Basic equations

Flood routing

Muskingum storage equation for flood routing, which assumes the storage to be proportional to a weighted value of the inflow and outflow, is given by

$$S = K [X I + (1 - X) O] \quad (1)$$

where S is the storage, I the inflow, O the outflow, K the factor with dimension of time, and X the weighting factor representing the relative importance of inflow or outflow on storage.

Electrical circuit

Referring to the basic circuit of Fig. 1 the total charge across the two condensers, C_1 and C_2 , can be shown to be given by

$$Q = 2 C_1 (R_1 + R_2) \left[2 \frac{R_1}{(R_1 + R_2)} i_1 + \left(1 - \frac{R_1}{(R_1 + R_2)} \right) i_2 \right] \quad (2)$$

if $R_1 = R_3$ and $C_1 = C_2$.

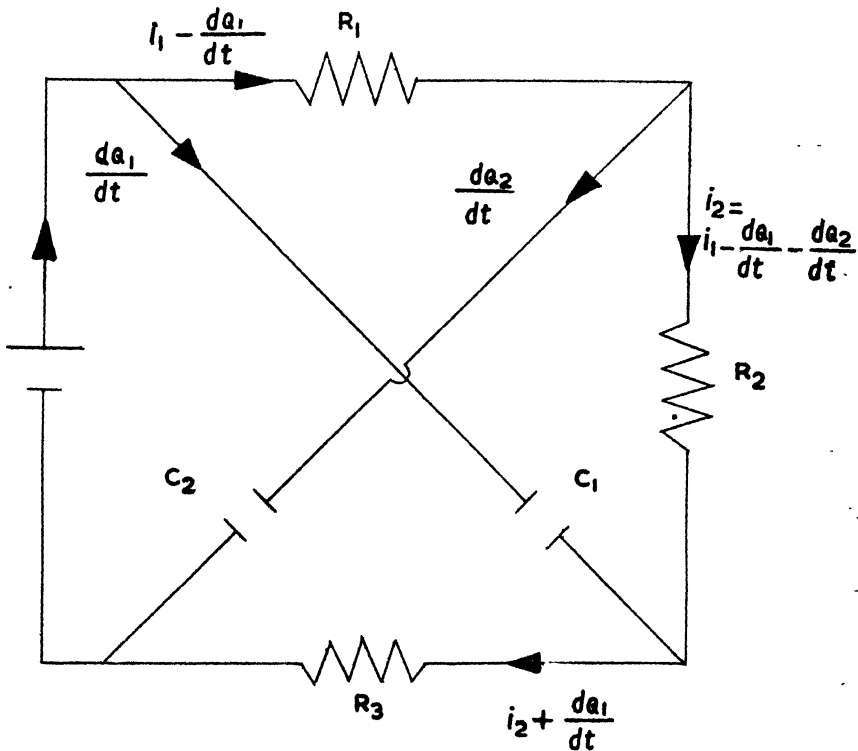


Fig. 1

Basic circuit

If the mathematical equations representing two physical phenomena are similar, then the two phenomena are said to be analogous. It can be seen that the equation (2) representing the electrical charge in the circuit is analogous to the Muskingum storage equation (1). If the total charge in the electrical circuit represents the flood storage, $2(R_1 + R_2) C_1$ represents K , $\frac{R_1}{2(R_1 + R_2)}$ represents X , the current i_1 represents the flow into the channel I , and the current i_2 represents the outflow, O . If the values of the resistors and condensers are so set as to suit a particular reach, as given by the values of K and X and a current i_1 , proportional to the inflow discharge hydrograph, is pumped into the above circuit, the current i_2 , represents the outflow discharge hydrograph. Thus, it is possible to obtain an outflow discharge hydrograph of a particular reach from the analogue, with a given inflow discharge hydrograph and given values of K and X , which are characteristics of the reach.

Method of determining the correct value of the source resistance

For tracing the outflow hydrograph, a current i_1 , proportional to the inflow discharge hydrograph, has to be pumped into the analogous circuit. For this purpose in the practical circuit given in Fig. 2, a battery with a series variable resistor has been used. In addition, as the analogue needs a constant current source, a fixed series resistor has been introduced. For evaluating the correct value of the series resistor, the following experiment has been performed. As an inflow discharge hydrograph, a cosine type of curve has been fed and the outflow traced, by keeping different values of the series resistor, from 1 megohm to 10 megohm. The Muskingum constants used are $K = 1.0$ and $X = 0.5$. Fig. 3 gives the inflow discharge hydrograph and outflow discharge hydrographs for different values of the series resistor. It can be seen that with the series resistor of 10 megohms the outflow discharge hydrograph is as desired, practically giving a peak of the same value as the inflow discharge hydrograph with a time displacement. It can also be seen that with the increasing value of the series resistor the peak increases, thus reducing the error. Having thus fixed the value of the series resistor as 10 megohms, the battery voltage and the variable resistor are chosen so that the pens of the potentiometric recorders connected across the 5 kilohm potentiometers will give a reasonably good scan.

3. Procedure for routing the outflow discharge hydrograph

Referring to Fig. 2, the values of the resistors, R_1 , and R_2 , are adjusted to suit the particular reach, according to the equations $K = 2 C_1 (R_1 + R_2)$ and $X = \frac{R_1}{2(R_1 + R_2)}$ and R_2 is put equal to R_1 . Two potentiometric recorders, 'Recorder I' and 'Recorder O' are connected across the 5-kilohm potentiometers to record the inflow and outflow discharge hydrographs respectively. The 83-megohm potentiometers are adjusted to be of maximum value and the switches S_1 , S_2 and S_3 are put on and both the 5-kilohm potentiometers are adjusted to give equal deflections at steady condition on the recorders. If now the inflow discharge hydrograph is plotted on the 'Recorder I' and the pen is made to trace it by slowly changing the 83-megohm potentiometer, the 'Recorder O' automatically traces the outflow discharge hydrograph. The analogue set-up is shown in Fig. 4.

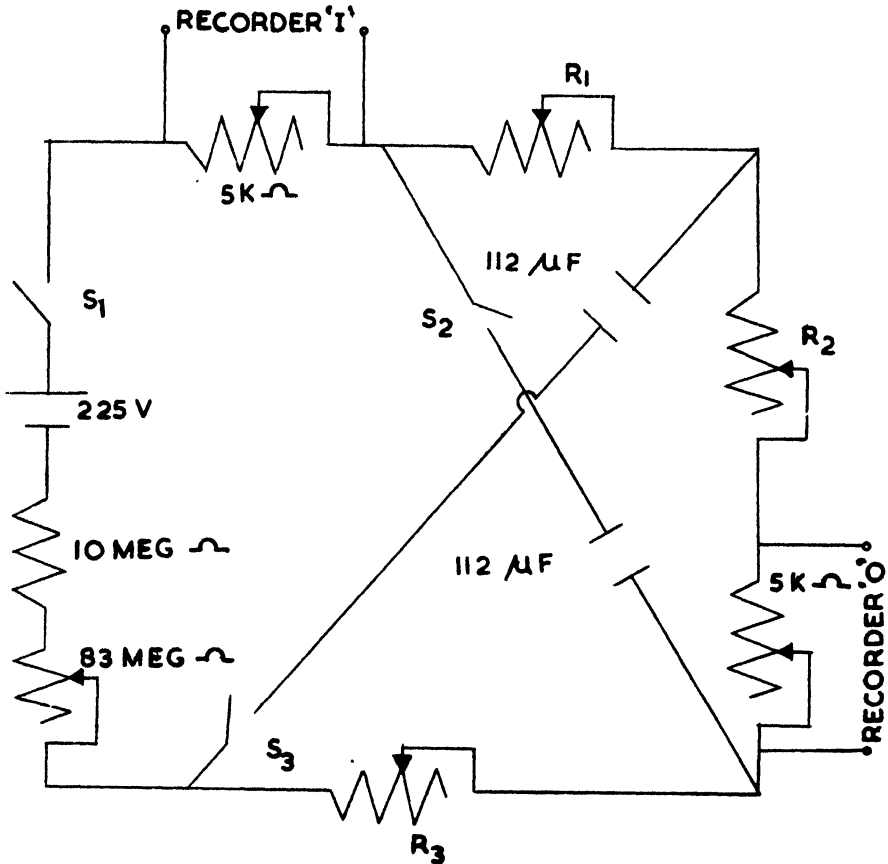


Fig. 2
Practical circuit

4. Discharge-stage converter

For some purposes, like flood forecasting, it is more desirable to obtain a stage hydrograph at the downstream point from the analogue. For this purpose a discharge-stage converter is developed. This is applicable only to simple ratings.

For a simple rating, the discharge-stage curve approximates to a parabola. In the low current region, the current *vs.* voltage curve of a selenium rectifier is a dropping one. This property can be utilized to advantage for the simulation of a discharge-stage curve. By a judicious choice of the rectifier and the current range, the curve of the current *vs.* voltage of the rectifier can be made to approximate the curve of discharge *vs.* stage. If then, the currents proportional to the discharges are fed to the rectifier, the voltages across it represent stages. If the rectifier having a similar current *vs.* voltage characteristic as the rating is inserted in place of the outflow potentiometer in the flood routing analogue and current proportional to the discharge hydrograph at the upstream point, according to the calibration curve of the rectifier, is pumped

into the analogue, the voltage across the rectifier will give directly the stage hydrograph at the downstream point. Fig. 5 is a forward current *vs.* voltage characteristic of a selenium 120 volts r.m.s. rectifier in the current range 2 to 18 micro-amp. As the resistance of this suitable rectifier in this current range is of the order of hundreds of kilohms, this cannot be directly inserted in place of the outflow potentiometer. To overcome this difficulty the voltages representing the outflow discharge hydrograph are amplified by a linear, high gain D.C. amplifier and fed to the rectifier. To limit the current through the rectifier to the suitable range a series potentiometer of 10 megohm is introduced. To facilitate calibration, a 5-megohm potentiometer is connected across the rectifier. The outflow in terms of stage is displayed on a digital

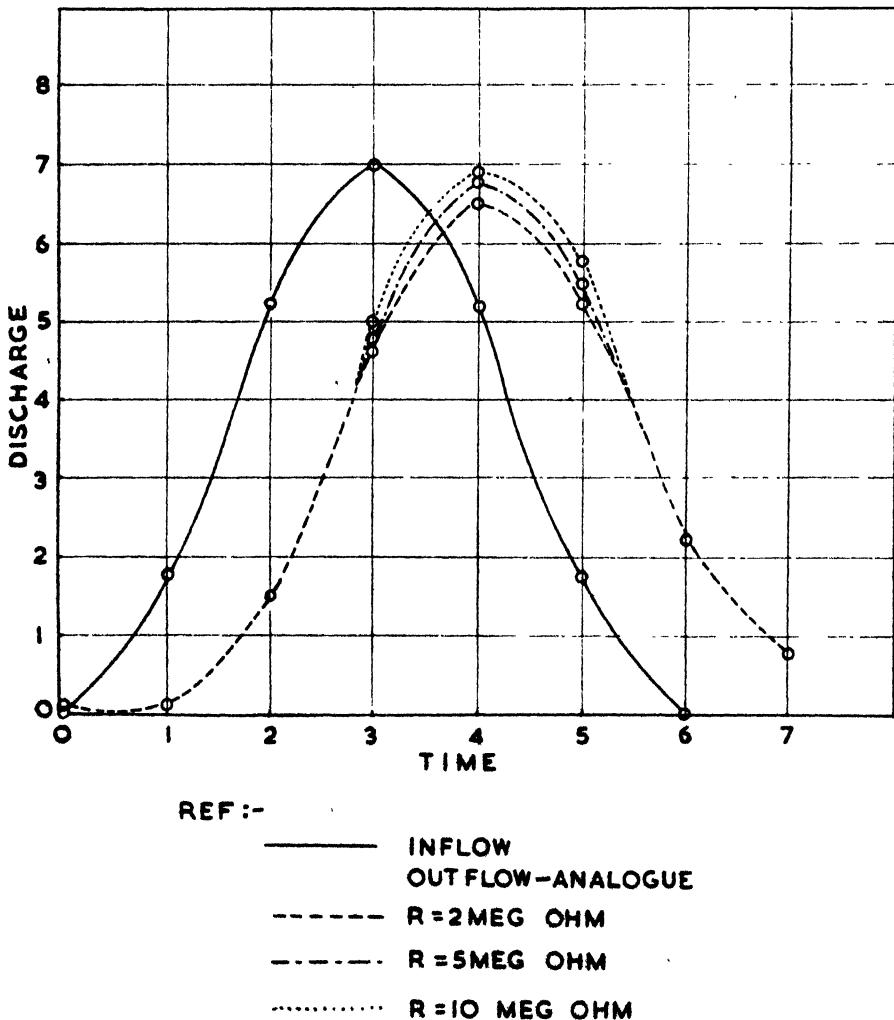


Fig. 3

Routing cosine type curve

voltmeter which gives directly in numbers either in ft. or in meters. The block diagram of the arrangement is shown in Fig. 6. The circuit of the discharge-stage converter is shown in Fig. 7. The analogue set-up with discharge-stage converter is shown in Fig. 8.

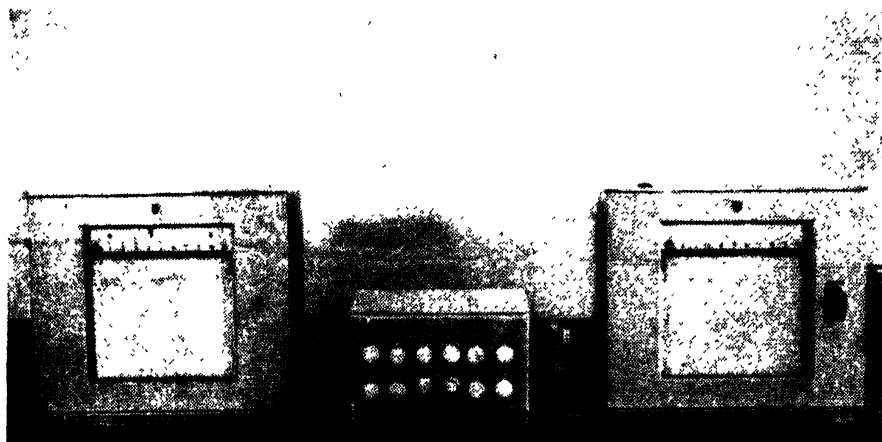


Fig. 4
Analogue set-up

5. Results

The analogue is tested for its applicability for the reach of about 97 km. in length between Baramul and Kaimundi of the River Mahanadi. The outflow discharge and stage hydrographs at Kaimundi are traced by feeding to the analogue, the inflow discharge hydrographs at Baramul. The inflow and outflow hydrographs are plotted from the available discharge and gauge data taken from the Water Year-books, published by the Central Water and Power Commission for the Mahanadi basin.

The flood hydrographs at Baramul plotted from the discharge data as observed daily thrice for the years 1948, 1949 and 1950 are fed to the analogue and the outflow discharge and stage hydrographs at Kaimundi traced. Figs. 9, 10 and 11 show the inflow discharge hydrographs at Baramul, observed outflow discharge hydrographs at Kaimundi and the ones given by the analogue. The outflow discharge hydrographs are traced with one set of constants, $R_1 = R_3 = 20$ kilohm and $R_2 = 160$ kilohm. It has been observed that when the constants for the years 1949 and 1950 are changed to $R_1 = R_3 = 40$ kilohm and $R_2 = 190$ kilohm, $R_1 = R_3 = 180$ kilohm and $R_2 = 1$ kilohm respectively, the results have improved. Figs. 12, 13 and 14 show the discharge hydrographs at Baramul, observed stage hydrographs at Kaimundi and the stage hydrographs given by the analogue for the years 1948, 1949 and 1950 respectively. The Muskingum constants used are $R_1 = R_3 = 20$ kilohm and $R_2 = 160$ kilohm for the year 1948, $R_1 = R_3 = 40$ kilohm and $R_2 = 190$ kilohm for the year 1949, and $R_1 = R_3 = 180$ kilohm and $R_2 = 1$ kilohm for the year 1950.

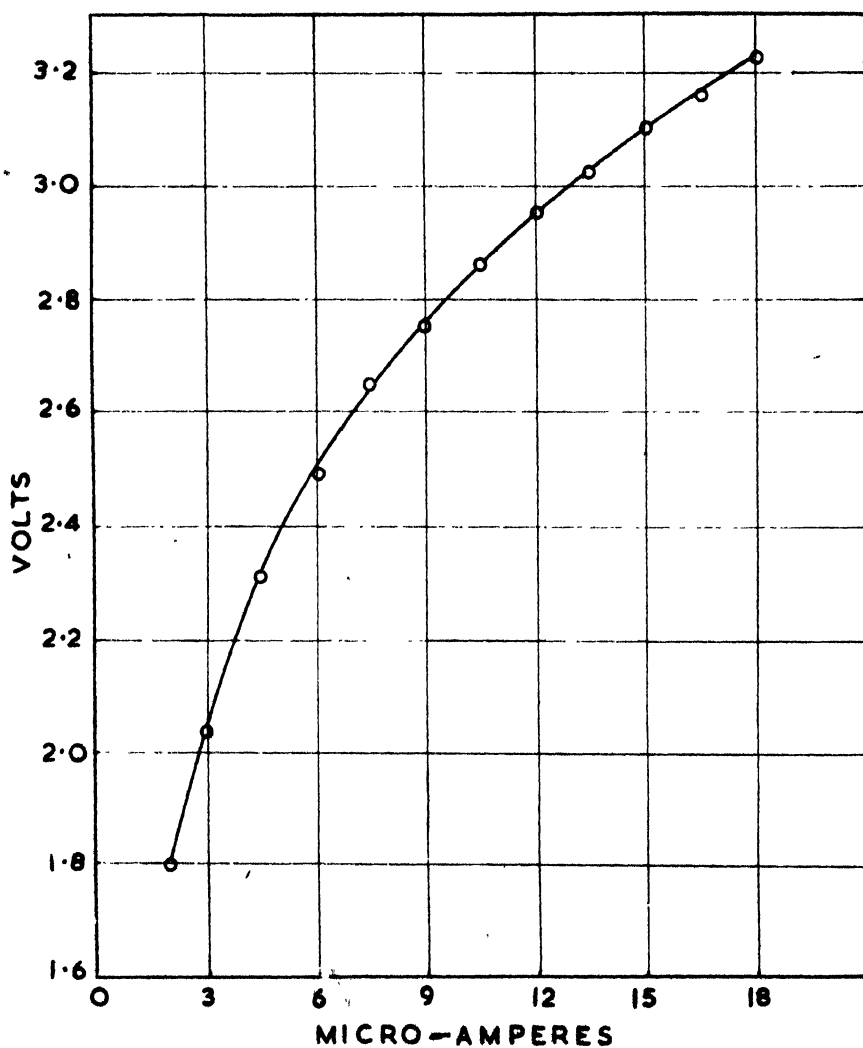


Fig. 5
Forward characteristic of a selenium rectifier

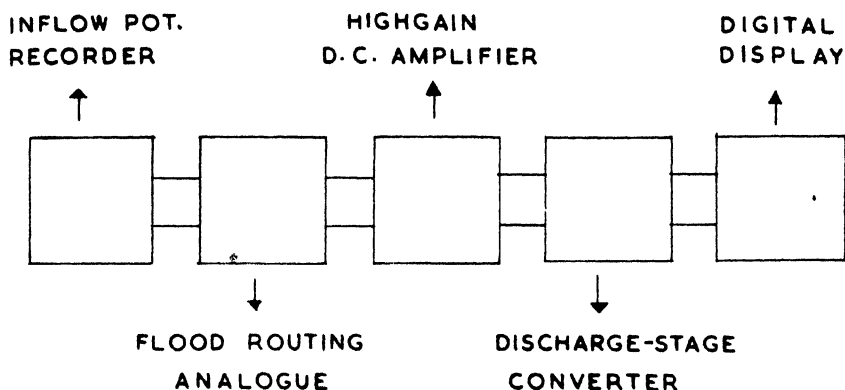


Fig. 6

Block diagram of the experimental arrangement

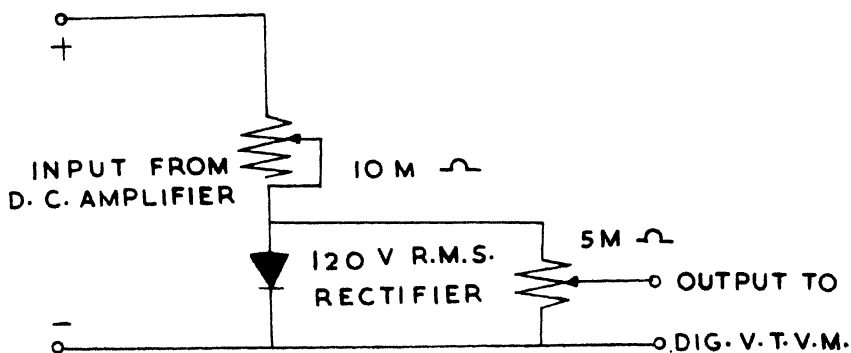


Fig. 7

Discharge-stage converter circuit

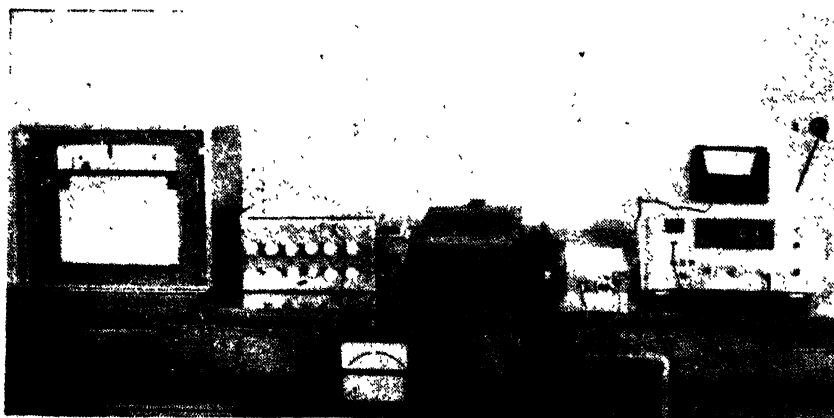


Fig. 8

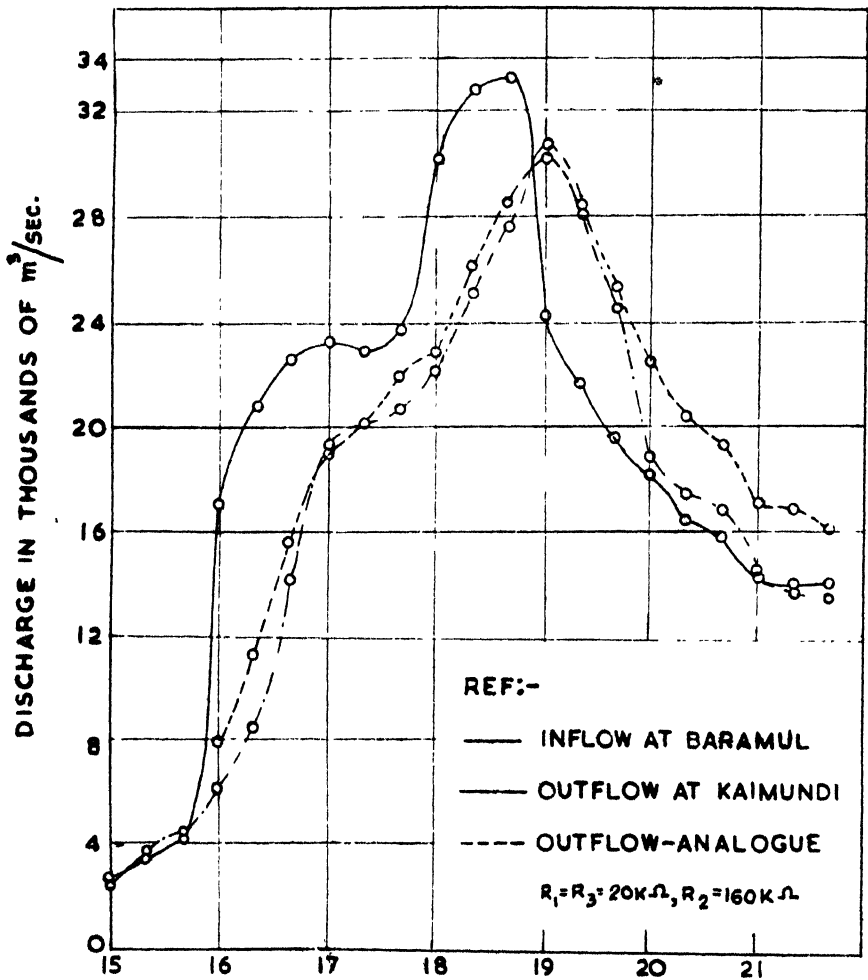


Fig. 9

Discharge hydrographs for August 1948

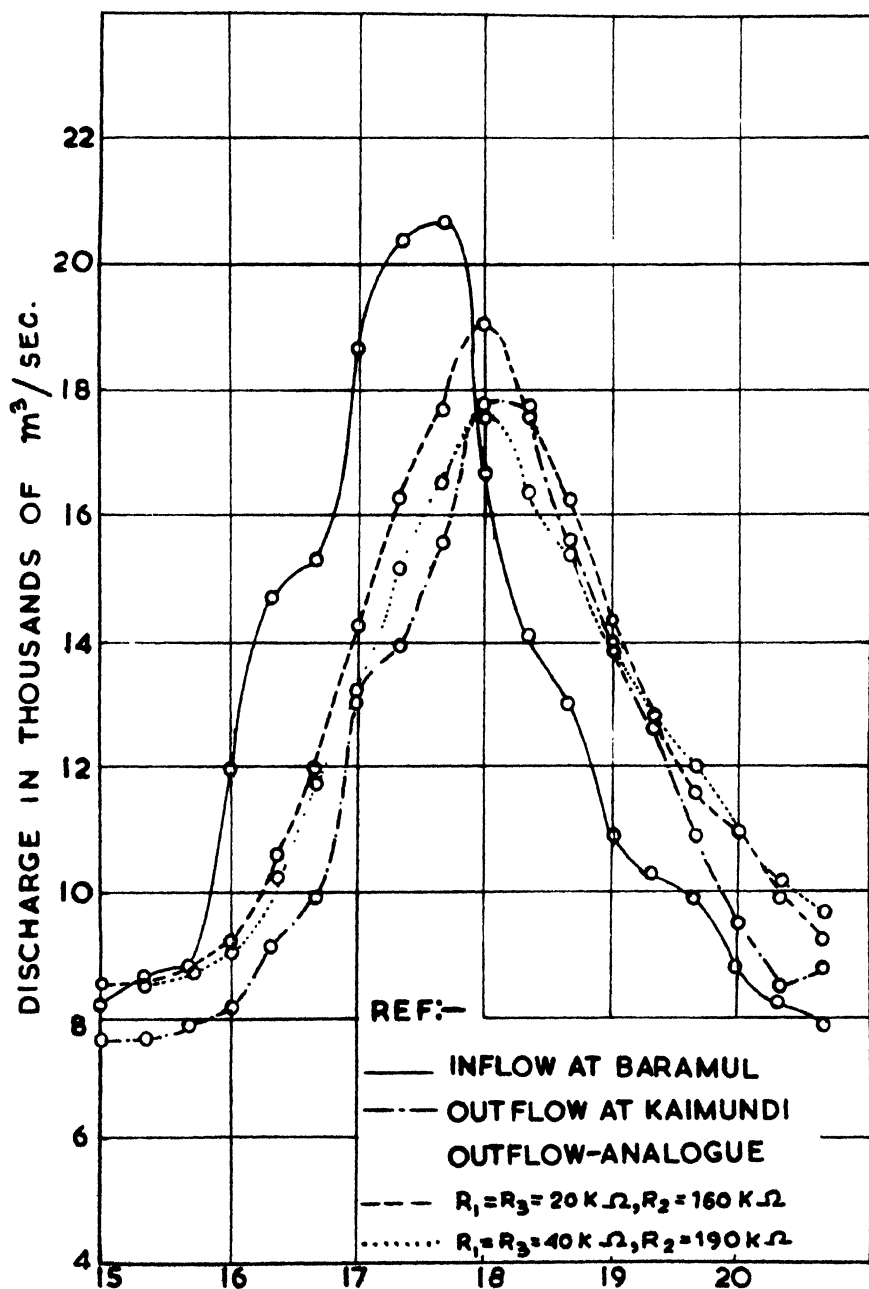


Fig. 10

Discharge hydrographs for August 1949

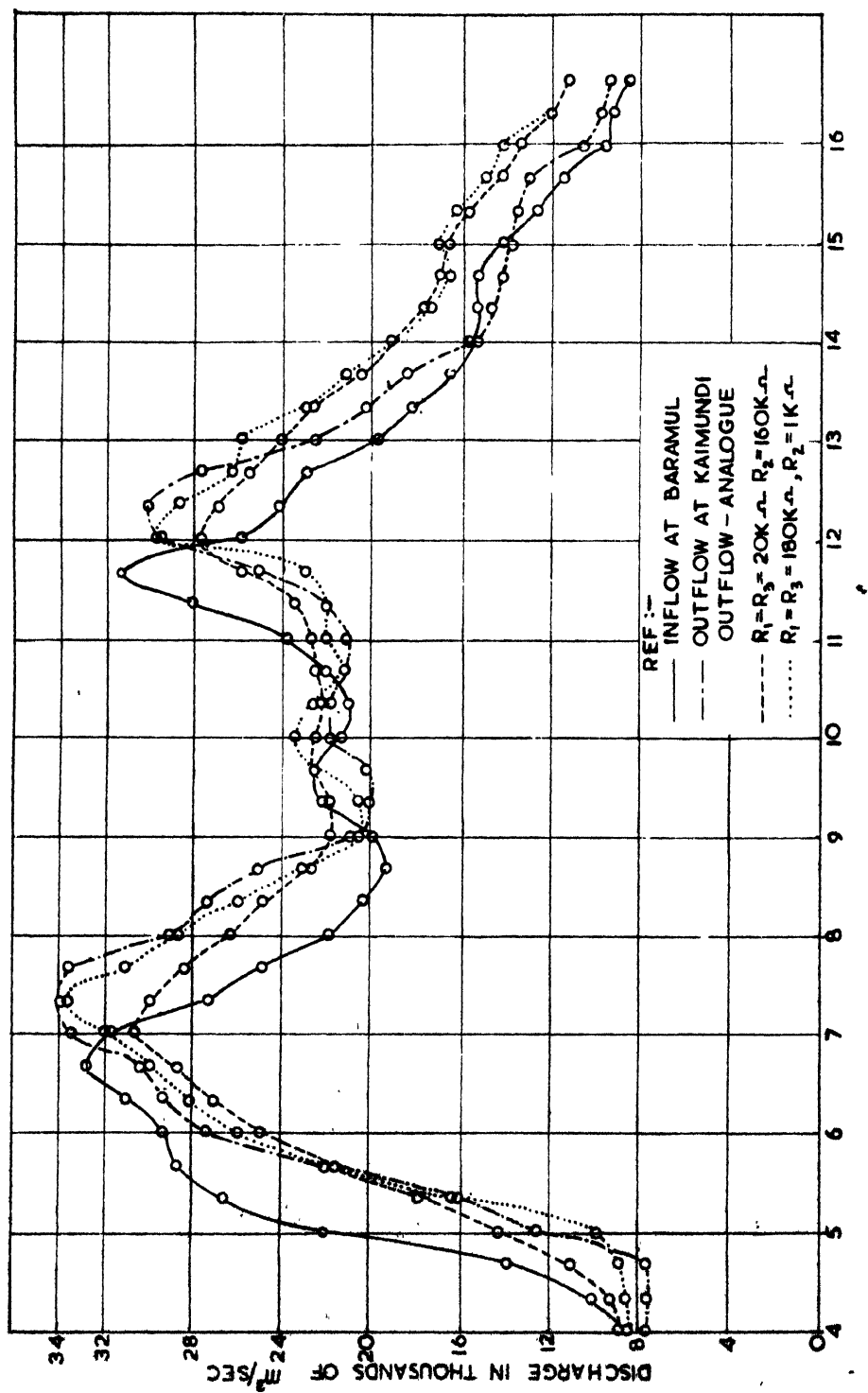


Fig. 11

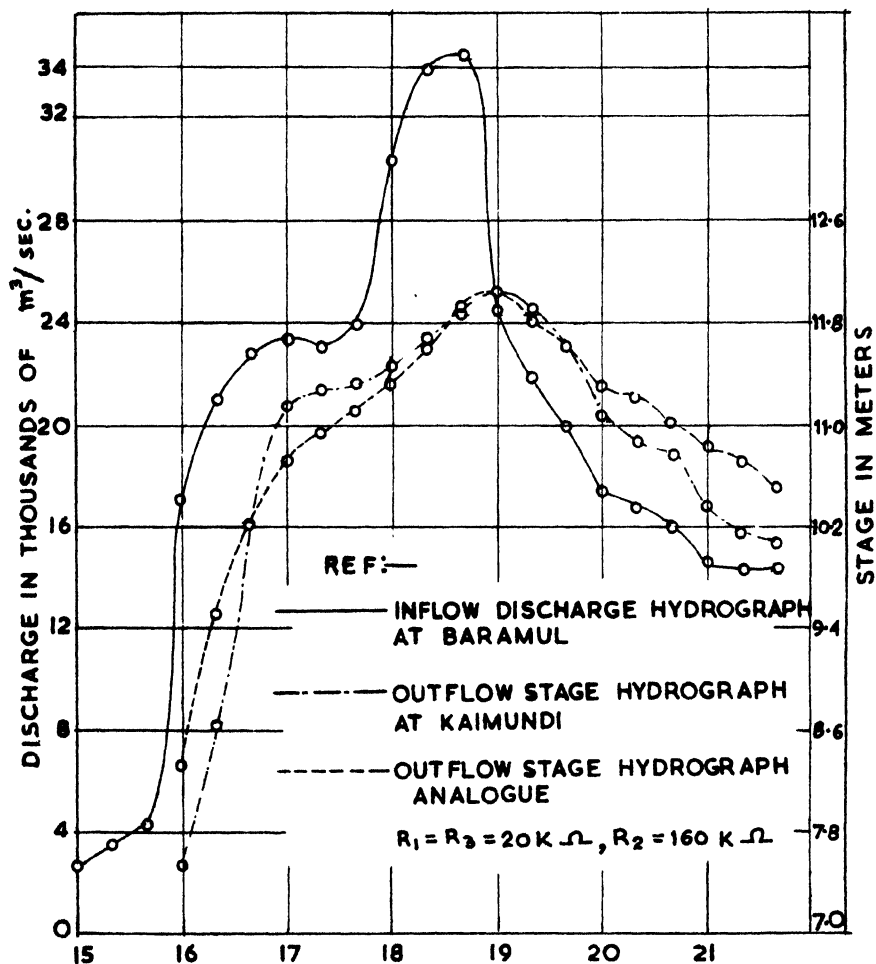


Fig. 12
Discharge and stage hydrographs for August 1948

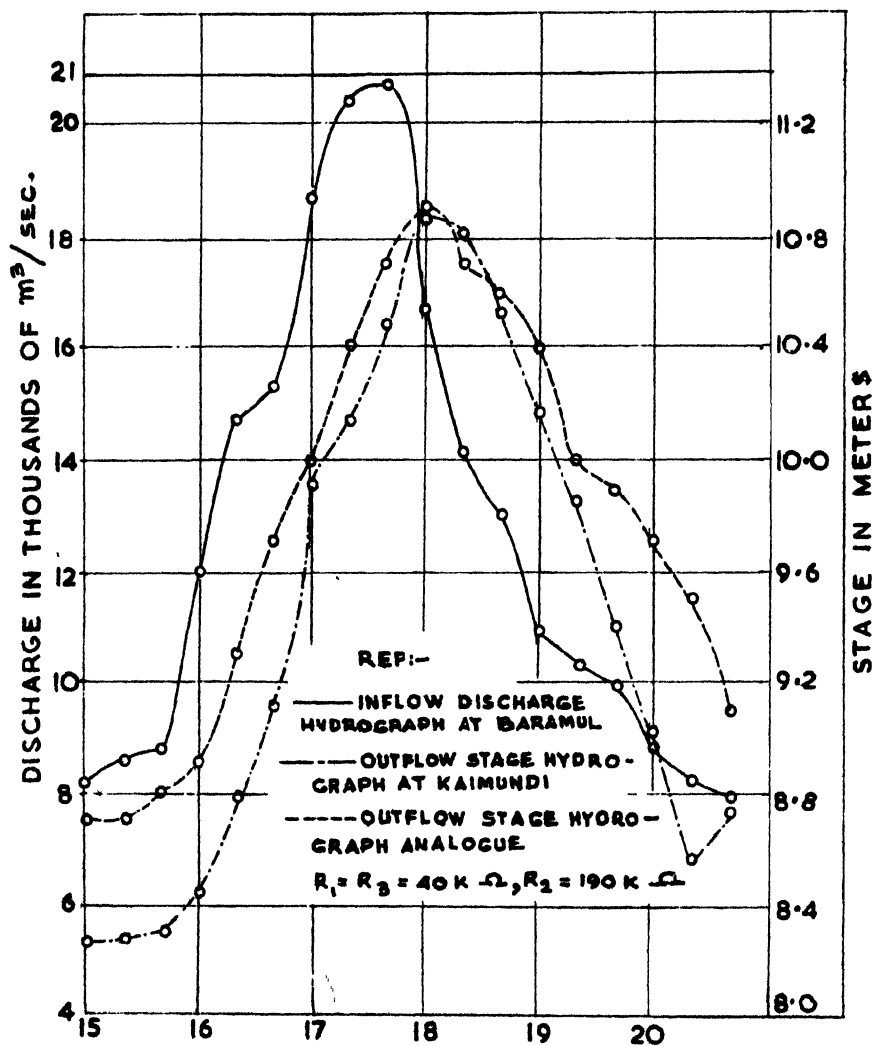


Fig. 13

Discharge and stage hydrographs for August 1949

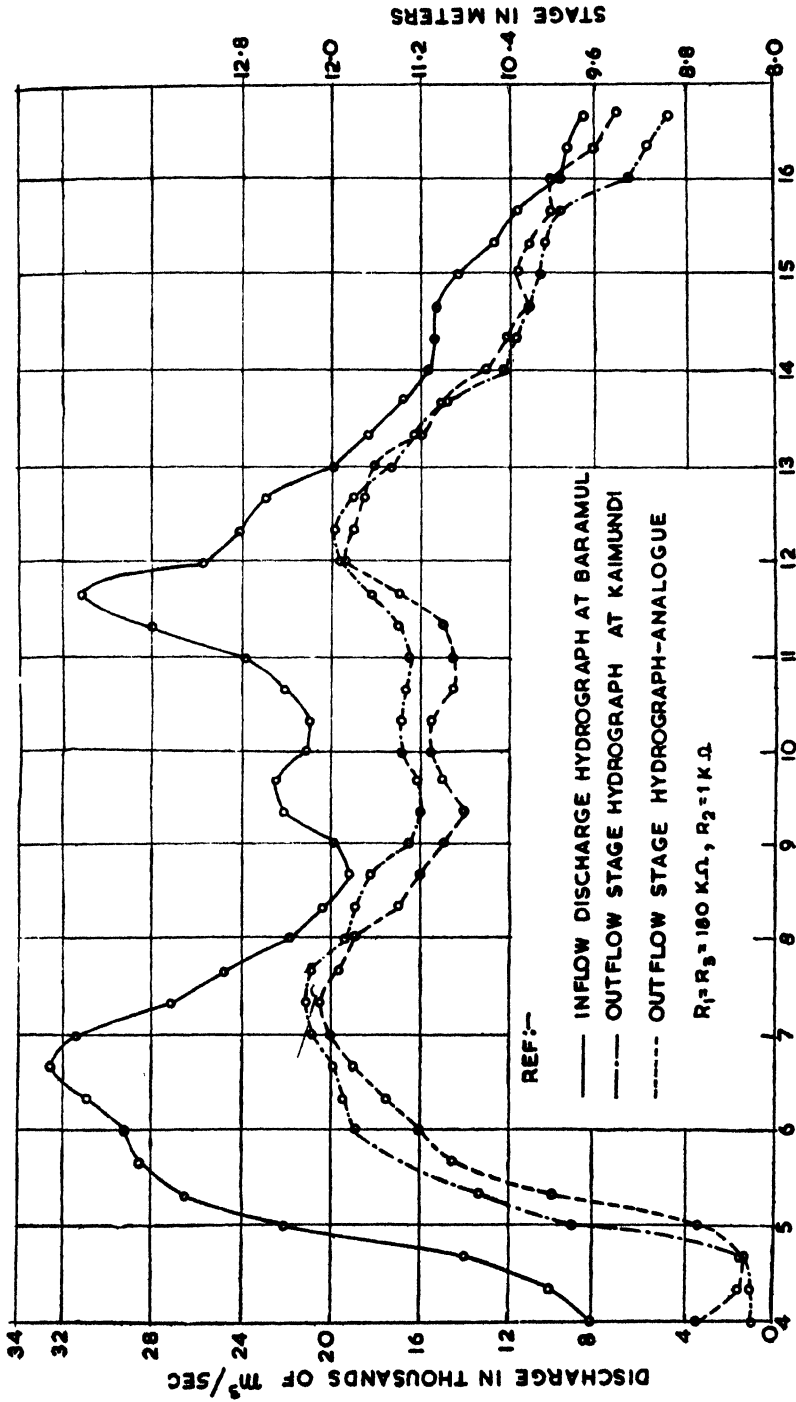


Fig. 14
Discharge and stage hydrographs for August 1950

6. Conclusions

The development of a direct discrete analogue for flood routing has been given. The analogue offers an efficient tool for flood routing purposes. As it is based on the Muskingum storage equation for flood routing, it will be applicable for all the river reaches where Muskingum storage equation holds good. If the rating at the downstream point is simple, the analogue can give either the discharge or the stage outflow hydrograph. For accurate prediction of the outflow hydrograph, a continuously recorded inflow discharge hydrograph has to be fed to the analogue.

7. Acknowledgments

The author is thankful to Shri C. V. Gole, Director, Central Water and Power Research Station, for his interest in this work. The assistance of Shri P. R. Belgal, Research Assistant, in carrying out the experiments is gratefully acknowledged.

8. References

1. R. K. Linsley, M. A. Kohler and L. H. Paulhus Joseph. 'Applied Hydrology'. *McGraw-Hill Book Co., Inc.*, 1st edition, 1949.
2. R. K. Linsley, L. W. Foskett and M. A. Kohler. 'Electronic Device Speeds Flood Forecasting'. *Engineering News Record*, vol. 141, no. 26, December 23, 1948.
3. M. A. Kohler. 'Electrical Analogies and Electronic Computers—Application to Stream Flow Routing'. *Transactions of the American Society of Civil Engineers*, vol. 118, 1953, p. 1028.

A TEMPERATURE REGULATOR FOR LOW CAPACITY BATHS***J. S. Gupta***Associate Member***Summary**

The problem of temperature regulation varies very widely. The actual design of the regulator depends on the system whose temperature is to be regulated as well as the accuracy desired. In this paper, the general development of the temperature regulators has been reviewed and a design procedure of a temperature regulator for low capacity bath has been illustrated by an example.

1. Introduction

Temperature regulation was one of the first problems to which automatic control was applied ; and it still remains one of the biggest fields of its application. The problem varies from keeping the room temperature at a reasonably constant value within a few degrees to those of process temperatures which require accuracies of the order of 0.01°C . or less. Starting from a simple bimetal thermostat, some of the most elegant methods of control have been devised. The methods of error detection as well as those of correction have advanced very much in recent years so that the temperature regulator has become a highly accurate instrument of very much improved performance. The actual design of the regulator depends on the system whose temperature is to be regulated as well as on the accuracy required.

2. On-off controller

The on-off type feedback control system is one of the most widely used types of control because of its relatively low cost. The temperature of a low capacity bath can conveniently be controlled with the help of thyatron. The performance of the controller can be explained with the help of Fig. 1. The output of the bridge detector is being fed to the grid of the thyatron through the amplifier. The thyatron is supplied by an A.C. voltage and the same is given to the bridge via a transformer. As the temperature of the bath rises above the reference value, the resistance of the non-linear resistors, RN_1 and RN_2 , falls and a voltage V_{AB} , 180° out-of-phase with the above voltage of the thyatron is fed to the grid of the thyatron. When the value of V_{AB} is sufficiently high, the thyatron stops firing and the flow of current in the heating element ceases. On the other hand, when the temperature falls below the reference value, V_{AB} reverses its phase and is consequently in-phase with the anode voltage of the thyatron. The thyatron continues to fire and the current keeps on flowing in the heating element.

* Written discussion on this paper will be received until April 30, 1967.

This paper was received on February 16, 1966.

It is seen that the signal at the grid of the thyatron has no effect on the value of the current supplied by it. The control is of the on-off type ; it behaves like a simple switch which either turns on a current or turns it off.

3. Phase lead and reversed lag application

The simple on-off controller has a fundamental defect that the system oscillates about its mean value of the temperature due to presence of time lags, and the desired temperature is never attained. The amplitude of these oscillations can be decreased by adding a phase lead network. If the frequency is very low, the principle of reversed lag¹ depending on the thermal process may be used.

4. A proportional controller

The oscillations of the on-off controller can altogether be eliminated by introducing a proportional control. The action consists in making the angle of lag between the grid and plate voltage vary continuously instead of being switched on between 0° and 180° . For this purpose, a second voltage is added to the grid of the thyatron through a phase-shifting network. The resultant voltage available at the grid with respect to the anode voltage of the thyatron is shown in Fig. 2.

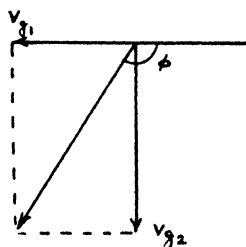


Fig. 2
Vector diagram for grid voltage

5. Analysis of the proportional controller

Since the system has a regulator, the disturbance in the inlet temperature due to changes in room temperature, etc. may be considered as input. Consequently the transfer function of the regulator works out to be,

$$\frac{\theta_2(s)}{\theta_1(s)} = \frac{1}{1 + \frac{K K_1 K_A K_3}{Q C_p V_{g1}^2} + T s}$$

where W is the weight of the water inside the bath, Q the rate of flow of water, T the time constant $\left(= \frac{W}{Q} \right)$ C_p the specific heat of water, θ_1 and θ_2 are the inlet and outlet temperatures, K is the constant in calories per amp., K_1 the constant of the detector in volt per $^\circ\text{C}$., K_A the gain of the amplifier, V_{g1} the amplified error voltage, V_{g2} the voltage output of the phase-shifting network, and K_3 the slope of the current *vs.* fire angle curve near 90° .

The block diagram may be drawn as shown in Fig. 3.

It can be seen that no instability exists in the above system, which is a first-order system only. The accuracy of the system is very high, because of the high gain in the feedback loop. All the above deductions exist, however, only for a small change from the values at balance point. For larger disturbances, these simple linear relationships do not exist any longer.

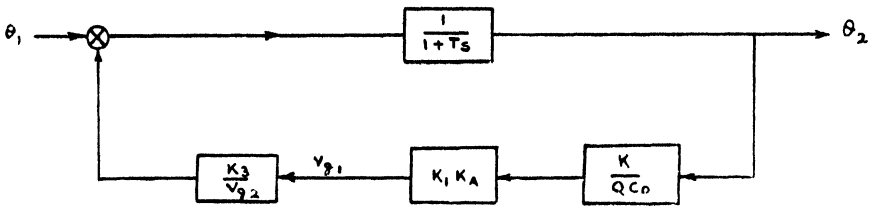


Fig. 3

Regulator block diagram

6. Reset control

Even though the accuracy of the regulator has been increased considerably by the proportional control with a high gain in the feedback loop, it is not possible to make the error absolutely zero. A small error in θ_2 is always brought in as a result of any disturbance θ_1 . This small error is called an 'off-set or droop' and it increases with increasing disturbances. This static error can be entirely eliminated by the introduction of the 'reset' or 'integral' control.

The transfer function of the feedback loop becomes

$$H(s) = K' \left(1 + \frac{1}{T_i s} \right)$$

after introducing the integral control, where

$$K' = \frac{K K_1 K_A K_2}{Q C_p V_{g2}}$$

Then, the closed loop transfer function from Fig. 4 is obtained as

$$\frac{\theta_2(s)}{\theta_1(s)} = \frac{s T_i}{K' + (1 + K')s T_i + s^2 T T_i}$$

The final value reduces to zero and hence the static error has been eliminated altogether.

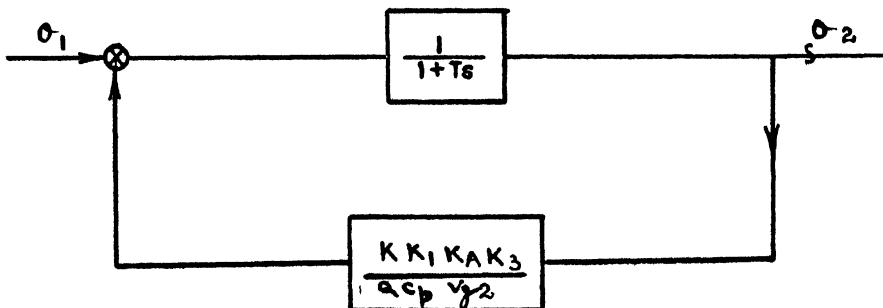


Fig. 4

Simplified regulator block diagram

7. Design procedure for off-on controller

Let us assume that a regulator is desired for regulating the temperature of a water bath having a capacity of about 6 litres per hr. in the range 50°C. to 100°C. within 0.5°C.

Heating system

Assuming the room temperature of 20°C., the power needed to effect a temperature rise of about 80°C. for 6 litres of water per hr. is given by

$$P = \frac{6 \times 1,000 \times 80 \times 4.18}{3,600} = 557 \text{ watts}$$

An immersion heater of 1,000 watts readily available may be chosen as a heating device. The length of the heater is about 25 cm. For keeping the clearance of about 7.5 cm., the height of the bath may be taken as 32.5 cm. The diameter of the bath may be taken as 25 cm. The empty annular space between the walls of the cylindrical bath is filled with glass-wools to prevent loss due to conduction. The error detecting elements are put in a thin aluminium container so that the time lag between the error voltage produced and the temperature measured is made practically negligible. The container is fixed in the top cover to sense the outlet temperature.

The thyatron tube BT₅, capable of carrying a steady current of 2.5 amp. and having a voltage drop of about 25 volts across it, may be chosen so that the necessary power develops in the heating element.

Detector

A Wheatstone's Bridge with two non-linear elements forming the opposite arms of the bridge may be chosen for the detection. The bridge may be supplied at 10 volts from the secondary of the transformer if the non-linear carbon resistors have the following specifications :

Power rating . . $\frac{1}{4}$ watt

Resistance . . About 1,500 ohms at room temperature

Resistance . . About 40 ohms at 100°C.

Response of the bridge is shown in Fig. 5. The rise in output voltage is approximately 2 millivolt per °C., the rise being better as the temperature difference increases.

Amplifier

From grid critical voltage and anode voltage characteristic of the thyatron shown in Fig. 6, it is observed that voltage of 3.5 volts (r.m.s.) is necessary at the grid to stop the tube firing when the plate voltage is 230 volts (r.m.s.). The output of the bridge detector is, however, of the order of millivolts; so an amplifier is required to get the necessary voltage.

The gain of the amplifier to achieve a correction within 0.5°C. would be about 700. The amplifier shown in Fig. 1 uses two stages of the tube 6SL7 of $\mu = 70$. An actual gain of 1,300 was obtained at 50 cycles per sec.

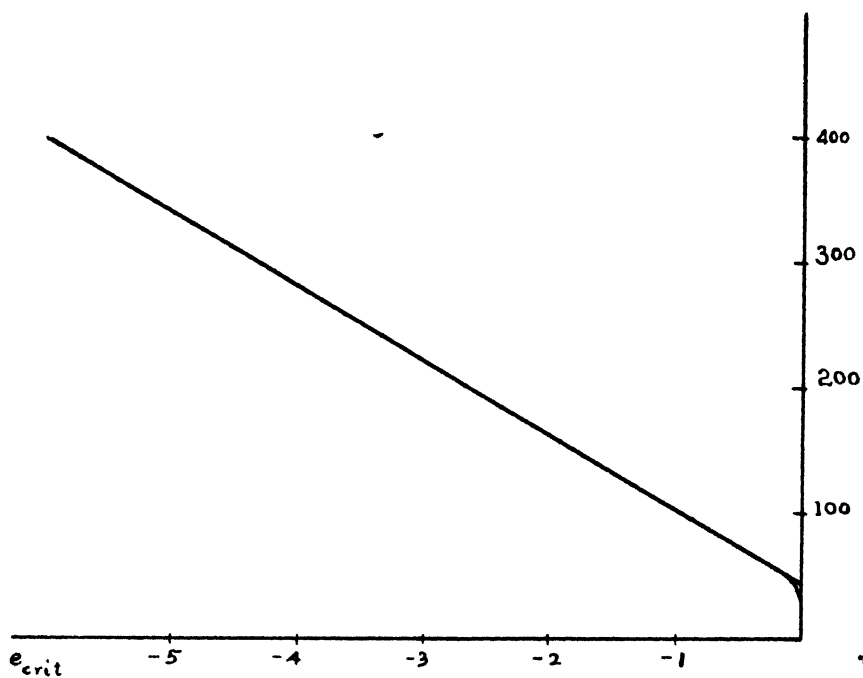


Fig. 5
Critical characteristic of the thyatron

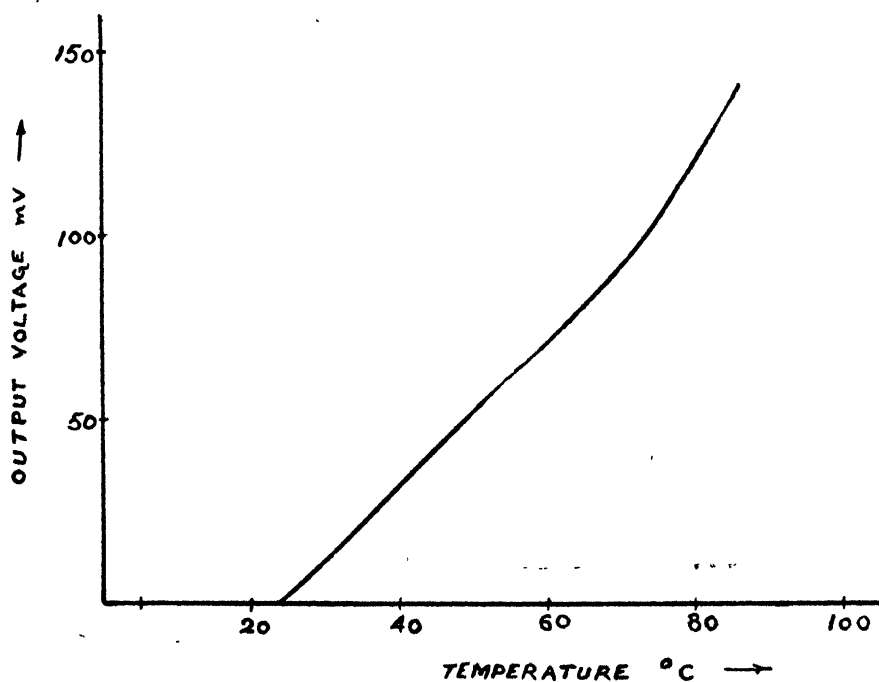


Fig. 6
Response of the bridge detector

8. The performance of the on-off controller

The on-off controller gave satisfactory results for temperature ranging from 36° to 75°C . At higher temperature the performance was not very satisfactory. The reasons may be as follows :

- (i) At higher temperature, radiation and conduction losses are appreciable and cannot be neglected ;
- (ii) The controller is not strictly of on-off type, because slight phase shifts of less than 180° are introduced by the transformer and the two amplifier stages. Consequently the firing angle of the thyatron, instead of commutating from 180° to 0° , varies over this range. The current changes continuously from the maximum of 2.5 amp. to zero ; and
- (iii) The bridge response is non-linear at the higher temperatures, the error voltage being more for the same change of the temperature. The thyatron is prevented from firing earlier and the current reduces.

9. Conclusions

- (i) A proper heat insulation should be provided for satisfactory working of the bath specially at the higher temperatures.
- (ii) For higher temperature range, either the voltage supplied to the bridge may be reduced or the bridge with only one non-linear arm may be used.
- (iii) A reversed time lag arrangement can be incorporated by providing a thick metal container in the bottom side of the bath itself near the heating element, the second pair of non-linear elements being enclosed in it.
- (iv) A proportional and reset control may be provided when high degree of accuracy has to be attained.

10. Acknowledgment

The author is grateful to Prof. N. Kesavamurthy of Electrical Engineering Department of I.I.T. (Kharagpur), Shri M. R. Mukherjee and Shri R. K. Sharma for the enlightening discussion and help.

11. References

1. H. Sutcliffe. 'The Principle of Reversed Lag Applied to On-Off Temperature Control'. *Proceedings of the Institution of Electrical Engineers*, vol. 107, no. 32, pt. B, March 1960, p. 209.
2. D. P. Eckman. 'Automatic Process Control'. *John Wiley and Sons, Inc.*, 1958.
3. M. H. Lajoy. 'Industrial Automatic Controls'. *Prentice-Hall, Inc.*, 1941.

TRANSIENT DESCRIPTORS DETERMINING THE PERFORMANCE OF LINEAR AND NON-LINEAR SYSTEMS*

T. R. Natesan

Non-member

Faculty of Electrical Engineering, College of Engineering, Guindy, Madras

Summary

This paper deals with the effect of 'transient descriptors' such as rise time, peak time, settling time, etc. on the performance of a closed loop linear and non-linear second order systems having synchro as error detector. These descriptors mainly depend on the figures of merit, viz., the damping ratio and the natural frequency of oscillation of the system. The non-linearity of the synchro is taken into account and a comparison is made between the linear and non-linear transient descriptors. It is reasonable and justified when non-linearity of synchro is ignored under steady state operation. But since the error is large during transient behaviour, it is necessary to consider non-linearity. The problem is analyzed for step and ramp input and the deviation of the results from being concurrent, is discussed. The graphs presented in the paper give these values quickly for linear and non-linear systems without compensation.¹

Notations

- J = moment of inertia in slug-ft.²,
- F = viscous friction in lb.-ft. per radian per sec.,
- K = open loop proportional gain of the system,
- δ = damping ratio,
- ω_n = undamped natural frequency of oscillation of the system,
- ω_d = damped natural frequency of oscillation of the system,
- ω_i = velocity of the reference input,
- θ_i = reference input,
- θ_o = controlled variable,
- ϵ = error of the system,
- ϵ' = first derivative of error,
- ϵ'' = second derivative of error,
- t_r = rise time,
- t_p = peak time,
- t_s = settling time,
- Δt = time interval at which numerical integration is carried out.

*Written discussion on this paper will be received until April 30, 1967.

This paper was received on September 2, 1966.

1. Introduction

In theory, all physical systems become non-linear under certain conditions of operations.² In certain cases the degree of non-linearity is so small that it can be ignored and the system can be treated as linear. In analyzing any linear system, the following conditions are assumed :

- (i) The magnitude of the response of a linear system to any disturbance is strictly proportional to the magnitude of the disturbance and its form is independent of that magnitude.
- (ii) The properties of the component elements of the system-inertia, friction, stiffness and so on are constant and in particular do not vary either with time or with the magnitude of the electrical or mechanical stresses impressed upon them.
- (iii) The component elements of the system are lumped. Question of wave motion due to properties distributed in space do not arise.³

A comprehensive and satisfying theory has been worked out only for linear systems. It is indeed fortunate that so many practical systems, in spite of the existence of non-linearities in them, do behave almost as if they were linear so that we can analyze them as if they were completely linear and yet get a reasonable approximation to their true behaviour. When the departure from non-linearity is small, it is often sufficiently accurate to treat a system as linear, using in the analysis the mean values of the system coefficients over the working range. But even when a system is markedly non-linear, a linear analysis is of considerable use and importance.

2. Error measurement

An important process in servomechanisms is the measurement of the error between input and output shafts, and the production of output signals in electrical form proportional to it. The processes of data conversion and subtraction are involved. It is possible to perform the subtraction first, *i.e.*, mechanically, and then to convert the difference into an electrical signal. Fig. 1 shows the application of the synchro to this problem of error detection, giving a system that is suitable only for A.C.

$$e(t) = E_a \sin \omega t \sin (\theta_i - \theta_o) = E_a \sin \omega t \sin \epsilon \quad (1)$$

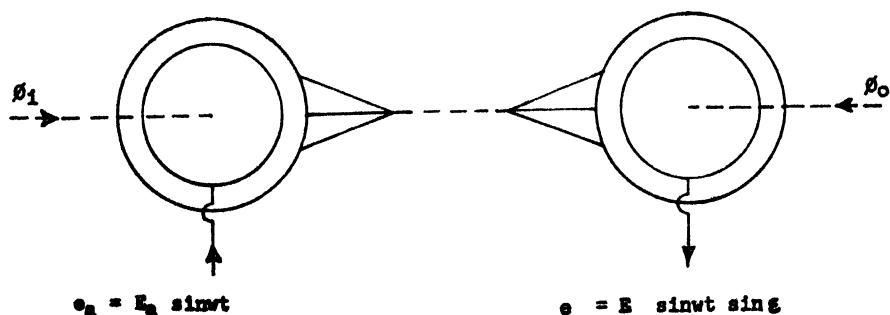


Fig. 1

Synchro system for obtaining a voltage dependent on error

From the servo point of view, the fact that this voltage is alternating is not of primary importance; its magnitude only gives the information required. Therefore, we may write

$$|e| = E_a \sin \epsilon$$

where $|e|$ denotes the magnitude of $e(t)$. When the error is very small, we may write

$$e = E_a \epsilon$$

that is, for small error as during steady state performance, the magnitude of the alternating voltage is proportional to the error, the latter being expressed in radians.

3. Closed loop response of linear system with ramp input

The closed loop transfer function is

$$\frac{\theta_0(s)}{\theta_i(s)} = \frac{1}{s^2 + 2\delta\omega_n s + \omega_n^2} \quad (2)$$

If the input to the system is a unit ramp, $R(s) = \frac{1}{s^2}$, the output is

$$\theta_0(s) = \frac{1}{s^2 (s^2 + 2\delta\omega_n s + \omega_n^2)} \quad (3)$$

for which the inverse transform is⁴

$$\theta_0(t) = t - \frac{2\delta}{\omega_n} + \frac{e^{-\delta\omega_n t}}{\omega_n \sqrt{1 - \delta^2}} \sin(\omega_d t + \phi) \quad (4)$$

where

$$\phi = \tan^{-1} \left[\frac{2\delta\sqrt{1 - \delta^2}}{2\delta^2 - 1} \right]$$

For step input, response time, peak time, settling time, etc. are defined with reference to the displacement of the controlled variable. But for a ramp input the abovementioned transient descriptors cannot be adjudged with reference to displacement. If the rise time, t_r , is to be determined based on the displacement of the controlled variable shaft, then from equation (4)

$$-\frac{2\delta}{\omega_n} + \frac{e^{-\delta\omega_n t_r}}{\omega_n \sqrt{1 - \delta^2}} \sin(\omega_d t_r + \phi) = 0 \quad (5)$$

i.e.,

$$2\delta\sqrt{1 - \delta^2} e^{\delta\omega_n t_r} = \sin(\omega_d t_r + \phi) \quad (6)$$

Determination of $\omega_n t_r$ from equation (6) is extremely laborious by analytical method. Therefore, a graphical procedure is followed. The exponential and sine curves are plotted for different values of $\omega_n t$ as shown in Fig. 2(i) and the point of intersection is determined. This is repeated for different values of damping ratio. From the sine and exponential curves, another graph is drawn as shown in Fig. 2(ii) connecting damping ratio and $\omega_n t_r$. It is seen from Fig. 2(ii) that the curve is asymptotic to a line $\delta = 0.29$. This observation leads to the conclusion that if the damping ratio is greater than 0.29, then the output shaft never reaches that of the input. However, for any

value of δ in the limit $0.29 < \delta < 1$, some variable in the system should have an overshoot. Therefore, to use displacement as the criterion to define the transient descriptors for the ramp input is incorrect and hence velocity has been chosen.

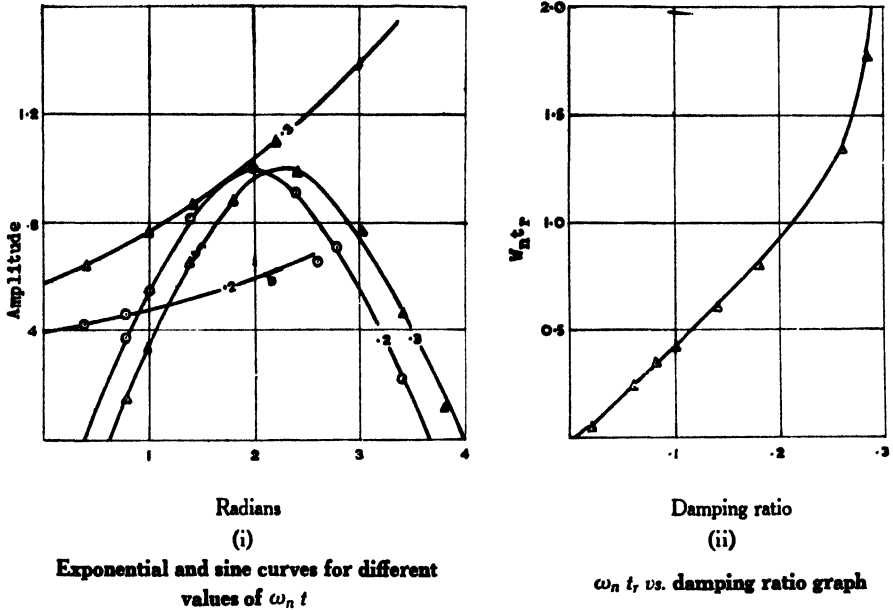


Fig. 2

4. Determination of descriptors

Differentiating equation (4) with respect to t , we get an expression for the velocity of the controlled variable.

Rise time

$$\frac{d\theta_0}{dt} = 1 - \frac{e^{-\delta \omega_n t}}{\omega_n \sqrt{1 - \delta^2}} [\omega_d \cos(\omega_d t + \phi) - \delta \omega_n \sin(\omega_d t + \phi)] \quad (7)$$

To determine the rise time, equate the exponential term in equation (7) to zero

$$\frac{e^{-\delta \omega_n t_r}}{\omega_n \sqrt{1 - \delta^2}} [\omega_d \cos(\omega_d t_r + \phi) - \delta \omega_n \sin(\omega_n t_r + \phi)] = 0 \quad (8)$$

i.e.,

$$\frac{e^{-\delta \omega_n t_r}}{\omega_n \sqrt{1 - \delta^2}} \neq 0$$

Therefore,

$$\frac{\omega_d}{\delta \omega_n} = \tan(\omega_d t_r + \phi)$$

$$\omega_n t_r \sqrt{1 - \delta^2} = \tan^{-1} \frac{\sqrt{1 - \delta^2}}{\delta} - \tan^{-1} \left(\frac{2\delta \sqrt{1 - \delta^2}}{2\delta^2 - 1} \right) \quad (9)$$

From equation (9), the values of $\omega_n t_r$ for different values of damping ratio are plotted as shown in Fig. 3.

Peak time

Similarly, the peak time is determined by equating the second derivative of equation (4) to zero

$$\begin{aligned}\frac{d^2\theta_0}{dt^2} &= \tan(\omega_d t_p + \phi) - \frac{2\delta\sqrt{1-\delta^2}}{2\delta^2-1} = 0 \\ \tan(\omega_d t_p + \phi) &= \tan \phi \\ \omega_d t_p &= \pi \\ \omega_n t_p &= \frac{\pi}{\sqrt{1-\delta^2}}\end{aligned}\quad (10)$$

Peak overshoot

Substituting $\omega_n t_p$ in equation (7), we have

$$\begin{aligned}\left(\frac{d\theta_0}{dt}\right)_{\max.} &= 1 - e^{-\frac{\delta\pi}{\sqrt{1-\delta^2}}} \\ \text{POR} &= 100 e^{-\frac{\delta\pi}{\sqrt{1-\delta^2}}}\end{aligned}\quad (11)$$

Settling time

Let us assume a tolerance band of F percent which is 2% in the problem chosen. The system is considered as having reached steady state, once the controlled variable stays confined within the tolerance band. The time required to do this is called 'settling time'. In equation (7), the exponential term should be equal to the tolerance band, i.e.,

$$\begin{aligned}\frac{100 e^{-\delta\omega_n t_s}}{\sqrt{1-\delta^2}} &= F \\ \omega_n t_s &= \frac{1}{\delta} \log\left(\frac{1}{F\sqrt{1-\delta^2}}\right)\end{aligned}\quad (12)$$

Equations (9), (10), (11), and (12) are expressed graphically in Fig. 3 for F equal to 2% with $\delta = 0.1$ to $\delta = 0.9$. Note that $0.1 \omega_n t_s$ and 0.1 POR are plotted to maintain a consistent scale. Values outside the plotted range can be calculated from equations (9) to (12).

5. Non-linear system with ramp input

Unlike a linear system, derivation of explicit expressions to study the behaviour of non-linear system is not possible. However, in cases where non-linear effects are large, analytical methods may not be adequate and solution may be possible only by numerical or graphical methods. A synchro is essentially a non-linear element. The differential equation of second order non-linear system using a synchro as the error detector is

$$J \frac{d^2\theta_0}{dt^2} + F \frac{d\theta_0}{dt} = K \sin \epsilon \quad (13)$$

where

$$\epsilon = \theta_i - \theta_0$$

Expressing equation (18) in terms of the error,

$$J \frac{d^2 \epsilon}{dt^2} + F \frac{d\epsilon}{dt} + K \sin \epsilon = J \frac{d^2 \theta_i}{dt^2} + F \frac{d\theta_i}{dt}$$

For a ramp input, $\frac{d^2 \theta_i}{dt^2} = 0$; and $\frac{d\theta_i}{dt} = \omega_i$, under all conditions for time $t > 0$.

The non-linear differential equation in terms of δ and ω_n is

$$\frac{d^2 \epsilon}{dt^2} + 2 \delta \omega_n \frac{d\epsilon}{dt} + \omega_n^2 \sin \epsilon = 2 \delta \omega_n \omega_i \quad (14)$$

Equation (14) can be written as

$$\epsilon'' + B \epsilon' + D \sin \epsilon = B \omega_i \quad (15)$$

where

$$\begin{aligned} \epsilon'' &= \frac{d^2 \epsilon}{dt^2} \\ \epsilon' &= \frac{d\epsilon}{dt} \end{aligned}$$

and B and D are constants.

Using Simpson's rule for integration,

$$\epsilon_n' = \epsilon_{n-2}' + [\epsilon_{n-2}'' + 4 \epsilon_{n-1}'' + \epsilon_n''] \frac{\Delta t}{3} \quad (16)$$

$$\epsilon_n = \delta_{n-2} + [\epsilon_{n-2}' + 4 \epsilon_{n-1}' + \epsilon_n'] \frac{\Delta t}{3} \quad (17)$$

Let

$$\epsilon = \epsilon_0 + \epsilon_0' t + \epsilon_0'' \frac{t^2}{2} + E t^3 \quad (18)$$

$$\epsilon' = \epsilon_0' + \epsilon_0'' t + 3 E t^2 \quad (19)$$

$$\epsilon'' = \epsilon_0'' + 6 E t \quad (20)$$

If ϵ_0 and ϵ_0' are the initial values, from equation (15), we get

$$\begin{aligned} \epsilon_0'' &= B \omega_i - B \epsilon_0' - D \sin \epsilon_0 \\ E &= - \frac{[\epsilon_0'' B + D \epsilon_0' \cos (\epsilon_0 + \epsilon_0' \Delta t)]}{6} \end{aligned}$$

The above numerical integration was carried out using the IBM 1620 electronic digital computer and the graphs were plotted for different values of damping ratio connecting the velocity of the controlled variable in terms of the input velocity and $\omega_n t$. From the family of response curves, the various non-linear transient descriptors were determined and the graphs plotted as shown in Fig. 3. It is seen from the graph that for ramp input the rise time and peak time for a non-linear system are larger than that for a linear system. But at the same time, a non-linear system has a smaller peak overshoot ratio and settling time. A non-linear system gives better performance than a linear system.

6. Linear system with step input

The equations for rise time, peak time, percentage overshoot ratio, and settling time can be derived in a similar manner as for the ramp input. Consider the time response of the controlled variable for a unit step,⁴

$$\theta_0(t) = 1 - \frac{e^{-\delta\omega_n t}}{\sqrt{1-\delta^2}} \sin(\omega_d t + \phi) \quad (21)$$

where

$$\phi = \tan^{-1} \frac{\sqrt{1-\delta^2}}{\delta}$$

Using equation (21), the following equations can be derived :

$$\omega_n t_r = \frac{\pi - \phi}{\sqrt{1-\delta^2}} \quad (22)$$

$$\omega_n t_p = \frac{\pi}{\sqrt{1-\delta^2}} \quad (23)$$

$$\text{POR} = 100 e^{-\frac{\pi \delta}{\sqrt{1-\delta^2}}} \quad (24)$$

$$\omega_n t_s = \left(\log \frac{1}{F\sqrt{1-\delta^2}} \right) \frac{1}{\delta} \quad (25)$$

Equations (22), (23), (24) and (25) are plotted in Fig. 4.

7. Non-linear system with step input

The non-linear differential equation describing the performance of the system is exactly the same as equation (13). Expressing the equation in terms of the damping ratio, natural frequency of oscillation and error, we have

$$\frac{d^2\epsilon}{dt^2} + 2\delta\omega_n \frac{d\epsilon}{dt} + \omega_n^2 \sin \epsilon = \frac{d^2\theta_i}{dt^2} + 2\delta\omega_n \frac{d\theta_i}{dt} \quad (26)$$

For a step input, $\frac{d^2\theta_i}{dt^2} = 0$ and $\frac{d\theta_i}{dt} = 0$, for all values of time $t > 0$.

The non-linear differential equation in terms of the error ϵ is

$$\frac{d^2\epsilon}{dt^2} + 2\delta\omega_n \frac{d\epsilon}{dt} + \omega_n^2 \sin \epsilon = 0$$

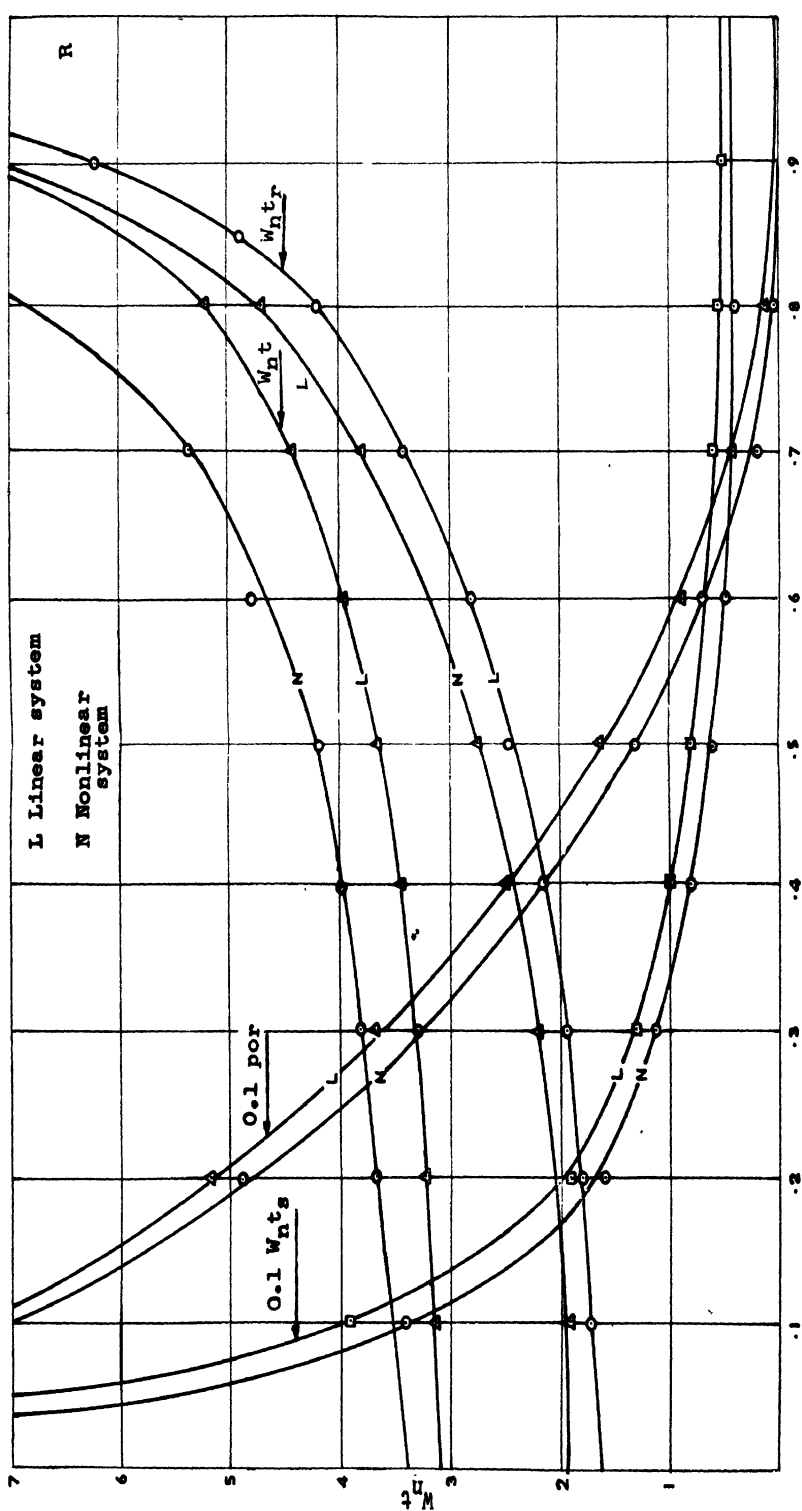
To solve equation (27) the same procedure of numerical integration was followed and the non-linear transient descriptors were determined and the graph is plotted as shown in Fig. 4.

Example 1

An uncompensated system subjected to a ramp input $R(s) = \frac{1}{s^2}$ gives

$$C(s) = \frac{16}{s^2(s^2 + 4s + 16)}$$

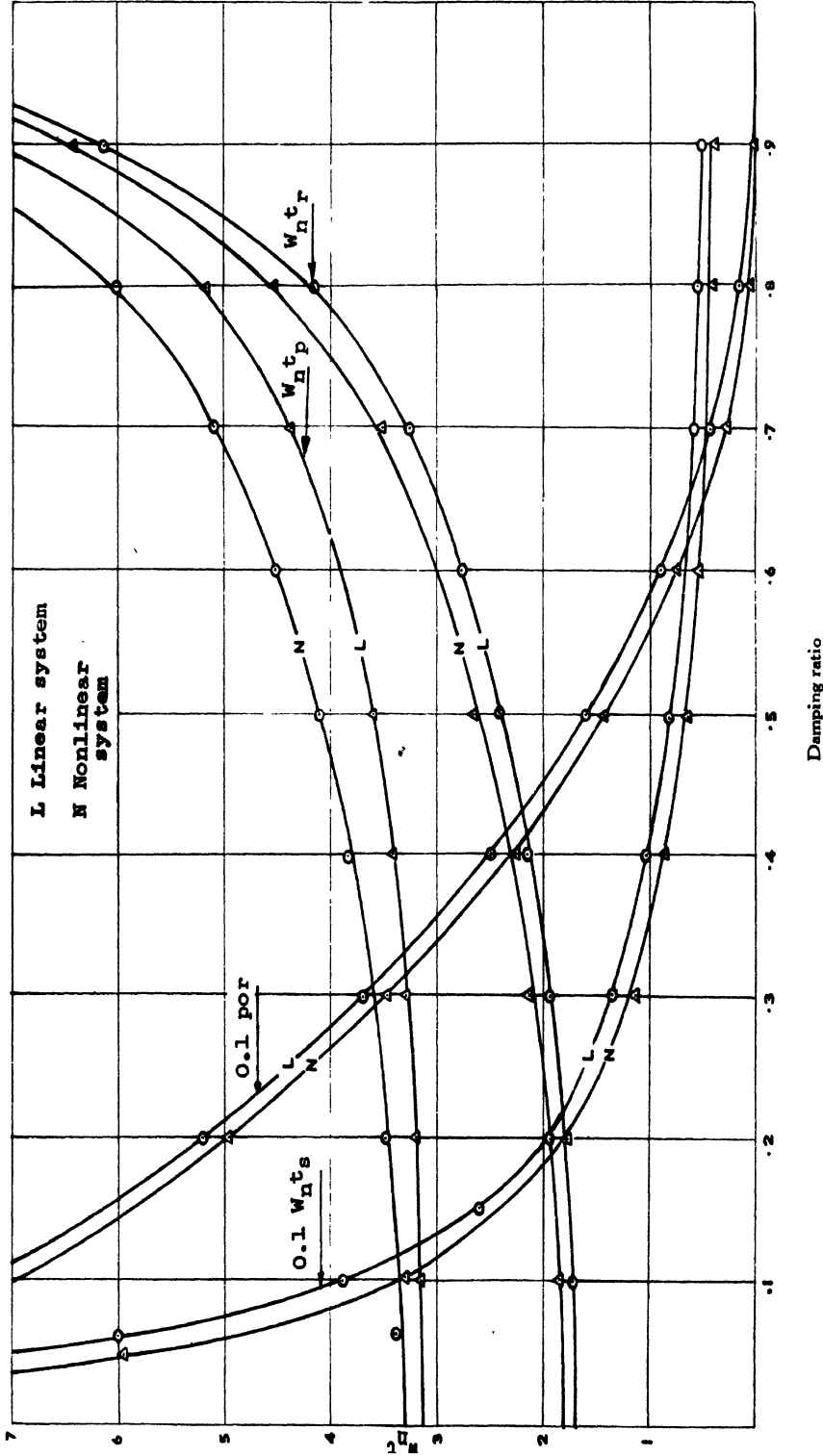
From this and equation (2), $\omega_n = 4$ and $\delta = 0.5$. Referring to the linear system in Fig. 3,



Damping ratio

Fig. 3

Values plotted give response of a second order linear and non-linear closed loop system for a unit ramp input



Response of a second order linear and non-linear closed loop system for a unit step input

$$\begin{aligned}\omega_n t_r &= 2.4, \text{ so, } t_r = 0.6 \text{ sec.} \\ \omega_n t_p &= 3.6, \text{ so, } t_p = 0.9 \text{ sec.} \\ 0.1 \omega_n t_s &= 0.8, \text{ so, } t_s = 2.0 \text{ sec.} \\ 0.1 \text{ POR} &= 1.6, \text{ so, POR} = 16\%\end{aligned}$$

Non-linear

$$\begin{aligned}\omega_n t_r &= 2.75, \text{ so, } t_r = 0.69 \text{ sec.} \\ \omega_n t_p &= 4.20, \text{ so, } t_p = 1.05 \text{ sec.} \\ 0.1 \omega_n t_s &= 0.60, \text{ so, } t_s = 1.5 \text{ sec.} \\ 0.1 \text{ POR} &= 1.30, \text{ so, POR} = 13\%\end{aligned}$$

Example 2

The above system is subjected to a step input $R(s) = \frac{1}{s}$.

Linear

$$\begin{aligned}\omega_n t_r &= 2.4, \text{ so, } t_r = 0.6 \text{ sec.} \\ \omega_n t_p &= 3.6, \text{ so, } t_p = 0.9 \text{ sec.} \\ 0.1 \omega_n t_s &= 0.811, \text{ so, } t_s = 2.03 \text{ sec.} \\ 0.1 \text{ POR} &= 1.600, \text{ so, POR} = 16\%\end{aligned}$$

Non-linear

$$\begin{aligned}\omega_n t_r &= 2.65 \text{ so, } t_r = 0.66 \text{ sec.} \\ \omega_n t_p &= 4.20 \text{ so, } t_p = 1.05 \text{ sec.} \\ 0.1 \omega_n t_s &= 0.72 \text{ so, } t_s = 1.8 \text{ sec.} \\ 0.1 \text{ POR} &= 1.50 \text{ so, POR} = 15\%\end{aligned}$$

8. Conclusions

It is easy to analyze a linear system but difficult to synthesize. A linear system is costly in design and gives a poor transient performance as seen from Figs. 3 and 4. The prime requisite of a control system is that it should have a small overshoot and settling time for a given damping ratio. From the graphs it is seen that a non-linear system has a better transient performance than a linear system. The rise time and peak time are found larger for a non-linear system. This may be due to the fact that the synchro gain is small when the error is large. Since the natural frequency of oscillation is proportional to the root of the gain, a small value of ω_n gives a large rise time and correspondingly a large peak time. For a given viscous friction, the damping ratio changes as the gain changes and, therefore, when the gain is small, the damping ratio is large and hence it gives a smaller overshoot. However, when the controlled variable is within the tolerance band, the gain of the synchro is large for the reason that the error is small. Therefore, ω_n is greater than what it was at the beginning and hence gives a smaller settling time.

9. Acknowledgments

The author expresses his deep sense of gratitude to the authorities of the Computer Centre in the Fundamental Engineering Research Establishment of the College of Engineering, Guindy, for having made available the services of the IBM 1620 electronic digital computer.

10. References

1. G. A. Jones. 'Finding Transient Descriptors Graphically-I'. *Control Engineering*, October 1965, p. 97.
2. Cunningham. 'Introduction to Non-linear Analysis'. *McGraw-Hill Book Co., Inc.*, New York, 1958.
3. P. L. Taylor. 'Servomechanisms'. *Orient Longmans, Ltd.*, 1960.
4. V. D. Toro and S. Parker. 'Control Systems Engineering'. *McGraw-Hill Book Co., Inc.*, 1960.

About the Authors

Shri J. S. Gupta

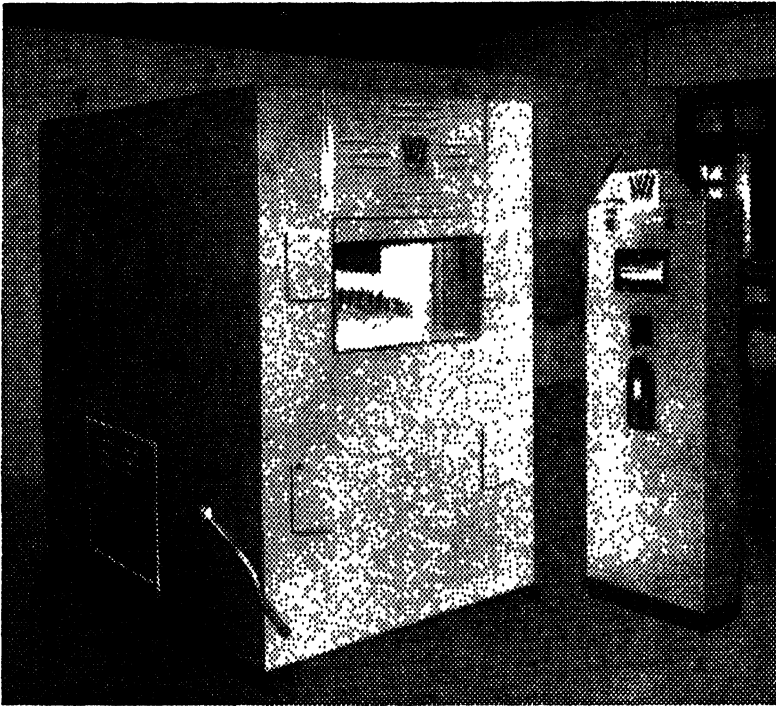
Shri Gupta graduated in Electrical Engineering from Rajputana University in 1951. After having industrial and practical experience of about 3 years, he worked in Patna University as Assistant Professor of Electrical Engineering from 1954 to 1960, and obtained his Master's degree in Technology in Control System Engineering in 1960. At present he is Reader in Electrical Engineering at the Banaras Hindu University, Varanasi.

Shri T. R. Natesan

Shri Thirumalaipatty Ramaswami Natesan had his high school and collegiate education at St. Joseph's College High School and College, Tiruchirappalli, from 1944 to 1953. He received the B.E. (Hons.) Degree in Electrical Engineering in May 1957. He entered College of Engineering, Guindy, in July 1957, and received the M.Sc. Degree in Engineering in August 1958. He was appointed as Lecturer in Electrical Engineering after the completion of training in October 1962. At present he is an Assistant Professor in Electrical Engineering and a Programmer in the Computer Centre of the College of Engineering, Guindy. His field of interest is control engineering.

Shri K. V. Rama Murthy

After having passed his M.Sc. in Applied Physics from Andhra University in 1958, Shri Murthy taught Applied Sciences for a short period in the Andhra Polytechnic, Kakinada. He then joined the Central Water and Power Research Station, Poona, as a Research Assistant and worked on hydraulic model experiments for over two years. During the period he developed a capacitive wave height recorder. He then joined the Research and Development Organization, Ministry of Defence, and worked about 1½ years on the development of homing devices for infra red guidance. He again joined the Central Water and Power Research Station as a research officer and is continuing in the same cadre now. He had worked on the development of direct discrete analogues apart from solving a number of specific problems of interest to the projects connected with river valley developments using the customary electrical analogue tray method. It is in this connection the flood routing analogue reported in the paper has been developed.



WELLMAN INCANDESCENT ELECTRIC BOX TYPE FURNACES ARE INSTALLED BY MAJOR ENGINEERING INDUSTRIES

10/11/55

More and more major industries are using Wellman Incandescent Standard Electric Box Type Furnaces. Normalising, Annealing, Hardening, Pack Carburising, Re-heating, Forging—all these are possible in the box type unit. For economical mass production or jobbing shop versatility these furnaces are equally suited. With small modifications these furnaces can be adopted for heat treatments requiring protective gas atmosphere.

Wellman Incandescent also manufacture standard electrode salt baths for all recognised treatments including cyanide hardening, isothermal annealing, straight hardening

and forced air circulation furnaces for tempering, subcritical annealing, ageing, solution treatment of aluminium alloys.

Some industries served by Wellman are : Aero Engine, Automobile, Ball & Roller Bearing, Foundry, Machine Tool, Spring, Tools & Dies, Transformer, Tube, Wire, Metal Working.



For further details please write to
**WELLMAN INCANDESCENT
INDIA LTD.**
8, Harington Street, Calcutta-16

NETWORKS REALIZING BISEXITIC MINIMUM POSITIVE REAL FUNCTIONS*

J. G. Advani

Non-member

and

P. K. Baokar

Non-member

Electrical Engineering Department, Faculty of Technology and Engineering, Baroda

Summary

Network structures containing seven, ten and twelve elements and capable of realizing bisexitic minimum positive real functions having $\text{Re. } \mathcal{Z}(j\omega) = 0$ at three real and distinct frequencies and also having $\mathcal{Z}(0) = \mathcal{Z}(\infty)$ are presented.

Conditions on the coefficients of given $\mathcal{Z}(s)$ so that it is realizable by any of these networks are found out. The values of the elements in the various networks are found out. The conditions on the coefficients of a bisexitic positive real function so that it has $\text{Re. } \mathcal{Z}(j\omega) = 0$ at three real and distinct frequencies are also presented.

1. Introduction

A good deal of work has been done on the realization of minimum biquadratic^{1,2,3} and biquartic^{4,5} functions having $\text{Re. } \mathcal{Z}(j\omega) = 0$ at one and two real and distinct frequencies respectively. All the workers on these functions have developed bridge type networks for the realization of such functions. Bridge networks require much less number of elements than those required to realize by by routine Bott-Duffin synthesis procedure. Realization of biquadratic and biquartic impedance functions by bridge networks is possible under certain conditions amongst the coefficients of the given function.

All the networks presented in the above said references have been developed by using a theorem from graph theory.⁶ This theorem is also used here to derive network structures for a bisexitic minimum positive real function. [A function $F(s)$ is a positive real function when (i) $F(s)$ is real for real s and (ii) $\text{Re. } F(s) \geq 0$ for $\text{Re. } s \geq 0$. A positive real function is said to be minimum if (i) it has no poles and zeros on frequency axis, and (ii) the $\text{Re. } F(j\omega)$ is zero at one or more real and distinct frequencies.] This theorem states that a network which does not contain (i) one-element path between input terminals, and (ii) one-element cutset of input terminals, can realize a minimum positive real function.

*Written discussion on this paper will be received until September 30, 1967.

This paper (re-drafted) was received on March 16, 1967.

For a bisextic minimum positive real function with $Z(0) = Z(\infty)$, at least one resistive and six reactive elements are required. The only possible 30 networks with seven elements and satisfying path and cutset requirements are shown in Figs. 1 to 8. Networks containing two resistive and eight or ten reactive elements are also presented.

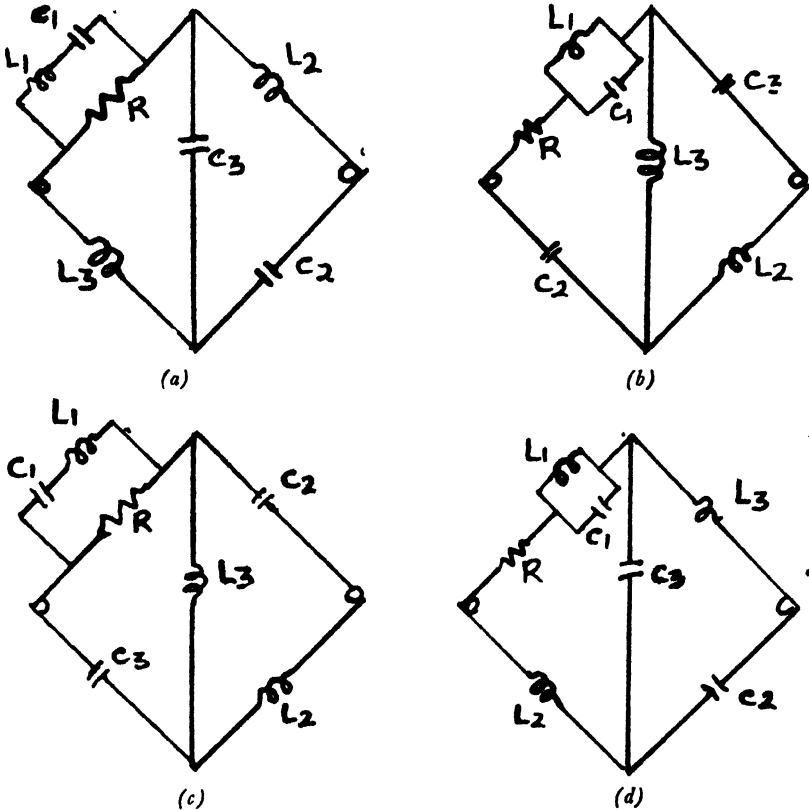


Fig. 1

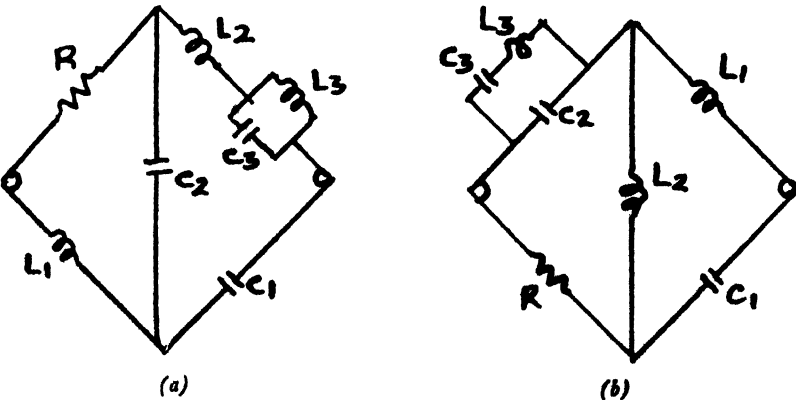


Fig. 2 (contd.)

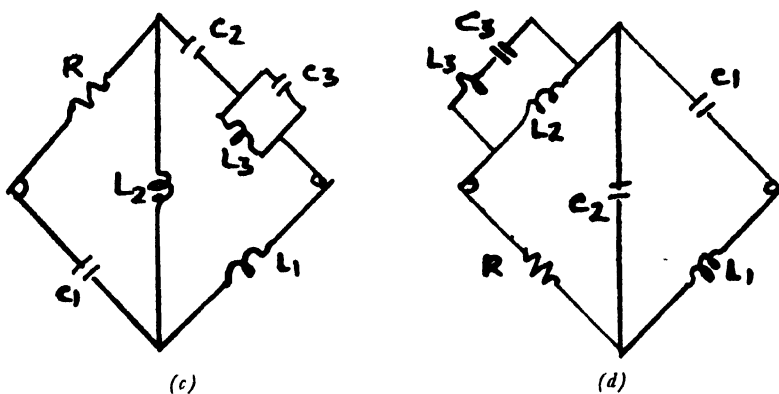


Fig. 2

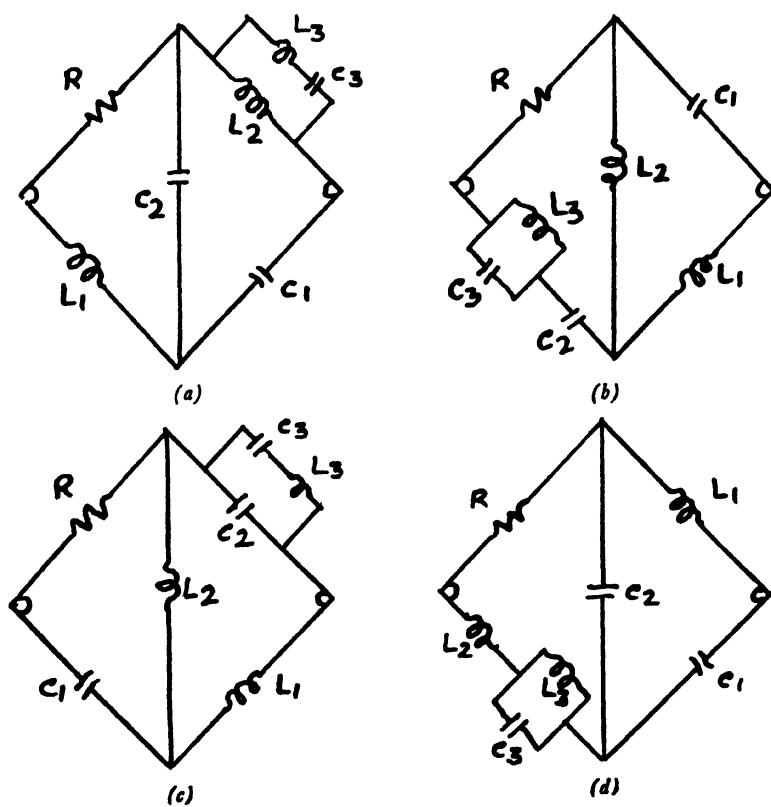


Fig. 3

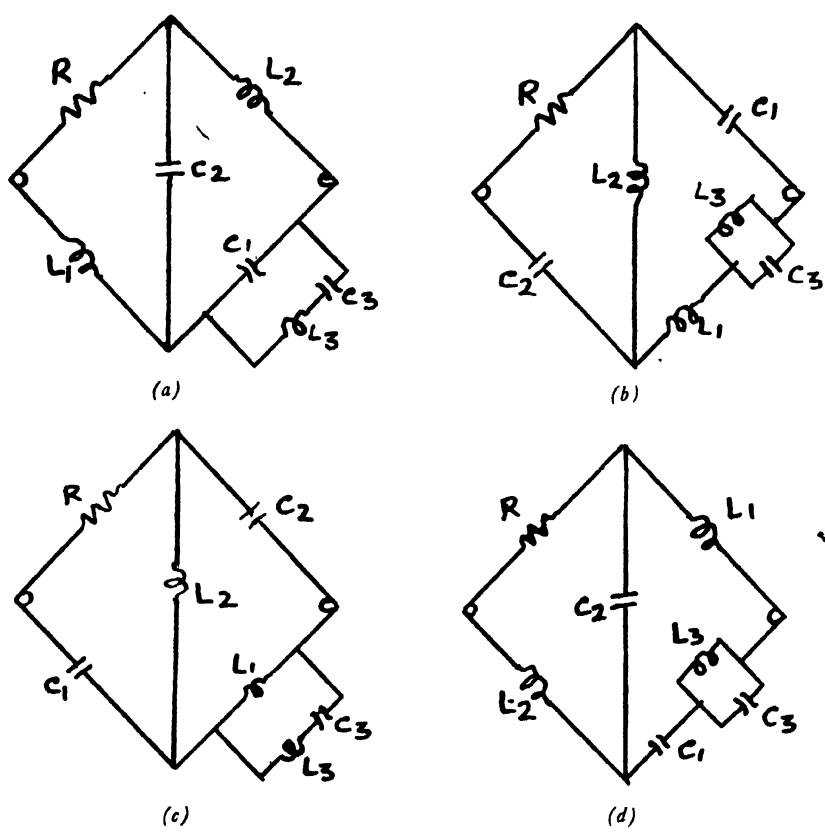


Fig. 4

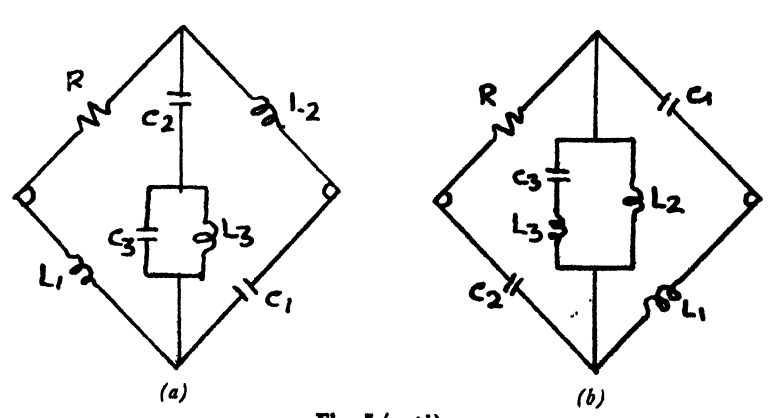


Fig. 5 (contd.)

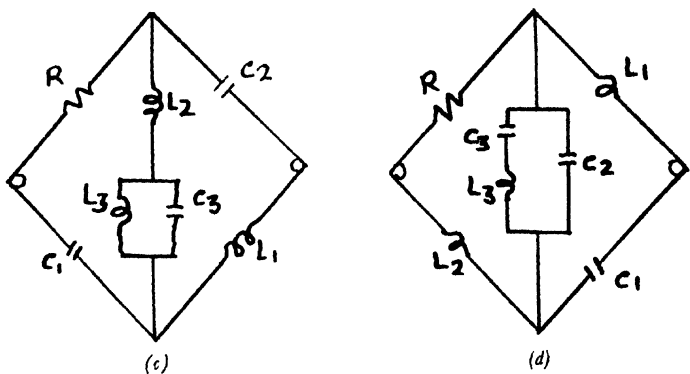


Fig. 5

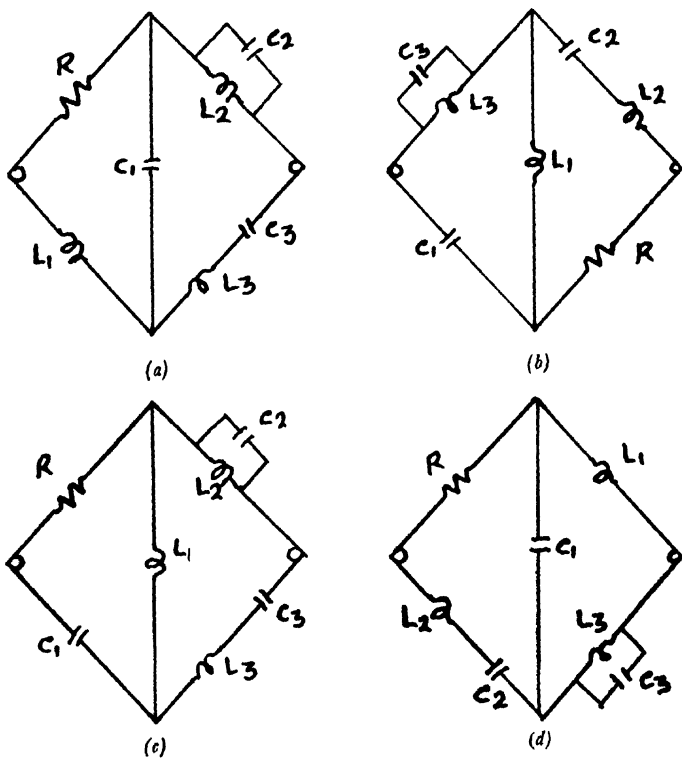


Fig. 6

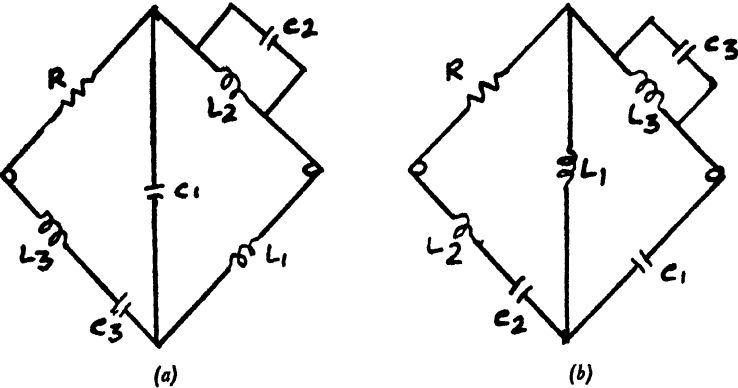


Fig. 7

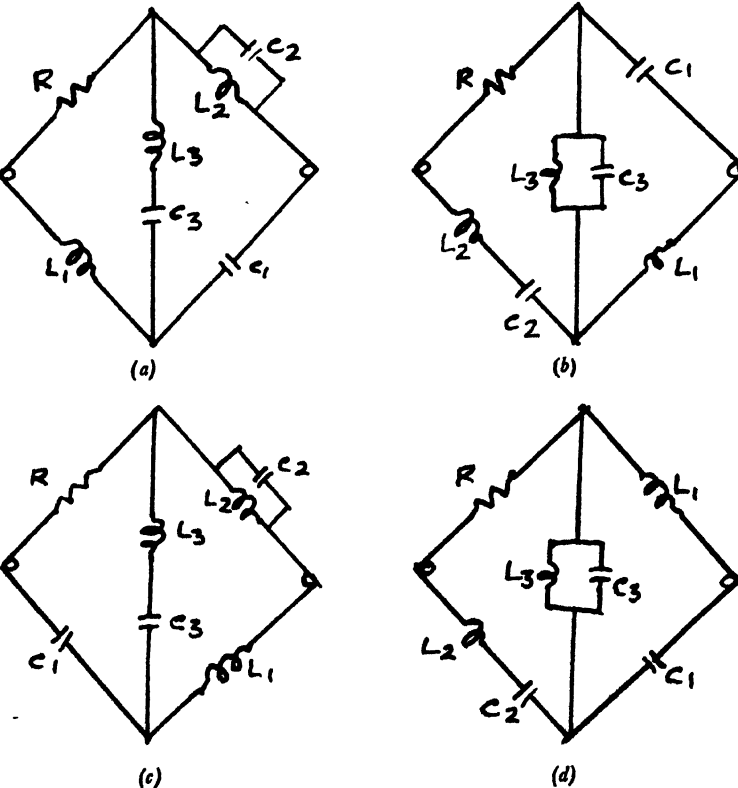


Fig. 8

2. Conditions on a bisexitic PR-function to have $\text{Re. } \mathcal{Z}(j\omega) = 0$ at three real and distinct frequencies

The bisexitic minimum positive real function,

$$\mathcal{Z}(s) = K \frac{s^6 + a_5 s^5 + a_4 s^4 + a_3 s^3 + a_2 s^2 + a_1 s + a_0}{s^6 + b_5 s^5 + b_4 s^4 + b_3 s^3 + b_2 s^2 + b_1 s + b_0} \quad (1)$$

will have its real part zero at three frequencies if the following conditions are satisfied:

$$\sqrt{a_0 b_0} (a_4 + b_4 - a_5 b_5)^2 + 4 (a_2 b_0 + b_2 a_0 - a_1 b_1) = 4 \sqrt{a_0 b_0} (a_2 + b_2 + a_4 b_4 - a_3 b_5 - b_3 a_5) \quad (2)$$

$$(a_4 + b_4 - a_5 b_5) (a_2 b_0 + b_2 a_0 - a_1 b_1) + 4 a_0 b_0 = 2 \sqrt{a_0 b_0} (a_0 + b_0 + a_4 b_2 + b_4 a_2 - a_5 b_1 - a_3 b_3 - b_5 a_1) \quad (3)$$

$$(a_2 b_0 + b_2 a_0 - a_1 b_1)^2 + 4 (a_0 b_0)^{\frac{3}{2}} (a_4 + b_4 - a_5 b_5) = 4 a_0 b_0 (a_4 b_0 + b_4 a_0 + a_2 b_2 - a_3 b_1 - b_3 a_1)$$

and the frequencies are assured to be real and distinct if

$$a_4 + b_4 - a_5 b_5 > 0 \quad (5)$$

$$a_2 b_0 + b_2 a_0 - a_1 b_1 > 0 \quad (6)$$

$$27 C_1^2 + 4 C_1 A_1^3 + 4 B_1^3 - A_1^2 B_1^2 - 18 A_1 B_1 C_1 < 0 \quad (7)$$

where

$$A_1 = \frac{a_4 + b_4 - a_5 b_5}{2}; \quad B_1 = \frac{a_2 b_0 + b_2 a_0 - a_1 b_1}{2 \sqrt{a_0 b_0}}; \quad C_1 = \sqrt{a_0 b_0}$$

3. Conditions and element-values

The $\mathcal{Z}(s)$ of equation (1) is considered. This impedance function can be realized by any one of the networks of Figs. 1 to 8, if and only if the coefficients of $\mathcal{Z}(s)$ satisfy certain conditions. These conditions and element-values are derived as given below. Considering the network of Fig. 1(a),

$$\begin{aligned} & s^6 + \frac{S_2 + S_3}{R} s^5 + \left(\frac{S_1 + S_2 + S_3}{L_1} + \frac{S_2 + S_3}{L_2} + \frac{S_2}{L_3} \right) s^4 \\ & + \frac{1}{R} \left(\frac{S_1 S_2 + S_2 S_3}{L_1} + \frac{S_2 S_3}{L_3} \right) s^3 + \left(\frac{S_2 S_3}{L_2 L_3} + \frac{S_2 S_3}{L_1 L_3} + \frac{S_1 S_3}{L_1 L_3} + \right. \\ & \left. \frac{S_1 S_2}{L_1 L_2} + \frac{S_1 S_3}{L_1 L_3} \right) s^2 + \frac{S_1 S_2 S_3}{R L_1 L_2 L_3} s + \frac{S_1 S_2 S_3}{L_1 L_2 L_3} \\ \mathcal{Z}(s) = R & \frac{s^6 + R \left(\frac{1}{L_1} + \frac{1}{L_3} \right) s^5 + \left(\frac{S_1}{L_1} + \frac{S_2 + S_3}{L_2} + \frac{S_3}{L_3} \right) s^4}{s^6 + \frac{S_2 + S_3}{R} s^5 + \left(\frac{S_1 + S_2 + S_3}{L_1} + \frac{S_2 + S_3}{L_2} + \frac{S_2}{L_3} \right) s^4} \\ & + R \left[\frac{(S_2 + S_3)(L_1 + L_3)}{L_1 L_2 L_3} + \frac{S_1 S_3}{L_1 L_3} \right] s^3 + \left(\frac{S_2 S_3}{L_2 L_3} + \frac{S_1 S_3}{L_1 L_3} + \frac{S_1 S_2}{L_1 L_2} \right. \\ & \left. + \frac{S_1 S_3}{L_1 L_3} \right) s^2 + R \frac{(S_1 S_2 + S_2 S_3 + S_1 S_3)}{L_1 L_2 L_3} s + \frac{S_1 S_2 S_3}{L_1 L_2 L_3} \end{aligned} \quad (8)$$

Comparing the corresponding coefficients of equations (1) and (8), thirteen equations are obtained. Values of seven elements in terms of the coefficients of $Z(s)$ of equation (1) can be found out from these equations. As there are thirteen equations and seven unknowns, six conditions on the coefficients of $Z(s)$ of equation (1) must be satisfied so that it can be realized by the network of Fig. 1(a). These conditions after manipulations and simplifications are as follows :

$$\frac{a_5 a_0 + a_5 b_5 + b_4 - a_4}{a_1} + \frac{a_1 b_1 + a_0 (b_2 - a_2)}{a_0 (a_5 b_5 + b_4 - a_4)} = b_3 \quad (9)$$

$$\frac{a_5 b_5 + b_4 - a_4}{a_1 b_1 + a_0 (b_2 - a_2)} + \frac{a_5 \{a_1 b_1 + a_0 (b_2 - a_2)\}}{a_0^2 a_1 (a_5 b_5 + b_4 - a_4)} = \frac{b_3}{a_0 a_1} \quad (10)$$

$$4 a_0^3 a_5 b_5 + a_1^2 b_1^2 - a_0^2 (b_2 - a_2)^2 = 4 b_3 a_1 a_0^2 \quad (11)$$

$$a_0 = b_0 \quad (12)$$

$$b_3 = \frac{a_0^2 (a_5 b_5 + b_4 - a_4)}{a_1 b_1 + a_0 (b_2 - a_2)} + \frac{\{a_1 b_1 + a_0 (b_2 - a_2)\} \{2 a_0 a_5 + a_1 (a_5 b_5 + b_4 - a_4)\}}{2 a_0 a_1 (a_5 b_5 + b_4 - a_4)} \quad (13)$$

$$\frac{a_0^2 a_1 (a_5 b_5 + b_4 - a_4) [(a_5 b_5 + a_4 - b_4) \{a_1 b_1 + a_0 (b_2 - a_2)\} - 4 a_0 a_1 b_5]}{\{a_1 b_1 + a_0 (b_2 - a_2)\} [a_5 \{a_1^2 b_1^2 - a_0^2 (a_2 - b_2)^2\} - 4 a_0 a_1^2 b_1]} = 1 \quad (14)$$

The element values are given in Table 1.

Table 1

Network of Fig. 1 (a)

Element-values :

$$R = K, L_2 = \frac{K a_1}{a_0}$$

$$S_1 = \frac{2 K a_0 a_1 [a_5 \{a_1 b_1 + a_0 (b_2 - a_2)\} - 2 a_0 a_1]}{a_5 \{a_1^2 b_1^2 - a_0^2 (a_2 - b_2)^2\} - 4 a_0 a_1^2 b_1}$$

$$S_2 = \frac{2 K a_0 a_1}{a_1 b_1 + a_0 (b_2 - a_2)}$$

$$S_3 = \frac{K [a_5 \{a_1 b_1 + a_0 (b_2 - a_2)\} - 2 a_0 a_1]}{a_1 b_1 + a_0 (b_2 - a_2)}$$

$$L_1 = \frac{2 K [2 a_0 a_1 - a_5 \{a_1 b_1 + a_0 (b_2 - a_2)\}]}{4 a_0 a_1 b_5 + \{a_1 b_1 + a_0 (b_2 - a_2)\} (b_4 - a_4 - a_5 b_5)}$$

$$L_3 = \frac{2 K [2 a_0 a_1 - a_5 \{a_1 b_1 + a_0 (b_2 - a_2)\}]}{\{a_1 b_1 + a_0 (b_2 - a_2)\} (a_4 - b_4 - a_5 b_5)}$$

Conditions :

1. $\frac{a_5 a_0}{a_1} + \frac{a_5 b_5 + b_4 - a_4}{2} + \frac{a_1 b_1 + a_0 (b_2 - a_2)}{a_0 (a_5 b_5 + b_4 - a_4)} = b_4$
2. $\frac{a_5 b_5 + b_4 - a_4}{a_1 b_1 + a_0 (b_2 - a_2)} + \frac{a_5 \{a_1 b_1 + a_0 (b_2 - a_2)\}}{a_0^2 a_1 (a_5 b_5 + b_4 - a_4)} = \frac{a_3}{a_0 a_1}$
3. $4 a_0^3 a_5 b_5 + a_1^2 b_1^2 - a_0^2 (b_2 - a_2)^2 = 4 b_3 a_1 a_0^2$
4. $a_0 = b_0$
5. $\frac{a_0^2 (a_5 b_5 + b_4 - a_4)}{a_1 b_1 + a_0 (b_2 - a_2)} + \frac{\{a_1 b_1 + a_0 (b_2 - a_2)\} \{2 a_0 a_5 + a_1 (a_5 b_5 + b_4 - a_4)\}}{2 a_0 a_1 (a_5 b_5 + b_4 - a_4)} = b_2$
6. $\frac{a_0^2 a_1 (a_5 b_5 + b_4 - a_4) [(a_5 b_5 + a_4 - b_4) \{a_1 b_1 + a_0 (b_2 - a_2)\} - 4 a_0 a_1 b_5]}{\{a_1 b_1 + a_0 (b_2 - a_2)\} [a_5 \{a_1^2 b_1^2 - a_0^2 (a_2 - b_2)\} - 4 a_0 a_1^2 b_1]} = 1$
7. $L_3 (S_2 + S_3)^2 > 4 L_2 S_2 S_3$
8. $\frac{S_1}{L_1} \neq \frac{(S_2 + S_3) \pm \sqrt{(S_2 + S_3)^2 - \frac{L_2 S_2 S_3}{L_3}}}{2 L_2}$

For the elements to be positive, the following inequalities should be satisfied :

$$a_5 (a_1 b_1 + a_0 b_2) > a_0 (a_2 a_5 + 2 a_1) \quad (15)$$

$$a_5 a_1^2 b_1^2 > a_0^2 a_5 (a_5 - b_2)^2 + 4 a_0 a_1^2 b_1 \quad (16)$$

$$a_5 b_5 > |b_4 - a_4| \quad (17)$$

$$(a_5 b_5 + a_4 - b_4) \{a_1 b_1 + a_0 (b_2 - a_2)\} > 4 a_0 a_1 b_5 \quad (18)$$

It can be proved that these inequalities could be automatically satisfied if the six conditions of equations (9) to (14) are satisfied and in addition $\mathcal{Z}(s)$ of equation (1) is a *PR*-function.

From the six conditions of equations (9) to (14) it is not guaranteed that $\mathcal{Z}(s)$ realized by this network has $\text{Re. } \mathcal{Z}(j\omega) = 0$ at three real and distinct frequencies. So for $\mathcal{Z}(s)$ to be realizable by this network and to have $\text{Re. } \mathcal{Z}(j\omega) = 0$ at three real and distinct frequencies simultaneously, all the six conditions given in equations (9) to (14) and those of equations (2) to (7) should be satisfied. It is possible that some of the conditions of these two sets might clash.

To clear this point the network of Fig. 1(a) is converted to network of Fig. 9 by delta-star transformation. The values of impedances appearing in Fig. 9 would be

$$\mathcal{Z}_1 = \frac{s L_2 C_3}{s^2 L_2 C_3 C_3 + C_2 + C_3} \quad (19)$$

$$\mathcal{Z}_2 = \frac{s L_2 C_3}{s^2 L_2 C_3 C_3 + C_2 + C_3} \quad (20)$$

$$\mathcal{Z}_3 = \frac{L_2 L_3 C_3 C_3 s^4 + L_3 (C_2 + C_3) s^2 + 1}{s (s^2 L_2 C_3 C_3 + C_2 + C_3)} \quad (21)$$

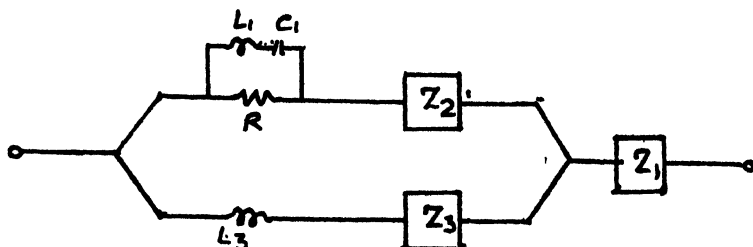


Fig. 9

The real part of $Z(s)$ of the network of Fig. 1(a) is zero at the zeros of $(s L_3 + Z_3)$ and $(s L_1 + \frac{1}{s C_1})$.

The zeros of $(s L_3 + Z_3)$ are given by equation (22).

$$s_2^2 \text{ or } s_3^2 = \frac{-L_3 (C_2 + C_3) \pm \sqrt{\{L_3^2 (C_2 + C_3)^2 - 4 L_2 L_3 C_2 C_3\}}}{2 L_2 L_3 C_2 C_3} \quad (22)$$

and that of $(s L_1 + \frac{1}{s C_1})$ is

$$s_1^2 = -\frac{1}{L_1 C_1}$$

The condition for the frequencies given by equation (22) to be real is given

$$L_3 (C_2 + C_3)^2 > 4 L_2 C_2 C_3 \quad (24)$$

and for these three frequencies to be distinct, the frequency given by equation (23) should not be equal to either of the frequencies given by equation (22).

$$s_1^2 \neq s_2^2 \text{ or } s_3^2 \quad (25)$$

Thus six conditions of equations (9) to (14) along with the two inequality conditions of equations (24) and (25) are sufficient conditions for $Z(s)$ of equation (1) to be realizable by network of Fig. 1(a) and to have $\text{Re. } Z(j\omega) = 0$ at three real and distinct frequencies simultaneously. These conditions are given in Table 1.

By similar procedure the conditions and element-values for other networks are found out and tabulated in Tables 2 to 8. The conditions and element-values for other networks [Figs. 1(b), 1(c), 1(d) 8(b), 8(c) and 8(d)] can be obtained from the principle of duality or by substitution of $s = \frac{1}{p}$.

Table 2

Network of Fig. 2(a)

Element-values :

$$R = K, L_1 = \frac{K}{b_5}$$

$$L_2 = \frac{2 K a_0 a_5^2 b_5}{a_0 a_5 b_5 (a_4 + b_4 - a_5 b_5) - 2 a_1 b_1}$$

$$\begin{aligned}
 L_3 &= \frac{K [a_0 a_1 a_5 b_5 (a_4 + b_4 - a_5 b_5) - 2 a_1^2 b_1 - 2 a_0^2 a_5^2 b_5]}{a_0^2 a_5 b_5 (a_4 + b_4 - a_5 b_5) - 2 a_0 a_1 b_1} \\
 S_1 &= \frac{K (a_5 b_5 + a_4 - b_4)}{2 b_5} \\
 S_2 &= \frac{K (a_5 b_5 + b_4 - a_4)}{2 b_5} \\
 S_3 &= \frac{2 K b_1 a_5 [a_0 a_1 a_5 b_5 (a_4 + b_4 - a_5 b_5) - 2 a_1^2 b_1 - 2 a_0^2 a_5^2 b_5]}{[a_0 a_5 b_5 (a_4 + b_4 - a_5 b_5) - 2 a_1 b_1]^2}
 \end{aligned}$$

Conditions :

1. $a_0 = b_0$
2. $4 a_0 a_5 b_5^2 = b_1 \{a_5^2 b_5^2 - (a_4 - b_4)^2\}$
3. $a_1 b_1 (a_4 - b_4) = a_0 a_5 b_5 (a_2 - b_2)$
4. $a_0^2 a_5 b_5^2 + a_1 b_1^2 = a_0 b_1 a_3 b_5$
5. $2 b_3 = b_5 (a_4 + b_4 - a_5 b_5)$
6. $\frac{b_1}{b_3} + \frac{2 a_1 b_5}{a_5 b_5 + b_4 - a_4} + \frac{a_0 a_5 b_3 - a_1 b_1}{b_1 a_5} = a_2$
7. $27 C_1^2 + 4 C_1 A_1^3 + 4 B_1^3 - A_1^2 B_1^2 - 18 A_1 B_1 C_1 < 0$

where

$$\begin{aligned}
 A_1 &= \frac{s_1}{L_2} + \frac{s_2}{L_3} + \frac{s_3}{L_3} \\
 B_1 &= \frac{s_3 (s_1 + s_2)}{L_2 L_3} + \frac{s_1 s_2}{L_1 L_3} \\
 C_1 &= \frac{s_1 s_2 s_3}{L_1 L_2 L_3}
 \end{aligned}$$

Table 3

Network of Fig. 3(a)

Element-values :

$$\begin{aligned}
 R &= K, L_1 = \frac{K}{b_5}, L_2 = \frac{K a_1}{a_0} \\
 S_1 &= \frac{K (a_5 b_5 + a_4 - b_4)}{2 b_5}, S_2 = \frac{K (a_5 b_5 - a_4 + b_4)}{2 b_5} \\
 L_3 &= \frac{2 K a_1 a_5 \{(a_4 - b_4)^2 - a_4^2 b_5^2\}}{8 a_1^2 b_5 + \{(a_4 - b_4)^2 - a_5^2 b_5^2\} \{a_1 (a_4 + b_4 - a_5 b_5) - 2 a_0 a_5\}} \\
 S_3 &= \frac{8 K a_1^2 a_5 b_5}{\{a_1 (a_5 b_5 - a_4 - b_4) + 2 a_0 a_5\} \{(a_4 - b_4)^2 - a_5^2 b_5^2\} - 8 a_1^2 b_5}
 \end{aligned}$$

Conditions :

1. $a_0 = b_0$
2. $a_0 a_5 b_5 (a_2 - b_2) = a_1 b_1 (a_4 - b_4)$
3. $b_1 \{a_5^2 b_5^2 - (a_4 - b_4)^2\} = 4 a_0 a_5 b_5^2$
4. $b_5 (a_4 + b_4 - a_5 b_5) = 2 b_3$
5. $a_1 (a_4 - b_4)^2 + a_5 (a_2 - b_2)^2 = (a_2 - b_2) (a_4 - b_4) a_3$
6. $a_1 b_1 \frac{(a_5 b_5 + a_4 - b_4)^2}{4 a_0 a_5^2 b_5^2} + \frac{a_0 b_3}{b_1} + \frac{b_1}{b_5} = a_2$
7. $27 C_1^2 + 4 C_1 A_1^3 + 4 B_1^3 - A_1^2 B_1^2 - 18 A_1 B_1 C_1 < 0$

where

$$A = \frac{S_1 + S_2 + S_3}{L_3} + \frac{S_1 + S_2}{L_2} ; B_1 = \frac{S_3 (S_1 + S_2)}{L_2 L_3} + \frac{S_1 S_2}{L_1 L_2} + \frac{S_1 S_3}{L_1 L_3}$$

$$C_1 = \frac{S_1 S_2 S_3}{L_1 L_2 L_3}$$

Table 4

Network of Fig. 4(a)

Element-values :

$$R = K, L_1 = \frac{K}{b_5}, L_2 = \frac{K a_1}{a_0}$$

$$L_3 = \frac{K a_0 \{a_5^2 b_5^2 - (a_4 - b_4)^2\}}{4 a_1 b_5 \{b_1 [a_5^2 b_5^2 - (a_4 - b_4)^2] - 4 a_0 a_5 b_5^2\}}$$

$$S_1 = \frac{K (a_5 b_5 + a_4 - b_4)}{2 b_5}, S_2 = \frac{K (a_5 b_5 - a_4 + b_4)}{2 b_5}$$

$$S_3 = \frac{K a_0 \{a_5^2 b_5^2 - (a_5 - b_4)^2\}}{b_1 \{a_5^2 b_5^2 - (a_4 - b_4)^2\} - 4 a_0 a_5 b_5^2}$$

Conditions :

1. $a_0 = b_0$
2. $4 a_0 a_1 b_5 = (a_5 b_5 + b_4 - a_4) \{a_1 b_1 + a_0 (a_2 - b_2)\}$
3. $2 a_4 b_5 = 2 b_3 + b_5 (a_5 b_5 + a_4 - b_4)$
4. $4 a_0 a_3 b_5 = 4 a_1 b_1 - a_0 \{a_5^2 b_5^2 - (a_4 - b_4)^2\}$
5. $\frac{a_0 \{a_5^2 b_5^2 - (a_4 - b_4)^2\}}{4 a_1 b_5} + \frac{2 a_1 b_5}{a_5 b_5 - a_4 + b_4} + \frac{b_1}{b_5} = a_2$
6. $\frac{a_0 a_5}{a_1} + \frac{2 a_1 b_1}{a_0 (a_5 b_5 - a_4 + b_4)} = \frac{b_3}{b_5} + \frac{4 a_1 b_5}{(a_5 b_5 - a_4 + b_4)^2}$
7. $27 C_1^2 + 4 C_1 A_1^3 + 4 B_1^3 - A_1^2 B_1^2 - 18 A_1 B_1 C_1 < 0$

where

$$\begin{aligned} A_1 &= \frac{S_1 + S_2}{L_2} + \frac{S_1 + S_3}{L_3} \\ B_1 &= \frac{S_1 S_2 + S_2 S_3 + S_3 S_1}{L_2 L_3} + \frac{S_1 S_2}{L_1 L_2} \\ C_1 &= \frac{S_1 S_2 S_3}{L_1 L_2 L_3} \end{aligned}$$

Table 5

Network of Fig. 5(a)

Element-values :

$$\begin{aligned} R &= K, L_1 = \frac{K}{b_5}, L_2 = \frac{K a_1}{a_0} \\ L_3 &= \frac{4 a_0^2 a_1 b_5 K [a_5 \{a_1^2 b_1^2 - a_0^2 (b_2 - a_2)^2\} - 4 a_0 a_1^2 b_1]}{\{a_1^2 b_1^2 - a_0^2 (b_2 - a_2)^2\}^2} \\ S_1 &= \frac{2 K a_0 a_1}{a_1 b_1 + a_0 (b_2 - a_2)} \\ S_2 &= \frac{2 K a_0 a_1}{a_1 b_1 - a_0 (b_2 - a_2)} \\ S_3 &= \frac{K [a_5 \{a_1^2 b_1^2 - a_0^2 (b_2 - a_2)^2\} - 4 a_0 a_1^2 b_1]}{a_1^2 b_1^2 - a_0^2 (b_2 - a_2)^2} \end{aligned}$$

Conditions :

1. $a_0 = b_0$
2. $4 a_0 a_1 b_5 = (a_5 b_5 + a_4 - b_4) \{a_1 b_1 + a_0 (b_2 - a_2)\}$
3. $\frac{a_0 a_5}{a_1} + \frac{a_1 b_1 - a_0 (b_2 - a_2)}{a_0 (a_5 b_5 + a_4 - b_4)} = \frac{(a_4 - b_4 - a_5 b_5)}{2}$
4. $a_1^2 b_1^2 - a_0^2 (b_2 - a_2)^2 + 4 a_0^3 a_5 b_5 = 4 a_0^2 a_1 b_3$
5. $\frac{2 a_1 b_3 \{a_1 b_1 + a_0 (b_2 - a_2)\} - 4 a_0^2 a_1 b_5}{\{a_1 b_1 + a_0 (b_2 - a_2)\}^2} + \frac{b_1}{b_0 b_5} = \frac{a_2}{a_0}$
6. $\frac{(a_5 b_5 + a_4 - b_4)}{a_1 b_1 + b_0 (a_2 - b_2)} \left[a_0 a_1 + \frac{a_0 a_5 b_5 (a_2 - b_2) - a_1 b_1 (a_4 - b_4)}{2 b_5} \right] + \frac{a_1 b_1}{a_0 b_5} = a_3$
7. $27 C_1^2 + 4 C_1 A_1^3 + 4 B_1^3 - A_1^2 B_1^2 - 18 A_1 B_1 C_1 < 0$

where

$$\begin{aligned} A_1 &= \frac{S_1 + S_2 + S_3}{L_2} + \frac{S_3}{L_3} \\ B_1 &= \frac{S_3 (S_1 + S_2)}{L_2 L_3} + \frac{S_1 (S_2 + S_3)}{L_3 L_3} \\ C &= \frac{S_1 S_2 S_3}{L_1 L_2 L_3} \end{aligned}$$

Table 6

Network of Fig. 6(a)

Element-values :

$$R = K, L_1 = \frac{K}{b_5}, L_2 = \frac{Ka_1}{a_0}$$

$$S_2 = Ka_5$$

$$L_3 = \frac{4Ka_0^2 a_1 a_5 b_5}{a_1^2 b_1^2 - a_0^2 (a_2 - b_2)^2}$$

$$S_1 = \frac{2Ka_0 a_1}{a_1 b_1 + a_0 (a_2 - b_2)}$$

$$S_3 = \frac{2Ka_0 a_1}{a_1 b_1 - a_0 (a_2 - b_2)}$$

Conditions :

$$1. a_0 = b_0$$

$$2. a_5 b_5 = a_1 - b_4$$

$$3. a_0 (a_3 b_5 + b_3 a_5) = a_1 b_1 + a_0 a_5 a_5 b_5 b_4$$

$$4. 2 a_0^2 a_5 a_1 b_5^2 = (a_3 a_0 b_5 - a_1 b_1) \{a_1 b_1 + a_0 (a_2 - b_2)\}$$

$$5. 2 a_0 (a_1 b_5 + b_1 a_5) + \frac{4 a_0^3 a_5^2 b_5^2}{a_1 b_1 + a_0 (a_2 - b_2)} + a_5 b_5 a_1 b_1 - a_0 (a_2 + b_2) = 0$$

$$6. \frac{a_1 b_1}{a_0 a_5} + \frac{a_0 a_5 b_5}{a_1} + \frac{a_1^2 b_1^2 - a_0^2 (a_2 - b_2)^2}{4 a_0^2 a_1} = b_3$$

$$7. 27 C_1^2 + 4 C_1 A_1^3 + 4 B_1^3 - A_1^2 B_1^2 - 18 A_1 B_1 C_1 < 0$$

where

$$A_1 = \frac{S_1 + S_2 + S_3}{L_3} + \frac{S_2}{L_3} + \frac{S_1}{L_1}$$

$$B_1 = \frac{S_1 (S_1 + S_3)}{L_1 L_3} + \frac{S_1 S_3}{L_1 L_3} + \frac{S_1 S_2}{L_1 L_2}$$

$$C_1 = \frac{S_1 S_2 S_3}{L_1 L_2 L_3}$$

Table 7

Network of Fig. 7(a)

Element-values :

$$R = K$$

$$L_1 = \frac{K \{a_0 a_3 b_1 b_5 - a_1 b_1^2 - a_0^2 a_5 b_5\}}{a_1 b_1^2 b_5}$$

$$L_2 = \frac{Ka_1}{a_0}$$

$$L_3 = \frac{K}{b_5}$$

$$S_1 = \frac{K \{a_0 a_3 b_1 b_5 - a_1^2 b_1^2 - a_0^2 a_5 b_5^2\}}{a_0 b_1 a_5 b_5^2}$$

$$S_2 = K a_5$$

$$S_3 = \frac{K b_0}{b_1}$$

Conditions :

1. $a_0 = b_0$
2. $a_5 b_5 = a_4 - b_4$
3. $a_1 b_1 = a_0 (b_1 - a_2)$
4. $a_0 (a_1 b_3 + b_1 a_3) = a_1 b_1 a_2 + a_0^2 a_5 b_5$
5. $a_0 (a_3 b_5 + b_3 a_5) = a_1 b_1 + a_0 a_5 b_4 b_5$
6. $-\frac{a_1 b_1^2 a_5 b_5^2}{a_0 a_3 b_1 b_5 - a_1 b_1^2 - a_0^2 a_5 b_5^2} + \frac{a_1 b_1}{a_0 b_5} + \frac{a_0 a_5 b_5}{a_1} = b_3$
7. $27C_1^2 + 4C_1 A_1^3 + 4B_1^3 - A_1^2 B_1^2 - 18A_1 B_1 C_1 < 0$

where

$$A_1 = \frac{S_2}{L_2} + \frac{S_1}{L_3} + \frac{S_3}{L_1} + \frac{S_1 + S_2}{L_1}$$

$$B_1 = \frac{S_1 S_2}{L_1 L_2} + \frac{S_3 (S_1 + S_2)}{L_1 L_3} + \frac{S_2 (S_1 + S_3)}{L_2 L_3}$$

$$C_1 = \frac{S_1 S_2 S_3}{L_1 L_2 L_3}$$

Table 8

Network of Fig. 8(a)

Element-values :

$$R = K, \quad L_1 = \frac{K}{b_5}, \quad L_2 = \frac{K a_1}{a_0}$$

$$L_3 = \frac{4 K a_0^2 a_1 a_5 b_5}{a_1^2 b_1^2 - a_0^2 (a_2 - b_2)^2}$$

$$S_1 = \frac{2 K a_0 a_1}{a_1 b_1 - a_0 (a_2 - b_2)}$$

$$S_2 = K a_5$$

$$S_3 = \frac{2 K a_0 a_1}{a_1 b_1 + a_0 (a_2 - b_2)}$$

Conditions :

1. $a_0 = b_0$
2. $a_5 b_5 = b_4 - a_4$
3. $\frac{a_1^2 b_1^2 - a_0^2 (a_2 - b_2)^2}{4 a_0^2 a_1 b_5} + \frac{a_0 a_5}{a_1} + \frac{a_3}{a_5} = a_4$
4. $\frac{a_1 b_1}{a_0 a_5} + \frac{2 a_0 a_1 a_5 b_5}{a_1 b_1 - a_0 (a_2 - b_2)} = a_3$

$$5. \quad \frac{a_1}{a_5} + \frac{b_1}{b_5} + \frac{2 a_1 (a_0 b_3 a_5 - a_1 b_1)}{a_5 \{a_1 b_1 - a_0 (a_2 - b_2)\}} = b_2$$

$$6. \quad a_1 b_1 + a_0 a_4 a_5 b_5 = (a_3 b_5 + b_3 a_5) a_0$$

$$7. \quad 27 C_1^2 + 4 C_1 A_1^3 + 4 B_1^3 + A_1^2 B_1^2 - 18 A_1 B_1 C_1 < 0$$

where

$$A_1 = \frac{S_1 + S_2 + S_3}{L_3} + \frac{S_1}{L_1} + \frac{S_2}{L_2}$$

$$B_1 = \frac{S_2 (S_1 + S_3)}{L_2 L_3} + \frac{S_1 S_3}{L_1 L_3} + \frac{S_1 S_2}{L_1 L_2}$$

$$C_1 = \frac{S_1 S_2 S_3}{L_1 L_2 L_3}$$

Networks containing two resistances and eight or ten reactive elements with $Z(0) = Z(\infty)$ are given in Figs. 10 to 12. Conditions under which these networks realize $Z(s)$ of equation (1) and the element-values are given in Tables 9 and 10.

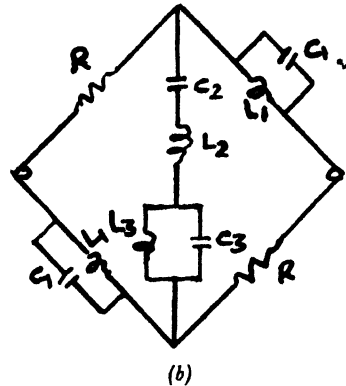
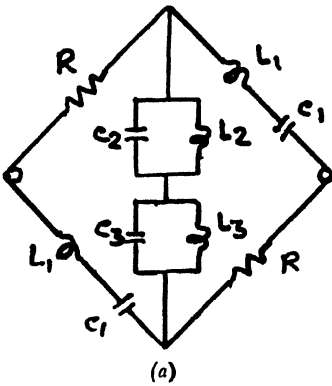


Fig. 10

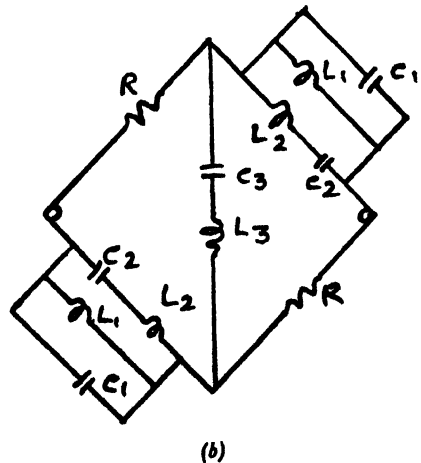
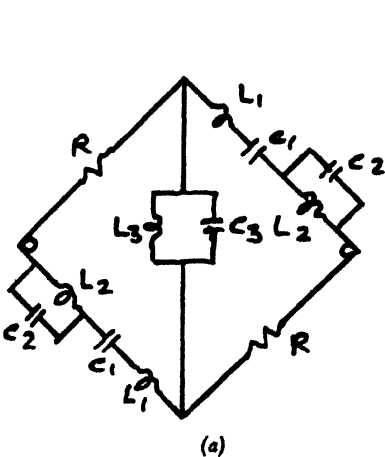


Fig. 11

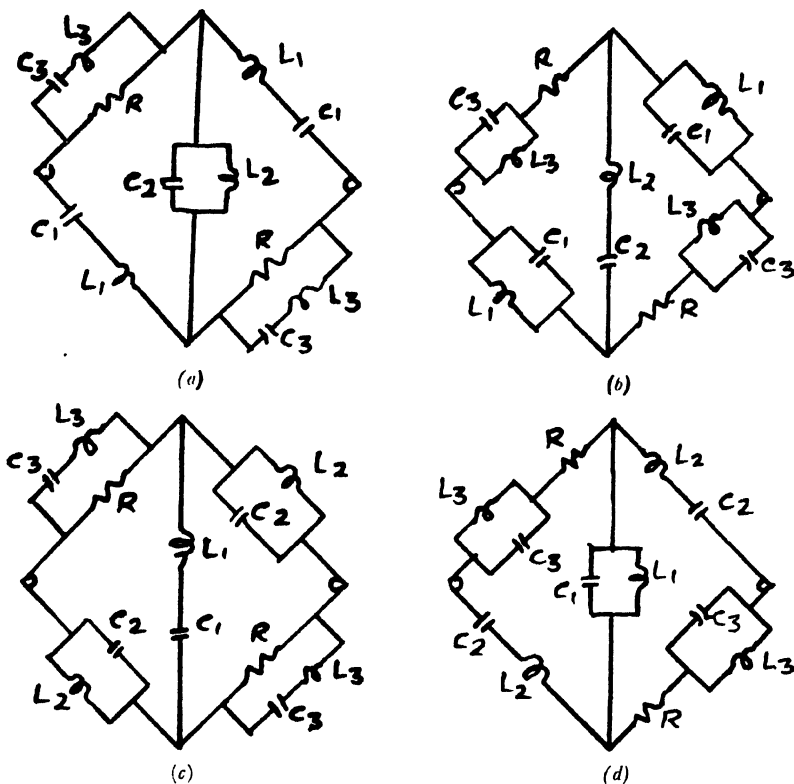


Fig. 12

Table 9

Network of Fig. 11(a)

Element-values :

$$R = \frac{K}{2}, \quad L_1 = \frac{K}{2b_5}$$

$$L_2 = \frac{K(b_0 b_1 b_5 a_3 - a_1 b_1^2 - b_0^2 b_5^2 a_5)}{2a_1 b_1^2 b_5}, \quad L_3 = \frac{K a_1}{a_0}$$

$$S_1 = \frac{K b_0}{2b_1}$$

$$S_2 = \frac{K(b_0 b_1 b_5 a_3 - a_1 b_1^2 - b_0^2 b_5^2 a_5)}{2b_0 b_1 a_5 b_5^2}$$

$$S_3 = K a_5$$

Conditions :

1. $a_0 = b_0$
2. $3a_1 b_1 = b_0 (b_2 - a_2)$
3. $3a_5 b_5 = b_4 - a_4$
4. $a_1^2 b_1 + a_0^2 a_5^2 b_5 = a_0 a_1 a_5 b_3$
5. $a_0 a_1^2 + 4a_1^2 b_1 a_5 + a_0^2 a_3 a_5 = a_0 a_1 b_2 a_5$
6. $a_0 a_5^2 + 4a_1 a_5^2 b_5 + a_1 a_3 = a_1 a_5 b_4$

Table 10

Network of Fig. 12(a)

Element-values :

$$R = \frac{K}{2}, \quad L_2 = \frac{K a_1}{a_0}$$

$$L_1 = \frac{2 K a_1 a_5^2}{a_1 a_5 b_4 - a_1 a_3 - a_0 a_5^2}$$

$$L_3 = \frac{2 K a_1 a_5^2}{4 a_1 a_5^2 b_5 + a_1 a_3 + a_0 a_5^2 - a_1 a_5 b_4}$$

$$S_1 = \frac{2 K a_0 a_1 a_5}{2 a_1 b_1 a_5 + \sqrt{4 a_1^2 b_1^2 - a_5^2 a_0^2 (a_1 a_5 b_4 - a_1 a_3 - a_0 a_5^2) (4 a_1 a_5 b_5 + \frac{a_1 a_3}{a_5} + a_0 a_5 - a_1 a_4)}}$$

$$S_2 = K a_5$$

$$S_3 = \frac{2 K a_0 a_1 a_5}{2 a_1 b_1 a_5 - \sqrt{4 a_1^2 b_1^2 a_5^2 a_0^2 - a_1 a_5 b_4 - a_1 a_3 - a_0 a_5^2} (4 a_1 a_5 b_5 + \frac{a_1 a_3}{a_5} + a_0 a_5 - a_1 b_4)}}$$

Conditions can be obtained by substituting the element-values in the following :

1. $a_n = b_n$
2. $\frac{S_1}{L_1} + \frac{S_3}{L_3} = \frac{a_3}{a_5}$
3. $S_2 \left(\frac{3}{L_1} - \frac{1}{L_3} \right) = 2 (b_4 - a_4)$
4. $\frac{1}{L_1 L_3} (S_1 + 2 S_2 + S_3) + \frac{S_2}{L_2} \left(\frac{1}{L_1} + \frac{1}{L_3} \right) = \frac{2 b_4}{k}$
5. $\frac{S_3 (S_1 + 2 S_2)}{L_1 L_3} + \frac{S_2}{L_2} \left(\frac{S_3}{L_3} + \frac{S_1}{L_1} \right) = b_2$
6. $\frac{S_2 (3 S_3 - S_1)}{L_1 L_3} = 2 (b_3 - a_2)$

4. Illustration

Let the impedance function,

$$Z(s) = 10 \frac{s^6 + 1.5 s^5 + 32 s^4 + 11 s^3 + 160 s^2 + 20 s + 200}{s^6 + 12 s^5 + 24 s^4 + 230 s^3 + 130 s^2 + 700 s + 200}$$

be considered.

The coefficients of $Z(s)$ of equation (26) satisfy the six conditions of equations (9) to (14). Hence, it is realizable by the network of Fig. 1(a).

Element-values are obtained by substituting the coefficients of $Z(s)$ of equation (26) in the expressions of element-values given in Table 1 and are as follows :

$$R = 10 \text{ ohms}, L_1 = 5 \text{ henry}, L_2 = 1 \text{ henry}, L_3 = 1 \text{ henry}, C_1 = 0.05 \text{ farad}, \\ C_2 = 0.1 \text{ farad}, \text{ and } C_3 = 0.2 \text{ farad}.$$

These element values satisfy the inequality conditions of equations (24) and (25) and hence the Re. $Z(j\omega) = 0$ at three real and distinct frequencies is given by equations (22) and (23). These values are $\omega_1^2 = 4$, $\omega_2^2 = 5$ and $\omega_3^2 = 10$.

5. Conclusions

Network structures containing seven elements (one resistive and six reactive) are the minimum element networks to realize a bisextic impedance function. The normal Bott-Duffin procedure would yield 43-element network.

6. Acknowledgment

The authors acknowledge the facilities offered by Prof. L.B. Shah, Dean, and Dr. S.M. Sen, Vice-Dean and Head of Electrical Engineering Department, Faculty of Technology and Engineering, M.S. University of Baroda for carrying out the present work.

7. References

1. M.E. Van Valkenburg. 'Special Class of a Bridge Equivalent of Brune Networks'. *Proceedings of the Institution of Radio Engineers*, vol. 44, November 1956, p. 1821.
2. R.M. Foster. 'Minimal Biquadratic Impedances'. *Transactions of the Institution of Electrical and Electronic Engineers*, vol. CT 10, December 1963, p. 527.
3. S. Seshu. 'Minimal Realization of Biquadratic Minimum Function'. *Transaction of the Institutions of Radio Engineers*, vol. CT 6, December 1959, p. 345.
4. W.H. Kim. 'Non-Series Parallel Realization of Driving Point Functions'. *Institution of Radio Engineers, National Conventions Records*, pt. 11, 1958, p. 76.
5. O.P. Gupta. 'Realization Techniques for Some Class of Minimum Positive Real Functions'. Mechanical Engineering Thesis submitted to the Birla Institute of Technology and Science, Pilani, 1964.
6. S. Seshu and M. B. Reed. 'Linear Graphs and Electrical Networks'. *Addison-Wesley Publishing Co. Inc.*, 1965.

STEREOPHONIC SOUND REPRODUCTION*

Lt-Col R. S. Attre

Member

Summary

The aim of this paper is to discuss stereo reproduction of sound and various systems used in stereo reproduction of sound with particular reference to the methods used in homes and large halls like cinemas and theatres. The latest techniques and equipment used in stereo reproduction of sound are also discussed.

Introduction

1. The word 'Stereophonic' (stereo) is derived from two Greek words, 'stereos' meaning solid, and 'phonics' meaning the science of sound or acoustics. When we put the two together we get 'solid sound' or three-dimensional sound—sound coming from different sources, at different locations, with different volume levels.

Definition

2. Stereo system is defined as an acoustic system in which sound recording and reproducing equipment employs a group of microphones and loudspeakers so arranged as to provide a sense of direction and thus enhance the degree of reality of the reproduced programme. It is analogous to stereoscopic vision in which a sense of depth adds realism to reproduced views.

Characteristics of the ear

3. With ideal amplification of sound the auditory impression of the reproduced sound should be exactly the same as that of the original source. This does not imply, however, that the amplified sound should correspond physically with the original. Differences in the response which cannot be detected by the ear are permissible, without detracting from the quality. In order to determine the practical requirements to be met by a sound system, it is necessary to know something about the characteristics of the human ear.

4. The ear responds to the pressure of sound; differences in pressure are transmitted to the basilar membrane, whence the auditory nerves convey the impression of sound to the brain.

5. Hearing, like vision, is subject to a certain amount of inertia, that is to say, an impression of sound persists for a short time after the source of sound has ceased, or, conversely, a sudden sound striking the ear drum only penetrates to our consciousness a brief interval later, in consequence of which fact sounds reaching the

*Written discussion on this paper will be received until September 30, 1967.

This paper was received on May 2, 1967.

ear within a very short time of each other, namely one-fifteeth sec. are not heard as separate sounds at all; the one tends to reinforce the other. Impressions of sound following upon each other at intervals of more than one-fifteen sec. are heard separately.

6. When we listen to a sound coming from a source which does not lie directly in front of the head, the sound does not reach both the ears simultaneously or at the same strength. It is mainly to these differences in time and intensity that we owe our sense of auditory direction or perspective; we are accustomed to associate sounds with a sense of space.

7. Composite sounds consist of a number of tones of different frequencies, intensity and phases, but the phases are not perceptible to the ear, so that, even in the ideal sound system, the phase of the various components may differ from that of the original composite sound.

Stereo reproduction

8. In a monophonic sound system, the sound usually emanates from only one location when being reproduced. Dual loudspeakers, large horns and location of the loudspeaker system in a corner of room can be used to spread the sound so that it is difficult to place the sound source at one point. These systems are likely to produce the impression that the sound is coming from a hole in the wall, with little feeling of the spatial extent or distribution of the original sound source. There is no stereo effect until two or more separate channels utilizing several microphones, amplifiers and speaker systems are used. Under these conditions the illusion of spatial orientation is completely convincing.

9. Modern stereo sound, with its directivity and depth perception adds the third dimension to the sound. The loss of dimensional effect can physically be experienced by covering one of the ears, say at a concert, then we can notice that a large part of the effect is destroyed by the absence of auditory perspective. To restore this perspective in the case of reproduced sound, recourse must be taken to stereo reproduction for which purpose at least two microphones, two channels of amplification and two loudspeakers are needed. If the original sound is not amplified direct, but is first recorded, the recording must also be stereophonic.

Aim

10 The aim of this paper is to discuss stereo reproduction of sound and various systems used in stereo reproduction of sound with particular reference to the methods used in homes and large halls like cinemas and theatres. The latest techniques and equipments used in stereo reproduction of sound will also be discussed.

Historical background

Early work

11. Both investigation into the mechanism of sound source-location and attempts to provide positional sense in a reproduced signal for entertainment purposes have been made since before the turn of the century. What might be said to be the very first stereo patent was granted to a Parisian engineer, Clement Ader, by

the German Patent Office on August 30, 1881. The patent described a system whereby telephone subscribers were to be equipped to receive relays of plays, opera and other productions direct from the stage or concert hall. The system consisted of two groups of telephone transmitters, mounted on the stage, a left group and a right one. The subscriber was to be provided with two receivers, one connected to each group, and by this means was able to follow the movements of the various characters on the stage.

Later developments

12. A number of other workers used similar techniques as those of Ader, to provide theatre relays. No considerable interest was shown in stereophony until early 1920's. In 1925, Ludwig Kapeller made an interesting improvement in the Ader system. He also suggested that the difficulty of supplying every subscriber with two telephone lines might be overcome by the use of two radio transmitters. Some experiments were made by the Berlin radio station using two channels on 505 meters.

13. Also in 1925, the American radio station WPAJ at Newhaven, Connecticut, conducted some experiments in stereo broadcasting. The transmissions were intended for headphone listening, and as such were extremely successful; the use of loudspeakers, however, did not produce such a startling effect, since the two channels became confused.

14. In 1926, the BBC also conducted similar experiments in stereo broadcasting using two medium frequency transmitters.

15. After these early beginnings, little more was done until the 1930's, when a great deal of activity took place in the stereo field on both sides of the Atlantic. The Bell Telephone Laboratories in the United States and the Columbia Gramophone Company in the United Kingdom set out to develop systems of stereo reproduction. It is from these systems produced by these organisations that all the present day techniques have grown.

16. In 1930, A.D. Blumlein, of the Columbia Company, demonstrated a complete system of two channel stereophony. In the following year, he filed British Patent No. 394325, which covered all aspects of stereo reproduction and has become a classic authority on the subject. The system designed by Blumlein was to be operated entirely by loudspeakers and at no time was headphone listening considered. He originally considered the problem as a means of improving sound in the cinema, but quickly foresaw the possibility of domestic sound reproduction in stereophony. His method was based on the fact that the interaural time differences can be produced at the head of a listener, by two loudspeakers, suitably placed, if these loudspeakers are fed with signals having an interchannel amplitude difference.

17. In 1932, Harvey Fletcher of the Bell Laboratories conducted a series of experiments, using a dummy head, into which two microphones had been inserted in front of the ears. Listening on headphones, this system was quite successful, but was not very good on loudspeakers as the reproduced images became confused.

18. Later, the experiments conducted by Steinberg and Snow, started on the hypothesis that if an infinite number of microphones were placed in front of the sound source, and each one of them was to be connected to the corresponding loudspeaker in a bank of a similar number of loudspeakers, the 'wavefront' leaving the sound source would be reproduced in the listening room exactly as it was in the original studio.

19. Bell Laboratories continued to work on the problem, and in 1936 they patented a disc cutter which could cut both hill and dale and lateral cuts at the same time in one groove. This was similar to that developed by Blumlein in the United Kingdom some years earlier, and like the Columbia one, could also be used to cut the 45°/45° system used today. A year later, in 1937, the first stereo tape machine was produced, using steel tape.

20. In the mean time, other workers were attempting to find a suitable system of stereophony to accompany the cinema film, and in 1937 a special demonstration film was shown in New York. This used only two channels, but was soon replaced by a three channel system, and this was used in the United States for the Disney Film 'Fantasia' in 1941. The early films used a separate 35 mm film to carry the various sound tracks, these being of the variable area optical type, magnetic sound on film having not yet been invented.

21. Little work was done in the United Kingdom or the United States during the war, but in Germany the first recording machines using magnetic plastic tapes were being developed, and the pioneers in this field were quick to appreciate that they could be used for multichannel as well as normal monophonic reproduction. Some important experiments were conducted in 1944 by Von Braunmühl and Ludwig Heck.

22. The first commercially available stereo recordings on sale to the general public in the United Kingdom were produced by the E.M.I. Company on magnetic tape in 1955. At the same time, many of the major recording companies were working on systems for recording stereophony on disc. The first stereo discs available to the public for domestic entertainments were issued in 1958, by the Pye group of Companies in the United Kingdom. At the same time suitable equipment for playing them was marketed by the same group. Other record companies quickly followed suit and at the present time a complete repertory of works is available on stereo discs.

23. The early system of using two separate transmitters was both uneconomic in terms of equipment and programme air time, and was 'incompatible' in that it did not give a signal usable by a monophonic listener, and in any case was not capable of the high standards of fidelity demanded at present. Other systems of stereophony from the radio were tried, for example an *AM* and an *FM* transmitter. Since 1961, a system developed by the General Electric and Zenith Companies is being used by over 300 stations broadcasting stereophony in the United States.

Producing a stereophonic effect

24. The intention of stereo sound reproduction is, by definition, to produce in the mind of the listener the illusion that he is listening in front of the original sound

source, with its own dimensions of width and depth, and with every individual part of the source sounding in its correct position in the whole. In order to do this, it is necessary to provide the ears with information sufficiently similar to that which would be present in real life that the brain cannot tell the difference, and the required illusion is created.

25. It would be possible to achieve the above mentioned result by using a large number of microphones and loudspeakers, so that each loudspeaker catered for a small part of the sound stage. This system is used in some theatre applications. but for domestic purposes it would seem to be impracticable on the grounds of space and cost.

Loudspeaker technique

26. Let us consider first the various types of information presented to a listener seated on the centre line between two loudspeakers. Suppose that both loudspeakers are fed with exactly identical signals. In other words, there will be no amplitude difference between the sounds, no frequency difference, and the loudspeakers will both 'speak' at the same time; all interchannel differences will be zero. It may be noted that the term 'interchannel' applies to the sound from the loudspeakers, whereas the term 'interaural' applies to the sound actually reaching the ears of the listener.

27. The only occasion where these two quantities are identical is when the loudspeakers are replaced by headphones, since at all other times the left ear hears a combination of sounds from both left and right loudspeakers, and vice versa. If the sound from the left hand loudspeaker is A , and that from the right is B , then at the two ears there will be the 'direct' signals AL and BR and the 'indirect' sounds AR and BL (Fig. 1). These indirect 'crossed' signals will be delayed by an amount, given by :

$$T_A \approx \frac{h}{v} \sin \theta,$$

where θ is the angle subtended by each loudspeaker at the ear of the listener.

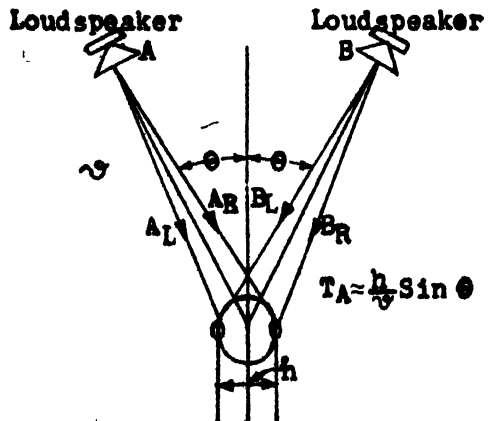


Fig. 1

Paired source listening equal signals
from both loudspeakers

28. If now the signal levels at the two loudspeakers are changed so that they are no longer equal, an interchannel intensity difference is produced. It can be seen that this will produce an interaural intensity difference, but due to the crossed signals an interaural time difference will also be present at low frequencies. Clark, Dutton and Vanderlyn, in a paper presented in 1957, derived an expression for this in terms of phase difference, phase and time difference being effectively the same at low frequencies. This expression was :

$$\text{Phase difference} = \frac{A - B}{A + B} \frac{2\pi}{\lambda} \sin \theta$$

Again, if the signal levels at the loudspeakers are kept equal, but a time difference is introduced, then again this interchannel time difference does not produce only an interaural time difference, because of the presence of the crossed signals.

29. The effect of interchannel intensity and time differences in two channel systems has been very fully investigated by D.M. Leakey. Fig. 2 shows the effect of interchannel intensity difference only, at low frequencies. The movement of the sound image was substantially independent of the type of sound, the level, or

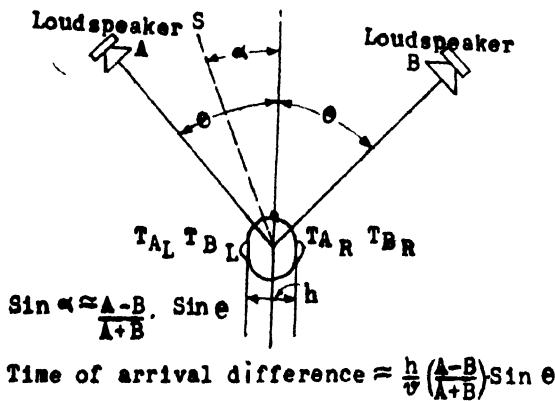


Fig. 2

Paired source listening producing an image at S

the particular listener, so long as the listener was seated exactly on the centre line, but there were noticeable variations as soon as the listener moved away from this point. Leakey derives mathematical expressions which are in reasonable agreement with the experimental results, and, with some approximation, the angle of incidence α of the sound image is given by :

$$\sin \alpha \approx \frac{A - B}{A + B} \sin \theta$$

30. Further arguments develop the theory at high frequencies, and point out the fact that, whilst correctly placed images can only be formed at low frequencies if the channels are in phase, phase reversal of one channel has little effect at high

frequencies when the angle θ is large. When θ is small, and more particularly when the loudspeakers are accurately matched, it becomes more necessary that the signals should be in phase at all frequencies.

31. From the results for one type of sound, wide band speech, when the listener moves away from the centre position, it is observed that the image becomes very poorly defined compared with central listening. The experiments with interchannel time differences alone show that the image can be moved in this way (by shifting the position of the listener). Furthermore such movement can to some extent be corrected by a suitable change in the interchannel intensity difference, at least for time differences upto about 2 milli-seconds. Such correction of position does not improve the image definition, however, and when the interchannel time difference is greater than this the impression of a single sound image is almost completely lost, the sound appearing to split into two separate parts.

Microphone technique

32. Microphone technique for stereophony falls into three main groups as follows :

(a) Omnidirectional microphone system

This system can be further subdivided into widely spaced (upto 20 ft.) and closely spaced. In this case interchannel intensity and time differences are both present, and the time differences can be readily calculated to be of considerable magnitude. The effect of these interchannel time differences will almost certainly blur the resultant images, and if the time differences are very great they may cause the images to separate into two sources, one in each loudspeaker, resulting in the now familiar 'hole in the middle'. These faults can to some extent be reduced by reducing the spacing of the microphones, thereby reducing the interchannel time differences for a given position of sound source, and the hole in the middle can be prevented with a centre microphone divided equally between the two channels, but random effects will still be caused in the final result.

(b) Dummy head system

In this stereo effect is produced by placing two microphones one on either side of a dummy head. The effect of the bulk of the head is to increase, especially at high frequencies, the interchannel intensity differences, and to a very much lesser extent, the interchannel time differences. The system is really only suitable for a reproduction by means of headphones, when it can give good results, except that the sounds will always be inside the head, and will move disconcertingly with head movement.

(c) The coincident system

In order to produce well defined images, in their correct places on the sound stage, strong, interchannel intensity differences are desirable,

with interchannel time differences kept to a minimum. This is, of course, still assuming a centrally seated listener. This type of signal can be produced by a pair of directional microphones, suitably oriented, and placed as close together as possible. If the listener is not exactly on the centreline of the loudspeakers, then some deterioration of the sound picture will result. The interchannel time differences introduced will move the images, and more seriously, cause them to become blurred. The intensity differences will also move the images. Movement can to some extent be corrected by suitable design of the loudspeaker polar response. An alternative method of correcting the movement of the images with off centre listening suggested by Vanderlyn is that a third, centre loudspeaker, fed with the sum of the left and right channels, at a lower level than the main loudspeakers, will improve matters. This loudspeaker is placed nearer to the listeners, so that the sound from it arrives at the listener from 1 to 30 milli-seconds earlier than the sound from the main loudspeakers. The level should be some 13 db below that of the main loudspeakers, and it is not necessary to reproduce low frequencies so the speaker can be quite small. By this means a two channel system can be made more satisfactory for a larger audience. Fortunately under domestic conditions only relatively few people will be listening in any one household, and they will not need to sit too far from the centre line, so the trouble may not be too serious.

Factors influencing sound-source location

General

33. The exact process by which the hearing system locates a given sound source is no more certain than that by which it perceives sound. The full use of both ears leads to the most accurate location, although with some experience, location can be achieved with one ear almost fully blocked. Movements of the head are then made, presumably to 'sample' the sound field in some way, as is done simultaneously by both ears, when these are operational.

34. In both cases, it is clearly necessary to consider the differences existing at two relatively adjacent points in the sound field. The presence of the head therein must also be significant, in its effect on these differences.

Intensity or loudness differences

35. For the source not in the median plane of the head, the head represents an obstacle between the source and the more distant ear. If a dimension ' d ' of the head is comparable with, or less than, the wavelength ' λ ' of a sound component, diffraction limits its effectiveness as an obstacle. Rayleigh treated the head as a sphere of circumference 2 ft. and calculated the intensity ratio at the two ears for a source on the ear-ear line. The ratio is then about 2 db at 2 kilo-cycles per sec. but less than 0.1 db at 150 cycles per sec. Direct measurement of the ratio confirms that there is no significant difference of intensity at frequencies below about 300 cycles per sec.

36. A further aspect of the diffraction effect is that, because it is a function of $\frac{d}{\lambda}$, the frequency spectrum, and hence also the loudness, of a complex sound will always in general be different at the two ears. It is not insignificant that location of a puretone source is less accurate than that of a complex tone source.

Phase and time differences

37. That the intensity difference at low frequencies is negligible, and that even in the mid-frequency (250—1500 cycles per sec.) range, the intensity difference required to produce location accuracy is quite different from that which occurs naturally leads to the supposition that other factors are also relevant. The difference in path—lengths from the ears to an oblique source leads immediately to a difference in time of arrival of a given wave front.

38. The ear-ear distance is approximately 20 cms. so that maximum time difference (*i.e.*, for a source on the ear-ear line) is about 0.6 milli-sec. It seems reasonable to suppose that this effect becomes completely unhelpful when the time difference becomes greater than 1 wave-period, in the limit, *i.e.* at $f \simeq 1.6$ kilocycles per sec.

Differences in ratio, direct sound/reflected sound

39. In any environment other than a perfectly symmetrical one, the sound incident on each ear will contain different proportions of directly and indirectly received energy. It is common experience that the brain is able, whether consciously or sub-consciously, to focus its attention on those portions considered relevant. Presumably, also, it can make use of this total information for location purposes.

Practical stereophonic systems

General

40. In addition to Blumlein's system, a number of other methods of producing stereo signals are in use. In the following paragraphs, the various systems in use are explained as well as one or two terms which may be noted, in order to put the stereo system in its correct context.

Monophonic system

41. A monophonic system is one in which the programme is transmitted through a single channel. More than one microphone may be used in the studio, but each of their outputs are combined to form essentially one audio channel.

Binaural system

42. A Binaural system is one in which two microphones are placed so as to occupy the normal ear positions, and connected to two separate channels, which are eventually led to two (separate) earphones at the listener's ears.

Stereo systems

43. Stereo system is a name originally given to a system involving a plurality of microphones, arranged so as to form a plane, intersecting the studio. Each

microphone feeds a separate channel, terminating in a loudspeaker placed at the corresponding point in a plane formed in the listening room. The term is now applied to any system employing more than one separate channel, each terminating in a loudspeaker.

44. Correction of the loss of spaciousness and perspective is possible by the use of two or more isolated channels. The greater the number of channels, the better is the stereo effect.

45. A satisfactory and practical approximation of the sound originating from an orchestra on a stage can be achieved if only three channels are used instead of many. One centre channel plus one on either side of the stage reproduces the effect of a live orchestra convincingly.

46. A two-channel system, however, is much more common in home systems than a three-channel system. The results obtained from a two-channel system are not as convincing as the results from a three-channel system, since there is likely to be difficulty from the lack of a real sound source in the centre of the speaker arrangement. Because of this difficulty, the two speakers must be spaced at a narrower angular distance from the listener's position than the outside speakers in a three channel stereo system.

47. Nevertheless, with only two channels, the improvement in spatial effect is quite marked in comparison to the results obtained with a single-channel system.

Pseudo-Stereo systems

48. A number of artifices have been applied to what is essentially a monophonic system in order to produce one or more stereo effects. They are characterized by having one channel and at least two separate loudspeaker systems. Relative frequency, phase, time or gain differences are introduced between the two separated loudspeaker channels.

49. With a stereo reproducing system there will be occasions when it is desired to reproduce monophonic material, and, depending on the nature of the material, some form of spreading—as obtained in pseudo-stereo—may be an advantage.

50. In the studio the use of 'spread' or 'delocalised' sounds derived from monophonic sources in two channel stereo productions has been found to provide a useful addition to the 'tools of the trade', particularly where dramatic effects are concerned. The general requirement can be divided into two parts, the first being the spreading of monophonic sources across the sound stage, and the second the production of a delocalised or disembodied sound. An example of the first could be the use of a monophonic recording of rain to provide an effect of rain over the whole stage, instead of its appearing as a point source, as it would if it were introduced via a panpot. The second, or delocalised sound, might be very useful for the narrator in a play or feature, when it is not desirable that he should appear on the sound stage as a part of the action.

Frequency splitting

51. Various attempts have been made to produce a pseudostereo spread of sound from a microphonic source. A simple method was to turn the single loud-

speaker to play into the corner of the room, so that all the sound was reflected (Fig. 3). This was not too satisfactory, however, since the lack of direct sound destroyed most of the sense of presence. An improvement on this was to use two loudspeakers, one facing the corner as before, and the other facing forwards to give the required presence. The West German radio service used for some time a monitoring loudspeaker whose high frequency units were mounted in a sphere, so that they radiated in all directions. This certainly produced a very diffused

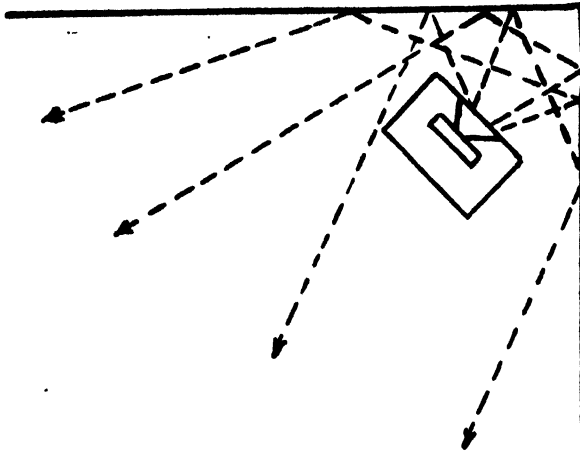


Fig. 3

Use of corner reflections to diffuse single loudspeaker

sound, indeed many users thought it too diffused, and the latest version has units facing forwards, upwards and sideways. At best the methods only gave a limited lateral spread of the sound. Another system, only intended for reproduction of orchestral music, proposed by Swiss Hermann Scherchen, uses electrical networks to divide the sound between the identical loudspeakers, and produces a more controllable spread.

Acoustic delay

52. A different method of approaching the problem is to arrange that a time delay is introduced between the sound fed to the two loudspeakers. One method of achieving this was marketed in the United States under the trade name 'Xo-phonic'. This consisted of an acoustic delay device introduced into the feed to one loudspeaker (Fig. 4). The output of the amplifier was split, one output going

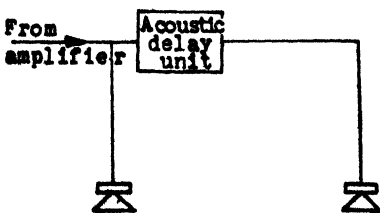


Fig. 4

**System of spreading
using acoustic delay line**

directly to one loudspeaker, and the other being fed to a small loudspeaker driver unit tightly coupled to the end of a 50 feet long coiled tube. The other end of the tube was coupled to a microphone unit, and the output of this was amplified and fed to the second loudspeaker. Due to the acoustic limitations, the frequency response of the unit was limited to the range of 200 to 3000 cycles per sec. The sound produced by the time delay method will tend to be a delocalised one rather than a spread source.

Phase shifting

53. It has been suggested that if the monophonic signal is fed to the two channels out of phase, the required spread of sound will be obtained. Whilst this is to some extent true, at low frequencies any way, the actual effect perceived by the listener seems to vary from one person to another. The BBC have tried a system of pseudo-stereophony (Fig. 5) whereby the monophonic sound itself is fed to both

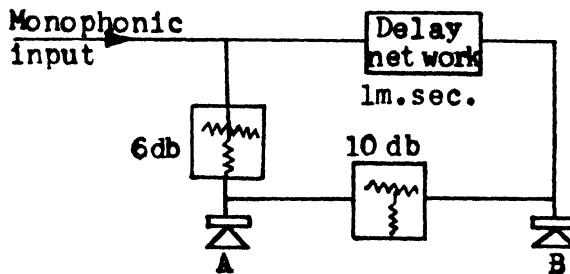


Fig. 5

Electrical spreader

channels, one being fed direct, the other through a phase shift network having a group delay of about 1 ms.

Summary of methods of generating stereophonic signals

54. The list which follows is not exhaustive, but distinguishes the various principles involved.

Time-intensity method

55. Two microphones are spaced apart by a distance much greater than the ear-ear distance, and a baffle is interposed between microphones, (Fig. 6). The angle θ , subtended by the line between centres of the microphones is also that which is subtended by the loudspeakers at the listener's head. The microphones receive signals which are functions of the respective path-lengths, and also of the intensity differences, which are exaggerated at the high frequencies by the baffle board.

Time method

56. Similar in arrangement to the previous method, but having no inter-microphone baffle. The distance between microphones is such that the time differences between wavefronts received at the separate microphones is not less than some acceptable minimum (3.5 ms typically for sound emanating from the extremes of the sound stage). In both of the above methods, some fraction of the output of

a third, central microphone may be combined with the L and R microphones in order to reduce the listener's impression of a concave stage ('hole in the centre effect').

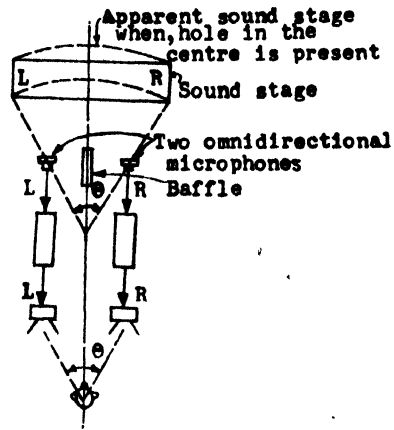


Fig. 6

Time intensity stereo system

Intensity method (stereosonic system)

57. Two microphones are made nearly coincident in space. The arrival-time differences for the two microphone signals are then very small; however, the intensity difference is made large by using directional microphones, typically velocity types having figure-of-eight polar diagrams. (Fig. 7). It can then be shown

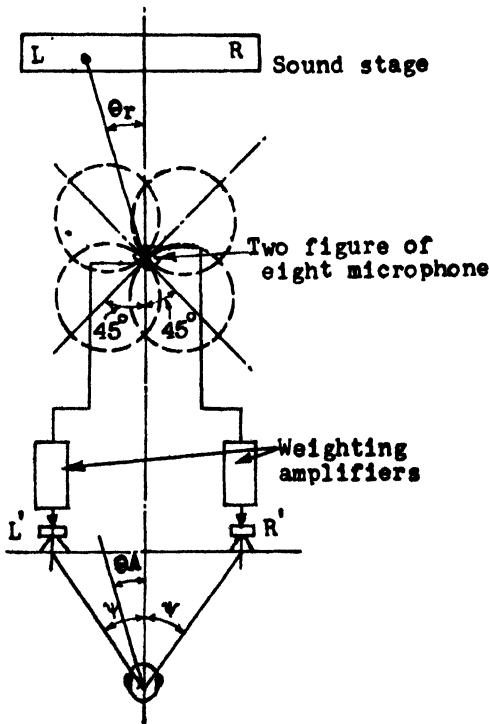


Fig. 7

Intensity 'stereosonic' system

that, with suitable weighting of the L and R signals, and taking the angles as defined by the figure.

$$\sin \theta_A = \tan \theta_T \sin \Psi$$

So that, provided θ_a is not too large, for a given listening distance and hence given Ψ ,

$$\theta_A \propto \theta_T, \text{ approximately}$$

This system is free from the 'hole in the centre' effect mentioned earlier.

Mid-side method

58. Two nearly coincident microphones are again employed, having figure-of-eight and cardioid polar diagrams respectively; these are oriented as shown in Fig. 8. With the figure-of-eight diagram normal to the centre-line of the sound

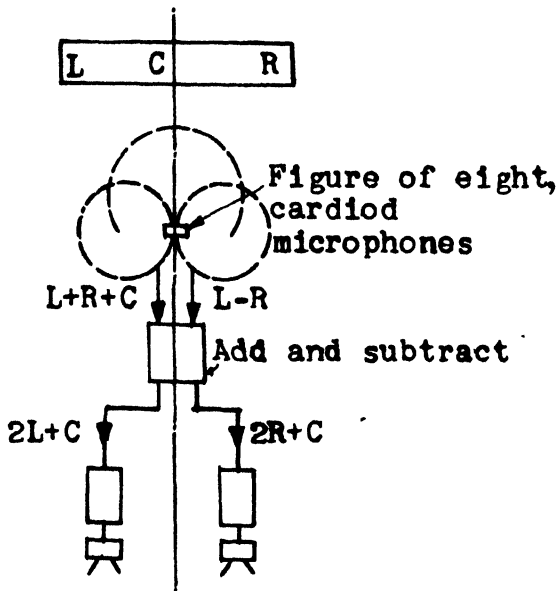


Fig. 8

Mid-side stereo system

stage, the microphone associated with this diagram produces an output proportional to $(L-R)$. The "cardioid" microphone receives a composite signal proportional to $(L+R+C)$. By adding these signals cumulatively and differentially, two signals $(2L+C)$ and $(2R+C)$ are derived.)

Stereophonic reproduction requirements

General

59. With certain exceptions referred to below, all methods of stereo-signal generation require identically similar treatment during the reproduction process. This identity refers in particular to the following :

(a) *Equal absolute gains of the channels and similar gain/frequency characteristics*

These equalities are clearly necessary, since, as discussed above, the stereo effect depends primarily on intensity and time effects, which should not be spuriously modified by the reproduction channels. The effects of channel unbalance depend somewhat on the generation method, but in general a gain difference of 2 db (such as would result from an individual channel tolerance of ± 1 db) will shift a properly central image by about 7 per cent of the stage width. Similarly, a time-delay difference leads to inaccuracy of location and estimation of "depth". If the maximum time-delay difference is put at 0.25 ms, the corresponding permissible phase-angle difference at 40 cycles per sec. is 3.6° .

(b) *Similar polar diagrams for the loud speakers at all relevant frequencies*

This requirement is really a concomitant of (a) above, for any listener situated outside the 'equal-field' area. It is also desirable that the polar diagram should not be notably directional at any region in the frequency range; with such directivity, the stereo effect changes more with the listener's position than is otherwise necessary.

Cross-talk

60. The cross-talk ratio is defined by

$$\text{Cross-talk ratio} = 10 \log_{10} \left(\frac{\text{power in one channel, maximum input}}{\text{power in other channel, zero input}} \right)$$

The presence of cross-talk leads to 'dilution' of channel identity, and it is found desirable to ensure that the cross-talk ratio is not less than 30 db.

Other requirements

61 The remaining other requirements, as given below, will be dealt with later separately either in domestic stereo reproduction or stereophony in large auditoria:

- (a) Stereo amplifier and pre-amplifier
- (b) Loudspeaker systems, their matching and placing
- (c) 'Balance' control

Domestic stereophonic reproduction

General

62. Equipment for the reproduction of stereo sound in the home can cost a modest amount, or a great deal of money, depending on the degree of enthusiasm in the project, or more likely, on the depth of the pocket.

63. Stereophony and high fidelity do not necessarily go hand in hand. It is possible to produce equipment which will give an acceptable stereo effect with only moderately good quality of reproduction. On the other hand, equipment capable of the highest possible reproduction quality can, if improperly installed, give very poor stereophony.

64. The requirements for high quality reproduction have been discussed at such lengths and by so many different authorities that there is little need to repeat them here. All that has been said concerning electronic equipment for monophonic sound reproduction applies equally to stereophony; it merely has to be doubled to produce the two channels. It is desirable that the various controls for both channels should be accurately gauged together in pairs, for if this is not done it will be difficult, as controls are varied, to preserve the exact balance between the two channels so necessary for perfect reproduction.

65. As with monophony, the two ends of the reproduction chain are the most critical if good quality is to be obtained. The loudspeakers in particular must be accurately matched, otherwise the positional information will not be faithfully reproduced and the listener will hear sounds in false positions on the sound stage. By false is meant a position other than intended by the producer of the recording or radio transmission. The relative position of the loudspeakers with respect to the listeners is also important for good reproduction of the programme material.

Power amplifier

66. There is no difference between an amplifier used for monophony and stereophony. Similar power handling requirements are necessary. These are mechanically similar and are physically disposed to minimise cross-talk.

67. It is interesting to point out, however, that many listeners have reported that for the same total power radiated into the room by the loudspeakers, a stereophonic system appears to produce an aurally louder impression than a monophonic one. It may be, therefore, that smaller power amplifiers can be used to produce an adequate volume level, thereby reducing the likelihood of offending neighbours.

Pre-amplifier

68. The pre-amplifier for stereo system ideally requires a few extra controls over and above those which would be found in monophonic equipment. (Fig. 9).

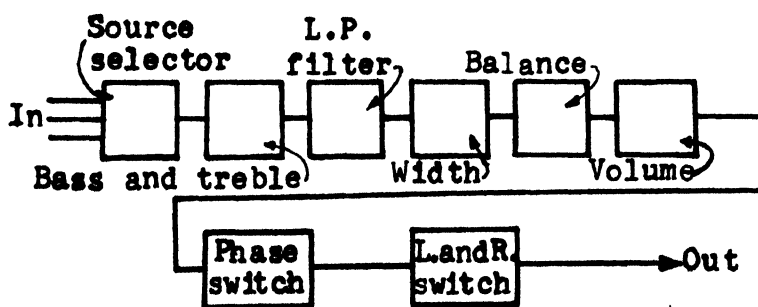


Fig. 9

Block schematic of stereo pre-amplifier

The normal volume and tone controls are of course desirable, these being gauged so that one knob operates the control for both channels. It is very necessary in

order to preserve the stereo picture, that when an adjustment is made to one channel, an identical adjustment is made to the other and hence considerable care must be taken in the gauging of the controls and the accuracy of the associated circuitry.

69. A balance control must be provided so that the overall gain of the two channels in the system can be adjusted relative to one another so that they are exactly equal. This is necessary to take into account any slight errors that may exist either in the system itself or in the programme material fed to it. It is possible also, by using this control, to compensate, to some extent, for listeners sitting away from the centre line of the loudspeakers, but only, of course, when they are all on one side.

70. A very useful adjustment which has not so far been applied to many domestic stereo systems is the width control. As with the studio equipment, in its simplest form this consists of a means of introducing some of the left hand channel into the right and vice versa. By this means the effective width of the reproduced picture can be reduced, no matter if the distance between the loudspeakers is large, to occupy a suitable amount of space between them.

71. Such a control is useful, for example, when a recording of a work of chamber music is played immediately after a recording of a full symphony orchestra. It is quite probable that the recording company will have recorded both works to occupy the full width of the space between the loudspeakers. In fact, however, the chamber music group will in the recording studio have occupied very much less space than an orchestra (Fig. 10) and so, in order to reproduce these to a

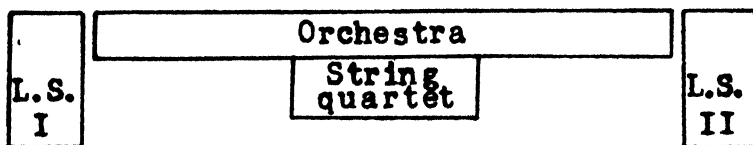


Fig. 10

Desirable relative widths for orchestra and string quartet

similar scale, it would be desirable to reduce the width of the reproduced picture of the smaller group. An increase in the width of the sound picture would seldom seem to be necessary, and would be difficult to achieve without special circuitry, except that in a receiver for multiplex stereo broadcasts, where a control on the difference signal could be used.

72. Two other controls are necessary. The first of these is a simple switch to reverse the phase of one channel. This may be considered a refinement since it should be possible to set this once and for all when the equipment is first set up. Accidents will occur, however, and some commercial recordings have inadvertently been issued with the two channels out of phase; such a switch would enable the error to be corrected without recourse to a soldering iron. In a similar way left and right channels have occasionally been reversed and a switch enabling the two channels to be interchanged would also prove useful,

Installation of equipment

73. Having decided on the equipment to be incorporated in our stereo system, it is necessary to give some thought to the way the various parts should be set up in the listening room. The control unit should preferably be mounted separately from either loudspeaker, and installed in such a way that it can be operated from the principal listening position. (Fig. 11). In this way settings of tone, volume

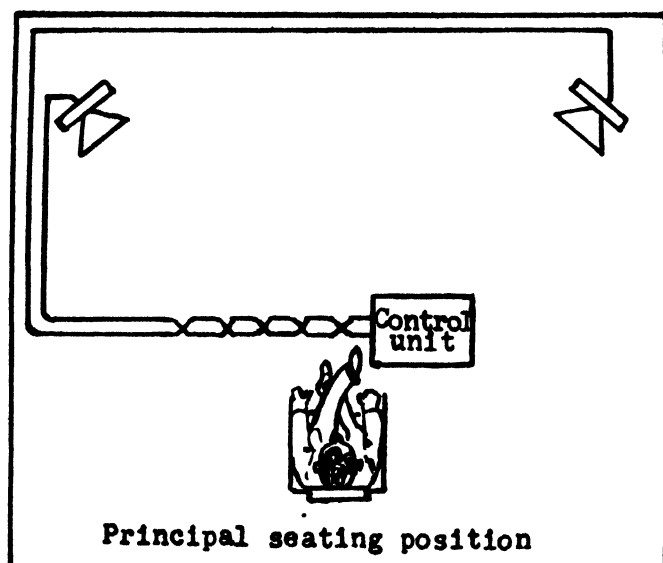


Fig. 11

Use of separate control unit

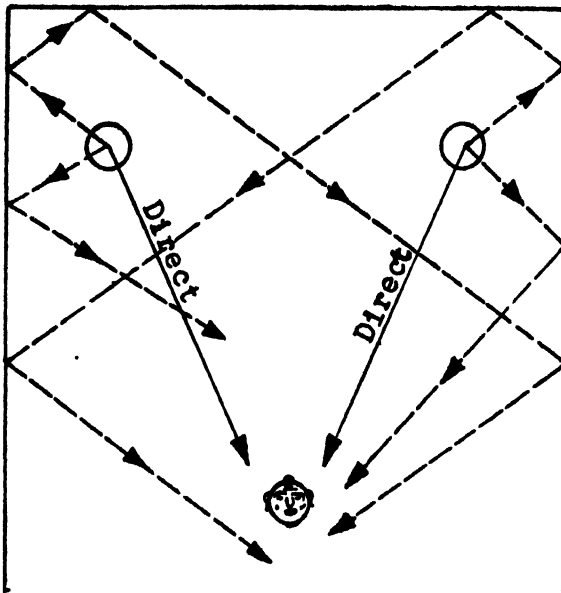
and balance controls can be adjusted with the minimum of trouble. If the control unit cannot be operated from the principal listening position it may be necessary to enlist the aid of a second person to turn the knobs in the balancing process, under the direction of someone in the best listening position.

74. The position of the control unit is not at all critical on any grounds other than those of operating convenience, but the position of the loudspeakers is in a corner, partly because it takes up less of the available space in the room if so installed, but also since the extra air loading due to the walls and floor of the room enables a better bass response to be obtained.

75. The most suitable place for loudspeakers for stereophony, then, would seem to be in two corners, preferably across the narrow end of a rectangular room. If the room is of such a size that placing them in this position would make the distance between them greater than 10 ft. or so, then the loudspeakers may have to be moved out of the corners, or it may not be possible to fuse the two sources into a complete sound picture.

Type of loudspeaker to be used

76. Much argument and discussion has taken place on the question of type of loudspeaker assembly to be used for stereophony. Some authorities insist that since the object is to spread the source of sound across the space between the loudspeakers, omnidirectional assemblies should be used. This misconception seems to stem from monophonic practice. With monophony, it is often desirable to spread the sound so that as far as possible it does not appear to come from the loudspeaker, and to this end a number of devices have been employed. They produce arbitrary, built in directional information which will be better than none at all. With stereophony, on the other hand, all necessary directional information should be contained in the transmitted signals, and so pseudo-stereo effects adding additional arbitrary information will only spoil the intended effect. (Fig. 12)

**Fig. 12**

Omnidirectional loudspeakers producing delayed reflections

Arrangement of loudspeakers

77. Loudspeakers arranged so that they direct their sound towards the listener and not at nearby walls and other reflecting surfaces are therefore desirable. It is usually found that the most satisfactory results are obtained if the loudspeakers are angled inwards, (Fig. 13) with their axes crossing some distance in front of the listeners, these axes making an angle of 90° with each other. This type of placing often enables the stereo effect to be enjoyed by more listeners than is possible when the loudspeakers are arranged so that their axes are pointing towards the principal listener.

78. The fact that it is desirable to reduce all reflected sound to a minimum means that not only are omnidirectional loudspeakers undesirable, but also that

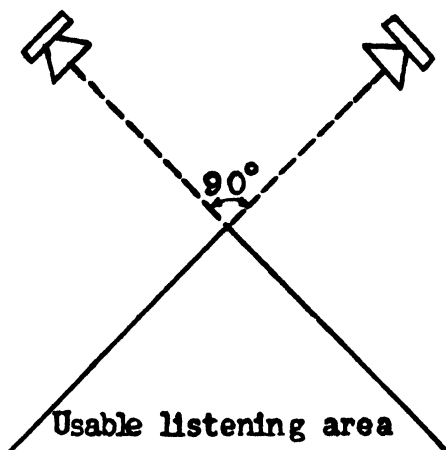


Fig. 13
90° loudspeaker placing

room reflections must be reduced to a minimum if the best possible stereo effect is to be obtained. Undoubtedly, the best stereo effect would be obtained if the reproduction took place in an acoustically dead room, since the original studio acoustic is well conveyed, if only in two dimensions. Such a room, however, would be most unpleasant to live in.

79. It is still desirable, however, to ensure that the area between the loudspeakers is as non-reflecting as possible, and also the area immediately to the sides. It is also helpful, though not essential, to reduce reflections from the wall opposite the loudspeakers as much as possible.

80. The need for non-reflecting surfaces around the loudspeakers does not necessarily imply expensive acoustic treatment. It will frequently be the case that the most convenient place for the loudspeakers is on either side of a window, and the simplest method of effecting the necessary treatment is to make the window curtains of suitably heavy material and hang them from ceiling to floor. This curtained area between the loudspeakers can have another effect; not acoustic, but psychological, in that the neutral area between the loudspeakers can help to give the listeners the effect of looking at a stage. A similar treatment of the wall opposite the loudspeakers will reduce reflections from that source to an acceptable value.

81. Even if there are no windows in that wall, the addition of curtains can add considerably to the interior decoration of the room. The space on either side of the loudspeakers can be similarly treated, or the absorption can be provided by placing soft upholstered furniture in this position.

82. Such makeshift acoustic treatment as described in the last paragraph does not, of course, preclude the use of any of the more professional types of sound

absorbers. Almost any of the standard acoustic tiles can be used in this application, as could glass fibre or rock wool, suitably mounted on a batton framework, and covered with some porous decorative material.

83. If the ultimate in stereo installations is desired, some thought might be given, not only to providing a suitable acoustic environment for the best sound reproduction, but also to the concealment of the loudspeakers. Many people find that it is easier to fuse the sounds from the two loudspeakers into a continuous sound picture if they cannot see the actual sound sources. There are, of course, many ways in which loudspeakers can be concealed such as by a net curtain or two sets of curtain etc. Whatever method is used, care must be taken that the concealing materials do not impede the sound to any significant extent, and that the loudspeakers are not boxed in with solid material in such a way that resonant cavities are produced.

Balancing the system—'balance' control

84. It cannot be too strongly emphasized that good reproduction cannot be obtained unless the balancing routine is carefully carried out. Having suitably placed the loudspeakers, a monophonic signal should be applied to both channels. This can be done from the radio, or from a recording, and probably the easiest method is to play a monophonic disc with a stereo pickup. This should result in an identical signal being fed to the two channels.

85. The volume is then turned upto a convenient level, and, sitting in the optimum listening position on the centre line between the two loudspeakers, the balance control is adjusted until all the sound appears to come from immediately in front, that is midway between the loudspeakers. The system is then correctly set for stereo reproduction.

86. This method of centralising will also give an indication of whether the two loudspeakers are correctly placed. If they are not, no central image will be possible, and equal signals from both channels will produce an odd effect, best described as a sound coming from above and behind the listener's head. The remedy for this is of course to reverse the connections to one loudspeaker.

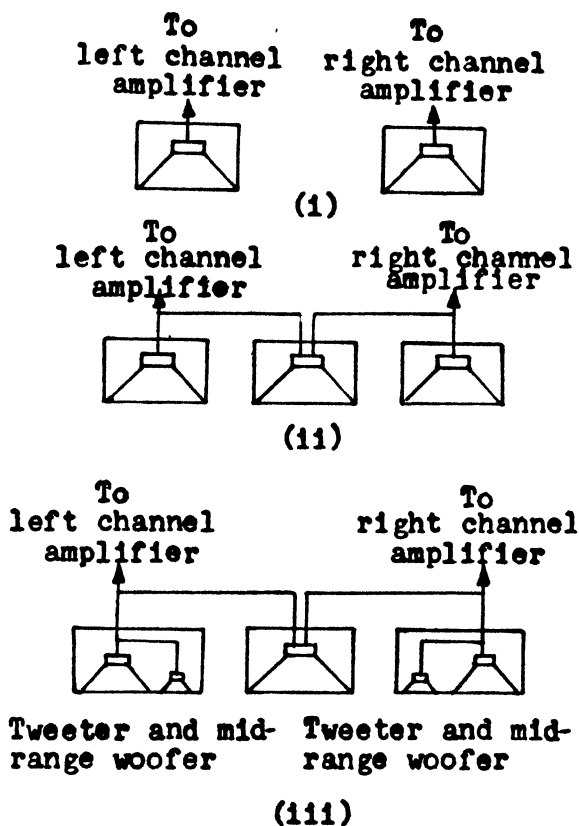
87. This is, incidentally, an excellent method of judging the 'goodness' of a stereo system, since the more accurately balanced the two channels are, the sharper will this centre image be. Small inequalities in frequency response between the two channels will result in a less distinct image, and if these irregularities are large, splitting of the image may occur.

88. Similarly, the technique can be used to find the optimum positions for the loudspeakers in a given room.

89. Various aids to achieving a good balance between the channels are commercially available. The simplest of these consists of a meter assembly designed to be connected across the loudspeakers. When the system is balanced the meter reads zero. There are other systems as well where the loudspeakers of equal sensitivity only can be used.

Stereo speaker systems

90. In the simplest stereo arrangement two similar speakers or two similar speaker systems are used, one for each channel. Fig. 14 (a) illustrates such an arrangement. In this case, two extended range speakers are used, each housed in its own enclosure. However, if the reproducer is to comprise a woofer and tweeter, or a woofer, midrange speaker and a tweeter, then each of the two enclosures will house identical sets of speakers.

**Fig. 14****Stereo speaker systems**

91. Usually the two speakers (or speaker systems) are placed 6 to 8 feet apart. This is the arrangement used in many 'packaged' stereo systems, but is not necessarily the best. Assuming that the two speakers are identical, it is quite possible that the acoustics of the room require that the spacing between speakers be something more or less than the 6 or 8 feet mentioned, in order to achieve the best stereo effect. Although most amplifiers have some arrangement for balancing, it is often impossible to achieve correct balance without altering the location of one or both speakers.

92. Another type of stereo speaker system is shown in Fig. 14 (b). Here a third speaker has been added. Signals from the left and right channels are fed to the third speaker, located between the other two, thus creating a third channel. This method seeks to avoid the 'hole in the middle' or "ping-pong" effect noted in some two-channel systems. A few amplifiers are equipped with a control for blending signals from the left and right channels in order to set up the third channel.

93. A variation of the system just described is shown in Fig. 14 (c). The left channel and the right channel use speakers covering all the musical range except the bass; that is, each speaker system consists of a mid-range speaker and a tweeter. The middle channel employs a woofer only; it receives only the lower tones from both the left and right channels. This "blended bass" system operates on the principle that the lower frequencies are non-directional and therefore only one sound source is needed for them.

Stereo from disc

General

94. Two-channel disc phonograph sound reproduction was commercialized in 1958. The stereo disc phonograph provides the reproduction of the original sound sources in auditory perspective, that is, the spatial relations in the original sound are substantially retained in the reproduction of the recorded sound.

Basic system

95. The simplest possible basic system for reproducing stereo disc recordings is shown in Fig. 15. It consists of a record player or changer utilizing a dual-element cartridge. If a variable reluctance type of cartridge is employed, the voltage-producing units will then be coils instead of crystal elements.

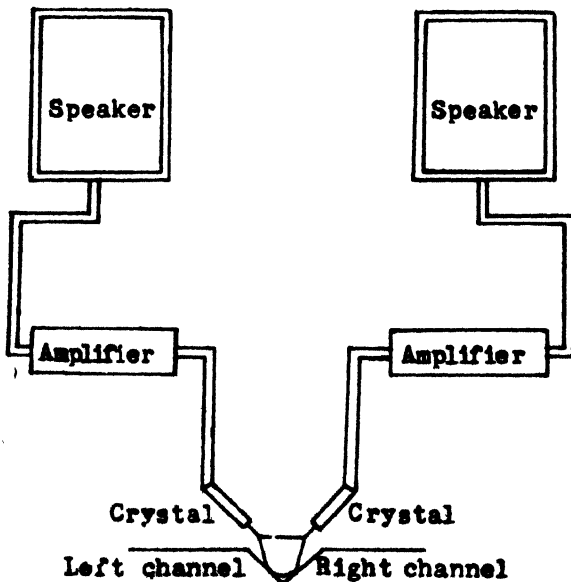


Fig. 15
Simple system for
reproducing stereo disc
recording

96. One crystal element (or coil) delivers the musical information it picks up from its side of the record groove to an amplifier; the amplifier voltages are then applied to a loudspeaker. The combination of crystal element, amplifier and speaker is referred to as a channel; we shall call this one the right channel, or channel A. The remaining crystal element delivers its voltage to a second amplifier and the amplified voltages are applied to a second loudspeaker. This combination of crystal element, amplifier and speaker is the left channel, or channel B.

97. With sufficient separation between the two speakers we shall then receive the impression that the sounds of the various instruments in the orchestra reach us from the proper directions and the overall result is a sense of realism not achieved by monaural high fidelity systems.

Stereo pick-ups

98. The difference between stereo and monophonic pickups is much more pronounced than in the case of tape replay-head. Two transducing elements at right angles are necessary to resolve the compound motion of the stylus into the separate channel components. Usually, the stylus cantilever is linked to a bridge-piece which transmits motion to both elements simultaneously. Therefore, the effective mass of the system tends to be doubled (relative to the equivalent monophonic pick-up) and the low frequency resonance frequency reduced by a factor $\frac{1}{\sqrt{2}}$ therefore mass-reduction must receive even closer attention by the designer.

99. The vertical compliance should be high in order to reduce the wear due to pinch effect. In a stereo pick-up it is essential that the vertical compliance be commensurate with the lateral compliance, since the modulation itself now has a vertical component. By the same token, the vertical component of the turntable 'rumble' typically several times greater than the horizontal component, must be considered. Fortunately, due to the intentional phase-reversal referred to above, the vertical 'rumble' component is largely cancelled.

100. A further factor which requires attention is the angle made by the axis of the pick-up with the record surface, this angle is sometimes referred to as the azimuth angle. If this is other than 90°, cross talk is introduced. Due to the imperfections of the mechanical construction, the cross-talk in any case cannot (in contemporary design, at least) be reduced to the values achieved in a tape system, and 20 db over the middle-frequency range appears to be considered good, even though at the extremes of the frequency range, the cross-talk may approach 0 db.

Reproducing system

101. The elements of a complete stereo disc reproducing system are shown in Fig. 16. There are two identical channels following a two-channel disc phonograph dynamic pick-up. Each element of the stereo pick-up consists of a transducer of the type employed in the single channel lateral dynamic pick-up. The arrangement is such that a vibration which excites one element will not excite

the other. Other types of pick-ups have also been developed. For example, in a ceramic pick-up two ceramic elements are arranged with the vibrating planes at right angles and coupled to the stylus in such a manner that a vibration which excites one element will not excite the other.

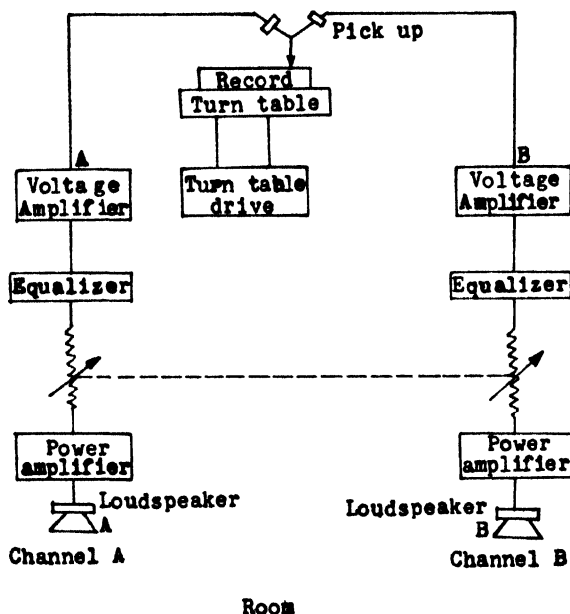


Fig. 16

Stereo disc phonograph reproducing system

102. The groove used for the stereo disc record is a fine groove. A stylus with a tip radius of 0.00075 in. is recommended for use in reproducing stereo disc records. Both diamond and sapphire styli are in use.

Compatibility

103. The word compatible means capable of existing together in harmony. Applied to stereo it refers to a disc recording that may be played on either a stereo or a monaural player. Monaural recordings may be played on stereo equipment without damage to either equipment or recording. Of course, since a monaural recording contains only one set of modulations, only one pick-up element, one amplifier and one loudspeaker functions during the playing of such a recording.

104. Unfortunately, the reverse situation is not true in present stereo recordings, although there are developments under way that may soon make this possible. Any attempt to playback a stereo recording on a player designed solely for monaural recordings will result in damage to the recording. This may not be evident to the non-critical listener after only one playing and the danger is that the listener may not notice the damage, may assume that none has resulted and may try it again. Almost certainly the recording will be ruined after several playings.

105. The reason why stereo recordings cannot be played on monaural equipment is due to the construction of the pick-up. A stereo stylus is free to move in two directions, as we have already seen. We might say that it has both vertical and lateral compliance. Compliance is merely a measure of how easily the stylus may be deflected from its rest position. A monaural stylus is free to move only laterally; we might say it has only lateral compliance. Consequently, when a stereo record is played on a monaural record player, one side of the groove is subjected to the action of a stiff, unyielding stylus and the delicate engravings in that side-wall are rapidly destroyed.

Stereo from tape

General

106. A two-channel magnetic tape stereo sound reproducing system employing pre-recorded magnetic tape was commercialised in 1956. 'Stereosonic' tape records, produced by EMI Limited of Britain, are becoming more popular as more people are buying tape recorders and converting them for stereo operation. Unlike the disc, however, which enjoys a considerably greater degree of popularity, stereo tape records are mainly of interest to the specialist.

107. Most stereo recorders of the home variety were, and still are, designed for playback only of stereo recordings, but they are capable of either recording or playback of monaural music.

Tape records

108. In Britain tapes are at present being made at tape speed of $7\frac{1}{2}$ in. per second, using half the tape width per channel, and they are treated electrically in a manner identical to that for monophonic tape records. The total playing time per tape is half that of the monophonic double-track tape of the same length. In the United States, two-channel stereo tapes using $\frac{1}{2}$ width per channel are readily available; with these the playing time is restored at the expense of a relative loss of output of 6 db.

Tape replay heads

109. The Principal criteria additional to those of the single track head are as follows :—

- (a) Accuracy of alignment of the gaps on a common azimuth line.
- (b) Accuracy of track-width and spacing, relative to the standards laid down.
- (c) Reduction of cross-talk; normally the upper track of the replay head will be used alternatively to scan monophonic records. The previously-mentioned figure of 30 db, for the minimum cross-talk is then quite unacceptable, since the spurious signal from the lower track bears no relation to the signal from the upper track and, moreover, occurs in reverse; 55-60 db should be achieved. This implies, in particular, the use of inter-track shielding within the head.

Reproducing System

110. The elements of a stereo magnetic tape reproducing system are shown in Fig. 17. There are two identical channels. The magnetic head is same as that used for stereo recording. The two-channel magnetic head is in reality two heads. The head is termed a stacked head because the gaps in the two heads are in a line. The stacked head is now the standard arrangement.

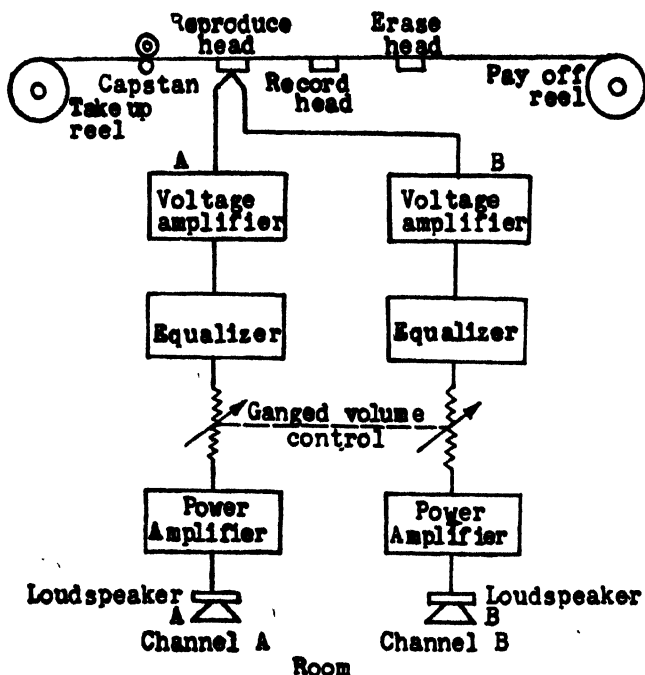


Fig. 17

Stereo magnetic tape reproducing system*Stereo radio**General*

111. Stereo radio reception is not, unfortunately, yet with us, although it is already an established practice in the United States, where a large number of local stations are transmitting two channels by means of the Zenith-General Electric system. In Europe, Working Party S of the European Broadcasting Union have proposed that the same system be adopted there also. However, 'Storecasting' has been excluded and a pre-emphasis of 50 μ s is specified.

Zenith-General Electric system

112. The design of a receiver for this system can take two different forms, and these are shown in block schematic. (Fig. 18). The first of these separates the monophonic signal, the sum of the two stereo channels, by the normal detection process. The pilot sub-carrier at 19 kilo-cycles per sec. is used to regenerate the

38 kilo-cycles per sec. sub-carrier, either by direct amplification and doubling, or by locking a 38 kilo-cycles per sec. oscillator. A band pass filter selects the side bands of the difference signal from the complex transmitted wave form and these side bands are combined with the generated 38 kilo-cycles per sec. sub-carrier to produce the difference signal after detection.

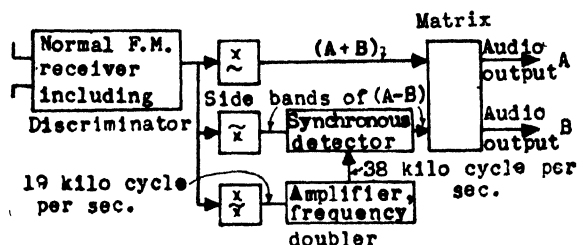


Fig. 18

Block diagram of basis decoder

113. Due to the time delay introduced into the difference signal by the band pass filter, it is necessary to delay the sum signal by an appropriate amount in order that the two signals shall be in exactly the same time relationship as when they were originally transmitted. If this is not done, then serious cross-talk will be introduced at high audio frequencies. Sum and difference networks then combine the two signals to produce the original left and right components.

114. The alternative design of receiver approaches the problem in a different way. It can be shown that the Zenith-General Electric system, originally described as a frequency division multiplex system using an amplitude modulated suppressed sub-carrier, is equivalent to a time multiplex system where the two sets of channel information are switched alternately to modulate the main transmitter, the switching occurring at the rate of the sub-carrier frequency.

115. It is thus possible to design a receiver (Fig. 19) in which the 19 kilo-cycles per sec. sub-carrier triggers an electronic switch operating at 38 kilo-cycles per sec. which will switch the whole output of the receiver either to one loudspeaker

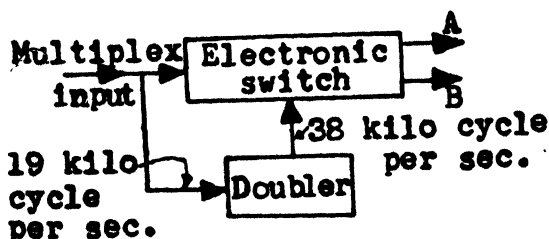


Fig. 19

Decoder using switching

chain or the other. A low pass filter is, of course, desirable to remove the 19 kilo-cycles per sec. pilot sub-carrier, and any higher frequency harmonics, from the feeds to the loudspeaker amplifiers, and to prevent interaction with the H.F. bias of domestic tape recorders.

116. It might be supposed that the circuitry outlined above for stereo reception could be applied after the normal detector of any V.H.F. sound receiver. Whilst

this is, of course, theoretically true, it is essential that the receiver circuitry shall be able to pass the highest frequency contained in the modulated wave form. In the Zenith-General Electric system, this is 53 kilo-cycles per sec. and so it is desirable for good operation of the stereo circuitry, that the 'audio frequency' pass band should be of the order of 60 kilo-cycles per sec. Note especially that this figure is not the radio frequency pass band of the receiver but the modulation frequency, after the normal discriminator.

117. It is further extremely important that the receiver shall pass the whole of the modulation spectrum without altering the time relationship of the various components, otherwise it will be impossible to combine the sum and difference signals to produce the original two channel signals.

Stereophony in large auditoria

General

118. The reproduction of stereo sound to a large audience in a cinema, theatre or concert hall presents a number of problems over and above those found under domestic conditions. An audience listening to stereophony at home will rarely exceed five or six in number, and these can be accommodated in the average room in such a manner that no one listener is too far from the centre line. Under these conditions, all the listeners will receive an acceptable stereo representation, from a two channel system

119. If a two channel system is employed in a large auditorium, however, with the two loudspeakers mounted, for example, on either side of the stage, there will be many listeners who will not be able to hear the reproduction properly. The listeners on or near to the centre line of the hall will, provided the reverberation time is short enough, receive a good stereo sound picture, but as the position of the listener moves away from the centre line the stereo effect will deteriorate progressively until in the side seats the sound will appear to originate in the nearest loudspeaker. Furthermore, there will again be a progressive deterioration of the stereo effect as the listener moves towards the back of the hall, due to the effect of even a small amount of reverberation.

Placing of loudspeakers

120. The important difference between the two kinds of system-domestic and large auditoria, is the fact that the listener sits at a great distance from the loudspeakers in an auditoria (except possibly those who sit in the front rows). The average listener is at a distance that is several wavelengths, even of the lowest frequency, from the loudspeaker grouping. Consequently some of things that may be said about stereo sound presentation in an idealistic sense, and which do not apply fully in the living room because of the limited dimensions, do apply, to a greater extent, in the large auditoria like a movie theatre.

121. On the other hand, the spacing between loudspeakers, even the three units generally employed behind the screen, is so great that it is impossible to base the presentation on phase difference effects, because the space in between loudspeakers represents several wavelengths of all except the very lowest frequency sounds.

Consequently the most satisfactory method of obtaining a suitable stereo sound track presentation in a theatre consists of using separate audio channels and synthesizing the individual tracks to represent the programme content.

122. Some improvement can be made for reducing the deterioration of stereo effect for listeners in the rear of the hall, by the addition of a number of extra pairs of loudspeakers, the actual number depending on the size of the hall. (Fig. 20). With the addition of these extra loudspeakers, the area of the auditorium over which an acceptable stereo effect can be obtained will be considerably increased.

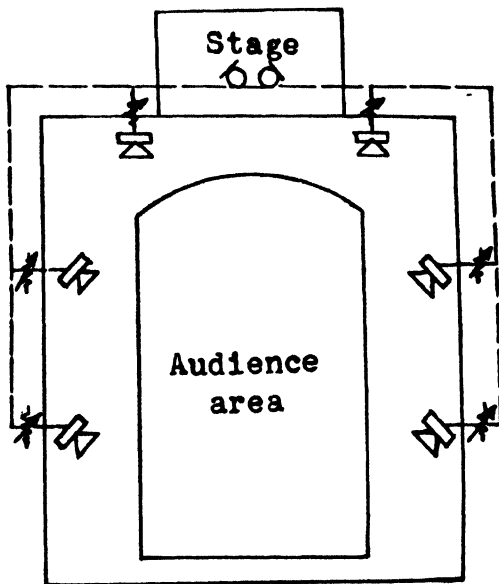


Fig. 20

Use of added pairs of loudspeakers

123. The adjustment of such a multi-speaker two channel system requires some care if the best results are to be obtained. A monophonic signal should be used, and each pair of loudspeakers should be balanced separately so that, listening on the centre line, all the sound appears to come from the centre of the stage. Having set this balance, it is then necessary to adjust the volume level of the individual pairs so that, listening still on the centre line, the sound always appears to originate in the centre of the stage as the listening position is moved towards the back of the hall. This will mean that the loudspeakers nearest the stage will be the loudest, the volume level being progressively reduced as the distance from the stage is increased. With accurate adjustment, the useful area for stereo listening can be extended to all except the seats at the extreme side of the hall.

Stereo motion pictures

124. Whilst the above method of reproduction of two channel stereophony can provide satisfactory entertainment in a large hall, further difficulties arise when the stereo sound has to be synchronised with a cinema picture. In this case, not only does the sound have to be audible stereophonically to a listener seated in any seat in the theatre, but at any given moment the position of the sound must match exactly the position of the source in the picture.

125. In order to fulfil this condition it is necessary to use a large number of channels so that the extra loudspeakers will provide fixed points across the stage from which the sound will come regardless of the position of the seat in the theatre. In pursuit of these fixed points, three, five, or even seven channels have been used, the greater the number of channels the more accurate the positional information available.

126. The idea of stereo sound in the cinema is almost as old as the sound film itself. At the same time as the early work was being completed on the optical method of sound on film recording, the basic work was going on, both in the United States and the Britain, to produce the first practical systems of stereophony, and it was natural that the two should be combined.

127. Twin track stereophony was used and a special demonstration film was shown, in 1937, covering several aspects of the cinematic art, from music to drama. The twin channel system, however, showed the shortcomings mentioned earlier, and the subsequent development by the Bell laboratories of the stereo sound on film system increased the number of channels to three. At this time magnetic sound recording was not developed to the point where it was practicable, and recourse had to be made to one of the two optical systems available.

128. The system chosen was the variable area sound track because this method of recording gave a greater dynamic range than was possible with the variable density system. In the first experiments the three channels were recorded on a separate film which was synchronised with the picture film. It was found, however, that the maximum signal to noise ratio available using this system was only some 50 db and it was decided that a dynamic range of 80 db was desirable if, realistic reproduction was to be obtained.

129. An automatic system was devised whereby the dynamic range was compressed at the time of recording and a control track was recorded, also optically, on the sound film; the information on the track corresponding to the amount of compression used. When the recording was played back the information from this track was used to control the gains of the three channel amplifiers so as to restore the full dynamic range required. In order further to reduce the background noise, high frequency pre-emphasis was added at the time of recording, a corresponding de-emphasis being used during the reproduction. The first demonstration of this system, which covered a frequency range of 20 to 14,000 cycles per sec. took place in April 1940. (Fig. 21).

Fantasound

130. About the same time as the Bell Laboratories were working on their system, the Walt Disney Studios in Hollywood, and the Radio Corporation of America were working on a system of stereo sound to accompany the musical Disney film 'Fantasia'. The particular system developed was appropriately termed Fantasound.

131. It was recorded optically on film and four tracks were used. Three of these carried the sound channels and the fourth a control track as in the Bell system.

The recording of the three sound tracks was, however, a much more complicated process. The original recording was made on eight separate tracks, six being individual microphones placed in front of the various sections of the orchestra, the seventh a mixture of these six and the eighth a more reverberant sound from a distant microphone. These eight tracks were specially mixed together to produce the three tracks for the final print.

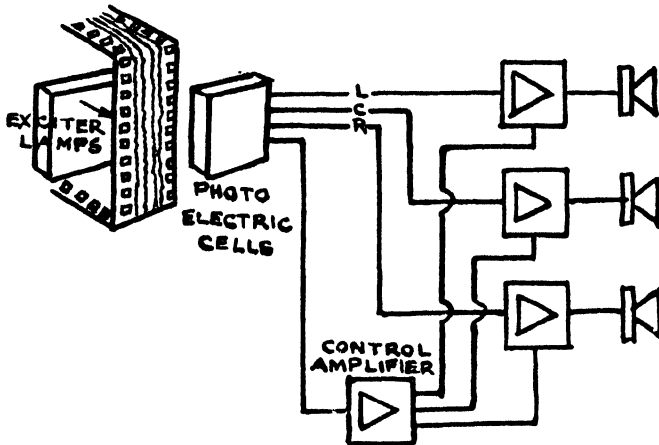


Fig. 21

Three channel sound system on film

Vitasound

132. In addition to this stereo technique used in "Fantasia", some items of the programme employed a form of pseudo-stereophony to produce particular effects. This pseudo-system which was also used in a number of other films at this period was called 'Vitasound'. It merely consisted of a number of loudspeakers in the auditorium area to the left and right of the audience which could be connected, again on the instructions of a control track, to the two outer loudspeakers behind the screen. (Fig. 22). This system, incidentally could be applied to a monophonic sound track, giving the illusion of a greater spread of sound when this was desirable to enhance the action.

133. During the war years, little development took place and it was not until the early 1950's when stereoscopic film became popular that an attempt was made to produce accompanying stereo sound. During the Festival of Britain, in 1951, the Telecinema showed film of this type where the sound was provided by three groups of loudspeakers behind the screen and a fourth at the back of the auditorium.

Stereo magnetic tape sound motion picture

General

134. During early 1950's much work was being done in the field of magnetic recording and the possibility of better sound quality which this system presented made it an ideal one for stereophony in the cinema.

135. The first presentations on Cinerama in 1952 used five magnetic sound tracks on a separate 35 mm film, running in synchronism with the picture film in a similar manner to the earlier Bell experiments. The five loudspeakers were suitably disposed behind the screen and the stereo effect was, at its best, very well worthwhile. Two other tracks were recorded on the sound film, one which operated 'effects' loudspeakers in the auditorium, the other being used as a control track.

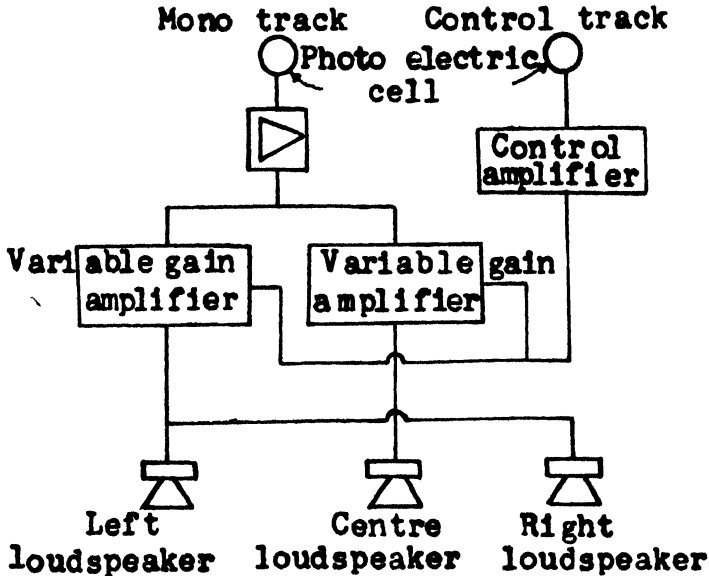


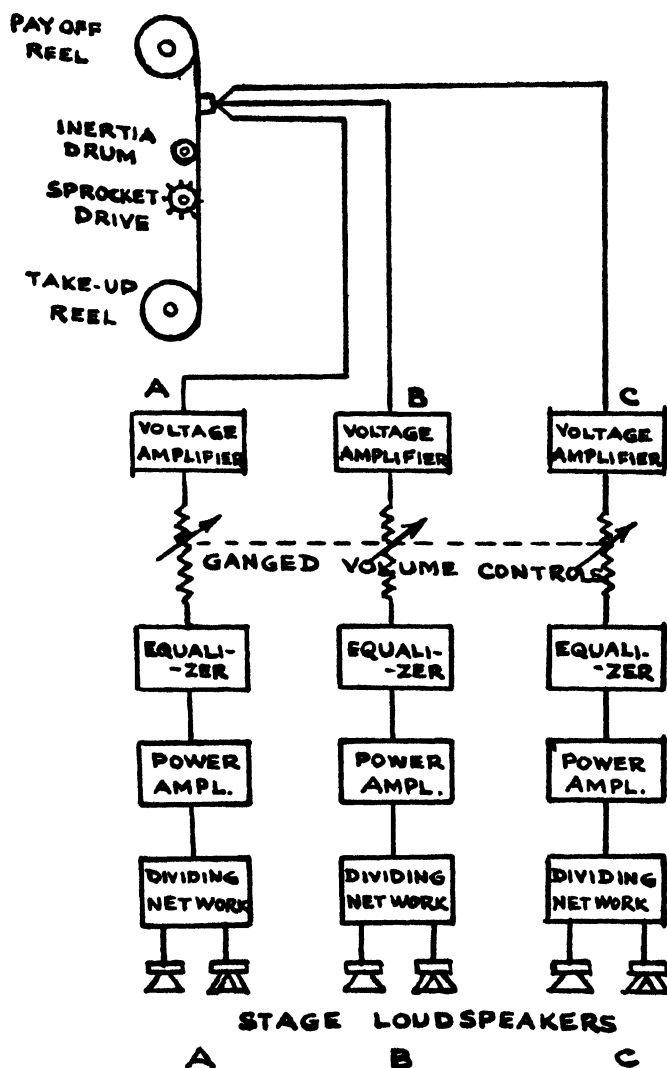
Fig. 22

Vitasound

136. Shortly after the appearance of Cinerama, in 1953, a number of three dimensional stereoscopic films were produced and it was natural to apply the stereo sound technique to these. In this case three channels were used, but the sound was not in fact truly stereo. This was particularly true of the speech, which was in fact monophonic in origin, an illusion of movement being obtained by panpotting the monophonic signal between the three channels. Music on the other hand was more nearly stereo, although since monophonic microphone techniques were still used for the most part, even this was often produced by spreading a monophonic sound rather than by true stereo methods.

137. The first commercial presentation of cinema stereophony to be made available on the major distribution circuits was introduced with the cinemascope productions in 1953. The earlier Cinerama productions had been limited to only a few theatres because of the special equipment needed both to project the three component parts of the picture and to reproduce the multi-track sound. In the case of Cinemascope, it was found possible to accommodate four narrow sound tracks on the picture film, thus doing away with the necessity for a separate synchronised film transport mechanism. The equipment in consequence was less costly, and it became possible to install it in more theatres.

138. The elements of a three channel magnetic-tape stereo sound motion-picture reproducing system are shown in Fig. 23. The output of the three-channel magnetic head is fed to three separate voltage amplifiers. The volume controls of the three channels are gauged so that the same amplification is maintained in the three channels



THEATRE

Fig. 23

Schematic arrangement of three-channel stereo magnetic-tape sound motion-picture reproducing system

three channels. The equalizers are used to adjust the frequency characteristics to those suitable for the best reproduction in the theatre. The output of power amplifiers feeds the three sets of loudspeakers, which are located behind the screen.

The Cinemascope system

139. The 20th Century-Fox Cinema Scope system uses, in so far as its sound medium is concerned, a three-channel main stereo system plus a fourth channel carrying special effects to be reproduced on loudspeakers in the auditorium area. The sound tracks, as mentioned above, are accommodated on four magnetic strips applied to the picture film, two on either side of each row of sprocket holes. The effects track, track four, is only half the width of the three main tracks, and, in consequence, will have a poorer signal to noise ratio. This track is only used intermittently, and carries a switching tone at 12 kilo-cycles per sec. whose function is to turn on and off the appropriate reproducing equipment. Thus the loudspeakers are prevented from reproducing interfering background noises when they are not required for effects. (Fig. 24).

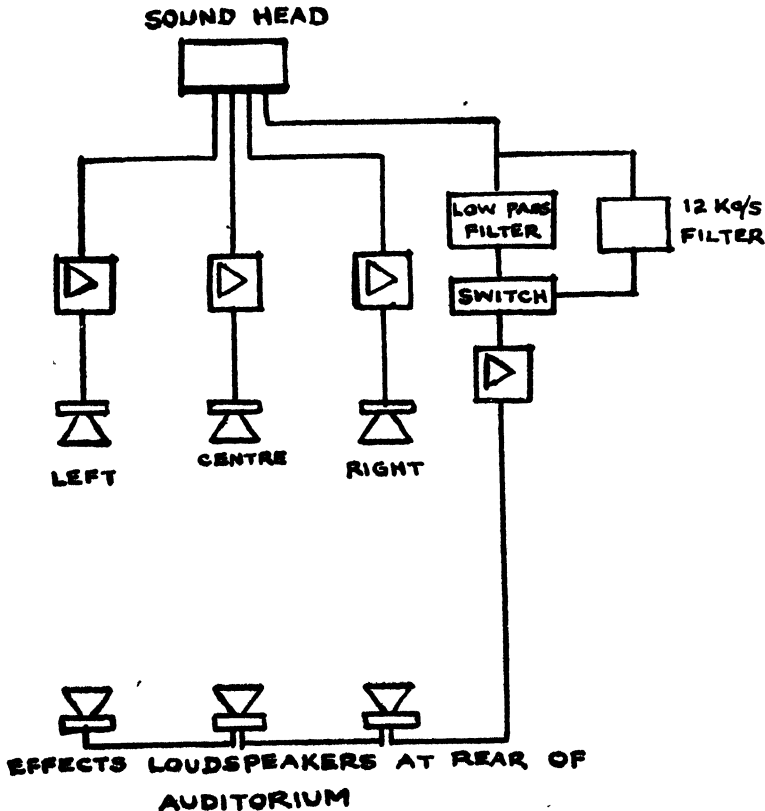


Fig. 24

Cinemascope system

140. The sound tracks are recorded in such a manner that the sound is 28 picture frames behind the picture in the gate. This is in contrast to the optical sound

system, where the sound is recorded in advance of the picture. In contrast to the optical sound head, which is after the picture gate, the magnetic sound head assembly is mounted as a separate unit between the picture projector and the upper film magazine, and the smoothing of the intermittent motion of the film transport system is accomplished by means of heavy fly-wheels and jockey pulleys. The fly-wheels are driven by the film itself, the drive to the film coming from the top sprocket in the picture projector. Wow and flutter can be reduced to an acceptable value by means of this system. Typical figures are 0.03% low frequency flutter and total RMS value within 0.15%, the generally accepted standard for cinema equipment.

141. The Cinema Scope release print, with its striped magnetic sound tracks, is capable of a high standard of reproduction. Unfortunately, in order to show such a film, a cinema must obviously be equipped with the appropriate reproducing apparatus. This may mean a costly conversion for the projectors as well as the additional loudspeakers required for the stage. The Cinema Scope print with magnetic sound track cannot be reproduced on projectors having only an optical sound system. The film is not compatible.

'Perspecta' sound system

142. In an attempt to make a film sound system which would give normal monophonic operation in a theatre equipped solely for single track optical sound reproduction, and from the same print give an impression of stereophony in a theatre with additional equipment, the Perspecta Sound system was devised. (Fig. 25).

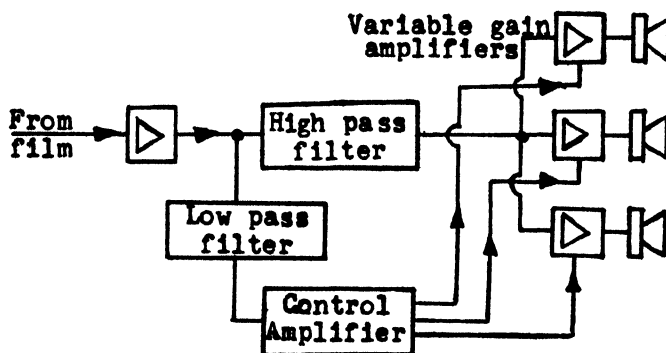


Fig. 25

Perspecta sound

143. In this system one sound track only is recorded on the film with the normal optical technique. In addition to the sound for the film, controlling signals at very low frequencies are recorded, the purpose of these being to control the individual gains of the channel amplifiers in the three channel theatre system. The control signals are at 30, 35 and 40 cycles per sec. the 30 cycles per sec. tone controlling the left speaker, the 35 cycles per sec. the centre and the 40 cycles per sec. the right hand speaker. The amplitude of these tones controls the level at which

the loudspeakers reproduce. Hence, depending upon which of the three tones are present, one, two or three loudspeakers will be in operation, all of them reproducing the same single track sound.

144. In this way it is possible for a sound to appear to move across the screen as the three channels are varied in sequence, or to produce a 'spread' effect when they are all present at once. Filtering prevents the control tones being heard in the theatre. Although this system is capable of producing a compatible release print, the electrical adjustment of the system is somewhat critical if perfect reproduction is to be obtained. This may be why few films have been made using the system and hence why few cinemas have been equipped to reproduce it.

Stereophonic reproduction in a car

General

145. Uptill recently, the technique of tape recording was not refined enough for good fidelity with 8 tracks narrow enough to go side by side on the quarter-inch tape. And duplication of the tapes would have been extremely difficult. But the art has been moving ahead fast. Low-noise tapes, excellent, low-cost playing heads, and other recent developments now give tape a dazzling potential for higher fidelity in very compact forms. This potential is one of the aspects that makes one of the latest developments in stereo reproduction—the car cartridge system, so exciting.

Stereo tape cartridge system

146. This system has been developed early this year for listening stereo music in a car. It has a reel of tape in a small, flat, plastic box, known the 'Cartridge', of size $5\frac{1}{2}$ in. \times 4 in. \times $\frac{7}{8}$ in. It has the speed of $3\frac{1}{4}$ inches per second and has 8 tracks having 4 complete stereo programme on each reel. Its playing time is 80 min.

147. The player is a small one and fits in the car very easily. It is rugged and reasonably simple in construction, with solid state electronics that should last virtually for ever : there are no tubes to replace. It is understood that, based on this development, a number of firms are trying to get home-style 8 track players developed and marketed soon.

148. Another reason for the way this system has zoomed in is one that most old hands in the recording industry did not anticipate. It is simply that people love the way stereo music sounds in a car. Stereo in the living room is a splendid thing, at its best creating a powerful sense of 'concert hall space' around the music. Stereo in a car creates a 'space' that is not so much like that of live music but is often very exciting on its own terms.

149. With the development of 8 track tape, it does not seem inevitable that stereo disc will die out soon. It is considered that 8 track tape and the stereo disc will undoubtedly co-exist for a long time. Over a long period, however, and by an orderly change over process, the 8-track cartridge system just might dethrone the disc, taking over the top spot in the living room that the disc has occupied since the turn of the century.

Conclusion

150. As the name implies, the object of stereo reproduction of sound is to reproduce sound in the "solid", with both depth and width, and with every part of the source sounding in its correct position in relation to the whole. The first patent for stereophony was granted in 1881, and stereophonic tapes and discs were produced in the 1930's; but it is only comparatively recently that the art reached its present high standard which is satisfying to the most discriminating.

151. The purpose of stereo sound is to present a true sense of the relative positions of the sounds being produced. Although a person hears a sound with both ears, the sound heard by each ear is slightly different. The brain utilizes this difference to determine, among other things, the direction of the sound. It is this feature of hearing that gives a sound depth as well as direction.

152. A short theoretical discussion on the theories of directional hearing and the creation of stereo effects has been given in the text for fully appreciating some of the technicalities which follow.

153. The advent of stereo stimulated quite a spate of ideas of pseudo-stereo : some means of 'deriving' stereo from earlier monophonic programme material. The success of any pseudo-stereo system must of necessity be measured against what its intention is. There are two main approaches. One merely seeks to give a sense of space by adding artificial reverberation. The other seeks to spread the apparent sound source by an adaptation of two or more speakers on the basic monophonic programme source.

154. In considering the potentialities of different systems of stereo reproduction and also examining the performance and the degree of realism they reproduce, we should keep in mind both the critical and the tolerant aspects of the human hearing faculty.

155. For the home user economy is an important factor. The system has to be made at a cost that a reasonable number of people can afford to buy, or it is not a commercial proposition. Closely associated with economy is compatibility. The system should be simple to use and should be able to present the fullest possible dynamic range in recorded material.

156. The exact requirements of loudspeaker placement, relative frequency response and relative power handling capabilities of the loudspeaker systems to be used are matters on which even the most respected authorities differ. This is probably because the placement of microphones at the source, the relative size of the source and the nature of sounds involved differ widely in the different programmes to be reproduced. One set of conditions cannot be optimum for all. Whatever the kind of programme material, the loudspeakers must be well-integrated, so that each loudspeaker gives a good impression of its source point, and does not itself sound like a spread-out source.

157. Different mediums that can be used to present the programme material over the stereo systems, as the home user sees them are disc, tape and radio. Each of these mediums has been discussed in the text. Stereo radio has still not reached

our country yet. With both tape and disc, the question of the ultimate in dynamic range seems to be a combination of two factors, namely, how much care and attention is given to the development of the system and better materials; and how much we are prepared to sacrifice, quantity—and price-wise, in achieving an increased dynamic range.

158. Stereo sound reproduction for large places like movie theatres and auditoriums have some peculiar problems of its own in addition to those found under domestic conditions. At present there are a number of wide-screen techniques employed in the movie presentations together with the corresponding sound presentations. Most of these have been described in the text.

159. The exhibitor's problems with multi-track presentation are very considerable. The movie projectors installed in the average theatre have the sound heads located in the correct position for standard optical track. To present stereo optical, which has additional sound tracks located somewhere else on the film, requires the addition of extra sound heads in the projector. This means the installation of a new section of the projector, thereby meaning additional expenses. The advent of magnetic tape-recording has made possible the application of the magnetic oxide to the actual movie film.

160. The various systems so far developed represent a tremendous advance in the stereo reproduction of sound and it is anticipated to show further improvements in the near future. This statement is fully justified by the latest techniques and equipments used in the modern stereo reproduction. Items like the development of stereo 'tape cartridge system' have not only brought stereo music on the open roads, but also may well revolutionize the construction, system and equipment of future stereo reproduction of sound.

161. Lastly, it must be emphasized that stereo reproduction is a part of high fidelity, not an 'additional feature'. Rather it can be said that stereo reproduction is a "fine point" in high fidelity.

References

1. Robert I. Sarbacher. 'Encyclopaedic Dictionary of Electronics and Nuclear Engineering'.
2. Norman H. Crowhurst. 'Stereophonic Sound'.
3. William F. Boyce. 'Hi-Fi Stereo'.
4. Morris Slurzberg and William Osterheld. 'Essentials of Radio Electronics'.
5. William R. Wellman. 'High Fidelity Home Music Systems'.
6. F. Langford Smith. 'Radio Designer's Handbook'.
7. Dr. N.A.J. Voorhoeve. 'Low Frequency Amplification'.
8. Norman H. Crowhurst. 'FM Stereo Multiplexing'.
9. A.T. Collins. 'Hi-Fi and Audio'.
10. D.L.A. Smith. 'Principles of High Fidelity sound Engineering'.

11. Norman H. Crowhurst. 'High Fidelity Sound Engineering'.
12. Gordon J. King. 'The Practical Hi-Fi Handbook'.
13. H. Burrell Hadden. 'Practical Stereophony'.
14. Munroe Upton. 'Inside Electronics'.
15. D.R. Khanna and R.S. Bedi. 'A Textbook of Sound'.
16. 'Encyclopaedia of Science and Technology'. *McGraw-Hill Book Co.*
17. 'Popular Electronics', March 1965.
18. 'Wireless World, March, April, May and June 1960, June and October 1962 and January and October 1963.
19. 'Proceedings of the Institution of Radio Engineers'. August and September 1950, May and November 1951 and July and October 1952.
20. 'Electronics Age', Spring 1966.

A DIRECT-COUPLED LOW-FREQUENCY PHASE METER***A. K. Mohanty***Non-member*

and

T. Natarajan*Non-member***Summary**

This paper describes a meter to read difference in phase between two electrical quantities which vary over wide range of frequencies, particularly low frequencies as encountered in servomechanisms. The meter is quite accurate, can pick up signals as low as 0.1 volt and its working is independent of the input waveforms.

1. Introduction

Phase meters have been constructed both for audio and radio frequencies utilizing several principles, namely,

- (a) Phase conscious rectifier systems as phase discriminators,¹
- (b) By neutralizing the phase introduced by the unknown network by means of a known network of variable phase,^{2,3,4}
- (c) Digital counting principle,⁵
- (d) Zero intercept phase comparison methods,^{6,7} and
- (e) Overlap phase meter.⁸

Many of these methods have some drawbacks in the sense that some are very frequency sensitive, some respond erroneously when harmonic content in the test signal is considerable and some are not direct reading while others are quite complicated.

A circuit based on principle (d) previously worked on by Kratzman⁶ and Yu⁷ for audio and ultrasonic frequencies can be simplified and, by means of direct coupling, use very low frequencies; but due to some difficulties to be indicated later, a different method was adopted.

2. Principle

A reference and a test signal of the same frequency are fed into two channels of electronic circuits as in Fig. 1. The amplified waveform, each one of them, is fed into an amplifier-comparator circuit which converts it to a square wave. The square waves feed into the grids of a summing amplifier and they produce current in the common plate resistance of this amplifier. Therefore, a voltage develops

*Written discussion on this paper will be received until September 30, 1966.

This paper was received on December 29, 1966.

in this resistance which is the algebraic sum of the square waves. Fig. 2 explains the operation involved. The duration of current flow in the above resistance is directly proportional to the phase angle.

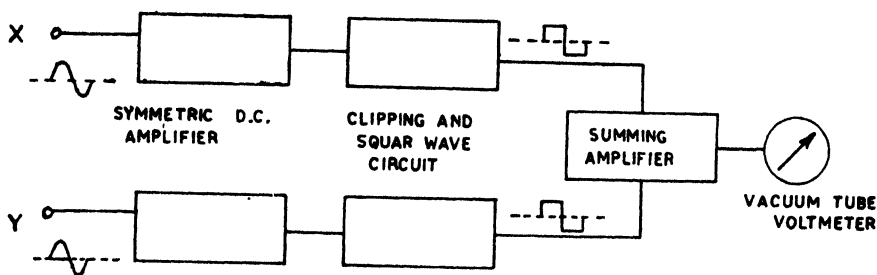


Fig. 1

Block diagram illustrating overlap phase meter

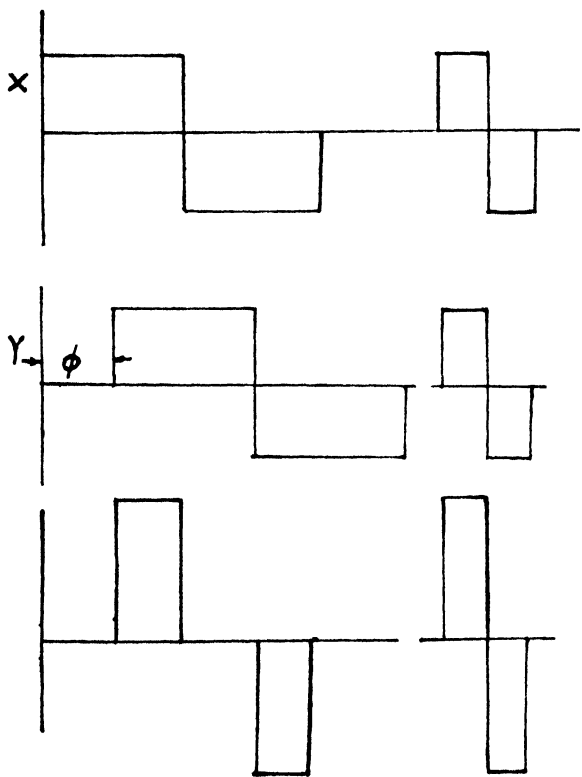


Fig. 2

Output waveform for different phase shifts

3. Different stages

3.1. Symmetric D.C. amplifier

The signal needs some amplification if its level is low, also the precision of the clipper or comparator circuit which converts the signal to a square wave is improved by a factor A , if the comparator is preceded by an amplifier of gain A . A paraphase difference-amplifier circuit adopted in the first stage provides

symmetric amplification, extreme linearity of operation, stability of quiescent D.C. voltage level, freedom from drift and a very high input impedance to act as a buffer to the signal source. The outputs of both halves of the amplifier are in pushpull. To obtain sufficient gain, another stage of D.C. amplification is adopted, the overall gain of both amplifiers being 1215.

3.2. The comparator circuit

The rectangular pulse producing circuit defines the instant when the waveform passes through a critical point by means of the stable and sharp break characteristics of a triode at cut-off. The zero of the wave is selected as the level of comparison as the slope is greatest here and the operation is then independent of the wave amplitude. Fig. 4 represents the cathode-coupled clipper⁹ circuit and the associated waveform. The grids are returned to approximately equal positive potentials for symmetrical clipping. For smaller inputs, the circuits act as a linear amplifier but on the positive half cycle of a large input signal to T_1 , the cathode potential rises and tube T_2 is cut-off. Once T_2 is cut-off a further increase in the input grid potential has no effect on the output. Similarly on the negative half cycle, T_1 is driven to cut-off because the plate current of T_2 holds the cathode potential at a high value and once T_1 is cut off the signal has no effect on the output.

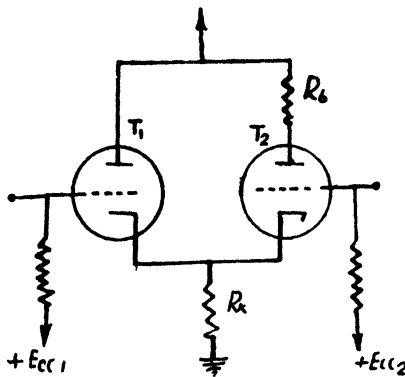
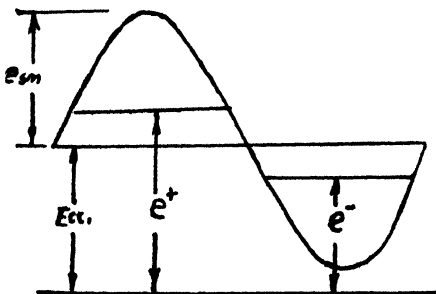


Fig. 4

Cathode coupled clipper circuit



The clipping level is 5 volt; maximum input voltage to the clipper is 40 volts or more.

3.3. Summing amplifier

In this, two amplifiers have a common load resistance. The square waves which are produced at the zero axis crossing of both the waveforms produce current in the common load. The tube operates either in class A or grid limited fashion.

3.4. Voltmeter circuit

The duration of current flow in the common load resistance as shown in Fig. 2, is a direct function of phase angle ϕ , i.e., it is proportional to $(180^\circ - \phi)$. The pulses of the figure can be rectified by means of a diode and fed into the grids of a most elementary balanced triode vacuum tube voltmeter. The reading of the meter in the plate circuit is proportional to the phase angle ϕ . It should be noted that for reading the phase at low angle frequencies, the meter requires special damping arrangements.

4. Calibration of the meter

The standard calibration network chosen for calibration purposes is a R - C network supplied from an oscillator balanced with respect to earth. The network along with the associated phasor relationships appear in Fig. 5 (a) and 5 (b).

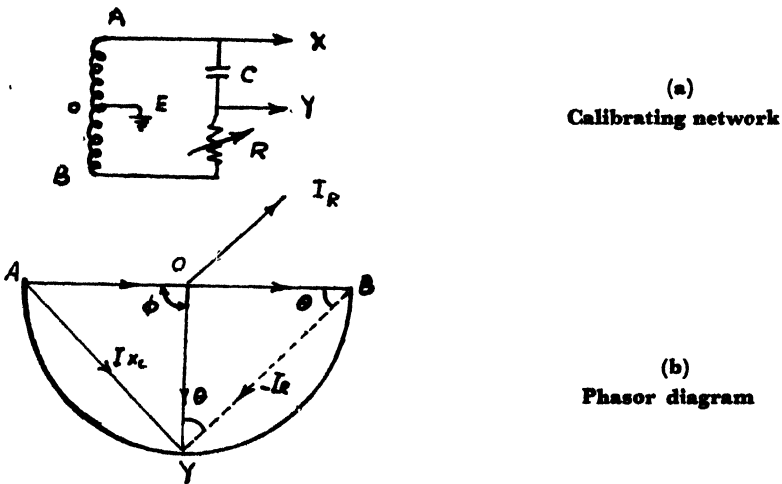


Fig. 5

Here ϕ , is the phase angle between V_{A0} and V_T , and $\phi = 2\theta$ where $\theta = \tan^{-1} \frac{X_c}{R}$.

Calibration was carried out with a 0.2 microfarad (polyester capacitor) 10% and a resistance box 10% tolerance. In the low frequency region, the meter reading was found to be substantially constant for a given phase angle irrespective of frequency. A curve of phase angle *vs.* meter reading is shown in Fig. 6.

5. Modified meter using a flip flop circuit

The meter based on the principle of overlap, suffers from a disadvantage, the meter reading is proportional to the magnitude of the phase difference or its

supplement and is ambiguous to the extent that one cannot distinguish between θ and $(360^\circ - \theta)$.

To obviate this difficulty, the circuit diagram to the right of the amplifier-comparator circuit is modified and appears as in Fig. 7(a).

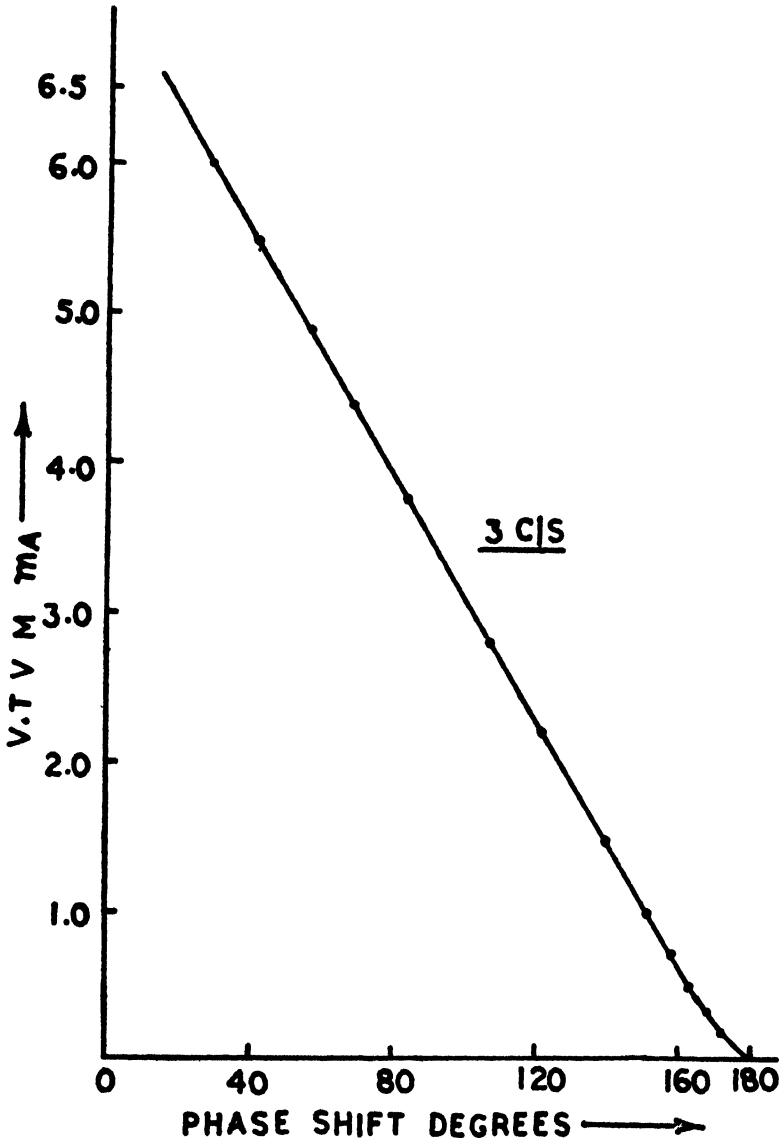
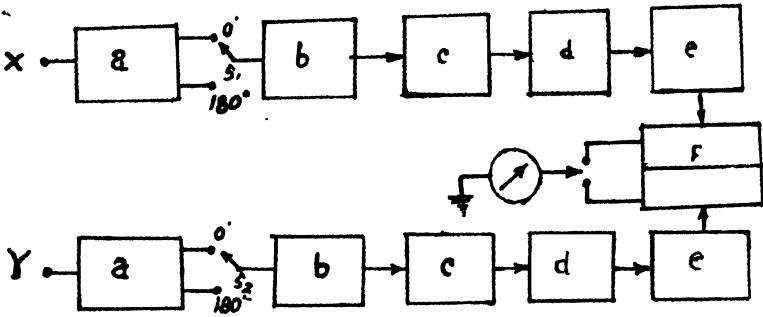


Fig. 6

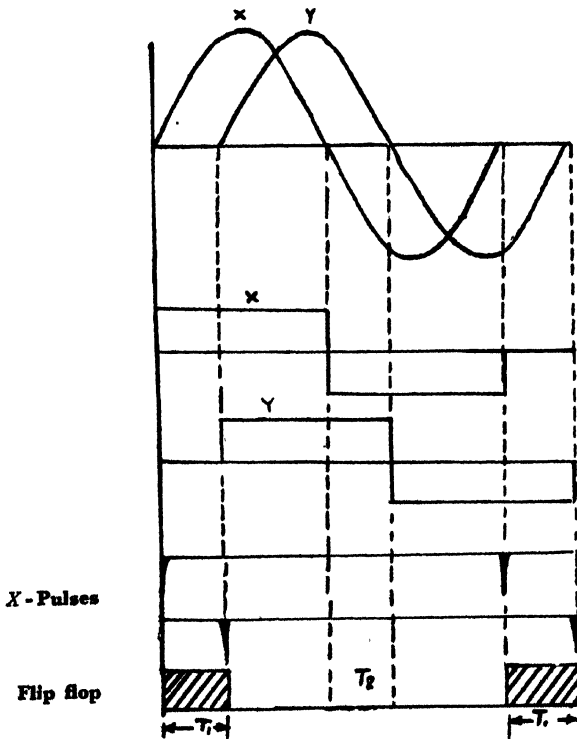
Overlap principle

The output of the comparator is fed into a differentiating network which produces pulses when the input wave crosses zero axis. The pulse train is amplified and fed into the grid of another amplifier which is biased to cut-off, so that



(a)

- a. Symmetrical D.C. amplifier
- b. Amplifier
- c. Comparator or clipper
- d. Differentiator-amplifier
- e. Amplifier
- f. Flip flop



(b)

Fig. 7

at its output a spike of negative pulse appear. The negative pulse from each channel are fed into each of the grids of a flip flop circuit. Each reference pulse triggers the flip-flop into 'on' for a time interval T_1 , until the similar pulse from the other channel arrives and triggers the tube to 'off' for a period T_2 and so on. The angle by which the reference signal leads the test signal is directly proportional to $\frac{T_1}{T_1 + T_2}$ and hence to the average current through the reference side of the trigger circuit. Likewise the test signal leads the reference by $\frac{T_2}{T_1 + T_2}$ and so the lead is proportional to the mean D.C. through the test signal side of the multivibrator circuit.

5.1. *Differentiator amplifier*

The grid of this amplifier is kept at zero bias so that the positive half cycle of the input square wave is grid-limited and only the negative half is amplified producing a positive going square wave at its output, the load R_L is kept deliberately very high compared to the plate resistance r_p so that it reacts sharply to positive going edges, producing large negative pulses of small duration of 1.5 microsec. at the R - C differentiator output.

5.2. *Direct coupled flip flop*¹⁰

It is a bi-stable trigger, and has been designed to ensure stability and speed of transition between stable states so that all transients die down in between the switching pulses. The design has taken into account the maintenance of stability when the components vary by $\pm 10\%$.

The modified circuit diagram is shown in Fig. 8.

Using the previous calibration network, the meter is calibrated and the phase angle *vs.* the meter reading is plotted in Fig. 9 and is seen to be linear.

6. **Conclusions**

Two types of phase meters constructed and tested have been described. The overlap type calls for a simplified circuit compared with the complicity and instability associated with the bi-stable multivibrator in the second method, as the bi-stable circuit showed triggering difficulty at low frequencies. The overlap meter was observed operating quite satisfactorily, from 3 cycles per sec. to 1000 cycles per sec. Below 3 cycles per sec. the meter damping was insufficient. Special damping can be provided either across the meter or at the grid of the balanced triode V.T.V.M. circuit in the form of a large capacitance.

The overlap meter reading is proportional to the magnitude of the phase difference or its supplement and is ambiguous to the extent that one cannot distinguish between θ and $360^\circ - \theta$. It can be overcome in the flip flop method in which the phase lead between X and Y or Y and X can be accurately determined from 0° to 360° by reading the current through both the sides of the flip-flap cathodes.

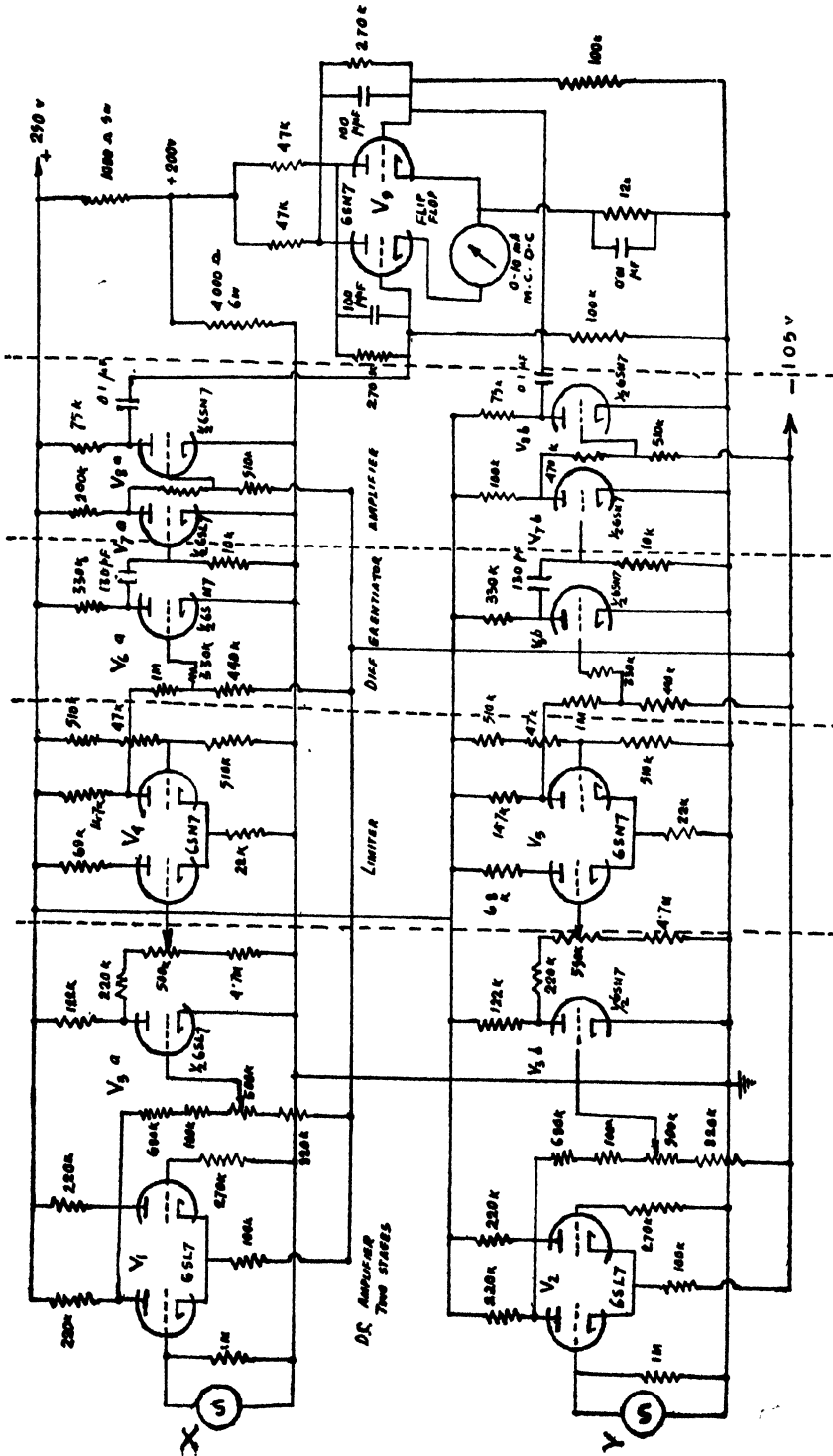


Fig. 8
Flip flop method

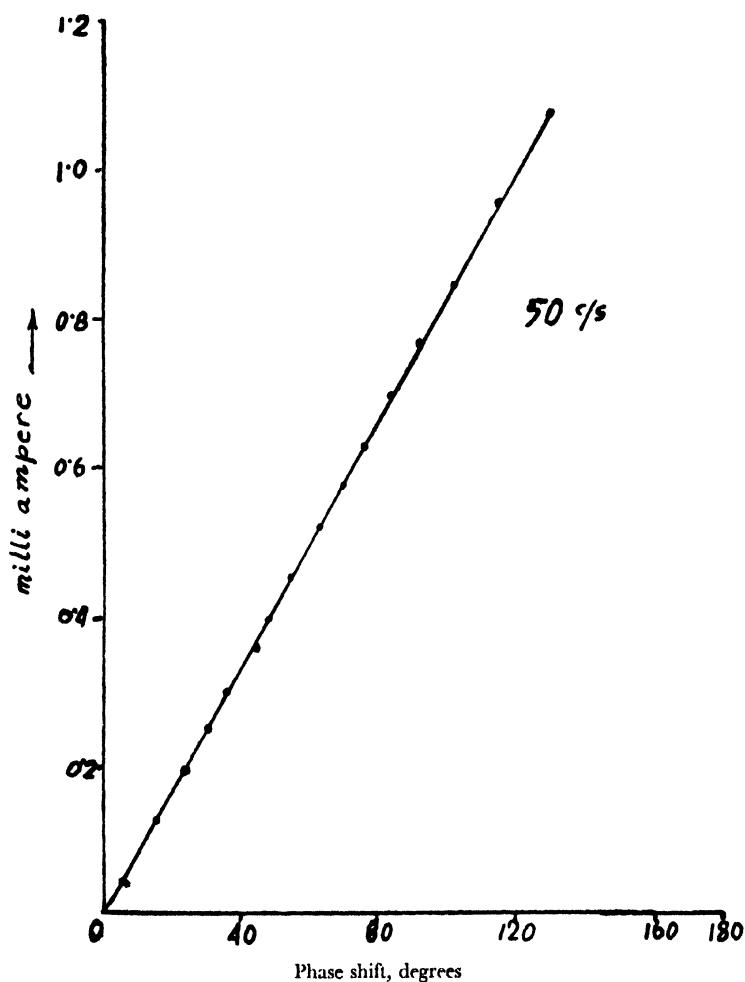


Fig. 9

Flip flop method

7. Acknowledgment

This project was undertaken in partial fulfillment of the M.Tech. degree in Electrical Engineering of the Indian Institute of Technology, Kharagpur. The authors are grateful to Prof. N. Kesavamurthy, Professor in Electrical Engineering Department, Indian Institute of Technology, Kharagpur, for valuable guidance and constant encouragement.

8. References

1. S. Krishnan. 'Diode Phase Detectors'. *Electronics and Radio Engineers*, vol. 35, no. 2, February 1959, p. 45
2. A.G.J. Holt. 'Measurement of Phase Shift at Audio Frequencies Using Magslip as a Calibrated Reference'. *Radio Electronics Engineers*, vol. , no. , October 1963, p. 305.
3. J.C. West and Potts. 'A Simple Variable Frequency Phase Measuring Device'. *Electronic Engineering*, September 1952.
4. B. Chatterjee. 'An Accurate Phase Meter for Terminal Networks'. *Indian Journal of Physics*, vol. 33, 1957, p. 541.
5. N. Hambley. 'A Low Frequency Phase Meter Electric Engineering'. vol. 37, no. 371, January 1959, p. 13.
6. E.R. Kratzman. 'Measuring Phase at Audio and Ultrasonic Frequencies'. *Electronics*, vol. 22, October 1949, p. 2.
7. Y.P. Yu. 'Zero Intercept Phase Comparison Method'. *Electronics*, November 1953.
8. D.J. Collins and J.E. Smith. 'Some Methods of Phase Measurement used in Transfer Function Analysis'. *Electronic Engineering*, vol. 30, April 1958.
9. L.A. Goldmuntz and H.L. Krauss. 'The Cathode Coupled Comparator Circuit'. *Proceedings of Institute of Radio Engineers*, vol. 36, September 1948.
10. R. Renwick and M. Phister. 'A Design Method for Direct Coupled Flip Flops'. *Electronic Engineering*, June 1955, p. 246.

LIMITATIONS ON THE PERFORMANCE OF A TELEVISION SYSTEM DUE TO PHOSPHOR DECAY*

P. S. Moharir

Non-member

Research Scholar, Electrical Engineering Department

The Indian Institute of Technology, Kanpur

and

K. V. Saprykin

Non-member

Leningrad Institute of Aviation Instruments, Leningrad, U.S.S.R.

Summary

The choice of phosphor for a picture tube screen is dictated by several considerations. But even if the decay characteristic were the only consideration, it can be shown that the full visual capacities of the eye cannot be satisfied. These limitations arise because of the contrast range allowed by the phosphor and the differential flicker due to its decay. The optimization conditions have been derived and it is shown that silicates and tungstates would be better for television use compared to sulphides.

1. Introduction

Several properties of phosphor are to be considered while selecting a phosphor for a picture tube screen. These properties are listed below:¹

1. Ease of applying phosphors to form screens of picture tube,
2. Ease of outgassing phosphors,
3. Secondary emission of phosphors,
4. Stability of phosphors against the effects of electron bombardment and associated thermal effects, contamination, exposure to moisture, light, air, tube processing (exhaust and baking) and high operating temperature,
5. Heat and infrared effects,
6. Emission spectra of phosphors,
7. Brilliance and efficiency of phosphors, and
8. Decay characteristics.

Obviously, as several other factors are to be considered while choosing the phosphor, the limitations set by the decay properties cannot altogether be avoided. But the point that needs appreciation is that, even if the decay characteristics were the only consideration some limitations have to be tolerated.

***Written discussion on this paper will be received until September 30, 1967.**

This paper was received on July 19, 1966.

The elementary types of phosphor decay curves can be represented by one of the following equations :

$$B = B_0 e^{-kt} \quad (1)$$

$$B = \frac{B_0 b^\alpha}{(b+t)^\alpha} \quad (2)$$

where B_0 is the luminance at time $t = 0$, and k, b, α are constants. Equation (1) holds true for monomolecular process, typical of silicates and possibly tungstates. Equation (2) holds true for bi- or poly-molecular process, typical of sulphides.

The intensity of phosphorescence is in both the cases proportional to the number of active centres, n . Thus,

$$B \propto n \quad (3)$$

But the rate of decay of active centres in monomolecular case is proportional to the number of active centres at any instant. Thus,

$$\frac{dn}{dt} = -kn \quad (4)$$

or

$$\ln n = -kt + \ln c \quad (5)$$

where c is an integration constant. Hence,

$$n = C e^{-kt} \quad (6)$$

or using equation (3),

$$B = B_0 e^{-kt} \quad (1)$$

Thus k is the decay constant of a monomolecular process.

In poly-molecular process

$$\frac{dn}{dt} = -a n^h; \quad h > 1 \quad (7)$$

where a and h are constants. Therefore,

$$n^{1-h} = -a(1-h)t + g \quad (8)$$

where g is integration constant related to initial value of n , and can be put in the form

$$g = -a(1-h)d \quad (9)$$

so that

$$n = \frac{\left[a(h-1) \right]^{\frac{1}{1-h}}}{(b+t)^{\frac{1}{h-1}}} \quad (10)$$

or using equation (9)

$$n = \frac{g^{\frac{1}{h-1}} b^{\frac{1}{h-1}}}{(b+t)^{\frac{1}{h-1}}} \quad (11)$$

Thus with $\frac{1}{h-1} = \alpha$, and using equation (3) this can be put in the form of equation (2). Thus α is a constant related to the order of decay in a poly-molecular process and b is a constant related to the order of decay as well as to the integration constant g . The purpose served by the constant b in equation (2) is to avoid singularity at $t = 0$ and to restore the value of B at $t = 0$ to B_0 .

However, neither equation (1) nor equation (2) can give any decay curve over its entire range.

2. Contrast limitations

Let $p(B_0)$ be the probability that at a particular point and at a particular time designated as $t = 0$, the luminance B_0 appears. Then the actual luminance at that point can be considered to be

$$\bar{B}_0 = \frac{\int_{B_0 \text{ min.}}^{B_0 \text{ max.}} p(B_0) B_0 dB_0}{\int_{B_0 \text{ min.}}^{B_0 \text{ max.}} p(B_0) dB_0} \quad (12)$$

This will decay according to equation (1) or equation (2). The decay continues for a time T after which another signal appears. T is then the frame period. At the end of time T the luminance would have decayed to a level \bar{B}_T .

Another signal appearing at this moment would produce some effect only if its luminance level is greater than B_T , otherwise, it would not be reproduced and the effect would be as if the luminance level of the signal appearing is \bar{B}_T . Thus the phosphor decay allows the maximum-contrast range of

$$C_p = \frac{B_0 \text{ max.}}{\bar{B}_T} \quad (13)$$

One minor effect of incomplete phosphor decay is neglected here. If a signal appears before the effect of previous signal is completely decayed, the luminance reproduced is slightly more than what would be reproduced if the second signal appears after the effect of previous signal is completely decayed. But this difference can be treated as a small distortion term and neglected.

Now the statistical area properties of a television scene are such that the first order luminance distributions tend to be uniform.² E. R. Kretzmer's findings³ indicate that the amplitude probability distribution of a television signal is nearly uniform. There is a tendency for black elements to predominate over white ones, but this trend is very slight. A. J. Seyler⁴ assumes that a measurement of a large number of typical television pictures would yield a uniform composite first order amplitude distribution. Therefore, we get

$$p(B_0) = \text{Constant} \quad (14)$$

Then, from equation (12)

$$\bar{B}_0 = \frac{1}{2} (B_{0 \max.} + B_{0 \min.}) \quad (15)$$

or

$$\frac{B_{0 \max.}}{\bar{B}_0} = \frac{2 C_n}{C_n + 1} \quad (16)$$

where C_n is the natural contrast range not limited by the phosphor decay, and is given by

$$C_n = \frac{B_{0 \max.}}{B_{0 \min.}} \quad (17)$$

Using equations (13) and (16), we get

$$C_p = \frac{2 C_n}{C_n + 1} \cdot \frac{B_0}{\bar{B}_T} \quad (18)$$

The phosphor would not limit the contrast range if

$$C_p \geq C_n \quad (19)$$

i.e., if

$$\frac{\bar{B}_0}{\bar{B}_T} \geq \frac{C_n + 1}{2} \quad (20)$$

The above discussion is expressed graphically in Fig. 1.

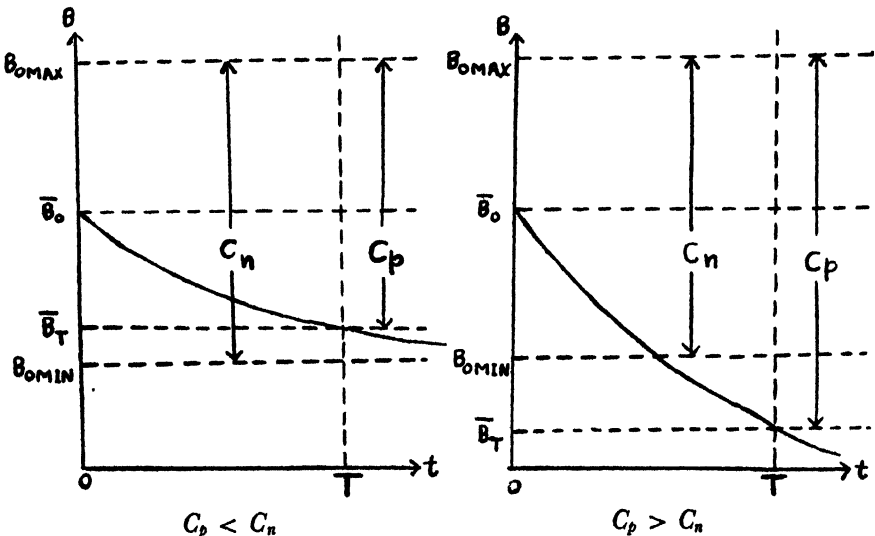


Fig. 1

Graphical explanation of contrast limitations due to phosphor decay. The thick line indicates the phosphor decay curve, the decay starting with \bar{B}_0 , the average initial scene luminance, and decaying upto luminance level \bar{B}_T in frame period T . $B_{0 \max.}$ and $B_{0 \min.}$ are the maximum and minimum initial luminance levels in a scene. If $\bar{B}_T > B_{0 \min}$ phosphor decay limits the contrast range, otherwise it does not.

It can be easily seen that equation (20) does not depend on the form of decay, *i.e.*, is valid for all forms of phosphor decay. This equation brings out clearly the fact that the higher the contrast range C that the kinescope should occupy, the more complete should be the phosphor decay in the frame period. Incidentally, the faithful reproduction on the receiver screen of fast moving images also demands the same thing.

3. Differential flicker considerations

There is yet another aspect of phosphor decay that is to be considered. Consider two luminance levels B_1 and B_2 in vicinity of each other that decay according to equation (1) or equation (2). Their difference ΔB will also decay similarly. Now defining⁵ the differential flicker as the ratio of the r.m.s. value of the A.C. component of ΔB to its average value, both the average and r.m.s. values being computed over the frame period T , it can be shown that the differential flicker is given for the exponential decay as⁵

$$f_{de} = \left[\frac{kT}{2} \coth \frac{kT}{2} - 1 \right]^{\frac{1}{2}} \quad (21)$$

and for the hyperbolic decay as

$$f_{dh} = \left[\frac{(1 - \alpha)^2 \frac{T}{b}}{1 - 2\alpha} \cdot \frac{\left(1 + \frac{T}{b}\right)^{1-2\alpha} - 1}{\left\{\left(1 + \frac{T}{b}\right) - 1^{1-\alpha}\right\}^2 - 1} \right]^{\frac{1}{2}} \quad (22)$$

The differential flicker f_{dh} is quite a complex function of two parameters α and $\frac{T}{b}$. It can be easily anticipated that as the differential flicker increases the needed differential luminance threshold for sure luminance discrimination also increases.

As the differential luminance threshold is a monotonously increasing function of differential flicker, it is legitimate to assume that the number of grey shades that can be discerned in a given contrast range would be a monotonously decreasing function of differential flicker. Therefore it can be written that

$$N = N_0 Q(f_d)$$

where N is the number of grey shades that can be discerned in a given contrast range when differential flicker and other factors are taken into account, N_0 is the number of grey shades that can be discerned in a given contrast range in a flicker-free situation and Q is a monotonously decreasing function of its argument. More about N_0 would be said soon.

4. Partial optimization of decay characteristics

The decay characteristics would be called optimum when the largest number of grey shades can be depicted. To derive the optimum conditions the

combined effect of contrast limitations and differential flicker is to be taken into account. It is shown in the Appendix that

$$N_0(\hat{B}, B_0, C) = \frac{1}{4.37 \times 10^{-3}} \int_{\hat{B}/C}^{\hat{B}} [(B + B_0) + 22.25(B^2 + B_0^2) + 2.88 \times 10^{-6}(B^4 + B_0^4)]^{-\frac{1}{2}} dB \quad (24)$$

where N_0 is the maximum number of gray shades that can be discerned by the light-adapted human eye with the adaptation level B_0 in a scene with limited contrast C and maximum luminance \hat{B} . Thus it is seen that as the limited contrast range increases the number of gray shades that can be discerned also increases.

This equation can now be used to get the optimum conditions.

Equation (18) can be written as

$$C_p = C_{p \text{ max.}} \cdot \frac{C_n}{C_n + 1} \quad (25)$$

where

$$C_{p \text{ max.}} = \frac{2 \bar{B}_0}{\bar{B}_1} \quad (26)$$

Therefore, for exponential decay

$$C_{p \text{ max.}} = 2 e^{kT} \quad (27)$$

and, for hyperbolic decay

$$C_{p \text{ max.}} = 2 \left(1 + \frac{T}{b}\right)^\alpha \quad (28)$$

Using equations (27) and (21), $C_{p \text{ max.}}$ and f_d can be calculated as functions of kT . Using equations (28) and (22) $C_{p \text{ max.}}$ and f_d can be calculated as functions of $\frac{T}{b}$ with α as a parameter. A value $\alpha = 2$ is used for calculations, because usually

$$0.8 \leq \alpha \leq 3 \quad (29)$$

and, hence $\alpha = 2$ forms a middle value. Results of calculations are shown in Fig. 2.

From Fig. 2 it is seen that as kT and $\frac{T}{b}$ increase, C_p and f_d also increase. The effect of increase in C_p is, naturally, to allow the larger number of gray shades on the kinescope screen, but simultaneously the effect of increasing differential flicker is to increase the needed differential luminance threshold for sure luminance discrimination. These two effects of increase in kT and $\frac{T}{b}$ thus go counter to each other as far as the maximum number of allowed gray shades is of concern.

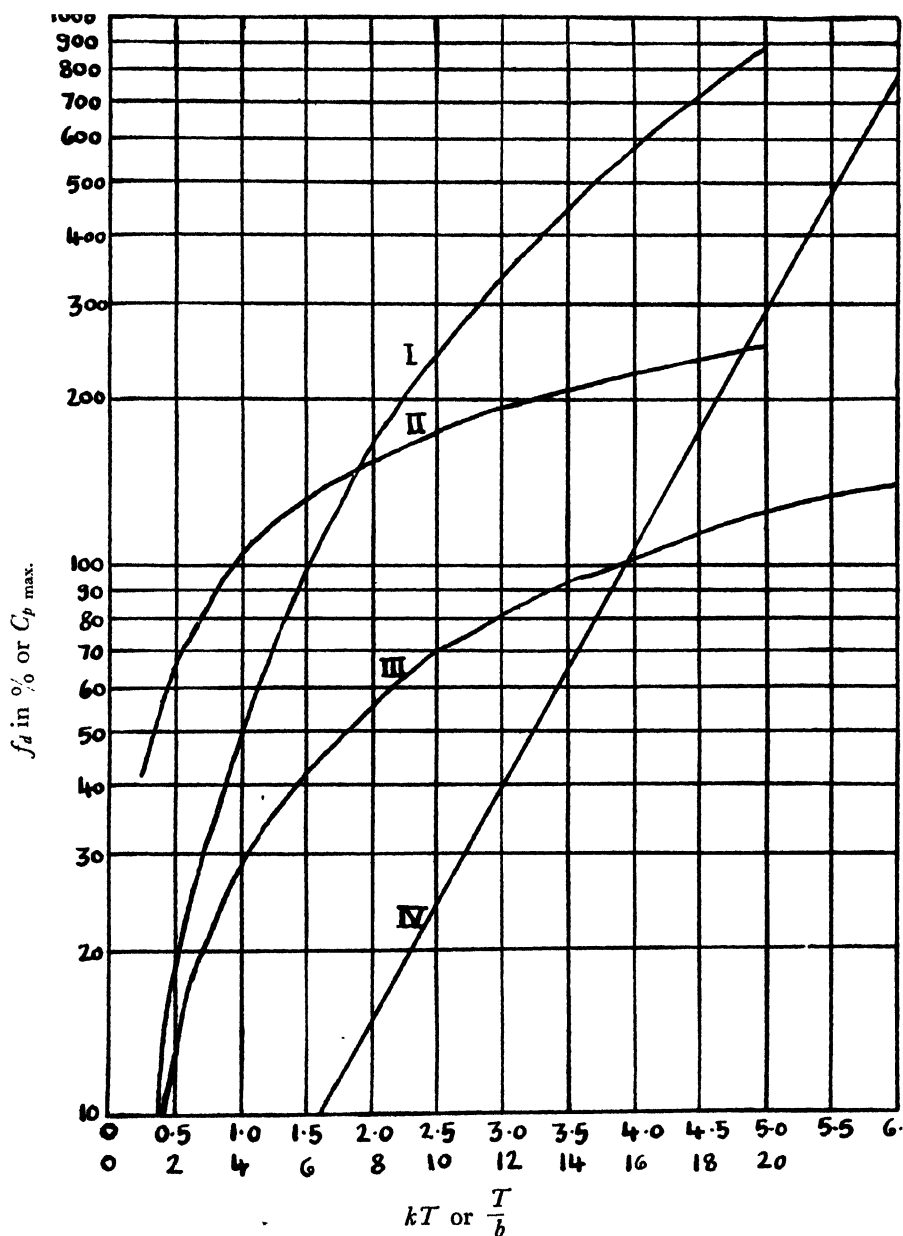


Fig. 2

I : $C_p \max.$ as a function of $\frac{T}{b}$ for hyperbolic phosphor with $\alpha = 2$, where C_p is phosphor limited contrast, T is the frame period and α, b are constants in the decay equation of a hyperbolic phosphor.

II : Differential flicker f_d as a function of $\frac{T}{b}$ for hyperbolic phosphor with $\alpha = 2$.

III : Differential flicker f_d as a function of kT for exponential phosphor where k is a decay constant of exponential phosphor.

IV : $C_p \max.$ as a function of kT for exponential phosphor.

For $C_p < C_n$, using equation (23), we get

$$N(\hat{B}, B_0, C_n \text{ and } kT \text{ or } \frac{T}{b} \text{ and } \alpha) = N_0(\hat{B}, B_0, C_p) Q(f_d) \quad (30)$$

Using equation (30), some sample calculations were done to calculate N as a function of kT or α and $\frac{T}{b}$. The form of $Q(f_d)$ assumed was

$$Q(f_d) = \frac{1}{1 + qf_d} \quad (31)$$

and some reasonable values of q were assumed. It was found that N goes through a maximum for very high values of kT or $\frac{T}{b}$. These values of kT or $\frac{T}{b}$ for which N is maximum are such that $C_p \simeq 1000$. But in actual natural scenes, eye makes use of the contrasts of the order of $C_n \simeq 100-200$ only.⁶ Thus, it may be said that for $C_p \ll C_n$, N continuously increases.

For $C_n \leq C_p$, equation (23) can be written as

$$N(\hat{B}, B_0, C_n \text{ and } kT \text{ or } \frac{T}{b} \text{ and } \alpha) = N_0(\hat{B}, B_0, C_n) Q(f_d) \quad (32)$$

It is immediately obvious that as the term N_0 is constant, whereas the term $Q(f_d)$ decreases as kT and $\frac{T}{b}$ increase, N continuously decreases for $C_p \geq C_n$.

Thus, it is seen that N goes through a maximum for

$$C_p = C_n \quad (33)$$

Thus, equation (33) gives an optimum phosphor decay condition.

For exponential phosphor, it becomes

$$e^{kT} = \frac{C_n + 1}{2} \quad (34)$$

and for hyperbolic phosphor it becomes

$$\left(1 + \frac{T}{b}\right)^\alpha = \frac{C_n + 1}{2} \quad (35)$$

From equation (23) it can be seen that the phosphor decay reduces the gray scale capacity of an eye by a factor of $Q(f_d)$. For $C_n \simeq 200$, this reduction factor under optimum conditions is $\frac{1}{(1 + 1.16 q)}$ for exponential phosphor and

$\frac{1}{(1 + 1.642 q)}$ for hyperbolic phosphor with $\alpha = 2$, if Q is assumed to be of the form given by equation (31). Thus even under optimum conditions phosphor decay does not allow full use of the gray scale capacity of human eye. Usually the optimum conditions would not be satisfied and this deviation from optimum conditions further limits the gray scale capacity of a television system.

5. Complete optimization of decay characteristics

The optimum condition given by equation (34) specifies optimum exponential decay uniquely. But the optimum condition given by equation (35) simply

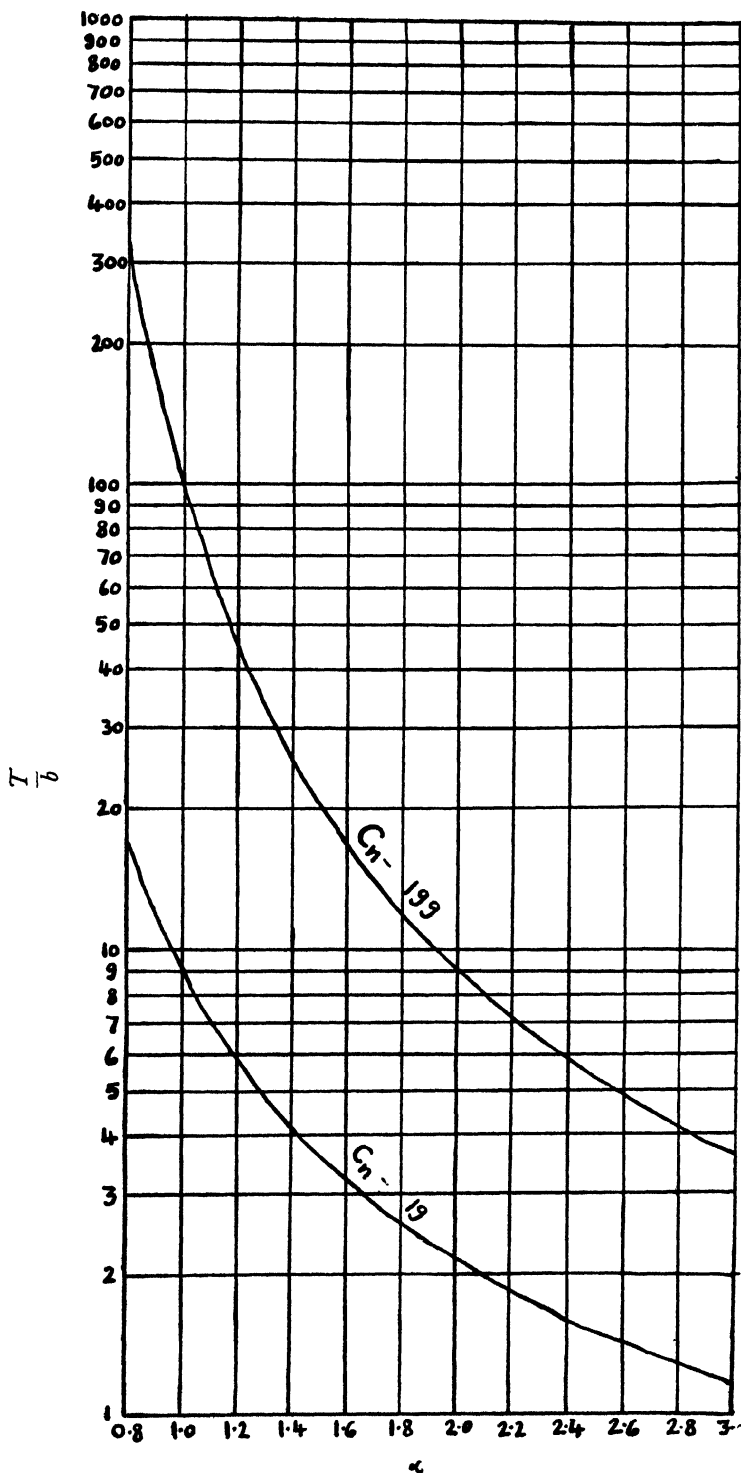


Fig. 3

Partial optimization relation $\left(1 + \frac{T}{b}\right)^\alpha = \frac{(C_n + 1)}{2}$ between α and $\frac{T}{b}$ for hyper-

specifies a relationship between α and $\frac{T}{b}$ for the hyperbolic decay. This relationship has been plotted in Fig. 3 for $C_n = 199$ and $C_n = 19$. To complete optimization, flicker should be calculated for every combination of α and $\frac{T}{b}$ given by equation (35). Then that combination for which flicker is least can be taken to identify optimum hyperbolic decay uniquely. The calculations were done for $C_n = 199$. The result is indicated in Fig. 4. The nature of this curve does not depend on C_n although the absolute values of flicker do. Optimum hyperbolic decay is at once obvious from Fig. 4.

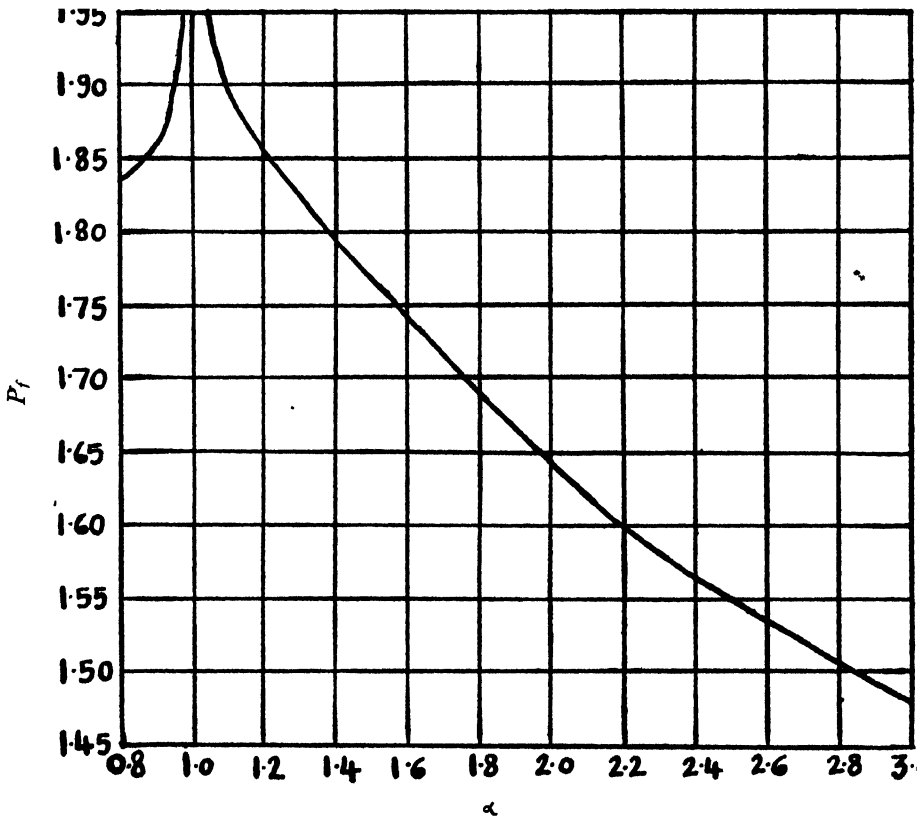


Fig. 4

Differential flicker f_d for hyperbolic phosphor as a function of α assuming that

$$\left(1 + \frac{T}{b}\right)^\alpha = \frac{C_n + 1}{2}$$

partial optimization relationship is satisfied for natural flicker-free contrast, $C_n = 199$. Here α and b are constants in the decay equation for hyperbolic phosphor and T is a frame period.

It can further be seen that flicker given by optimum exponential decay is always less than that given by hyperbolic decay. Thus exponential decay is superior to hyperbolic one as far as optimization of gray scale capacity of a television system is concerned.

6. Conclusion

It can be seen that exact form of function Q in equation (23) need not be known. Only thing that is necessary for the validity of the argument is that number of discernible gray shades decreases as the differential flicker increases and that decrease in number of discernible gray shades due to increase in differential flicker is more than outbalanced by the increase in number of discernible gray shades due to increase in C_p for $C_p \leq C_n$. Also, it can be seen that contrast and differential flicker considerations can always lead to complete optimization. It is also seen that optimum exponential decay allows the maximum gray scales capacity. This means that silicates and tungstates would be better for television use compared to sulphides. For those types of phosphor decay which cannot be represented either by equation (1) or by equation (2), it easily follows that attempt should first be made to satisfy condition (33), i.e., to have

$$\frac{\bar{B}_0}{\bar{B}_1} = \frac{C_n + 1}{2} \quad (36)$$

and then out of the phosphors that satisfy this condition a particular one which yields minimum differential flicker should be chosen.

7. Acknowledgment

Part of the work reported here was done at The Indian Institute of Technology, Bombay for Master's degree for the junior author.

8. References

1. H.W. Leverenz. 'Cathodoluminescence as Applied in Television'. *Radio Corporation of America Review*, vol. 5, no. 2, October 1940, p. 131.
2. S. Nishikawa, R.J. Massa and J.C. Mott-Smith. 'Area Properties of TV Pictures'. *Institute of Electrical and Electronic Engineers' Transactions on Information Theory*, vol. IT 11, no. 3, July 1965, p. 348.
3. E.R. Kretzmer. 'Statistics of Television Signals'. *Bell System Technical Journal*, vol. 31, 1952, p. 751.
4. A.J. Seyler. 'Channel Capacity Utilization of Television Relay Links'. *Forts. der Hochfrequenztechnik*, vol. 5, 1960, p. 263.
5. Sid Deutsch. 'Pseudo-Random Dot Scan TV Systems'. *Institute of Electrical and Electronic Engineers, Transactions on Broadcasting*, vol. BC 11, no. 1, July 1965, p. 11.
6. O.H. Schade. 'Electro-optical Characteristics of TV Systems'. *Radio Corporation of America Review*, vol. 9, no. 1, March 1948, p. 5.
7. P.S. Moharir. 'Fluctuation Theory of Luminance Discrimination for the Light-Adapted Eye and Its Particular Application to the Television Case'. *Journal of the Institution of Engineers (India)*, vol. 47, no. 1, September 1966, p. 17.
8. S. Hecht. 'The Visual Discrimination of Intensity and the Weber-Fechner Law'. *Journal of General Physiology*, vol. 7, 1924, p. 241.

Appendix

If the two areas are simultaneously viewed by the eye, one with luminance B and the other with luminance $B + \Delta B$, there exists a minimum value of ΔB , necessary for the eye to be able to recognize the two luminances as distinct ones. Rather than studying ΔB as a function of luminance B , the fraction (ΔB) is generally studied. This fraction depends on number of factors such as the luminance B , the adaptation luminance level, B_0 , of the eye, the area, A , under view, the time, T , for which the scene is viewed. It has been shown that⁷

$$\left(\frac{\Delta B}{B}\right)_L = K (fTA)^{-\frac{1}{2}} \left[\frac{1}{B} \left(1 + \frac{B_0}{B}\right) + f t_0 \left(1 + \frac{B_0^2}{B^2}\right) + (\Delta t_0)^2 t_0 f^3 B^2 \left(1 + \frac{B_0^4}{B^4}\right) \right]^{\frac{1}{2}} \quad (37)$$

where K is constant in the range 3-5, f is the number of photons that enter the eye per unit area per unit time per unit luminance. t_0 is the refractory period of the nervous transmission channels, and Δt_0 is the random fluctuation in t_0 and subscript L is used to denote light adaptation.

If B_0 is equated to zero in equation (37), the fraction $\left(\frac{\Delta B}{B}\right)_d$ for dark-adapted eye results, subscript d denoting dark-adaptation. $\left(\frac{\Delta B}{B}\right)_d$ has been studied experimentally by S. Hecht.⁸ It has also been shown that⁷ using only the data for dark-adapted eye it is possible to evaluate $K(fAT)^{-\frac{1}{2}} f t_0$ and $(\Delta t_0)^2 t_0 f^3$.

Using S. Hecht's data following values were obtained.⁷

$$K(fAT)^{-\frac{1}{2}} = 4.37 \times 10^{-3} \quad (38)$$

$$f t_0 = 22.25 \text{ millilamberts}^{-1} \quad (39)$$

$$(\Delta t_0)^2 t_0 f^3 = 2.88 \times 10^{-6} \text{ millilamberts}^{-3} \quad (40)$$

Substituting these values in equation (37)

$$(\Delta B)_L = 4.37 \times 10^{-3} \left[(B + B_0) + 22.25 (B^2 + B_0^2) + 2.88 \times 10^{-6} (B^4 + B_0^4) \right]^{\frac{1}{2}} \quad (41)$$

Now the number of gray shades N_0 that can be discerned by the light adapted human eye with the adaptation level B_0 and restricted to luminance levels in the range $B_1 - B_2$ is

$$N_0 = \int_{B_1}^{B_2} \frac{1}{(\Delta B)_L} dB \quad (42)$$

If B is the maximum scene luminance and C is the contrast accommodated,

$$B_2 = \hat{B} \text{ and } B_1 = \frac{\hat{B}}{C}$$

Combining equations (41) and (42) we get equation (24).

ON NONEQUI-RIPPLE APPROXIMATION*

S. N. Rao

Non-member

Department of Mechanical Engineering, Indian Institute of Science, Bangalore?

Summary

Equal-ripple or Chebyshev approximation for the ideal low-pass filter characteristic is well known. This paper suggests a magnitude function which gives a nonequi-ripple approximation and considerably reduces the ripple in the passband with only a slight increase in the 3-db bandwidth. The proposed magnitude responses are drawn for the third, fourth and fifth order approximations and compared with the respective Chebyshev approximations.

The magnitude of a function which approximates the ideal low-pass filter characteristic is given¹ by

$$\left| G_n(jw) \right| = \frac{1}{\sqrt{1 + \epsilon^2 C_n^2(w)}} \quad (1)$$

where ϵ is a small real number, w is the normalised frequency and $C_n(w)$ is the Chebyshev polynomial of order n . The value of ϵ is determined from the tolerable ripple in the passband and the value of n is determined from the rate of cut-off (*i.e.*, the slope of the function at high frequencies) required in the stopband.

Consider the magnitude function defined by

$$\left| F_{nk}(jw) \right| = \frac{1}{\sqrt{1 + \epsilon^2 w^{2k} C_{n-k}^2(w)}} \quad (2)$$

where $k = 1, 2, 3, \dots (n/2)$, as an approximating function for the low-pass filter characteristic. Comparing the magnitude function given in equation (1) with that given in equation (2), it can be seen that the approximation obtained by using equation (2) has considerably reduced ripple inside the passband since

$$|w^k C_{n-k}(w)| < 1 \text{ for } |w| < 1$$

whereas $|C_n(w)| \leq 1$ for $|w| < 1$.

Note that the slope of the magnitude function given in equation (2) at high frequencies in the stopband is same as that of equation (1). While the maximum deviation from the ideal characteristic occurs at a number of frequencies (depending on the value of n) inside the passband by using equation (1), it occurs only at $w = 1$ by using equation (2). The magnitude of the function given in equation (2) at $w = 0$ is unity for all orders whereas that of the function given in equation (1) is unity only for odd orders.

*Written discussion on this paper will be received until September 30, 1967.

This paper was received on August 26, 1966.

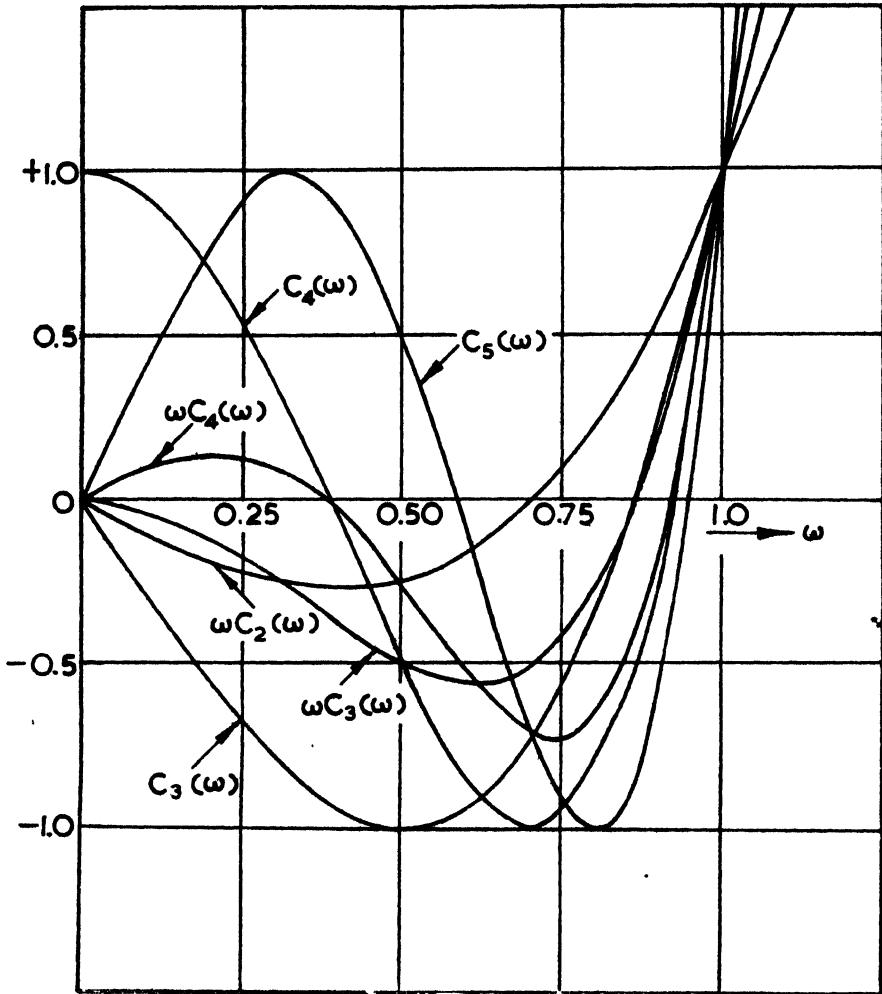


Fig. 1

Plots of $w C_2(w)$, $C_3(w)$, $w C_3(w)$, $C_4(w)$, $w C_4(w)$ and $C_5(w)$

The following discussion is confined to the case where $k = 1$. Since the case $n = 2$ is trivial in the sense that equation (2) reduces to equation (1), it is further assumed that n is greater than 2.

The plots of $w C_2(w)$, $C_3(w)$, $w C_3(w)$, $C_4(w)$, $w C_4(w)$ and $C_5(w)$ against the frequency w are shown in Fig. 1. Comparing the plots of $w C_2(w)$, $w C_3(w)$ and $w C_4(w)$ with those of $C_3(w)$, $C_4(w)$ and $C_5(w)$ respectively, it is obvious that the ripple can be reduced inside the passband by replacing $C_3(w)$ by $w C_2(w)$, $C_4(w)$ by $w C_3(w)$ and $C_5(w)$ by $w C_4(w)$ in equation (1). The result of this replacement in its general form gives equation (2).

Table 1

w	$G_s(jw)$	$F_{31}(jw)$	$G_4(jw)$	$F_{41}(jw)$	$G_5(jw)$	$F_{51}(jw)$
0.000	1.000	1.000	0.895	1.000	1.000	1.000
0.212					0.917	0.998 (local min.)
0.250	0.946	0.995	0.9665	0.990	0.910	0.9985
0.308					0.895 (local min.)	0.999
0.3828			1.000	0.9848	0.916	1.000
0.408	0.9025	0.991 (local min.)				
0.500	0.895 (local min.)	0.992	0.970	0.970	0.970	0.9925
0.588					1.000	0.965
0.6124			0.9161	0.9625 (local min.)		
0.7071	0.9425	1.000	0.895 (local min.)	0.970		
0.745					0.914	0.94 (local min.)
0.810					0.895 (local min.)	0.955
0.866	1.000	0.978	0.970	1.000		
0.924			1.000	0.9848	0.985	1.000
0.950					1.000	0.990
1.000	0.895	0.895	0.895	0.895	0.895	0.895
1.250			0.2416	0.3665	0.124	0.196
1.500	0.217	0.356	0.085	0.1466		
2.000	0.0767	0.1415	0.0206	0.0386	0.0055	0.0103

It can be easily seen that the polynomials $w C_{n-1}(w)$ or in general $w^k C_{n-k}(w)$ do not exhibit equal-ripple behavior. A little thought comparing equations (1) and (2) will convince anyone of the fact that the ripple (distance from the maximum of unity to adjacent minimum on the right) in the plot of equation (2) grows progressively (from cycle to cycle) as frequency approaches unity, but this ripple is always less than that given by equation (1). Thus the approximation obtained by using equation (2) is not equal-ripple.

Table 1 compares the magnitude functions given in equations (1) and (2) for $n = 3, 4$ and 5 , $k = 1$ and $\epsilon^2 = 0.25$ (which approximately corresponds to one db ripple in the Chebyshev approximation). The amplitude responses given

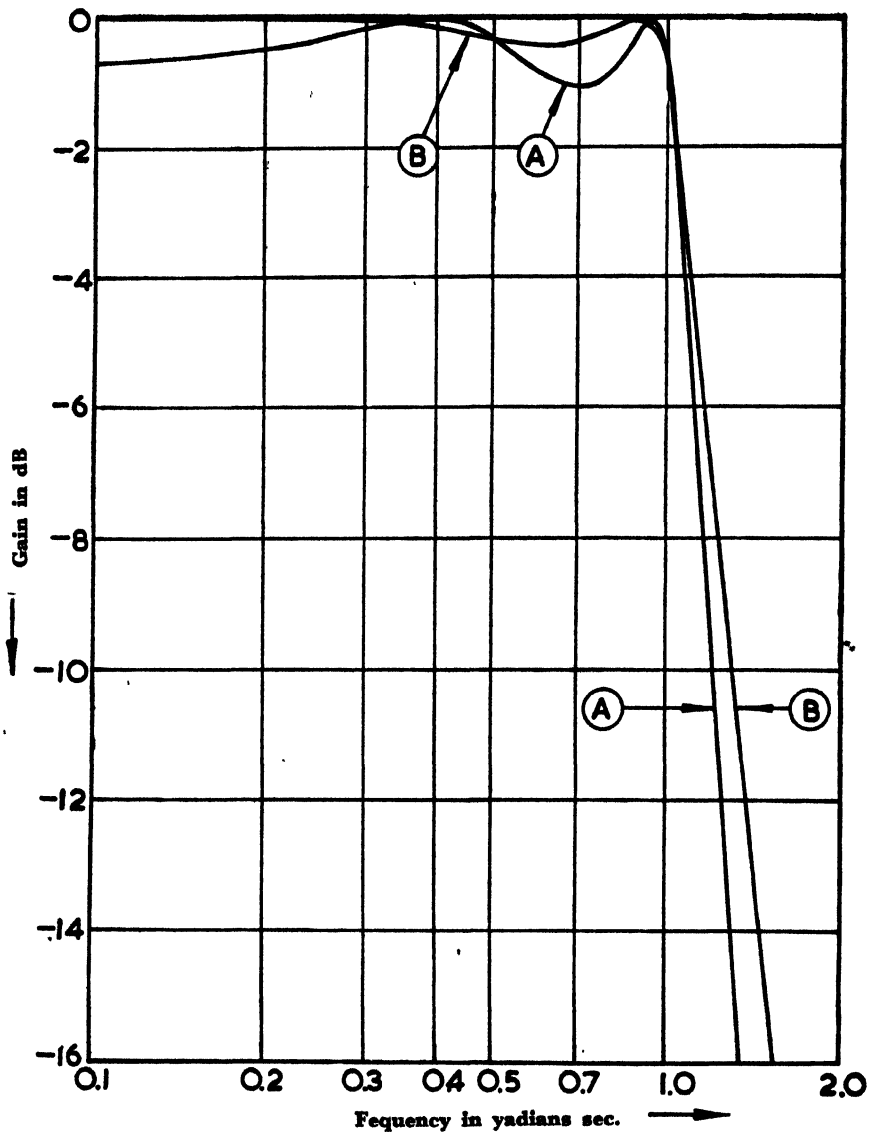


Fig. 2

Plots of equations (1) and (2) for $n = 3$ and $\epsilon^2 = 0.25$

in equations (1) and (2) for $n = 3$, $k = 1$, $\epsilon^2 = 0.25$ are shown in Fig. 2 (plotted from Table 1) by curves A and B respectively and the corresponding responses for $n = 4$ and 5 , $k = 1$, $\epsilon^2 = 0.25$ are shown in Figs. 3 and 4. It can be seen from Fig. 2, 3 and 4 that the ripple inside the passband of the curve B is considerably less than that of the curve A and the 3-db bandwidths of the curves A and B differ very little. This reduction in ripple in the amplitude response shortens² the settling time because the ripples in the amplitude response usually give rise to prolonged ringing in the step response.

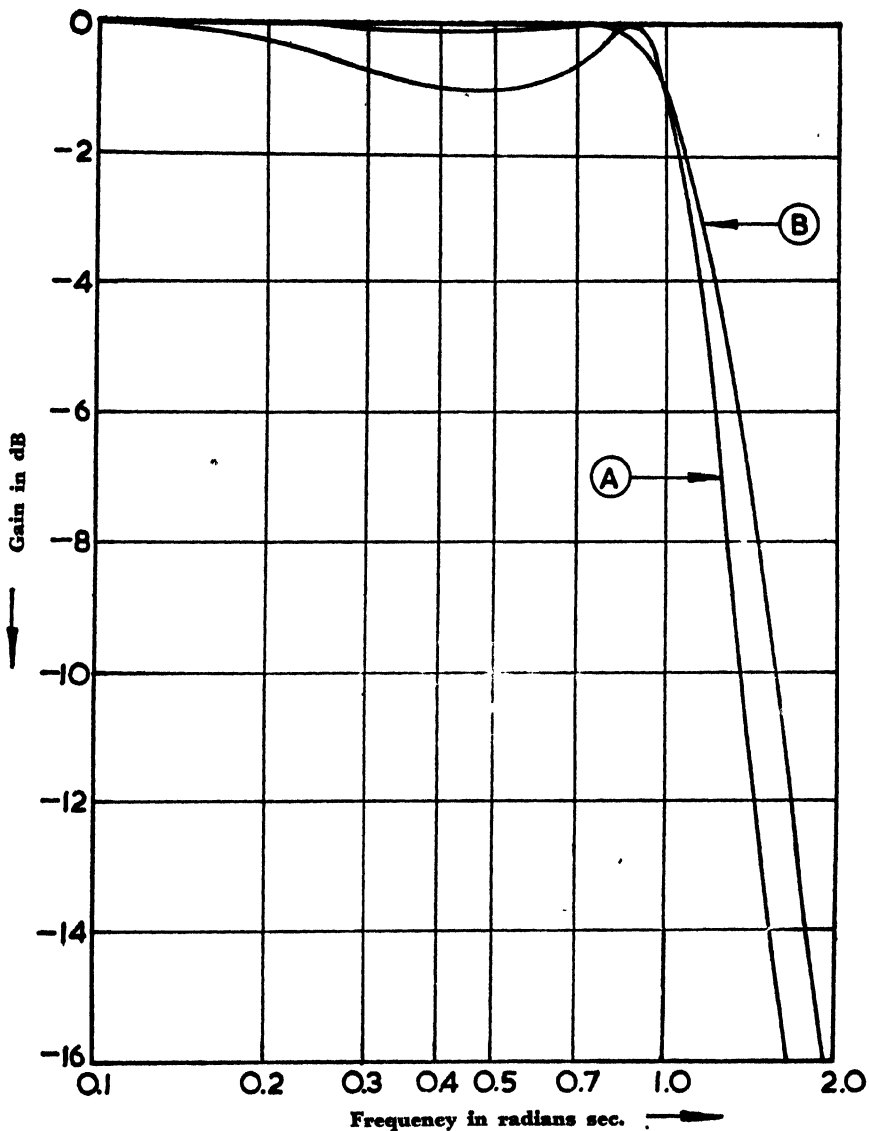


Fig. 3

Plots of Equations (1) and (2) for $n=4$ and $\epsilon^2=0.25$

The slopes of the different approximating functions at $w = 1$ are compared in Table 2. The table shows that the magnitude of the slope of the proposed approximating function at $w = 1$ is larger than that of the Butterworth approximation (except for third order case) and smaller than that of the Chebyshev approximation of the same order. It may be noted that the magnitude of the slope of the third order proposed approximating function at $w = 1$ can be increased at the expense of a little more ripple in the passband by increasing the value of ϵ^2 .

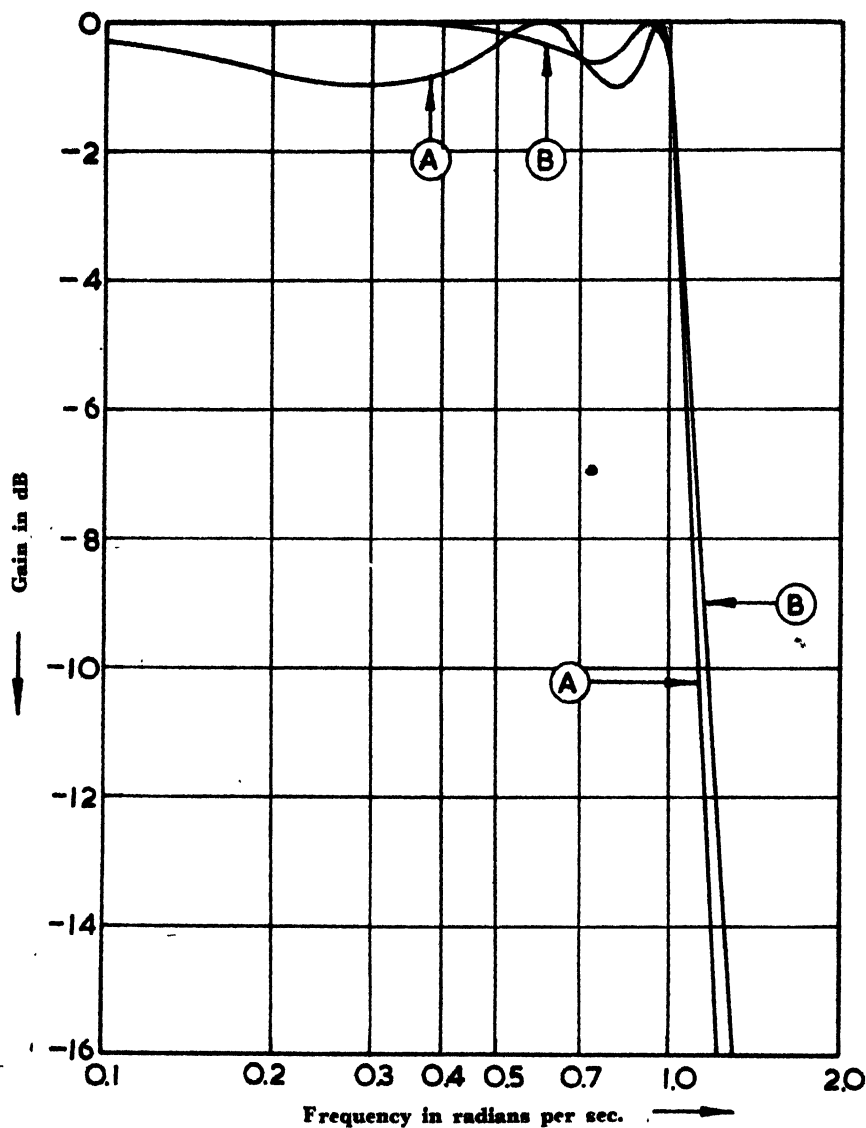


Fig. 4
Plots of equations (1) and (2) for $n = 5$ and $\epsilon^2 = 0.25$

Table 2

n	Slope at $w = 1$ of		
	Butterworth approximation	Chebyshev approximation, $\epsilon^2 = \frac{1}{4}$	Proposed approximation, $\epsilon^2 = \frac{1}{4}$
3	- 1.06065	- 1.611	- 0.89444
4	- 1.4142	- 2.8625	- 1.78888
5	- 1.76775	- 4.4722	- 3.042

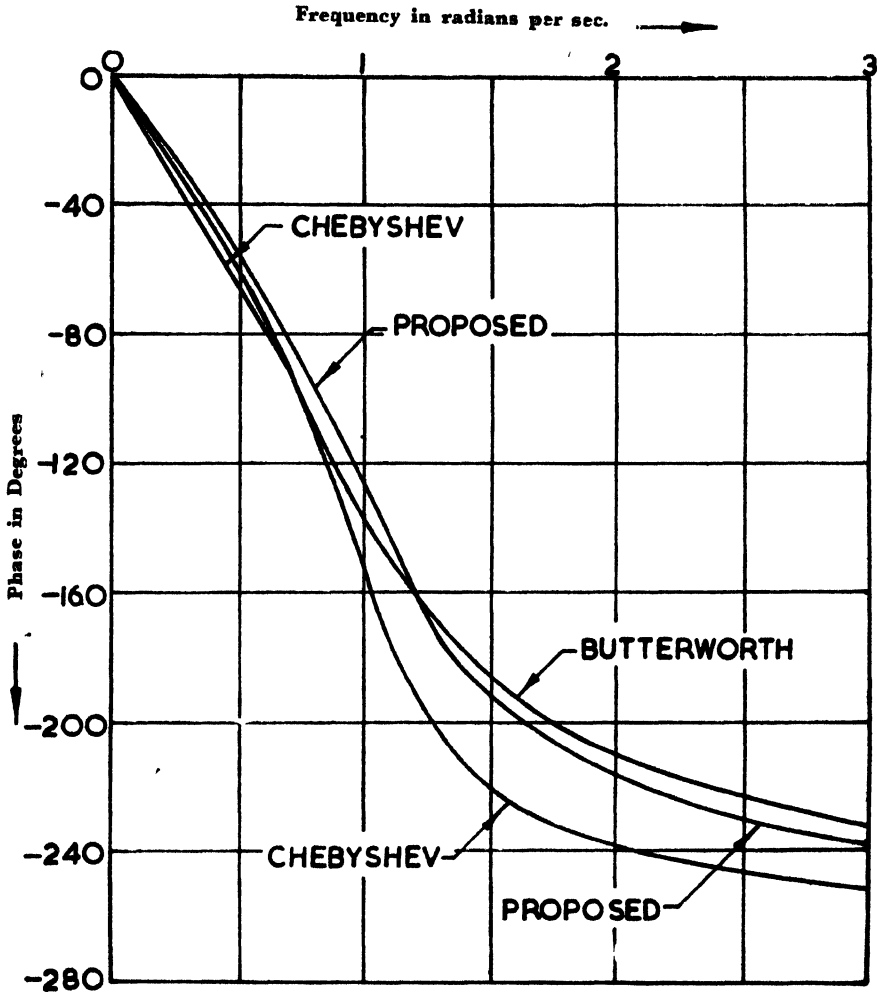


Fig. 5

Phase responses of Butterworth, Chebyshev and proposed approximations of order three for $\epsilon^2 = 0.25$

The system functions whose amplitude responses are given by curves *A* in Figs. 2, 3 and 4 are respectively:

$$G_3(s) = \frac{1}{2(s + 0.5)[(s + 0.25)^2 + (0.968)^2]}$$

$$G_4(s) = \frac{1}{3.58[(s + 0.14076)^2 + (0.9844)^2][(s + 0.3398)^2 + (0.40775)^2]}$$

$$G_5(s) = \frac{1}{8(s + 0.293)[(s + 0.0905)^2 + (0.991)^2][(s + 0.237)^2 + (0.6125)^2]}$$

and the system functions whose magnitude responses are given by curves *B* in

Fig. 2, 3 and 4 are respectively

$$F_{31}(s) = \frac{1}{(s + 0.835) [(s + 0.4175)^2 + (1.012)^2]},$$

$$F_{41}(s) = \frac{1}{2[(s + 0.21825)^2 + (0.99856)^2] [(s + 0.5825)^2 + (0.3741)^2]}, \text{ and}$$

$$F_{51}(s) = \frac{1}{4(s + 0.5249)[(s + 0.13125)^2 + (0.9958)^2][(s + 0.39325)^2 + (0.5637)^2]}$$

By comparing the pole locations of $F_{31}(s)$, $F_{41}(s)$ and $F_{51}(s)$ with those of $G_3(s)$, $G_4(s)$ and $G_5(s)$ respectively, it can be concluded¹ that the phase responses of the functions $F_{31}(s)$, $F_{41}(s)$ and $F_{51}(s)$ will be more linear than those of functions $G_3(s)$, $G_4(s)$ and $G_5(s)$ respectively. This fact is borne out in Fig. 5 where the phase angle of $F_{31}(s)$ is compared with those of third order Butterworth and Chebyshev approximations.

It is well known that the poles of the system function whose magnitude is given in equation (1) are all located on an ellipse in the s -plane. No such simple closed geometric curve for the location of the poles of the system function whose magnitude is given in equation (2) could be obtained.

Finally, it can be concluded that the magnitude function defined in equation (2), while having the same slope at high frequencies in the stopband, considerably reduces the ripple inside the passband compared with the usual equal-ripple approximation given in equation (1). It may be noted that a generalization of the problem obtained by replacing the weighting function w^k in equation (2) by a general polynomial in w is worth investigating.

References

1. M.E. Van Valkenburg, 'Introduction to Modern Network Synthesis'. *John Wiley & Sons, Inc.*, 1960.
2. F.F. Kuo. 'Network Analysis and Synthesis'. *John Wiley & Sons, Inc.*, 1962.

ABOUT THE AUTHORS

Shri A. K. Mohanty

Shri Mohanty is Lecturer in the Electrical Engineering Department, Regional Engineering College, Rourkela. The present work was undertaken in partial fulfilment of the M. Tech degree in Control Engineering of the I.I.T., Kharagpur, in 1965.

Shri T. Natarajan

Shri Natarajan is engaged as Lecturer in the Electrical Engineering Department, P.S.G. College of Engineering, Coimbatore. The present work was undertaken in partial fulfilment of the M. Tech degree in Control Engineering of the I.I.T., Kharagpur, in 1965.

Prof. K. V. Saprykin

Prof. Saprykin was with the Leningrad Television Research Institute from 1936 to 1941 and again from 1945 to 1951. The break from 1941-45 is due to his war service. From 1951 onwards he is on the staff of the Leningrad Institute of Aviation Instruments. From 1955 to 1957 he had been to Peking on deputation. He was visiting UNESCO Professor in I.I.T., Bombay, from August 1965 to December 1966. At present he is on the staff of the Leningrad Institute of Aviation Instruments. He was associated with the work reported here when he was Visiting Professor at I.I.T., Bombay.

Shri P. S. Moharir

Shri Moharir got his M.Sc. degree in Physics with specialization in Electronics from the Nagpur University in 1964. He got his M. Tech. degree in Television Engineering from the Indian Institute of Technology, Bombay, in 1966. He is at present a research scholar in Electrical Engineering at the I.I.T., Kanpur. The work reported here was done for his Master's degree at the I.I.T., Bombay.

Dr. S. N. Rao

Dr. Sunkara Nageswara Rao obtained his B.E. (Elec.) degree with honours from the University of Madras in August 1957. He joined the Graduate College of the University of Illinois in September 1958 and obtained the M.S. and Ph.D. degrees in Electrical Engineering in August 1959 and February 1962 respectively. He was employed as an Assistant Professor of Electrical Engineering at Villanova University, Villanova, U.S.A. from February 1962-64. Since March 1964, he has been working as Assistant Professor of Instrumentation and Control in the Department of Mechanical Engineering at the Indian Institute of Science, Bangalore. His interests are in the areas of Network Theory and Control Systems.

CORRIGENDA

TO VOL. 47, No. 5, PT. ET 2, JANUARY 1967

Page 66, line 22, instead of 'results, a continuously recorded inflow discharge hydrograph was fed', please read as 'results, a continuously recorded inflow discharge hydrograph has to be fed'.

Page 69, line 10, instead of 'low current region, the current vs. voltage curve of a selenium rectifier is a dropping', please read as 'low current region, the current vs. voltage curve of a selenium rectifier is a drooping'.

Page 97, line 19, instead of 'Shri K.V. Rama Murthy', please read as 'Shri K.V. Ramana Murthy'.

Page 97, line 22, instead of 'He then joined the Central Water and Power Research Station, Poona, as a Reaearch Assistant and worked on Hydraulic Model experiments for over two years', please read as 'He then joined the Central Water and Power Reserch Station, Poona, as a Research Assistant and worked on the development of electronic instruments for hydraulic model experie~~m~~ents for over two years'.

EDITOR'S NOTE

Emphasising that the right role of the Institution of Engineers (India) remains in the promotion of genuine advancement of Engineering Technology and Engineering Science, Major General S.P. Vohra, the President of the Institution, stressed during the 448th Meeting of the Council held in Bombay on February 26, 1967, that, as a regular feature, at the time of every quarterly Council Meeting, one of the Engineering Divisions should hold a symposium on a topic which would have special significance and importance considering the engineering activities in and around the location of the Meeting.

Accordingly, a symposium on 'Roads and National Highways' was organized during the 449th Meeting of the Council held in Srinagar on May 26-28, 1967. It hardly needs emphasis that the road construction and maintenance activities launched in the Jammu and Kashmir State has been accorded supreme importance in the present-day efforts of the Nation. The proceedings of the Symposium has been published in *Journal*, vol. 48, no. 1, pt. C1 1, September 1967.

The next one in the series—the Symposium on 'Modern Electronic Communication Techniques', as decided by the Andhra Pradesh Centre of the Institution—records not only India's progress in a modern world, but also brings into limelight the unique role of the City of Hyderabad as the epi-centre of electronic activities of the Nation.

The Symposium, held on August 26, 1967, concurrently with the 450th Meeting of the Council in Hyderabad (August 26-28, 1967) was well attended by electronic engineers. Lively discussions followed the presentation of papers by engineer-authors, who came as representatives of the various organizations engaged in modern electronic communication techniques.

This special issue of the Electronics and Telecommunication Engineering Division part of the *Journal*, containing the speeches, papers and discussions by eminent engineers and research workers of the country is, therefore, expected to serve as a launching base for further moves in 'Modern Electronic Communication Techniques'.



MAJOR GENERAL S. P. VOHRA (M.),
President, The Institution of
Engineers, India



PROF. S. P. CHAKRAVARTI (M.),
Chairman, Electronics and
Telecommunication Engineering
Division, and Chairman, First
Session of the Symposium



SHRI O. LAXMIYAH (M.), Chairman,
Andhra Pradesh Centre



BRIG. M. K. RAO (M.), Member,
Electronics and Telecommuni-
cation Engineering Division
Board and Chairman, Second
Session of the Symposium



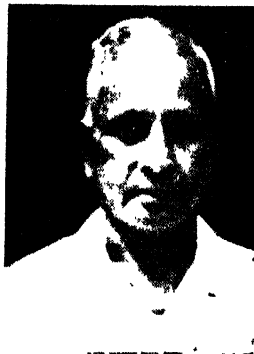
BRIG. C. L. SESHAGIRI (M.) Chairman,
Symposium on 'Modern Electronic
Communication Techniques'



LT. COL. B. BHASKAR, Member, Symposi-
um on 'Modern Electronic Communi-
cation Techniques'



LT.-COL. S. B. LAL, Member, Symposi-
um on 'Modern Electronic Communi-
cation Techniques'



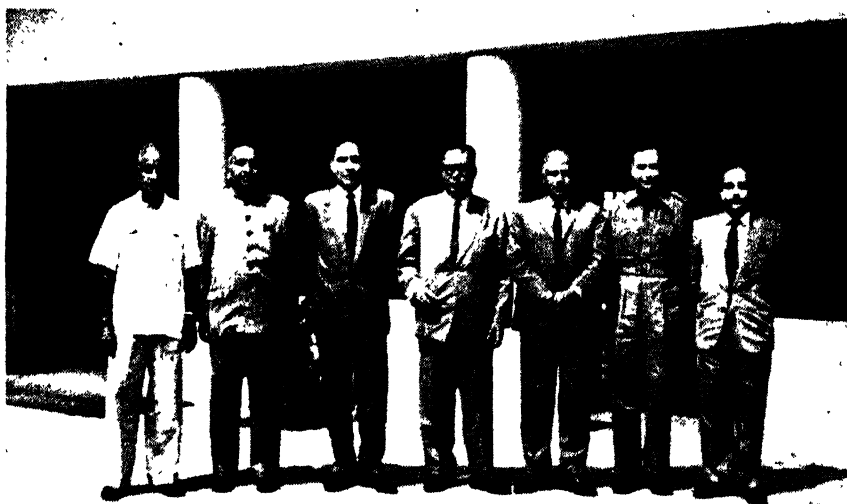
N. SUBBA RAO (M.) Member, Symposi-
um on 'Modern Electronic Communi-
cation Techniques' and Honorary
Secretary, Andhra Pradesh
Centre

SEMINAR ON 'MODERN ELECTRONIC COMMUNICATION TECHNIQUES', HYDERABAD, AUGUST 26, 1967

The day-long session of the army and civilian engineers over the electronic communication techniques is regarded by many eminent engineer-members as a unique occasion and is sure to pave the way for many more of such symposia to enliven the quarterly Council Meetings.

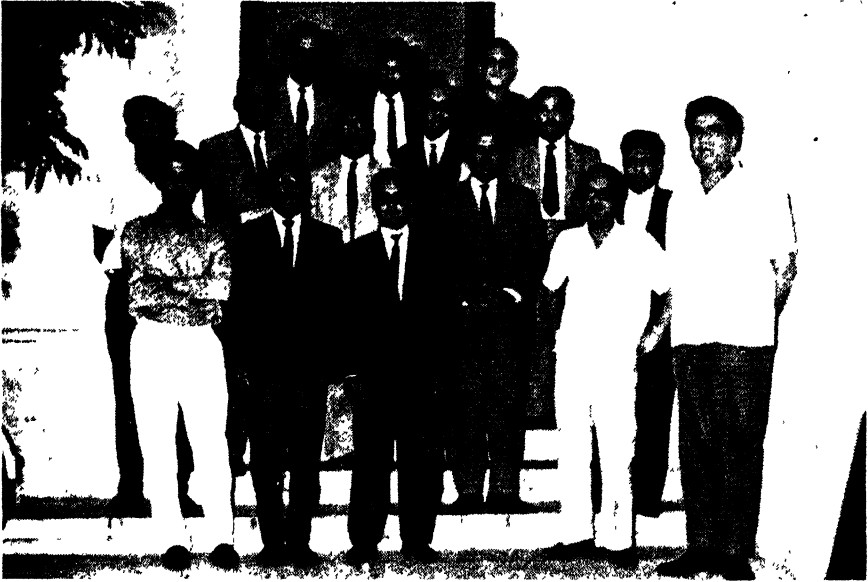
Herein below are given a few photographs taken on the day of the Symposium at the Andhra Pradesh Centre of the Institution to provide a visual depiction of the Proceedings.

ORGANIZING COMMITTEE OF THE SYMPOSIUM



L.R. 1. SHRI N. SUBBA RAO, HONORARY Secretary, ANDHRA PRADESH CENTRE 2. SHRI O. THIMMAIAH, Chairman, ANDHRA PRADESH CENTRE 3. MAJOR GENERAL S.P. VOHRA, President of the Institution 4. PROF. S.P. CHAKRAVARTI, Chairman of the Electronics and Telecommunication Engineering Division of the Institution 5. Brig. C.L. SESHAGIRI, Chairman, Organizing Committee 6. Lt.-COL. S.B. LAL, Member, Organizing Committee 7. Lt.-COL. B. BHASIN, Member, Organizing Committee

PARTICIPANTS IN THE SYMPOSIUM



1st row L.R. 1. SHRI A.K. MUKHERJEE 2. SHRI S.V.R. NAIDU 3. SHRI C.R. CHAKRAVARTHY 4. BRIG. C.L. SISHAGIRI 5. SHRI CHATTERJEE 6. DR. M.N. FARUQUE

2nd row L.R. 1. SHRI C. SAIYANARAYANA 2. BRIG. M.K. RAO 3. PROF. V.V.L. RAO 4. SHRI S. A. SRINIVASAN 5. LT.-COL. B. BISAIN 6. PROF. A. PRABHAKAR

3rd row L.R. 1. WG.-CDR. R. NAGARAJA RAO 2. SHRI G. KANTIAH 3. MAJOR R.K. JOSHI

WELCOMING THE AUDIENCE



SHRI O. TIJIMMAIAH (Standing), CHAIRMAN, ANDHRA PRADESH CENTRE, welcoming the audience and President to inaugurate the Symposium. (Sitting) L.R. MAJOR GENERAL S.P. VOHRA, President of the Institution and PROF. S.P. CHAKRAVARTI, Chairman of the Electronics and Telecommunication Engineering Division of the Institution and Chairman for the morning session

INAUGURATION OF THE SYMPOSIUM



MAJOR GENERAL S.P. VOHRA, PRESIDENT (Standing) inaugurating the symposium (Sitting I.R. SHRI O. THIMMAIAH, Chairman, Andhra Pradesh Centre and Prof. S.P. CHAKRAVARTI, Chairman, Electronics and Telecommunication Engineering Division)

AUDIENCE AT THE SYMPOSIUM IN THE HALL OF ANDHRA PRADESH CENTRE



Sitting in the front row:

- (1) SHRI K.K. NAMBIAR, a Council member (2) SHRI DILDAR HUSAIN, a Past-President
- (3) SHRI V.Y. KAMAT, a Council member (4) DR. G.P. CHATTERJEE, a Council member and Chairman, Mining and Metallurgy Division of the Institution (5) SHRI B.P. KAPADIA, a Past-President

Second row : Senior members of the Institution along with other members and participants in the Symposium.

INAUGURAL ADDRESS

BY

MAJOR GENERAL S. P. VOHRA (M.), PRESIDENT

'Shri Thimmaiah, Prof. Chakravarti and Brother Engineers,

The primary aim of the Institution of Engineers (India) is to promote the genuine advancement of Engineering Technology and Engineering Science and their application.

I feel that one of the ways by which this can be increased is to create the right atmosphere at different Centres to hold technical seminars and symposia at the time when the Council Meetings take place. It was with this object, we decided that in addition to the normal activities of the Council at the time of the Council Meeting, we should have these technical seminars or symposia.

It was the object of this meeting that the engineers and educationists should also participate in such symposia and contribute papers and ideas whenever discussions take place.

The first Council Meeting, after I took over as the President of the Institution, was held at Srinagar. At the time of Srinagar Session, we held a Technical Symposium on 'Roads and National Highways'. I must say that it went off very well.

While selecting the subject for the symposium here, on electronics, one felt that it is one of the important fields in which considerable development has to take place, if I may say so, in the next decade or so. Secondly, we have the Defence Electronics Research Laboratory, EME School, College of Engineering (Osmania University), Electronic Corporation of India, Bharat Heavy Electricals and similar electronic establishments located around Hyderabad.

I must congratulate the Organizing Committee that within a short time they have printed a very good booklet giving important subjects selected by them. I do not, myself, belong to Electronic Wing, but there appears to be considerable original work and the papers are of very high standard.

Similarly, steps have already been taken to hold a Seminar during the next Council Meeting, which will be held sometime in November this year and the venue will most probably be Poona. In this connection, I have already written to the Chairman of Poona Centre to hold a technical symposium depending on the activities of that area.

Gentlemen, you would agree with me, that only by having these discussions, we would be able to fulfil the primary role of the Institution and will henceforth enhance the prestige and understanding of the Institution.

The symposium, as you all know, is being held in two Sessions. I am afraid, we have to curtail the second-half of the Session. But that does not mean that we should curtail the discussions on papers. However, it will

be left to the Chairman of the Session. The first Session will be presided over by Prof. S. P. Chakravarti and the second Session by Brig. M.K. Rao.

Prof. Chakravarti is the Chairman of the Electronics and Telecommunication Engineering Division of the Institution. I very much liked to have his assistance in organizing the technical symposium here. I thank him on behalf of the Institution and my personal capacity that though the time was limited, the Chairman was able to come here and preside over the session.

Prof. Chakravarti is well-known in the field of electronics and is associated with different divisions. He has also assisted actively in furthering the activities of the Committee.

I am sure, the participants will show keen interest in making this technical Symposium a success.'

WELCOME ADDRESS

BY

**SHRI O. THIMMAIAH (M.) CHAIRMAN,
ANDHRA PRADESH CENTRE**

‘General Vohra, Brother Engineers, Delegates, Ladies and Gentlemen,

On behalf of the Institution of Engineers, I have great pleasure in extending a hearty welcome to brother engineers, participants of the symposium and other Senior Members to this great City of Hyderabad. The Institution has endeavoured best to make your stay in the City of Hyderabad as comfortable as possible, and if any inconvenience has been caused, we request to be pardoned.

Hyderabad, as ex-Capital of Nizam’s Dominion, is noted for its hospitality. However, if the level of hospitality has not been maintained, it is partly due to the present trying circumstances.

During the 449th Council Meeting held at Srinagar, the President along with Council Members had decided that a symposium should be held at the next Council Meeting, that is the present one, and the subject should be appropriate to the development taking place in and around the region where it is to be held. We have in Hyderabad the following institutions engaged in electronic field : (i) the Defence Electronics Research Laboratory, (ii) A.E.C’s Electronic units (iii) E.M.E. Shool (South), (iv) Hindusthan Aeronautics, Ltd. Besides these, there are several private entrepreneurs devoting considerably on the subject. The local committee of the Andhra Pradesh Centre discussed the subject and finally selected the topic ‘Modern Electronic Communication Techniques’ as the most appropriate subject to cover the developments taking place in and around the city of Hyderabad. A Sub-Committee consisting of Brig. Seshagiri and Lt. Col. B. Bhasin was formed for organization, selection of papers, etc. Invitations were sent to various institutions for contribution of papers and participation in this symposium. We are happy to announce that a great interest was shown by the various institutions to participate in the Symposium. Sixteen papers have been received. Nine papers have been printed complete in the form of a booklet along with the abstracts of other papers. Three papers were received late and arrangements are being made to print them also.

The Institution congratulates the Sub-Committee for the good work done by them in a very short period under the supervision of Brig. C.L. Seshagiri, Commandant, EME School, especially in organization, selection of papers, printing, etc. The Institution extends its special thanks to Lt. Col. S.B. Lal for the excellent work done in getting the papers vetted and printed in record time. Our thanks are also due to the Deccan Press for their cooperation.

The Institution also congratulates all those who have contributed the papers at short notice.

The Institution congratulates the Honorary Secretary, Joint Honorary Secretary and the sub-committees and members of the Local Committee for their help and cooperation in making the symposium and Council Meeting a success.

Gentlemen, you are aware that the Electronics Science is a 'must' both during the war time and peace time. Electronics has its wide applications in: (i) radar; (ii) modern transmission system with high frequency; (iii) data processing, solving complicated equations by digital and analogue computers and measurement of distances and in spacecraft. The Andhra Pradesh Centre of the Institution of Engineers (India) is proud that the Engineers, both Civil and Army, are meeting on a common platform to discuss the utilities of the electronics and electronic equipment, both for peace time and war time.

We are happy to note that most of the equipment required in the electronic field are now being manufactured in India in a short period and the discussions will go a long way in the development of the electronic technology and the speedy manufacture of electronic equipment required to enable India to be self-sufficient.

The Institution of Engineers (India), Andhra Pradesh Centre, and the participants are proud that Major General S.P. Vohra, President, who himself is the Director of Corps of Electrical and Mechanical Engineers in the Army, has been responsible for the maintenance of the electronic equipment in the Army and has consented to inaugurate the symposium. I welcome you all to participate in the symposium and make the function a grand success.'

**OPENING ADDRESS OF PROF. S. P. CHAKRAVARTI (M.),
CHAIRMAN, ELECTRONICS & TELECOMMUNICATION
ENGINEERING DIVISION**

ON

MODERN ELECTRONIC COMMUNICATION TECHNIQUES

1. Introduction

Although the Electronic Age has dawned with the opening of the present century, the era of 'Modern Electronics' may be said to have commenced from 1945 with the cessation of the Second World War.

Considerable developments in electronics made during the war period, which had remained secret at that time, were released for use during the post-war period, and further new inventions and outstanding contributions in electronics have also been made since 1945.

The development of modern 'Electronic Communication Techniques' has therefore been the outcome of all these available contributions during the war period as well as post-war period.

The developments have been mostly in V.H.F., microwave and still higher frequency (I.R. and Optical) ranges. The application of new techniques has generally produced equipment having wide-band characteristics, low noise, very high stability (a few parts in 10^{10}), low energy consumption, small size and considerable robustness.

The principal contributions which influenced the development of modern techniques since 1945 as well as the specific systems in which they have been applied are presented in brief in the Sections given below.

2. High frequency electron tubes on entirely new principles

As the tubes developed prior to 1940 were unsuitable for use at decimetric, centimetric and millimetric wavelengths, high frequency electron tubes based on entirely new principles have been evolved/improved for use at frequencies 1,000 megacycles per sec. to 300 kilomegacycles per sec. (30 cm. to 1 mm.).

Broadly they have been of three types as given below.

(a) Tubes based on interaction of beam and cavity

Klystron is the most important tube of this class, developed during 1937-39. A two-cavity Klystron operates as amplifier, frequency multiplier and also as self-excited oscillator (with a feedback loop) in the decimetric and centimetric ranges. Three- and multiple-cavity Klystrons operate as high power pulsed oscillators in microwave range.

Reflex Klystron was developed about 1940, used for generating low power oscillations in the centimetre range.

Due to simplicity and reliability of electron tuning, wide applications of reflex Klystrons in various circuits of centimetre range equipment (e.g., local oscillator in radar receivers) have been made. A reflex Klystron can also be used for multiplying and dividing the frequency of oscillation. About 3 years ago, power reflex Klystron tubes suitable for large scale systems use covering the band, 18 to 100 kilomegacycles per sec., have been developed by Standard Telecommunication Laboratories, Ltd. At 35 kilomegacycles per sec. (3.5 mm.) an output of 2.5 watts was obtained corresponding to an efficiency higher than 3%.

Superiority of Klystrons over Magnetrons

In recent years, the Klystron has begun to displace the Magnetron. Modern radar systems obtain considerable information from the phase characteristics of the returning echo but require accurate phase control of the outgoing pulse. The Magnetron, which is only an oscillator and cannot amplify, is unable to satisfy this criterion.

Klystron, which can amplify, has no such limitation. Modern high power Klystron amplifiers even approach the Magnetron in efficiency, achieving 40 to 45 %.

The Klystron amplifier of Stanford University designed for ballistic missile early warning radar is perhaps the world's largest electron tube and can deliver a peak output power of $1\frac{1}{2}$ million watts or a continuous power output of 100 kW.

(b) Tube based on interaction of beam and circuit (slow wave structure)

Travelling-wave tube is the most important tube of this class.

In these tubes, the electrons interact with travelling electromagnetic waves, but unlike the Magnetron the wave does not travel in a circle but length-wise through the tube. The wave gathers the electrons into bunches. The electrons bunched by the wave excite electromagnetic oscillations in the output compartment of the tube. For the interaction of the electrons with the wave to be sufficiently efficient, it is necessary for the velocity of electrons to be near to that of the electromagnetic wave. Therefore deceleration of electromagnetic wave has been achieved by sending it along a wire spiral. To pass the narrow spiral, the whole tube is placed inside the coil of an electromagnet. The electromagnet consumes a high power and weighs hundreds of times more than the tube itself.

Spiratron

In the U.S.S.R., a new version of TWT which does not require a magnetic focusing coil has been developed. Inside the decelerating spiral and along its axis, the tube uses a thin taut wire which is kept at a potential somewhat higher than that of the spiral.

TWT has been mostly employed as amplifiers of low and medium level signals and also as high power pulse generator in centimetric wave range. They have proved very suitable as amplifiers on 'communication satellites'.

(c) *Tubes based on interaction in crossed fields*

Magnetron is the most important tube of this class.

A typical high power pulsed magnetron gives a power output of more than 1,000 kW at 10 cm. wavelength when supplied with pulses of 100 amp. at 40 kV and aligned in a uniform magnetic field of approximately 1,500 Gauss.

The essential features of such a Magnetron are given below.

An indirectly heated oxide cathode is supported from a glass insulator by tungsten rods along which enter the input pulses and heater supply. The anode with 13 segments which is resonant circuit with a like number of poles is fashioned from a copper block with water jacket on the outside. Loops are provided for accepting R.F. power from the resonant circuit and leading it through co-axial lines, a loop aerial and a vacuum tight window to the output wave-guide feeder.

The conversion of energy from steady current input to R.F. output occurs in the 'interaction space' in which circulate the electrons that form the connecting links in the process.

Magnetrons are used to produce high power pulsed oscillations in the microwave range in communication and radar equipment.

3. Low noise amplifiers at microwave frequencies—Masers and 'Parametric amplifiers'

Very low noise figures obtained in amplifiers (receivers) of these types make them suitable for use :

- (i) In receiver portion of radar sets, employing low peak powers or with given peak power for longer range service;
- (ii) In tropospheric scatter communication system;
- (iii) In microwave relay links employing non-optical ranges, where the signal intensity is low;
- (iv) In the repeater (amplifier) located on the active satellite, in satellite communication system; and
- (v) In accurate measurement of 'cosmic noise' in microwave range.

The types of 'low noise amplifier' developed since 1955-56 are :

- (i) Gas maser (molecular amplifier);
- (ii) Solid state maser (paramagnetic amplifier of transmission cavity and travelling wave types); and
- (iii) Parametric amplifier.

Paramagnetic amplifiers operate at the temperature of liquid Helium ($< 4.2^\circ\text{K.}$). One of the amplifiers can operate at 1.25°K. That is why amplifiers built on this principle possess much less internal noise.

The typical noise figures for the above are given in Table 1.

Table 1
Typical noise figures

Amplifier	Noise figure in dB
Gas maser	0.16
Solid state maser	0.10
Parametric amplifier	0.80 to 9.4 (depending upon variable reactance element used)

4. Pulse modulation systems—P.P.M. and P.C.M.

In pulse modulation system, information is conveyed by modulating some parameter [either amplitude, or duration (width) or position in time] of the transmitted pulse.

Of these, 'pulse position modulation' (P.P.M.) or, 'pulse time modulation' is of particular interest. Compared with P.D.M, P.P.M. conserves power.

The P.P.M. is most suitable for 'time division multiplex communication systems' on wire and radio channels.

P.C.M. (pulse code modulation) system

In P.C.M, the signal is sampled, and the magnitude of each sample is rounded off to the nearest one of finite set of permitted values (*i.e.*, the samples are quantized).

Further, the quantized samples are translated into 'codes' as in telegraph systems. At receiving end, original wave is obtained.

The P.C.M. is suitable for time division multiplex and also for secret communication system. A very high grade secrecy device can be obtained by use of P.C.M. technique.

5. Digital communication systems

Considerable advancement has been made in digital techniques and their application during last 10 years.

Digital modulation provides the following advantages :

- (i) Good relaying capability: Can be relayed many times without deterioration of signal /noise ratio ;
- (ii) Reliable quality output can be achieved;
- (iii) Gives security in communication (suitable for defence);
- (iv) Has anti-jamming characteristics;
- (v) Suppression of interference;
- (vi) Adaptable in integrated circuits;
- (vii) Reduction in transmission errors; and
- (viii) Provides spectrum conservation.

6. Applications to V.H.F. and microwave communication

(i) *Multi-channel V.H.F. broadcasting*

For details of this system, a reference may be made to the paper entitled 'Multiplex Broadcasting' by Greig, published in the *Proceedings of the American Institute of Electrical Engineers*, January 1946.

The P.P.M. was employed to obtain the combined pulse series from 10 stations. The band-width for 10 channels is about 2.5 megacycles per sec. which modulates a V.H.F. carrier by amplitude modulation for radiation.

(ii) *Multi-channel V.H.F. telephone and telegraph system*

After the Second World War, multi-channel, frequency modulated V.H.F. systems have been developed for simultaneous transmission of a number of telephone and telegraph channels.

The equipment (as manufactured in Great Britain) are of two types :

- (a) A six-channel system handles six 4 kilocycles per sec. wide bands in each direction.
- (b) Twelve/twenty-four channel system handles a band either of 60-108 kilocycles per sec., or, 12-108 kilocycles per sec. in each direction.

The composite bands frequency modulate V.H.F. transmitter of 100 watts at frequency within the band 70-88 megacycles per sec. This band is free from noise, both natural and man-made and slightly greater distances than the line-of-sight distance can be used.

Since 1948, a multi-channel frequency modulated V.H.F. link has been developed in Switzerland for 6 channels. Transmission is effected with a frequency modulated V.H.F. carrier in the range 150-200 megacycles per sec.

(iii) *Multi-channel microwave systems—microwave relay systems*

(A) *For communication over optical range*

- (a) After the close of the Second World War, basic experiments were carried by I.T.T. Corporation to develop a multi-channel microwave link, employing P.P.M. A composite band, 2.8 megacycles per sec. arises out of 23 channels. Microwave frequency range of 1,000-3,000 megacycles per sec. has been considered most suitable. Repeaters of un-attended type have been placed at intervals of 20 to 30 miles.
- (b) Around 1948, I.T.T. Corporation developed their FTL 10B system which provides a maximum of 23 V.F. channels and operates in 1,825-2,100 band. The modulating band arising out of 23 channels by P.P.M. is 2.8 megacycles per sec. and transmitted frequency band is 5.6 megacycles per sec. in width. The overall signal-noise ratio is better than 50 dB.

To produce microwave frequencies, a special Magnetron or Turbator has been used, and it gives extremely low noise figure, high stability and clear tunability.

Later improvement includes use of 'low noise amplifiers (parametric amplifier)' in receivers at the repeaters.

(B) *For communication beyond optical range*

- (a) Since 1941 and particularly since 1950 many experimental and theoretical studies have been made regarding microwave tropospheric propagation beyond the optical range.

A 900 megacycles per sec. P.P.M. system for beyond-the-horizon multi-channel link for 91 miles path was successfully installed. Parabolic reflectors, 28 ft. across, and a diplexing illuminating horn have been installed at each terminal. Vertical polarization is used for transmission and horizontal for reception.

The 23-channel P.P.M. equipment have been used with bandwidth restricted to 1 megacycles per sec.

- (b) Canadian Westinghouse Co. has developed a new system of long distance multi-channel microwave communication, known as 'Tropospheric Scatter System' which can provide reliable communication across 100 to 200 miles without a repeater.

(C) *6,000 megacycles per sec. radio system*

This multi-channel system has been developed in the U.S.A. to handle industrial bands.

New components as described below, have been devised that make microwave communication above 2,000 megacycles per sec. practical and economical.

- (a) Klystron is now widely used at frequencies upto 25,000 megacycles per sec. and performs more efficiently than any other tube;
- (b) Waveguides not only operate as transmission lines, but are designed to operate as capacitance, inductance, filter or hybrid.

This system is affected most by atmospheric conditions. Importance is given to the sensitivity and noise figure of receivers, because of the deep fading.

7. Transistors and tunnel diodes

The invention of the transistor in 1948 marked the beginning of a new era in electronics.

Junction-transistor, photo-transistor, surface barrier and field effect transistors, junction diodes and photo-diodes were discovered, followed by an array of new semi-conducting devices.

In 1958, 'tunnel diode' was discovered and this has unusual significance in electronics.

Tunnel diodes, unlike transistors and conventional diodes have no frequency limitations, require one-hundredth of the power of a transistor, have their switching times as short as 10^{-12} of a sec., are unaffected even when exposed to nuclear radiation and temperature extremes. In addition, they take very tiny space.

Transistors and tunnel diodes are also most suitable for miniaturization and micro-miniaturization along with 'evaporated' components developed for this work.

Applications

Transistors have found application in electronic telephone exchanges, carrier and V.F. communication systems, A-43 transistor portable television receiver, 9-transistor broadcast receiver, transistorized loud-speaking system, and hearing aids.

Point-contact transistors were employed in operator tone-dialling equipment. Point-contact transistors and photo-transistors were employed in direct distance-dialling equipment.

Transistors were widely used in digital computers, in digital data transmission and missile control systems.

8. Lasers

Laser stands for 'light amplification by stimulated emission of radiation'.

The laser is a device for producing a very powerful monochromatic beam of light in which the waves are coherent or in step and with this it is now possible to control the light waves in much the same way as is possible to control electromagnetic radiation at lower frequencies.

In conventional light, the spontaneously emitted photons are all random in phase and direction giving rise to an incoherent wavefront.

An atom in the excited state—if it be struck by an outside photon having precisely the energy of the one that would be emitted spontaneously—can be stimulated before its voluntary drop to emit a photon.

The stimulated photon joins precisely in phase with the photon that triggered its release and travels in the same direction as the incident photon. The incoming photon is, as a result, augmented by the one given up by the excited atom and the emitted wavefront, is coherent.

After Maiman's announcement of a 'Ruby Laser' in 1960, many new laser materials have been discovered. These are crystals other than ruby, glasses, plastics, liquids, gases, semi-conductors and plasmas.

Solid state laser (ruby laser)

The laser was made from a single crystal of pink ruby and aluminum oxide, coloured pink by addition of about 0.05% chromium. It was machined into a rod of about 4 cm. long \times $\frac{1}{8}$ cm. across. The ends were polished optically flat

and parallel and were partially silvered. To provide an intense source of 'bumping' light, a powerful electronic flash tube was coiled round the ruby. An intense beam of red light flashes out from the ends of the rod.

Gas laser

It consists of a discharge tube (100 cm. long \times 1.5 cm. diameter) with two small optically flat mirrors (reflectors) at the ends and is filled with a mixture of gases (He at 1 mm. and Ne at 0.1 mm.). A wave that starts out near one mirror and travels along the axis of the system grows by 'stimulated emission' until it reaches the other mirror, whence it will be reflected back into the active medium, so that growth continues.

The gas lasers can be designed to produce output beams over a wide range of wavelengths.

Applications

(a) Laser communication systems

In the communication field, laser offers unusual advantages for the following types of communication:

- (i) Between two different parts of the world : On a carrier wave of 10^{14} cycles per sec., 4×10^{10} channels each 10 kilocycles per sec. wide with spacing of 5 kilocycles per sec. could be carried, enabling one-half of world's population to hold high-fidelity conversations with the other half at one and the same time.
- (ii) Between Earth and Moon : If and when the Moon becomes colonized and industries beneficial to inhabitants of Earth developed thereon, a laser beam will provide telephone, teleprinter, and television channels between Earth and Moon over a distance of about 200,000 miles.

Optical radar ranging

A coherent light beam detecting and ranging system called 'Colidar' was developed. Successful ranging was reported at more than 16 miles (30,000 m.) in daylight and 63 miles (112,000 m.) at night.

It is not suggested that pulsed laser will displace radar but it offers the advantages of a narrow beam and relative freedom from interference.

9. Satellite communication

Preliminary experiments on Moon-relay communications were carried out in the U.S.A. in early fifties. Further, planned studies during 1958-61 used fixed ground stations to conduct experiments using Moon and other artificial satellites like Echo 1 and Echo 2 as reflectors. These together with later broad-band experiments with 'active satellites' provided ample useful data to establish reliable world-wide communication systems (for telephone, teleprinter and television channels) with different active satellites. The use of passive satellites is now considered to be of no commercial value.

At the present moment, there is a number of such communication satellites over Europe, U.S.A., Atlantic, Pacific and Indian Oceans. In India, we are having one over Ahmedabad.

The experimental work started about 1958 with launching of Score, the first communication satellite. The Telstar was launched in July 1962 and demonstrated the successful broadband communication across the Atlantic in decimetric and centimetric bands.

With regard to active satellites, opinion has differed on the orbit systems for world-wide communications—synchronous orbit or lower altitude random and phased orbit. The present opinion is for stationary (synchronous) orbit for international and national communication links. Syncom-2 was launched into a synchronous equatorial orbit which made it stationary with respect to any point on earth.

The first Intelsat commercial satellite—‘Early Bird’ (weight 85 lb.)—was put over the Atlantic in April 1965. Its effective radiated power is about 15 dB above 1 watt, it has an antenna beam width of 10° and provides 240 telephone channels.

The second series of Intelstat-2 satellites consists of two ‘Blue Birds’ (weight 155 lb.) one over the Atlantic (to give 100 voice channels) and another over the Pacific (to give 180 voice channels plus 6 voice/data channels for NASA) since 1966. The effective radiated power of Blue Bird is about 16 dB above 1 watt, its beam width is 15° . The transponder on the satellite includes 4-stage tunnel diode amplifier and four 6-watt travelling-wave-tube-amplifiers for operation in parallel. The satellite transmitter frequency is in band 4.06-4.18 gigacycles per sec., and receiver frequency in band 6.28-6.40 gigacycles per sec.

Brief details of equipment at ground are given below.

Ground station

The typical transmitter includes local oscillator, frequency-modulator and 10-kW R.F. power amplifier. The power amplifier uses a Klystron to generate an output of 10 kW from 50-milliwatt carrier input. The various channel bands are translated into higher frequency bands by subcarriers to give an overall broad-band to modulate the microwave carrier.

The carrier frequencies of the transmitter for ground-to-satellite communication are 6,390 and 2,299.5 megacycles per sec. for Telstar and Moon satellites respectively. For satellite-to-ground communication, frequency of 4,170 megacycles per sec. has been used in case of Telstar.

UNIDIGIT PCM SYSTEM***Dr. M.N. Faruqui***Non-member**Assistant Professor, Department of Electrical Engineering,
Indian Institute of Technology, Kharagpur***Summary**

Instead of attempting to quantize the amplitude and representing each quantized amplitude level by a multidigit binary or ternary code, the unidigit systems quantize the slopes of any waveform by a binary $1/0$ or ternary $1/0/-1$ pulses. These pulses after integration build up a replica of the input waveform in terms of small segments of varying slopes. Ideally any waveform may be broken up into segments, and then each segment is approximated by straight lines. The approximation may be kept within close limits or the error can be made as small as we please by employing negative feedback. Naturally, for good approximation it is also necessary to have large number of segments or the length of the segments has to be small with a consequent increase in the P.R.F.

Based on the above a practical system has been developed and called 'slope-quantized P.C.M. (SQ-PCM) system'. The binary SQ-PCM employs a comparator with a threshold and an integrator, together with a response shaping network in the feedback loop. An approximated signal is built up by the feedback network and the difference between the original waveform and the approximated waveform gives rise to an error signal which is sought to be reduced by the feedback. The comparator working on the error signal gives $(a+1)$ output only when the error exceeds a reference threshold, otherwise an 'O' is generated. The negative slopes of the signal are matched by the cumulative negative slopes built up by the feedback network. The approximation thus is fairly satisfactory.

The system above could be easily converted, by employing two threshold comparator circuits, into a ternary SQ-PCM system generating $+1/0/-1$ pulses: the ternary SQ-PCM system gives a much better approximation than the binary system. The transmission properties of the SQ-PCM systems have been investigated and it is seen that the SQ-PCM-PM system is the most efficient from the power and communication efficiency viewpoint.

A further improvement of the signal-noise ratio and input-output characteristics of the SQ-PCM has been made possible by employing a second feedback loop. The system called 'hybrid-unidigit PCM system' offers the optimum performance and is equivalent to a 7-digit PCM system (approximately 60 kilocycles per sec. PRF) at 40 kilocycles per sec. PRF only.

*Presented at the Symposium on 'Modern Electronic Communication Techniques' held in Hyderabad on August 26, 1967.

SESSION I

CHAIRMAN : PROF. S.P. CHAKRAVARTY (*M.*)

Paper 1 : Unidigit PCM System. Dr. M.N. Faruqui, <i>Non-member</i>	...	204
Paper 2 : Survey of Developments in Digital Communication Systems. V. Narayana Rao, <i>Non-member</i> , and C.R. Chakravarthy, <i>Non-member</i>	218
Paper 3 : Digital Filters. A. Prabhakar, <i>Non-member</i>	231
Paper 4 : Shift Register Sequences. C. Satyanarayana, <i>non-member</i>	...	237
Paper 5 : Satellite Communications. Major R.K. Joshi, <i>Associate Members</i>		245
Paper 6 : Decoding of Pseudo-Random Coded Sequences. A. Mukherjee, <i>Non-member</i>	262

1. Introduction

The general problems of communication and signal processing may be classified broadly into two groups: (i) signal transformation, and (ii) their subsequent transmission. For efficient communication both signal processing and the RF modulation techniques have to be optimized. The paper discusses the relative merits of different quantized systems and also of different modulation techniques as used in pulse communication systems. Quantization and coding of the analogue signals ensure an almost error-free and efficient transmission in the channel.

A multilevel quantization has many difficulties, both in transformation and transmission, due to lack of multistate storage and switching device and their vulnerability to noise interference. Currently binary codes have found wide applications and notable binary systems which use quantization in time and amplitude are PCM¹, ΔM ², and $(\Delta - \Sigma M)$.³ However, it has been shown that a ternary code,⁴ even with the use of binary devices to generate the code, will have a larger channel capacity and will require lesser equipment. An amplitude quantization of the signal waveform and a subsequent coding into three levels (+1, 0, -1) seems to be a reasonably attractive idea, but unfortunately this will lead to elaborate and complicated circuitry. A uni-digit system, somewhat similar to ΔM , where the slopes of the signal waveform could be quantized into three level (+1, 0, -1) pulses will be simple in circuitry and will offer the advantages of ternary over binary. A system has been developed along the above lines and called 'ternary slope-quantized PCM', or, SQ-PCM system.⁵ In this system, the values of the slopes of the signal waveform at sampling instants, sampling being done at a rather high rate, are quantized into +1, 0, -1 pulses by using two threshold devices in parallel. A simple expedient of building up an approximated signal and then comparing it with the original input in a negative feedback loop improves the quality of approximation considerably.

Using the above idea of a threshold comparator a binary SQ-PCM system⁶ has been developed, where a 1/0 coding of the slopes of the signal waveform is employed. Like the ternary system, the encoder compares the original signal with the approximated one built up by the feedback network and tries to reduce the error of quantization. The impulse response of the feedback network is such that it decays exponentially in a certain manner and the step by step modification of the cumulative positive and negative slopes matches the input waveform fairly well. The binary SQ-PCM system has a satisfactory performance for most of the signals but suffers from a little frequency distortion. A modification of the system called HU-PCM⁷ improves the signal/noise ratio (SNR) considerably and does not have any frequency distortion.

Finally, the transmission properties of these systems have been studied⁸ and it has been shown that the communication efficiency and power efficiency of these systems are fairly high or comparable to normal PCM systems, at least upto 7-digit PCM systems.

2. Ternary SQ-PCM system

A staircase approximation of a signal waveform could be written as

$$f(t) \simeq \sum_n \Delta B_n U(t - t_n)$$

where

$$\Delta B_n = f_n - f_{n-1}$$

and

$$U(t - t_n) = \text{Unit step at } t = t_n = \frac{n}{f_r}$$

when f_r is the pulse repetition frequency (P.R.F.).

The first derivative of this approximation will be

$$f'(t) = \sum_n \Delta B_n \delta(t - t_n)$$

The parameter, ΔB_n is proportional to the slopes between the sample points and could be positive, negative or almost zero. If the slopes are now quantized into a ternary code, the approximated waveform will be

$$f'(t) \approx \sum_n B_0 \delta(t - t_n) = f'(t)$$

where B_0 takes the discrete values of $+1, 0, -1$ according as

$$\begin{aligned} B_0 &= \pm 1, \text{ if } |\Delta B_n| \geq \text{Threshold value} \\ &= 0, \text{ if } |\Delta B_n| < \text{Threshold value} \end{aligned}$$

A practical scheme to implement this quantization is shown in Fig. 1(i) where the boxcar circuit produces the staircase signal which is further processed as shown. The system, as it is, produces a level compression which is a serious drawback. A feedback is provided to improve the quality of matching of the input with the output by a continuous comparison between the signal and its approximation. The feedback loop, necessarily therefore, contains a local receiver which essentially is an integrator. With the integrator in the feedback loop, the overall effect is of a double differentiation of the signal at the transmitter while at the receiver only a single integrator is used. An integrator type of equalizer, therefore, is included in the transmitter as shown in Fig. 1(ii). The forward circuit now has an integrator and differentiator and a re-adjustment of the blocks leads to circuit in Fig. 1(iii).

In Fig. 1(iii) the error signal $E(t)$ is sampled with a bi-symmetrical sampling circuit to give an output $S(t)$. The comparator quantizes $S(t)$ into $+1, 0, -1$ pulses $0(t)$. This is feedback degeneratively through an integrator whose output $B(t)$ is compared with $f(t)$, the input signal, to produce the difference or error signal $E(t)$. At the distant end receiver, the sequence of ternary pulses are just integrated and filtered to give the approximated signal. The $f(t)$ follows $f(t)$ linearly and for zero signal input the stationary pattern is $1/0/-1$

pulses. Feedback increases the dynamic range of the signals that can be handled by the system and also reduces the errors to the minimum possible under the given conditions.

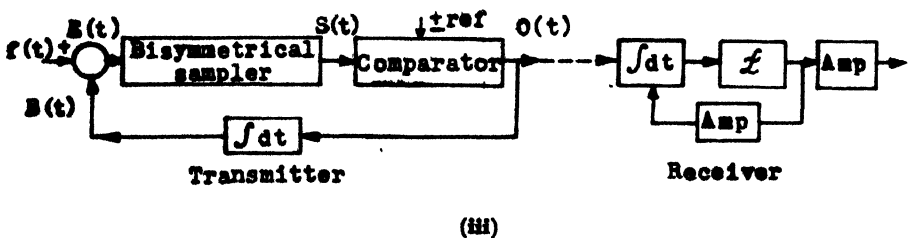
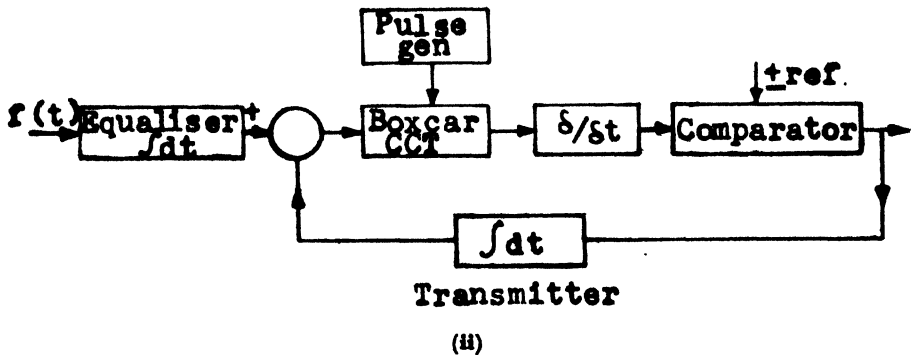
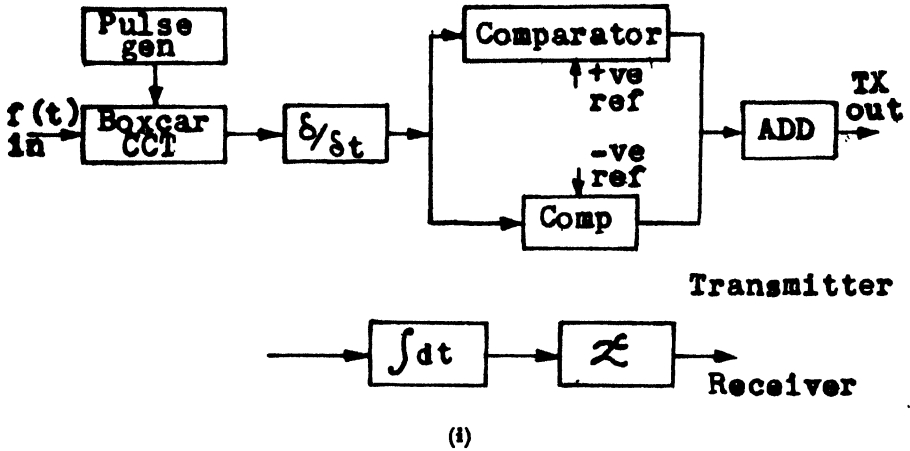


Fig. 1

Ternary SQ-PCM system

An analysis of the signal to quantizing noise characteristics of the system⁹ shows that with the use of an optimum threshold, the error waveform has a peaky distribution of amplitudes, and, if a truncated Gaussian distribution with an average crest factor of 4 is assumed, the SNR is given as

$$\left[\frac{S_o}{N_o} \right] = \frac{K \cdot f_r^{\frac{3}{2}}}{f_o^{\frac{1}{2}} \cdot f_m}$$

where f_o is the filter bandwidth, f_m the frequency of the message signal, f_r the PRF, and K is a factor of proportionality ($= 1$ for optimum input level).

The SNR is seen to be proportional to $f_r^{\frac{3}{2}}$ and inversely proportional to f_m . Two factors are worth mentioning here. One is the overload which occurs for inputs larger than the optimum and gives rise to saturation or overload distortion, and the other is the break point of the integrator in the feedback loop. In the calculation above an ideal integrator has been assumed, but in practice an integrator with a breakpoint at 1,000 cycles per sec. is chosen, so that the dependance of SNR on f_m is not pronounced. As f_m increases, the overload occurs at lower input levels and there will be some frequency distortion due to saturation.

The performance characteristics of the ternary SQ-PCM system is very satisfactory. Fig. 2 shows the SNR with the input level variations at a PRF of 40 kilocycles per sec. The optimum SNR for 0 dB input level is 42 dB, and the dynamic range for the SNR above 25 dB is 30 dB. Fig. 3 shows the variation of SNR with PRF and it is seen that the SNR improves by about 9 dB per octave change in PRF. Fig. 4 shows the output *vs.* f_m (sinusoidal signals) and the frequency distortion is seen to be negligible. The dynamic range of the system could be increased by using an 'instantaneous compandor'.

3. Binary SQ-PCM system

If we use an interpolating function similar to the one used in the ternary system, we can match only the positive and zero slopes of the signal. To match the negative slopes of the waveform, therefore, the cumulative effect of decaying an interpolating function has to be used. It is shown⁶ that

$$\tilde{f}(t) = \sum_n C_n r(t - t_n)$$

where

$$\begin{aligned} C_n &= +1, \text{ if } |C_n| \geq \text{Threshold value} \\ &= 0, \text{ if } |C_n| < \text{Threshold value} \end{aligned}$$

$$C_n = \frac{1}{2W_m} \int_{-W_m}^{W_m} \frac{f(w)}{R(w)} \cdot e^{-j\frac{\pi n w}{W_m}} dw$$

when $r(t - t_n)$ is the impulse response of the interpolating filter to impulses occurring at $t = t_n$, and $f(w)$ and $R(w)$ are the frequency domain characteriza-

tion of the signal and filter respectively. It is thus possible to process the signal in a way similar to that shown in Fig. 1, and a block diagram of the system is shown in Fig. 5(i). The impulse response of the feedback network is such that its cumulative effect matches the negative slopes of the waveform. The error signal is sampled at the desired PRF and compared with an optimum reference level to produce 1/0 pulses $0(t)$ at the output. The feedback loop consists of an integrator and a response shaping network, and at its output the approximated signal $B(t)$ is compared with input $f(t)$ to give rise to the error signal $E(t)$. The optimum reference of the comparator and the feedback network response are so adjusted that the error signal is minimized. The distant receiver is a replica of the network in the feedback circuit and, hence, the output of the receiver is fairly close to $f(t)$.

The signal-to-noise characteristic of the binary SQ-PCM are derived in a manner similar to the ternary SQ-PCM system and

$$\left[\frac{S_v}{N_v} \right] = 0.5 \frac{K f_r^{\frac{3}{2}}}{f_0^{\frac{1}{2}} f_n}$$

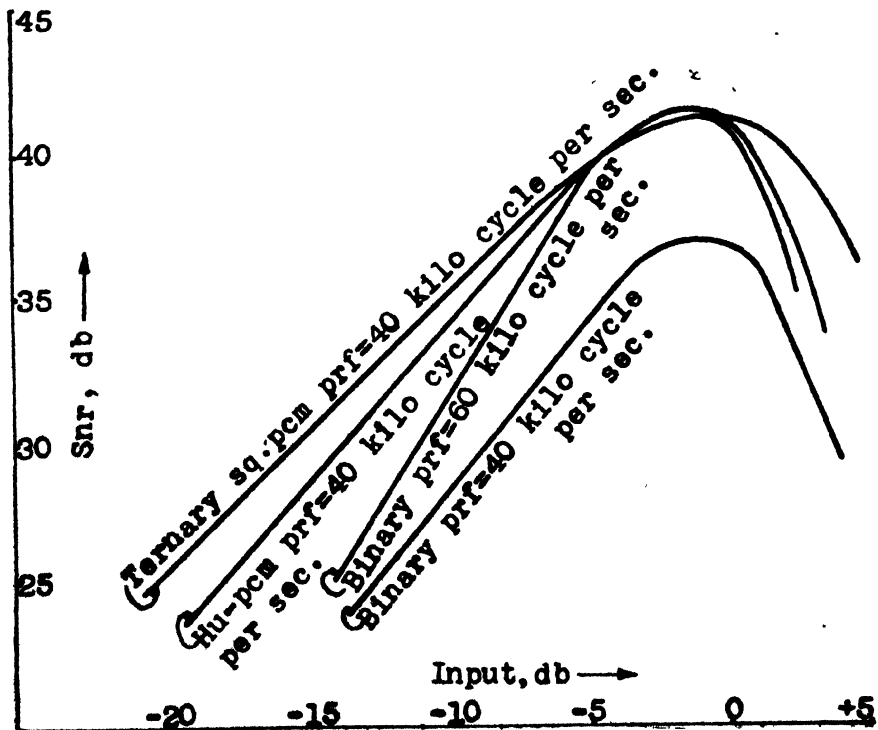


Fig. 2

Variation of SNR with input level

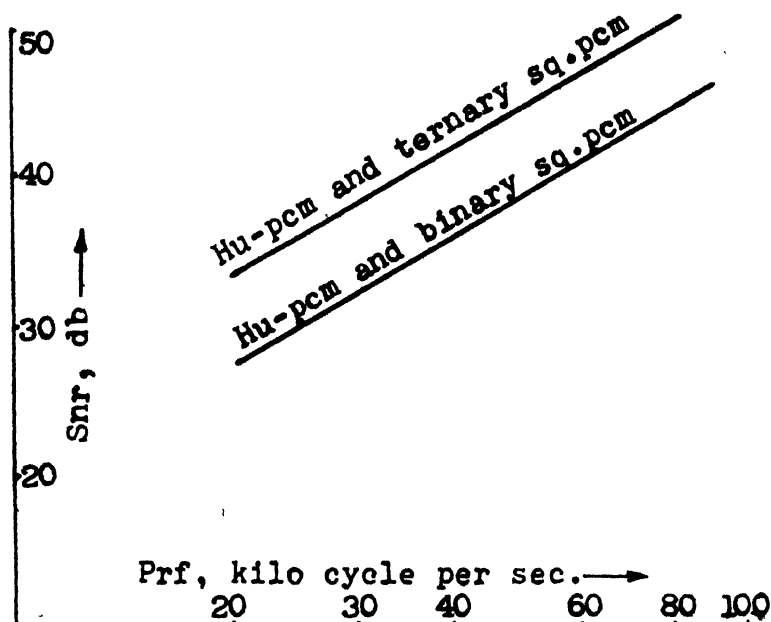


Fig. 3

Variation of SNR with PRF

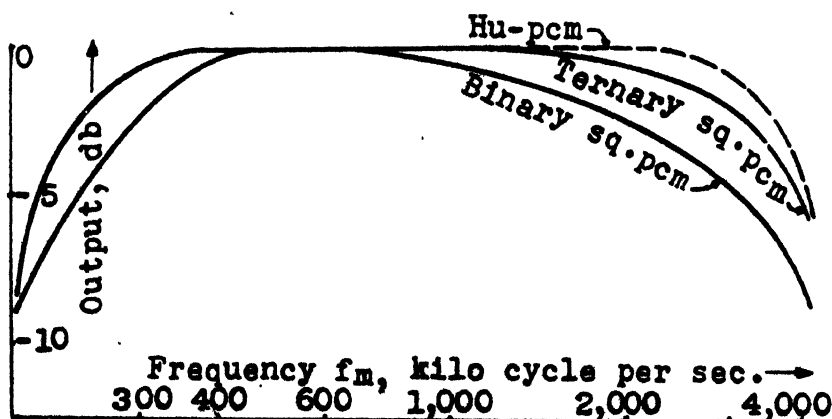


Fig. 4

Output vs. frequency

This shows that the results of the binary SQ-PCM are poorer by 6 dB as compared to those of the ternary SQ-PCM system for the same PRF and f_m . The frequency distortion due to overload at higher f_m is more pronounced in the binary SQ-PCM system, and the dynamic range is smaller. The optimum SNR at 40 kilocycles per sec. PRF is 37 dB and dynamic range is 23 dB. Fig. 2 shows the SNR with input variation at 40 kilocycles per sec. PRF, Fig. 3 shows the variation of SNR with PRF and Fig. 4 shows the output vs. f_m . It is seen

that at higher f_m the output falls by about 6 dB as compared to the lower f_m and the SNR at higher frequencies is poorer, again because of overload. This system is quite suitable for message signals like speech etc., and the dynamic range could be increased by using an instantaneous compandor. To equalize the output and SNR at the higher end of the band, some modifications can be made and the system optimized.

4. Improvement of the binary SQ-PCM system

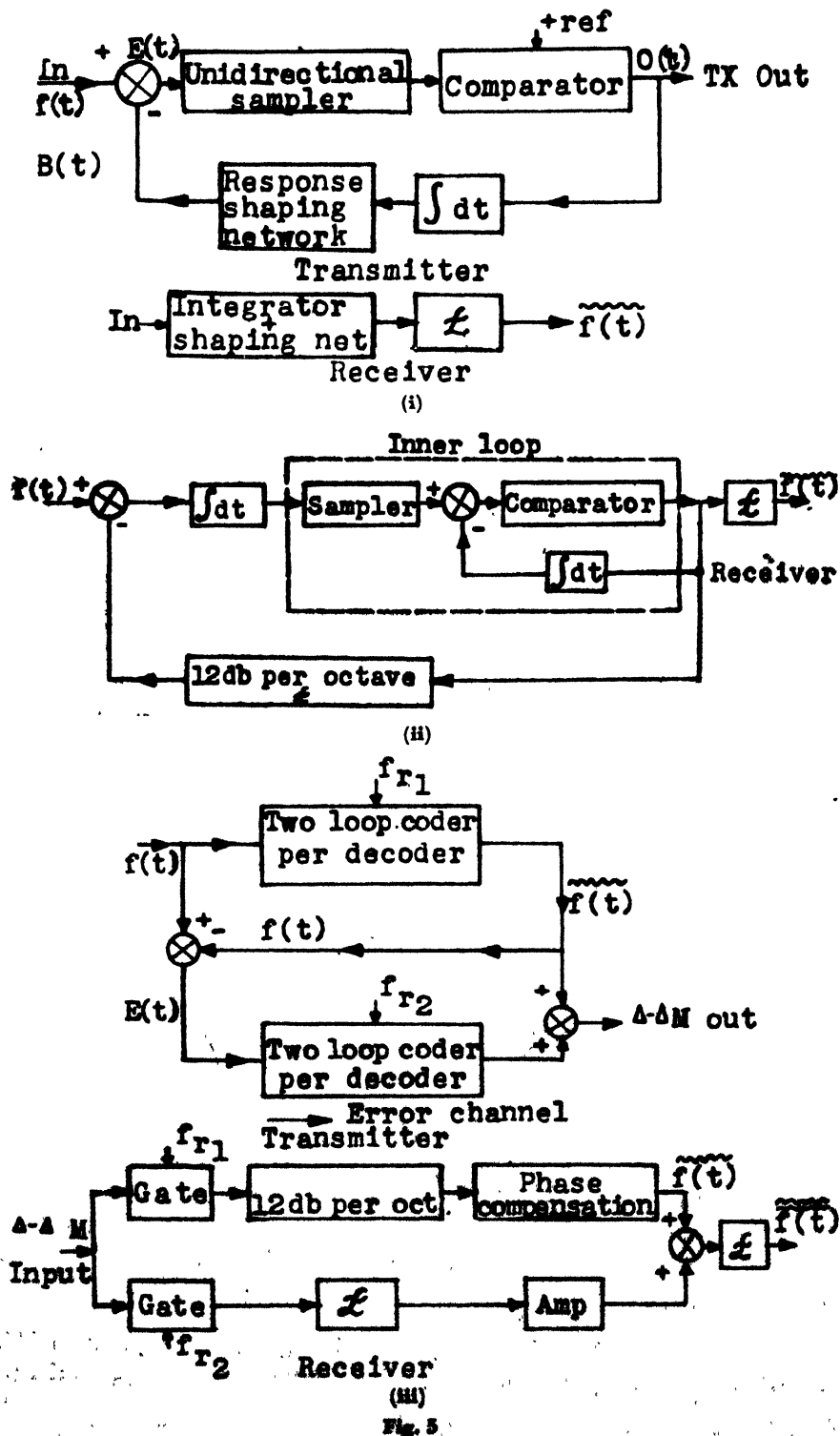
It is seen that in $\Delta - \Sigma M^2$, the SNR and output are equalized in the useful band at the cost of lower overall SNR. To improve and optimize the system, therefore, various secondary feedback loops have been tried, and it is found that a two-loop system using a modified inner loop has very satisfactory performance. The basic two loop quantizing circuit [Fig. 5 (ii)] has an inner loop similar to that of the binary SQ-PCM system, except that the sampler is taken outside the loop. The equalization of SNR and output is obtained by an integrator before the sampler and a simple feedback in a manner similar to the $\Delta - \Sigma M$. The sampler outside the inner feedback loop avoids the large aliasing error introduced when the error waveform inside the loop is sampled, and the inner loop quantizer maintains the superiority of the SQ-PCM system. The secondary loop, now optimizes the performance of the system which has been called the 'hybrid unidigit PCM' (HU-PCM). The SNR is 41 dB at a PRF of 40 kilocycles per sec., and there is no frequency distortion. Fig. 2 shows the SNR *vs.* input variation, Fig. 3 the SNR *vs.* PRF and Fig. 4 shows the output *vs.* f_m . The SNR is constant for all f_m at a certain input level.

The HU-PCM reduces the quantizing noise by using a secondary feedback loop but other hybrid PCM systems have also been suggested which obtain some improvements in SNR by utilizing auxiliary discrete channel to transmit information regarding the coding error separately. For $\Delta - M$ such an auxiliary discrete channel has been developed where the error due to the primary coder is recoded in a secondary coder, and a two stage $\Delta - M$ called $\Delta - \Delta M$ system is obtained. The overall SNR of this complex $\Delta - M$, shown in Fig. 5 (iii), increases considerably and result of a two stage $\Delta - \Delta M$ are similar to the HU-PCM.

The results and performance of the three systems discussed above show that the ternary SQ-PCM at 40 kilocycles per sec. PRF is equivalent in terms of performance to a 7-digit normal PCM system. The binary SQ-PCM system at 40 kilocycles per sec. PRF is equivalent to a 6-digit PCM system and with the modification made in HU-PCM, the system at 40 kilocycles per sec. PRF is equivalent to a 7-digit PCM system (equivalent PRF 60 kilocycles per sec. An instantaneous compandor-compressor in forward path and an expander in the secondary loop increases the dynamic range of these systems considerably.

5. Transmission characteristics

The coded signals of the ternary or the binary SQ-PCM system could be transmitted as video pulses on cables, or modulated into some RF carrier be-



fore transmission. The channel will introduce some noise and interference during the transmission and the correct detection of the signals in presence of noise is of great significance. The signal power necessary to achieve this with a given amount of noise in the channel can be calculated from a knowledge of the statistic of the noise, the probability of error which is acceptable and type of modulation-demodulation scheme used. A set of graphical relationships between channel input SNR and system output SNR have been calculated for the video, —AM, —FSK and —PM modes of transmission. The SNR at the output of the system is limited by the quantizing noise introduced, to start with, at the time of coding.

There are many ways of evaluating the transmission characteristics of the systems, prominent among these is the power efficiency and communication efficiency. For the same rate of information transmitted an ideal system will require a much smaller CNR than the actual system. Power efficiency, therefore, gives an idea of the extra power needed by the actual system in comparison to the ideal. Considering a practical channel of bandwidth W , a certain CNR at the input of the detector is necessary to give an output $\left(\frac{S_o}{N_o}\right)$ of, say, 45 dB—a figure slightly higher than the limiting quantizing noise. The rate of information at the output of the receiver is

$$H' = W_m \log_2 \left(1 + \frac{S_o}{N_o} \right)$$

where W_m is the message bandwidth.

To signal at this rate, the ideal system will require a certain CNR — $\left(\frac{S_i}{N_i}\right)_{\text{ideal}}$ and, hence,

$$H' = W_m \log_2 \left(1 + \frac{S_o}{N_o} \right) = W \log_2 \left[1 + \left(\frac{S_i}{N_i}\right)_{\text{ideal}} \right]$$

or,

$$\left[\frac{S_i}{N_i}\right]_{\text{ideal}} = \text{Anti-log} \left[\frac{W_m}{W} \log_2 \left\{ 1 + \frac{S_o}{N_o} \right\} \right] - 1$$

The actual $\left(\frac{S_i}{N_i}\right)_{\text{actual}}$ is known from the curves previously mentioned and

$$\begin{aligned} \eta &= \text{Power efficiency} \\ &= \frac{\text{Power transmitted in an ideal system}}{\text{Power transmitted in the actual system}} \\ &= \frac{\left(\frac{S_i}{N_i}\right)_{\text{ideal}}}{\left(\frac{S_i}{N_i}\right)_{\text{actual}}} = \frac{\left(\frac{S_i}{N_i}\right)_{\text{ideal}}}{\left(\frac{S_i}{N_i}\right)_{\text{actual}}} \end{aligned}$$

if the noise is assumed to be same in both cases. Table 1 shows the power efficiency calculated from the above. For the purpose of comparison, the

power efficiency has been calculated for the 7-digit PCM and delta-modulation (RC-shaped signal)⁹ systems also.

The other way of evaluating the transmission characteristics is the determination of minimum signal energy required for each information bit transmitted in the presence of Gaussian noise of uniform spectral density. The communication efficiency,

$$\beta = \frac{E_{\min.}}{\epsilon^2}$$

where $E_{\min.}$ is the minimum energy required per bit, and ϵ^2 the noise spectral density.

This can be rewritten as

$$\beta = \frac{P_{\min.}}{\epsilon^2 H} = \frac{P_{\min.}}{\epsilon^2 W} \cdot \frac{W}{H} = \frac{S_i}{N_i} \cdot \frac{W}{H}$$

where $P_{\min.}$ is the minimum power required and H is the bit rate. For any transmission mode, $\frac{S_i}{N_i}$, W , and H for a $\frac{S_0}{N_0}$ of 45 dB are known and, hence, β is calculated and shown in Table 2. The table also shows the β for the 7-digit PCM and Δ -M (RC-shaped signal) for the purpose of comparison.

6. Conclusions

It is thus seen that the SQ-PCM method of quantizing and uni-digit coding gives rise to very simple and efficient digital systems. The uni-digit ternary code seems to be very promising as it can be generated simply and its coding and transmission characteristics are fairly good. The communication and power efficiencies of ternary SQ-PCM-FSK and SQ-PCM-PM are equal or higher than other binary systems at a comparable PRF, its dynamic range is large, and the stability of the system is better than other systems. A secondary feedback loop around the quantizer, like the HU-PCM, will improve the performance of the system and it is expected that the PRF can be reduced to 30 kilocycles per sec. for an optimum SNR of 42 dB.

The binary SQ-PCM system is quite suitable for speech and data transmission, etc., but consequent with its improvement, the HU-PCM system seems to be best amongst the binary systems developed so far (in the range of 45 dB quantizing noises). The power and communication efficiencies are the highest and dynamic range could be increased to 40 dB. One of the disadvantages of these systems is that the SNR increases only at the rate of 9 dB per octave change of PRF as compared to the exponential increase of SNR in normal PCM systems. The limiting effect, therefore, is that in comparison to a 9-digit PCM the PRF required in HU-PCM to give a similar performance is much higher.

7. Acknowledgments

The author wishes to thank Prof. G.S. Sanyal and Prof. J. Das for their encouragement and keen interest in the work.

Table 1
Calculated values of power efficiency

System	SNR quan- tizing	PRF, kilo- cycles per sec.	dB — Video			dB — AM		dB — FSK			dB — PM			
			$\left(\frac{S_i}{N_i}\right)$ actual	$\left(\frac{S_i}{N_i}\right)$ ideal	η , dB	$\left(\frac{S_i}{N_i}\right)$ ideal	$\left(\frac{S_i}{N_i}\right)$ Actual	η , dB	$\left(\frac{S_i}{N_i}\right)$ actual	$\left(\frac{S_i}{N_i}\right)$ ideal	η , dB			
7-digit PCM	43	60	12.4	3.99	-8.58	-0.58	15.4	-15.9	-	4.32	13.15	-17.47	9.4	9.98
Binary SQ-PCM	42	60	12.7	3.58	-9.12	-0.98	15.7	-16.68	-	4.68	13.4	-18.08	9.7	10.68
Δ -M (RC- shaped) signal	42	60	12.7	3.58	-9.12	-0.98	15.7	-16.68	-	4.68	13.4	-18.08	9.7	-10.68
HU-PCM	42	40	12.7	6.8	-5.9	1.49	15.7	-14.21	-	2.57	13.4	-15.97	9.7	-8.21
Ternary SQ-PCM	42	40	16.4	6.8	-9.6	1.49	16.4	-14.9	-	4.66	13.15	-17.81	10.64	-9.15

$W_m = 4$ kilocycles per sec, $W = \frac{1}{2} f$, for video case.
 $W' = f$ for AM and PM; $W = 2 f$ for FSK-binary; $W = 3 f$ for FSK-ternary.

Table 2
Calculated values of communication efficiency

System	dB SNR quan- tizing	kilo- cycles per sec. PRF	— Video			— AM			— FSK			— PM		
			$\frac{S_i}{N_i}$	$\frac{W}{H}$	β	$\frac{S_i}{N_i}$	$\frac{W}{H}$	β	$\frac{S_i}{N_i}$	$\frac{W}{H}$	β	$\frac{S_i}{N_i}$	$\frac{W}{H}$	β
7-digit PCM	43	60	12.4	0.5	8.69	15.4	1.0	34.67	13.15	2	41.3	9.4	1.0	8.71
Binary SQ-PCM	42	60	12.7	0.5	9.31	15.7	1.0	37.15	13.4	2	43.76	9.7	1.0	9.33
Δ -M (RC- shaped) signal	42	60	12.7	0.5	9.31	15.7	1.0	37.16	13.4	2	43.76	9.7	1.0	9.33
HD-PCM	42	40	12.7	0.5	9.31	15.7	1.0	37.15	13.4	2	43.76	9.7	1.0	9.33
Ternary SQ-PCM	42	40	16.4	0.315	13.78	16.4	0.63	27.5	13.15	1.89	39.0	10.64	0.62	7.42

The bandwidths W , are the same as given in Table 1.

The H for ternary case is $40 \log 2^3 = 63.2$ kilobits per sec.

8. References

1. W.M. Goodall. 'Telephony by Pulse Code Modulation'. *Bell System Technical Journal*, vol. 26, 1947, p. 395.
2. F. de Jager. 'Delta Modulation—a Method of PCM Transmission Using the 1-Unit Code'. *Philips Research Reports*, vol. 7, 1952, p. 442.
3. H. Inose and Y. Yasuda,. 'Unity Bit Coding Method by Negative Feedback'. *Proceedings of the Institute of Electrical and Electronics Engineers*, vol. 51, no.11, November 1964, p. 1524.
4. W. Alexander. 'The Ternary Computer'. *Electronics and Power*, vol. 10, February 1964, p. 36.
5. M.N. Faruqui and J. Das. 'A Slope Quantized Ternary Pulse Code Modulation'. *Transactions of the Institute of Electrical and Electronics Engineers, PG Communication System*, June 1964.
6. M.N. Faruqui. 'A Slope Quantized Binary Pulse Code Modulation'. *Electronic Engineering*, vol. 38, 1966, p. 31.
7. J. Das and P.D. Sharma. 'Optimized Hybrid Unidigit PCM System'. *Electronics Letters*, vol. 2, no. 1, January 1966.
8. M.N. Faruqui. 'Studies on Unidigit PCM Systems'. Ph.D. Thesis submitted to the Indian Institute of Technology, Kharagpur, 1964.
9. J.B. O'Neal, Jr. 'Delta Modulation Quantizing Noise—Analytical and Computer Simulation Results for Gaussian and Television Input Signals'. *Bell System Technical Journal*, vol. 45, no. 1, January 1966.

SURVEY OF DEVELOPMENTS IN DIGITAL COMMUNICATION SYSTEMS*

V. Narayana Rao

Non-member

and

C.R. Chakravarthy

Non-member

Defence Electronics Research Laboratory, Hyderabad

Summary

A major trend during the past decade has been the increasing digitalization of electronics. Digital modulation techniques have been utilized in all the modern communication systems in order to achieve full exchange of bandwidth to signal-noise ratio, effective utilization of channel capacity, and the available frequency spectrum. Digital modulation systems have the distinct advantages such as good relaying capability, immunity to jamming, ease of adaptability to secure transmission and utilization of solid state circuits, reduction of errors in transmission and a high degree of reliability. In this paper, a brief introduction has been given to the PCM, delta modulation, concepts of modern communication systems such as the random access discrete address systems utilizing the time-frequency matrix addressing technique and the pseudo noise coding method, the Autovon and Autodin and the applications of digital modulation for space communications have been discussed briefly.

1. Introduction

A major trend during the past decade has been the increasing digitalization of electronics. There have been and continue to be dramatic improvements in the components for digital circuits so that ever increasing degrees of reliability, operating speed, miniaturization and precision in data handling become attainable. Digital devices are generally free from calibration problems and can be designed or programmed to perform complicated functions which might otherwise be unattainable. For most aspects of space communications, the digital approach is rapidly becoming mandatory, as the high degree of reliability required for missions of long durations and high degree of precision for data transmission and tracking of space vehicles can be achieved by the utilization of digital modulation techniques. The digital modulation is the only preferred technique in all modern communication systems for it provides the advantages give below.

*Presented at the Symposium on 'Modern Electronic Communication Techniques' held in Hyderabad on August 26, 1967.

- (i) Good relaying capability: digital modulation can be relayed many times, easily without deterioration of signal-noise ratio.
- (ii) Uniform and reliable output: uniform and reliable quality output can be achieved as it is a sharp transmission threshold system.
- (iii) Secure transmission: it is easily adaptable to secure or secret transmission which is of great significance for application to defence communication systems.
- (iv) Anti-jam characteristics: as it is a wide-band communication system with a sharp threshold and provides redundancy in transmission, more powerful and sophisticated type of equipments have to be used to jam as compared to the narrow band communication systems.
- (v) Suppression of interference: digital modulation permits excellent suppression of interference as long as such interference is weaker than the transmitted pulse. However, modern concepts of statistical communication theory have proved that suitable types of coded transmission systems will provide effective communication even in the presence of noise.
- (vi) Ease of adaptability to integrated circuits: since most of the digital circuits are of repetitive type, a modular construction is possible by utilization of the solid state integrated circuits. In these circuits simplicity of design is associated with a high degree of reliability in operation, reduction in the cost and increase of the ease of maintenance of the equipment.
- (vii) Spectrum conservation: the digital modulation systems provide a very good exchange of band width to signal to noise ratio and hence provide a very efficient use of the frequency spectrum.
- (viii) Reduction in transmission errors: the probability of errors can be reduced to a minimum by the selection of suitable modulations, waveforms and utilization of the appropriate error correcting and detecting codes.

2. Pulse modulation systems

The various types of pulse modulation systems are described below.

'The Sampling Theorem' states that a continuous message waveform that has a spectrum of finite bandwidth can be recovered from a set of discrete samples whose data is slightly higher than twice the highest signal frequency. It is this principle that forms the basis of all pulse modulation systems. In pulse-amplitude modulation, the series of periodically recurring pulses are modulated in amplitude by the instantaneous sample of the input voice or information signal. In the pulse width modulation or pulse duration modulation, the time of occurrence of either the leading or trailing edge of each pulse or both is varied

from its unmodulated position by the instantaneous sample of the modulating wave. In pulse position modulation, the amplitude of each instantaneous sample is used to vary the position in time of a pulse relative to its unmodulated time of occurrence. Pulse width modulation and pulse position modulation exhibit the feature of trading bandwidth for signal-noise ratio which is characteristic of FM. These are illustrated in Fig. 1.

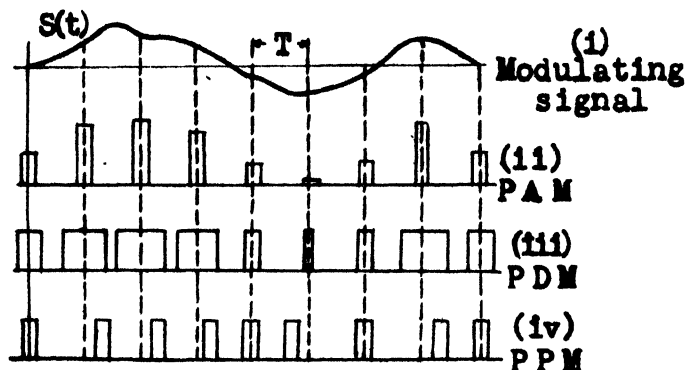


Fig. 1

Unquantized pulse systems

Pulse code modulation represents a major break-through in the art of communication. Each modulating wave is sampled periodically at a rate in excess of twice the highest frequency component present in it. These samples are quantized into certain discrete levels. Each quantized sample is assigned a code pattern of a series of pulses which are transmitted by the pulse carrier. At the receiver end, each code pattern is identified, decoded and used to produce a voltage proportional to the original quantized sample. This is illustrated in Fig. 2. PCM lends itself to time division multiplexing and is considered to be the most efficient among the existing communication systems.

The more recent pulse modulation system which requires wider bandwidth than PCM but has much simpler circuitry as compared to the complex PCM is known as the delta modulation. Delta modulation is also designated as an 'uni-digit PCM' system. Delta pulses represent binary decisions determined by the polarity of the difference between the modulating signal and the approximation of the original signal (*vide* Fig. 3). Thus, in a delta modulation system the transmitted pulses carry the information corresponding to the derivative of the amplitude of the modulation signal, and at the receiver these pulses are integrated to obtain the original waveform of the signal. A comparison of the two systems, delta and PCM will show that delta modulation is more advantageous under certain conditions for voice communications, from the point of view of both quality and simplicity. It comprises of simplified circuitry and also is capable of tolerating higher percentage transmission errors than the pulse code modulation. However, delta modulation requires much wider band-

width (Fig. 4) than PCM if the desired quality of voice transmission is high. PCM can be used for transmission in multiplex speech communication systems, data and facsimile signals, whereas, delta modulation is suitable for single channel systems. Delta modulation is finding increasing areas of application in many modern wideband communication systems, which would be discussed later.

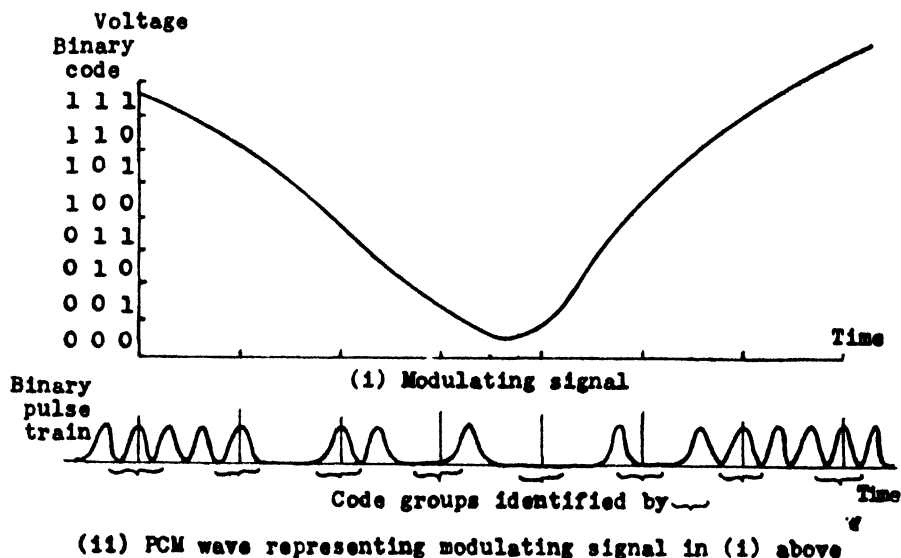


Fig. 2

Modulating signal and 3-digit binary PCM wave utilizing uniform quantum levels for a single-channel system

3. Wideband communication systems

Modern trend in all present-day communication systems is to utilize the broad band technique for effective utilization of channel capacity. J.P. Costas, a pioneer scientist in the field of communication system design, has analytically shown that broad band techniques have definite advantages for both civil and military applications and that they result in far more efficient spectrum utilization than conventional narrow band systems. With regard to military communications, he has also shown that the ability for a communication system to resist jamming varies in direct proportion to the transmission bandwidth for a fixed data or information rate. Hence, narrow band techniques lead progressively to more expensive communication systems and to less expensive jammers. Utilization of the broad band techniques for military communications is hence not only desirable, but also often mandatory.

The design of communication systems took a revolutionary change after the initiation of the 'Science of Statistical Communication Theory' by the pioneers, Wiener, Shannon, Fano, Costas and others. This theory certainly

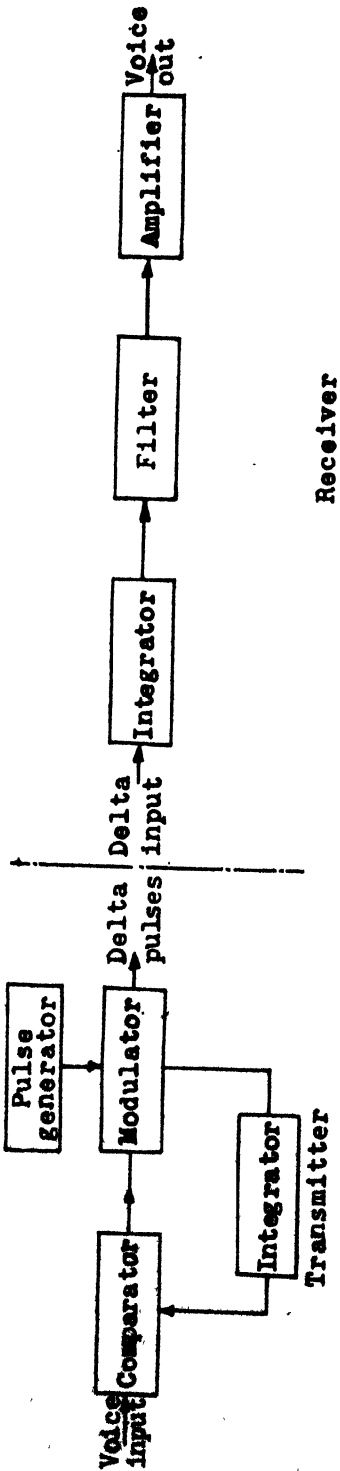
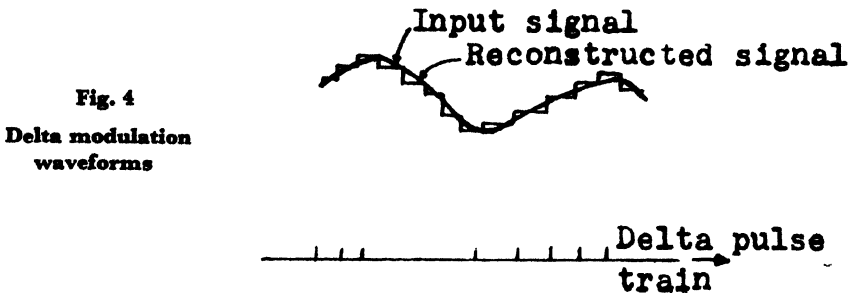


Fig. 3
Block diagram of delta modulation system

has not only brought about a turning point in the design of communication system but also has enabled one to compute the efficiency of a given system, as well as the hypothetically maximum of efficiency which any system could attain. The advent of this theory has resulted in the development of modern wideband communication systems such as 'address communication systems, Code-division multiplex systems, M-ary binary digital communication systems, coherent and non-coherent reception techniques'.



4. Address communication systems

One of the most significant concept of communication system design since the end of Second World War is the evolution of the random access discrete address system more popularly known as the 'RADA'. It can be defined as a system in which many users can send independently different messages over a common wideband frequency channel at the same time, and in the same geographical area, by utilizing a technique of continuously addressing each communication. In such a system many messages will coexist and will carry not only different modulating signals but also different addresses so that each one can be distinguished from all others. For a typical address communication system, the transmitter has to perform two separate functions, viz., modulation and addressing. This is in contrast to the usual radio transmitter where only modulation is required to send messages. Again the modulation of voice or other information could be performed on either an analog or digital basis. In the analog modulation class, both PPM as well as PFM are considered suitable for the implementation of the address communication systems. Among the digital modulation systems, the delta modulation as well as the pulse code modulation are considered compatible for the implementation of the same. However, digital modulation systems are preferred in view of all the various advantages they provide, which have already been enumerated earlier.

The addressing technique could be implemented by utilization of the time-frequency matrix or the pseudo noise codes. The time-frequency matrix is represented in Fig. 5. The voice or any other information is converted into a train of pulses which can be called modulation pulses. Each modulation pulse is transmitted as a group of three or four short RF pulses (bursts of RF energy). Each RF pulse is usually sent on different frequencies and in different

time relationships to the other pulses. The combination of the time and frequency slots in which RF pulses are transmitted is selected from what is known as the 'time-frequency address matrix' (TF matrix) and this combination constitutes an address which is continually recognized by the receiver of the particular user from the maze of other addresses. Only by transmitting a particular address can any desired user or receiver be reached. From Fig. 5 it is seen that the combinations $F_1 T_1$, $F_4 T_3$, $F_2 T_7$ and $F_5 T_1$, $F_1 T_5$ and $F_3 T_8$ constitute two different addresses. The size of the time frequency matrix determines the total number of unique addresses. One can obtain a very large number of addresses even from a relatively small time-frequency matrix. The total number of unique addresses available from a time frequency matrix is given by

$$A = \frac{{}^{FC_N} \frac{|F|}{|F-N|} \frac{{}^{T-1}P_{N-1}}{|T-N|}}{|F-N| |N|}$$

where A is the number of address.

For example, if $F = 6$, $T = 16$ and $N = 3$,

$$A = \frac{\frac{|6|}{|3|} \frac{|15|}{|3|}}{|3|} = 6.30$$

If N is increased to $N = 4$,

$$A = \frac{\frac{|6|}{|2|} \frac{|15|}{|12|}}{|4|} = 40,950$$

The size of the time-frequency matrix also determines the total bandwidth occupied by the system. One can obtain any desired number of addresses by a suitable design of the time-frequency matrix. These addresses can be changed by a simple dial-like procedure. The address communication system provides a private hot-line inter-communication service between various subscribers on an immediate direct basis without any delay, in a manner comparable to today's telephone service. This system is particularly suitable for military mobile communications below the division level where modern concepts of mobile warfare place a heavy burden on communications, civilian mobile telephone service, satellite communications, aircraft traffic control systems and other multiple access communication systems.

The address communication system, if successfully implemented will solve many of the pressing combat communication problems for they provide the following advantages such as conservation of bandwidth, immediate direct access, secure transmission, immunity against jamming, graceful degradation, higher degree reliability, high degree of flexibility, low equipment cost and long term military survivability.

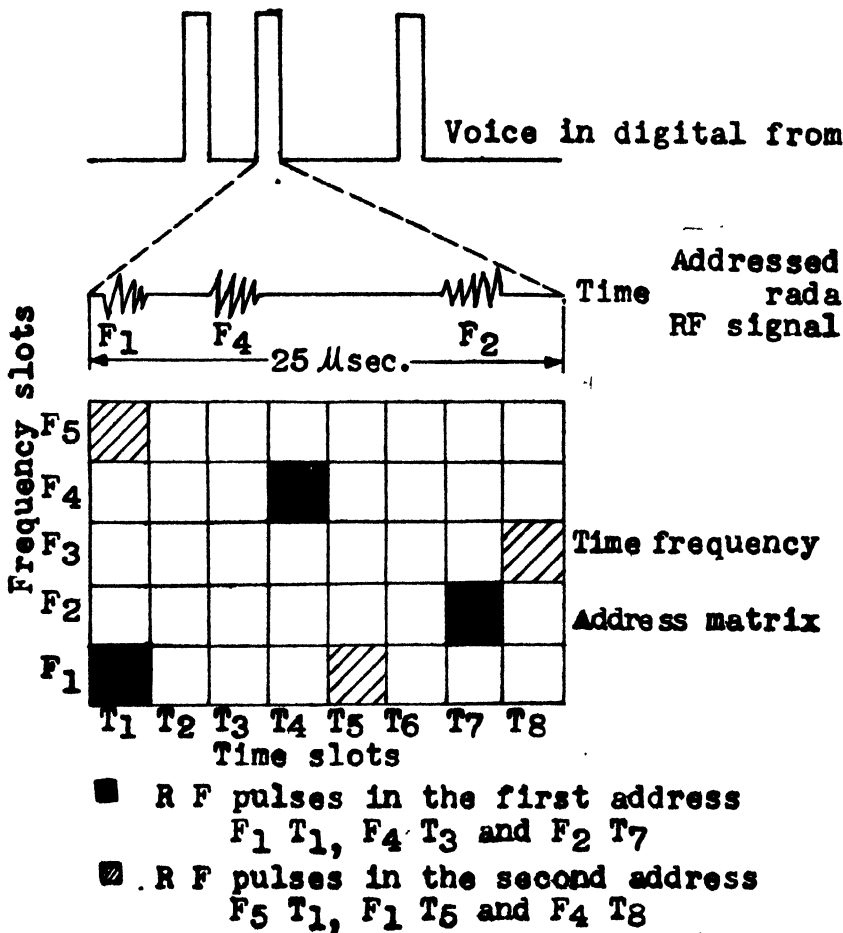


Fig. 5

Representation of time-frequency matrix

5. Pseudo noise code addressing technique

The concept of address communication systems can also be accomplished by the utilization of the pseudo noise codes generated by shift register with linear feedback. Different portions of a long shift register sequence can be assigned as characteristic addresses of a large number of users or the subscribers. The receiver will recognize only the particular address for which it has been set. This can be accomplished by the utilization of digital matched filters or suitable correlation detection techniques. When the pseudo noise code has been completely read into the digital matched filter of the intended receiver, an output pulse modulation is obtained from which voice is recovered.

Experimental sets have been developed by utilizing the PN code as the addressing technique to accomplish the RADA concept in the U.S.A. which can provide about 1,000 subscribers. An experimental VHF portable radio

set has been developed in the U.S.A. by the IBM utilizing pseudo noise codes the addressing technique to accomplish the RADA concept in a particular geographical area, for a capacity 1,000 subscribers.

The implementation of the concept of address communication systems is still in the experimental stage as is revealed from the available information. Only a few experimental systems and equipment have been developed in more advanced countries but relatively large military RADA systems are in the design and planning stage in the U.S.A. It is claimed that there are experimental indications, that this concept will be very successful and will be one of the most important communications system concept in the future. Equipment like RADEM and RACEP have been developed and subjected to evaluation in the U.S.A.

6. Autovon and Autodin

The military communication systems in the U.S.A. are now being re-organized for automatic computer control circuits and several schemes have been developed, almost all of which utilize digital techniques. Autovon and Autodin are two different systems catering for instantaneous communication between different points of the globe which are included in the network.

Autovon is an automatic voice network which handles voice and graphic communication on an automatic switching basis for the United States defence stations in the U.S.A. and outside the U.S.A. It consists of automatic switching equipment, transmission facilities and terminal equipment. It is one of the most significant and comprehensive telecommunication programmes undertaken ever by the United States Defence Department. It works on a four-wire switching system with customers competing for services on a priority basis. The main features incorporated in Autovon are:

- (i) Direct distant dialling,
- (ii) Four levels of pre-emption;
- (iii) Off-hook service;
- (iv) Direct four wire subscribers;
- (v) PBX subscribers;
- (vi) Conference facilities;
- (vii) Broadcast facilities;
- (viii) Automatic testing,
- (ix) Recording announcement,
- (x) Reprogrammable common control;
- (xi) Dial assistance operator;
- (xii) Confirmation signals;

- (xiii) Wideband switching; and
- (xiv) Abbreviated dialling.

The implementation of full programme of Autovon will be completed by 1970.

Autodin provides a smooth and efficient flow of information through the network. Autodin centre utilizes both circuit and message switching. Circuit switching is the common practice of connecting the calling party directly to the person being called. However, to improve handling of large number of digital traffic, message switching allows storage of incoming messages until they can be forwarded to the next switching centre or to their ultimate destination. In this way, as soon as a switching centre has relayed a message to another centre it is free for a new incoming call. The technique avoids long delays under busy conditions and prevents world-wide circuits from being tied up while one message is being completed. Autodin switching centre is similar to that of Autovon, although its needs and functions are specialized for handling data type digital signals rather than voice. Overall control of the centre is maintained by the communication data processor unit. In addition, the circuit and message switching units are inter-connected.

Four types of services can work into Autodin through the switching centre. They are identified as compound magnetic tape high speed teletype and standard teleprinter terminals. The compound terminal transmits and receives teletype and punch card messages. The magnetic tape terminal serves to connect computers to the system. High speed teletype terminal operates similarly to the compound terminal except that the rate of transmission is higher.

In the United States and wherever else possible, facilities for Autovon and Autodin are being leased by the Government from existing telephone and telegraph companies. Facilities outside the United States are also mostly owned by the United States Government. A total of 182 major and minor illustrations will serve the network with about 2,200 tributary stations connected with it. Both Autovon and Autodin networks will rely on every means of transmission available, including telephone cable microwave link, HF radio, troposcatter and under sea cable. Feasibility of utilizing synchronous satellites is also being investigated.

7. Application of digital techniques for space communications

One of the primary problems of space communications is the transmission of information or data at as high a rate as possible with a minimum of errors through a channel perturbed by stationary Gaussian noise. The trading of band width to signal to noise ratio is very important for all space communication systems. If we examine the various methods of modulation, we find that these fall naturally into two classes of uncoded and coded transmission systems. It is well known that for the efficient utilization of the frequency spectrum and

effective utilization of channel capacity, reduction of probability of errors, for the detection of weak signals in the presence of noise, one has to take recourse to the coded transmission systems.

Data may be presented to the transmitter in a variety of forms. Data is generated as a random sequence of binary symbols. Each symbol contains one bit of information. These data vectors are transformed into coded vectors by utilizing a coder. Various types of codes with special correlation properties have been utilized for the encoding of data and detection of signals. Codes such as orthogonal codes, bi-orthogonal codes, trans-orthogonal codes, the PN codes have been utilized for space communications depending on the requirements. In modern space communication systems the principles of coherent communication have found increasing areas of application.

In the M -ary digital communication system, there are available at the transmitter $M = 2^k$ signals to be transmitted. Each one of the data vectors is generated as a binary sequence of k consecutive data symbols. These data vectors are transformed into the code vectors by utilizing the various codes or signal waveforms which have very good correlation properties. At the receiver, all the M -signals are received but it has to decide, as to which of the M transmitted data signals has been transmitted. Hence, 'Optimal receivers' utilizing the 'maximal likelihood detection techniques' which decide on the maximum posterior probability criterion is used. Thus for coherent reception in white noise, a bank of M -correlators consisting of M -multipliers and integrators associated with a decision device is utilized for optimal decoding at the receiver.

The error probability, P_E , i.e., the probability that an error occurs in one or more bits of a sequence of K bits for uncoded and coded transmission systems is illustrated in Figs. 6 and 7. It is seen from Fig. 6 that for a fixed data rate, noise density N_0 and $P_E = 10^{-5}$, the required signal power is reduced almost by a factor of 2 (about 2.5 dB) for $K = 5$. If $K = 10$, the signal power is reduced by almost a factor of 4, i.e., about 5 dB for the same data rate as illustrated in Fig. 7. Hence, it is evident that coded transmission systems bring about the conservation of power which is of vital importance for space communication and also permit approximately doubling the data rate for $K = 5$ and quadruple it for $K = 10$. Thus utilization of coded transmission systems, associated with coherent reception techniques provide an effective communication in the presence of noise.

8. References

1. H.E. Rowe. 'Signals and Noise in communication System'. Bell Telephone Laboratories Series. *Van Nostrand Co., Inc.*, 1965.
2. P.F. Panter. 'Modulation, Noise and Special Analysis Applied to Information Transmission'. *McGraw-Hill Book Co., Inc.*, 1965.
3. A. Lender and M. Kozuch. 'Single Bit Delta Modulating System'. *Electronics*, vol. 34, no. 46, November 17, 1961, p. 125.

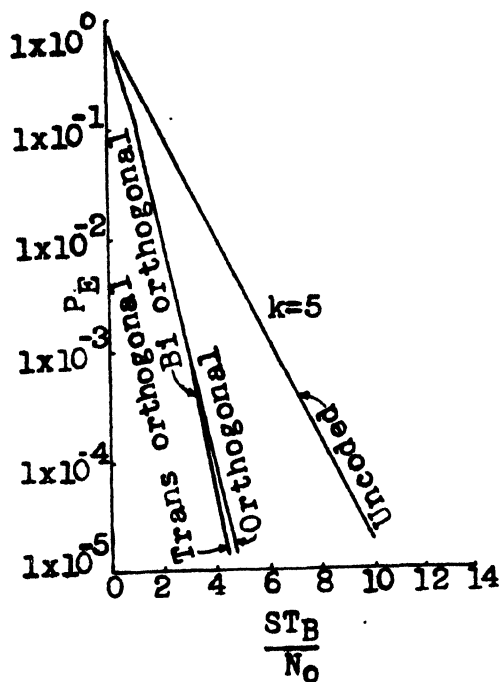


Fig. 6
Error probability sequences for
coded and uncoded transmission
systems

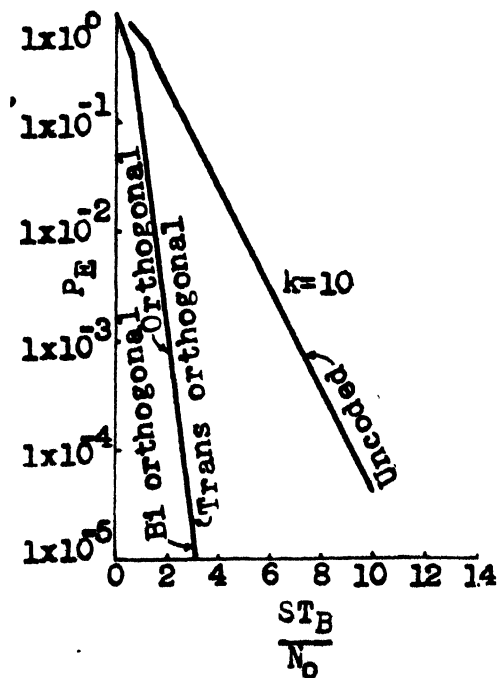


Fig. 7
Error probability sequence
for coded and uncoded
transmission systems

4. 'Magnuski, Henry, Motorola's Contribution to Random Access Techniques'. *Motorola Engineering Bulletin*, vol. 11, nos. 1 and 2, November 2, 1963, p. 1.
5. F. Corr, R.C. Field and J. Marchese. 'A Pulsed Pseudo-Noise VHF Radio Set'. *IBM Journal of Research and Development*, vol. 9, no. 4, July 1965, p. 256.
6. S.W. Golomb. 'Digital Communications with Space Applications'. *Prentice Hall, Inc.*, 1964.
7. A.J. Viterbi. 'Principles of Coherent Communication'. *McGraw-Hill Book Co., Inc.*, 1966.
8. A. Mark. 'AUTOVON-Inception to Implementation'. *Signal*, March 1966, p. 9.
9. R.A. Bovrcy. 'AUTODIN-World Wide Automatic Digital Network'. *Signal*, March 1966, p. 1.
10. H.E. McGuire. 'RACEP Manpack Designed for Military'. *Signal*, vol. 17, no. 3, November 1962, p. 10.
11. H.C. Van De Hulst, C. de Jager and A.F. Moore (Ed.). 'Space Research II'. *Proceedings of the Second International Space Science Symposium*, Florence, 1961.

DIGITAL FILTERS***A. Prabhakar***Non-member**Professor, Department of Electronics & Communication Engineering,
Osmania University, Hyderabad***Summary**

Digital filters are attractive for use both in communication systems and in sampled data control systems. In communication, they fulfil the need of sharp cut-off filters, while in control systems, they offer the designer great flexibility in choosing the transfer characteristics of the controller element. The latter facility is particularly useful in the design of control systems to suit wide variations in the environmental conditions and in the strength of the control signal. This paper briefly reviews the problem of digital filter synthesis and presents the experimental results obtained in the Defence Research Laboratory, Hyderabad.

1. The digital filter

The digital filter consists of a sampler, a coder, a digital computer and decoder as shown in Fig. 1. Here the analogue signal $E_i(t)$ is sampled and the output from the sampler $E_i^*(t)$ is quantized and coded in an analogue digital converter, and is later modified by a suitable digital programme, which yields an output member series $E_o^*(t)$ related to the input member series $E_i^*(t)$. The main problem in the synthesis of a digital filter is the determination of the digital programme of the computer, equivalent to the frequency characteristics of the corresponding analogue filter. The logical step would be to find the pulse transfer function of the sampled data system $G(Z)$ from the transfer function of the analogue filter, and realize this pulse transfer function by a suitable digital programme in the computer. A few examples will make this approach quite clear.

2. Synthesis of pulse transfer functions

Suppose it is desired to synthesize a digital filter having the properties of an ideal integrator. The frequency characteristics of an ideal integrator are shown in Fig. 2 and the transfer function of an ideal integrator should be of the form $G(s) = \frac{K}{s}$, where K is a constant. The pulse transfer function $G(Z)$ of the corresponding sampled data system is given by

$$\sum_{n=0}^{n=\infty} g(nT) Z^{-n}$$

*Presented at the Symposium on 'Modern Electronic Communication Techniques' held in Hyderabad on August 26, 1967.

where $g(t)$ is the impulse response of the ideal integrator, and Z is defined as e^{Ts} and T the sampling interval. Since it is known that the impulse response $g(t)$ of an ideal integrator is the constant K , we can substitute this value in the expression for $G(Z)$. Then, we get

$$\begin{aligned}
 G(Z) &= \sum_{n=0}^{n=\infty} K Z^{-n} \\
 &= K (1 + Z^{-1} + Z^{-2} + \dots) \\
 &= \frac{KZ}{Z-1}, \text{ or, } \frac{K}{1-Z^{-1}}
 \end{aligned} \tag{1}$$

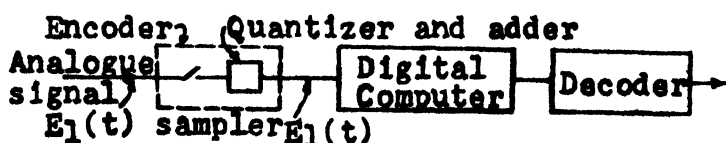


Fig. 1
Schemate diagram of a digital filter

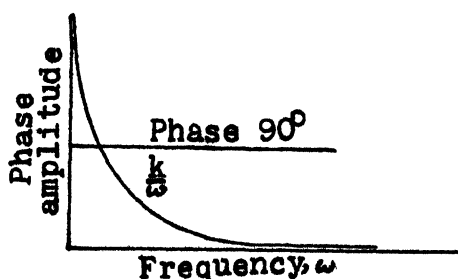


Fig. 2
Frequency characteristics of an integrator

The digital programming of the computer has therefore to be done to yield the output input relationship of the sample data system as

$$\frac{E_o(Z)}{E_i(Z)} = \frac{K}{1-Z^{-1}}$$

or,

$$E_o(Z) - E_o(Z) Z^{-1} = K E_i(Z)$$

From the above equation, we get

$$E_o^*(t) = E_o^*(t-T) + K E_i^*(t) \tag{2}$$

The computation involved in equation (2) can readily be performed by a conventional digital computer. Clearly the programme for equation (2) will involve either additions or subtractions and one delay operation. For

more sophisticated filters, the programming will be complicated. An example of the synthesis of a low-pass filter will be considered next.

3. The ideal low-pass filter

The impulse response of an ideal low-pass filter having a cut-off frequency f , is given by

$$\frac{\sin 2\pi f t}{2\pi f t}$$

This function which is plotted in Fig. 3 shows a non-zero response before $t = 0$. This is obviously contrary to fact, and arises because an ideal low-pass filter is not physically realizable and cannot be made. In order to be realizable, the ideal low-pass filter transfer characteristic may be approximated to the Butterworth function, $\frac{1}{(1 + w^{2N})^{\frac{1}{2}}}$ where N represents the order of the function.

The higher the value of N chosen, the better will be its approximation to the ideal filter. To illustrate the principle of synthesis, a third-order Butterworth will be considered. The impulse response of such a filter having a cut-off frequency of 1 radian per sec. is found to be

$$e^{-t} - \frac{2}{\sqrt{3}} e^{-\frac{1}{2}t} \left[\cos \left(\frac{3}{2}t + \frac{\pi}{6} \right) \right]$$

and is shown plotted in Fig. 4. Replacing t by nT , we get for the Z -transform of the impulse response as

$$\sum_{n=0}^{\infty} \left(e^{-nT} \right) Z^{-n} = \frac{2}{\sqrt{3}} \sum_{n=0}^{\infty} e^{-\frac{nT}{2}} \left[\cos \frac{2}{3} n T + \frac{\pi}{6} \right] Z^{-n} \quad (3)$$

Fig. 3
Plot of $\sin \frac{2\pi f t}{2\pi f t}$

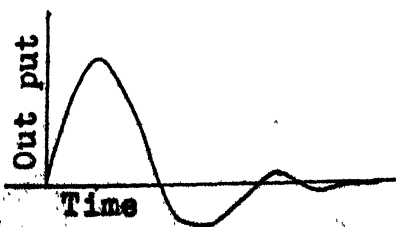
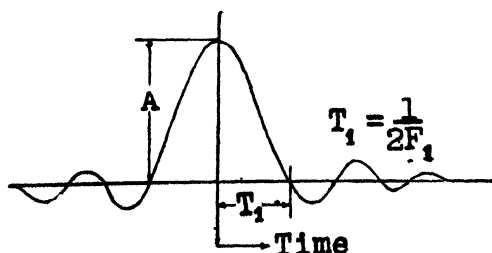


Fig. 4
Output vs. time

If, in this example, it is assumed that the input frequency spectrum F_1 stretches up to twice the cut-off frequency of the filter, the sampling interval T , according to Shannon's sampling theorem would be $\frac{1}{2F_1}$ (in this case, $\frac{\pi}{2}$ sec.). Substituting this value in equation (3), we get

$$\frac{E_0(Z)}{E_1(Z)} = 0.358 Z^{-1} + 0.265 Z^{-2} + 0.03 Z^{-3} + \dots \quad (4)$$

It will be seen that only three terms of the series are significant. In most practical filters this will be the case, as the series is rapidly convergent and hence the practical utility of this method. The programming of the digital computer has therefore to be done according to equation (4) which gives the relationship between $E_0^*(t)$ and $E_1^*(t)$ as

$$E_0^*(t) = 0.358 E_1^*(t - T) + 0.265 E_1^*(t - 2T) + 0.03 E_1^*(t - 3T) \quad (5)$$

The computation involved in equation (5) is simpler than that in the ideal integrator described earlier.

4. An alternative approach

An alternative approach to the problems of digital filter synthesis would be the convolution of the instantaneous samples with the impulse response of the filter. However, the convolution integral must be evaluated from $-\infty$ to $+\infty$ and this would be an impossible task even for a high-speed digital computer. Fortunately, we can make simplifications, since in the case of practical filters the impulse response decays to a negligible value within a reasonable interval from the time of excitation so that finite limits may be set to the convolution sum which may give rise to very small arbitrary error. Perhaps this can best be illustrated by the example of the synthesis of the third-order Butterworth low-pass filter.

As in the case of Z -transform analysis we shall assume that the signal has a band width F_1 , and it is desired to filter this with a low-pass filter having a cut-off frequency F_2 , where F_1 is necessarily greater than F_2 (otherwise there would be no point in filtering). Then the procedure to be followed would be to sample the input signal at sampling rate $2F_1$, and programme the digital computer to substitute for each sample the sum $-T_1$ to $+T_1$ of all samples multiplied by the appropriate impulse response of the filter.

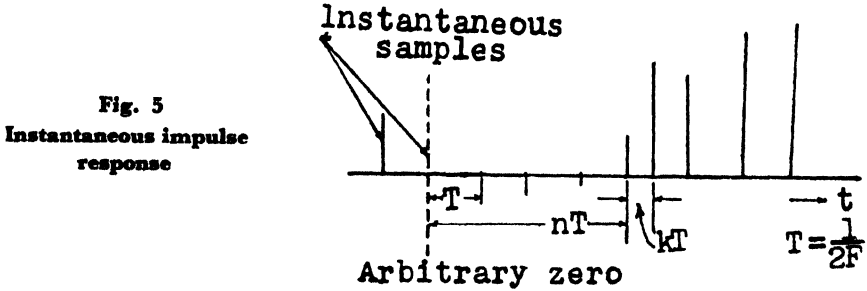
In our case, the impulse response would be

$$e^{-t} = \frac{2}{\sqrt{3}} e^{-\frac{t}{2}} \left[\cos \left(\frac{3}{2} t + \frac{\pi}{6} \right) \right]$$

where $\pm T_1$ are the limits on the convolution sum set by accuracy considerations. Fig. 5 represents the situation in our example, if the output signal at any time t_1 is given by $E_0(t_1)$, where $t_1 = nT + kT$ is measured from an arbitrary zero.

Then

$$E_0(t) = \sum_{s=-s_1}^{s=s_1} E_1(n+S) T \left[e^{-(k-s)T} - \frac{2}{\sqrt{3}} e^{-\frac{(k-s)T}{2}} \cos \frac{3}{2}(k-S)T + \frac{\pi}{6} \right] \quad (6)$$



Referring to Fig. 4, if T_1 is the time at which impulse response decays to a negligible value, then $S T$ need not exceed T_1 .

i.e.,

$$S = \frac{T_1}{T}$$

Now T_1 and T are known from the conditions of the problem and the limits on S can easily be determined to be S' , say. Equation (6), therefore, reduces to

$$E_0(t) = \sum_{s=-s'}^{s=s'} E_1(n+S) T \left[e^{-(k-s)T} - \frac{2}{\sqrt{3}} e^{-\frac{(k-s)T}{2}} \cos \left(\frac{3}{2}(k-S)T + \frac{\pi}{6} \right) \right] \quad (7)$$

The impulse response of the filter would probably have to be calculated by a sub-routine.

5. Experimental results

The method outlined above has been tested with the aid of the general purpose computer available at the Defence Research Laboratory, Hyderabad. An ideal low-pass filter normalized to a cut-off frequency of 1 radian per sec. was synthesized by programming its impulse response as a sub-routine. The inputs to the computer were sinusoidal signals ranging from 0 to 5 radians per sec. The sampling time of the signals was 1 sec. and limits of summation S' chosen were ± 6 . The output from the computer which is a time-series was decoded by recovering the envelope of the amplitude modulated pulses. The same computer was also used to synthesize other types of filters and compensating networks.

6. Proposed digital controller

Fig. 6 shows the schematic model of the digital controller for sampled data systems being planned at the Osmania University, Hyderabad. The analogue error signal $A(t)$, is combined with a pulse generator output in a standard transistorized multiplier circuit. The sampled output $A(nT)$ is coded in the binary form in an analogue digital converter. In the controller proposed, four samples can be stored in the register on the top and the storage

capacity can be increased with the number of samples desired. Four samples of the impulse response are stored in the preset shift register, and the input series and the impulse response series are multiplied and added according to equation (7). The output from the output register is converted again into the analogue form before being passed on to the controlled system.

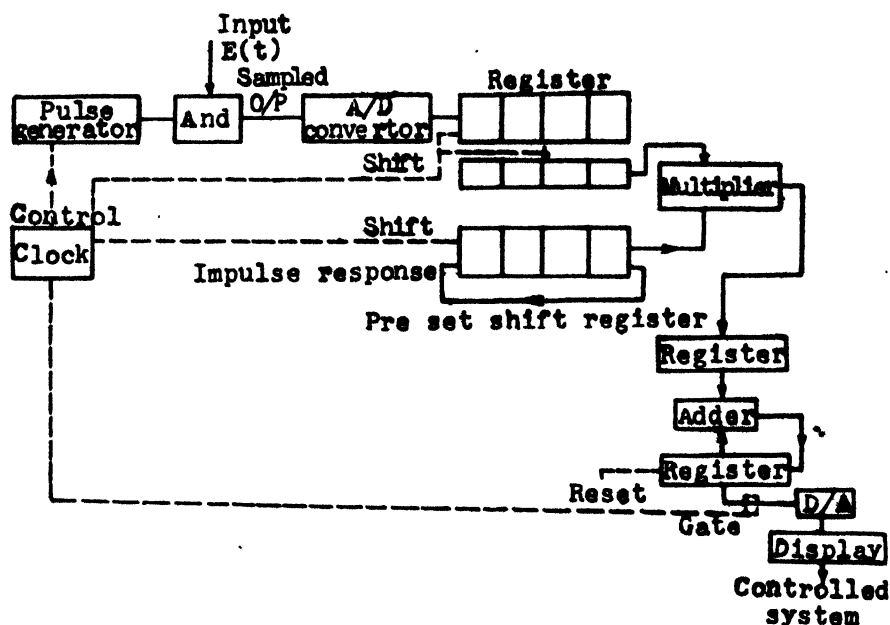


Fig. 6

Schematic diagram of a digital controller data system

7. Conclusion

There are two general difficulties about the convolution method. The signal bandwidth must be known fairly accurately. It is also necessary to store S' samples before interpolation can begin. This means that even if instantaneous computation were possible, there would always be a delay of $S' T$. Perhaps real time filtering is more feasible with Z -transform method than with the convolution method. Apart from this, both the approaches are apparently applicable to any filter response whether analytical or not.

8. Acknowledgments

The author wishes to express his deep gratitude to Mr. G.H. Stearman of the College of Aeronautics with whom he had several stimulating discussions on the subject.

9. References

1. Lawrence, Jespersen and Lamp. *Journal of Research National Bureau of Standards*, vol. 65D, no. 4, July-August 1961, p.351.
2. J. Tou, 'Digital and Sampled Data Control Systems,' McGraw-Hill Book Co. Inc., 1964.

SHIFT REGISTER SEQUENCES***C. Satyanarayana***Non-member**Lecturer, Department of Electronics and Communication Engineering,
Osmania University, Hyderabad***Summary***In this paper the construction, generation, properties of m-sequences and their applications for ranging, information transmission, synchronization etc., have been considered.***1. Simplex codes**

If a code is such that its maximum correlation between two distinct code words is equal to the average correlation, then the code is called a 'simplex' code. Thus, for a simplex code,

$$\begin{aligned}
 C(V_i, V_j) &= \text{Average } C(V_i, V_j) \quad [i \neq j] \\
 &= -\frac{1}{P-1} \quad \left. \vphantom{\begin{aligned} C(V_i, V_j) &= \text{Average } C(V_i, V_j) \quad [i \neq j] \\ &= -\frac{1}{P-1} \end{aligned}} \right\} \text{ if } P \text{ is even} \\
 &= -\frac{1}{P} \quad \left. \vphantom{\begin{aligned} C(V_i, V_j) &= \text{Average } C(V_i, V_j) \quad [i \neq j] \\ &= -\frac{1}{P} \end{aligned}} \right\} \text{ if } P \text{ is odd}
 \end{aligned}$$

For $i = j$, average of $C(V_i, V_j) = 1$, where $V_i, i = 1, 2, \dots, P$ are the code words. The correlation function of a simplex code is shown in Fig. 1. Because the correlation function assumes two values the sequence is also known as a two-level sequence.

There are four known types of two level sequences giving rise to simplex codes. These are the sequences corresponding to the following values of word length P :

- (i) $P = 2^k - 1$, Maximal length linear shift register sequences or m -sequences
- (ii) $P = 4t - 1$ is prime quadratic residue or legendre sequences.
- (iii) $P = 4t - 1 = 4x^2 + 27$ is prime, Hall sequences.
- (iv) $P = Q(Q + 2)$ where both Q and $(Q + 2)$ are prime, twin prime sequences.

Out of these, the m -sequences are easy to generate by means of a shift register, with suitable logics. The sequences consist of $(+1)$ s and (-1) s or $(+1)$ s and zeros.

*Presented at the Symposium on 'Modern Electronic Communication Techniques' held in Hyderabad on August 26, 1967.

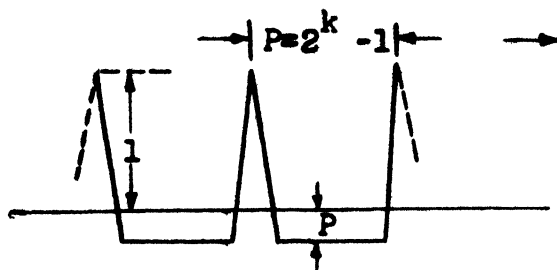


Fig. 1

Correlation function of a simplex code for n odd

2. Construction of m -sequences

The m -sequences are maximal length linear recurring sequences. The theory of linear recurring sequences provides a method of construction of m -sequences. If m -sequence of period $2^k - 1$ is desired any irreducible k th degree polynomial over GF (2) having period $2^k - 1$ can be used to give a recursion formula. Applying the recursion formula to any k -tuple other than $0 \dots 0$ provides an m -sequence of the desired type.

Associated with the polynomial,

$$f(x) = \sum_{i=0}^k C_i x^i = C_0 \oplus C_1 x \oplus \dots \oplus C_k x^k = 0 \quad (1)$$

is the recursion relationship

$$\sum_{i=0}^k C_i x_{j-i} = C_0 x_j \oplus C_1 x_{j-1} \oplus \dots \oplus C_k x_{j-k} = 0 \quad (2)$$

which gives

$$X_j = \frac{1}{C_0} [C_1 x_{j-1} \oplus \dots \oplus C_k x_{j-k}] \quad (3)$$

The symbol \oplus denotes 'exclusive or'.

As an example, for $k = 4$, an irreducible polynomial of period $P = 2^k - 1 = 15$ is

$$x^4 \oplus x^3 \oplus 1 = 0 \quad (4)$$

The recursion is given by

$$x_j = x_{j-3} \oplus x_{j-4} \quad (5)$$

Applying this recursion to the vector 0001, the following sequence is obtained :

$$000100110101111 \dots \quad (6)$$

3. Generation of the m -sequence

To generate the m -sequence of period P , not exceeding 2^k a shift register of degree k , can be employed. If the shift register is linear, the period of the sequence is at most $2^k - 1$, and any output sequence achieving $P=2^k - 1$ is called a maximum length linear shift register sequence. A shift register of degree k , is a device consisting of k consecutive binary storage positions, which shifts the contents of each position to the next position down the line, in time to the regular beat of a clock. In order to prevent the shift register from emptying by the end of k clock pulses, a 'feedback term' may be computed as a logical function of the contents of the k positions and fed back into the first position of the shift register. The general block diagram of such a register with feedback and also external logic is shown in Fig. 2. With this set-up any pre-assigned binary sequence can be obtained as the output, given suitable choices of k , f and the initial state of the shift register. The most important special case of Fig. 2 which has been analyzed in great detail is the 'linear' case in which $f(x_1, \dots, x_k)$ is a parity check function on some or all of its k inputs.

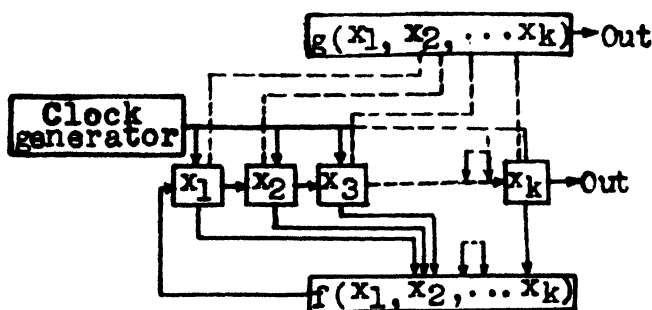


Fig. 2

General shift register of degree with logical feedback

External logic, $g(x_1, \dots, x_k)$ can also be added to the set-up in Fig. 2, as shown by the dotted lines. The principal advantage of this configuration is that the 'internal or direct logic', $f(x_1, \dots, x_k)$ in conjunction with the k -position register can be used to establish a period P , and the 'external or output logic', $g(x_1, \dots, x_k)$ can modify the sequence of period P , already generated to any other sequence of period P .

As an example, the sequence constructed above for $k = 4$ can be generated by a 4-stage shift register with the feedback logic :

$$f(x_k) = x_{k-3} \oplus x_{k-4} = x_{k-3} \bar{x}_{k-4} + \bar{x}_{k-3} + x_{k-4}$$

The symbol '—' over a parameter stands for complementation. If the initial vector is 1000, then the succession of states will be :

1000, 0100, 0010, 1001, 1100, 0110, 1011, 0101, 1010, 1101, 1110, 1111, 0111, 0011, 0001.

The output (the last position of each state) is the sequence [same as in equation (6)]

000100110101111

repeating periodically with period 15.

4. Properties of m -sequences

Even though the sequence in equation (6) is generated by a deterministic device, it satisfies several most obvious randomness tests and hence the sequence is also known as 'pseudo-random' or 'pseudonoise' sequence.

Randomness tests

- (i) The balance property: In each period of the sequence, the number of 1's differ from the number of zeros by at the most 1.
- (ii) The run property: Among the runs of 1's and zero's in each period, one-half the runs of each kind are of length one, one-fourth of each kind are of length two, one eighth are of length three, and so on, as long as these fractions give meaningful numbers of runs.
- (iii) The correlation property: If a period of the sequence is compared, term by term, with any cyclic shift of itself, the number of agreements differ from the number of disagreements by at the most 1.

It can be easily verified that the postulates, 1 to 3, are satisfied by the sequence considered. Postulate 3 is a precise characterization of the maximum length linear shift register sequences.

The randomness of these sequences refers to the *a priori* conditions, under which the sequence was produced, rather than to the *a posteriori* consideration of what the sequence looks like, or what properties it exhibits.

- (iv) Cycle and add property : Given a PN code of length 2^k-1 and any cyclic permutation of the same PN code the modulo 2 sum is another cyclic permutation of the PN code. As an example for the code sequence in equation (6) if we add a cyclic shift of itself, the result is

000100110101111

001001101011110

001101011110001

Another cyclic shift of sequence in equation (6).

5. Applications of m -sequences

Ranging

For range radar application in environments with extreme background noise, a shift register modulated pulse train using a maximum length sequence has the property that its auto-correlation function is recoverable despite a noise-to-signal excess of many decibels.

For a range radar, if a single pulse is transmitted, the returned pulse amplitude will be very small as the range increases. To enhance the echo, a pulse train can be transmitted. If the repetition period of the pulses is less than the time required for the signal to travel to the target and back, there will be ambiguity, which can be avoided by using m -sequences since the period of a m -sequence can be made longer than the time required for the echo to return. Good accuracy and resolution can be obtained by transmitting sequences whose time bandwidth products are 10^3 or more. The m -sequences with periods in the range of billions and trillions can be generated with ease by shift registers. Such long sequences are especially useful in radar astronomy because the delay involved between the transmitted and returned signal is large. For example, the Venus ranging experiment of M.I.T.'s Lincoln Laboratory in 1959 and 1961 used a m -sequence of length $2^{13}-1 = 8191$, to determine whether to transmit 'pulse' or 'no pulse' in consecutive time intervals. The two-way transit time for the pulse is 247 sec. for the planet Venus.

For good range resolution, the pulse repetition rate should be large. Hence, there will be large amount of delay involved in determining the phase of the returned sequence by correlation with a locally generated sequence. If the sequence is of million digits length, $\log_2 10^6$ 'yes-or-no' questions have to be asked to obtain the correct phase. Sequences have been found which have the property that the phase can be determined by correlation using far fewer than the full number of trails. These sequences are found by combining several short PN sequences, digit by digit. If the periods of the several sequences have no common divisors, the period of the combined sequence is the product of the periods of the several sequences. It is possible to determine the phase of the combined sequence by determining separately the phases of the component sequences. This requires at the most $(P_1 + P_2 + \dots + P_n)$ trial correlations to determine the phase of a sequence whose length is $P_1 P_2 \dots P_n$ where P_i are the lengths of the component sequences.

As an example of construction of a combined sequence, consider the two sequences with periods P_1 and P_2 :

$$\begin{array}{ll} 110100 & P_1 = 7 \\ 111100010011010 & P_2 = 15 \end{array}$$

The combination is formed by the logical function add of the two sequences, digit by digit. The combination sequence with period 105 is 1110000100010001101000100100101010000100000100100000000101010010001001100000011010011100000010000.

The auto-correlation function of the combined sequence has peaks for all values of phase shift which are divisible by the period of either component. Also the correlation, when both components are out of phase, is not $-\frac{1}{P_1 P_2}$. This is a consequence of the fact that the combination sequence is very unbalanced, with 73 zeros to 32 ones. Combination sequences can be constructed preserving the auto-correlation properties of a single PN sequence,

The applicability of a waveform for radar can be judged by considering the ambiguity function plots. The ambiguity function is the Fourier transform of the product of the transmitted and received waveforms into the Doppler domain or the inverse Fourier transform of the product of the spectra of transmitted and received waveforms into the time (delay) domain. The 'Bed of nails' magnitude squared ambiguity function or ψ -function for the m -sequence of period $P = 4$ is shown in Fig. 3. For no-delay and Doppler shifts, the maximum value P^2 occurs. Along the delay axis, the value drops to $\frac{1}{P^2}$ of the maximum and for delay and Doppler shifts not equal to zero, the value is $\frac{(P-1)}{P^2}$ of the maximum.

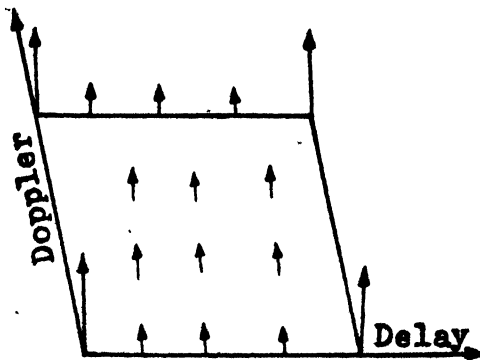


Fig. 3

ψ -Function of the m -sequence corresponding to period 4 : 111-1

If the periodic impulses of the sequences are replaced by a bandpass a periodic signal the contours of $|A|$ function for $P=4$ is shown in Fig. 4.⁴ Here the $|A|$ function lies below the central spike by at least the half-power time bandwidth product. As the period of the m -sequence used is increased, there will be more uniform distribution of the ambiguity and hence the peaks at points for delay and Doppler not-zero are reduced since the total volume enclosed above the delay Doppler plane is a constant and equal to unity.

Coding for information transmission

In information transmission each message symbol is encoded into n binary digits. It can be shown⁵ that as n is made larger and larger, $H_n(x)$, the entropy of the input to the channel, approaches the channel capacity C ; the relationship is expressed as

$$H_n(x) = C - \frac{1}{n} \log_2 n$$

To each message symbol, any one of 2^n code vectors can be assigned randomly. The number of binary digits for N message symbols will be $N 2^n$. As N and n are increased there arises the problem of storage of these binary digits, particularly for a spacecraft transmitter. This can be overcome by employing

a shift register encoder to construct binary code signals which possess two level correlation.

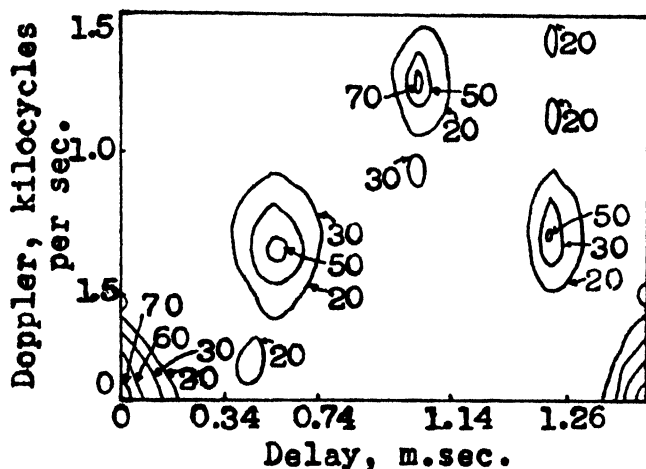


Fig. 4

|A|-Function contours for the code sequence 111-1

Synchronization

The two level correlation of PN code makes it attractive for using in synchronization techniques. A maximal length linear shift register is used in conjunction with phase lock techniques to obtain both bit and word synchronization as well as a coherent demodulation reference. Also by employing a shift register the complexity of the decoding equipment can be reduced.³

Let the PN code clock generator frequency be $2f_s$, where

$$2f_s = f_i \oplus f_s / 90^\circ$$

APN* code is defined as $PN^* = PN \oplus f_s$

Since PN is of odd length and there is a half-cycle of f_s for each PN bit, PN^* will have a cycle length of $2P$, being composed of a code of period P , followed by its complement.

The auto-correlation function $R(T)$ of the PN^* code is shown in Fig. 5. The maximum correlation cycle between $+1$ and -1 and occur for each cycle of the PN code component.

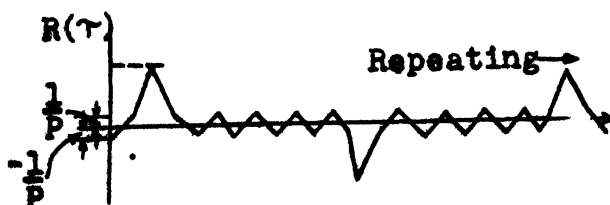


Fig. 5

PN^* auto-correlation function

The auto-correlation properties of PN* codes provide the basis by which two identical PN code generators operating from independent clock sources can be locked in time synchronism. The cross-correlation between $PN \oplus 2f_i$ and PN is shown in Fig. 6. From Fig. 6 it is seen that an S curve is generated each time the PN code passes through its point of maximum correlation; otherwise, the function is zero. This property is ideal for employing phase lock techniques to synchronize the two PN code generators, with the cross-correlation function forming the loop error signal

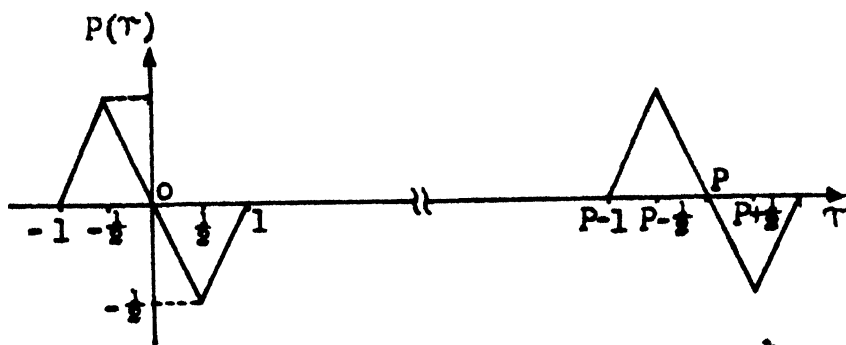


Fig. 6

Cross-correlation function between $PN \oplus 2f_i$ and PN

Besides the applications mentioned above, the shift register sequences can also be used in enciphering, where it acts as the 'key', multiple address coding where different portions of a long sequence can be assigned to different stations for position identification. As an example of the latter, different 10-bit segments of a sequence of length 1023 have been assigned to each of 64 outlying weather stations to monitor rainfall information in the vicinity of Calcutta. Another interesting application is in the generation of random numbers for Monte-Carlo techniques.

6. References

1. S.W. Golomb (Ed.) 'Digital Communications with Space Applications'. Prentice Hall, Inc., 1964.
2. F.M. Reza, 'An Introduction to Information Theory'. McGraw-Hill Book Co., Inc., 1961.
3. Balakrishnan (Ed.). 'Advances in Communication Systems, Theory and Applications'. Academic Press, 1965.
4. C. Satyanarayana. 'The Ambiguity Function'. Master's degree thesis submitted to the Electrical Engineering Department, Indian Institute of Technology, Kanpur, 1966.

SATELLITE COMMUNICATIONS***Major R.K. Joshi***Associate Member**Instructor in Radar Engineering Wing, EME School (South),
Secunderabad***Summary**

This paper deals with general system concepts and design trends in satellite communications. The subject has been built up by discussing the development of communications satellites in the chronological order and the present-day thinking in regard to the multifarious applications of satellite communications. This has been done so that the design trends may be well-appreciated keeping the above background in mind. The military applications and the impact on the growing communications needs of India have also been discussed in brief.

1. Introduction

During the year 1950, roughly one million telephone conversations took place from the U.S.A. to the countries overseas. Over the following ten years, this number rose to four millions. It is expected to reach 20 millions by 1970 and climb close to 100 millions by 1980.

Although the above figures are for one of the most developed countries of the world, nevertheless, they speak of a definite trend in the growth of telephone traffic throughout the world which has forced the communication engineers to look for additional means of communication. Furthermore, besides the telephone and telegraph communications, endeavours are being made to develop the transmission of long distance television broadcast—a possibility which by permitting mutual exchanges of programmes between countries will bring the people of the world close to each other and will be a great landmark in the history of this shrinking world.

Although until lately most of the inter continental communications traffic has been handled by means of cables and HF radio links, there can be no question but that these means alone will not suffice to meet future requirements. Submarine cables, because of the restricted number of telephone channels available for use, offer but limited possibilities, and as far as broad band transmission is concerned (television), they are not suitable. Besides this, the HF spectrum is already so overloaded that no further frequencies are available for additional radio links. In the circumstances, there seems to be no alternative but to resort to the use of long-range communication satellites for bridging long distances and transmitting broad-band signals.

*Presented at the Symposium on 'Modern Electronic Communication Techniques' held in Hyderabad, on August 26, 1967.

In addition to the civil authorities demanding an increased capacity of means of communication, the military authorities in some of the countries (like the U.S.A. and western European countries) have for some time felt the need for substantial number of long-range communication links affording utmost reliability and immunity to jamming by a potential enemy. Since this dual interest is particularly prevalent in the U.S.A. it was reasonable to expect that the United States would take the lead in exploring the possibilities offered in this field by satellite this is all the more so as they are in a better position than other countries to provide the financial means to carry out the work entailed in the research, development, construction and launching of experimental satellites.

2. Short history and development of satellite communications

The history of satellite communication dates from October 21, 1957, the day of successful launching of the 'Sputnik' by the U.S.S.R. It is only since then, that the communication engineers could have started dreaming realistically of putting up an artificial satellite in space which could either act as passive reflector for VHF and SHF radio waves or as an active repeater station in space, thereby increasing the range of communications to thousands of miles at these frequencies, thus replacing the cumbersome network of ground based repeater stations. Problem with these repeater stations becomes very complicated when two ground stations are separated by a stretch of sea.

The experimental work on the communication satellites began around the year 1958 with the launching of 'Score' the first experimental communication satellite on December 18, 1958. First test of communication transmission was conducted by means of this satellite. Since then a large number of experimental communication satellites both active and passive have been launched. The notable landmark in the history of development has been the launching of Telstar-1 on July 10, 1962, which demonstrated the successful transmission of broad-band communications across the Atlantic Ocean in SHF range for the first time.

At this stage there remained no doubt in the minds of the experts that the construction of satellites for world-wide communications would not only be feasible but also commercially worth while. On the other hand, opinion had been far from unanimous as to how such a satellite communication system should be designed technically. Very little experience was available at this stage and in view of the many different theoretical possibilities it remained to be seen which one would offer the best prospects of success.

The use of passive satellites has been considered to be of no commercial interest despite satisfactory results achieved with Echo 1 and 2, for the reason that the signals reflected back to ground stations even with high power transmitters are extremely weak and because the possible bandwidth is not sufficient for satisfactory transmission of television signals. With regard to the design of active satellites the opinion differed widely on the orbit systems for

world-wide communications network. The opinion was chiefly divided in favour of the following systems:

- (i) Synchronous orbit; and
- (ii) Lower altitude random and phased orbits.

The points advanced in favour of the first system were fixed antennas at the ground station which are much cheaper than the steerable antennas required for the second system and lesser number of satellites required for establishing world wide communications. The points against the system were the delay period of 0.6 sec., in duplex transmission, echo effect, problems of station keeping (*i.e.*, keeping the satellite in exact orbit so that its time period of rotation is that of earth, *i.e.*, 24 hr.) and the very high power requirements for the satellite.

However, to gain practical experience on these problems a number of experimental satellites were planned for launching. Of these, Syncom 1 and need special mention as they were the first synchronous satellites launched by Hughes Aircraft Co. (the chief proponents of synchronous orbits). Syncom-2 was launched into a synchronous equatorial orbit which makes the satellite stationary with respect to any point on earth.

The results obtained from the launchings of Syncom-1 and Syncom-2 were so satisfactory that they proved even better than its proponents, once outnumbered, had expected. The result of this has been that opinion has now more or less crystallized in favour of the stationary orbit concept for international and national commercial communications links.

The growth of the satellite communications since then has been very swift. In February 1963, Communications Satellite Corporation (COMSAT) was incorporated in the U.S.A. The Corporation has the virtual monopoly on the growth of commercial systems.

As a number of nations started showing interest in the global communications by satellites, International Telecommunications Satellite Consortium (INTELSAT) was formed which has 55 member nations now. Communications Satellite Corporation (COMSAT) is the manager for developing the space segment of the (INTELSAT) global system. India is one of the member nations of INTELSAT.

3. Operational systems

The first INTELSAT commercial satellite 'Early Bird' was put up by COMSAT over the Atlantic in April 1965, and it is still operational. Built and developed by Hughes, the satellite has been launched in synchronous orbit. The weight of the satellite is 85 lb. The effective radiated power is 14.5 dBW (14.4 dB above 1 watt). It has an antenna beam width of 10° and is capable of providing 240 voice channels.

Coming up next on the schedule of COMSAT was the deployment of an uprated satellite 303A the Hughes-built, which is also being called INTELSAT-2 and Blue Bird. Two Blue Birds have been launched by now, one over the

Atlantic and the other over the Pacific. Besides six voice/data circuits for National Aeronautic and Space Agency (NASA). Blue Bird has opened commercial links in the Pacific with nearly 180 channels and the one on the Atlantic has augmented the Early Bird's existing 240 channels with another 100.

Although heavier (155 lb. *vs.* 85 lb. in orbit) and more powerful (15.5 dBW *vs.* 14.5 dBW) than Early Bird. Blue Bird is rated at the same 240 channels because its antenna beam width has been increased from 10° to 15° in order to cover a greater surface area of the earth. Bandwidth has been increased to about 125 megacycles per sec. by using single conversion transponder that includes a four-stage tunnel-diode amplifier and four 6-watt travelling-wave-tube-amplifiers which can be operated in parallel. In the satellite the receiver operates in the band 6.285-6.405 gigacycles per sec. and the transmitter in the band 4.06-4.18 gigacycles per sec.

The Blue Bird has a rated three years operational life and will fill up the time gap between now and the upcoming third phase of global system (INTELSAT-3) for international television and telephony links.

It may be pointed out that the satellite for Pacific (Blue Bird) was first launched in October 1966, but the apogee motor failed to put it into the required geo-stationary orbit 22,300 miles above the earth and the space craft is now travelling in an elliptical orbit. It was while this 'rough' satellite was temporarily above Indian Ocean in November 1966, that Britain was able to transmit live television pictures to Australia. The replacement for this 'rouge' Pacific satellite has been launched in January 1967, and has been successfully injected into synchronous orbit.

4. Intelsat-3

The first and the second phase being over, COMSAT is now shooting for early 1968 for the third phase of global system (INTELSAT-3). This will provide three new satellites: one above the Atlantic, one above the Pacific and one above the Indian Ocean (*vide* Fig. 1). Each will have a capacity of 1,200 two-way telephone channels estimated to handle projected telephone circuit needs through the early 1970's.

The Intelsat-3 satellites are being constructed by an American Company TRW systems and six are on order. These will have slightly greater transmitter power than that of Intelsat-2 but because the aerial beam will not be an all-round toroidal one but will have all the radiated energy directed in a cone towards earth the erp will be substantially greater—about 22 dBW. The directional beam will be achieved by an electronically despun aerial system which will counteract the effect of the stabilization spin of the satellite by cyclically switching the RF energy to the aerial elements as the satellite rotates. The greater capacity of these satellites will be provided by the wider band width 500 megacycles per sec. instead of INTELSAT-2's 125 megacycles per sec. the receiving band being 5.925 to 6.425 gigacycles per sec. and the transmitting band 3.700 to 4.200 gigacycles per sec. Each of the satellites will weigh 260 lb. and measure 56 in. by 37 in.

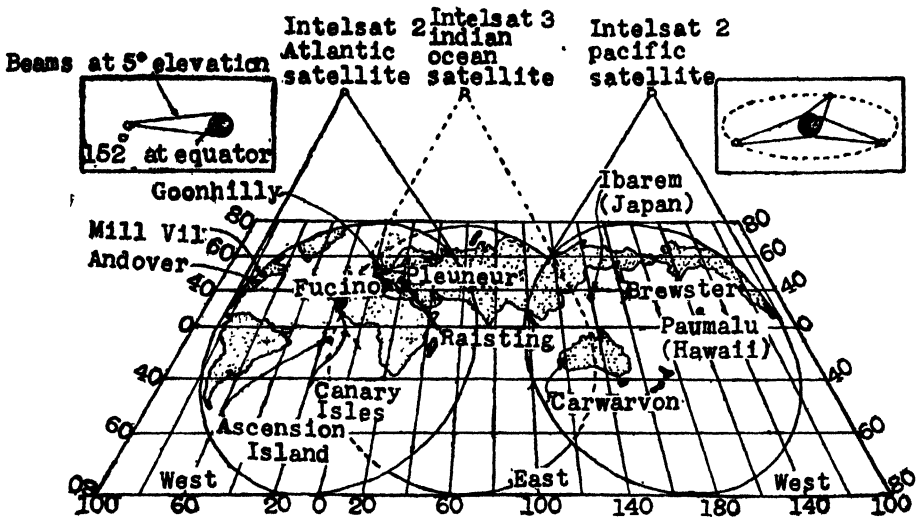


Fig. 1

Location of communication satellites over the earth

5. Multifarious applications of satellite communications

The completion of project INTELSAT-3 is not the end but just the beginning of multifarious activities in satellite communications.

Planned for launching in 1967 is a 210 lb. synchronous aeronautical satellite that will provide voice communication relay to commercial aircraft over the Atlantic where currently used links such as high frequency are least, effective. This means working with lower performance aircraft receivers the use of VHF and very low gain aircraft antennas. Initially two transportable ground stations with 42-ft. antennas will be used with COMSAT guaranteeing two communication channels. Once this initial aeronautical satellite proves out, it will expand quickly into a global system. Such a system would provide to trans-oceanic flights such services as aircraft location, traffic density information and in flight telephone hook-up for passengers. This means in early 1970's when the supersonic transports begin flying, all the anticipated problems would be solved especially when the pilots are passing over empty stretches of land and water.

COMSAT is also considering the design studies for a large multipurpose satellite that may well end up providing both aeronautical (air traffic control as well as communications) and television as early as 1968 or 1969. The satellite would weigh about 800 lb. in orbit. It may have as many as three narrow beam antennas and 10 to 12 repeaters to accomplish its varied tasks. With a planned 500 megacycles per sec. bandwidth and erp of 40 dBW the satellite will have capacity of about 5,000 to 6,000 twoway telephone channels.

One of the most exciting applications of satellites is considered to be data transmission in near future. It is difficult to say when the computer-to-computer hook-ups *via* satellite will be big business but the experts feel that the data transmission one day will be the biggest source of revenue from satellites.

Direct television broadcast from satellite to home receivers is also being considered. If the detailed design studies were started now, the Radio Corporation of America (RCA) believes that it could demonstrate large area telecasting into home receivers by 1969. RCA would use a synchronous satellite with a single TV channel capacity. This practical demonstration would be made at a frequency of 800 megacycles per sec. Using a 40-ft. dish antenna at the ground station and a transmitter power of 5 kW on the satellite would provide an acceptable signal for home receivers modified by an outside antenna and booster amplifier both costing under 100 dollars.

Another job for communications satellites will be to collect meteorological information from a world wide network of weather observation stations—from ocean buoys to aircraft—and feed their data into a master computer complex to obtain the world weather pictures. The analysis and forecast in turn could be distributed to cities and towns throughout the world by the same satellite network. Three or four synchronous satellites could pick up virtually all weather stations, excluding only the polar areas. Such a satellite network could also take pictures of cloud cover over the earth in the manner of Nimbus and Tiros meteorological satellites.

6. Future trends in satellite design

The future trends in satellite design and the problems encountered can be considered under the headings given below.

Satellite size

Hughes Aircraft Co. is in the process of developing high powers satellites—HS 307 family. One of the satellites of this family proposed by them for television broadcast is 9 ft. in diameter and 8 ft. long, would weight about 1,550 lb. and provide an effective radiated power of 40 dBW. Hughes have considered larger satellite configurations and concluded that the improvements gained do not seem to be worth the increase in size. By doubling the satellite length to 16 ft. an erp of 43 dBW was expected which the experts do not consider to be worth the increase in size. The size of HS 307 family and its power output is considered adequate for the commercial communications satellites for the next decade.

Synchronous orbit

Since a single synchronous orbit is visible from about one-third of the earth's surface, ground stations do not need to handover traffic from one satellite to another. By going to lower orbits handover becomes a big problem. Such orbits also require more satellites, perhaps 6 to 12, for a phased orbit and 18 to as many as 48 for a random system. The cost of ground station also goes up because of the complex tracking system. The motion of satellites at lower

altitudes introduces Doppler shifts, variation in path lengths, and irregular periods of mutual visibility between stations. This makes it difficult or impossible to allow one satellite to cover several ground stations simultaneously, that is to provide, multiple-access.

On account of all these factors the future systems are likely to be synchronous except where some special purpose systems are required like the satellites required for military use where reliability and security of messages and freedom from enemy interference are very important considerations.

In the stationary orbit, which is synchronous, circular and equatorial, periodic control can reduce satellite excursions to less than 0.03° from its desired position, a precision approached by the Syncom-3 and Early Bird. The sun and the moon exert a continuing pressure on the satellites changing its orbit inclination. To counteract this and keep the satellite on station a total of about 170 ft. per sec. of control velocity is needed each year. This is not a burdensome design requirement and the advantages in ground station design where fixed antennas can then be used are expected to warrant such control in the future systems.

Stabilization and altitude control

Spin stabilization where the satellite spins about one of its axes to prevent tumbling is considered to be the most rational choice for a practical communications satellites design. The spin axis is perpendicular to the orbit plane so that the directions of the earth towards which maximum antenna gain is desired is perpendicular to the satellite axis throughout its orbit. This is considered very good from the point of view of the problem of thermal control. Because of the averaging effect of spinning on the heating of its surface due to thermal radiations of the sun the satellite operates at a temperature of nearly 25°C . In the other method, *i.e.*, earth oriented, the satellite creates a number of problems like active thermal control and requirement of a servo loop to keep the solar cell array pointed towards the sun, of the two methods therefore, the spin stabilization is preferred.

The problem of antenna directivity in spin stabilized satellites has been overcome by electronically despun phased array antenna designs (*vide* Fig. 2).

Power sources

One of the pacing technologies in building practical communications satellites has been the power system. But surprisingly enough, most specialists agree that for next five to ten years, possibly even longer, satellites will use solar cells or photo-voltaic systems. The solar cellwritten-off time and again in recent years by engineers for large power sources in space, is now being seriously considered for systems in kW ranges. For 1975 flights hardware, 40 to 50 kW photo voltaic systems are being considered practical and realizable. These kilowatts will be obtained out of deployable array that unfold or expand in space. Only problem is the structural dynamics of these solar cell assemblies.

Hughes is now getting 6 watts per lb. out of its solar array (structural material, solar cells and diodes). The Company has been proposing to equip its HS 307 satellites with 550 watts of D.C. power and they feel it can be increased to 700 to 800 watts still using skin mounted cells.

The TRW systems engineers say that the best way to go is to have existing solar cells mounted on light weight deployable structures of rigid foldable panels. By using this method it is felt that 20 watts per lb. of raw power can be obtained. Thin film solar cells are also being developed which would reduce the weight further. With today's state of art 10 to 50 kW of power can be obtained from a solar array as large as 500 sq. ft. or more of solar cells.

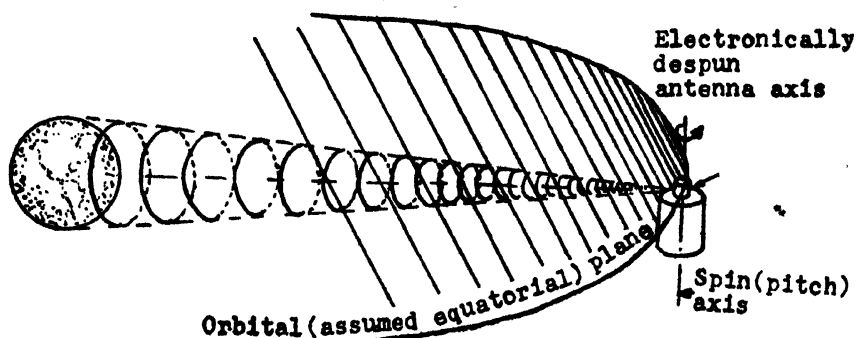


Fig. 2

Design of electrically de-spun phased array antenna

The other power supply sources being considered are nuclear sources but reactor weights, including their shielding, make them unattractive on the basis of lb. per watt output and their use in communication satellites is unlikely for some time.

Satellite power

Considerable work is being done currently on higher power travelling wave tubes for communications satellites. However, Hughes is taking a different track to increase the RF power output. They are using a number of 6 watts TWTs in parallel. By staying with lower power devices in its parallel approach, Hughes engineers believe that they can reach the 100-200 watt range of RF power in one satellite. And if one of the small TWTs quits working there will be a modest degradation of power and not the complete outage that will result if a single high power tube fails. Engineers were worried about the TWT life four or five years ago but now the tube designers are talking about 200,000 and 300,000 hours life time of 6 watts TWTs.

Antenna design

The already operational synchronous communications satellites have used toroidal beam to increase antenna gain. Most of the power is radiated nearly

perpendicular to the satellite spin axis but with no directivity in this plane. This technique limits antenna gain to 8 dB at most if the beam is to cover the entire visible portion of the earth.

By going to a pencil beam antenna gain can be increased to as much as 19dB and still cover the entire visible area of the earth's surface. But this means the antenna system design must provide for despinning the beam, the beam must rotate relative to the satellite at the spin speed (plus or minus the orbital angular velocity) to cancel the satellite spin and keep the beam on earth.

The two basic design solutions to the beam despin problems are the mechanically despun antenna and electronically phased array. Both are active contenders, for an advanced satellite system and each has its own set of advantages and disadvantages.

The primary advantage of the mechanically despun antenna is that the received beam can also be despun with minimal additional complexity, but there are two disadvantages. Bearings are required and the long term reliability of these components in vacuum has not been fully established. Secondly it is difficult to provide the toroidal beam radiation pattern as a back up in case of failure of the despin mechanism. This capability is desirable not only as a back up, but during the initial descent phase of orbit injection where it greatly simplifies satellite acquisition by ground stations.

Two configurations both of which avoid the use of rotary joints are shown in Fig. 3.

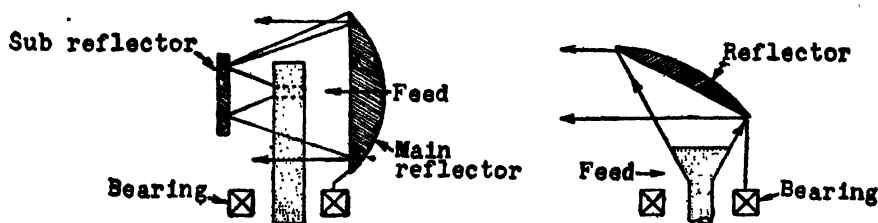


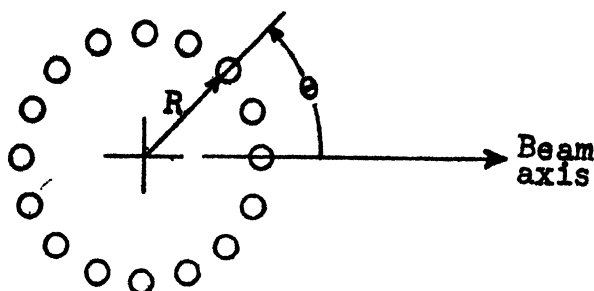
Fig. 3

Configurations for avoiding rotary joints

A phased array antenna (*vide* Fig. 4) is made up of radiating elements spaced uniformly around a cylinder. The shape of the beam in the spin axis plane is determined by the pattern of an individual element. Each element is excited at phase chosen so that the signals due to all elements add in the direction corresponding to the centre of the beam. If R' is the radius of the array and, θ the angle between the beam axis and one of the elements, the phase angle for the drive in radians is $2\pi R' \cos \theta / \lambda$, where λ is the wave length. Total gain of the antenna is the product of one element's gain and gain improvement factor which increases roughly proportional to the number of elements and to the radius of the array. Variation in the geometry of the elements relative to

the beam, however, results in undesirable spin modulation which is periodic at a frequency equal to the number of elements N times the spin speed. Thus, for example, when the radius is increased without adding more elements, there is an increase in spin modulation. A suitable design is to make the radius R , approximately equal to $\frac{\lambda N}{16}$ where N equals twelve or more, the resulting spin modulation is only a few hundredths of a decibel.

Fig. 4
A phased-array antenna



The phase of the antenna elements can be controlled by ferrite phase shifter supplied with appropriate voltages. Such phase shifters provide two outputs with phase shifts equal in magnitude but opposite in sign. The two outputs can drive diametrically opposite elements, so that the number of phase shifters needed is $\frac{N}{2}$. Each phase shifter requires two drive voltages, which vary as $\sin \left(2 \pi R \cos \frac{\theta}{\lambda} \right)$ and $\cos \left(2 \pi R \cos \frac{\theta}{\lambda} \right)$. This would give an electronically de-spun beam.

Multiple access

When the aim is to service about one-third of the earth with a single satellite repeater, it is important that as many ground stations as possible be able to communicate simultaneously with the satellite. By sharing a single satellite repeater, among many users service costs can be reduced and small and large ground terminals with differing communication requirements can participate at the same time. This is in fact the reason that the developing countries which cannot afford extensive microwave or cable system will find satellite system an inexpensive substitute. To obtain such multiple access, the trend in repeater configurations has been to the linear wideband translator that can handle an entire 500 megacycles per sec. common carrier band. In the future global system the multiple access technique being used is frequency division multiplexing.

Ground stations

The design of ground antennas and ground terminal equipment will have a great effect on the performance of communications by satellites. The steerable antenna systems required for non-stationary orbits are more expensive

than the stationary antennas required for stationary orbits. The latter cost only about one-third to one-half as compared with the former system. The INTELSAT agreement calls for joint ownership of the satellites by member countries whereas each member country will own its ground stations.

It has been estimated that 80 to 100 new ground stations will be needed over the next few years (*vide* Fig. 5). Each ground station will cost about Rs. 21 millions or more. As a result of this a number of companies both in the U.S.A. and Britain are trying to specialize in the building and installations of these stations.

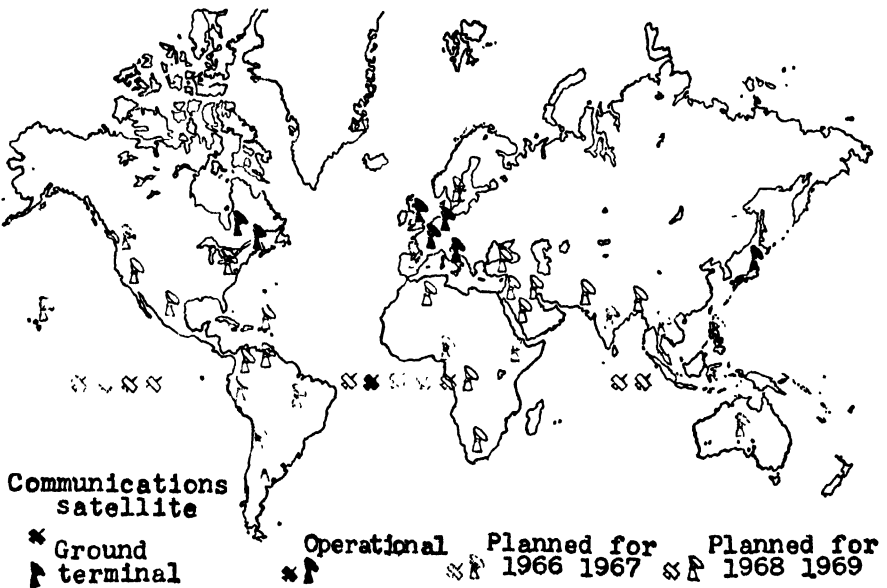


Fig. 5
Proposed new ground stations

Most of the ground stations are being built having reflecting bowl 85 ft. in diameter for commercial use. This is the minimum size necessary to satisfy a receiving performance figure of merit recommended by INTELSAT:

$$\frac{\text{Aerial gain}}{\text{System noise temperature in } ^\circ\text{K.}}$$

expressed in decibels. A typical figure for an 85 ft. diameter aerial bowl, British design station (Fig. 6) is 40.7 dB with 5° aerial elevation at the reception frequency of 46 gigacycles per sec. The basic problem is, of course, the strictly limited radiated power from the satellite and the irreducible noise level of the system (sky noise plus man-made radio interference plus receiving equipment noise). In practice this means that the aerial bowl should be 85 ft. in diameter to collect sufficient RF energy from the satellite, the station could not operate with an aerial beam lower than 5° elevation and the system noise temperature must be brought down to 50° to 60° K.

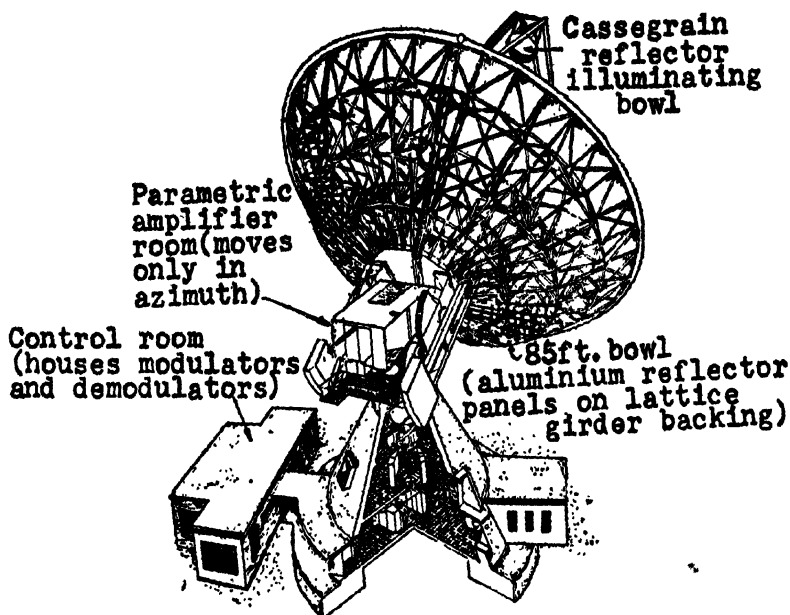


Fig. 6

A typical ground station aerial bowl

Where special requirements are concerned such as for military communications (where the ground stations are to be mobile) smaller stations with antenna diameters 6 to 60 ft. are being constructed. Channel capacity will vary from 1 voice channel with a 6 ft. dish to four voice channels with a 40 ft. dish.

The International Radio Consultative Committee (CCIR) has recommended a channel quality of $50 \text{ dB} \frac{\text{Test tone}}{\text{Noise}} \left(\frac{T}{N} \right)$ for satellite systems. To obtain this quality an effective ratio of carrier power to receiver noise temperature of 172.7 dBW per °K. is required for a single channel. On the basis of this calculation, the satellite erp required per channel is shown as a function of antenna diameter in Fig. 7.

Sample calculations for 85-ft. antenna are shown in the Table below.

Table

Calculation of erp of satellite in synchronous orbit for one CCIR voice channel

$$\left. \begin{array}{l} \text{Effective carrier power to receiver noise} \\ \text{temperature for } 50 \text{ dB } \frac{\text{Test tone}}{\text{Noise}} \text{ quality} \end{array} \right\} = \begin{array}{l} 172.7 \text{ dBW per} \\ \text{°K. per channel} \end{array}$$

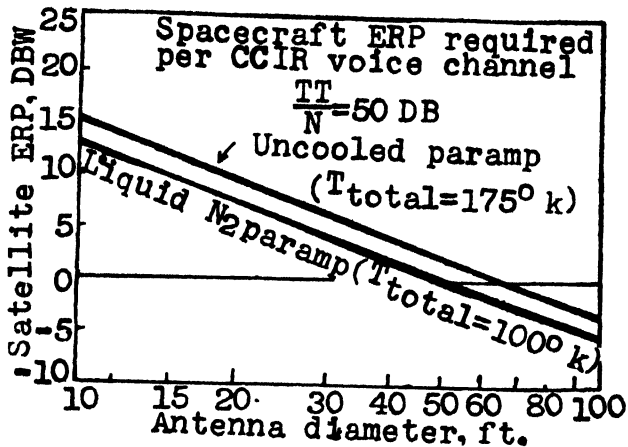


Fig. 7
Satellite erp vs. antenna diameter

Add losses :

(i) Receiver noise temperature $100^\circ \text{K.}/175^\circ \text{K.}$ (uncooled/liquid H_2 PARA-AMP)	= 20 dB/22.4 dB
(ii) Ground-to-space noise contribution	= 1.0 dB
(iii) Intermodulation degradation and reduction in powder due to it	= 4.2 dB
(iv) Rain margin	= 4.0 dB
(v) Space loss	= 196.9 dB
Total losses	= 226.1 dB/228.5 dB
Add ground antenna gain* (85 ft. antenna 50% efficiency)	= 58.1 dB
Nett losses	= 168.0 dB 170.4 dB
Erp required* per channel	= 4.7 dBW/—2.3 dBW

Fig. 8 represents the required ground transmitter power per channel as a function of antenna diameter calculated on similar lines.

7. Communication satellites for military uses

The communication satellites for military uses have more stringent conditions of operation as compared to the commercial ones because they should provide exclusive access to satellites, security of communications, uninterrupted and reliable operations at all times and under all conditions (even during nuclear black-out of high frequency radio) protection against jamming and they should be capable of working with relatively smaller and mobile ground

stations. As regards the channel capacity the military communications systems require relatively small channel capacity between a large number of stations rather than follow the commercial long haul approach of supplying a large trunk capacity between fewer stations.

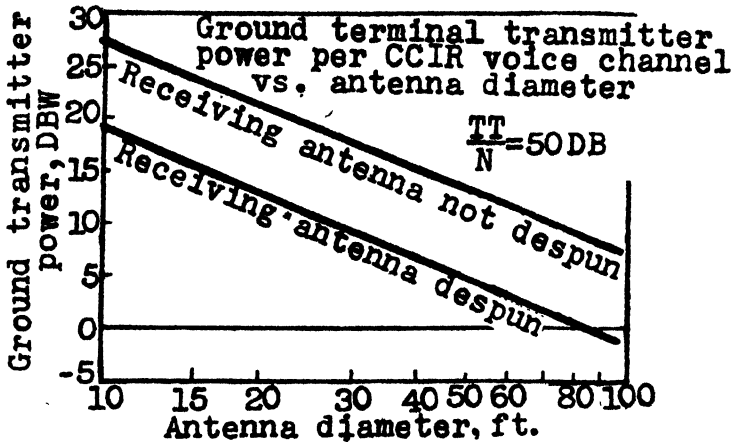


Fig. 8

Power required for ground transmitter vs. antenna diameter

With the above requirements in view the U.S. military authorities have begun a project (initial defence communications satellite project) of launching about 22 satellites in a near-synchronous altitude. These satellites will be in several altitudes in the vicinity of 21,000 miles. Fifteen of these have already been launched in two phases. At this altitude an earth station located at 35° latitude would view the same satellite for about $4\frac{1}{2}$ days.

The random orbital configuration has been chosen to provide two important advantages.

First it assumes that if one satellite malfunctions another satellite will eventually be in a place to provide communications capability. Secondly, the satellites can operate without station keeping controls, thereby preventing an enemy from changing the orbit of the satellites and disrupting communications.

As regards communication reliability, it depends heavily on the number of satellites in orbit. It has been found that reasonable reliability will be attained with 15 satellites. Reliability will be almost 100% on the link Heel-mano, Hawaii to Camp Roberts. Reliability will be 93% on west European link.

The satellites are operating as real time repeaters receiving signals at some classified frequency in the band between 7.975 and 8.025 gigacycles per sec. and transmitting the signals between 7.250 and 7.300 gigacycles per sec.

The antenna used in the satellites is omnidirectional with respect to the spin axis. It has a beam width of 25° in the other direction. Spin stabili-

zation will maintain the satellite's axis normal to the plane of the orbit. A large portion of energy is radiated into space due to the antenna being omnidirectional with respect to spin axis.

The satellite will require 26 watts of power. Over 8,500 solar cells mounted on the surface of a 3-ft. diameter satellite will initially supply about 42 watts. The solar cells' efficiency will slowly decrease with time. The power system has done away with batteries for more reliability.

The satellites permit multiple access by a number of ground stations. However, no ground station can use a satellite unless it is scheduled. United States has offered to its NATO partners the opportunity to participate in communications *via* these satellites. The ground stations being set up are using smaller antennas 6-60 ft. Standardized air transportable ground stations using 40 ft. antennas are being developed by the U.S. firm, Hughes Aircraft Co., and the British firm, Marconi. The Hughes built station can be air transported and set up on a prepared site by a 27-man station crew in 48 hours. The cassegrain antenna contains a four-horn-feed that permits the terminal to track the satellites signal by simultaneous lobing (monopulse) techniques. This terminal station can transmit or receive at least four high quality voice channels and four tele-type messages. A high quality channel has a signal to noise ratio greater than 53 dB.

A more transportable terminal that uses a four-dish cluster with a total outside diameter of about 15 ft. is in development. These antennas are also able to track the satellite. Each terminal can be air-lifted and set up by a six man crew in about two hours with a minimum of site preparation. The terminal is valuable for remote areas and for emergency operation and will provide one tactical quality voice channel, $\frac{S}{N} = 30$ dB, 64 duplex telegraph channels or four-vocoded voice channels.

A vocoder reduces the voice bandwidth by transmitting only those frequencies in the speech signal that will allow the speech to be reconstructed at the receiver.

One of the aims of this project is to gain information and experience for design of an advanced system (ADSCP) in early 1970s. No details of this presumably highly sophisticated system have been released although it is known that it would provide highly secure, many wide band mobile communications channels. Probably the satellites would be both synchronous and fully stabilized for maximum erp.

An area of growth necessary in military systems will be anti-jamming capability and message security as pointed out earlier. This will possibly be achieved by using data processing in the satellite. Two future possibilities are direct signal processing which means extracting signal from the jamming and noise, and commanded antenna switching, permitting a transmitter to make the satellite aim high-gain beams at particular localities. This would

of course require thousands of added parts compared to less than a thousand now in a simple repeater.

8. Conclusions

The growth of trunk traffic in India is taking place at a very fast rate. In Bombay city alone the present rate of daily trunk calls is about 8,000 and it has been estimated to go up to 120,000 by the end of the Fourth Plan (*vide* report published in the *Times of India* dated July 30, 1967). There is a plan to cover about fifty major cities by direct dialling system. Satellites offer very attractive prospects to meet these growing requirements effectively and economically.

As regards the international traffic, India is one of the members of IN-TELSAT. One ground station is already being set up at Ahmedabad and one or two more are proposed by 1970s. Whereas this might cater for the growing international traffic in, addition to the already existing high frequency links, the problem still remains for the growing domestic traffic.

The talk about putting up large capacity synchronous satellites for domestic services in various countries is gaining such a momentum that some of the countries like the U.S.A. might have such a satellite in the next two to three years with circuit capacities ranging from 3,000-12,000.

Studies have been conducted on the effects of individual nations putting up their own domestic communications satellites and it has been found that such systems would not necessarily interfere with global communication network, or communications links of the near by countries. The Hughes Aircraft Co., which has conducted a number of studies in this area, say, Japan for example, could put up its own satellite and not illuminate China or even Philipines with its signal.

Once a multiple satellite is an operational success it will be useful for India to go in for such a satellite. Such satellite could be put in a synchronous orbit and illuminate the territorial limits of India alone. Such a satellite would provide one or two television channels in additon to the voice channels needed to meet the increasing traffic.

This would mean the growth of television services could be much faster. With a few broadcast stations the entire country could be serviced with television broadcast either by a network of ground stations or by direct television broadcast depending on the system employed. International television channels could also be used to broadcast programmes from other countries.

The need for reliable and secure military communications cannot be over emphasized. A country like India with its border, stretching 2,000 miles, a few channels for long distance secure communications are required to handle military traffic. Some of the channels could be leased off for exclusive military use from this multipurpose satellite. This would workout more economical than setting up conventional micro wave links which are more prone to disruption by sabotage than satellites. As regards the security and anti-jamming

facilities of communications for military use it may be pointed out that the suggested satellite would only be accessible to ground stations with in the country and the chance of jamming by any potential enemy are considerably reduced. Messages of course would have to be coded (in cases where secrecy is involved) while making use of such a satellite.

8. References

1. 'Situation Report on Communications Satellites'. *Interavia*, June 1962, p. 749.
2. S. G. Lutz. 'Satellite Communications and Frequency Sharing'. *Interavia*, June 1962, p. 753.
3. 'Telstar—The Private Venture Satellite'. *Interavia*, June 1962, p. 760.
4. R. Henkel. 'Communications Satellites 1966 and Beyond'. *Electronics*, May 1966, p. 83.
5. J. J. Cohen. 'Military Services Satellites will Ring the Earth'. *Electronics*, May 1966, p. 96.
6. F.C. White. 'For a Pilot over the Ocean a Satellite Link to Have'. *Electronics*, May 1966. p. 100.
7. D. D. Williams. 'Communications Satellites Part 2, Design Choices for the Future'. *Electronics*, May 1962, p. 109.
8. W. Kowin and G.G. Chadwick. 'Latest Word in Space Talk, It Can Come from Anywhere'. *Electronics*, May 1966, p. 117.
9. H. Rosen. 'Future of Satellite Communications'. *Space Light*, vol. 8, no. 12, December 1966, p. 414.
10. 'Military Space Communications'. *Space Light*, vol. 9, no. 3, March 1967, p. 101.
11. 'World Satellite Communications'. *Wireless World*, February 1957, p. 71.

DECODING OF PSEUDO-RANDOM CODED SEQUENCES***A. Mukherjee***Non-member**Electronics and Electrical Communication Engineering Department,
Indian Institute of Technology, Kharagpur***Summary**

In this paper the different methods of decoding and detection of pseudo-random (P.R.) codes used in wide-band communication and the relative advantages arising out of them are discussed.

1. Introduction

It is known that PR sequence can be used for ranging application, time-modulation, binary modulation and M -ary modulation especially in the cases when signal-noise ratio (SNR) is quite low. Such sequences find an important use in random access communication systems (Fig. 1).

The M -ary modulation technique will be considered in this paper. In this technique, one of the M alternative sequences is transmitted according to state of the message source. The receiver decides which of the M sequences has been transmitted. It is important to observe that decoding is considerably more difficult than coding. It is therefore considered worthwhile investigating how the complexity of the decoder may be reduced.

2. Coding of the sequences

The signal to be transmitted which may be in the form of analogue signal or digital data is first converted into binary code by an analogue digital converter or a pulse code modulation (P.C.M.) coder. This coded signal is then used as the initial condition of a sequence generator. The minimum length of the sequence will obviously be determined by the number of digits in the P.C.M. In a 5-bit P.C.M., for example, the length of the sequence is clearly $2^5 - 1 = 31$.

(i) Parallel decoder

In such a system the received input signal is multiplied with all the possible sequences simultaneously. The product is integrated, the integrated output is then sampled and the samples are fed to a decision circuit to determine the maximum. Fig. 2 shows the block diagram of such a system.

The selection of amplitude corresponding to which the value of the product is maximum may be achieved by providing common degeneration combined with an individual amplitude dependent regeneration to a set of amplifiers. This accentuates the difference in level between the outputs of different lines. This may further be improved by biasing the amplifier with the average of the outputs to eliminate all but the largest component.

*Presented at the Symposium on 'Modern Electronic Communication Techniques' held in Hyderabad on August 26, 1967.

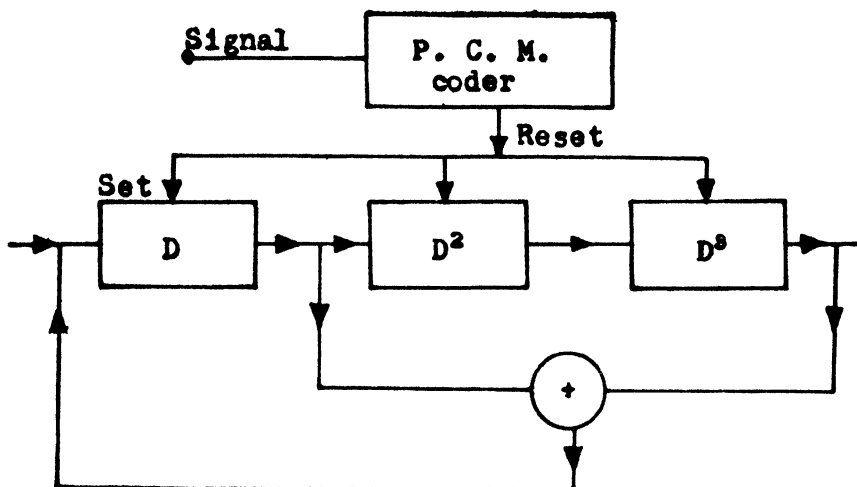


Fig. 1

Circuit diagram of a PR sequence generator used as a coder

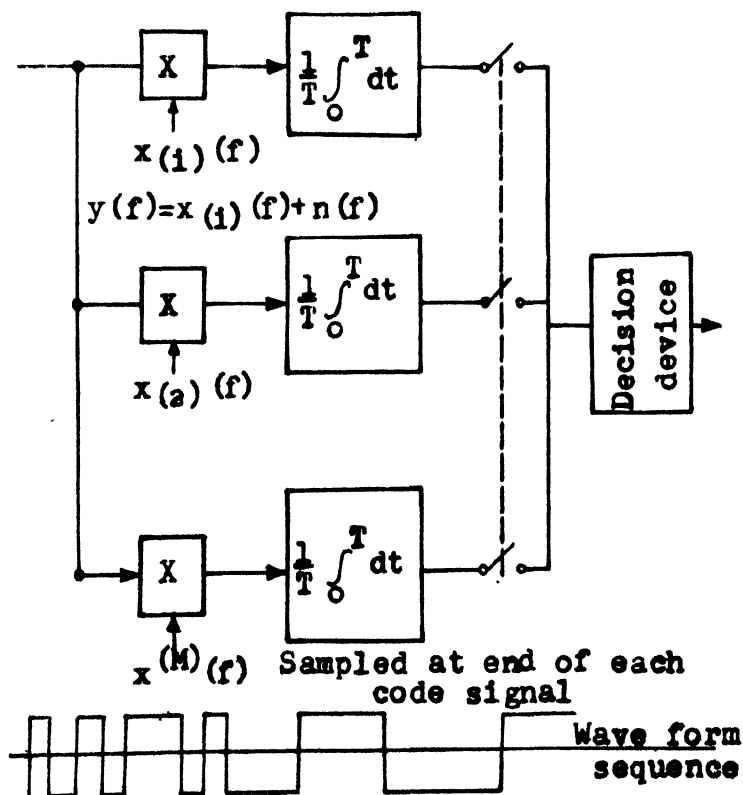


Fig. 2

A parallel decoder

Such a scheme is rather impractical when the length of the sequence is large. For example, we may consider a 5-unit code of length 31. If all the possible 31 sequences are transmitted, then as many multipliers, integrators and samplers would be required. The maximum amplitude selector will also need 31 amplifiers with common degeneration. The number of multipliers, integrators and samplers can be reduced to one only whatever be the number of the possible sequences if we adopt the following technique instead.

(ii) *Serial decoding*

The testing in such cases is done one after the other, *i.e.*, serially. For such a serial scheme since all the correlations are to be completed within one symbol period, both the received signal and the reference sequences must be compressed in time by a factor equal to the number of sequences being used. For a 5-unit code of length 31, the compressed sequence of 31 bits will have to occupy a time period equal to the original bit period. The other point to be noted is that the received sequence be made to repeat as many times in one symbol period. So a delay line type circulator has been used. After all the sequences are tested the delay line must be discharged. And so during coding process a time gap is kept between two sequences for the discharge of the delay line. The block diagram is shown in Fig. 3. The outputs of the multiplier are integrated and tested for maximum amplitude.

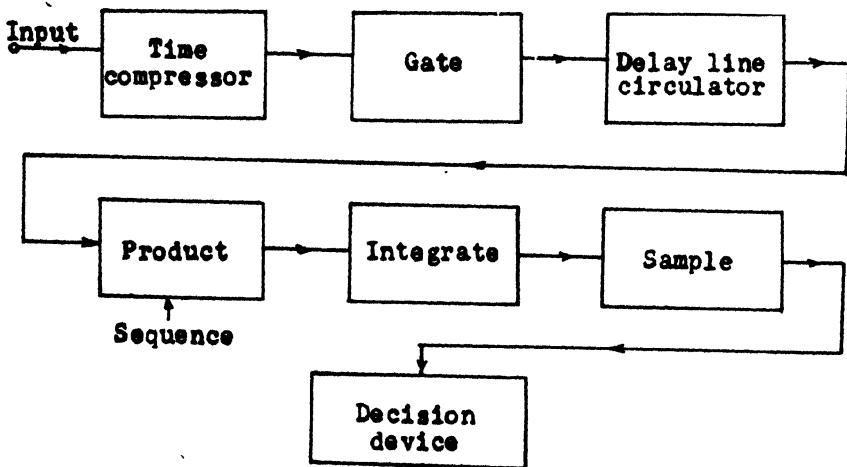


Fig. 3

A serial decoder

Maximum amplitude selection

The aim here is to select the sequence corresponding to which the value of the product is the maximum. The method for determining the maximum amplitude (Fig. 4) is to reset a voltage sawtooth with matched filter output sample. The input pulses are applied to a peak charging diode, the input is then compared with the peak charging device. This will give an output (a short pulse) when the input is greater than the peak charging device. This short pulse

is used to reset the sawtooth generator. The synchronous voltage of the sawtooth generator is obtained from a B.R.F. generator. Thus if the time of occurrence of a particular receiver sequence is known then a relation can be established between the amplitude of the sawtooth and the receiver sequence. The maximum value of the product will then give us the idea of the sequence received.

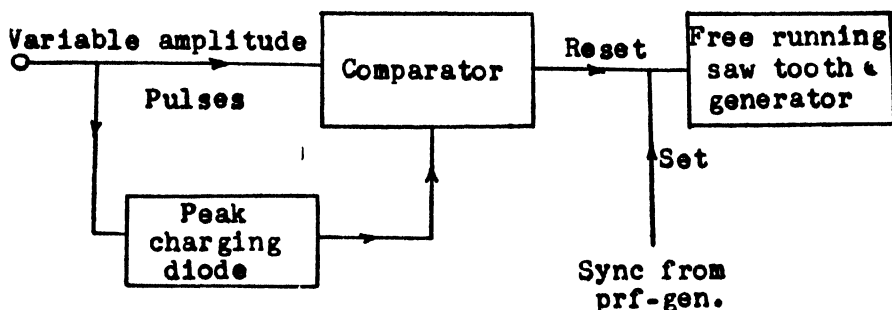


Fig. 4

A maximum amplitude selector

Time compression

It has been discussed earlier that the sequence received is to be compressed in time to the extent of original bit period. The block diagram of the scheme employed is shown in Fig. 5.

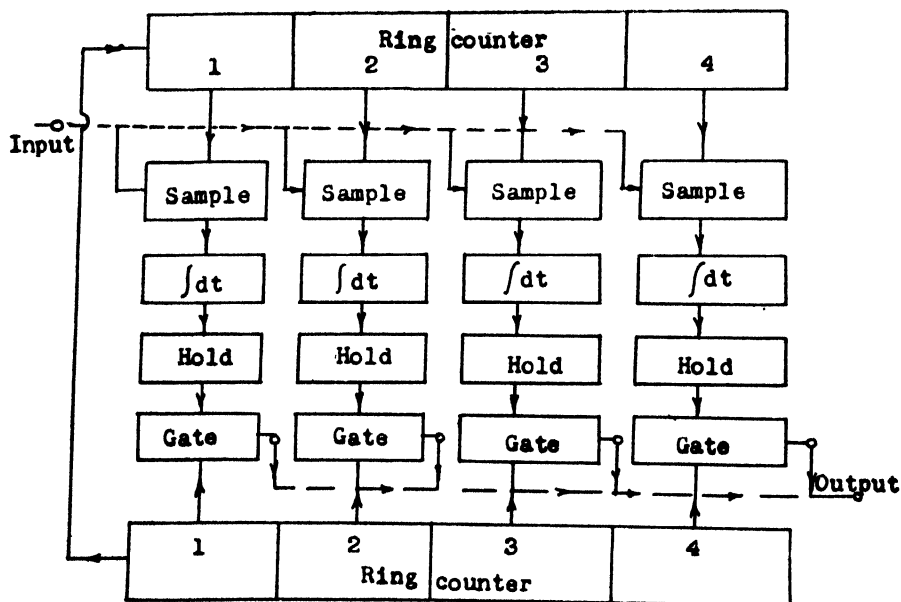


Fig. 5

Block diagram of a time compressor

Let a simple sequence of length 7 be considered, the structure being 11-11-1-11. A sample of the bit is taken at the end of each bit period. The gating pulse is applied from a ring counter of order 7. The sampled amplitude are then 'hold'. There is another ring counter shown (B_n) which gives pulse at the rate of 7 times the P.R.F. of the first set of ring counter. This is used to sample the hold output again thus we see that after a repetition of 7 bits the desired sequence is repeated in a time corresponding to one bit period. The other bit period contains the time shifted replica of the same sequence.

The other method of time compression uses a delay line. The loop [Fig. 6 (i)] stores and compresses the signals as they arrive and has available in the compressed form an output at any time during the operation. The loop consists of controlling 'AND' gates and a delay section. The signal passes 'AND' gate 1 only when a sample pulse coincides. The complement of the 'AND' 1 sampling pulse controls the gating action of 'AND' gate 2 at its inhibit input. This is a re-circulation gate which, with the 1 megacycle per sec. clock pulse, allows the content of the delay line to re-circulate continuously between sample pulses. When the next sample pulse arrives to enter a new signal bit the inverted replica of the sample pulse gives a proper signal at the inhibit input to the recirculating gate to inhibit the gate for the duration of the sample pulse. This action allows a new data bit to enter the delay line while the oldest data bit in the line is erased simultaneously at the re-circulating gate. The time relationship of waves and pulses of Fig. 6(i) is shown in Fig. 6 (ii). A portion, T , of the signal is sampled at T intervals. The loop accomplishes compression by the following sequence. The delay line receives sample a, a One, which undergoes a complete circulation of the loop. One micro-sec. after re-circulation sample b (a Zero) is inserted alongside sample a. Both the samples circle the loop. One micro-sec. later, sample c is inserted alongside sample b. This process continues filling the line with pulses that represent the polarity of the signal at the time of sampling. This process compresses T , the interval between pulses to the clock interval; for example, 1,000 micro-sec. becomes 1 micro-sec. In other words, g samples are compressed into time T . After the storage line is filled the oldest sample is continuously replaced by a new sample. Thus, the stored information is constantly up-to-date.

The advantage obtained in such cases is the reduction of the cost of equipment and simplification of circuitry. The number of multipliers, integrator and sampler is reduced to one only, whatever be the number of the possible sequences. The maximum amplitude selector is also quite simple compared to one that is used in the case of parallel detection method. This is achieved only because the amplitudes are occurring after a regular time-interval.

The only disadvantage of the system is that the circuitry must be quite fast.

(iii) *Sequential technique*

The correlation function of the P.R. sequence does not give any indication of the time shift required for the local replica to bring about coincidence when it is outside the working zone. The method discussed earlier is thus

based on trial correlation of all the possible sequences and select the maximum amplitude of the correlator detector. The acquisition time in such cases is rather high compared to the information bits. When the SNR is sufficiently high the number of trials may be minimized to a great extent if the code is made up of several short sub-codes.

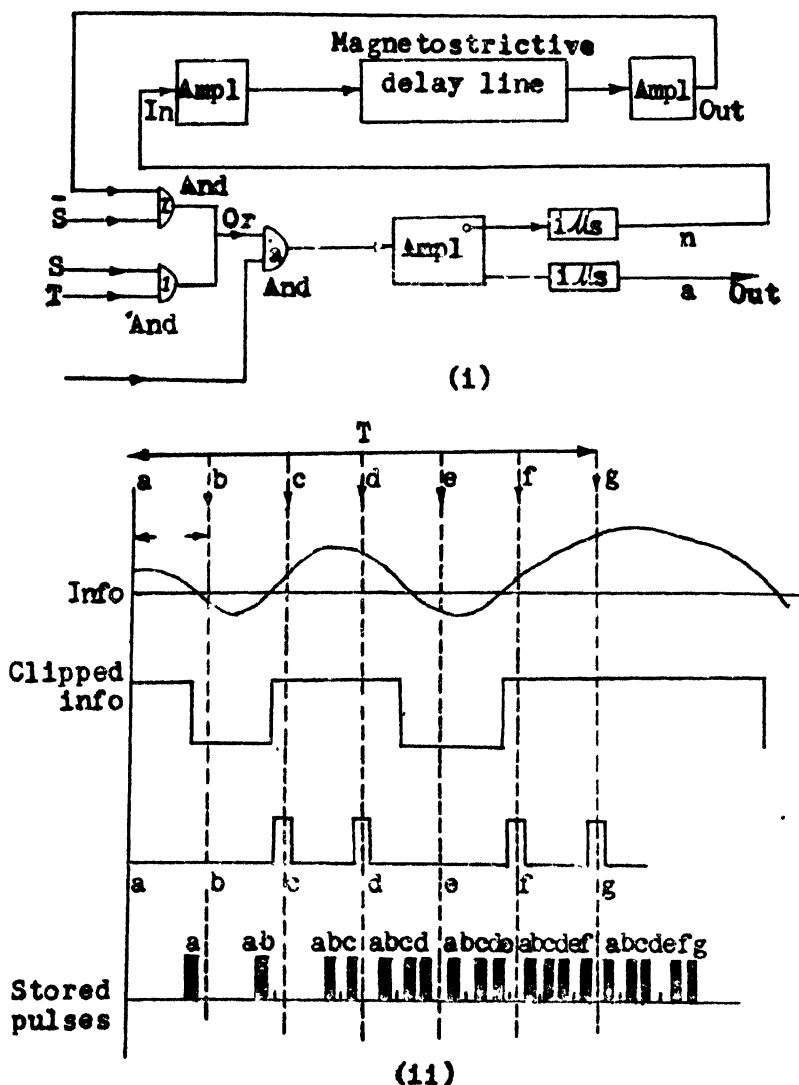


Fig. 6
Block diagram of a time compressor

In analyzing a sequence it is seen that the sequence is determined by the initial condition and these are the first five bits of the sequence in case of sequence of length 31. In this technique the first five received bits are used as

the initial condition of a receiver sequence generator. This is correlated with receiver sequence to see whether the estimate is correct. If the agreement is not good fresh data may be introduced and the process repeated. The data obtained in different trials may be investigated to obtain the decision about which sequence is transmitted. The advantage of this system is a very small acquisition time. The length of the trial is kept above a certain threshold to avoid false dismissal or false alarm and it depends solely on input SNR.

3. Conclusion remarks

Detailed experimental investigation is being conducted on serial and sequential detection techniques to simplify the circuitry and reduce the acquisition time.

4. Acknowledgment

The author is grateful to Prof. N.B. Chakraborti of the Department of Electronics and Electrical Communication Engineering, Indian Institute of Technology, Khargpur, for his valuable guidance.

5. References

1. W. Jackson (*Ed.*). 'Group Synchronization of Binary Digital System—Communication Theory' by R.H. Barker. *Academic Press Inc.*, 1953.
2. S.W. Golomb. 'Digital Communication with Space Application'. *Prentice Hall Inc.*, 1965.
3. C. Cherry (*Ed.*). 'The Synthesis of Linear Sequential Coding Network' by Huffman. 'Third Symposium on Information Theory, London. *New York Academic Press, Inc.*
4. S. Weber. 'Modern Digital Circuits'. *McGraw Hill Book Co., Inc.*, 1964.

SESSION II

CHAIRMAN : BRIG. M.K. RAO (*M.*)

Paper 1 : Microwave Communication along Railway Routes and Radio Patching of Train Traffic Control System with 400 megacycles per sec. Equipment in the U.H.F. Band. S.A. Srinivasan, <i>Non-member</i>	269
Paper 2 : Speech Compression and Expansion. S.V.R. Naidu, <i>Non-member</i>	277
Paper 3 : Speech Bandwidth Compression. G. Kanttaiah, <i>Non-member</i>	291

MICROWAVE COMMUNICATION ALONG RAILWAY ROUTES AND RADIO PATCHING OF TRAIN TRAFFIC CONTROL SYSTEM WITH 400 MEGACYCLES PER SECOND EQUIPMENT IN THE U.H.F. BAND*

S.A. Srinivasan

Non-member

Chief Signal and Telecommunications Engineer, South Central Railway, Secunderabad

Summary

This paper briefly reviews the communication systems presently used in the Indian Railways and indicates the growing limitations of the existing methods on the face of increasing complexity of the railway networks. It refers to the growing use of microwave communication system in the advanced countries of the world and stresses the need for introduction of this system in the Indian Railways. It presents a typical microwave network for a railway zone and discusses the various aspects of operation and efficiency as well as the problems associated therewith.

1. Introduction

The very nature of a railway zone, which can be described as a complex facility operating continuously over several thousands of miles of traffic, demands a steady flow of information and data over a wide geographical area apart from specifically designed direct control and feedback systems for regulating the movement of trains. Railways in India at present use almost every form of conventional communications such as, Morse telegraphy, teleprinters, talk-back speakers, telephone exchanges and H.F. radio, both single and double sideband.

Morse telegraphy on open line wires is used for a variety of purposes: station-to-station messages, inter-wire between groups of large stations and through-wire between important junctions. The H.F. radio communication is provided between all divisional headquarters, divisional headquarters and railway headquarters, railway headquarters and Delhi, and between divisional headquarters and important stations. Mobile vans carrying H.F. transmitters and receivers are available at all divisional headquarters for meeting emergencies. The wireless equipment is intended for the transmission of data, both on C.W. and R.T., which is vital for the control of freight and coaching stock and for routine managerial tasks.

A train traffic control system, in its simplest form, uses a pair of copper wires to provide an omnibus speech circuit for the controller at the divisional headquarters to communicate with every Station Master on a section which

*Presented at the Symposium on 'Modern Electronic Communication Techniques,' held in Hyderabad, on August 26, 1967,

may vary in length from 100 to 350 miles. The controller is provided with selective calling apparatus based on a total code principle which employs positive and negative pulses at $3\frac{1}{2}$ cycles per sec. A similar omnibus circuit is also provided for linking stations of operating importance with a deputy controller at the divisional headquarters. The main purposes of these control systems are to control the movement of trains in such a manner that the tracks and rolling stock are put to optimum use and passenger services run to time.

A network of trunk lines link railway exchanges at headquarters with similar exchanges at all divisional headquarters. Teleprinters are employed between marshalling yards to provide advance information of trains and wagon destinations to enable the receiving marshalling yard to be ready to receive the freight train and plan the marshalling operations in advance. Marshalling yards as well as large stations are provided with extensive public address equipment and where required with V.H.F. links.

Other operational circuits in use are for teleprinters/facsimile, power control, stock control and data processing. The purposes of the stock control circuit is to transmit data on rolling stock over teleprinters or facsimile. This data in the case of the Railway Board will be received by a central computer in Delhi which will serve two immediate purposes:

- (i) To locate special types of wagons, and
- (ii) To decide on the best method among several alternatives of ensuring optimum usage of stock.

At railway headquarters, computers have so far been used only for accounting purposes. But it is only a question of time before they are extended for vital operating purposes. In any event whatever be the data processing system adopted, the need for a completely reliable and efficient system of communications for data transmission can only be provided in the UHF and SHF ranges and by using on an extensive scale teleprinters and facsimile.

2. Microwave communications system

The HF spectrum which became overcrowded some years ago is not immune from atmospheric disturbances. The efficiencies of line wires which are expensive to maintain are subject to the vagaries of nature and indeed have now become much less reliable because of copper wire thefts on a large scale. The only economical alternative is to integrate all communications into one radio relay system in the UHF or SHF range. Such systems are noted for exceptional reliability, large capacity and when adequately planned would yield a good return on investment. The railways in the U.S.A., Canada, Japan and other advanced countries, in spite of being the largest users of microwave communications in their respective countries, are now considering the pros and cons of satellite relay stations *vs.* laser. Private microwave has already spread to 24,000 route miles in the U.S.A. and is expected to cover 50,000 route miles in another six years. The Japanese Railways with 398,497 channel miles are the largest single users of microwave in that country. The Indian

Railways too, are inevitably committed to the installation of large scale microwave networks for reasons of economy and efficiency. Microwave frequencies are chosen for areas where a large system capacity is required and UHF for areas where the demand in the near future will not exceed about 24 channels.

A typical microwave network for a railway zone is shown in Fig. 1. It will be noted that the speech channels are planned on a liberal scale because in a railway system, time is of the essence and correspondence is expensive. The microwave network of each railway must fit into the networks of contiguous railways systems; most of the radio relays must inevitably follow the railway route; and operational requirements demand the dropping of channels at several points along the route. The same system, therefore, must provide for both short-haul and long-haul communications and this calls for some ingenuity

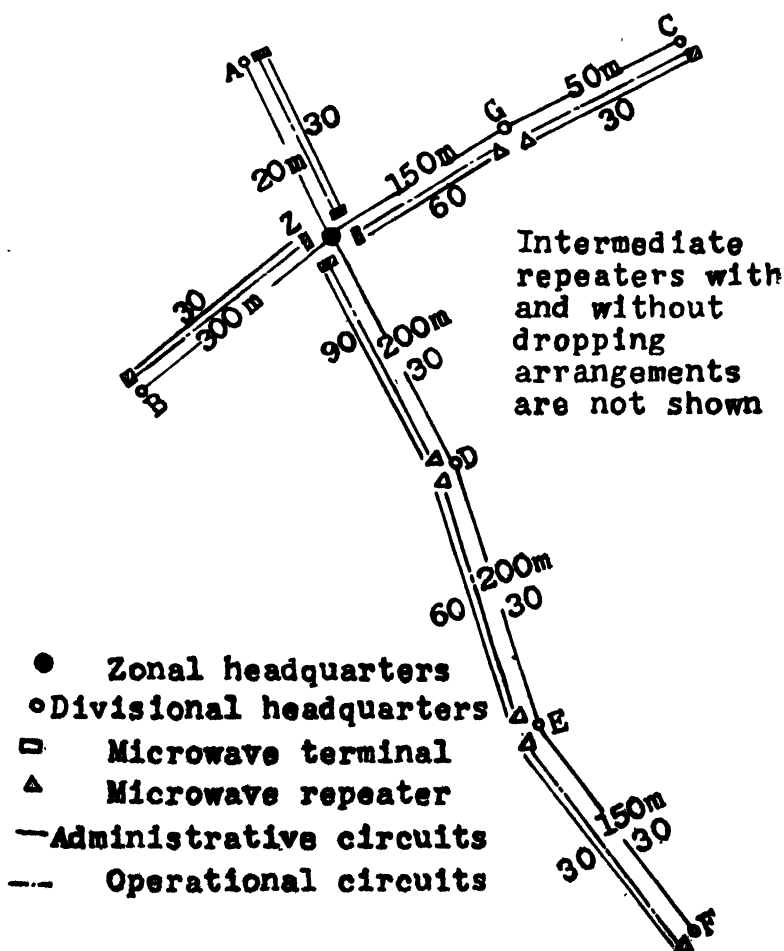


Fig. 1

A typical microwave network for a railway zone

in design. One of the various solutions is to employ the leak principle, *i.e.*, at repeating stations, the channels to be dropped would be allowed to leak through so that the $\frac{S}{N}$ ratio of the long-haul circuits is within the acceptable limits. Various other solutions to the problem of integrating short-haul with long-haul circuits are under consideration.

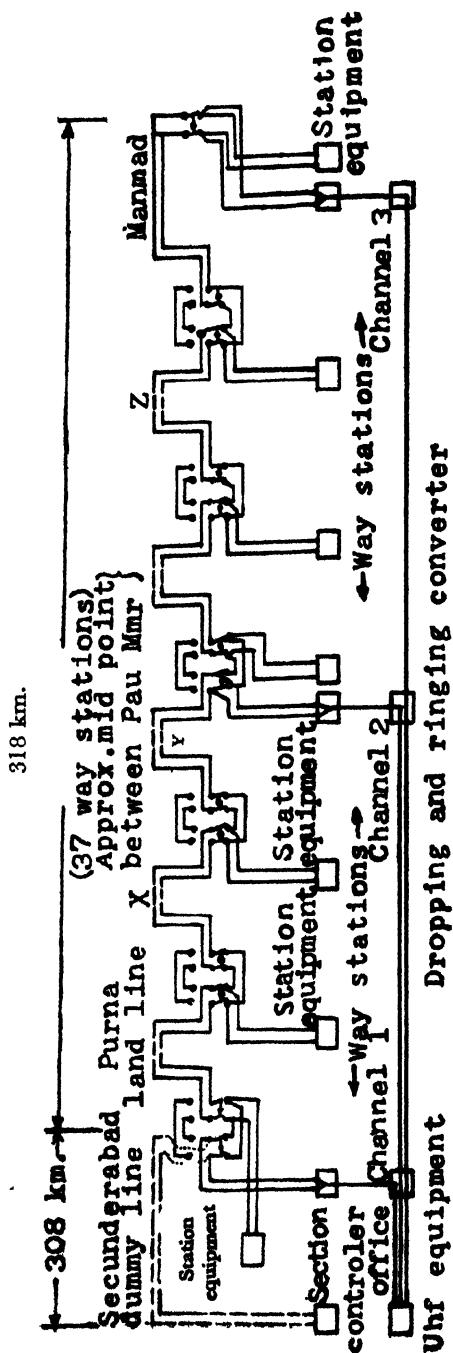
An important operational circuit is the radio patching of section and deputy controls in which the line wires cannot be eliminated altogether, because of the very close spacing of railway stations. Radio patching as conceived at present and shown in Fig. 2 implies the use of radio channels for dummy lines, feeding the line at an intermediate point as well as at the remote point. Conversations would take place over radio most of the distance but on line wires over the last lap which will be limited to about 50 miles. When faults occur, line wire terminations will be switched to isolate the faulty section. The technical problems that would arise from radio patching are obvious:

- (i) Conversion from 4-wire radio circuits to 2-wire line wire circuits would have to be carefully designed; and
- (ii) Compatibility with the present selective calling system and arrangements for ensuring that the ringing tone is fed back to the controller.

The UHF relay systems will be employed in areas which do not warrant the use of more than 24 channels. The frequencies employed for the microwave are in the 7 kilomegacycles (kmc) per sec. range and for UHF in the 400 megacycles per sec. range. Each frequency in the 7 kmc range can yield as many as 960 audio channels although, in the first instance, the railways would not require more than about 120 channels. It will, of course, be possible to double these figures by using special equipment. Recent research has shown that the 400 megacycles per sec. band has some peculiar properties which make it eminently suitable for railway purposes.

The teleprinter is at a handicap where the transmission of figures are involved because of the inherent limits of the Murray code which does not provide for redundancy and as a result every mutilated coding element may form an accepted character. Error correcting code systems are unfortunately expensive and, therefore, facsimile must replace teleprinters in due course. In facsimile transmission a message may be blurred or slightly distorted but one transmitted character cannot reproduce an unintended character.

The use of teleprinters will be restricted to reservation messages and, in a well planned network, for replacing the typewriter in the office by a teleprinter system. The signed draft when typed in a teleprinter will automatically be transmitted to the next office, and in each office the carbon copy would become the record copy. The despatch section in a divisional office will then consist of teleprinters and inter-railway correspondence will never be posted by train. In the zonal headquarters teleprinter messages can be directly routed to the respective departments *via* a manual teleprinter exchange. Drawings and tabulated statements can be dealt with in a central office at headquarters, *viz.*, facsimile.



Note :

Repeating stations to be provided as required by the terrain and equipment

Fig. 2
Proposed radio patching between Secunderabad and Manmad

The final choice of a radio relay system would depend not only on the initial cost but also on recurring costs and obsolescence. The first type of obsolescence is the equipment wear out, in which the life of the equipment is reduced by a breakdown of the unit or the system itself. Transistorization has been a significant factor in making the wear out factor unimportant. First costs depend on how the system is laid out especially the position and types of repeaters of various links. Where a large number of channels are to be used for operational circuits, the repeaters may have to be of the modulator/demodulator type, rather than heterodyne. But this has an important bearing on the noise performance of the system. The C.C.I.R. has laid down certain guidelines in this regard.

The hypothetical reference circuit established by the C.C.I.R. provides a standard for systems engineers and equipment designers. This circuit is 2,500 km. (1,550 miles) long, divided into 9 equal sections of 6 hops, each interconnected at base band frequency, resulting in 9 modulation/demodulation processes in 54 hops. The recommended limitation for radio equipment, excluding multiplex of the mean noise power in any hour is 7,500 picowatts, sophometrically weighted. Breaking this down further, each section is 173 miles long consisting of six 28.8 mile hops, the noise power for each section being within 833 picowatts. The six feeder sets will introduce 150 picowatts while the group delay equalization network may account for 100 picowatts. Each modulator/demodulator may contribute approximately 37 picowatts. Subtracting, this leaves an allowable contribution for six repeaters of 546 picowatts, or 91 picowatts per repeater. This hypothetical system cannot, of course, match a real life system, but it provides a basis for comparing the equipment performance against the C.C.I.R. recommendations. A modulator/demodulator repeater cannot normally measure up to this demand, while a heterodyne can, but it should be remembered that the recommendations are for a long haul system.

In spite of the complexity of the problem of noise assessment, in most cases, it should be necessary to clinch only three significant parameters in order to determine with adequate precision the limits of noise performance which a microwave system will have to cope with under actual operating conditions taking into account the effects of both fading and busy hour loading. These parameters are :

- (i) Receiver input level at which the noise in the worst derived voice channel reaches 631,000 picowatts;
- (ii) The required fade margin in decibel, dB. This affects noise performance since it determines what the receiver median input level corresponding to non-faded condition must be. Addition of fade margin and threshold level gives median input level; and
- (iii) Noise in the worst derived voice channel with median input to the receiver, measured with the radio base band loaded with white noise power equipment to the busy hour load for the full channel capacity of the system.

There is wide agreement that 631,000 picowatts (30 dB), should be the value at which a voice channel should be taken out of service, and 42 dB should be taken out of service, and 42 dB should be the typical value easily achievable with conventional microwave and antenna for fade margins. However, it should be reiterated that these two parameters are characteristics of the individual hops rather than the system. The third parameter is the one which describes the day-in and day-out noise performance of the system. The most important contribution to this parameter is intermodulation distortion. It is in this case that the real objectives of the system are yet to be stipulated. This is an important area of decision for the users and manufacturers alike, for it seriously affects the cost of the system as well as the scope of the technical problems that have to be solved.

It may be relevant in this case to consider the practices adopted in telephone systems for guidance in this respect. Telephone systems make a distinction between long haul and short haul systems with the dividing point at about 200 miles. C.C.I.R. and Bell systems provide guidelines for short-haul. Both these systems treat permissible noise for a system longer than 200 miles as directly proportional to length. The C.C.I.R. system allows 3 picowatts per Km. for microwave contribution and 1 picowatt for carrier contribution, making a total of 4 picowatts per Km. for the complete system. In terms of miles, this would mean 4.8 picowatts per mile for microwave alone and 6.4 for microwave and multiplex. The Bell system provides for 6.3 picowatts per mile as compared to C.C.I.R.'s 6.4 picowatts per mile. It would, therefore, be seen that as far as long-haul systems are concerned, both the recommendations are almost identical. For short-haul systems, the practice is quite different. The usual method is to specify signal noise for such systems regardless of the number of hops. This figure is at present 2,000 picowatts for microwave plus multiplex noise, or, 1,500 picowatts for microwave alone. This would give 7.5 picowatts per mile for a maximum length system of 200 miles, 15 picowatts per mile for 100 miles system and even more for shorter systems.

It will be noted from the above that the 7.5 picowatt per mile figure for the most stringent case in short haul system is only 2 dB less stringent than the 4.7 picowatt per mile for long haul. But for system planning, the important criterion is the picowatts per hop, since the microwave noise power is approximately proportional to the number of hops rather than to the number of miles. Hence if the long haul standard of 4.7 picowatts per mile is considered, one would get 117.5 picowatts for a 25-mile hop, another 141 picowatts for a 30-mile hop, and 188 picowatts for a 40-mile hop. On the basis of short-haul figures of 7.5 picowatts per mile, the above would be 187.5, 225 and 300.

Reverting again to the C.C.I.R. recommendations for actual circuits, no recommendations exist for sections shorter than 250 km. But it is stated that in conjunction with the length L , greater than or equal to 250 km. noise power shall not exceed the mean value $3L$ picowatts per km. at zero relative level within any hour of the month, and also 47,500 picowatts must not be

exceeded for more than $\left(\frac{L}{2500} \times 0.1\right)\%$ of the time of a month which is purely a design objective.

However, these figures do not have any real meaning unless one is able to subjectively rate the noise power value and a 'feel' for this value could be obtained by a reference to the levels of noise power in telephone transmission. The details are given in the table below.

Noise power at zero relative level, picowatts	Subjective impression in the telephone receiver of subscriber
10,000	Noise just noticeable
100,000	Noise still allows voice communication even with soft talkers.
1,000,000	Noise very much in evidence and voice communication is affected

3. Conclusions

It may, therefore, be stated that although microwave systems standards are established by the telephone industry providing the basis for establishing adequate performances, the distinction between short-haul and long-haul requirements becomes valid for private industrial communication networks. Unless a short-haul system is eventually to become a part of long-haul system, there is no need to set a standard higher than 2,000 picowatts for an 8 hop system or an average value of 250 picowatts per hop.

Since channel dropping systems are to be used extensively in railways, back-to-back repeaters, as already stated, have a positive advantage, since full base band is available at every point. If the criterion is relaxed to 7.5 picowatts per mile, the requirements can be met fairly easily with this type of repeaters. Again in operational circuits, it is to be remembered that every circuit will be a composite one with a radio bearer line and a physical line, the latter being an omnibus telephone circuit with a number of tappings. The overall noise level will, therefore, be determined by the line wire.

SPEECH COMPRESSION AND EXPANSION*

S.V.R. Naidu

Non-member

*Senior Workshop Officer (Assistant Professor), Radar Engineering Wing,
EME School (South), Secunderabad*

Summary

The characteristics of speech energy and a method of compressing the same is explained with special reference to speech communication. The COMPANDOR is introduced and the process by which it increases the signal-to-noise ratio and eliminates cross talk is dealt with at length. An expression for the noise advantage obtained due to the use of Compandors has been derived. The possibilities of application have been outlined, and two typical circuits, one a valve version and the other a transistorized version, of compression-expansion systems are studied. It is shown that the Compandor offers toll quality speech transmission over lines which otherwise could not have been used either due to the noise content or due to near-end cross talk.

Part 1 : The principles

1.1. Introduction

A survey of the field of electrical communications reveals that progress in this field was mainly a relentless fight against interference caused by noise and cross talk. The development and use of a device, known as a COMPANDOR, has made possible quality voice transmission over telephone circuits which otherwise would have been unsuitable because of either excessive noise or cross talk. This paper is a general introduction to COMPANDORS. It includes a brief discussion of their theory, circuitry and application.

1.2. Characteristics of speech energy

In all voice transmission systems sound energy is first converted to electrical energy. The resulting electrical signal consists of a complicated wave made up of tones of different frequencies and intensities. When designing a voice transmission system it is these fundamental signal characteristics of speech that must be considered.

The volume or intensity range depends on two factors :

- (i) The talker; and
- (ii) The words or syllables spoken.

The average talker produces an intensity range of 30 dB to 40 dB. However, the difference between the loudest syllable of a loud talker and the weakest syllable of a soft talker can be as much as 70 dB.

*Presented at the Symposium on 'Modern Electronic Communication Techniques', held in Hyderabad, on August 26, 1967.

Intensity ranges of such magnitudes present a serious problem to transmission systems design. The weakest signal must be amplified and transmitted at a level higher than noise and cross talk likely to be encountered in the transmission path. At the same time the strongest signal must not overload the amplifier used. These factors set the upper and lower limits of the power range that can be handled. System with a wide intensity range of signals and also noise and cross talk protection are not always practical or economical.

The necessity of a system which can overcome the effects of noise and cross talk cannot be overstressed. The search for such a system ultimately, yielded a device called the 'COMPANDOR'.

1.3. The Compandor

A Compandor consists of an intensity range compressor and an intensity range expander, from which its name is derived. The idea of speech compression and expansion was not new. The technique existed in a restricted form in the field of recording and reproduction of disc records, to give them a greater dynamic range. But extensive use of the compandor in voice communication systems is relatively recent.

The compressor section of the Compandor compresses the intensity range of the input speech signals by amplifying the weak signals more than the strong signals. At the receiving end, the expander section performs the opposite function and restores the original range of intensity.

1.4. Principle of the Compandor

The Compandor consists of two devices: the compressor at the transmitting end and the expander at the receiving end of the same circuit. The basic block diagram of the Compandor is shown in Fig. 1.

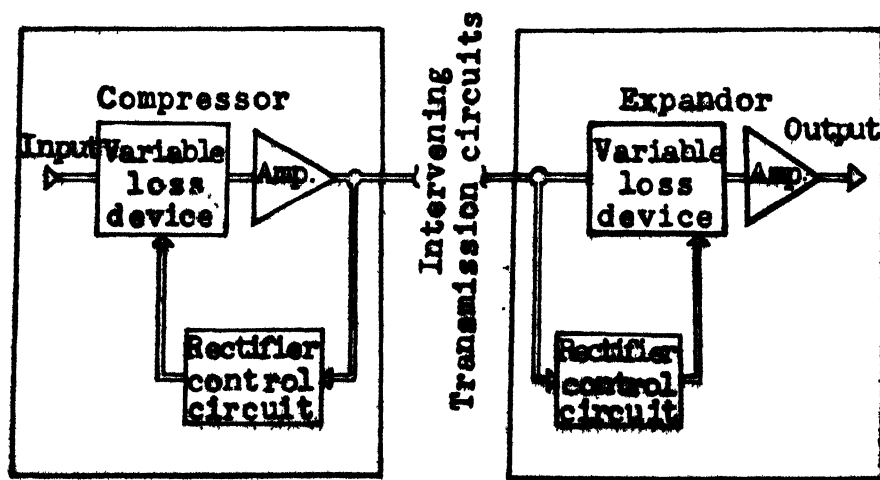


Fig. 1

Block diagram of a Compandor

Speech signals entering the compressor pass through a variable loss device, called a 'varioloesser' and reach the amplifier. A part of the speech energy output of the amplifier is fed to a control circuit where it is rectified. The resulting direct current is applied to the varioloesser circuit and controls the amount of signal attenuation. The amount of this D.C. feedback is directly proportional to the input speech energy. For weak signal inputs the control current fed back is small and the attenuation of the varioloesser is small. If the input speech energy increases, the attenuation of the varioloesser increases in direct proportion. This results in compression of the speech energy range.

In the expander, a portion of the input speech energy (rather than the output energy as in the compressor) is fed to the rectifier control circuit which provides the direct current control signal to the varioloesser. The attenuation of this varioloesser is inversely proportional to the level of the D.C. control signal.

The expander thus introduces a loss which is inversely proportional to the level of the input speech energy and equal to the gain introduced by the compressor. This action, being complementary to that of the compressor, restores, to the speech signal, its original intensity range.

The performance of a compandor depends on three factors :

- (i) The compression-expansion ratio;
- (ii) The companding range; and
- (iii) The attack and recovery times.

1.5. Compression-expansion ratio

The degree to which speech energy is compressed or expanded is expressed by the ratio of the range of input power to the range of output power (expressed in dB). With this definition the compression ratio is always greater than 1 and the expansion ratio is always less than 1. For undistorted transmission it is obvious that the product of the compression and expansion ratios must be equal to 1.

Proper selection of these ratios involves a compromise. While a large compression ratio will give a large signal-to-noise ratio, it is likely to magnify minor irregularities in performance and therefore cause distortion. But if the compression ratio is too small the range of speech energy will not be sufficiently compressed to realize the signal-to-noise ratio that the system is capable of giving. A compression ratio of 2:1 and an expansion ratio of 1:2 provides satisfactory performance of compandors used for telephone transmission.

1.6. Companding range

Theoretically companding action must occur over the entire intensity range of speech energy. Distortion will occur if the companding range is less than the intensity range of speech signals. In practice however a companding range of 50 dB to 60 dB is adequate to keep distortion within acceptable limits and to provide sufficient signal to noise ratio. Either very high or very low signals present outside this range are few and can be attenuated without loss of intelligibility.

The effect of a Compressor, with a 2:1 compression ratio, on various power levels is shown in Fig. 2. It will be seen therein that compression and expansion occur around a level of +5 dB. This is called the unaffected level or the focal point. Speech energy at this level passes through the compressor and expander with zero loss or gain; *i.e.*, unaffected by companding action.

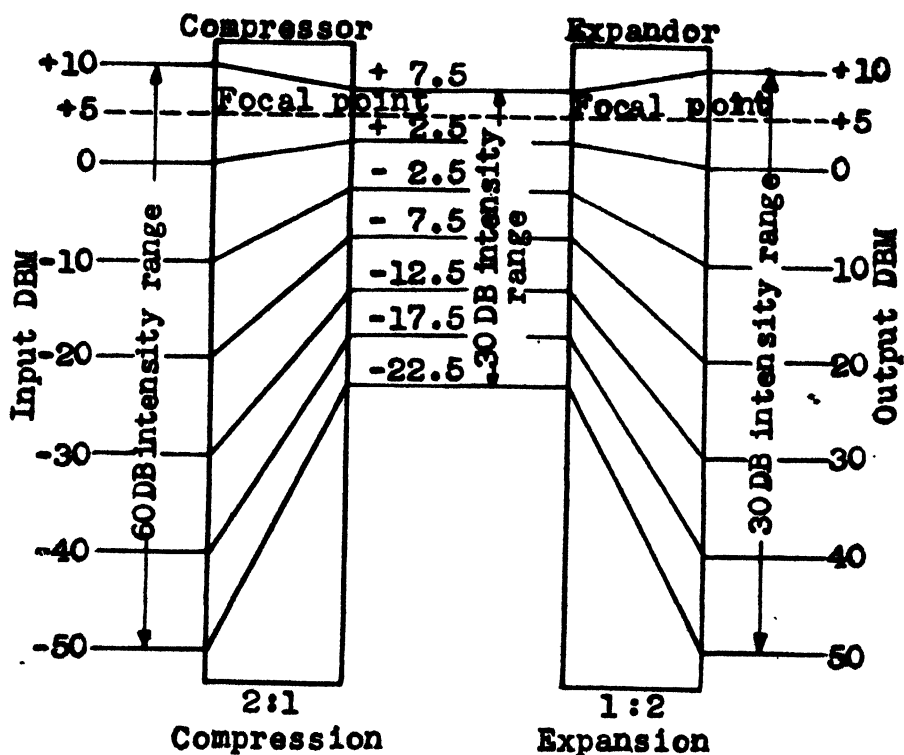


Fig. 2

Effect of a Compressor on various power levels

Fig. 3 shows the input power *vs.* output power relationship for the compressor, expander and the compandor as a whole. The focal point and companding range are clearly shown.

The maximum noise advantage is obtained if the focal point coincides with the highest level of the companding range. When such is the case, all speech levels below the focal point will be amplified by the compressor (and attenuated in the expander). A raise in the mean power of the signal being fed into the transmission line will occur. This may increase intermodulation noise and also cause overloading. The focal point is, therefore, kept 10 dB to 15 dB below the top of the companding range. Actual choice of the focal point will depend on the noise advantage desired and the power level that the particular system is capable of handling.

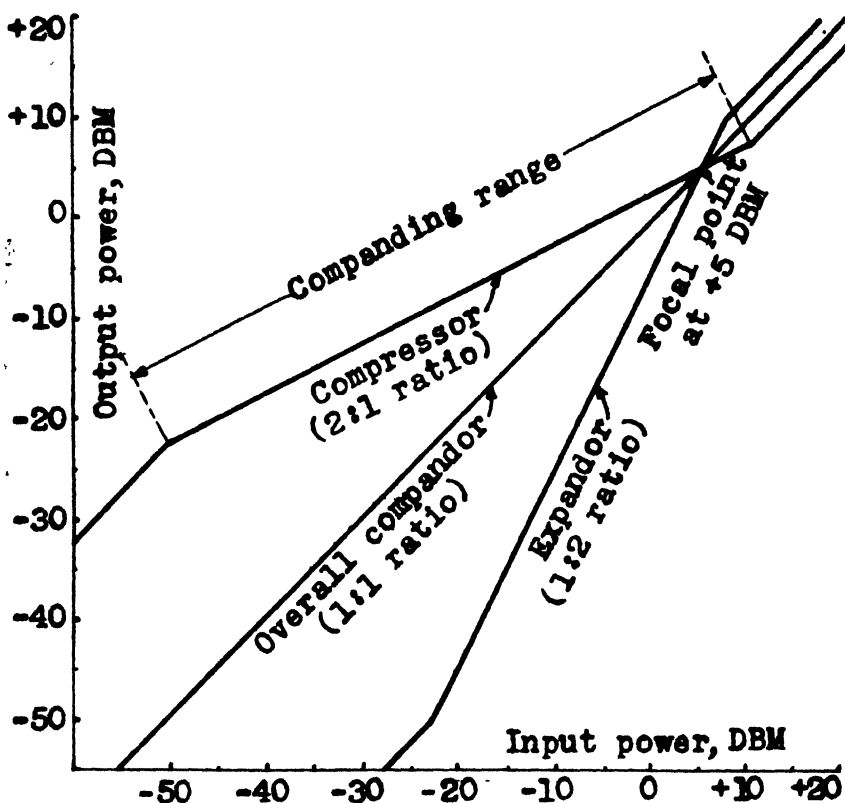


Fig. 3

Relationship of Input vs. Output power for a Compressor

Attack and recovery times

If the gain or loss of a Compressor used in a speech transmission system varies instantaneously with a change in input signal considerable distortion will occur. To avoid this, the time constant of the Compressor is set so that the gain or loss varies as a function of the speech signal envelope and not the instantaneous amplitude. The gain or loss is thus controlled by syllabic variations of the input signal and not by individual speech peaks.

The attack time is defined as the interval between the instant when the power of a test signal, applied to the compressor input, is increased from -16 dBm0 to -4 dBm0 and the instant the output voltage envelope of the compressor reaches 1.5 times its final steady-state value.

The recovery time is defined as the interval between the instant when the test signal is reduced from -4 dBm0 to -16 dBm0, and the instant when the compressor output voltage reaches 0.75 times its final steady-state value.

Similar definitions apply to the expander.

Attack and recovery times of 3 milli-sec. and 13.5 milli-sec. respectively are normally used. If the attack and recovery times are short, modulation products may cause distortion. Long attack time can mean mutilation of the initial parts of the syllable. If the recovery time is too long the full loss of the expander will not be inserted between syllables and noise quieting is not achieved. The recovery time must be short enough for the compressor to operate at the syllabic rate, *i.e.* to recover between syllables of words.

Irrespective of the attack and recovery times actually adopted it must be ensured that the attack and recovery times of the compressor and expander coincide exactly. This will avoid overshoots.

The attack and recovery times are some times referred to as operate and release times respectively.

1.7. Noise advantage

The effect of a Compandor on the signal-to-noise ratio in a typical speech transmission channel is shown graphically in Fig. 4. It compares the operation of two carrier channels : Fig. 4 (ii) is with a Compandor and Fig. 4(i) is without the same. For explanation, a line noise intensity of -51 dBm is assumed to exist at the input to the receiving carrier terminal.

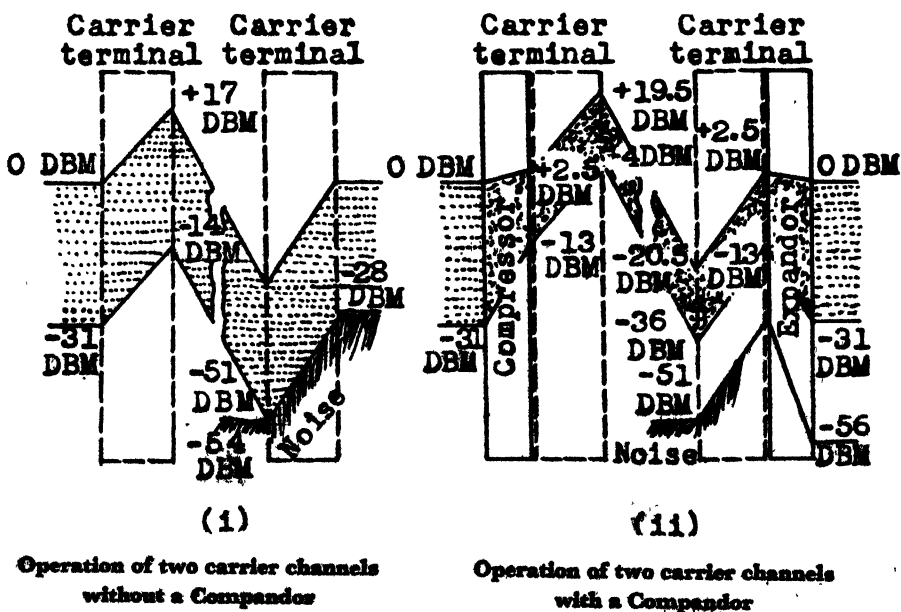


Fig. 4

Effect of a Compandor on the signal-to-noise ratio

Let the Fig. 4(i) be considered. The low intensity signal starting with a level of -31 dBm reaches the receiver terminal at -54 dBm, *i.e.*, 3 dB below the assumed noise power. But for intelligible transmission the signal level must be at least 20 dB above the noise. Hence, in this example, noise predominates,

Now consider Fig. 4(ii). The same low intensity signal is raised in level by the compressor by +18 dB, so that it now reaches the receiving carrier terminal at a level of -36 dBm, *i.e.*, the weakest signal is +15 dB above noise level. Now, both the signal and the live noise are amplified 23 dB and enter the expander. The noise, being weak is attenuated more than the signal. Therefore, the margin between the signal and the noise increases to 25 dB. This figure is sufficient to ensure quiet listening conditions.

1.8. Expression for noise advantage

Compressors and expandors may also be defined as nonlinear four terminal devices whose transmission factors are connected with the input voltage V_1 , by the relationship,

$$\frac{V_2}{V_1} = K_o \left[\frac{V_1}{C_1} \right]^\alpha - 1 \quad (1)$$

where K_o is the value of the transmission factor when the input voltage V_1 has the value C_1 , V_2 is the output voltage of the device and α is a regulation coefficient, which, if undistorted transmission in the channel is desired must satisfy the following conditions:

- (i) For the compressor : $\alpha =$ a constant less than unity;
- (ii) For the expander, using β instead of α ; $\beta =$ a constant greater than unity; and
- (iii) $\alpha \beta = 1$

In the case of a linear four-terminal network $\alpha, \beta = 1$.

From this relationship, we have the output voltage of the compressor to be

$$V_2 = K_{oc} C_1 \left[\frac{V_1}{C_1} \right]^\alpha \quad (2)$$

To this output an additional noise signal will be added before it reaches the expander input. We shall assume that there is no inherent noise in the compressor input or the compressor itself. Then, if V is the noise voltage in the channel, the expander input voltage V_3 will be

$$V_3 = \sqrt{(K_{ol} V_2)^2 + V^2} \quad (3)$$

where K_{ol} is a coefficient of the transmission line.

The expander output voltage V_4 , will be given by

$$V_4 = K_{op} C_3 \left[\frac{V_3}{C_3} \right]^\beta \quad (4)$$

where K_{op} is the fixed transmission factor of the expander when the voltage C_3 is applied to its input.

Also,

$$C_3 = K_{ol} C_1$$

where $C_3 = K_{ol} C_1$.

Substituting equations (2) and (3) into equation (4) successively, we get

$$V_4 = C_3^{1-\beta} K_{ol}^\beta K_{oc}^\beta C_1^\beta \left[\frac{V_1}{C_1} \right]^{\alpha\beta} \left[1 + \frac{V_2}{K_{ol} K_{oc} C_1 \left[\frac{V_1}{C_1} \right]^\alpha} \right]^{\frac{\beta}{2}}$$

which may be put as

$$V_4 = A V_4 \left[1 + \frac{V_2}{B V_1^{\alpha\beta}} \right]^{\frac{\beta}{2}}$$

where A is a constant.

The righthand side can be expanded into a series. Assuming that $V \ll V_1^\alpha$ which is normally the case in commercial telephony and therefore neglecting the terms containing $\frac{V^2}{V_1^{\alpha}}$ we can put the expression in the form

$$V_4 = A V_1 + q$$

The second term here represents the added noise and has a value equal to

$$\frac{\beta}{2} \frac{K_{op}}{K_{ol} K_{oc} C_1^{2(1-\alpha)}} V^2 \frac{1}{V_1^{2(\alpha-1)}}$$

Since signal and noise are independant of each other and both are random processes, we can write for the average value of q per min. as

$$\bar{q} = \frac{\beta}{2} \frac{K_{op}}{K_{ol} K_{oc} C_1^{2(1-\alpha)}} \bar{V}^2 \left(\frac{1}{V_1^{2(\alpha-1)}} \right)$$

By a similar process the average noise per min. without a compandor can be

$$\bar{n} = \frac{1}{2} \frac{K_{op}}{K_{ol} K_{oc}} \bar{V}^2 \left(\frac{1}{V_1} \right)$$

Therefore,

$$\text{Noise advantage} = \frac{\bar{n}}{\bar{q}}$$

$$= \alpha \frac{\left(\frac{C_1}{V_1} \right)}{\left[\left(\frac{C_1}{V_1} \right)^{2\beta-1} \right]}$$

This expression shows that the noise advantage is a function of the compression regulation factor.

For reasons which are beyond the scope of this paper, $\alpha = \frac{1}{2}$ is regarded as optimum.

1.9. Cross talk advantage

In normal speech transmission cross talk is mostly due to the high speech signal peaks. The compressor reduces the amplitude of such loud signal peaks, thus preventing cross talk to adjacent channels due to circuit overloading.

Cross talk advantage is also realized due to the expander. Cross talk like noise, is objectionable during silent periods and is not noticeable during speech. Since the expander introduces a condition of maximum loss when signals are not present (*i.e.*, only when cross talk and noise exist) cross talk and noise are attenuated greatly and do not disturb the telephone listener.

Part 2 : The Circuitry

2.1. Basic valve circuit

Simplified circuit of a typical valve operated compressor is shown in Fig. 5 which shows only the parts essential to compressing action.

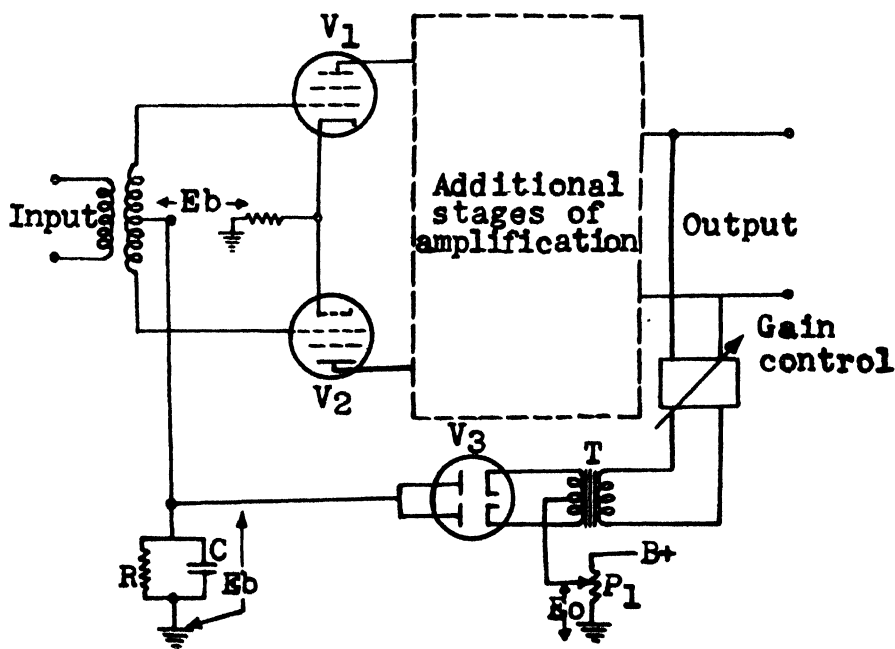


Fig. 5
Simplified circuit of a Compressor

The device consists of a conventional amplifier with the addition of a control-circuit. With very small signal inputs V_2 , is ineffective due to the positive bias on its cathodes from P_1 . Once the signal reaches a certain threshold level rectification at V_3 occurs and the increased negative bias on the variable mu tubes V_1 and V_2 reduces their gain. This results in an input-output characteristic as shown in Fig. 6 with the compression starting at A.

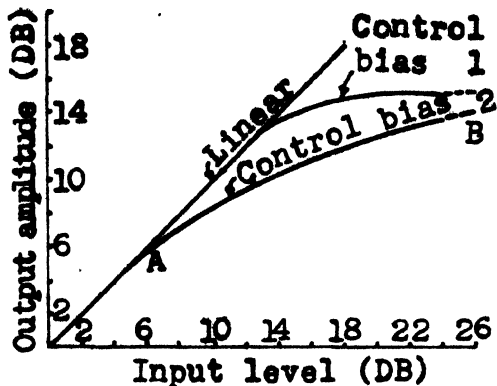
The reciprocal of the slope of the AB is the compression ratio. In practice the mutual conductance *versus* bias voltage relationship for variable mu tubes is such that the line AB is slightly curved; but this nonlinearity is negligible.

To specify the shape of the compression curve, two quantities are necessary:

- (i) The compression ratio; and
- (ii) The point at which the compression starts.

The changing of the gain of the control circuit (gain control in Fig. 5) will change the starting point only and will have no effect on slope. If the gain is increased by n dB, then the compression will start at n dB lower signal level.

Fig. 6
Relationship between input level
and output amplitude



The changing of the bias voltage E_0 , effects both the compression ratio and the starting point (Fig. 6). An increase of E_0 will produce a higher compression ratio and also a higher starting level. A given characteristic can therefore be obtained by several successive adjustments of E_0 and the control gain.

The values of C and effective impedance of the charging circuit decide the attack time. The recovery time is determined by the time constant of R and C .

The changing of the polarity of the control voltage will give us an expander, with characteristics as shown in Fig. 7.

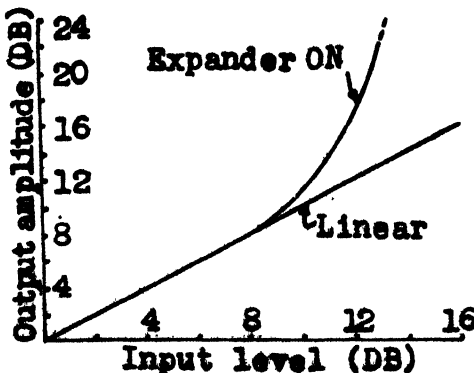


Fig. 7
Relationship between input
level and output amplitude

2.2. A transistorized circuit

A 2:1 compression ratio is achieved if, over the required range of signal levels, the control current is directly proportional to the level of the signal at the input to the rectifier and the gain of the variable loss network is inversely proportional to the control current.

In the expander a ratio of 1:2 results if the control current is directly proportional to the level of the signal at the input to the rectifier and the gain of the variolower is directly proportional to the control current.

In the circuit to be discussed, the controlled elements in the variolosses, both in the compressor and expander circuits, are the A.C. resistances of the emitter-base junction of the germanium junction transistors. Fig. 8 shows the fundamental property of such a junction.

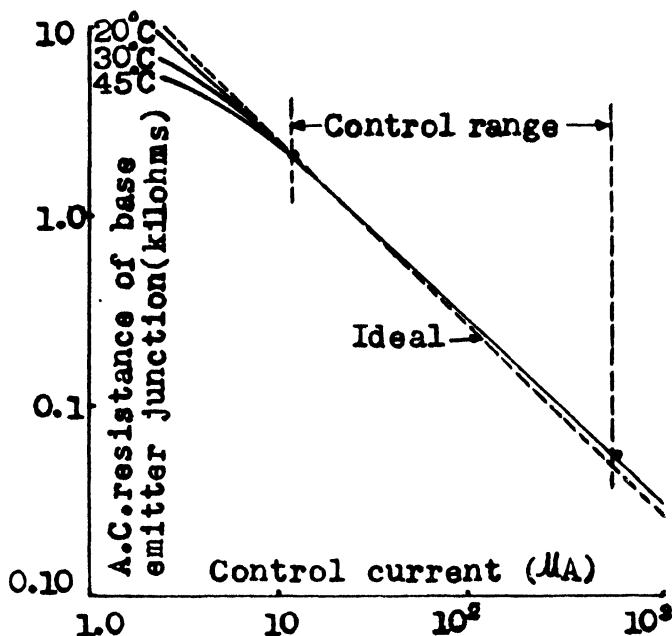


Fig. 8

Fundamental properties of a germanium junction

It shows that the A.C. resistance of the junction is inversely proportional to the unidirectional current flowing in it. Over the control range extending from 10 micro-amp. to 500 micro-amp. (*i.e.*, a range of over 30 dB) the A.C. resistance is inversely proportional to the control current to within an accuracy of 0.5 dB.

2.3. Variolosses

The variolosses circuits used are shown in Fig. 9.

In the compressor circuit the A.C. resistances of the two junctions are used in series as a shunt between the input and output transformers, each of whose impedances is much greater than the greatest value reached by the junction resistances.

In the expander circuit, the transistors used also provide useful gain. The circuit is basically a single stage push-pull amplifier. The gain of such an amplifier, when operating into a constant load resistance, is almost exactly inversely proportional to the input resistance of the transistors. As already seen, this varies inversely as the control current. Hence the gain of the circuit

will be directly proportional to the control current if the source resistance is kept low compared to the junction resistances.

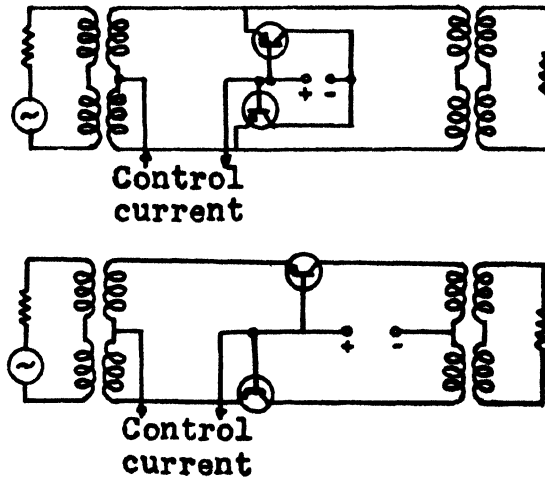


Fig. 9

The variolossor circuits

Since the variable loss elements are non-linear some distortion will occur. This can be kept low by ensuring that the ratio of control current to signal current is large.

2.4. Control current rectifier

This is shown in Fig. 10.

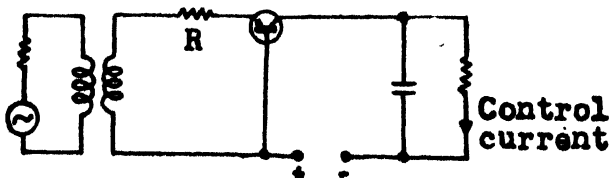


Fig. 10

Schematic diagram of a control current rectifier

Half-wave rectification takes place in the emitter-base junction. The input-level/control-current characteristic of the rectifier is shown in Fig. 11.

The departure from the ideal at low currents and high ambient temperatures is due to the collector cut-off current augmenting the control current at low signal levels. This is compensated accurately by causing the collector cut-off current of a similar transistor flow in the rectifier load circuit in opposition to the control current.

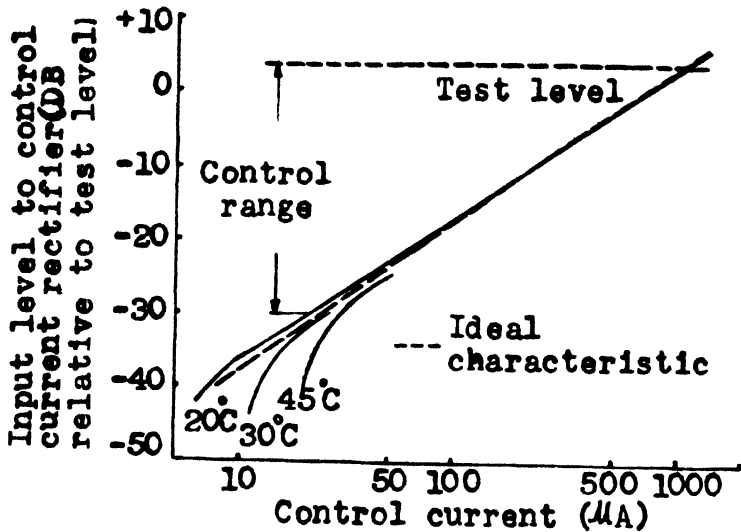


Fig. 11

Characteristic curves of a rectifier

Complete circuits of the compressor are reproduced as Figs. 12 and 13 respectively.

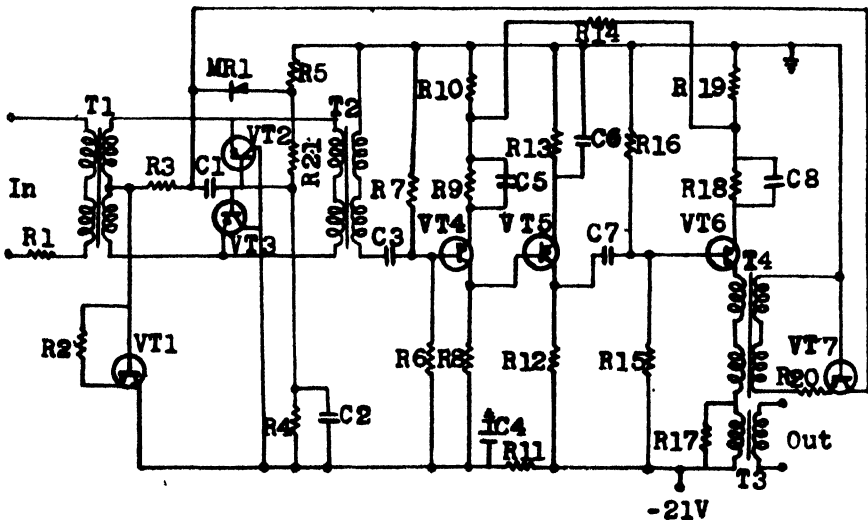


Fig. 12

Circuit diagram of a Compressor

Part 3 : Applications

Componders are used in telephone voice channels to make noisy circuits satisfactory for toll transmission service. On physical and phantom voice-frequency circuits the Compondor is particularly valuable in compensating for the effects of power line induction and noise pickup from other random sources.

Many older circuits which have fallen below transmission standards can be restored to toll quality by using Compondors.

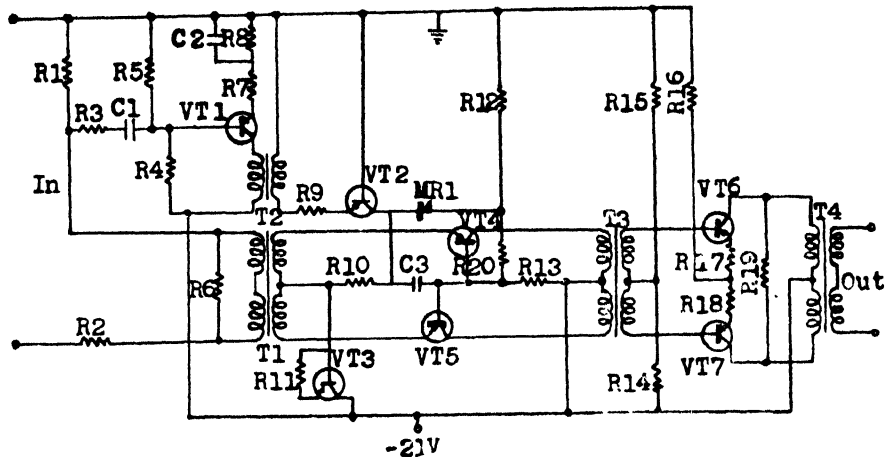


Fig. 13

Circuit diagram of a Compressor

Compondors are employed effectively on amplitude-modulated carrier systems to reduce the effects of cross talk as well as to improve the signal-to-noise ratio. Repeater spacing of carrier systems operating over wire lines or cable pairs is often limited by line noise conditions or excessive near-end cross talk. With the noise advantage offered by Compondors, repeater spacing may be limited only by the maximum system gain.

Multi-channel microwave radio carrier systems can achieve greater fading margins, longer transmission paths, and make use of more repeaters to extend the system because of the additional signal-to-noise advantage of the compandor. Such an advantage can also reduce the radio antenna gain requirements, thus permitting the use of smaller antenna systems.

Because of the noise and cross talk improvement, design requirements of line filters, in addition to other carrier terminal and repeater equipment, can be lowered—resulting in lower equipment costs. Substantial savings can therefore be realized in designing and manufacturing carrier systems with compandors built into the channel equipment.

Part 4 : Conclusions

Under idle circuit conditions, Compondors provide a noise advantage equal to the maximum gain of the compressor. For the Compondor characteristics shown in Fig. 4(ii), the noise advantage would be 28 dB. In actual practice, however, the effective noise advantage is always less than the value achieved during idle conditions. Typical values range from about 20 dB to 25 dB. The actual noise advantage depends on such factors as the speech power level, the noise level, the compandor focal point, and the companding range.

The Compondor offers relief from the disturbing effects of noise and cross talk the principal enemies of communication. It is, therefore, a remedial device that offers a practical method of improving the quality of voice transmission over otherwise marginal or unsatisfactory telephone circuits.

SPEECH BANDWIDTH COMPRESSION***G. Kanttaiah***Non-member**Defence Electronics Research Laboratory, Hyderabad***Summary**

Compression of speech bandwidth is being constantly attempted in the field of telephone communication to enable the release of more channels for expansion purposes. This paper briefly indicates the mechanism of speech production and its transmission over long distance. It describes the recent developments in speech transmission, namely, Vobanc, Codimex, Vocoder, and the Phonetic-element systems.

1. Introduction

Since the invention of telephone communication, the scientists were interested in compression of speech bandwidth so that more channels can be realized with existing facilities. As early as 1930, the Bell Telephone Laboratories started a research programme on speech bandwidth compression. The speech signal is redundant in nature so that it does not require the full bandwidth of 4,000 cycles per sec. of a present telephone channel. But the redundant nature of speech makes it intelligible even in a very noisy background.

The mechanism of a speech production may be described adequately in terms of the physiological structure of the vocal tract. The mouth and throat form an acoustic cavity which is bounded by the tongue and the roof of the mouth on the bottom and top, by the lips and teeth on the front and the vocal cords and glottis on the back. This cavity is a multiple resonant system whose resonances are function of its dimensions. In comparison with the music of a symphony orchestra, human speech is a relatively simple type of signal. Vocal sounds are more like the tonality of a single string of a stringed instrument, since their component vibration constitute only one fundamental and one series of harmonically related overtones. Thus, according to the information theory, speech does not require full telephone bandwidth that is now used. During the last fifty years, lot of effort was put in to investigate the nature of speech and many theories were put forward to explain the mechanism of speech. The three dimensional speech waveforms called 'sonograms' (Fig. 1), are thoroughly studied and analyzed. Different types of speech band width systems are developed based on several different theories making use of a particular aspect of speech signal. It is not possible here either to explain or to list all of the systems that were tried and explained in the literature. The systems aiming at speech band compression can be broadly divided into two categories: (i) Spectrum-alteration systems; and (ii) Vocoder (voice coding) systems.

*Presented at the Symposium on 'Modern Electronic Communication Techniques' held in Hyderabad on August 26, 1967.

Spectrum alteration systems can achieve only the compression ratios of the order of 3 to 5 whereas Vocoder type of systems can achieve great compression ratios as high as 10 to 20.

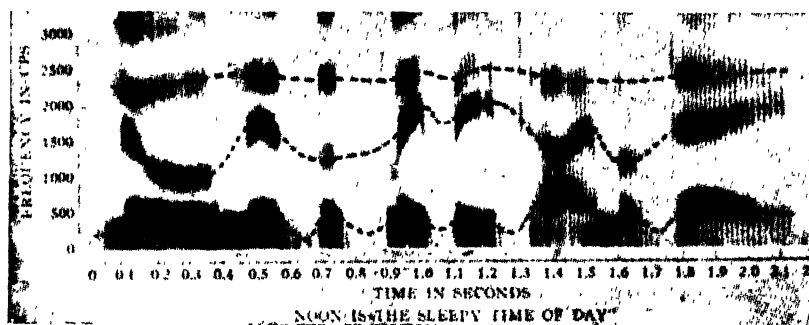


Fig. 1
Three-dimensional waveforms

Spectrum alteration systems are mainly based on the fact that the speech signal consists of three formant frequencies which appear as zones of concentrated energy in the graphic representation of sound signals. The three formant frequencies fall into three bands, *i.e.*, 0.2 to 1 kilocycles per sec., 1 to 2 kilocycles per sec. and 2 to 3.2 kilocycles per sec. bands and a sort of frequency division technique is adopted to compress each of the formant frequency band to achieve the bandwidth compression of speech signal. At the receiving end the frequency is multiplied to the original frequency bands to get back the speech. The Vobanc and Codimax belong to this category which are explained in detail subsequently.

Homer-Dudley of Bell Telephone Laboratories developed and demonstrated the first channel vocoders, a bandwidth compression system using a bandwidth of 300 cycles per sec. Channel vocoder depends upon the principle that the power spectrum changes slowly at a rate of few cycles per second. Since the advent of the first channel Vocoder, the vocoders have undergone many improvements in several respects. A high fidelity channel vocoder has been explained in detail in the later part of this paper.

2. Vobanc and Codimex systems

Vobanc (voice band compression) and Codimex (compression division multiplication expansion) fall in the category of formant tracking devices. In Vobanc the speech band is divided into three parts (0.2-1, 1-2 and 2-3.2 kilocycles per sec. bands.) Each of these bands usually contain three principal vowel formants. The signal in each band is passed through a regenerative modulator which halves the frequency. Thus, the frequency band is compressed. At receiving end, the frequencies are doubled to get back the speech signal. The block diagram of Vobanc system which achieves a compression ratio of 1:2 is shown in Figs. 2 and 3. The transmitting terminal of Vobanc consists of a modulator to shift the frequency band of 0.2 to 3.2 kilocycles per sec. upto 107.8 to 104.8 kilocycles per sec. the lower side band being used. The

output of the modulator is fed into three amplifiers each of which is connected to an 'A'-filter. The A_1 -filter transmits from 107.8 to 107 kilocycles per sec. and its output generally contains the lowest vowel formant. The A_2 -filter transmits from 107 to 106 kilocycles per sec. and contains the second vowel formant. The A_3 -filter transmits from 106 to 104.8 kilocycles per sec. and contains the third formant and the higher frequencies. The outputs of A-filters are amplified and each is then connected to regenerative modulator, the block diagram of which is shown in Fig. 4. The regenerative modulator consists of a balanced modulator, the carrier supply being derived from the modulator output. This feedback arrangement halves the input frequency and the output is proportional to the input over a certain range. The output of regenerative modulators are filtered by B-filters which have got half the band width of corresponding A filters. The output of the B-filter is brought down to voice band by suitable modulators. The combined output of three B-filters are accommodated either in the band of 75-1,925 cycles per sec. or in the band of 2,075-3,925 cycles per sec. Thus the speech band of 4,000 cycles per sec. accommodates the two channels.

The receiving terminal of Vobanc (Fig. 5) consists of a group of three modulators which shift 2 kilocycles per sec. band back upto 52 to 54 kilocycles per sec. Another set of B-filters separates the three channels. Each B-filter is connected to a frequency-doubler circuit, which consists essentially of a full-wave rectifier. The operation of the frequency doubler is inverse to that of regenerative modulator. The desired output of 104-108 kilocycles per sec. is filtered from the combined output of three frequency doublers and demodulated to voice frequency band.

In Vobanc only one stage of compressor divider is employed. Any attempt to compress further will result in elimination of voice harmonics surrounding the formant. A different type of compressor divider is employed in Codimex system, two stages of which can give a compression ratio of 1 : 4 and three stages of which can give compression ratio of 1 : 8 Codimex system is similar to Vobanc in all respects except the compressor divider. In the Vobanc system the instantaneous amplitude is maintained whereas with the Codimex system the amplitude under-goes an operation linked to that applied to the frequency. The waveforms of compressor divider are shown in Fig. 5. Waveform (i) is the single side band containing the audio signal. The waveform (ii) is the same as waveform (i) but clamped to positive level. Then the amplitude is reduced to its logarithmic value in waveform (iii). At the points where the signal passes through zero, a trigger switches a flip-flop producing a division by 2 waveforms (iv). At each triggering the flip-flop output operates a commutator which reverses the sign thus giving wave form (v) which is the compressed output of original signal. At receiving end the reverse operation is carried out by a multiplier expander which is essentially a full wave rectifier.

3. High fidelity channel Vocoder

Transmitter of a channel Vocoder is a sort of speech analyzer which samples the speech signal in frequency domain by using a set of continuous

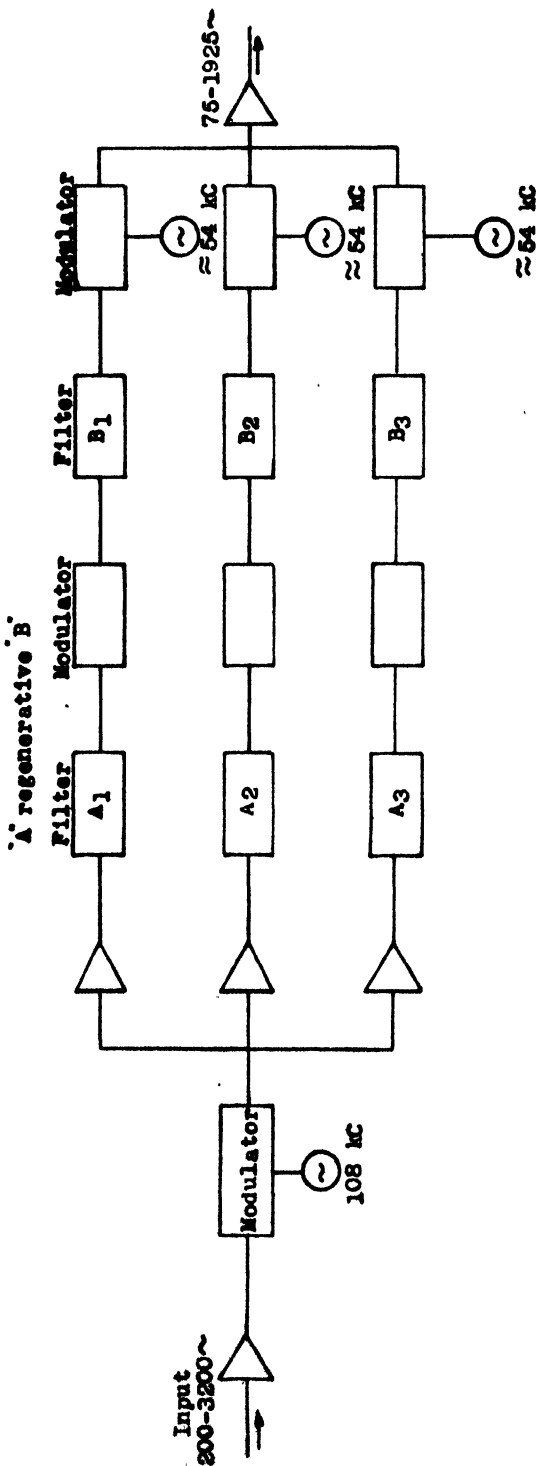


Fig. 2
Block diagram of the transmitting terminal of the Vobanc

bandpass filters to produce values of short-time frequency spectrum for a series of discrete frequency bands. The channel Vocoder also differentiates the speech sounds which are either voiced as a vowel or unvoiced as a sibilant or, 'S' sound. It also contains a pitch extractor that develops varying voltage output whose amplitude is proportional to the basic pitch frequencies of the voiced sound.

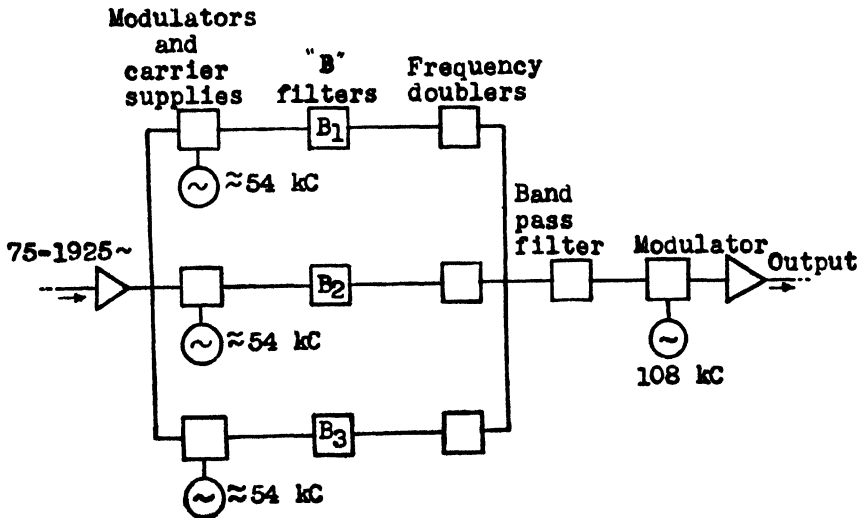


Fig. 3

Block diagram of the receiving terminal of the Vobanc

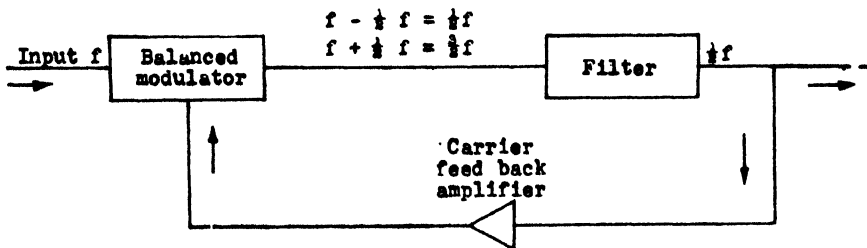


Fig. 4

Block diagram of the regenerative modulator frequency divider

In Fig. 6, the transmit terminal is composed of a voice operated gain adjusting device (Vogad), the spectrum channel analyzer circuits, the voicing indicator circuits, and the pulse-code modulation (PCM) circuits for digital encoding.

The talker's speech signal is generated in a special microphone that has a relatively flat response, and ranges from 70 to 3,800 cycles per sec. The signal is fed into the Vogad, which has a 22-dB range of adjustment. This range is

controlled in 1.5-dB increments by a digital counter that is responsive to the drive pulses sent to it from the voiced-unvoiced indicator gate in the voicing indicating circuitry. The gate operates at the interval rate set by the precise points of time at which successively articulate segments of speech, occur and in a fashion that is identifiable in terms of differential amplifier 'cross-overs'. The output of the Vogad is held at a relatively constant value by this automatic gain control.

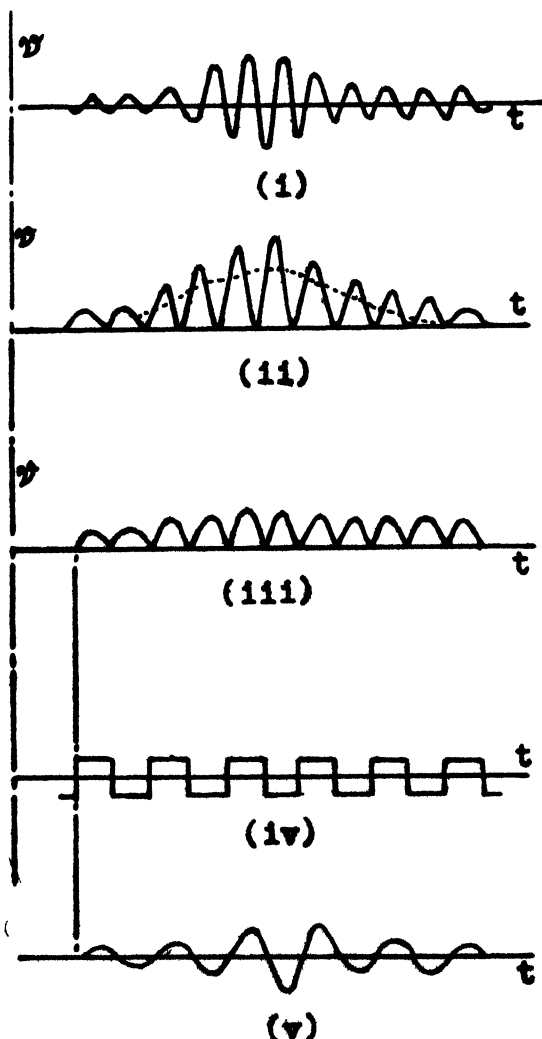


Fig. 5

Waveforms of compression divider of the Codimex system

This Vocoder has 16 spectrum channels, each of which contains a band-pass filter, rectifier, and a low-pass filter. Each filter passes a narrow band of voice frequencies, and this energy is rectified and inserted into a 25 cycles per

sec. low-pass filter. The output of the low-pass filter is a slowly varying signal that describes the energy content during a given period of time in the portion of the speech spectrum to which the channel is tuned. As different sounds are made by the talker, the outputs of the spectrum channels correspond to the spectral distribution of energy.

By the use of filters and differential amplifiers, the voicing indicator circuits detect whether the speech input is voiced or unvoiced. The signal from the Vogad is separated into high- and low-frequency segments, each of which is amplified and rectified one to a positive D.C. level and the other to a negative D.C. level. These levels are combined and added in the differential amplifier, and the positive or negative resultant determines whether a voiced or unvoiced condition exists. The output of these circuits is then included in the PCM code for transmission to the receiver.

The pitch-tracking circuitry also receives the signal from the Vogad, and this circuitry includes a variable frequency filter that automatically tunes to the pitch frequency of the talker's voice by means of a feedback control loop. The output of the pitch-tracking filter is then amplified and limited to detect the lowest frequencies present. A frequency-to-amplitude (voltage) converter is used for driving the low-pass filter. The output of this filter is a voltage that is proportional to the fundamental pitch-frequency of the voice, and it controls the frequency of the variable tuning filter. The pitch information is used only when the differential amplifier indicates a voiced condition.

Signals from the spectrum channel, together with the voiced-unvoiced decision and pitch channel, are multiplexed and pulse-code modulated into the output. In this Vocoder, each spectrum channel output is represented by a three bit ($2^3 = 8$ values) code, and the pitch channel is represented by a six-bit ($2^6 = 64$ values) code. The information contained in the 16-spectrum channels and the pitch channel, together with the voiced-unvoiced decision, comprise a 54-bit-per-frame PCM code. At a frame sampling rate of 44-44 frames per sec. a total transmission bit rate of 2,400 bits per sec., is attained.

At the receiving terminal (*vide* Fig. 7), the PCM signal—which includes timing synchronization—is decoded and framed for proper channel synthesizer low-pass filter is a replica of the corresponding analyzer output before encoding.

The decoded pitch extractor channel signal controls a voltage to the 70-300 cycles per sec. buzz-generator voltage-to-frequency converter. Since the voltage output of the pitch detector is directly proportional to the fundamental frequency of the voice, the buzz-generator produces periodic pulses that occur at the fundamental voice frequency. The hiss generator, which produces sounds for use in synthesizing unvoiced speech is essentially a white-noise generator.

The buzz-hiss gate is controlled by the decoded PCM signal element that relates the voiced unvoiced indication in each frame. The output voltage from each low-pass filter to its associated modulator determines the level of energy fed into each bandpass filter. These receiver filters are identical to

their counterparts in the channel analyzer sections of the transmitter. Thus, the output frequencies and energy content are representations of the frequencies and energy inserted into the analyzer filters at the transmitter.

The signals from the 16-synthesizer channels are combined, amplified and applied to the receiver of the listener's telephone set, which is a synthesized replica of the talker's speech.

4. Phonetic-element system

Phonetic-element systems aim at the machine recognition of spoken language rather than the bandwidth compression. Phonetic element systems require very small bandwidth of the order of 50 cycles per sec. Phonetic element systems which are also known as phonetic Vocoders work on the principle of Vocoders, *i.e.*, sampling in the frequency domain to determine the short term frequency spectrum. Phoneme is a shortest distinct sound of spoken word.

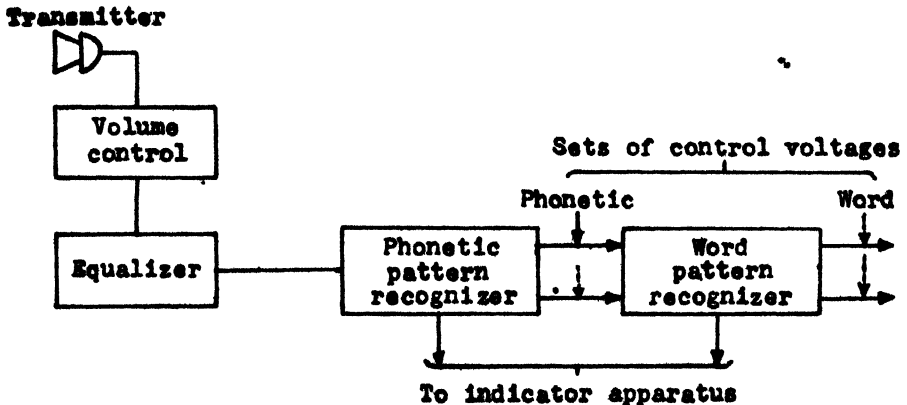


Fig. 8

Block diagram of the electronic word recognizer

Block diagram of an electronic word recognizer is shown in Fig. 8. The speech signal passes from transmitter of a telephone set to a volume control and an equalizer. Next, the speech signals enter the phonetic pattern recognizer where the spectrum of speech is continuously compared with a number of stored spectra of phonemes and the best fit is determined. The phonetic pattern recognizer contains a set of continuous band pass filters. Each band pass filter contains an amplifier, a rectifier and a lowpass filter to smooth the speech power to syllabic rate. Now the phonetic pattern information is fed to word pattern recognizer. The word pattern recognizer should contain in its store the phonetic-pattern of all the words which are to be recognized. Phonetic pattern is compared with stored phonetic-patterns of each word and the word is thus recognized. It can be easily seen that a large amount of hardware is required to store the data of all phonemes and words. A word recognizer having a capacity of 10 words has been built and demonstrated successfully.

Still it is long way off to build a versatile word recognizer which can recognize any spoken word.

5. References

1. H. Dudley. 'The Carrier Nature of Speech'. *Bell System Technical Journal*, vol. 19, 1940, p. 495.
2. J.L. Flanagan. 'Automatic Extraction of Formant Frequencies from Continuous Speech'. *Journal of Acoustical Society of America*, vol. 28, 1956, p. 110.
3. J.L. Daquet. 'Speech Compression Codimex System'. *Transactions of the Institute of Electronics and Electrical Engineers*, August 11, 1963, p. 63.
4. B.P. Hogert. 'The Volanc—a Two-to-One Speech Bandwidth Reduction System'. *Journal of Acoustical Society of America*, vol. 28, 1956, p. 399.
5. P.G. Edwards and J. Clapper. 'Better Vocoders are Coming'. *Institute of Electronics and Electrical Engineers, Spectrum*, vol. 1, September 1964, p. 119.
6. H. Dudley and S. Balachek. 'Automatic Recognition of Phonetic Patterns in Speech'. *Journal of Acoustical Society of America*, 1965, p. 721.

TROPOSPHERIC SCATTER COMMUNICATION***Major P.P. Chawla***Associate Member**Officer Commanding, Field Workshop Company, EME School (South), Secunderabad***Summary**

Considerable investigation is in progress regarding tropospheric scatter communication technique which relates to the establishment of radio communication with UHF or SHF bands, between two points on earth's surface separated by moderate distances of within 1,000 km. This paper briefly defines the scope of such a type of communication system, and describes the tropospheric propagation mechanism, the scatter characteristics and effect of atmospheric conditions. It also deals with the tropo system parameters and indicates its advantages and cost economics. In the end, it mentions about the details of the present installations of tropo system and indicates the future trend of development.

1. Introduction

Tropospheric scatter communication may be defined as a method or system of transmitting, within the troposphere, microwaves in the UHF or SHF bands to effect radio communication between two points on the earth's surface separated by moderate distances of from 120 to 1,000 km. Such a span or hop may be augmented by other spans in tandem to permit end-to-end or through circuits upto many thousands of km. The name 'tropospheric scatter communication' is now usually referred to in the engineering vocabulary simply as 'Tropo'.

A conventional sketch of a Tropo span is shown in Fig. 1. This graphic representation is merely symbolic, and indicates in a general way that the circuit utilizes high power and large directional antennas, may be duplexed, can surmount ground obstacles of considerable magnitude, and will span a relatively large distance over the earth's surface.

With accuracy, Tropo can be termed a 'gap filler'. It provides a means of radio communications at distances not covered either by the short-range UHF or SHF line-of-sight systems, and the medium frequencies, or by the HF and long range LF system. Since ionospheric scatter communication is usually not effective on paths under 600 km. and since microwave links, because of terrain, are sometimes not practicable on long paths tropospheric scatter communication fills a gap in communication system at present used by the armed forces of the western countries. A summary of the above is shown in Fig. 2 where the principal characteristics of 'microwave' communication as utilized

*Presented at the Symposium on 'Modern Electronic Communication Techniques' held in Hyderabad on August 26, 1967.

OTHER PAPERS RECEIVED FOR SYMPOSIUM

Paper 1 :	Tropospheric Scatter Communication.	Major P.P. Chawla,					
	<i>Associate Member</i>	300
Paper 2 :	Cassegrain Aerial.	C.R. Ramachandran Nair,	<i>Non-member</i>	...			310
Paper 3 :	Frequency Synthesis in Communication Equipment.	P.R. Santhanam,	<i>Non-member</i>	317
Paper 4 :	A Pitchfinder Circuit for Use in Vocoders.	P. Baskaran,	<i>Non-member</i>	323
Paper 5 :	Tropospheric Scatter Communication Systems.	M.S.V. Gopal Rao,	<i>Non-member</i>	329
Paper 6 :	Satellite Communication System.	Wing Cdr. R. Nagaraja Rao,	<i>Non-member</i>	336
Paper 7 :	Delta Modulation.	G.V. Subba Rao,	<i>Non-member</i>	...			354

today over the surface of the earth is shown, and indicates the relationship of tropo to the other modes in the microwave band (70 M Hz to 20 G Hz). Satellite communication are intentionally omitted from this figure as the propagation mechanism is somewhat different in space.

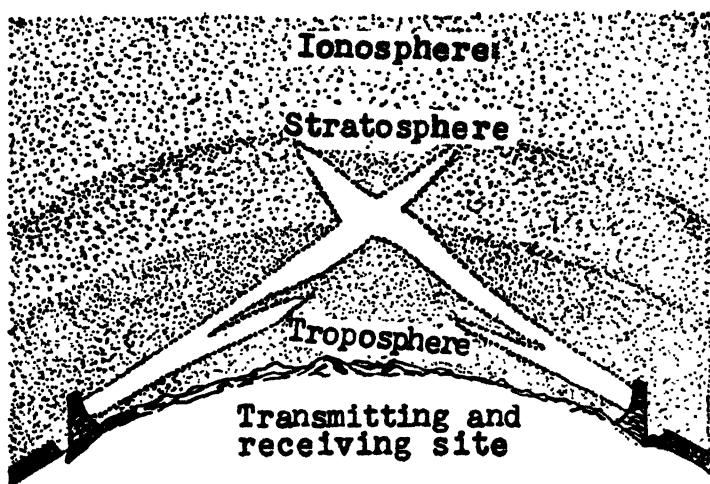


Fig. 1

Graphic representation of a Tropo span

Systems of multiple spans in tandem, composed of tropo links and extending even to thousands of miles or kilometres, are now in operation in many parts of the world, providing a reliable multi-channel communication. Most of these are shown in Fig. 3. The gap represented by our country may be readily seen. Tropo is also used in several special applications. The ability of Tropo to span hundreds of km. of inhospitable terrain with circuits of relatively high traffic density ensures a continuing need for this type of transmission.

2. The tropospheric propagation mechanism

A number of theories have been proposed to explain the nature of tropospheric scatter. To the present time, however, no single theory has been universally accepted as a complete explanation. Each theory, while acceptable in most respects has at least one disadvantage that prevents it from being completely acceptable. Some theories have been withdrawn because of new data and experimentation with this phenomenon. The theory presented here is probably the most widely used and also the most conservative presented to date. It has been compiled from the latest and most reliable reports and articles.

The phrase, 'tropospheric forward scatter' describes the hypothesis that has been suggested to explain the mechanism that enables the propagation of usable microwave radio signals well beyond line-of-sight distances. Diffraction theory does not account for the substantial electro-magnetic fields that

are produced at these ranges, nor does atmospheric ducting explain the time availability of these fields.

The troposphere is the region of the earth's atmosphere that extends from the ground to a height of slightly over 10 km. It lies several kilometre below the stratosphere and the ionosphere. The difference as we all know between the ionosphere and the troposphere is that there is practically no ionization of the air molecules in the troposphere.

The ability of the troposphere to act as a smooth refractive medium is based upon the variation of the dielectric constant. The greater the decrease in dielectric constant, the greater the bending of the beam towards the earth. Water vapour content is the main cause of the variation of the dielectric constant. The greatest variation in heating and cooling take place near the surface of the earth; therefore, the greatest variations in the dielectric constant also occur near the surface of the earth. It can be said that the vapour variations play no great part above 6 km. and have serious effect on predicting the performance of tropospheric propagation.

As the earth's atmosphere is in a constant state of motion with respect to the earth, small irregularities or eddies occur. These irregularities occur in 'blobs' that are large compared to the wavelength used in scatter communications. Thus they present a different index of refraction from that of the surrounding medium. The changes in the refractive index are a result of the variations in the dielectric constant. These variations are as a result of the turbulent air motion and the water content.

This abrupt change in the index of refraction produces a 'scattering' of the electromagnetic wave. However, most of the propagated energy continues in the forward direction, although enough energy is scattered towards the earth to be usable. Effectively, the blob has re-radiated the signal towards the earth. The signals received will be affected by the actual conditions of the atmosphere, since scatter depends upon the turbulences in the atmosphere. The number of blobs in the volume common to both the transmitting and receiving antenna beams (Fig. 4) determine the amplitude of the signal received. The scatter model shown is idealized to indicate the path geometry. Notice that both the receiving and transmitting antennas are directed at the horizon. A certain volume of the atmosphere is common to both antennas. It is within this volume that the scatter phenomenon takes place.

It can be proved mathematically that the scatter angle θ , in Fig. 4, is the most important factor in determining the received power. The angle θ , represents the angle between a ray from the transmitter antenna and one to the receiving antenna. If the scatter angle is increased, the received power falls off rapidly. With wide-beam antennas, the effective scatter volume is increased, but the effective power received is decreased. With narrow beam antennas, the entire common volume contributes significantly to the received signal. For each ray of the entire beamwidth considered, a slightly different angle exists. It is necessary to sum up the infinite number of rays over the volume to obtain

the sum of the individual contributions. It is correct to assume, therefore, that the scatter radiation comes from an infinite number of small scatterers within the common volume and that each scatterer effectively reradiates according to the amount of energy impinging upon it.

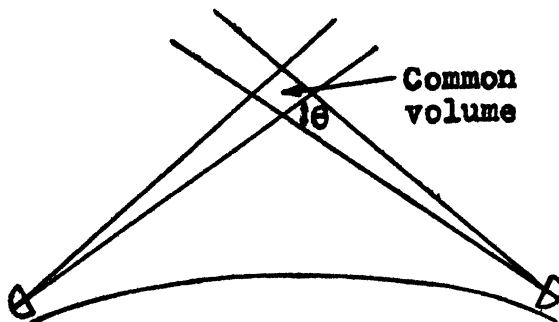


Fig. 4

Path of tropospheric beams

3. Scatter characteristics

Regardless of the true mechanism of propagation, much is known concerning the characteristics of the microwave energy field propagated beyond the horizon. It has been learnt through observation of a large mass of empirical data collected from operational tropo links.

Firstly, it is known that the average amplitude of the field propagated beyond the horizon is greatly attenuated with respect to the transmitted field. The amount of attenuation can be calculated as a function of the angular distance between the transmitting and receiving sites.

Secondly, the amplitude of the received field varies substantially with time over a given path. For convenience these amplitude variations are separated into short-term and long-term distributions. Short-term amplitude time distributions are those measured over periods shorter than a few minutes. The long-term distribution represents the variation of hourly medium levels over a longer period of time—usually a month, a season, or a year. Determination of parameters and design are usually based on the worst propagation month of the year—usually February or March in the northern hemisphere.

Thirdly, it is known that when a wide band of the frequency spectrum is utilized for the transmission of intelligence, any existing multipath propagation introduces a factor that is evidenced as a signal distortion. It is a result of phase differentials that appear across the frequency band when signals are received over the longer path of the multipath routes as well as over the direct path. This distortion places an upper limit to the band width that can be transmitted successfully.

4. Scatter capabilities

Tropospheric scatter may be called upon to transmit any type of signal, although voice transmission is usually used. Normally, some teletype will be

transmitted using equipment that feeds four teletype channels into one voice channel. With modifications to certain equipment, facsimile, telemetry, video, and other types of communications may be transmitted and received.

5. Atmospheric consideration

The atmosphere that surrounds the earth is stratified, and all the strata have varying characteristics and relationships. Scattering blobs are actually relatively small volumes in space at which the index of refraction varies from the surrounding atmosphere. Usually they are caused by meeting of moisture laden air masses and warm air masses, which affects a change in refractive index. Rain, snow and similar weather conditions do not have persistently noticeable direct effect on VHF and UHF waves.

Cosmic noise has an effect on radio propagation. Cosmic noise encompasses radio interference caused by the eruptions from sun and stars. Eruptions cause an abnormal ionization of the strata affecting reflection and refraction conditions necessary for propagation. It is impossible to predict accurately the nature of these disturbances or even the phenomena. But, at the frequencies used in tropospheric scatter, cosmic noise and cosmic interference are usually so small that they do not interrupt communications. Man made noise at the tropospheric scatter frequencies are usually of some consequence, however, and must be considered in the design and location of scatter systems. Usually the least costly and simplest solution is to locate the system away from vehicular traffic, aircraft, machinery, electrified fences, power lines and other sources of man-made interference.

6. System considerations

All high quality, long-distance multichannel communication systems have two requirements: (i) reliability; and (ii) delivery of a favourable SNR (signal-noise ratio) to the user. The signal components usually are amplified, as required to overcome the various losses in the system. The big problem for the communicator is the accumulation of noise. Every time the signal is processed there is some contribution to noise, which adds on a cumulative basis. The result is that long-haul systems require sharp attention to the details of noise accumulation if the resulting SNR is to meet requirements.

Signal-noise ratio is a complex subject, and a technical discussion would be out of place in this type of paper. For high toll quality telephone voice circuit in multichannel system it is usually prescribed that the minimum SNR of 45 dB be delivered to the user at the termini of 10,000 km. system, with the noise contributions from individual spans pro-rated on the basis of distance as a percentage of 10,000 km.

It was pointed out previously that tropospheric forward signals are subject to amplitude time variations, separated into short-term and long-term distributions. In practice, the two types of signals fading are not compensated individually, since the resultant fading is a combination of both types, usually

referred to a monthly median level. Methods known as diversity techniques have been developed to counteract this fading and afford the prescribed propagational reliability.

Diversity can be defined as the utilization of more than one independent and uncorrelated transmission path over a single span of tropo to afford greater reliability than that provided by a single transmitter and receiver at each end. In each type of diversity now in common use, certain additional equipment is required.

One of the most effective methods is known as 'space diversity', in which two antennas, separated in space by 100 wavelengths or more, are used to receive the signals and reduce the effect of fading, since signals separated in space by this distance show a complete absence of correlation (Fig. 5).

Another method in wide use is known as 'frequency diversity' wherein two frequencies, separated by about 1-10% depending upon the frequency band in use, are transmitted over the span from the transmitting to the receiving station. Here, again, there is a minimum of correlation between signals received on the two frequencies. As an example, a separation of 10 to 12 M Hz at a frequency of 1,000 M Hz should be adequate (Fig. 6).

Other types of diversity, which are little used at the present time include circular polarization and differences in azimuth orientation of antennas (angle diversity).

Although space and frequency diversity may be utilized independently (dual diversity), both may also be used simultaneously to afford quadruple diversity. For high reliability circuit requirements and in applications where the span length otherwise might produce a marginal circuit, quadruple diversity is the preferred solution, despite additional equipment necessary. It is therefore used in the vast majority of fixed station systems installed till now (Fig. 7).

7. Tropos system parameters

The logistical and engineering requirements of a forward tropospheric scatter facility are little different from those of most radio systems. The scatter equipment requires 130 to 400 kVA of power, the amount depending upon the type of system that is chosen. As with similar facilities, high level land areas are best suited for installation and operation of this type of communications.

Each tropo communication system must be individually designed, because the operating command has specific requirements. The most important consideration usually decided by the operating command, is the reliability of the system. Two factors control the design of the system reliability. A breakdown of the equipment will lower the reliability of the service, but this condition may be minimized by providing dual equipment. The second factor, which is completely a design function is propagation reliability.

The system is generally designed with enough flexibility to obtain a reasonable degree of reliability. Over a 500-km. path, reliability of 99.99% may

be attained, although certain factors may limit the number of voice channels or require high power and large 'dish' antennas. The important fact, however, is that this type of communications may be achieved. When the reliability requirement is lower, the number of voice channels may be increased and the use of smaller antennas and lower power may prove sufficient. Reliability is a function of path distance and path conditions, then, to which all computations and design requirements are made to conform.

For non-strategic voice transmission, 95% reliability is considered adequate, this lower reliability usually results in considerable saving. For missile guidance system, 95% reliability could prove disastrous; therefore, such a system requires a higher reliability. The reliability is determined from the type of service required. Various bandwidths and numerous channels can be used. Many special systems exist today in which the propagational reliability may vary from 99.9% to 99.99% for 120 to 300 voice channel capacity over path lengths of 150 to 300 km. There are also systems of 48 to 96 voice channels with the same reliability operating upto span lengths of 500 km. and a few circuits that span 500 to 1,000 km. but are limited to 12 to 48 channels.

The tropo terminal equipment is compatible with voice systems that terminate in telephone line pairs and use 600-ohm and 135-ohm line circuits for ring down.

8. Antennas

Because of the high gain requirements encountered in troposcatter transmission, highly directional antennas must be used. They usually take the form of large parabolic reflectors with horn feeds. The larger the parabolic surface the higher the gain until a point of diminishing returns is reached.

Two basic antenna systems are associated with tropo systems now in use. A wide variety of communication facilities is provided by the combination of these antenna systems with other equipment. It is possible to use either a 28-ft. or a 60-ft.-parabolic reflector illuminated by either a vertically or a horizontally, polarized feed horn. If two reflectors are used, a vertically polarized feed horn to one reflector and a horizontally polarized feed horn to the other will provide a higher order of diversity. However, this necessitates cross-polarized feed horns for reception at both terminals.

Due to narrow beam width of the antennas, it is necessary that the equipment be made capable of changing both elevation and azimuth.

9. Advantages of Tropo

Tropo has been developed over the past ten years into a highly successful method of radio communication which offers certain advantages not possessed by other modes. These are :

- (i) It provides high-grade multi-channel service over distances between 100 to 1,000 km. in a single span, thus reducing the number of stations or terminals required in a line-of-sight system;

- (ii) With a properly designed system it will offer a circuit of high propagational reliability on a year round basis. This reliability compares favourably with that of line-of-sight circuits and is generally far superior to that afforded by current high-frequency techniques;
- (iii) It can be utilized in rugged or otherwise inhospitable terrain where it is impracticable or impossible to provide other means of communication; and
- (iv) It provides a high degree of spectrum utilization while simultaneously minimising frequency allocation problems incident to radio interference in a high density location.
- (v) It offers a relatively high degree of security as compared with other methods of communication. Radio interference, deliberate or otherwise, is reduced to the minimum unless the interfering transmission is within the beam and range of any one station in the tropo system. Further, there are in a Tropo system fewer stations that are subject to jamming or link impairment. From a physical viewpoint, the surreptitious destruction of a tropo link is more difficult than the cutting of a submerged cable or unattended line-of-sight span. As for security obtained in a tropo link and that obtainable in a satellite circuit, it remains to be seen whether latter can be developed to the point where destructive radio interference or radio interception can compare with the security achievable on Tropo system.

Undeniably and under certain conditions, tropo offers certain over riding advantages. When the cost of Tropo system is considered, these advantages must be weighed against the cost of other systems that may lack the advantages peculiar to tropo.

10. Present installations

Operational system route distance now in commission	80,160 km. with
or being installed	... 257,000 voice channels
Experimental route distance now in commission	... 2,500 km. with
	60,000 voice channels
Average route distance per system	... 1,027 km.
Average voice channel km. per system	... 52,800
Average number of tropospans per system	... 4.1
Average length per span	... 251 km.

11. Tropo costs

In general, it cannot be said categorically that tropo is either cheaper or more expensive over the long haul period than any other mode of communication. It all depends on the conditions surrounding any individual project. It is practically impossible to compare tropo channel/km. costs with those of other communications, since no firm basis for comparison exists. The future development of lower cost solid state tropo equipment for commercial and common carrier use will go far towards furnishing a more definitive answer to the cost problem.

12. Correct equipment trends

The present trends in the current development of tropo equipment can be summarized as given below:

- (i) Completion of transformation of all tropo equipment from tube types to solid state, though still retaining power tubes in power amplifiers;
- (ii) Further efforts to decrease size, weight, and main power requirements for solid-state equipment. These efforts include development of relatively high output powers utilizing only solid-state devices, thus eliminating power tubes;
- (iii) Additional development to reduce size and increase efficiency of Klystron tubes. Utilization of travelling wave tubes in power amplifiers where economical;
- (iv) Investigation of various new types of power tubes;
- (v) Development of cheaper and lighter antennas, particularly for transportable and technical Tropo equipment, where weight storage, and ease of assembly in the field are paramount;
- (vi) Investigation of alternatives to parabolic antennas;
- (vii) Advances in further modularization of solid state equipment, including use of integrated circuitry, to reduce size and weight and increase accessibility;
- (viii) Further development of automatic fault indicator and performances monitoring equipment to facilitate maintenance and reduce maintenance personnel;
- (ix) Development of a light weight, easily transportable Tropo terminal which better meets the tactical requirements of the military and which can be set up in the field in a minimum time. It must be easily transportable by all types of helicopters.
- (x) Development of a reliable and relatively cheap type or types of equipment, conforming and capable of incorporation into national communications systems without degradation of the system; and

- (xi) Further studies and investigations of the Tropo-propagation mechanism to determine its exact nature and behaviour, and thus afford designers a stronger base for development of improved equipment and perhaps better bandwidth for increased channel capacity.

13. The future of Tropo

For commercial or common-carrier purposes, there appear to be many nations that are beginning to realize the value of Tropo in places where the nature of terrain presents obstacles and, in addition, where there is no need for circuit drop requirements at intermediate points between stations. It can be assumed that during the next ten years there will be a steady, if limited demand for common-carrier Tropo systems.

The continued and additional employment of new and advanced types of Tropo for military purposes will, of course, depend upon the international situation. As pointed out previously, the accent is now on development and procurement of light tactical types for utilization in jungle, guerrilla, or amphibious warfare, with some additions or upgrading of existing or planned strategic systems.

There is no doubt that Tropo is here to stay, and will occupy its own niche in the array of various types of communication systems. Under certain conditions its employment is now indispensable; the future may well add to these conditions to augment its value to later use in both worldwide and domestic communications.

14. References

1. F.E. Terman. 'Radio Engineers' Handbook'.
2. 'Electronic Circuit Analysis'. United States Air Force Manual.
3. G.L. Grisdale and D.A. Paynter. 'A Tropospheric Scatter Link Over a 200 Mile Path Point-to-Point'. *Telecommunication*, October 1960.
4. P.F.J. Foakes. 'The Potentialities of Thin Line Tropospheric Scatter'. *Point to Point Telecommunication*, October 1965.
5. Gunther. 'Tropospheric Scatter Communications'. *Institute of Electronics and Electrical Engineers, Spectrum*, September 1966.

CASSEGRAIN AERIAL***C.R. Ramachandran Nair***Non-member**Instructor, Radar Engineering Wing, EME School (South),
Secunderabad***Summary**

The SHF aeriels based on the optical Cassegrain principle are found to be somewhat superior to conventional paraboloidal aeriels. For the same performance they are cheaper and smaller in size. The design of the complete system is simpler and the assembly is rugged. With these advantages Cassegrain aeriels should replace existing designs of paraboloids.

1. Introduction

The need for high performance, low cost aerial and feeder system was appreciated from the start of the development of microwave multichannel telephony and the satellite communication. In the latter case the size reduction is also of great importance. The normal paraboloid aeriels used in radar sets did not meet the requirements fully.

This paper discusses the principle of Cassegrain type of paraboloidal aeriels that are found to satisfy the requirements. A comparison table is provided at the end of the paper for a Cassegrain aerial and an ordinary horn reflector, both designed for a frequency in the range of 6 kilomegacycles per sec.

2. Theory of Cassegrain aeriels

In the design of microwave aeriels, attempts were made to use many of the principles in optics. The Cassegrain aerial is one such adaptation of the optical Cassegrain principle. In the Cassegrain telescope (Fig. 1), light proceeding to first real image I, is intercepted by a hyperbolic mirror M, whose focus coincides with that of the objective and made to pass through a hole in the centre of the objective to form the real image, I. By this arrangement the focal length is folded and the effective focal length is large for small physical size. This increased effective focal length in comparatively smaller space helps in reduction of dimensions.

This method is adapted in the case of Cassegrain aeriels also. The principal advantages are flexibility in design, improved performance in terms of efficiency, polar diagram and band-width and simplicity of primary feed design.

*Presented at the Symposium on 'Modern Electronic Communication Techniques' held in Hyderabad on August 26, 1967.

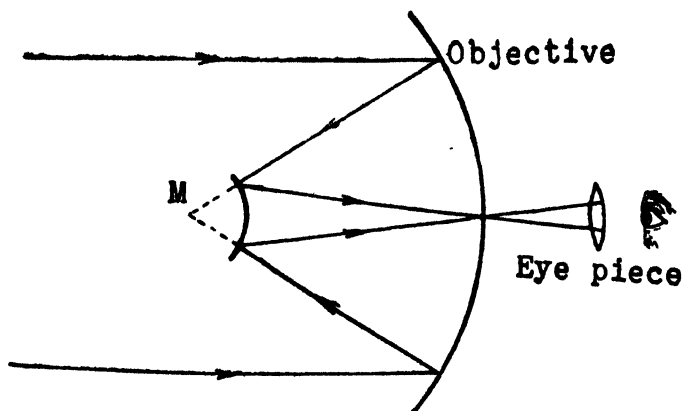


Fig. 1

Principle of a Cassegrain telescope

3. Principle of Cassegrain aeriels

The feed is located at the vertex of the parabolic reflector and a hyperbolic sub-reflector is located in front of the parabola between vertex and focus (Fig. 2). Parallel beam falling on the parabolic reflector is made convergent and brought to focus F , if the hyperbolic reflector were absent. In the presence of the hyperbolic surface, this reflects this to the point, F' . The virtual image at F formed by the parabolic surface serves as the object for the hyperbolic surface which produces the real image at the feed, F' .

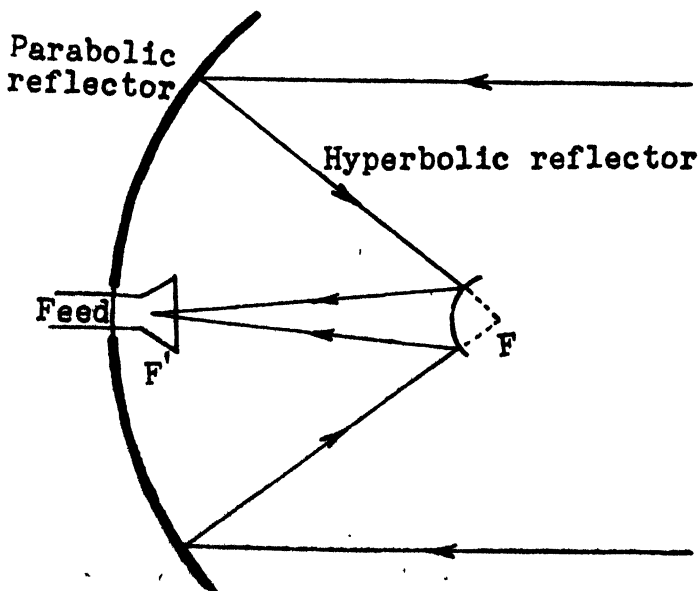


Fig. 2

Principle of a Cassegrain aerial

The points, F and F', are the conjugate foci of the hyperbolic sub-reflector. Convergent spherical waves centred at F and incident on the hyperbola will be reflected as a second set of convergent spherical waves centered at F'. This property it there for any hyperbola with foci, F and F'. A large number of such hyperbolic surfaces, which will be suitable as a sub-reflector, can be obtained.

Let us consider the action of the sub-reflector as a hyperbolic mirror which images the feed to a point behind the sub-reflector at the focus of the hyperbola. The magnification of a hyperbolic mirror is

$$(\epsilon + 1) (\epsilon - 1)$$

where ϵ is the eccentricity (the magnification is also equal to the distance from sub-reflector to real focus divided by the distance from the sub-reflector, to the virtual focus). The eccentricity of the hyperbola is always greater than unity (this is the ratio of the distance between the two foci to the constant difference between the two focal radii). The effective focal length of the Cassegrain aerial is equal to the distance between F and F' times the magnification. Magnification will be between 2 and 5 for practical structures, for which eccentricity is between 3 and 1.5.

4. Primary feed

The easiest form of primary feed is a circular horn. As in any other radiator, its dimensions in terms of a wavelength determine the beam width, the beam width decreasing as the size of the horn increases.

As far as possible, all the energy radiated by this horn must be reflected by the hyperbolic sub-reflector, i.e., the spillover of energy must be minimum. This requires that the sub-reflector must intercept energy upto about 10 decibels (dB) below the maximum. This then means that if the horn size is reduced, the angle subtended by the sub-reflector at the horn will be large and *vice versa*. If this reflector is not to interfere much with the parabolic reflector, the size cannot be large. The results obtained on the basis of principles of geometric optics do not agree completely with the practical results because the ratio of diameter of the sub-reflector to wavelength is not large enough.

5. Hyperbolic sub-reflector

The image of the primary horn produced by the reflector serves as the basic feed for the paraboloid. A convex hyperbolic sub-reflector causes immediate divergence of the signal and consequently reduces the energy reflected back into the primary feed. The amount of energy reflected to horn is greatest if the feed is close to the sub-reflector. The reflection can be reduced by proper matching techniques. The normal matching methods cause cancellation of energy reflected towards axis and is effective over a broad band. With this matching, the region of strong illumination of parabolic reflector becomes an annulus in which the maximum field strength occurs at an angle from the axis. This pattern of illumination leads to high efficiencies but also increase the level of first side lobe.

If the sub-reflector size is increased, the axial length of the antenna can be reduced, because in that case the sub-reflector will be nearer to the parabolic reflector. But, with this the aperture blocking also will be more and this is not desirable. The blocking of the aperture can be reduced by using a smaller sub-reflector. But then this will be at a greater distance from the parabolic reflector and the mechanical structure becomes complicated. Thus, the choice of the sub-reflector size must be a compromise.

It is a known fact that the phase errors are reduced proportionately with the size of the basic feed of the paraboloid. With a convex hyperbolic surface, the virtual image of the horn formed will be reduced in size compared to the actual horn. The size reduction varies with the hyperbola as shown (Fig. 3).

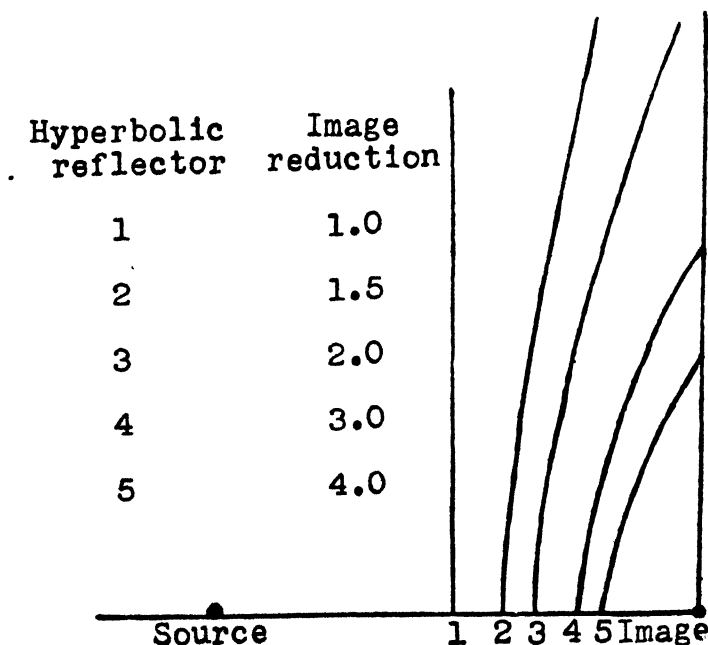


Fig. 3

Reduction of image in a hyperbolic reflector

The horn feed and the sub-reflector can be sealed against moisture (in a perspex or fibreglass housing) and is robust enough to withstand any rough treatment occurring during transport and assembly. Due to wide aperture of the paraboloid, the horn lies inside the rim of the dish and is not exposed to damage from falling ice (Fig. 4).

6. Performance comparison

Efficiency of a Cassegrain aerial is about 60% which can be achieved with a conventional paraboloid also. But in the latter case the size of the aerial (especially the focal length) becomes very large. Reflection from the Cassegrain aerial designed for 6 kilomegacycles per sec. band is found to be less

than 2% from 5.9 to 6.4 kilomegacycles per sec. A horn reflector aerial is better in this respect having reflection less than 1% over a band of 4 to 11 kilomegacycles per sec. Cassegrain aerial is circularly symmetrical and therefore the reflecting surface can be made by spinning it in one piece. This technique minimizes tool costs. This method is satisfactory up to a diameter of 4 m. and avoids all problems of sealing joints. At present manufacturing costs for a horn reflecting aerial are 3 to 4 times those of a Cassegrain aerial.

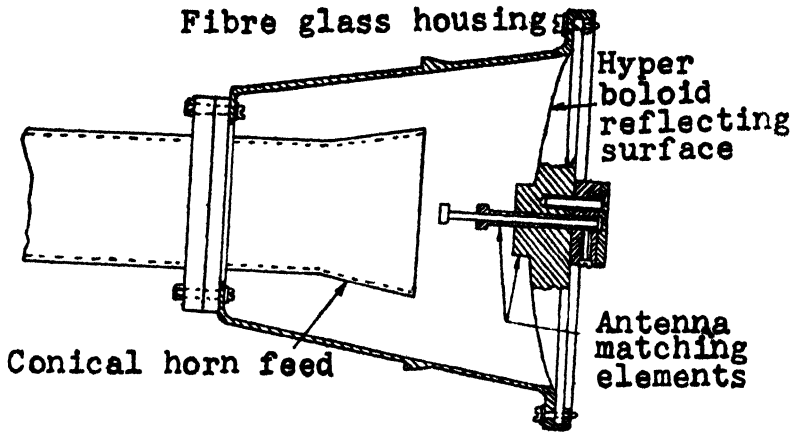


Fig. 4

Horn feed in a fibre glass housing

An important advantage of a Cassegrain aerial is that when it is used at a place where various routes are converging, like in a city centre. For a 1,800-channel system operating on the same frequency, it is estimated that aerial discrimination of 65 dB is required. In a Cassegrain aerial two routes can operate at same frequency and polarization at angles greater than 85° .

7. Cassegrain aerial for single polarization

One drawback with the Cassegrain aerial discussed is that the sub-reflector blocks the parabolic aperture. This can be reduced by using a grating of wires as shown (Fig. 5) called 'polarizing screen'. This polarizing screen favours a single-plane of polarization to which it is transparent, and on receipt, only this plane polarized wave passes through to the plane converter.

If the sub-reflector has horizontal grating of wires, this will pass vertically polarized waves with negligible attenuation, but will reflect horizontally polarized wave sent by the feed.

The horizontally polarized wave reflected from the polarizing screen is incident on the plane converter kept in place of the paraboloid and at the converter this is shifted through 90° in space. The screen is transparent to this reflected energy from the plane converter.

The polarizing screen consists of parallel strips or rods, with spacing small compared to wavelength for which it is considered. For a wave with polarization in the plane of the rods, the rods are in the same plane as the electric field and act as a reflecting surface because they are closely spaced, screen may be either flat or of any shape as required. The plane converter consists of a number of parallel slats mounted on a reflecting surface. The slat depth is $\frac{\lambda}{4}$ for the design wave length and the slats are at an angle of 45° to the accepted plane of polarization.

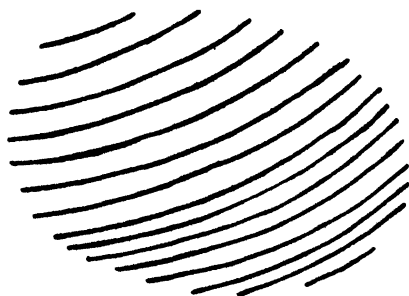


Fig. 5

Cassegrain aerial as a 'polarising screen'

Cassegrain aerial with single polarization is very useful because two channels operating at same frequency and side by side can have very good isolation if operated at an angle of about 15° and for different polarization. But manufacture of main and sub-reflectors are quite costly.

Comparison of Cassegrain and horn reflecting aerials

Parameter	Cassegrain	Horn reflector
Gain, dB ...	45	45
Radiating area, m. ² ...	11.2	10.2
Windage area, m. ² ...	11.7	17.8
Height, m. ...	3.8	7.6
Width, m. ...	3.8	4.3
Depth, m. ...	1.5	3.6
Weight, kg. ...	417	771
Operating band, kilomegacycles per sec. ...	5.9-6.45	3.8-4.2 5.9-6.45 10.7-11.7

8. References

1. P. W. Hannan. 'Microwave Antennas Derived from the Cassegrain Telescope'. *Transactions of the, Institute of Radio Engineers* vol. AP-9 no. 2, March 1961, p. 154.
2. Ware and Stemp. 'Microwave Radio System for Multichannel Telephony and Television in 64 Gigahertz Range: Part 4—Cassegrain Antenna'. *Electrical Communication*, vol. 40, no. 2, 1965.
3. L. Schwartzman and R. W. Martin. 'A Monopulse Cassegrain Antenna'. *Institute of Radio Engineers, Inter Convention Record*, vol. 8, pt. 1, 1960.

FREQUENCY SYNTHESIS IN COMMUNICATION EQUIPMENT*

P.R. Santhanam

Non-member

Lecturer, Communication Engineering Wing, EME School (South), Secunderabad

Summary

In the vehicle-borne communication systems, wherein high power transmitters and sensitive receivers operate simultaneously and in close proximity, it is imperative that the spurious signal should be at least 100 dB below the wanted signal, to avoid mutual interference. This paper states the problem of frequency stabilization, and illustrates the principle of direct frequency synthesis by analysis of a working circuit. However, it concludes by comparison that a pure VFO output is characteristic of a partial synthesizer which uses a phase-locked oscillator as its output frequency generator.

1. Introduction

In our country, radio communication is being used on a large scale by military, police and other services. Within a short time we can expect the HF and the VHF bands to become overcrowded. Hence, it will be very essential to achieve good frequency accuracy in transreceivers so as to use every available channel in a given frequency spectrum. Accurate frequency control is also needed in S.S.B. transmitters and receivers. Any frequency error in pilot carrier S.S.B. system will increase the AFC capture problem and in a suppressed carrier system it results in a frequency offset of the demodulated signal thereby decreasing intelligibility.

To achieve good frequency stability, crystal oscillators may be used. Most crystal oscillators, without means for temperature control and uncompensated, can provide frequency accuracy of 0.005% over a range of -55° to 105°C . Much better accuracies are possible when the temperature range is reduced, e.g., at room temperature or when temperature compensation is used. But where the range of communication is large, as for example, in the case of a transreceiver covering a frequency range of 1 to 30 megacycles per sec. with 1 kilocycles per sec. channel spacing 29,000 crystals will be needed if a separate crystal is required for each channel. This method is impractical. Instead of this arrangement, it is possible to generate the desired frequencies by successive addition and subtraction of frequencies derived from crystal oscillators or from combinations of frequency standards and frequency dividers. The output frequencies are in effect synthesized from a number of constituent parts. An example will illustrate the method.

*Presented at the Symposium on 'Modern Electronic Communication Techniques' held in Hyderabad on August 26, 1967.

2. Direct frequency synthesizer

Fig. 1 illustrates the block diagram of a direct frequency synthesizer used in Stromberg Carlsen transreceiver SC 900A. Four groups of frequency injection signals are fed into mixers and filters. They are marked I, II, III and IV in the figure. The dials can be set for any output frequency within the range of 1.0 to 30 megacycles per sec. in 1 kilocycles per sec. steps.

The upper line of mixers is actually in the signal path of the receiver (Fig. 2). This follows the usual practice in which the signal mixers are used to provide heterodyne points at which the desired increments of frequency are injected progressively as the signal is translated up or down in frequency. As is clear from the block diagram the principle of operation is one of successive mixing and filtering to achieve the desired output frequency.

It is important to remember that mixers produce spurious modulation products in addition to the major sum and difference frequency components. The output of mixer contains the input frequencies, harmonics of input frequencies and the sum and difference of these harmonics in all sorts of combinations. Though the output circuit is tuned so as to select only the sum or the difference frequency component, it is impossible to attenuate completely those frequency components which coincide with the desired frequency or one very near to it. Experiments performed on a balanced multiplicative mixer system under best operating conditions of bias and input signal levels show that there are eight harmonics and thirty-two products which are within 80 dB of the desired ($f_2 \pm f_1$). This is shown in Table 1. It is, however, required to suppress the spurious frequencies to a level more than about 80 dB below the desired signal output. So, in choosing f_1 and f_2 , it should be borne in mind that their spurious modulation products are not nearly coincident with the desired frequency. The choice of f_1 and f_2 becomes difficult if the requirements of purity of output waveform are stringent.

It should also be borne in mind that the range of frequencies derived from a harmonic generator is limited; the stability of the tuned circuits limit the number which can be cascaded to discriminate between high order adjacent harmonics. Wadley has suggested a method of selecting high order harmonics (Fig. 3) and this is now being used in a number of communication equipment. The drift cancelled oscillator should be set very close to 21st, 22nd, 23rd or 24th harmonic to get 15th, 16th, 17th, or 18th harmonic respectively. To illustrate the function, let us assume that the 16th harmonic is desired. The drift cancelled oscillator is set close to 22nd harmonic. The output of mixer 1 will contain a difference frequency component close to 6 megacycles per sec. and this will be passed on by the narrow band filter to mixer 2, to which the output from the drift cancelled oscillator is also fed. The difference frequency passes through the BP filter and is the desired harmonic. If the frequency of the drift cancelled oscillator increases by a small amount Δf the first mixer output will decrease by Δf . However in the second mixer the Δf cancels out and hence drift free output is obtained.

Table 1
Measured attenuation values of modulation products in relation to $(f_2 \pm f_1)$ in an approximately balanced system. The input frequencies are assumed to be pure sine waves.

f_1	8dB	f_2 $f_2 + f_1$ $f_2 - f_1$	30dB 0dB 0dB	$2f_2$ $2f_2 + f_1$ $2f_2 - f_1$	30dB 37dB	$3f_2$ $3f_2 + f_1$ $3f_2 - f_1$	33dB 49dB	$4f_2$ $4f_2 + f_1$ $4f_2 - f_1$	58dB 68dB
$2f_1$	35dB	$f_2 + 2f_1$ $f_2 - 2f_1$	38dB	$2f_2 + 2f_1$ $2f_2 - 2f_1$	47dB	$3f_2 + 2f_1$ $3f_2 - 2f_1$	69dB	$4f_2 + 2f_1$ $4f_2 - 2f_1$	72dB
	42dB	$f_2 + 3f_1$ $f_2 - 3f_1$	63dB 65dB	$2f_2 + 3f_1$ $2f_2 - 3f_1$	68dB 66dB	$3f_2 + 3f_1$ $3f_2 - 3f_1$	73dB 72dB	$4f_2 + 3f_1$ $4f_2 - 3f_1$	79dB 78dB
$4f_1$	57dB	$f_2 + 4f_1$ $f_2 - 4f_1$	60dB 58dB	$2f_2 + 4f_1$ $2f_2 - 4f_1$	72dB 70dB	$3f_2 + 4f_1$ $3f_2 - 4f_1$	77dB	$4f_2 + 4f_1$ $4f_2 - 4f_1$	78dB

3. Alternative approach to direct synthesis technique

In the direct frequency synthesizer discussed above, the frequency accuracy of any output generator is the same as that of the frequency standard. But mixers produce spurious frequencies and even with complex filters it is not possible to suppress these frequencies and generate signals of absolute purity. In practice these spurious products are of too high a level for a communication equipment except where narrow frequency spectrums meet the communication requirements.

An alternative approach to the direct synthesis technique is to derive the required frequency from a locked oscillator by a partial synthesis process.

Fig. 4 shows the frequency synthesizer system (FSS) used in a transceiver operating in the frequency range of 30 to 75.95 kilocycles per sec. This range is in two bands. The channel spacing is 50 kilocycles per sec. The FSS is used for both transmission and reception. The block diagram shows that a closed loop automatic phase control system is used to lock the variable frequency oscillator (VFO).

By mechanical differential motion the VFO tuning shaft is set to the required position corresponding to the selected frequency setting. This is done by the kilocycles per sec. and megacycles per sec. switches on the front panel. For illustrative purposes, the frequencies at different points in the synthesizer are shown for two received frequencies 33.10 megacycles per sec. (low band) and 68.45 megacycles per sec. (high band). While transmitting the frequencies will be 50 kilocycles per sec. less at these points unless otherwise stated.

The frequency range of VFO is 41.5 to 64.45 megacycles per sec. The VFO generates 11.5 megacycles per sec. above the carrier frequency on low band and 11.5 megacycles per sec. below the carrier frequency on high band. The VFO output passes through two isolating stages, FSS buffer, and FSS 1st mixer buffer. During transmission, the VFO frequency is shifted 50 kilocycles per sec. lower than during reception.

The output of 1 megacycles per sec. crystal oscillator is fed to the pulse generator where it is distorted. The output of the pulse generator is a frequency spectrum ranging from 1 megacycles per sec. to 12 megacycles per sec. in 1 megacycles per sec. increment. The frequency spectrum remains unchanged during transmission.

The pulse generator output is applied to FSS first mixer. The beat frequencies of FSS first mixer are applied to 53 megacycles per sec. filter which has a band width of 2 megacycles per sec. centred at 53 megacycles per sec. Hence the sum or the difference frequency which lies within this range will be passed by 53 megacycles per sec. filter to FSS second mixer.

The output of the 100 kilocycles per sec. interval oscillator ranges from 46.85-47.75 megacycles per sec. in 100 kilocycles per sec. increments. This is independent of receive-transmit condition. The specific frequency depends on the frequency selected by kilocycles per sec. tuning knob; that is whichever

50 or 100 kilocycles per sec. channel point is selected. If the channel point selected is in terms of 100 kilocycles per sec. the 100 kilocycles per sec. interval oscillator frequency is obtained by adding 46.85 megacycles per sec. to the specific 100 kilocycles per sec. channel point. If it is 50 kilocycles per sec. channel point, 46.9 megacycles per sec. should be added to the specific 50 kilocycles per sec. channel point to arrive at the frequency of 100 kilocycles per sec. interval oscillator. Only in the case of 95 megacycles per sec. channel point, this relationship does not hold good. In this case the oscillator frequency is 46.85 megacycles per sec. The interval oscillator frequencies for various setting of tuning knob is given in Fig. 4.

The output of the second mixer is the difference between the two input frequencies. It is easily seen that the FSS-IF will always be 5.65 megacycles per sec. at 100 kilocycles per sec. channel point and 5.60 megacycles per sec. at 50 kilocycles per sec. channel point. The values are 50 kilocycles per sec. lower during transmission.

The IF-signal after amplification and limiting in FSS-IF amplifier is applied to the frequency discriminator and to the phase comparator (Fig. 5). The output from 50 kilocycles per sec. interval oscillator is also applied to phase comparator. The 50 kilocycles per sec. interval oscillator generates one of the three frequencies 5.55 megacycles per sec., 5.60 megacycles per sec., or 5.65 megacycles per sec. If the kilocycles per sec. tuning knob is set in terms of 50 kilocycles per sec. the oscillator frequency will be 5.60 megacycles per sec. and if the knob is set in terms of 100 kilocycles per sec. the oscillator frequency is 5.65 megacycles per sec. During transmission, the frequencies will be 50 kilocycles per sec. lower. The output of 50 kilocycles per sec. interval oscillator which serves as reference is fed to the phase comparator. The phase comparator also receives signal from FSS-IF amplifiers.

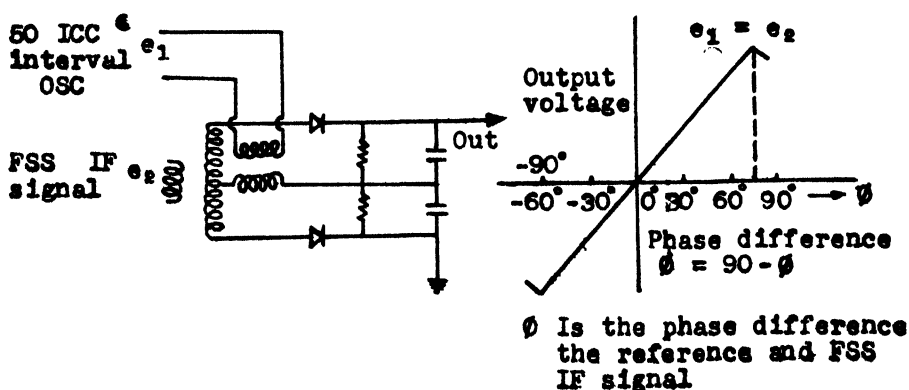


Fig. 5

The output of the phase comparator is a D.C. voltage proportional to the phase difference between the reference signal and FSS-IF signal. This D.C. error voltage which is part of the automatic phase control (APC) voltage is

applied to the APC modulator. The APC modulator is a varicap (voltage variable capacitance diode) device. Its capacitance value changes in accordance with the D.C. error voltage applied to it. Since this is across the tuned circuit of the VFO, the frequency of VFO is altered accordingly. Hence the error signal from the phase comparator causes the VFO to phase lock to the required frequency.

The capture range of the APC loop is limited. If VFO drifts too far from the correct frequency, then the phase discriminator becomes ineffective and cannot bring VFO to the correct frequency. The capture range is also reduced by insertion of the anti-hunt network.

To extend the capture range, a frequency discriminator is used in addition to the phase discriminator. Since the sensitivity of the frequency discriminator is low near the centre frequency, it has little effect there and operation is governed in this range by the phase discriminator. Beyond the capture range of the discriminator, however, the frequency discriminator delivers the required voltage to reduce the error to a point where the phase discriminator can take control.

The necessity for a pure VFO output is particularly stringent for the receiver in a communication system where the spurious signal should be at least 100 dB below the wanted signal. This is especially required to avoid mutual interference in vehicle borne installations which call for high power transmitters and sensitive receivers to operate simultaneously and in close proximity. A pure output is characteristic of the partial synthesizer described above which uses a phase-locked oscillator as its output frequency generator.

4. References

1. H.J. Finden. 'Developments in Frequency Synthesis'. *Electronic Engineering*, vol. 25, no. 303, May 1953, p. 178.
2. H.J. Finden. 'The Problem of Frequency Synthesis'. *The Journal the British Institution of Radio Engineers*, vol. 21, no. 1, January 1961, p. 95.
3. R.T. Cox and E.W. Pappenfus. 'A Suggestion for Frequency Conservation'. *Transactions of the Institute of Radio Engineers*, December 1956.
4. A.F. Evers. 'A Versatile Digital Frequency Synthesizer for Use in Mobile Radio Communication Sets'.
5. S. Krishnan. 'Diode Phase Detectors'. *The Electronic and Radio Engineer*, vol. 36, no. 2, February 1959, p. 45.
6. E.W. Pappenfus, W.B. Bruene and E.O. Schoenike. 'Single Side Band Principles and Circuits'. *McGraw-Hill Book Co., Inc.*, 1964.

A PITCH FINDER CIRCUIT FOR USE IN VOCODERS***P. Baskaran***Non-member**Department of Electrical Engineering,
Indian Institute of Technology, New Delhi***Summary**

A pitch finder circuit has been developed to find instantaneously the pitch of voiced sounds. The circuit utilizes the fact that a voiced speech wave contains a large peak at the onset of each pitch period. The circuit consists of a chain of amplifiers, each one of them acting like an instantaneous expander, expanding the larger amplitude components while suppressing the smaller ones. Two monostable circuits are added to the chain of amplifiers, to shape the output and provide error free operation in enabling the circuit to provide one rectangular pulse for each pitch period of the input wave. An AGC amplifier at the input ensures optimum performance of the circuit under varying speech levels.

1. Introduction

Speech can be broadly classified into two classes of sound, voiced and unvoiced. Voiced sounds are produced by vibratory movement of the vocal cords interrupting the smooth flow of air from the lungs resulting in a transmission of energy in the form of a series of periodic impulses, to the vocal cavities. The waveform of these pulses gets modified by the resonances of vocal and nasal cavities through which energy flows out into the open air producing vowels and vowel-like consonants. The unvoiced sounds are produced by the flow of air through constrictions in the vocal tract which cause turbulence. While the voiced sounds exhibit certain periodicity and well-defined frequency resonances, the unvoiced sounds contain rather broad bands of energy and do not have any periodicity.

A speech compression system or a vocoder (voice coder) usually is comprised of: (i) means for analyzing the speech wave, and extracting the important acoustic parameters which are vital for intelligibility at the transmitting end; (ii) means for transmitting these parameters through the transmission channel in some code to the distant end; and (iii) means for decoding the received input at the receiver, and synthesizing speech. In short any speech compression system must have means for real time analysis and synthesis of speech.

It has been very well recognized that the low frequency periodicity which the voiced sounds exhibit and which is called the 'pitch' of the voice, constitutes an important factor in the intelligibility of speech. Hence, an accurate

*Presented at the Symposium on 'Modern Electronic Communication Techniques' held in Hyderabad on August 26, 1967

and precise determination of pitch is of vital importance in Formant and channel vocoders which utilize pitch for synthesis of voiced speech.

Fig. 1 shows an electrical analogue for production of waveforms analogous to those of voiced sounds. The pitch pulses produced by the vocal cords are roughly of the sawtooth waveshape and the three tuned circuits correspond to the predominant resonances taking place in the cavities of the vocal tract. Each pulse produces basically a damped oscillation in the vocal tract. It is obvious that the output will contain a fundamental periodicity equal to the pitch pulses, and that the commencement of each fundamental cycle of sound is characterized by the maximum amplitude.

Some typical voiced speech waveforms are given in Fig. 2. A study of a large number of voiced speech waveforms, reveals that the amplitude of the wave reaches the maximum, and decays to a low value during every pitch period of a voiced sound and that the value of these maxima during the various pitch periods is the same for the duration of any one voiced sound. The circuit used to find the pitch, discriminates the largest amplitude peak during any one pitch period from the other amplitude peaks occurring during the same period, and produces one pulse at the output corresponding to the time of occurrence of the largest amplitude peak during the pitch period.

2. Working of the pitch finder

Fig. 3 shows the block schematic diagram of the pitch finder circuit. The microphone with proper polarity is connected to a preamplifier and followed up by an AGC amplifier which gives a reasonably constant output irrespective of the position of speaker near the microphone. The output of the AGC amplifier is fed to a chain of seven expander amplifiers in cascade (the term 'expander' is used rather loosely for want of a better term to signify its operation) isolated by emitter followers between each of them.

The expander amplifier

The principle of working of this amplifier is extremely simple. It utilizes the non-linear input characteristic—input voltage *vs.* input current ($U_b \simeq I_b$) of a common emitter transistor configuration (Fig. 4).

Hence, if a common-emitter transistor amplifier with D.C. base bias current approaching zero is driven from a constant voltage source (low impedance source) the collector current $I_c (= \beta I_b)$ will exponentially rise with increase in the base voltage. Hence for an A.C. input under the above condition, the output will be zero for the negative portions of the input, and will be an expanded form of input for the positive portions. The larger amplitudes are considerably enhanced due to the non-linear characteristic, compared to lesser amplitude components. For example, if a waveform of the type given in Fig. 2 (i) is fed at the input, with peak A, just larger than B, the output will contain a peak corresponding to A, much larger than B. The rectification of the wave that takes place in the amplifier, due to class B-like operation is of no consequence to us as we are only interested in the amplification of the peaks, and their subsequent discrimination.

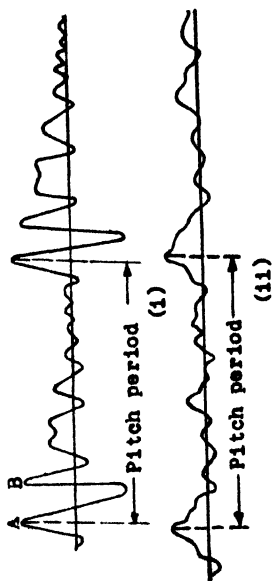
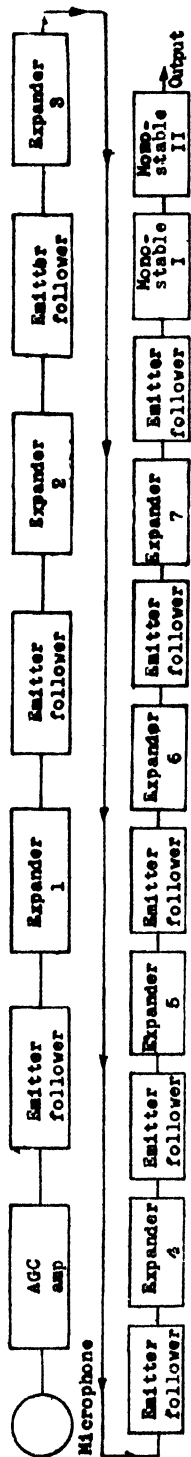


Fig. 1 |

Production of waveforms analogous to voiced sound

Fig. 2
A typical voice-speech waveformFig. 3
Block diagram of a pitch finder

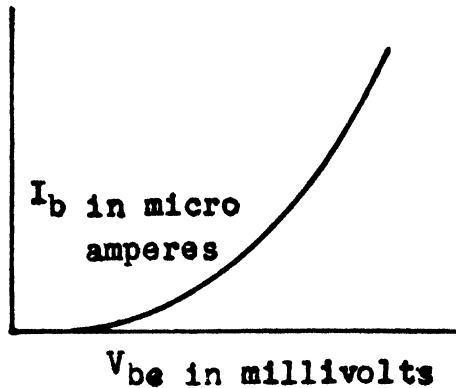


Fig. 4

Input voltage vs. input current

As the first approximation, we may consider that each expander amplifier of the type described has an output roughly proportional to the square of the input. If we cascade seven such amplifiers, the output will be proportional to (input)¹²⁸.

For example, if a wave like the one in Fig. 2 (i) is fed in at the input of this expander chain, and if the ratio of amplitudes, $\frac{A}{B} = 1.01$, then at the output, $\frac{A}{B} \simeq 2.5$. This means that even if the amplitude of the largest peak is just 1% more than its neighbouring peaks in the input wave, the largest peak will be more or less able to swamp the neighbouring peaks completely at the output. This fantastic enhancement of the differences of amplitude levels at the input makes this portion of the circuit, the heart of the pitch finder

3. The monostable multis

There are still some difficulties to be overcome, before reliable pitch pulses can be produced by the circuit at the rate of 1 pulse per pitch period. Firstly, the circuit should be made to respond only to the largest peak and no output should be produced for the subsequent smaller peaks. Secondly, if, as occasionally happens, a second peak of almost identical amplitude equal to the largest peak, occurs within a pitch period, the pitchfinder should not respond to it. To design a circuit which will carry out this task, we will have to make a closer study of the speech waves. Such a study reveals that whenever two identically large maximum peaks occur within a pitch period, they are usually separated by not more than one-tenth of a pitch period, but never in any case by more than one-fifth of a pitch period. This fact coupled with our knowledge that the pitch frequency rarely exceeds 300 cycles per sec. enables us to design two monostable-multivibrators to be added to our expander chain in cascade, to eliminate the production of faulty pulses occurring at the output.

The first monostable triggered by the output of the expander chain produces pulses of 3 millisecon. duration. The trigger level can be conveniently adjusted to make the monostable immune to the output of the expander chain corresponding to the minor and secondary peaks. As the recovery time of the multi is more than 3 millisecon., a second largest peak, even if it occurs during a pitch period, will not be able to trigger the multi. The second monostable is driven by the first and produces, sharp pulses of 20 microsecon. duration each at the output.

Some important factors taken into consideration in the design of the expander chain deserve mention.

Firstly, each expander amplifier has to be driven from a constant voltage source (a very low impedance source) if it has to function properly. Hence, each amplifier is driven by an emitter follower.

Secondly, no amplifier should be allowed to saturate at the amplitude peaks. This is likely to occur, as the large amplitude peaks, undergo tremendous amplification. Hence the input level for each stage, and the collector resistance of the stage have to be carefully adjusted for eliminating any possibility of saturation. Variable resistances in series with fixed resistances were used in all the emitter leads of the emitter followers to tap out the optimum voltage for input to each expander amplifier.

Thirdly, as each amplifier, produces a phase reversal of 180° and as the expander amplifier responds only to unipolar signals, NPN and PNP transistors were used alternately to make up the expander chain.

Fourthly, as there are a large number of stages being cascaded, very large values of coupling condensers have to be used for eliminating appreciable phase shift or delay.

The operation and adjustment of the AGC circuit has been found to be rather critical for optimum performance.

4. Comments

The distinctive feature of the circuit described is the fact that no time delay elements like integrators have been used here. Hence pitch pulses are detected without delay from the speech wave.

If the pitch period requires to be indicated, then a circuit of the type described by Anderson² may be added to the circuit described.

This circuit with some addition can also perform the task of voiced-unvoiced decision making which is of vital importance in conventional vocoders. The energy and the amplitude levels of the unvoiced sounds are rather small compared to those of voiced sounds. Because of the property of the circuit to completely suppress all low amplitude components, the pitch finder circuit will give no output when it is fed by unvoiced speech inputs. The absence of any output from the pitch finder for a period of more than 50 millisecon. can

be made to trigger a circuit with a built-in delay to indicate the absence of a voiced sound.

5. Acknowledgments

The author owes a deep debt of gratitude to Dr. P.V. Indiresan, Professor and Head of the Department, Department of Electrical Engineering, Indian Institute of Technology, Delhi, for the suggestion of this problem and the continued help and guidance which he extended for the execution of this project.

6. References

1. L.O. Dolansky. 'Instantaneous Pitch Period Indicator'. *Journal of Acoustic Society of America*, vol. 27, no. 1, January 1955, p. 67.
2. F. Anderson. 'Pitch Indicator for Training Deaf Scholars'. *Journal of Acoustic Society of America*, August 1960, p. 1065.

TROPOSPHERIC SCATTER COMMUNICATION SYSTEMS***M.S.V. Gopal Rao***Non-member**Defence Electronics Research Laboratory, Hyderabad***Summary**

Historical evolution of tropospheric scatter communications and the present state of art and knowledge related to the system design parameters are outlined. Modern trends in equipment design, transmitter powers, channel capacities, diversity reception, reliability and security aspects are discussed. Possibilities of application and potentialities of tropo-scatter systems in India for both civil and military purposes are described.

1. Introduction

Radio wave as a vehicle of communication is well known. Ever since the early days of radio the 'communication engineer' has been focussing his attention on two basic problems: first, in getting over the curvature of the earth which is as old as modern; and secondly, in the utilization of higher and higher frequencies of the radio spectrum to provide greater traffic handling capacity. The ionosphere and H.F. communication has been fully exploited during the past several years and a stage of saturation has been felt. As a result of the fantastic technological growth during the Second World War and later with the advent of satellites, new avenues have opened up in the field of communication systems employing U.H.F. and microwave frequencies. Tropospheric scatter and the satellite communication systems are among the important modern ventures aimed at the same basic problems.

In this paper, the evolution of tropo-scatter systems, their capabilities and limitations, the propagation and system design parameters and the present state of art in the field are discussed.

2. Historical background

As early as 1933, Marconi, working in the frequency range 500-600 megacycles per sec. has realized the possibility of 'tropospheric communication' beyond the horizon distances and foresaw considerable scope for its use. However, this work was not followed up vigorously until 1949. At this time the knowledge of tropospheric fields occurring beyond the radio horizon distances was considered inadequate and for this reason the expansion programme of television service in the U.S.A. had to be frozen for some time. This has created the necessary background and pressure on various laboratories and companies to collect more data on the tropospheric scatter fields. Several of the resulting studies,¹⁻³ have indicated the occurrence of radio field strength at a much higher level than could be expected by the 'smooth earth diffraction

*Presented at the Symposium on 'Modern Electronic Communication Techniques,' held in Hyderabad on August 26, 1967.

theory'. The violent Rayleigh type of fading of the received signal is taken to suggest some scattering mechanism of propagation. There are, however, other theories based on internal reflections and partial reflections from large inhomogeneities in the troposphere. Although the mechanism of propagation is still considered debatable, much data has accumulated on the characteristics of propagation, such as, path losses, frequency dependence, fading, etc. By about 1952 it has been realized that this mechanism can be utilized for highly reliable point to point communication with a considerable bandwidth capability. The first practical system known as 'pole vault' has been engineered in the year 1954 in Canada. From this time onwards there has been a continuous and rapid growth of technology and several firms have started making a number of commercial troposcatter systems, to meet a variety of defence and civilian requirements. By about 1965 it is estimated that a total of about-53,600 route-miles and a total of 2,687,000 channel-miles are covered by troposcatter systems.

3. Propagation parameters

The tropospheric signals beyond the horizon arrive with maximum intensity in the horizontal direction along the great circle route so that the transmission and reception are usually carried out by means of large parabolic reflectors with narrow beamwidths. The typical propagation path profile is shown in Fig. 1. It will be seen that the transmitter and receiver beams will be looking into a common volume in the troposphere at a certain height depending on the angular distance between the transmitter and receiver locations. The variation of the height of this common volume with increasing distance between the terminals is shown in Fig. 2. Calculation for this is made assuming that $4/3$ of the true radius of the earth to allow for the standard downward curvature of the radio waves due to the decrease of atmospheric refractive index with height. From this figure, it will be seen that maximum single hop distance of the order of 800-1,000 km. will be possible when the common volume reaches the levels of the 'tropopause'. Beyond this distance the losses will be much more and the systems become un-economical. For this reason, long distances are usually covered by a number of links connected in tandem. The signal strength variation with distance and the frequency as observed in the U.S.A. are shown in Figs. 3 and 4. These figures depict a comparison of the troposignals with respect to the signals expected by 'smooth earth diffraction theory'. Comparison is also made with the losses, encountered in 'ionosphere scatter circuits.'

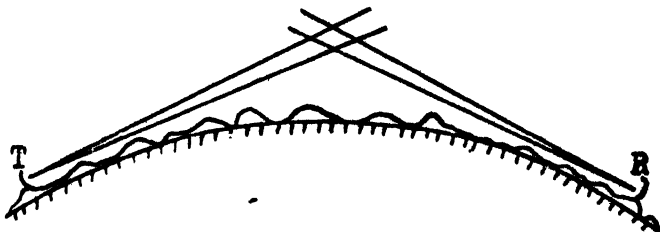


Fig. 1

A typical propagation path of a tropo-scatter system

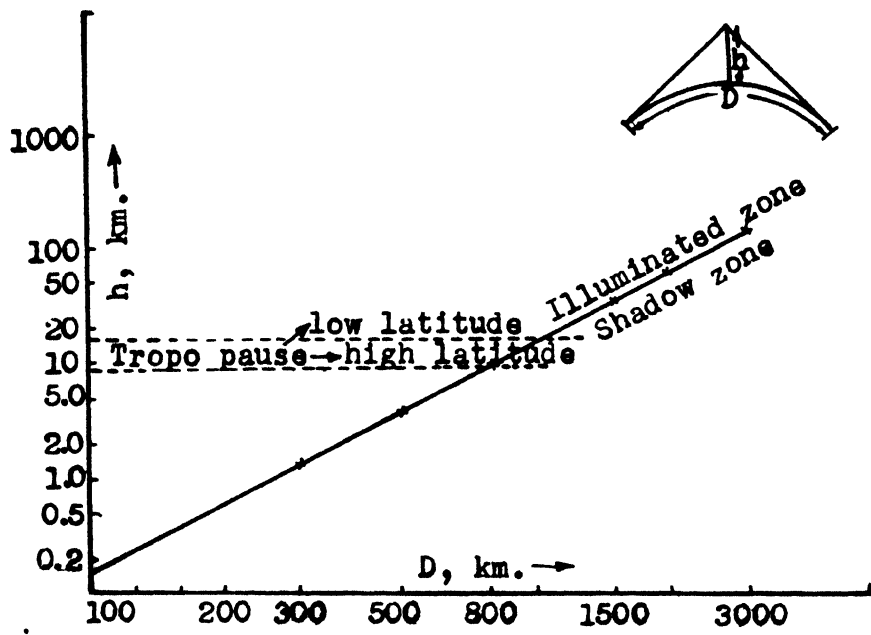


Fig. 2

Variation of height with increasing distance between terminals

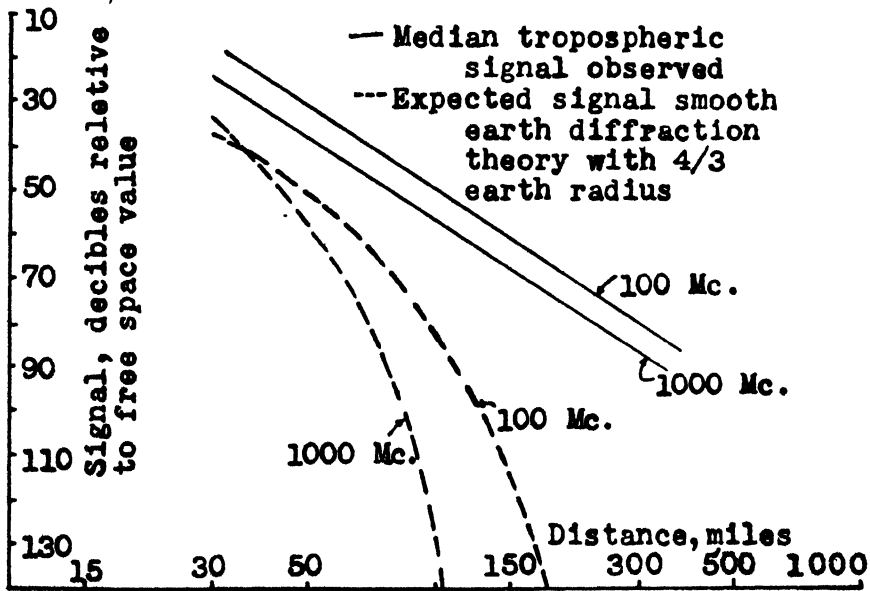


Fig. 3

Variation of tropospheric signal with distance

The tropomedium being non-dispersive in nature, larger bandwidth capabilities are achieved. The useful bandwidths at points far beyond the horizon are at least one-tenth of corresponding bandwidths obtained in line-of-sight links.

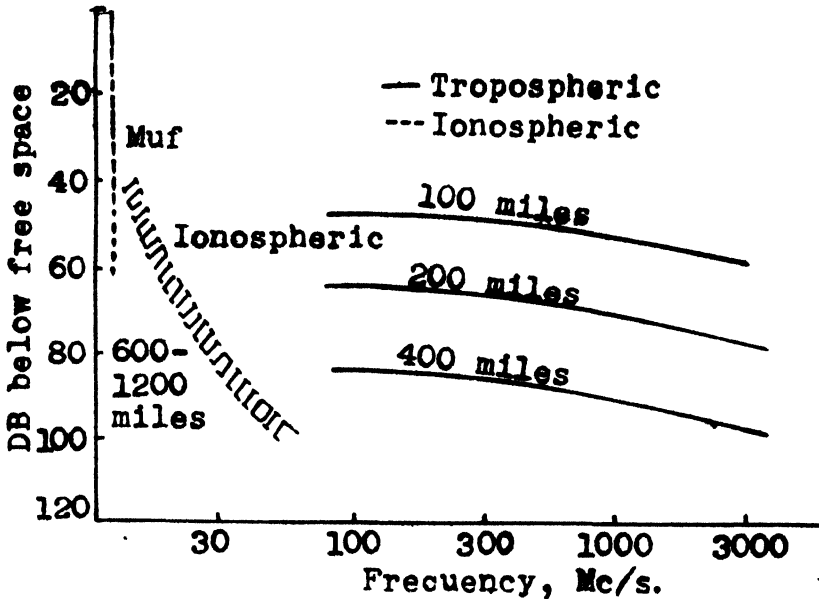


Fig. 4

Variation of tropospheric signal with frequency

The signal strengths are generally higher during night than during day. Marked diurnal variations are observable only at the low percentiles, generally in the lower decile. The diurnal curve generally flattens out in 93-99% values, showing that the propagation is relatively independent of the time of the day. The median 50% curve shows a range of 6 dB variation between the maximum and the minimum.

In the seasonal variation, the field intensity tends to be higher in summer premonsoon period and lower during monsoon and winter periods. From the upper air data analysis⁴ of the radio meteorological parameter, ΔN the difference in refractivity in the first kilometre height shows that the annual range can be much larger in India than that observed in the U.K. This range can be as high as 21 dB at Bangalore while this is only 4.5 dB in the U.K. These ranges are computed based on the ranges observed in ΔN and the effective earth's radius factor, K . This study has further revealed that there is practically no correlation between the surface refractivity N_s and the difference, ΔN . This feature has been reported from other tropical regions in Africa also. The data from the U.S.A., U.K. and Germany indicate that there is a strong correlation between N_s and ΔN . This had led to the design of tropo-systems based on N_s as an important radio meteorological parameter. This

evidently will not be possible for tropical conditions in India. In general, the systems are to be designed for the worst conditions of propagation loss which might occur during certain months in the year. The annual ranges in N_s , ΔN , K and ΔE the computed range of signal strength at different stations in India are shown in Table 1. In view of the fast fading experienced in these circuits, it will be necessary to use diversity reception techniques employing either space diversity or frequency diversity or both.

Table 1
Annual ranges of N_s , ΔN , K and ΔE

Station	N_s	ΔN	K	E , dB
Ahmedabad	298-392	30-69	1.24-1.78	18
New Delhi	300-394	28-64	1.22-1.69	18
Bangalore	284-338	30-77	1.24-1.96	21
Visakhapatnam	342-400	50-95	1.63-2.52	15
Bombay	334-388	50-94	1.63-2.48	15
Port Blair	368-390	40-68	1.33-1.76	12
British Isles	318-346	39-49	1.32-1.45	4.5

Because of large path losses, large transmitter power and highly sensitive receiving equipment is necessary for reliable communication. In the frequency range of interest, only the receiver noise will be the limiting factor. So the receiver thresholds are sometimes improved, by adopting parametric amplifiers and tunnel-diode amplifier at the front end.

4. Equipment description

A block diagram of the equipment normally used at one of the tropo terminals is indicated in Fig. 5. Frequency division multiplex and FM transmission is the normal practice followed. The several voice channels are translated in frequency and arranged in adjacent slots of 4 kilocycles per sec. bandwidth, which forms into what is known as a 'baseband signal'. This signal will be initially amplified and used to frequency-modulate an intermediate frequency such as 30 or 70 megacycles per sec. A FM index of 3 is normally employed. This intermediate frequency is upconverted to desired carrier frequency by mixing with a steady local oscillator. Now this upconverted signal is amplified in power to generate about 1 watt of power which will be used to drive the power amplifier stage. All these functions are carried out in the portion of the circuit called 'exciter'. The power level obtained at this level can be straightaway utilized in line-of-sight operation. The final stage of power amplifier consists of a high power Klystron along with its power supplies and protection system. Depending on the type and the capacity of the Klystron,

power of the order of 1 to 100 kW are generated. This power is fed through an isolator and a duplexer to the antenna feed system. For quadruple diversity reception, the information is transmitted on two different frequencies f_1 and f_2 and received on two other frequencies, f_3 and f_4 . This requires the use of two antennas separated by a distance of more than 100λ , at each of the terminals. The antenna consisting of a dual-feed system and a parabolic reflector gives rise to substantial gain increasing the effective radiated power and confining the radiation to a narrow beam. Theoretically, this gain will be more at higher frequencies and with larger reflector diameters. However, in tropo systems in practice, an antenna gain beyond about 40 to 45 dB could not be achieved due to what is termed as 'antenna-to-aperture coupling loss'.

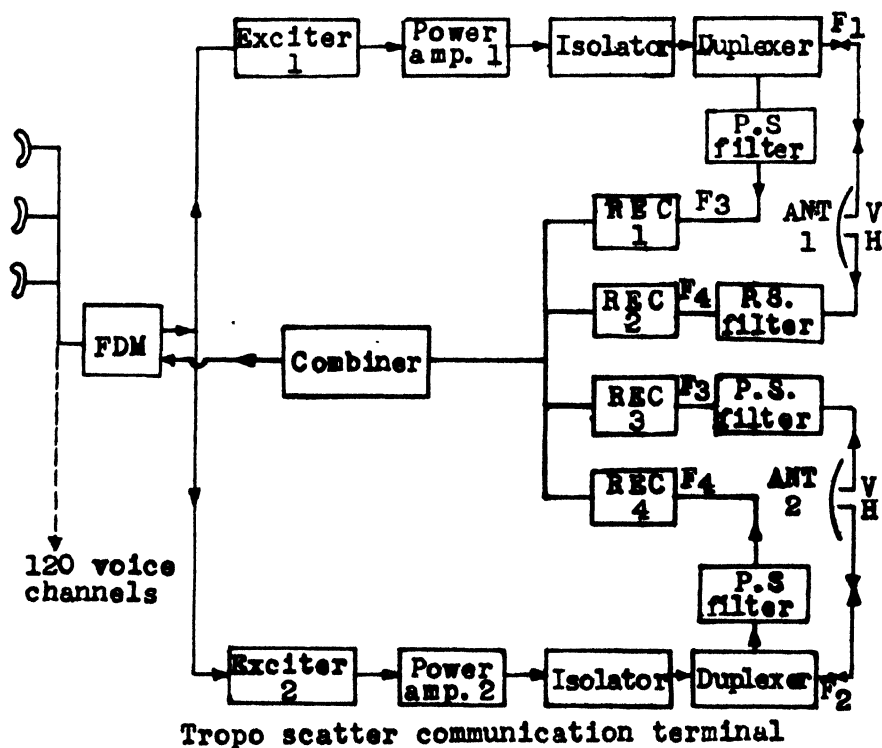


Fig. 5

Block diagram of a typical tropo-scatter communication terminal

In the receiver the signals are first taken through bandpass filters known as 'preselectors' and then to a tunnel-diode amplifier or parametric amplifier and a mixer to bring down the carrier frequency to an IF of 30 or 70 megacycles per sec. The signal is amplified in the IF chain and finally demodulated by means of conventional circuits. The demodulated signal now consists of the baseband which is a composite traffic of incoming voice channels. The baseband signals from all the four receivers are combined in a suitable circuit to counter-act the fading effects.

In the latest designs solid state devices are employed to the maximum extent and some flexibility of the equipment is provided for the users to change the operating frequency, output power and antenna dishes in order to meet any special requirement or situation. This is achieved by adopting common equipment upto IF chain in both transmitter and receiver circuits and adopting modular construction for the excitor and the power amplifier circuits. A maximum number of 300 voice-channels can be handled in these systems requiring a bandwidth of about 10 megacycles per sec. in the receivers. However depending on the distance between the terminals and the path losses involved, the maximum channel capacity has to be worked out.

5. System design parameters

In designing an operational system, two approaches can be followed. One is to design a system for a specific requirement of the channel capacity and a fixed path and to calculate the required transmitter power and the equipment configuration. In the other approach, equipment is designed with standard specifications of power, antenna dishes and channel capacity and work out the radio gain and applicability in different paths. In the first approach, the system losses are to be evaluated. The losses consist of free space loss, tropo loss, and cable losses. Once the total system loss is known and the carrier to noise ratio requirement at the receiver is known, the equipment requirements are worked out. In the second approach the receiver noise threshold, the signal-noise ratio, the transmitter power, and antenna gains available are combined to yield the total system gain or radio gain. With this available gain, the designer computes the probable coverage of distance and the percentage reliabilities to be expected with such a system.

6. Conclusions

In conclusion, it may be stated that with a large number of tropo links already commissioned in different parts of the world, the system design has reached a near-perfect stage except that certain variations in tropo loss, which are likely to occur in the tropical regions, are not yet fully established.

7. References

1. K. Bullington. 'Radio Propagation Variations at VHF and UHF'. *Proceedings of the Institute of Radio Engineers*, vol. 38, no. 1, January 1950, p. 27.
2. I.H. Gerks. 'Propagation at 412 Megacycles from a High-power Transmitter'. *Proceedings of the Institute of Radio Engineers*, vol. 39, no. 12, November 1951, p. 1374.
3. K. Bullington. 'Radio Transmission beyond the Horizon in the 40 to 4000 Mc. Band.' *Proceedings of the Institute of Radio Engineers*, vol. 41, No. 1, January 1953.
4. M.S.V. Gopal Rao and K.V. Ranga Rao. 'Radio Meteorology Variation of Radio Refractive Index with Height in the Lower Troposphere in India.' *Journal of the Institution of Telecommunication Engineers*, vol. 12, no. 7, July 1966, p. 369.

SATELLITE COMMUNICATION SYSTEMS***Wing-Cdr. R. Nagaraja Rao***Non-member**Defence Research Laboratory, Hyderabad***Summary**

Various stages in the development of communication satellites have been described. Technical characteristics of important satellites have been mentioned. Their military applications are discussed. Modern trends in their design have been indicated. Characteristics of the Experimental Satellite Earth Station, recently established at Ahmedabad, have been mentioned.

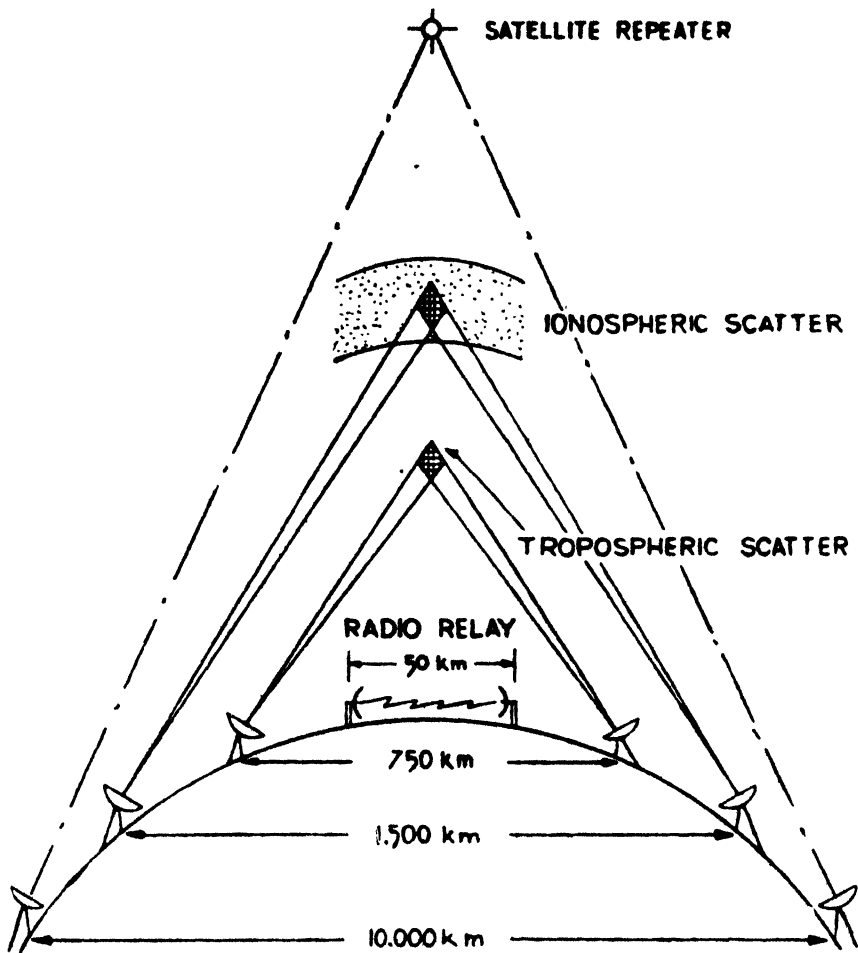
1. Introduction

The space age started on October 4, 1957, with the launching of the satellite Sputnik by the Russians. This was followed in rapid succession by many such satellites for various scientific observations. The Score satellite was first used to receive and re-transmit wireless messages. Since then Courier, Echo, Relay and Syncom and numerous other communication satellites are being successfully used as links for establishing communications between distant stations. In this paper, a discussion on the techniques used for the successful operation of these satellites, their performance, capability and modern trends in their design and applications have been discussed.

2. Need for communication satellites

The steady and rapid growth of internal and oversea telephone and telegraph traffic are saturating the existing land and underwater cable systems and wireless communication systems. These conventional systems cannot be expanded to meet these requirements due to overloading of channels, and the vagaries of the transmission media. The cost of cable links has increased enormously. The bandwidth offered by cables is not sufficient for wideband systems like the TV. The transmission of even a single wideband TV message is not possible through the Atlantic even if all the existing undersea telephone channels are used. A new system of using the wideband capabilities of microwaves was required. The two present systems of communication, namely, (i) troposcatter system, and (ii) satellite communication system, fill this need. Each has got its own merits and demerits. The satellite communication system has the advantage that a single satellite can be used by a number of ground stations widely separated apart. In view of their flexibility, huge capacity and reliability, communications satellites have pervaded the field of communication in a big way. Fig. 1 shows the transmission path of various types of communication systems.

*Presented at the Symposium on 'Modern Electronic Communication Techniques' held in Hyderabad on August 26, 1967.

**Fig. 1**

Modes of wireless communication systems

3. Types of systems

Communication satellites could be broadly divided into two categories, passive and active. The passive communication satellite has a reflecting surface which merely reflects the signal received from one point on the earth to a second point on the earth. It does not contain any active electronic equipment. The active satellite contains a radio receiver which receives the radio signal from one point of the earth, amplifies the signal and by means of a transmitter re-transmits it to another point on the earth at a different frequency. A passive system has no capability for amplification within the satellite, and as such requires more powerful ground transmitters. However, the absence of any electronic parts in a passive system makes it more reliable.

Passive satellites

Experiments have been carried out with two types of passive satellites. The first type called 'Echo' was a large spherical structure made of 100 ft. diameter aluminized mylar plastic, and was put into an elliptical orbit. The second type was the 'Westford' type, in which a large volume of space was filled with a number of tiny passive satellites (metallic foils).

An isotropic reflector like the 'Echo' is wasteful of energy, as only a small part of its surface reflects energy in the useful direction (*i.e.*, towards the ground receiving station).

In the 'Westford' type of satellites, the individual elements are small compared to a wavelength and millions of them are distributed in a volume of space. These are not suitable in their present state for commercial exploitation. For commercial use, an 'advanced passive combat' is being designed.

Active satellites

These could be considered under two basic types : delayed repeater (store and forward) and line-of-sight (real time) repeater. In the delayed type, a ground station transmits a message to a satellite passing overhead. The message is stored on a tape recorder in the satellite and then played back through the satellite transmitter when the satellite passes over the appropriate ground receiving station. These are low altitude types, and the motion of the satellite is essential for getting the message from place to place. In this system, the message is delayed the period of delay depending upon the distance between the two stations and the trajectory of the satellite. The Score (December 1958) and 'Courier' (October 1960) belonged to this category. The line-of-sight ((real time) type of active satellite can be either of the synchronous altitude type or of the intermediate altitude type. 'Telstar' (July 1962) and 'Relay' (December 1962) were of the intermediate altitude type whereas 'Syncom' (July 1963) and 'Early Bird' (April 1965) were of the synchronous type. Brief particulars of some of the important communication satellites already launched and planned for future launching are given in Appendix 1. The calendar showing the landing of major communication satellites is given in Appendix 2.

4. Orbits

A satellite has to be put into its proper orbit by a suitable launching vehicle. Orbits may be circular or eccentric (elliptical). A circular orbit requires a specific combination of velocity, direction and altitude and is difficult to achieve. Natural orbits are generally eccentric.

The 'six orbital elements' defining a satellite orbit in space are given in Fig. 2.

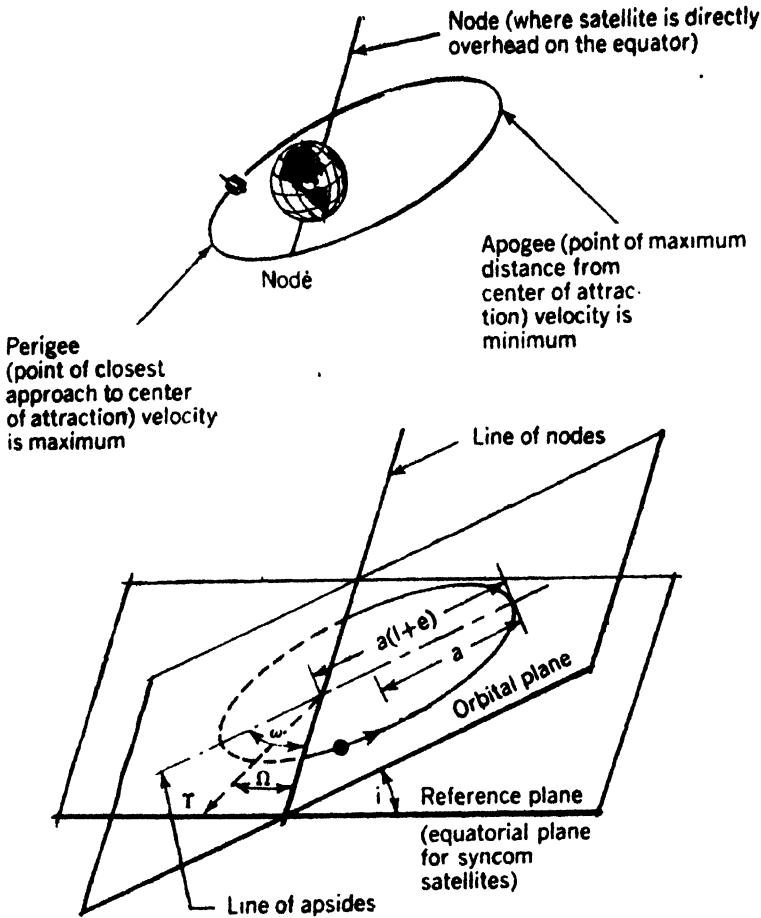


Fig. 2

Orbital parameters for specifying location of orbit in space relative to earth

The satellite will be in circular orbit if the centrifugal force associated with the satellite in motion is equal to the gravitational attraction between earth and satellite.

$$\text{Centrifugal force} = m_s \frac{V^2}{r}$$

$$\text{Gravitational force} = f \frac{m_e m_s}{r^2}$$

Equating the two,

$$\frac{m_s V^2}{r} = f \frac{m_e m_s}{r^2}$$

i.e.,

$$V = \sqrt{\frac{f m_e}{r}} = \frac{1.996 \times 10^{10}}{\sqrt{r}}$$

where v is the satellite velocity (in cm. per sec.), m_e the earth mass, m_s the satellite mass, f the gravitational control (6.67×10^{-8}), and r the distance from centre of mass of earth to centre of mass of satellite (in cm.).

Hence, for a circular orbit, a required velocity exists at every satellite altitude. If satellite velocity is less than this circular velocity, satellite orbit will be an ellipse, with apogee at circular altitude. If satellite velocity is greater than the circular velocity, the satellite orbit will be an ellipse with perigee at circular altitude.

For a given altitude, there is a specific velocity required for a satellite to occupy a specific orbit. The act of providing this velocity is called 'injection into orbit'. The direction of injection velocity is tangential to desired orbit.

One of the methods employed for bringing a satellite to a circular orbit is to use an 'apogee kick' technique. This is shown in Fig. 3, for a 'Syncom'. First the satellite is injected into a highly eccentric ellipse. When the target reaches apogee at the desired altitude for circular orbit, the velocity is less than the velocity required for circular orbit at that altitude. This velocity is made up to the required velocity for circular orbit at that altitude by firing an additional rocket, in a direction parallel to earth's surface. The satellite is placed in circular orbit. The intermediate elliptic orbit is called the transfer orbit.

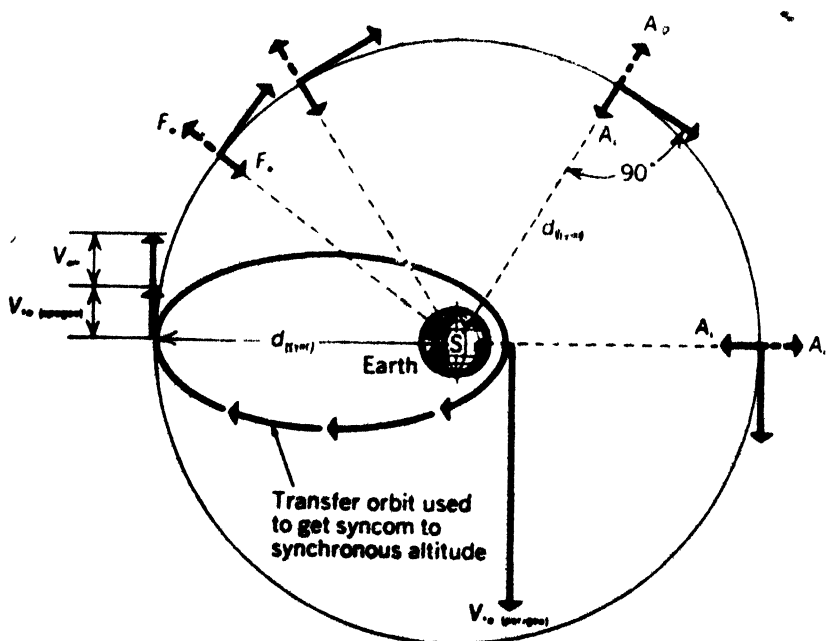


Fig. 3

Mode of putting 'SYNCOM' into synchronous orbit

Syncom orbit

Project 'Syncom' was designed to develop the capability of launching satellites into synchronous orbit and demonstrating their utility.

The basic three-stage booster could place 150 lb. in elliptical orbit at an apogee of 22,300 miles, with the load spin stabilized with the spin axis in the

orbital plane. An 'apogee kick' rocket motor carried in the satellite gave velocity increment to place satellite in circular orbit at 22,300 mile altitude, with a final weight of 78 lb. In the final stage of Syncom I and II, the satellite was in synchronous orbit inclined 33 degrees to equator with a period of 24 hours.

After spin axis has been placed in final orientation perpendicular to the orbital plane, velocity corrections are accomplished by using a lateral 'thruster'.

Syncom III was put into a truly 'stationary orbit' instead of the inclined synchronous orbit of Syncom II by using a more powerful third stage rocket. The sub-satellite point or earth track described by Syncom II is a figure of eight moving north and south of the equator every 24 hours by an amount equal to the inclination of the orbit in degrees. Since Syncom III has zero inclination, (*i.e.*, lines in equatorial plane) its earth track is a stationary point on the earth's equator.

Random orbits

The Initial Defence Satellite Communication Programme (IDSCP) planned for strategic communication consists of a worldwide network of ground stations and about twenty satellites in randomly spaced near-synchronous equatorial orbits. These satellites will be at several altitudes near 18,300 nautical miles. The distance between satellites varies continuously. However orbital parameters have been so chosen that satellites will never bunch. Since they are not at synchronous altitude, they will drift slowly across the earth at about 30° per day. There is little difference between coverage angles at altitudes of 15,000 to 21,000 nautical miles. The drift is below 50° per day for altitudes above 1,700 nautical miles. Fig. 4 shows drift and coverage as a function of altitude.

Near-synchronous random orbits ensure that if one satellite malfunctions, another satellite will eventually be in place to provide communication capacity. Also such satellites can operate without station keeping controls, thus preventing the enemy from changing the orbit of the satellites and disrupting communications.

5. Stabilization

To improve the gain, directional antennas are being introduced in satellites. This necessitates methods to stabilize the satellite to direct the antenna towards the earth. In 'spin' stabilization, the satellite is spun about the axis of symmetry at 10 to 150 revolutions per min. The satellite is gyro-stabilized and the spin axis is inertially oriented in space. If spin axis is perpendicular to the plane of satellite's orbit, an antenna beam (a figure of rotation about the spin axis) will continuously impinge upon the earth. An antenna with a pencil beam just subtended by the earth will give the maximum gain. Use of such antenna requires complete stabilization of the satellite. Fig. 5 shows the relative communication capacity for various types of stabilization. In practice, it is very difficult to obtain full stabilization.

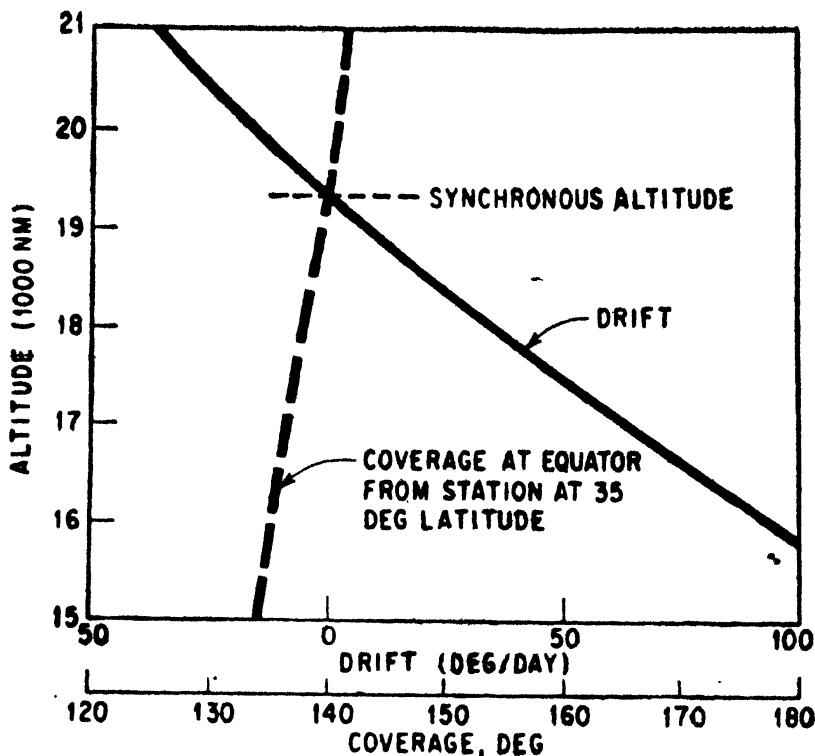


Fig. 4

Drift of a non-stationary satellite as a function of altitude

Since antenna is omnidirectional about spin axis, a large portion of the energy is radiated into space. To eliminate this loss, de-spun antennas are used. De-spinning can be achieved mechanically or by electronic scanning, so that the unidirectional beam is rotated opposite to the spin of the satellite. This ensures that the beam will remain stationary with respect to the earth, radiating all the power towards the earth.

Another method of stabilization is the 'gravity gradient stabilization (G.G.S.)'. This is based on the tendency of a body in orbit to align itself with its long axis (*i.e.*, the axis of minimum moment of inertia) pointing towards the earth, because of the variation in gravitational attraction with distance. The G.G.S. enables earth oriented synchronous satellites to remain within about 3° of the desired orientation. Better orientation is not possible, due to the torque produced by thrusters used for station keeping.

The G.G.S. has been tested upto about 600-mile altitude. Whether it will work at synchronous altitude is yet to be seen, since the pull at synchronous altitude is only $\frac{1}{200}$ of the pull experienced by it at 600 miles.

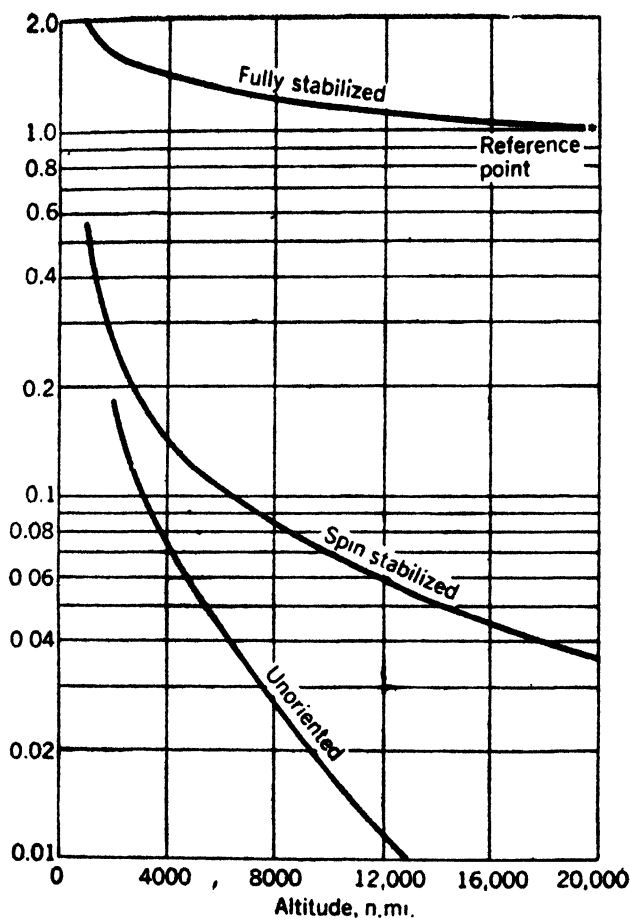


Fig. 5

Relative communication capacity vs. altitude and altitude stabilization

6. Coverage

To cover a certain portion of the earth for communication purposes, the number of satellites required when orbiting at higher altitudes is fewer than the number required for orbits at lower altitudes. The mutual visibility can be calculated by spherical geometry. The zone of visibility can also be described in terms of a slant range from satellite to horizon, ground station's separation and the satellites beamwidth as shown in Fig. 6.

The probability of service (in percentage) as a function of separation between ground stations and orbit altitude is shown in Fig. 7. Reliability of service can be increased by using a larger number of satellites. This is shown in Fig. 8 which is based on circular orbits for both random and synchronized spacing of satellites.

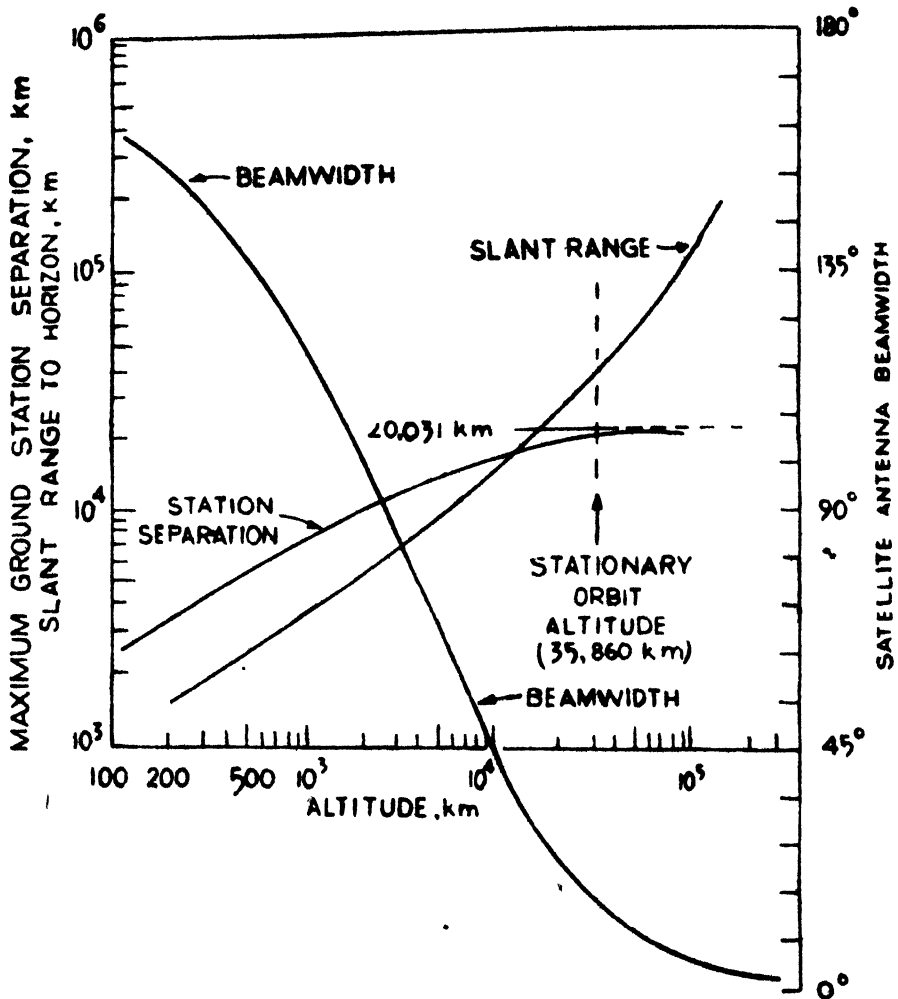


Fig. 6

Circuit length slant range and beamwidth as a function of altitude

7. Design of ground stations

Ground station is an important part of satellite communication system. Since the satellite is at a great distance from the ground station, and can radiate only a small amount of power, the ground station equipment must be extremely sensitive.

A sensitive receiver, of high-gain directional antenna, and an accurate antenna mounting and pointing device are essential components of a 'ground station'. Since the beam intensity decreases rather rapidly from the centre toward the edges, it is necessary to point the antenna with greater accuracy than one beamwidth ($\frac{1}{4}$ to $\frac{1}{10}$ is a good practical value). Some of these stations are equipped with digital computers to convert orbital data for a

satellite into pointing directions. A non-stationary satellite system, requires more than one antenna system, for 'hand over' capability.

Parabolic antennas are generally used for ground stations, some of them with Cassegrain feed.

Noise temperatures of antenna and front end of receiver are important factors in ground station sensitivity. Antenna noise temperature depends on the degree to which its design permits radiation from extraneous noise sources to get into the system. (A typical figure is 0.5°K for a large horn antenna; and 5°K to 10°K for a Cassegrain type at the zenith). Fig. 9 shows the noise temperature as a function of frequency for a number of common receiver front ends. The maser gives the lowest noise contribution, but is the most complex and expensive. This is used in large stations with high communication capacity. Both maser and cooled parametric amplifiers require artificial cooling to temperatures near absolute zero.

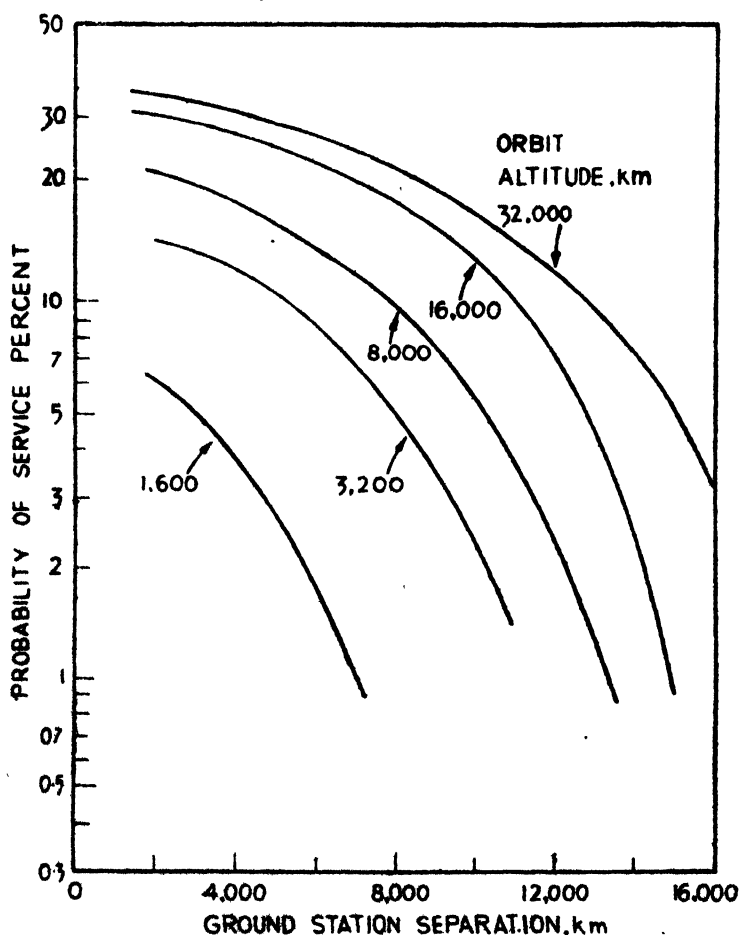


Fig. 7

Probability of service from a single satellite

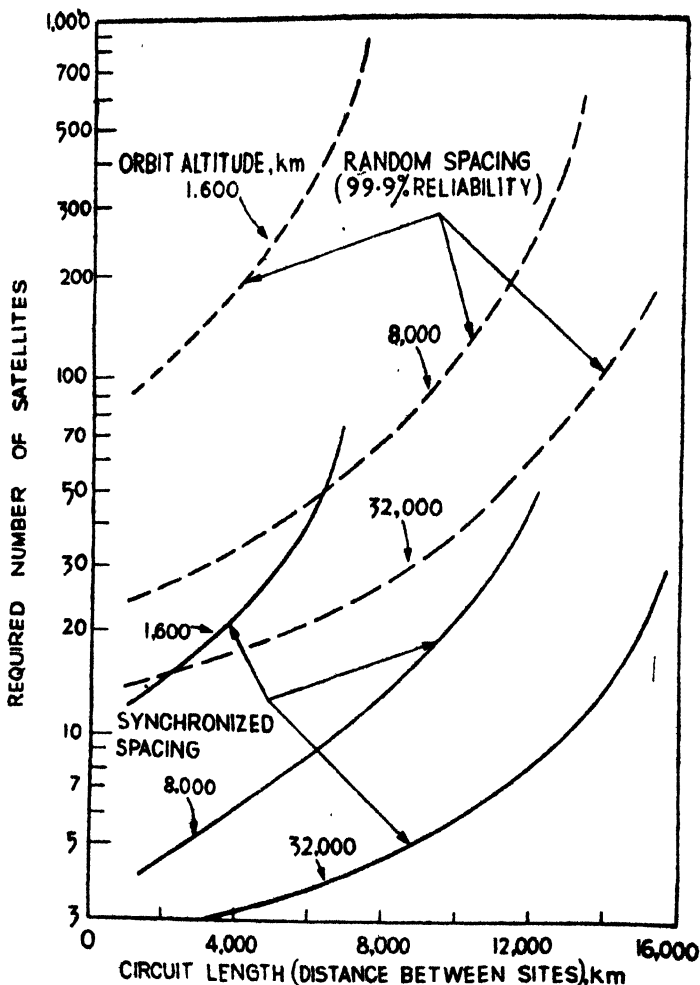


Fig. 8

Number of satellites required for synchronized and random orbital spacing

Transmitter powers are of the order of 5 to 20 kW, over a wide bandwidth. Generally either TWTS or Klystrons are used in the output stage of transmitters.

8. Satellite communication in India

India is entering the field of global communication through satellites by establishing two ground stations. The installation of the first station has just been completed at Ahmedabad. This is called the 'Experimental Satellite Communication Earth Station', and has been constructed by the Department of Atomic Energy, Government of India, at a cost of Rs. 1.75 crores with partial financial assistance from the United Nations Special Fund. This station will track and operate with communication satellites, participate in tests and demonstrations with other countries having similar facilities on a mutual basis

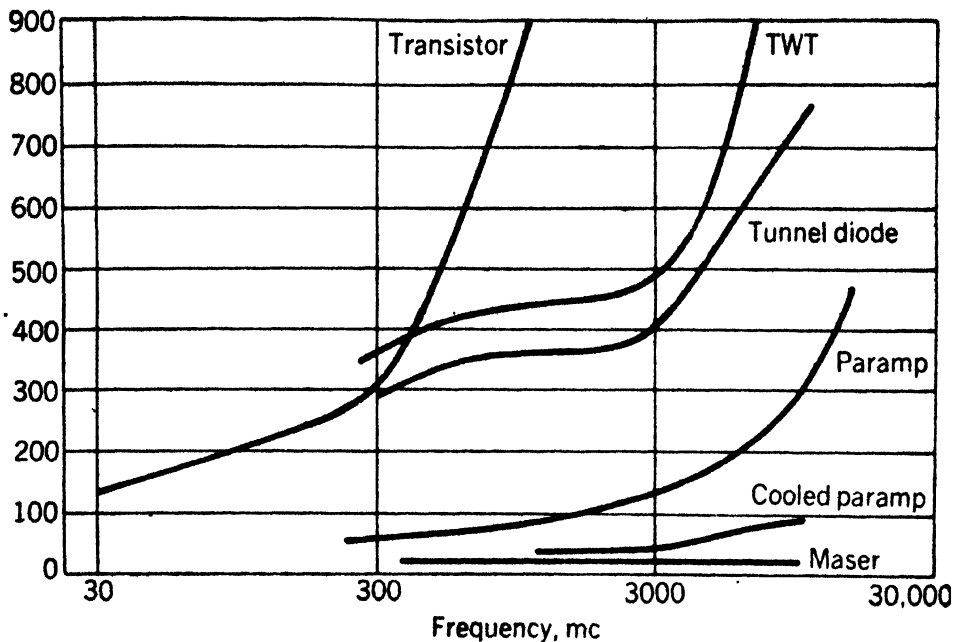


Fig. 9

Noise performance of low noise paramplifiers

and provide training and research facilities for engineers and technicians from India and foreign countries. Tests will initially be carried out by collaborating with N.A.S.A., U.S.A., using 'Application Technology Satellites', on transmission of multichannel telegraph, speech, TV, digital data and facsimile signals on two separate modes of operation : frequency translation and multiple access.

The main satellite communication equipment was supplied by Nippon Electric Company. The multiplexing equipment has been supplied by the Indian Telephone Industries, Bangalore. The transmitter works in the frequency range of 6,200-6,315 megacycles per sec. using a Klystron giving a frequency-modulated power output of 5 kW. The receiver works in the frequency range of 3,700-4,200 megacycles per sec. with an frequency-modulated of 70 megacycles per sec. (IF bandwidth is 25 megacycles per sec. and RF bandwidth is 90 megacycles per sec.). The pre-amplifier stages consist of one liquid nitrogen cooled parametric amplifier, one uncooled parametric amplifier and one tunnel diode amplifier. The antenna consists of a 14-m. parabolic dish with Cassegrain feed, with a gain of 55.5 dB for transmission frequencies and 52.3 dB for reception frequencies. Facilities for manual tracking and servo-controlled auto-tracking are provided, with facilities for rotation of $\pm 360^\circ$ in azimuth and -2° to $+93^\circ$ in elevation.

The second station is being set up near Poona by the Overseas Communications Service for normal commercial traffic.

9. Military applications

Military systems all over the world are planning the utilization of active satellite repeaters to have a highly reliable communication system free from atmospheric and ionospheric effects and invulnerable to countermeasures.

The military systems require such systems for their long range point-to-point (strategic) and short range (tactical) communication systems. Till these systems are fully established, leased channels on commercial satellites will be used for long haul, point-to-point administrative traffic.

The strategic communication system involves a worldwide distribution network of communication trunks utilizing diverse transmission media interconnected by appropriate switching centres. The system should provide communication for command, control, logistics, intelligence, weather, administration, etc. For strategic system the Initial Defence Communication Satellite Programme (IDCSP) is being introduced initially in the U.S.A. These consist of a total of twenty-four (97-lb.) satellites, launched eight at a time by a Titan 3-C booster, near equatorial predetermined orbits of 18,200 nautical miles. The RF output will be 2.5 to 3 watts, with a circularly polarized biconical array having 25° beamwidth, continuously illuminating the earth segment below. The experience gained will be used to launch eight Advanced Defence Communication Satellites (ADCSP) with each satellite having 30 times more capability than IDCSP, and anti-jamming facilities. Such ADCSP satellites will have mechanical/electrical de-spun antennas, with multi-access facilities and will use Crypto-secure codes with keystream generation. The long range systems use will big and sophisticated ground stations (fixed or transportable).

The short range 'tactical' system are required for use between a number of stations at shorter distances like troops in field, ships and aircraft. These tactical Satcom programmes will be taken up later with satellites (weighing 1,500-1,800 lb.) in near-synchronous equatorial orbits working on VHF band as well as on 7,925 to 8,025 megacycles per sec. for reception and 7,250 to 7,300 for re-transmission. The ground stations (which will be transportable) will be simplified at the expense of a complicated satellite. Such satellites will be used by thousands of users for communicating short bits of information. The near-synchronous altitude random orbits will be utilized for this system.

For military use, a frequency band of 7.9 to 8.4 gigacycles per sec. has been allotted for ground transmissions, and 7.25 to 7.75 gigacycles per sec. for the satellite transmissions.

10. Modern trends in the design of satellites

The design of communication satellites is undergoing rapid changes as experience is gained on the satellites in orbit. Some of the modern trends in the design of such satellites are indicated below.

Physical specifications

The size and weight of the satellite have been continuously on the increase to obtain greater channel and performance capabilities. Some of the active

satellites planned or the 1970s weigh as much as 1,600 lb. (ATS) and 3,000 lb. (Advanced domestic cosmat). Advanced passive cosmat is likely to weigh as much as 120,000 lb.

Various types of stabilization of satellite antennas are being tried out. The present spin-stabilized antennas will be replaced by an electronically or mechanically de-spun phased array antennas or gravity gradient stabilized antennas, both of which are under development. Another type of antenna projected is a steerable horn antenna. To obtain a higher antenna gain, plans are under consideration to unfold at synchronous altitude, foldable 'Sunflower' antenna dishes 15 ft. in diameter. The unfolding may be done by pneumatic system. Antennas will be continuously controlled so that they are always directed towards the earth.

Launching of satellites is being economized by launching upto eight satellites by a single booster vehicle.

Technical specifications

The RF output from the communication satellite is being increased by either using more powerful TWTs or using a number of low power TWTs in parallel (which incidentally ensures the continuity of service even if one TWT fails), while TWTs of 6-watt output are being used at present, TWTs with 30-watt output are being experimented. The RF output of the order of 4 kW is being planned for next generation of satellites.

With the increase of RF power output, the total input power requirements of the satellite are rapidly increasing. The physical size of the satellite becomes too unwieldy if the solar cells are greatly increased in number to cater for increased power requirements. To keep down the size of the satellite, a number of foldable panels carrying the solar cells may be attached to the main body. The efficiency of solar cells in orbit is progressively reduced due to a variety of environmental factors. The later generation of power supplies may use solar thermo-electric systems, solar dynamic systems or SNAP (System for Nuclear Auxiliary Power) nuclear reactors, to meet the large power requirements.

The SNAP system is unaffected by satellite altitude, orientation, and Van-Allen belt radiation.

At present the frequency of operation (for civil use) is being concentrated in 6 gigacycles per sec. band transmission from ground and 4 gigacycles per sec. band transmission from satellite. For military systems, 7 and 8 gigacycles per sec. bands are being used. For aeronautical comsats the VHF band is being utilized and proposals for shifting over to UHF band are being considered. The microwave bands are getting congested due to the large bandwidths required for multi-channel and multi-access satellites. The use of 16 gigacycles per sec. and 36 gigacycles per sec. bands is being envisaged to avoid ground network interference and obtain the higher bandwidth possible at higher frequencies. The atmospheric attenuation at these frequencies is likely

to be offset by the increased antenna size. The ATS-E will be exploring the utility of these millimetre bands.

Tunnel-diode front ends are being employed to increase the satellite receiver gain.

The predicted life of the satellites now in orbit are of the order of one to two years. The life of the satellite is estimated from the life of some of the critical components like the TWT, solar battery, degradation, moving parts, if any, the depletion of gas used for precession jets, etc. With alround improvements taking place in these fields, a forecast of a much longer life of the order of 10 to 30 years is predicted for the future satellites.

Applications

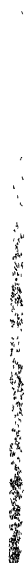
In the field of utilization, there is a trend towards multipurpose satellites capable of performing more than one function (like communications, air traffic control, TV, etc.). The number of channels available in a single satellite is being progressively increased. For example, in the 'Advanced Domestic Comsat' being planned, a total of 24 TV channels plus 60,000 voice-circuits are being catered for. By sharing a single satellite among many users service costs can be reduced and small and large ground terminals with differing communication requirements can participate at the same time. The first ATS-B satellite will test the multiple-access technique using frequency division multiplex (FDM). The FDM requires huge bandwidth, sometimes of the order of 500-megacycles per sec. and use of linear wideband tunnel-diode amplifiers on the satellite. Other methods like the Time Division Multiplex (TDM) and Pulse Code Modulation (PCM) are proposed for future systems. The PCM requires each carrier to be coded with a pseudo random 'key' in addition to voice information. Receivers with correct 'key' receive the desired signals while undesired signals appear as a slight increase in background noise. This method permits many access to be made on the same frequency without interference, the combined signal in satellite appearing like background noise. The security provided by this system makes it particularly useful for military systems.

One of the most exciting applications would be the possibility of data transmission by satellites, *e.g.*, computer-to-computer hook-ups *via* satellites. Distribution of the Central TV programmes to a network of local TV stations will be carried out *via* satellites instead of through ground links, as is being done at present. Direct satellite-to-home television service would be possible in the near future.

Communication satellites will be used for collecting meteorological information from a world wide network of weather observation stations and feed the data to a master computer complex to obtain the world weather picture. The same satellite network will be used to distribute the met analysis and forecast to cities and towns all over the world.

11. World wide satellite communication network

Fig. 10 shows the network of satellite ground terminals, and communication satellites which are operational, being built or in the planning stage.



Appendix 1

Name	Function	Launching date and results	Orbit	Technical specifications	Weight and dimensions
ECHO	Passive reflector, inflatable balloon of Gore construction, aluminized	1. August 12, 1960, still in orbit 2. January 25, 1961	Passive satellites 1. 1049/945 miles	1. Reflected 960 and 2,390 megacycles per sec. Contact between the U.S.A. and the U.S.S.R. Launch vehicle carried a TV camera, movie camera and a transmitter	1. 100 ft. diameter, 150 lb. 2. 135 ft. diameter, 550 lb.
WEST FORD	Passive reflection by volume dispersed randomly oriented dipoles	May 9, 1963 Disadvantages were: range smear and Doppler smear due to common volume of two antennas).	Circular	Tested on 8,350 and 7,750 megacycles per sec.	$\frac{1}{2}$ in. long, 0.0007 in., 20 kg.
SCORE	Delayed repeater (receives stores, and retransmits)	December 18, 1958 (12 days' life), delays upto 2 hr.	Active satellites 114 miles	1. Transmitter 132 megacycles per sec., 8 watts 2. Receiver 150 megacycles per sec; both receiver and transmitter duplicated; dry battery operated	150 lb.
COURIER	Delayed repeater	October 4, 1960 Can handle 69,000 words per min. Control system failed, after 18 days	578 miles 758 miles	Four transmitters Four receivers Five tape recorders Two telemetry transmitters plus command and control system 19,200 solar cells	Spherical, 51 in. diameter, 500 lb.
OSCAR	Orbital satellite carrying amateur radio built by amateurs	March 9, 1965 (Oscar 3) 1. 30 days' life 2. 30 days' life 3. 17 days' life	200 miles Circular	1,2. Transmitter only 114 megacycles per sec. 100 milliwatt output 'H' dry cells 3. Receiver 144.1 megacycles per sec. Retransmit 145.9 megacycles per sec. Beacon 145.85 megacycles per sec.	10 lb. (Oscar 1 and 2) 35 lb. (oscar 3) 12 in. x 18 in. x 8 in.
TELSTAR	Real time repeater to obtain scientific data on space environment by telemetry equipment	1. July 10, 1962 2. May 7, 1963 1. Fault in operation repaired by ground command	1. 3,514 miles 592 miles 2. 6,719 miles, 604 miles Period 1. 157.8 min. 2. 225.4 min. Spin stabilized	600 FM voice channel or 1 TV, or, 12 two-way telephony channel Spin stabilized 3,600 solar cells (15 watt) 19 nickel-cadmium cells Transmit 4,170 megacycles per sec. (2.25 watt) Receiver 6,390 megacycles per sec. Telemetry Tx 136 megacycles per sec. Rx 120 megacycles per sec. Beacon Transmitter for Tracking : 4,080 megacycles per sec.	34.5 in. diameter 170 lb. (1) 175 lb. (2)
RELAY	Medium altitude repeater scientific measurements	1. December 13, 1962 2. January 21, 1964 Still working	1. 4,630 and 822 miles, 185 min. 2. 4,606 miles, 1,298 miles 195 min.	All equipment duplicated Receiver : 1,725 megacycles per sec. Transmit : 4,170 megacycles per sec. Beacon : Tx 126 megacycles per sec. Rx 184 megacycles per sec. Spin stabilized omniantenna 8,216 solar cells (60 watts) TV or 300 voice telephony	175 lb. 8-sided cylinder truncated at one end 32 in. tall 29.5 in. diameter
SYNCOM	Active real time repeater. To study synchronous orbit operation : (now in military use)	July 26, 1963	22,230 miles, 22,230 miles, 23 hr. and 55.9 min. Truly stationary orbit	Spin stabilized Receiver 7,362 megacycles per sec. Transmitter 1,815 megacycles per sec. 3,750 solar cells (25 watts) 9 sun.	78 lb.

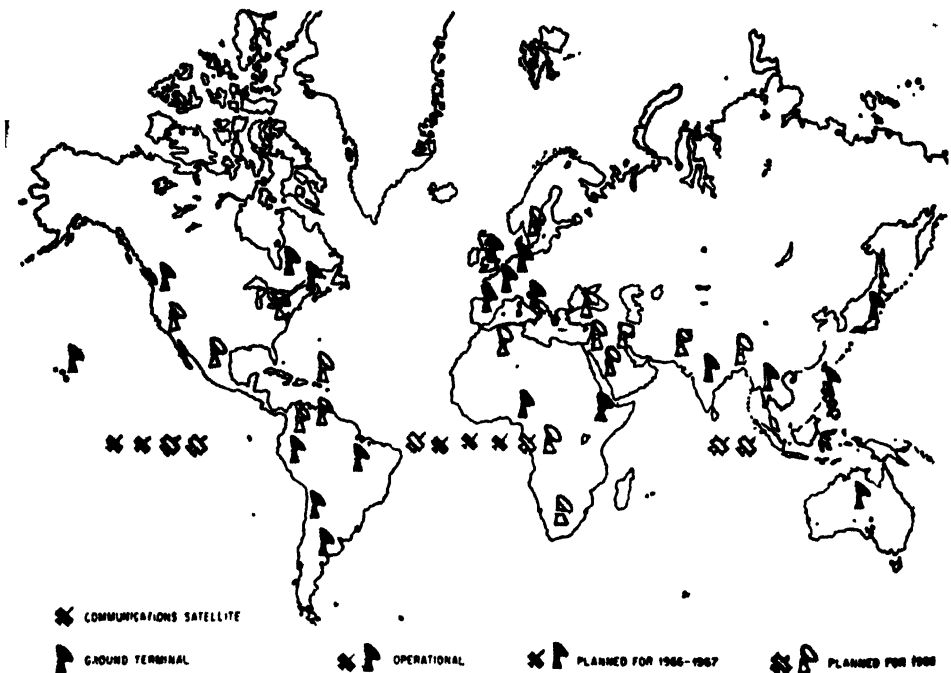


Fig 10

Proposed worldwide network of satellite ground terminals

12. References

1. L. Jaffee. 'Communications in Space'. *Holt, Reinhart and Winston Inc.*, 1966.
2. Gatland. 'Telecommunication Satellites'. *Iliffe Books Ltd.*, 1965.
3. Balakrishnan. 'Space Communications'. *McGraw-Hill Book Co. Inc.*, 1966.
4. Carter. 'Communication Satellites'. *Academic Press*, 1964.
5. Krussner and Michael. 'Introduction to Space Communications'. *McGraw Hill Book Co. Inc.*, 1965.
6. 'Satellite Communication Issue'. *Bell System Technical Journal*, July 1963, p. 739.
7. 'Communication Satellites Part—1'. *Electronics*, May 2, 1966, p. 83.
8. 'Communication Satellites—Part 2'. *Electronics* May 30, 1966 p. 109.
9. 'Aerospace in Perspective Utilization'. *Space and Aeronautics*, January 1967, p. 80.
10. S.K. Chatterjee. 'Satellite Communication'. *Electro Technology*, October 1965, p. 155.

Appendix 2

Calendar of major communication satellites

ECHO : Large self inflating spheres for passive communications :

Echo 1 : Launched in 1960

Echo 2 : Launched in 1964 (still working)

RELAY : Two active Comsats in medium altitude elliptic orbits :

Relay 1 : Launched in December 1962

Relay 2 : Launched in January 1964

SYNCOM : Three active in synchronous orbit :

Syncom II : Launched in July 1963, still used by the U.S. Defence Department

Syncom III : Launched in August 1964, still used by the U.S. Defence-department

INTELSAT I, (Early Bird)—First commercial Comsat (851 lb.) in synchronous orbit, April 1965, Link Europe and North America, 240 two-way voice channels 50 megacycles per sec. bandwidth.

INTELSAT 2, (Lani Bird) : Interim global commercial Comsat launched in December 1966. Failed to achieve synchronous orbit. Another to be launched in 1967.

INTELSAT 3, (Advanced Global Comsat) : Commercial global communication satellite, in synchronous orbit, launch due in 1968, 1,200 to 1,500 voice two way voice channels to cover Atlantic, Pacific and Indian oceans.

AERONAUTICAL COMSAT : Spin stabilized, similar to Intelsat 3 or ATS-B with aircraft to satellite VHF Link and ground to satellite microwave link, in synchronous orbit to provide air traffic and operational control communications over North Atlantic and Pacific traffic lanes for commercial aircraft. To be operational in 1969.

INTERIM DOMESTIC COMSAT : Two to four Intelsat—3—type satellites in synchronous orbit to provide TV, voice and teletype relay for continental U.S.; 12 TV or 6,000 to 9,300 voice channels (4 and 6 gigacycles per sec. bands) per satellite. To be operational in 1969.

ADVANCED PASSIVE COMSAT : To develop system parameters and technology to exploit multiple access, wide bandwidth and long life times of passive communications reflectors. Inflatable double lens configuration with gravity gradient, solar emissivity and low thruster stabilization. Synchronous and 2,000 nautical mile configurations in study. Will be launched in 1970s. Synchronous Comsat weighs 40,000 lb., and 2,000 nautical miles, Comsat weigh 120,000 lb.

ADVANCED DOMESTIC COMSAT: Domestic communications via four second generation comsats (in 3,000 lb. range) in synchronous orbit. Microwave and millimeter band carrier with PCM and FM modulation with 24 TV and 60,000 voice channel per satellite. To be launched in 1972, by Titan 3c.

APPLICATIONS TECHNOLOGY SATELLITES: Multi-mission 'Engineers' Satellites for research and development in communications, navigation, meteorology and spacecraft technology in synchronous and medium altitude orbits. Weight 1,600 lb. Spin stabilized ATS-B launched in December 1966, ATS-C to follow in late 1967; Gravity gradient stabilized ATS-A to be launched in mid-1967; ATS-D&E in 1968. ATS-E will explore the mm. bands (16 gigacycles per sec. and 36 gigacycles per sec.)

DELTA MODULATION***G.V. Subba Rao***Non-member**Defence Electronics Research Laboratory, Hyderabad***Summary**

Delta modulation is a novel coded modulation system. It is a differential pulse code modulation or unidigit code PCM and is as efficient as PCM, requires wider band-width but has a much simpler circuitry. In delta modulation, in contrast to PCM where n-digit binary code is used to transmit information, a code comprising of only one digit is used. The transmitted pulses carry the message information corresponding to the derivative of the amplitude of the message function and at the receiving end these pulses are integrated to obtain the original waveform. One of the significant difference between PCM and delta modulation is the relative simplicity and the low cost of the coding equipment in the latter. This paper covers the basic principles of delta modulation, its inherent quantizing noise, signal-to-noise performance and basic circuitry involved. Several variations like 'delta sigma modulation' and 'high information delta modulation' which overcome the deficiencies of the delta modulation will be introduced.

1. Introduction

The advantages of the digital communication techniques, namely, minimization of the influences of the interferences in the transmission path, relaying capability, uniformity and reliability of the output irrespective of the transmission distances involved and ease of adaptability to solid-state circuits have been very well known. In pulse modulation systems, the unmodulated carrier is usually a series of regularly recurrent pulses: information is conveyed by some parameter of the transmitted pulses such as amplitude, duration, time of occurrence or shape of the pulses. Pulse code modulation is considered to be the most efficient among the existing communication systems. A more recent pulse modulation system which has much simpler circuitry but is almost as efficient as PCM is the 'delta modulation'.

Delta modulation was invented in the ITT French Laboratories by E.M. Delorairé, S. Van Mierlo and B. Derjavitch. Considerable amount of work has been done on the delta and allied modulation systems by F. de Jager at Philips Laboratories, A. Lender at ITT French Laboratories, Inose and Yasuda at the Tokyo University and Zetterberg at Ericsson Laboratories. In India considerable contribution in this field is done by Dr. J. Das, Dr. M.N. Frauqui and others of the Indian Institute of Technology, Kharagpur.

*Presented at the Symposium on 'Modern Electronic Communication Techniques,' held in Hyderabad on August 26, 1967.

In delta modulation, a code comprising of only one digit is used and the information signal is converted into a sequence of binary pulses in such a manner that a reconstruction of it is obtained by applying these pulses to a linear network. The modulator output pulses carry the information corresponding to the derivative of the amplitude of the modulating signal.

Delta modulation is the simplest and cheapest known digital modulation system. It is not quite as efficient as its rival PCM in getting the maximum quality out of a given pulse rate. It does not lend itself to multiplexing, economically. The disadvantages of delta modulation that it can be used only for such signals as speech which do not contain a D.C. component and have less energy in high frequencies, and that its dynamic range and signal to noise ratio are inversely proportional to the signal frequency are overcome in the modified delta modulation systems like delta sigma modulation system and the high information delta modulation system.

As far as is known, delta modulation has not yet been used commercially. Motorola, Inc., of the U.S.A. has been trying to use delta modulation as the modulation technique in its random access discrete address system but that equipment has not been accepted by the Defence Department yet.

2. Theory of delta modulation

The basic circuit for delta modulation is shown in Fig. 1. It consists of a pulse generator, a modulator, an integrating network and a comparator and is essentially a quantized feedback system. The modulator sends out either positive or negative pulses at the clock rate depending on whether the output of the comparator is positive or negative. One input to the comparator is the message signal. The second input is derived by synthesizing the modulator output pulse train by passing it through the integrating network in the feed back path. The comparator output, which is the difference between these two inputs decides what the polarity of the output pulses should be in order to correct for the difference between the two voltages. The feed back system tends to reduce the difference, so that the synthesized signal follows the message

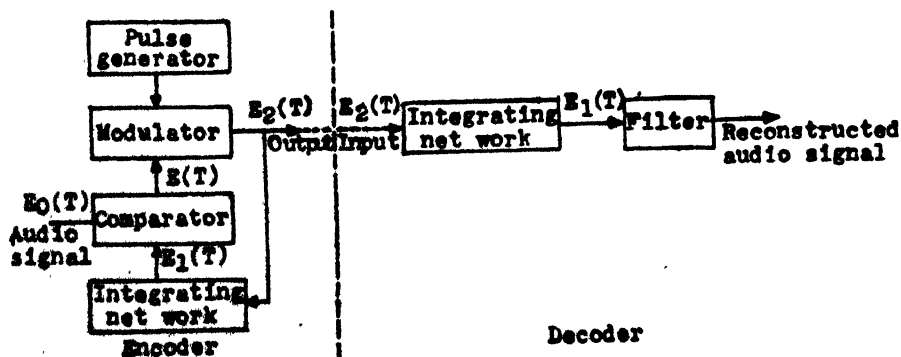


Fig. 1

Block diagram of a delta modulator

signal. Sampling of the difference signal is done at a constant rate by the pulses from the pulse generator.

In practice the negative pulses of the output signal are omitted without affecting the signal to noise ratio.

The decoder consists of an integrating network followed by a low pass filter and an amplifier. The output of the integrator is the original message signal plus noise components due to sampling. These are eliminated by the low-pass filter. The difference between the original and the reconstructed signal gives rise to quantizing noise which can be decreased by increasing the pulse frequency. In contrast to the quantization principle of PCM, the information is quantized in a one-unit code and the 'sampling frequency' is made equal to the pulse frequency. This results in very rough quantizing, which is compensated by the fact that the signal samples are taken as often as indicated by the pulse interval and thus n times as often as for PCM at the same pulse frequency, where n equals the number of pulses in the PCM code group.

The simplest system of delta modulation is obtained by using an integrating network in the feedback path. This network has a large time constant and its response to an impulse is practically an unit step function. The waveforms using single integration are shown in the Fig. 2. This simple integrator results in coarse quantization and large quantizing noise. At a pulse frequency of 40 kilocycles per sec. the intelligibility of speech will be good but the quantizing noise will have an effect on speech which is called by de Jager 'sandiness'.

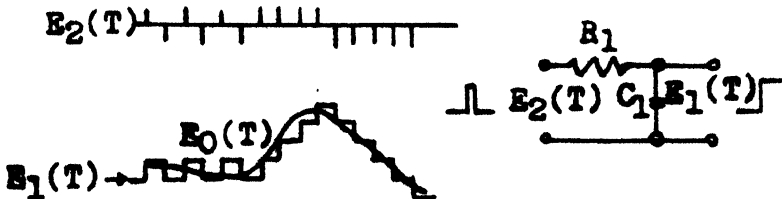


Fig. 2

Delta modulation waveforms using single integrator

The large quantization noise resulting from the usage of single integrator can be reduced by the usage of the double-integrator circuit shown in Fig. 3. The time constants, $R_1 C_1$ and $R_2 C_2$, are large so that the response to a pulse is a step at C_1 and a voltage of constant slope at C_2 . The effect of this circuit is to change the slope of the output with every pulse input. As is seen in the figure the resulting waveform is much smoother than for the case of single integration where every received pulse has the effect of increasing or decreasing the level of the received signal by a unit step. When the output of the double integrator is smoothed by passing through a low pass filter, it will approximate the original message function much closer than single integrator. Another modification is done to the feedback network utilizing the principle of prediction. This overcomes the disadvantage of delay in recognizing the changes in the message shape encountered in other types of feedback networks. The modification consists of a prediction time constant T , made arbitrarily equal to

the pulse interval. With this prediction the response of the circuit is a step followed by a voltage of constant slope. By means of this step, the output of the network knows in advance what the voltage at the capacitor is rising to. This is equivalent extrapolation. The advantage can be seen in Fig. 3, the two approximating curves $e_1(t)$ for the same signal, $e_0(t)$.

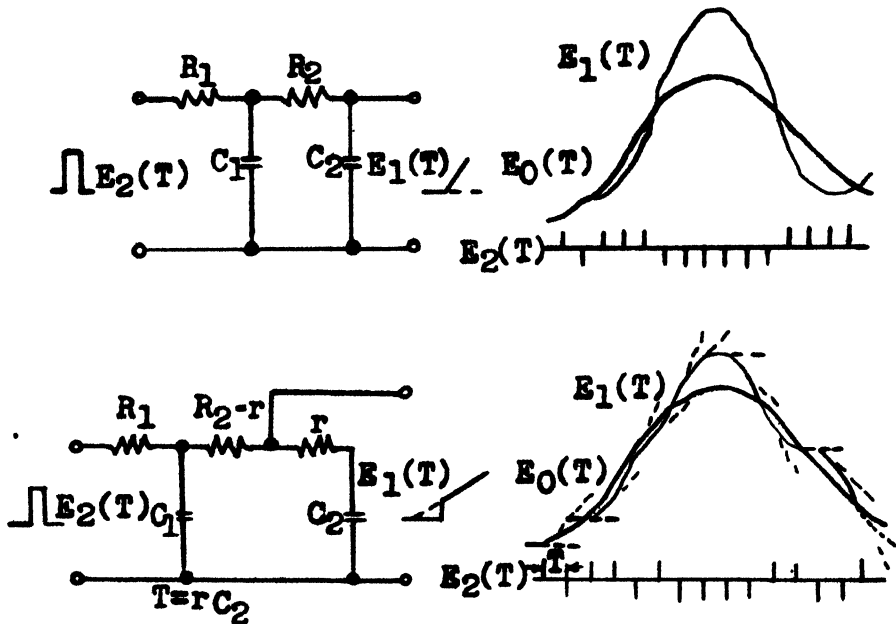


Fig. 3

Use of a double integrator circuit

3. Problem of overloading

The problem of 'overloading' is different in delta modulation system compared to others. In delta modulation system, the information contained in the transmitted pulses is mainly correlated to changes of input signal and not to its amplitude. However, since the synthesized wave can change only one level per clock pulse, delta modulation has no fixed maximum amplitude but overloads when the slope of the signal is too large. The largest slope the system can reproduce is one changing by one level or step every pulse interval, so that the maximum signal power depends on the type of signal. If the magnitude of one quantum step is σ volts and the time between sampling instants is $T_s = \frac{1}{f_s}$ sec., then the maximum rate of change of amplitude it can register is $\frac{\sigma}{T_s}$ or σf_s volts per sec.

For a sine wave of angular frequency, $\omega = 2\pi f$ the maximum slope is $A\omega$, where A is the peak amplitude. Therefore, for a sine wave of frequency

f_s , applied to the integrator, the maximum amplitude which can be transmitted is

$$A_{\max.} = \frac{f_s \sigma}{2 \pi f}$$

Thus, both the maximum amplitude and the number of distinguishable levels decrease with increase of frequency to be transmitted. This limitation is minimized in the case of speech where the higher frequencies contain less energy than the lower ones so that in this respect an integrating network is well adapted to the transmission of speech.

It has been observed experimentally that the delta modulation system can transmit a speech signal without overloading, if the amplitude of the signal does not exceed the maximum sine wave amplitude that can be transmitted at a frequency of 800 cycles per sec.

4. Signal-noise ratio in delta modulation

System of single integration

Lender has shown that the quantizing noise power is approximately given by

$$N_s = \frac{1}{3} \left(\frac{f_m}{f_s} \right) \sigma^2$$

The maximum amplitude which can be transmitted without overload with single integration is given by

$$A = \frac{f_s \sigma}{2 \pi f}$$

Therefore, the average signal power is given by

$$S_s = \frac{A^2}{2} = \frac{f_s^2 \sigma^2}{4 \pi^2 f^2}$$

Therefore, the signal-noise ratio for single integrator system is given by

$$\frac{S}{N} = \frac{1}{3} r^2 \left(\frac{f_m}{\pi f} \right) = C_1 \frac{f_s^3}{f_m^3 f^2}$$

Quantizing noise in the system of double integration Lender has obtained the signal-noise ratio as

$$\frac{S}{N} = \frac{1}{3} r^2 \left(\frac{f_m}{\pi f} \right)^4 = C_2 \left[\frac{f_s^5}{f_m^3 f^4} \right]$$

The improvement in signal-noise ratio varies with f_s^3 for system with single integration, whereas it varies with f_s^5 for system with double integrators.

5. Bandwidth consideration

F. de Jager has experimentally established that with a pulse frequency of 100 kilocycles per sec. very good reproduction of speech is possible. In this case,

a bandwidth of 50 kilocycles per sec. is required. For PCM of a code of n digits,

$$\frac{S}{N} = 20 \log_{10} 2^n \text{ dB}$$

For $\frac{S}{N}$ of 50 dB, $n = 8$.

Taking a sampling frequency of 8 kilocycles per sec. the clock frequency is 64 kilocycles and so the bandwidth required is 32 kilocycles per sec., about 50% of what is required for delta modulation.

Fig. 4 shows the relationship between signal-noise ratio, sampling rate and the frequency. With speech confined to frequency of 4 kilocycles per sec. the signal-noise ratio of PCM and delta modulation are 44 dB and 29 dB for a pulse frequency of 56 kilocycles per sec. and 74 dB and 33 dB for pulse frequency of 96 kilocycles per sec.

6. Delta sigma modulation

Delta modulation is incapable of transmitting D.C. signals, its dynamic range and signal-noise ratio are inversely proportional to the signal frequency and the integration at the decoder results in accumulative error in the demodulate signal when the system is subjected to transmission disturbance such as noise. The delta sigma modulation system overcomes these defects and meets the requirements for digital transmission of video signals and the like which are characterized by more uniform spectra with D.C. components through adverse transmitting conditions. Delta sigma modulation system is due to Inose, Yasuda and others of the Tokyo University. The delta sigma modulator is shown in Fig. 5. The output pulse p , is fed back to the input and subtracted from the modulating signals. The difference signal $\Delta = s - p$, is integrated and the integrated difference signal, $e(t) = \int \Delta(t) dt$, is compared in amplitude with a predetermined reference. If the integrated difference signal is larger than the reference signal a pulse is sent out. The negative feedback always keeps the integrated difference signal near the reference. Thus output pulses carry data corresponding to the input amplitude.

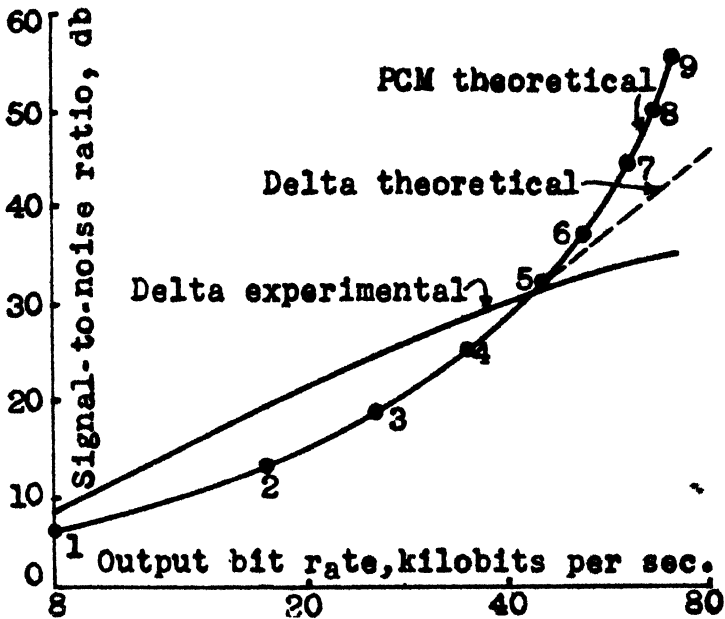
Decoding consists of only reshaping the pulses and passing them through a low pass filter. No integration is involved so that no cumulative error resulting from transmission disturbances occurs.

The signal-noise ratio with single integration is given by

$$\frac{S}{N} \propto \frac{f_s^3}{f_m^3}$$

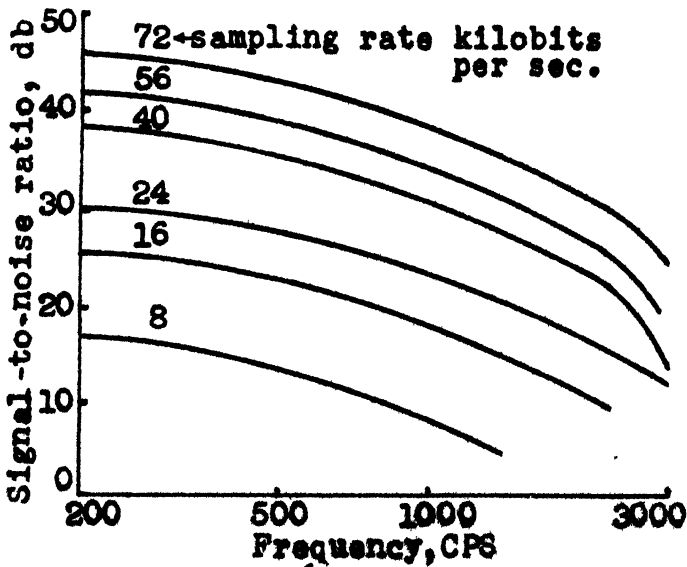
The $\frac{S}{N}$ ratio for delta modulation is proportional to $\frac{f_s^3}{f_m f^2}$. The same relationship to the pulse repetition frequency exists in both the cases but the signal frequency has no relation to the signal to quantizing noise ratio in the delta sigma modulator.

With double integration, the signal to noise ratio is proportional to f_s^5 .
For k integrators the signal-noise ratio is proportional to f_s^{2k+1}



(i)

Signal to noise ratio for delta modulation and PCM



(ii)

Fig. 4

Signal-to-noise w. frequency

7. High information delta modulation (HIDM)

The HIDM which is another variation of delta modulation provides greater dynamic range than ordinary delta modulation and can be used for voice communication with excellent results upto 20 kilocycles per sec. This modification is due to Winkler.⁷

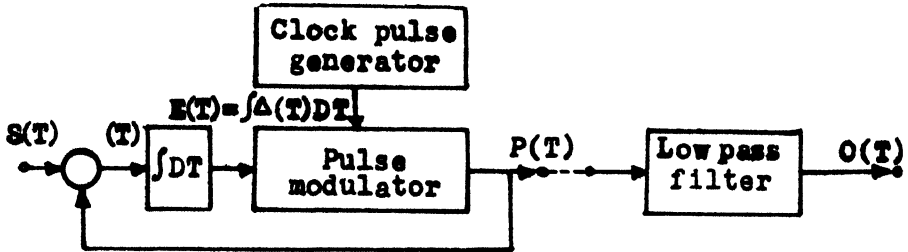


Fig. 5

Block diagram of the delta-sigma system

In the ordinary delta modulation, the amplitude level after the integrator can rise only linearly. To reach an amplitude level of 40 units, say, it will take 40 pulse periods.

In HIDM, the counting of the amplitude levels is performed in binary steps, resulting in an exponential variation of 2^n of amplitude levels due to a sequence of pulses of one polarity. So in less than a period of 7 pulses the magnitude of $39\frac{1}{2}$ is exceeded. The circuit of the HIDM is similar to that of a delta modulator except for the demodulator. The block diagram of the HIDM demodulator is shown in Fig. 6. The flip-flop takes a state depending on the polarity of the pulses. The exponential generators are used alternately, one generating positive waveform and the other negative waveform. The impulse device delivers the proper initial impulse to the exponential generators. The output of the exponential generators consists of a series of exponential ramp signals which are summed in an integrator to provide the desired

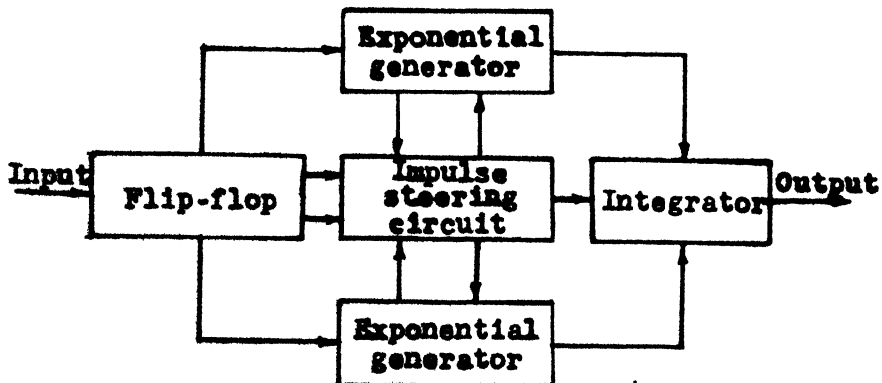


Fig. 6

Block diagram of a HIDM modulator

demodulator output. It has been shown by Winkler that the dynamic range of HIDM with slope limiting of 11.1 levels per pulse period is much greater than the dynamic range of ordinary delta modulation and equivalent to 7 bit PCM with linear quantizing. The HIDM response to step function is shown in (Fig. 7).

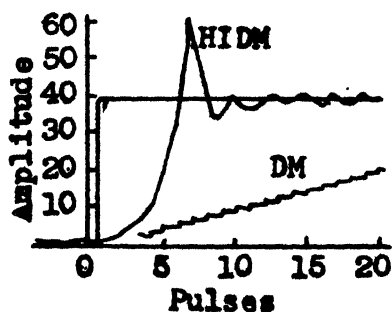


Fig. 7

HIDM response to step function

8. Conclusion

With a number of modifications for the basic delta modulation system coming up to make it sophisticated enough to compete with its rival PCM it is sure delta modulation will very soon occupy a better place than the modest place it occupies presently in the world of communications.

9. References

1. P.F. Panter. 'Modulation, Noise and Spectral Analysis'. McGraw-Hill Book Co., Inc., 1965
2. F. de Jager. 'Delta Modulation—a Method of PCM Transmission Using the 1-Unit Code'. *Philips Research Reports*, vol. 7, 1952, p. 442.
3. A. Lender and M. Kozuch. 'Single Bit Delta Modulation System'. *Electronics*, vol. 34, no. 46, November 17, 1961, p. 125.
4. J.F. Schouten, F. de Jager and J. A. Greefkes. 'Delta Modulation System for Telecommunication'. *Philips Technical Review*, vol. 13, no. 9, March 1952, p. 237.
5. F.K. Bowers. 'What Use is Delta Modulation to Transmission Engineers?'. *Communications and Electronics*, no. 29, March 1957, p. 142.
6. H. Inose, Y. Yasuda and J. Murakami. 'A Telemetering System by Code Modulation—Delta Signal Modulation'. *Transactions of the Institute of Radio Engineers, Space Electronics and Telemetry*, vol. 8, September 1962, p. 204.
7. M.R. Winkler. 'High Information Delta Modulation'. *Institute of Radio Engineers Convention Record*, 1963.

PROCEEDINGS OF THE SYMPOSIUM ... 363

PROCEEDINGS

The Symposium on 'Modern Electronic Communication Technique' started with a welcome address by Shri O. Thimmaiah (*M.*), Chairman of the Andhra Pradesh Centre of the Institution. The Symposium was inaugurated by Major General S.P. Vohra, M.I.E., President of the Institution of Engineers (India).

Prof. S.P. Chakravarti (*M.*), Chairman of the Electronics Division of the Institution, took the chair for the first session and six papers were read in that session by various speakers.

Opening the Session, Prof. S.P. Chakravarti thanked the President, Major General S.P. Vohra, and Shri O. Thimmaiah for organizing such a Symposium on the 'Modern Electronic Communication Techniques' which is a very good subject and covers the developments in communication from 1954 onwards till date. He was very much pleased to note that there has been a very good response from the various institutions in India and very good papers have been received. Seventeen papers have been received but due to paucity of time only a few selected papers in the two sessions could be presented on separate subjects.

• Prof. Chakravarti said, 'Before I call the authors to present their papers I would like to specially thank Brig. C.L. Seshagiri and Lt. Col. S.B. Lal for the very good work done by them in getting the pre-prints of papers ready in such a record time. I want to express my personal thanks to Lt.-Col. B. Bhasin who is an Associate Member of the Institution and also a member of the Local Committee of this Centre, in organizing this Symposium. He has been a live-wire and due to his personal efforts the symposium has come up with such a good response of papers from various leading institutions in India. I would also like to thank the Local Centre for the very good arrangements made for the Symposium.'

Prof. Chakravarti then delivered a brief resume of the modern techniques in the field of electronic communication after which he requested the authors to come and present their papers.

The following papers were presented in Session 1:

1. 'Unidigit PCM System' by Dr. M.N. Faruqui, Assistant Professor, Department of Engineering, Indian Institute of Technology, Kharagpur.
2. 'Survey of Developments in Digital Communication Systems' by Shri C.R. Chakravarti, Senior Scientific Officer, Defence Electronics Research Laboratory, Hyderabad.
3. 'Digital Filters' by Prof. A. Prabhakar, College of Engineering, Osmania University, Hyderabad.
4. 'Shift Register Sequences' by Shri C. Satyanarayana, Lecturer in Department of Electronics, College of Engineering, Osmania University, Hyderabad.

5. 'Satellite Communications' by Maj. R.K. Joshi, Instructor in Radar Engineering Wing, EME School (South), Secunderabad.
6. 'Decoding of Pseudo-Random Coded Sequences' by Shri A. K. Mukherjee, Assistant Professor, Department of Engineering, Indian Institute of Technology, Kharagpur.

Session 2 was presided over by Prof. V.V.L. Rao, Principal (Retd.), Regional Engineering College, Warangal. Prof. V.V.L. Rao was very kind enough to agree to take the Chair as Brig. M.K. Rao who was to preside over the session was held up and was unable to come in time. Prof. V.V.L. Rao declared the session open and requested the speakers to come and present their papers.

The following papers were presented in Session 2 :

1. 'Microwave Communication along Railway Routes' by Shri S.A. Srinivasan, Chief Signal and Telecommunications Engineer, South Central Railway, Secunderabad.
2. 'Speech Compression and Expansion' by Shri S.V.R. Naidu, EME School (South), Secunderabad.
3. 'Bandwidth Compression of Speech' by Shri G. Kanttaiah, Senior Scientific Officer, Defence Electronics Research Laboratory, Hyderabad.

Prof. V.V.L. Rao, in the end, summed up the lectures and thanked the various authors who presented the papers during the afternoon session.

Each author was allowed 20 minutes time to present his paper and 10 minutes were given for discussions. There had been very lively discussions after the presentation of each paper and various important issues emerged from the discussions for the benefit of the participants.

Brig. C.L. Seshagiri, Commandant, EME School, at the conclusion of Session 2 thanked all the authors and participants for making the symposium a grand success and especially expressed his thanks to Prof. V.V.L. Rao who very kindly had agreed to preside over Session 2. The Symposium concluded with a vote of thanks to all.

All the papers received for the Symposium were printed in a booklet form and distributed to all members and participants attended during the 450th Council Meeting of the Institution of Engineers (India) held at Hyderabad from August 24-28, 1967.

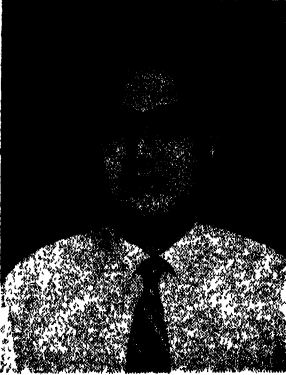
The following were the members of the Organising Committee for the Symposium :

- Brig. C.L. Seshagiri, M.I.E., Commandant, EME School, Secunderabad and Chairman of the Organising Committee.
- Lt. Col. B. Bhasin, C. Eng., A.M.I.E., A.M.I.T.E., A.M.M.E.A., Assistant Director, DLRL, Hyderabad 5, and Member of the Organising Committee.
- Lt. Col. S.B. Lal, Non-member, EME School (South), Secunderabad, and Member of the Organising Committee.

ABOUT THE AUTHORS

Dr. M.N. Faruqi

Dr. Nasim M. Faruqi received the B. Tech. (Hons.) degree in Electrical Engineering (Communication) and the M. Tech. degree in UHF and Microwave Engineering from the Indian Institute of Technology, Kharagpur, in 1956 and 1961 respectively. He received the Ph.D. Degree for his work on 'Studies on Unidigit PCM Systems' in 1964 from the Indian Institute of Technology, Kharagpur. He took one year's training in Overseas Communication Service, Bombay, and joined the Indian Institute of Technology, Kharagpur, in 1958. Presently he is an Assistant Professor there and is engaged in research on Communication Systems.



Shri C.R. Chakravarthi

Shri Chakravarthi received the B.Sc. (Hons.) Degree with Physics as the special subject from the Central College, Bangalore, of the Mysore University in 1957 and the Post Graduate Diploma of Indian Institute of Science, Bangalore, in Electrical Communication Engineering in 1960. He joined the Research and Development Organization, Ministry of Defence, in 1960, and was employed in the Aeronautical Development Establishment, Ministry of Defence, Bangalore, wherein he was engaged in developmental work in the field of aviation electronics for about one year and eight months. Since 1962, he has been engaged on various research projects in the field of development of advanced techniques applied to digital communication systems at the Defence Electronics Research Laboratory, Hyderabad.



Shri A. Prabhakar

Shri Alladi Prabhakar graduated in Electrical Engineering from the Madras University in 1948 securing a First Class. He was Research Scholar at the Indian Institute of Science, Bangalore, from 1950 to 1951 and Junior

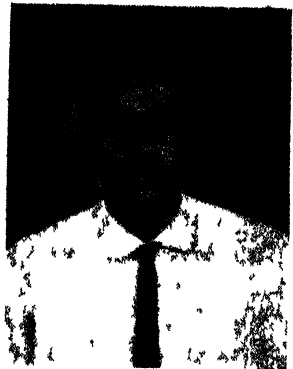


Scientific Officer at the Defence Science Laboratory, Delhi, from 1951 to 1952. He then served as Lecturer and Assistant Professor, Institute of Armament Technology, Kirkee, from 1952-1954. In 1965, he proceeded to the United States where he got his Master's Degree in Electronics from the Harvard University. In 1960 he was deputed to attend the NATO Advanced Guided Missile Course at Cranfield, England. In 1964 he was appointed Professor of Electronics and Communication Engineering at the Osmania University, Hyderabad. His specialization is in the field of Analogue Computers and Servomechanisms. He

has published about 20 papers in Indian and foreign Journals.

Shri C. Satyanarayana

Shri Satyanarayana obtained the B.E. Degree in Electrical Communication Engineering from the Indian Institute of Science, Bangalore, in 1963. For about an year he worked as Associate Lecturer at the College of Engineering, Osmania University. After obtaining the M. Tech. Degree in Electrical Engineering from the Indian Institute of Technology, Kanpur, in 1966, he joined as Lecturer in the Department of Electronics and Communication Engineering, College of Engineering, Osmania University, Hyderabad.



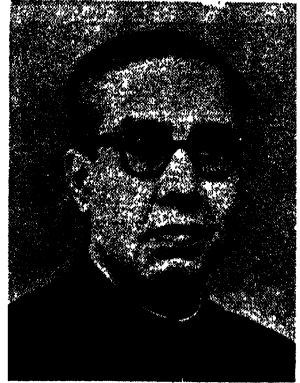
Major R.K. Joshi



Major Joshi graduated in 1959 from the Indian Institute of Technology, Kharagpur, and was commissioned in the Army in 1960. He has done an advanced course in communication engineering from the Military College of Electronics and Mechanical Engineering, Secunderabad. Later on, he has done a course abroad and is presently employed as an instructor in the Radar Engineering Wing of the Military College of Electronics and Mechanical Engineering, Secunderabad.

Shri S.A. Srinivasan

Shri Srinivasan is the Chief Signal & Telecommunication Engineer of the South Central Railway. He was the Chief Signal & Telecommunication Engineer of the Southern Railway till this new Railway was formed. He has organized a Signal Engineering & Telecommunications Training Institute for the Officers and Inspectors of the Indian and Nigerian Railways and became its Principal in 1957. Prior to that he had worked in various capacities on the Central, Western and North Eastern Railways and in the Railway Board. He was also associated with the design and installation of the early route relay inter-lockings and multiple aspect upper quadrant installations on the Indian Railways.

**Major P.P. Chawla**

Major Chawla obtained his B.Sc. (Engg.) Degree in Electrical Engineering from the Bihar Institute of Technology, Sindri, in First Division with distinction in 1956. He got his commission in the Army immediately thereafter and has undergone various courses which includes one on 'Earth Moving Machinery' and a 'Junior Commandors' Course. Recently he underwent a 16-months Electronic Specialist Course. He has also served as Workshop Officer and Officer Commanding of various types of field workshops both in peace and field. He saw active service in one of the workshops against the Chinese in 1962. At present he is commanding a field workshop.

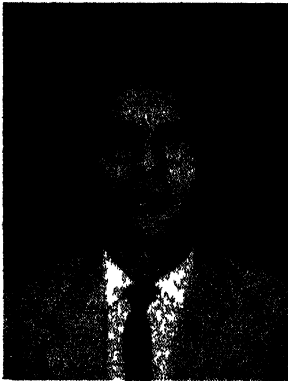
**Shri C.R. Ramachandran Nair**

Shri Nair passed his B.Sc. examination with Physics as main subject from the Kerala University in 1959. He obtained his B.E. Degree in Electrical Communication Engineering from the Indian Institute of Science, Bangalore, in 1962. He joined the Research and Development Organization, Ministry of Defence, where he worked till 1964. He is now working as Workshop Officer in the Military College of Electronics and Mechanical Engineering, Secunderabad.



Dr. M.S.V. Gopal Rao

Dr. Rao received his degrees of B.Sc. (Hons.) in Physics, M.Sc., and D.Sc., degrees from the Andhra University, Waltair, in the years 1954, 1955 and 1960.

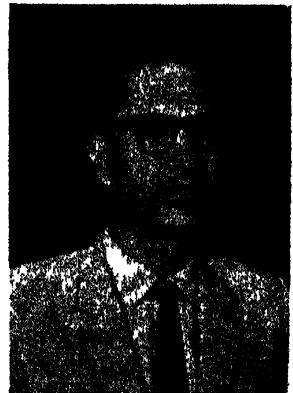


He was awarded the Metcalf Medal (1955) of the Andhra University. He has worked as a Lecturer in Physics (1959-60) and as a Senior Research Fellow (CSIR) (1960-61) at Andhra University. He has served on the Faculty as a visiting Assistant Professor of Electrical Engineering at Cornell University, Ithaca, New York (1961-62). He was a Pool Officer in Physics at the Indian Institute of Technology, New Delhi. He joined the Defence Research and Development Organization (1963) as Senior Scientific Officer at Defence Electronics Research Laboratory, Hyderabad. He has been specializing in the fields

of Radio Wave Propagation, Communications and Electronics.

Wing Commander R. Nagaraja Rao

Wing Commander Nagaraja Rao obtained his B.E. Degree in Electrical Engineering in 1948 from the Engineering College, Bangalore, and the D.I.I.Sc. in Communication Engineering from the Indian Institute of Science, Bangalore. He worked for more than two years at the High Power Transmitters, All India Radio, New Delhi. He then joined the I.A.F. as Technical Signal Officer in August 1951. He has been working in Air Force in several capacities as Maintenance Engineer, Instructor, etc., in the field of ground and airborne electronic and radar equipment. He was deputed to France for specialized training on aircraft equipment in 1953. He passed the post-graduate Diploma Course in Aircraft Electrical Engineering at the College of Aeronautics, Cranfield, U. K., in 1960. He is presently employed as an Assistant Director at the Defence Electronics Research Laboratory, Hyderabad.



PUBLICATION FOR SALE (*continued from Cover ii*)

5. Proceedings of the Symposium on 'Economy and Efficiency of Engineering Enterprises in India.' The Institution of Engineers (India). 242 pages. Rs. 15.00.

In an age dedicated to productivity, the need for economy and efficiency in Indian enterprises is well understood. Nevertheless, obstacles abound on the way. In this *Proceedings* 'The problem has been stated, the maladies described; and the solution suggested—unanimously by the engineers in the country'.

6. Proceedings of the Symposium on 'Prestressed Concrete'. The Institution of Engineers (India). 265 pages. Rs. 15.00.

In this *Proceedings*, the papers presented in the Symposium held on February 21, 1955, at Hyderabad, under the joint auspices of the Institution and the Concrete Association of India, have been compiled.

7. Proceedings of the Symposium on 'Prestressed Concrete'. The Institution of Engineers (India). 226 pages. Rs. 15.00.

In this *Proceedings*, the papers presented in the Symposium held by the Institution on February 4-7, 1960, at New Delhi, have been compiled.

8. An Engineering Wizard of India. Dildar Husain, Past-President, The Institution of Engineers (India). 163 pages. Rs. 10.00.

This book, dedicated 'to all those Corporate Members of the Institution of Engineers (India) who face the future with confidence, drawing inspiration from the example of Sir Mokshagundam Visvesvaraya, who devoted his life and services to the country, for a creative tomorrow', is a memorial volume published on the occasion of unveiling of the statue of Sir Mokshagundam Visvesvaraya at Hyderabad.

* These publications can be obtained from the Institution on payment of the charges in advance by cheque drawn in favour of 'The Secretary, The Institution of Engineers (India)'. Postage will be charged extra.

I. A. R. I. 75.

IMPERIAL AGRICULTURAL RESEARCH
INSTITUTE LIBRARY
NEW DELHI.

[illegible]